

Hepatocellular carcinoma with obstructive jaundice: diagnosis, treatment and prognosis

Lun-Xiu Qin, Zhao-You Tang

Lun-Xiu Qin, Zhao-You Tang, Liver Cancer Institute and Zhongshan Hospital, Fudan University, Shanghai, China
Correspondence to: Zhao-You Tang, M.D., Professor & Chairman, Liver Cancer Institute, Fudan University, 136 Yi Xue Yuan Road, Shanghai 200032, China. zytang@srcap.stc.sh.cn
Telephone: +86-21-64037181 **Fax:** +86-21-64037181
Received: 2002-10-09 **Accepted:** 2002-11-25

Abstract

Obstructive jaundice as the main clinical feature is uncommon in patients with hepatocellular carcinoma (HCC). Only 1-12 % of HCC patients manifest obstructive jaundice as the initial complaint. Such cases are clinically classified as "icteric type hepatoma", or "cholestatic type of HCC". Identification of this group of patients is important, because surgical treatment may be beneficial. HCC may involve the biliary tract in several different ways: tumor thrombosis, hemobilia, tumor compression, and diffuse tumor infiltration. Bile duct thrombosis (BDT) is one of the main causes for obstructive jaundice, and the previously reported incidence is 1.2-9 %. BDT might be benign, malignant, or a combination of both. Benign thrombi could be blood clots, pus, or sludge. Malignant thrombi could be primary intrabiliary malignant tumors, HCC with invasion to bile ducts, or metastatic cancer with bile duct invasion. The common clinical features of this type of HCC include: high level of serum AFP; history of cholangitis with dilation of intrahepatic bile duct; aggravating jaundice and rapidly developing into liver dysfunction. It is usually difficult to make diagnosis before operation, because of the low incidence rate, ignorance of this disease, and the difficulty for the imaging diagnosis to find the BDT preoperatively. Despite recent remarkable improvements in the imaging tools for diagnosis of HCC, such cases are still incorrectly diagnosed as cholangiocarcinoma or choledocholithiasis. Ultrasonography (US) and CT are helpful in showing hepatic tumors and dilated intrahepatic and/or extrahepatic ducts containing dense material corresponding to tumor debris. Direct cholangiography including percutaneous transhepatic cholangiography (PTC) and endoscopic retrograde cholangiopancreatography (ERCP) remains the standard procedure to delineate the presence and level of biliary obstruction. Magnetic resonance cholangiopancreatography (MRCP) is superior to ERCP in interpreting the cause and depicting the anatomical extent of the perihilar obstructive jaundice, and is particularly distinctive in cases associated with tight biliary stenosis and along segmental biliary stricture. Choledochoscopy and bile duct brushing cytology could be alternative useful techniques in the differentiating obstructions due to intraluminal mass, infiltrating ductal lesions or extrinsic mass compression applicable before and after duct exploration. Jaundice is not necessarily a contraindication for surgery. Most patients will have satisfactory palliation and occasional cure if appropriate procedures are selected and carried out safely, which can result in long-term resolution of symptoms and occasional long-term survival. However, the prognosis of icteric type

HCC is generally dismal, but is better than those HCC patients who have jaundice caused by hepatic insufficiency.

Qin LX, Tang ZY. Hepatocellular carcinoma with obstructive jaundice: diagnosis, treatment and prognosis. *World J Gastroenterol* 2003; 9(3): 385-391
<http://www.wjgnet.com/1007-9327/9/385.htm>

INTRODUCTION

Jaundice presents in 19 % to 40 % of patients with hepatocellular carcinoma (HCC) at the time of diagnosis and usually occurs in later stages. In most situations, it is due to diffuse tumor infiltration of liver parenchyma, hilar invasion, or progressive terminal liver failure (advanced underlying cirrhosis)^[1]. Obstructive jaundice as the main presenting clinical feature is uncommon. Only 1-12 % of HCC patients manifest obstructive jaundice as the initial complaint^[2]. Identification of this group of patients is clinically important, because surgical treatment may be beneficial.

Mallory *et al.* described the first such case in 1947, in which HCC invaded the cystic duct and gave rise to obstructive jaundice caused by hemobilia from the tumor thrombi^[3]. Thereafter, there have been few and scattered reports of such presentations of HCC in English literatures^[4-11]. In 1975, Lin *et al.* clinically classified such cases as "icteric type hepatoma", which manifested as obstructive jaundice in the early stage before the tumor became discernible or palpable^[12]. Okuda classified these patients as "cholestatic type of HCC"^[13].

Thrombus in bile duct (BDT) is one of the main reasons of obstructive jaundice. The incidence was 1.2-9 % in previous report^[4,12-15]. Huang *et al.* collected the cases from the newly diagnosed HCC patients of the admission registration database, and found the incidence of this type HCC was only 0.53 %^[16]. Variation in the biological behavior of HCC may partly account for the difference in incidence. It is reported that the incidence is increasing in patients with HCC, and transcatheter arterial chemoembolization (TACE) therapy could increase the possibility of common bile duct obstruction of tumor thrombi^[17].

PATHOLOGICAL FEATURES

HCC may involve the biliary tract in several different ways: tumor thrombi, hemobilia, tumor compression, and diffuse tumor infiltration. Infrequently, jaundice may also result from the external compression on the major bile ducts by direct tumor encasement or by the metastatic lymphadenopathy at the porta hepatis^[18,19].

BDT might be benign, malignant, or a combination of both. Benign thrombi could be blood clots, pus, or sludge. Malignant thrombi could be primary intrabiliary malignant tumors, HCC with invasion to bile ducts, or metastatic cancer with bile duct invasion. HCC invasion into bile duct may be due to one of the three mechanisms: (1) a distal tumor may grow continuously until it fills the entire extrahepatic biliary system; (2) a fragment of necrotic tumor may separate from the proximal intraductal growth, migrate to the distal common bile

duct and cause an obstruction; (3) hemorrhage from the tumor may partially or completely fill the biliary tract with tumor-containing blood clots^[4, 14-16, 20, 21]. In this type of HCC, blood clots are inevitably mixed with fresh tumor debris. However, Shimoji *et al.* reported one case suspected recurrent HCC during the choledochotomy after left hepatectomy for HCC, no HCC was detected by either macroscopic or intra-operative ultrasonographic examination. The course of hemobilia thus remained unclear until the autopsy was performed. Hemorrhage from a ruptured branch of the portal vein into the intrahepatic bile duct, filling the entire common bile duct with solid casts of blood, is uncommon. The hemorrhage into intrahepatic bile duct may be secondary to a portal vein rupture from: (1) a rupture of the engorged or variceal proximal portal vein leading directly into the intrahepatic duct; (2) necrosis of a cirrhotic liver nodule adjacent to both the intrahepatic bile duct and the vein; or (3) either cholangitis or an abscess in the proximal intrahepatic bile duct. Despite the remarkable recent improvements in various diagnostic modalities, hemobilia is still often incorrectly diagnosed as biliary tract carcinoma or stones. The etiologic diagnosis of jaundice in patients with cirrhosis, either with or without HCC, is thus of great clinical importance^[22].

Fragments of tumor in the bile duct, as described by Edmondson and Steiner, are usually fragile, fleshy, and grayish-white, having the appearance of chicken fat^[23]. BDT often grows faster than the primary cancer. The parenchymal tumor could be not continuous with the extrahepatic bile duct tumor. The bile duct tumor might attach to the mucosa of the bile duct with a thin stalk, without invasive growth into the submucosa^[24]. Most of the primary tumors are pathologically confirmed as HCC, however, the growth of mixed type of liver cancer (HCC and cholangiocarcinoma) into the common bile duct (CBD) has also been found, which may differ from the underlying mechanism of the development of icteric type HCC^[25].

In most cases, hepatic tumors can not be palpated from the liver surface because they are deep-seated and small, or because the liver is cirrhotic^[12, 18, 21, 26]. Intraductal HCC growth is mostly caused by direct invasion from the primary lesion and occasionally from an adjacent massive tumor thrombus in the portal vein^[27]. Icteric type HCC may occur even with no primary detectable lesion^[21, 28]. Most primary lesions of icteric type HCC patients are grossly infiltrative type or mixed infiltrative and nodular type. Usually, no tumor capsule formation could be found in the primary tumors. The infiltrative nature of this particular type of HCC may in part explain their invasion of the biliary tree and portal veins early in their growth without regard to tumor size or type^[19, 29].

CLINICAL MANIFESTATION AND DIAGNOSIS

Clinical features

The common clinical features of this type of HCC include: high level of serum AFP; the history of cholangitis with dilation of intrahepatic bile duct; aggravating jaundice and rapidly developing into liver dysfunction. It is usually difficult to make diagnosis before operation, because of the low incidence rate, ignorant of this disease, and the difficulty for the imaging diagnosis to find the BDT preoperatively.

Just as other types of HCC, no specific symptoms could be found in the early stage. Only when intraductal tumor growth occurs in the common hepatic duct and/or the common bile duct does obstructive jaundice become a clinical concern. Hemobilia due to intraductal tumor growth is occasionally observed.

Besides jaundice, right upper quadrant pain is one of the major presenting features. In cirrhotic patients, unexplained hemobilia could be the initial complaint without any

manifestation of primary tumor, which can reveal a small, potentially curable, HCC that has spread to the biliary tree^[30]. Sometimes, this kind of patient is manifested as acute pancreatitis^[31].

The serum total bilirubin level can rise very rapidly and correlates well with ALP and GGT levels^[16, 32]. It is important to evaluate carefully when dealing with patients with intrabiliary tumor thrombi, even though they may show negative for viral hepatitis infection.

There are still difficulties and challenging problems in differential diagnosis of this type of HCC. The presence of an elevated AFP level and positive HBV markers are helpful to establish the diagnosis. The absence of these findings, especially with no primary hepatic tumor being detected, a variety of other diagnoses will be entertained. Despite remarkable recent improvements in the imaging tools for diagnosis of HCC, such cases were still incorrectly diagnosed as cholangiocarcinoma or choledocholithiasis^[4, 14-16, 21, 33, 34]. Ultrasonography (US) and CT are helpful in showing hepatic tumors and dilated intrahepatic and /or extrahepatic ducts containing dense material corresponding to tumor debris.

Ultrasonography (US)

Abdominal US is valuable as an initial investigation and for differentiation of patients with these presentations. Using US, it is able to suspect patients with icteric type HCC, even before other diagnostic strategies. Dilatation of proximal biliary tracts developed inevitably with time. Distension of the gallbladder was occasionally seen if the thrombus was located below the common hepatic duct (CHD). Tumor thrombi of bile duct could be easily identified on US as low-, iso-, or high-echogenic masses. At times, vascular signals could be detected on a Color Doppler sonography (CDS). Regarding biliary tract tumor thrombi, icteric type HCC should be strongly suspected whenever liver tumors exist. Moreover, pathological proof of thrombi can be obtained with an US-guided approach.

CDS is a non-invasive method in liver hemodynamic studies. Because HCC is known to be a hypervascular tumor, CDS is useful in detection of blood flow in HCC and helpful in differentiating it from other liver tumors. For the detection of tumor vascularity, spectral Doppler sonography guided by CDS is shown to be useful in the differential diagnosis of liver tumors. It is also useful in detection of blood flow within portal vein thrombosis in liver cirrhosis. It is a useful method for differentiating malignant from benign portal vein thrombi in liver cirrhosis, with 45-90 % sensitivity and 95-100 % specificity^[35]. Wang *et al.* found blood flow in bile duct tumor thrombi in 7 of 8 patients (87.5 %) with HCC and bile duct infiltration. Power Doppler sonography, a technique based on the integrated power of the Doppler spectrum, is more sensitive than CDS in depicting vascular flow in HCC. Its utility in detection of vascularity of bile duct tumor thrombi in patients with HCC might be more sensitive than that of CDS^[36].

Endoscopic sonography could show a tumor thrombus with central echogenicity and a "nodule-in-nodule" pattern, could provide more accurate evidence for the correct diagnosis^[37].

Computed tomography (CT)

Although CT is useful in patients with obstructive biliary disease, axial CT is not an effective method of demonstrating biliary anatomy. Because of the cross-sectional orientation of the CT images, the anatomy is fragmented and CT alone is less accurate in providing information of complex anatomic relationships. 3D CT cholangiography demonstrated the dilated bile ducts but could not depict nondilated peripheral bile ducts not seen on 2D axial images. On 3D CT cholangiography with miniIP, grades for anatomic details of biliary system were over

grade 4: visualization up to third-order branches. 3D CT cholangiography with miniIP determined the cause and level of all patients. Grades for anatomic visualization of the biliary tree corrected with an attenuation difference between bile ducts and enhanced hepatic parenchyma. Therefore, maximal hepatic parenchymal enhancement is one of the most important factors for 3D cholangiography with miniIP. Appropriate dilatation of the biliary tree is also necessary to extract pixels of bile ducts for 3D cholangiography. Focal disruptions of peripheral bile ducts were in all patients. However, the limitation of resolution in demonstrating a normal size of bile duct and focal disruption do not interfere with the determination of the level of obstruction, contiguity of ducts between different hepatic segments, and the presence or absence of isolated hepatic segment. 3D CT cholangiography correctly show the presence of biliary obstruction. Moreover, there is complete agreement between 3D CT cholangiography and PTC in the determination of obstruction level and cause in all patients. Spiral CT cholangiographic findings were also in agreement with those of direct cholangiography with regard to the site and extent of obstruction^[38].

Direct cholangiography

Although sonography and CT are sensitive in detecting biliary tract obstruction, direct cholangiography including percutaneous transhepatic cholangiography (PTC) and endoscopic retrograde cholangiopancreatography (ERCP) remains the standard procedure to delineate the presence and level of biliary obstruction. Nevertheless, direct cholangiography is operator dependant and invasive, with a higher complication rate in patients (up to 9 %) with obstructive jaundice^[39,40]. The complications, such as pancreatitis, sepsis, hemobilia, and biliary proliferation, can be life threatening and can delay or even diminish the chance of managing the primary disease. ERCP and PTC are useful in the diagnosis of intrabiliary thrombi, and intraductal filling defects resulting in partial or complete obstruction and ductal dilatation are shown in 70 % of bile invasion by HCC. However, these cholangiographic features are not diagnostic for bile duct invasion by HCC; therefore, ERC and PTC are limited in their usefulness for characterization of BDT.

Magnetic resonance cholangiopancreatography (MRCP)

The MR features of intraductal tumors, bile duct obstruction with an associated hepatic mass or localized intrahepatic duct dilatation within wedge-shaped areas, indicated intraductal tumor extension. The enhancement of intraductal masses on dynamic MR images shows an extension of HCC rather than blood clots. MR cholangiography is recently shown to be superior to ERCP in detecting the presence of biliary obstruction, but it is relatively ineffective for interpretation of icteric-type HCC.

MRCP was introduced in 1991 by Wallner *et al*^[41]. It is an absolutely noninvasive imaging modality, allowing demonstration of the biliopancreatic system by means of data acquisition and images post-processing reconstruction presenting at the coronal planes similar to conventional cholangiography. It requires neither contrast medium injection, nor biliary endoscopic intervention; therefore, it completely avoids the formidable complications inherent to conventional cholangiographic examinations. Both primary liver tumors and dilatation of biliary system could be demonstrated in MRCP. Recent studies have demonstrated that MRCP can accurately depict abnormalities in the hepatobiliary system, and claimed a high accuracy in depicting various biliary and pancreatic disease entities, with reported sensitivities approaching 90-95 % for biliary and pancreatic ductal dilation and stricture^[42].

Presence of intraluminal soft tissue at the bile duct, and enhancement of the intraluminal soft tissue in the arterial phase are two typical features of HCC with tumor thrombi in bile duct. Sometimes, the simultaneous presence of an intraluminal tumor in the portal trunk and CHD could be found in this type of patients. Three different MRCP features could be found: (a) an oval defect in the hilar bile duct(s) with dilated intrahepatic ducts. A bulky intraluminal-filling defect resulting from either tumor fragments or blood clots obstructing the major bile duct is the most common cholangiographic finding of icteric type HCC. This feature has been reported in about 70 % of this type of patients. It most frequently occurs in the hepatic or common bile ducts, causing partial or complete obstruction. The bile ducts containing tumor fragments are visualized because the impacted tumor appears dark on MRCP and there is no surrounding bile. A comparison of direct cholangiography with MRCP showed that the non-visualized bile duct in type I MRCP corresponded well in size, contour, and location to the intraluminal filling defect on conventional cholangiography; (b) dilated intrahepatic ducts with missing major bile ducts, and (c) localized stricture of the hilar bile duct(s). It is an unusual cholangiographic feature of icteric-type HCC, and an incidence of 9-15 % has been reported. The stricture is short, smooth, and confined to the porta hepatis, in contrast to the multiple, long segmental dilatations and "rat-tail" stricture seen in cholangiocarcinoma. The localized stricture is probably the result of bile duct encasement by the large infiltrative tumor in the caudate lobe and hepatic hilum and the enlarged hilar lymph nodes. However, it may be very difficult to differentiate from hilar cholangiocarcinoma or cystic duct cancer in a patient presenting with type III MRCP, because of the very similar cholangiographic appearance. Other imaging modalities are required for additional information about the extent of the tumor, the extraluminal tumor compression, and the presence of enlarged lymph nodes. The presence of one or more of the following features in multiplanar MRI and MRCP help to identify this rare, specific type of HCC: (a) the presence of an intraluminal tumor in both the portal trunk and the common hepatic duct, (b) enhancement of the intraluminal tumor in the CHD on the arterial phase, (c) type I MRCP feature, and (d) hemobilia, blood clot within the gallbladder, and/or type II MRCP feature^[29, 42-45].

Both ERCP and MRCP are excellent for confirming the presence of malignant perihilar biliary obstruction that has been suggested by sonography and CT. Nevertheless, MRCP is obviously superior to ERCP in interpreting the cause and depicting the anatomical extent of the perihilar obstructive jaundice. It is particularly distinctive in cases associated with tight biliary stenosis and along segmental biliary stricture. For this kind of patients, an undue pressure and retention of contrast medium imposed on a diseased biliary tree might deteriorate the pre-existing biliary tract infection. Therefore, the amount of injected contrast agents given is below the optimal dose needed to appropriately visualize the biliary tree cephalad to the lesion site. Complementary PTC is warranted to remedy this problem. Certainly, the procedure-related risk increases synergically. Furthermore, in cases with separate biliary obstruction, detailed opacification of the intrahepatic biliary system may have necessitated multiple PTC sessions before the MRCP era. For deeply jaundiced patients with renal insufficiency, an iodinated contrast material is particularly dangerous; whereas MRCP is also satisfactorily delineate the dilated biliary system irrespective to the serum bilirubin level and renal function. In addition, the nonopacified area on the direct cholangiography, such as a sequestered bile duct or gallbladder as a result of tumor invasion, can be depicted clearly by MRCP.

Icteric type HCC represents the most difficult disease entity to correctly diagnose using either MRCP or ERCP. The

characteristic cholangiographic feature of bile duct involvement by a ruptured HCC is a large expanding intraluminal filling defect with an irregularly lobulated outline and ground-glass radiolucency of the filling defects, which may be smooth or irregular, usually seen in the common hepatic duct^[14,44,45]. The differential diagnoses of this type of cholangiography include papillary type cholangiocarcinoma, intraductal polyps or mucin-hypersecreting intrahepatic biliary neoplasm. It still relies on other information, such as the presence of liver cirrhosis, hepatitis markers, tumor markers (AFP, CEA), the fluctuation of jaundice, and hemobilia. The presence of an encapsulated mass with a central scar or internal fat may also be helpful to diagnose icteric HCC. MRCP and direct cholangiography provide the equivalent diagnosis information that segmental bile ducts are not visualized and the CHD is partially opacified because of migrating tumor thrombi. Furthermore, by means of T2-weighted axial and coronal plane of MR images, tumor thrombi that ruptured from the primary tumor into both intrahepatic and extrahepatic bile ducts could be perfectly depicted. This novel diagnostic modality makes the diagnosis of icteric HCC more straightforward and certain than ever before^[46].

Choledochoscopy

Choledochoscopy is an alternative diagnostic technique applicable before and after duct exploration. Choledochoscopy can differentiate obstructions resulting from intraluminal mass, infiltrating ductal lesions or extrinsic mass compression. Yamakawa first introduced intra-operative fiber optic choledochoscopy (IOC), using an improved fiberoptic choledochoscope, in 1976. Chen *et al.*^[47] used IOC to visualize the nature of obstruction of the bile duct.

Characteristic cholangiographic findings of HCC invading into the bile duct include intraluminal expanding hilar mass density. Jan *et al.* found the main choledochoscopic findings were a yellowish intraluminal nodular mass and tumor thrombus in the CBD. These features may allow differential diagnosis from hilar papillary type cholangiocarcinoma^[14].

Bile duct brushing cytology

Bile duct brushing cytology is another useful technique in the diagnosis of malignant biliary strictures. In HCC with obstructive jaundice due to invasion of the biliary tract, a striking feature of the brushing is the prominent capillary vascular pattern associated with the tumor cells. This is a cytologic feature that has been noted in fine-needle aspirates of HCC as well, and is distinct from the expected findings in adenocarcinoma^[48].

TREATMENT STRATEGIES

Surgical treatment

Jaundice is not necessarily a harbinger of advanced disease and a contraindication for surgery. Patients with primary liver cancer and jaundice due to migrated tumor fragments in the bile duct may benefit from surgical resection. Most patients will have satisfactory palliation and occasional cure if the appropriate procedures are selected and carried out safely, which can result in long-term resolution of symptoms and occasional long-term survival.

The goals of operative intervention are biliary decompression with removal of tumor debris or tumor-containing blood clots, and, if possible, curative resection of the hepatic tumor. The commonly used operative methods are lobectomy (including the primary tumor and the tumor thrombi in bile duct), hepatectomy plus thrombectomy, choledochotomy with T-tube drainage alone, internal biliary stenting, or biliary diversion. The ideal treatment of these patients is hepatic resections^[18,33,34,49-51].

“Curative” resection is possible in some patients with obstructive jaundice. The overall survival of patients with HCC with obstructive jaundice might be similar to those patients who present with no clinical detectable jaundice, and is much better than those with jaundice due to hepatic insufficiency^[52].

There are numerous techniques that can be employed for biliary decompression and drainage^[26]. The decision to perform what kind of operations or interventions should be based on the nature and location of the main tumor mass, severity of the symptoms, associated neoplastic strictures, the patient's overall status, and the experience of the surgeon. Wang *et al.* reported 10 cases with gross evidence of tumor thrombi in the bile duct were treated with different resection methods and interventions. Eight out of the 10 patients underwent exploratory laparotomy (right lobectomy with extrahepatic bile duct resection in 2 cases, right lobectomy with tumor thrombectomy in 2 cases, left lobectomy and caudate lobectomy with extra-hepatic bile duct resection in 2 cases including T-tube drainage in 1 case and biopsy only with post-operative internal biliary stent in 1 case). Survival time of these patients was 39 months (still alive); 38 months (still alive); 8 months (died); 8 months (died); 8 months (still alive); 1 month (still alive); 14 months (died); 8 months (died), respectively. Of the 2 non-surgical cases, 1 underwent PTBD only and the other had endoscopic removal of the thrombi. Their survival time was 18 days (died) and 24 months (still alive with recurrence), respectively. The 4 cases, with right lobectomy or left lobectomy including extrahepatic bile duct resection, had relatively long-term disease-free survival (39 months, 38 months, 8 months and 1 month after operation, respectively). However, there were no differences in survival between the partial hepatectomy procedure with removal of tumor thrombi and the simple drainage procedure without tumor resection. So, they suggested that, for the improvement of survival, it was necessary to perform major hepatic resection with removal of the extrahepatic bile duct. If hepatic resection could not be accomplished with bile duct resection due to limited liver function, non-surgical modalities should be considered instead of surgery because there was no difference in prognosis between the 2 groups^[53]. Hu *et al.* reviewed 18 patients with obstructive jaundice by tumor emboli from HCC during a 15-year period of time. Types of surgical procedures were choledochotomy with T-tube drainage alone in 9 patients, choledochotomy with T-tube drainage followed by hepatectomy in six, and T-tube drainage followed by TACE in the remaining three patients. The mean survival time for 9 patients with external drainage alone was 4.5 months. For the 3 patients with T-tube drainage and TACE, the mean survival time was 11 months. Six patients who had undergone hepatectomy had a better postoperative survival time, with 1 surviving for more than 3 years and another alive for 70 months, without evidence of recurrence at the moment^[54]. Tantawi *et al.* reported 5 patients underwent liver resection associated with biliary exploration, clearance and T-tube drainage, 4 of them received major hepatectomy. All of the patients survived more than 1 year with a median survival of 29 months. There were 2 long-term survivors without recurrence at 29 and 80 months^[51].

Intraoperative identification of the nature and location of intraluminal biliary obstruction is crucial for the initial assessment and planning of operative strategy. In this respect, IOC, cholangiography, and intraoperative US are important adjuncts to formal common bile duct exploration. Direct endoscopic visualization of bile ducts will facilitate differentiation of neoplastic stricture from filling defects demonstrated in cholangiograms. Removal of gross tumor debris as much as possible from the luminal of the bile duct through manual extraction and irrigation is one of the key procedures to the prognosis. This can often be verified at the end of the procedure either by repeated cholangioscopy or

cholangiography. Using intra-operative US on the surface of the liver, small or deeply seated tumor and intrahepatic metastasis can be found and an adequate tumor resection margin can be marked out accurately. IOC reveals the characteristic finding of an intraluminal yellowish nodular mass in patients with malignant obstruction of the bile duct due to HCC. Liver resection with a free margin of the involved hepatic duct can be achieved by a choledochoscopically guided operation^[14].

It is not difficult to remove such tumor casts at operation in most cases. However, active hemorrhage occurred during operation in some cases, possibly because of the continuity of the intraductal tumor debris with the main intrahepatic tumor. Suturing, electrocauterization, compression, Pringle's maneuver, or hepatic arterial ligation usually can achieve hemostasis. When noncalculous material is found to be obstructing the extrahepatic ducts, even no obvious primary hepatic tumor was found, tumor embolus must be considered and the material sent routinely for pathological evaluation.

The role of preoperative biliary drainage (PBD) before liver resection in the presence of obstructive jaundice remains controversial. Cherqui *et al.* found major liver resections without PBD were safe in most patients with obstructive jaundice. Recovery of hepatic synthetic function was identical to that of no jaundiced patients. Transfusion requirements and incidence of postoperative complications, especially bile leaks and subphrenic collections are higher in jaundiced patients. Whether PBD could improve these results remains to be determined^[55]. Teda *et al.* thought a combination of biliary drainage and subsequent TAE is a recommended pre-operative strategy for the successful surgical treatment of Icteric type HCC. Nine of the 10 patients achieved sufficient reduction of the jaundice preoperatively. After the evaluation of liver function, 8 patients underwent hepatectomy without any appreciable morbidity or mortality. The median survival time of the resected cases was 18 months^[56].

Non-surgical treatments

Although successfully resected cases of Icteric type HCC have been reported, most of this type of patients are inoperable^[49-52,57]. The alternative treatment strategy is palliative in intent, including palliative treatment for the tumor and thrombi, and alleviating the jaundice. Palliative treatment strategies, including TACE and/or radiotherapy (R/T) show a beneficial effect in improving the survival.

Biliary drainage is usually used as the initial treatment because of overt cholangitis. Early and effective biliary drainage (percutaneous transhepatic biliary drainage, PTBD) might be necessary in this group of patients with limited hepatic function to prove the prognosis^[58].

To some extent, for icteric type HCC patients with poor and complicated conditions, the palliative strategies are chosen based on experience. In icteric type HCC patients with sufficient reserved liver function, TACE is effective and should be tried as a first choice of therapy^[59]. The median survival time among those eight patients who received palliative treatment was 13.4 months (a range of 8-26 months), which was significantly longer than for the other two patients without treatment (2 and 4 months).

External beam radiation therapy may be beneficial in some patients with unresectable icteric-type HCC. Also, US-guided localized radiotherapy, particularly on the critically located CBD and CHD thrombi, could be effective^[60,61]. Huang *et al.* demonstrated that radiotherapy could be an effective adjuvant strategy in those who showed limited response to TACE or those who had poor liver reserve function. The median survival time of those 8 patients receiving palliative treatment (TACE

alone, or radiotherapy alone, or in combination) was longer than that the other two patients without treatment (13.4 months vs. 3 months)^[16]. When combined with other conventional therapies (such as TACE), radiation therapy may play an important role in the treatment of HCC^[62].

Endoscopic biliary drainage (EBD) for unresectable HCC associated with obstructive jaundice remains controversial because of the short survival of these patients. Some reports suggest EBD is one of the most effective treatments for patients with unresectable malignant biliary stenosis, and even for patients with obstructive jaundice caused by liver metastasis. However, EBD is often difficult in HCC patients with obstructive jaundice and may fail because of proximal biliary obstructive at the hilum, underlying liver cirrhosis, and a poor hepatic functional reserve. Consequently, it is not a commonly used procedure in patients with advanced inoperable HCC and obstructive jaundice, and the indications for EBD in these patients are also controversial because of their short survival^[63].

ERCP can be both diagnostic and therapeutic. Biliary stenting can relieve jaundice and allow further chemotherapy, but at additional expense and potential morbidity. Martin *et al.* retrospectively analyzed 26 patients with HCC and jaundice undergoing ERCP after CT or US, and found in selected patients, stenting could safely relieve jaundice and allow subsequent chemotherapy. CT or US accurately predicted lesions that responded to stenting. ERCP and stenting provided no benefit in the absence of biliary dilation on CT or US^[64]. Placement of metallic stents is the procedure of choice for palliation of malignant biliary obstruction. Stents show a favorable patency rate with regard to patient survival. In patients with hilar obstruction, the clinical efficacy of metallic stents is superior to that in patients with CBD obstruction^[65]. In the palliative treatment of HCC patients, a large stent may be necessary, as used in reports of HCC successfully treated by metal stents, if the hepatic functional reserve is not too poor^[66,67].

EBD is more effective for palliation in the patients with obstructive jaundice caused by tumor fragments and/or blood clots or with tumor protruding into the CBD lumen than in the patients who mainly have tumor invasion. So it is important to understand the causes of obstruction on cholangiograms before performing EBD. And it is difficult in most patients with direct tumor invasion involving both hepatic ducts, and multiple tumors in both lobes. It is important to determine the site, extent, and nature of the obstruction, as well as liver function and the presence of portal thrombus, before performing EBD. In patients with tumor involvement of both the right and left intrahepatic ducts, EBD should be avoided because of the low successful drainage rate and short survival. In HCC patients with obstructive jaundice, considering the progression of hepatic insufficiency, it is important to achieve complete drainage at the first stenting procedure. In patients with CBD bifurcation tumors, drainage of both lobes should be achieved, if possible. However, attempted drainage of all obstructed liver segments may cause cholangitis or sepsis if it is unsuccessful^[68,69].

The combination of palliative methods may relieve jaundice, ensure a good quality of life and possibly prolong survival of this type of HCC patients. Lauffer *et al.* reported 1 case received combination treatment with surgical segment III drainage, TACE and radioembolization with Yttrium-90 resin particles and endoscopic stenting was performed. With these combined procedures, relief of jaundice and a survival time of 32 months could be achieved^[70].

PROGNOSIS

The prognosis of icteric type HCC patients is generally dismal, but is better than those HCC patients who have jaundice caused by hepatic insufficiency. Cholangitis secondary to tumor

obstruction is found to be the major cause of death in these patients.

The prognosis of this type of HCC patients is closely related to the stage of disease, the location and extension of tumor thrombi in bile duct. In 1994, Ueda *et al.* classified HCC with BDT into 4 types. Type I: BDT located in the secondary branch of the biliary tree. Type II: BDT extending to the first branch of the biliary tree. Type III: BDT extending to the common hepatic duct (CHD) (IIIa); an implanted tumor growing in the CHD (IIIb). Type IV: floating tumor debris from the ruptured tumor in the CBD^[71]. They also found that the patients with type I, IIIb and IV of BDT had a relative better prognosis than other types.

Different therapies also influence the prognosis of this type of patients. Lau *et al.* reported that patients who received curative liver resection had a much better survival rate than those without resection (with a median survival of 25.3 vs. 2.1 months, respectively)^[72]. Huang *et al.* studied 9 patients who had a patent portal vein and reported that the mean survival of 4 patients with curative resection was 35.8 months, but that of the 5 patients with palliative treatment was only 4.5 months. Thus, the ideal treatment for HCC associated with obstructive jaundice is to reduce the jaundice with preoperatively and perform hepatic resection, but the prognosis of patients who are inoperable is extremely poor^[73]. Kojiro *et al.* reported that 2 of their patients died 40-60 days after the development of obstructive jaundice^[4]. In a study of 49 HCC patients with obstructive jaundice, Lau *et al.* reported that 9 patients received curative resection, 35 had biliary stents, and 5 had supportive treatment, and the overall survival of these patients was similar to that of HCC patients without jaundice. They concluded that good palliation and occasional cure were possible with proper treatment^[52]. For biliary drainage in patients with unresectable HCC, the mean survival time of patients with only EBD was 3.9 months^[29], and the patients with external drainage alone was 4.5 months^[54].

CONCLUSIONS

Obstructive jaundice as the main presenting clinical feature of HCC is uncommon. The prognosis of this type of HCC is generally dismal, but is better than those HCC patients who have jaundice caused by hepatic insufficiency. Jaundice is not necessarily a harbinger of advanced disease and a contraindication for surgery. Patients with primary liver cancer and obstructive jaundice due to migrated tumor fragments in the bile duct may benefit from surgical resection. Most patients will have satisfactory palliation and occasional cure if appropriate procedures are selected and carried out safely, which can result in long-term resolution of symptoms and occasional long-term survival.

REFERENCES

- 1 **Becker FF.** Hepatoma-nature's model tumor. A review. *Am J Pathol* 1974; **74**: 179-210
- 2 **Kew MC, Paterson AC.** Unusual presentations of hepatocellular carcinoma. *Trop Gastroenterol* 1985; **6**: 10-22
- 3 **Mallory TB, Castleman B, Parris EE.** Case records of the Massachusetts General Hospital. *N Eng J Med* 1947; **237**: 673-676
- 4 **Kojiro M, Kawabata K, Kawano Y, Shirai F, Takemoto N, Nakashima T.** Hepatocellular carcinoma presenting as intrabiliary duct tumor growth. A clinicopathological study of 24 cases. *Cancer* 1982; **49**: 2144-2147
- 5 **Ishikawa I, Kobayashi K, Odajima S, Takada A, Takeuchi J.** Primary hepatic cancer with recurrent episodes of obstructive jaundice and distended gall bladder. A case report and review of the literature. *Am J Gastroenterol* 1973; **60**: 496-503
- 6 **Ihde DC, Sherlock P, Winawer SJ, Fortner JG.** Clinical manifestation of hepatoma. A review of 6 years' experience at a cancer hospital. *Am J Med* 1974; **56**: 83-91
- 7 **Roslyn JJ, Kuchenbecker S, Longmire WP Jr, Tompkins RK.** Floating tumor debris. *Arch Surg* 1984; **119**: 1312-1315
- 8 **Okuda K, Kubo Y, Okazaki N, Arishima T, Hashimoto M.** Clinical aspects of intrahepatic bile duct carcinoma including hilar carcinoma. *Cancer* 1977; **39**: 232-246
- 9 **Wang JH, Wang LY, Lin ZY, Chen SC, Kang SC, Chuang WL, Lu SN, Hsieh MY, Tsai JF, Chang WY.** Doppler sonography of common hepatic duct tumor invasion in hepatocellular carcinoma: report of two cases. *J Ultrasound Med* 1995; **14**: 471-474
- 10 **Jureco S, Kim H.** Extrahepatic biliary obstruction by hepatocellular carcinoma. *Am J Gastroenterol* 1980; **74**: 176-178
- 11 **Terada T, Nakanuma Y, Kawai K.** Small hepatocellular carcinoma presenting as intrabiliary pedunculated polyp and obstructive jaundice. *J Clin Gastroenterol* 1989; **11**: 578-583
- 12 **Lin TY, Chen KM, Chen YR, Lin WS, Wang TH, Sung JL.** Icteric type hepatoma. *Med Chir Dig* 1975; **4**: 267-270
- 13 **Okuda K.** Clinical aspects of hepatocellular carcinoma: analysis of 134 cases. In: Okuda K, Peters RL, eds. *Hepatocellular carcinoma*. New York: John Wiley 1976: 387-436
- 14 **Jan YY, Chen MF.** Obstructive jaundice secondary to hepatocellular carcinoma rupture into the common bile duct: choledochoscopic findings. *Hepatogastroenterology* 1999; **46**: 157-161
- 15 **Lau WY, Leung JW, Li AK.** Management of hepatocellular carcinoma presenting as obstructive jaundice. *Am J Surg* 1990; **160**: 280-282
- 16 **Huang JF, Wang LY, Lin ZY, Chen SC, Hsieh MY, Chuang WL, Yu MY, Lu SN, Wang JH, Yeung KW, Chang WY.** Incidence and clinical outcome of icteric type hepatocellular carcinoma. *J Gastroenterol Hepatol* 2002; **17**: 190-195
- 17 **Spahr L, Frossard JL, Felley C, Brundler MA, Majno PE, Hadengue A.** Biliary migration of hepatocellular carcinoma fragment after transcatheter arterial chemoembolization therapy. *Eur J Gastroenterol Hepatol* 2000; **12**: 243-244
- 18 **VanSonnenberg E, Ferrucci JT.** Bile duct obstruction in hepatocellular carcinoma (hepatoma)-clinical and cholangiographic characteristics. Reports of 6 cases and review of the literature. *Radiology* 1979; **130**: 7-13
- 19 **Soyer P, Laissy JP, Bluemke DA, Sibert A, Menu Y.** Bile duct involvement in hepatocellular carcinoma: MR demonstration. *Abdom Imaging* 1995; **20**: 118-121
- 20 **Afroudakis A, Bhuta SM, Ranganath KA, Kaplowitz N.** Obstructive jaundice caused by hepatocellular carcinoma. *Dig Dis* 1978; **23**: 609-617
- 21 **Buckmaster MJ, Schwartz RW, Carnahan GE, Strodel WE.** Hepatocellular carcinoma embolus to the common hepatic duct with no detectable primary hepatic tumor. *Am Surg* 1994; **60**: 699-702
- 22 **Shimoji H, Shiraishi M, Hiroyasu S, Isa T, Kusano T, Muto Y.** Common bile duct blood clot: an unusual cause of ductal filling defects for calculi. *J Gastroenterol* 1999; **34**: 420-423
- 23 **Edmondson HA, Steiner PE.** Primary carcinoma of the liver, study of case among 43900 necropsies. *Cancer* 1954; **7**: 462-502
- 24 **Narita R, Oto T, Mimura Y, Ono M, Abe S, Tabaru A, Yoshikawa I, Tanimoto A, Otsuki M.** Biliary obstruction caused by intrabiliary transplantation from hepatocellular carcinoma. *J Gastroenterol* 2002; **37**: 55-58
- 25 **Saito M, Hige S, Takeda H, Tomaru U, Shibata M, Asaka M.** Combined hepatocellular carcinoma and cholangiocarcinoma growing into the common bile duct. *J Gastroenterol* 2001; **36**: 842-847
- 26 **Kuroyanagi Y, Sawada M, Hidemura R, Aoki S, Kato H.** Common bile duct obstruction by hepatoma. *Am J Surg* 1977; **133**: 233-235
- 27 **Kojiro M, Nakashima T.** Pathology of hepatocellular carcinoma. In: Okuda K, Ishak KG, eds. *Neoplasms of the Liver*. Tokyo: Springer Verlag 1987: 81-107
- 28 **Cho HG, Chung JP, Lee KS, Chon CY, Kang JK, Park IS, Kim KW, Chi HS, Kim H.** Extrahepatic bile duct hepatocellular carcinoma without primary hepatic parenchymal lesions-a case report. *Korean J Intern Med* 1996; **11**: 169-174
- 29 **Tseng JH, Hung CF, Ng KK, Wan YL, Yeh TS, Chiu CT.** Icteric-type hepatoma: magnetic resonance imaging and magnetic resonance cholangiographic features. *Abdom Imaging* 2001; **26**: 171-177
- 30 **Cajot O, Descamps C, Navez B, Lacreman D, Druez P.** Hemobilia disclosing very small hepatocellular carcinoma ruptured into the biliary ducts. *Gastroenterol Clin Biol* 1997; **21**: 426-429
- 31 **Tseng LJ, Jao YT, Mo LR.** Acute pancreatitis caused by hemobilia secondary to hepatoma with bile duct invasion. *Gastrointest Endosc* 2002; **55**: 240-241

- 32 **Lai ST**, Lam KT, Lee KC. Biliary tract invasion and obstruction by hepatocellular carcinoma: report of five cases. *Postgrad Med J* 1992; **68**: 961-963
- 33 **Tsuzuki T**, Ogata Y, Iida S, Dasajima M, Takahashi S. Hepatoma with obstructive jaundice due to the migration of a tumor mass in the biliary tract: report of a successful resection. *Surgery* 1979; **85**: 593-598
- 34 **Matzen P**, Malchow-Moller A, Brun B, Gronvall S, Haubek A, Henrksen JH. Ultrasonography, computed tomography and cholescintigraphy in suspected obstruction jaundice. A prospective comparative study. *Gastroenterology* 1983; **84**: 1492-1497
- 35 **Dodd GD III**, Mernel DS, Baron RL, Eichner L, Santiguida LA. Portal vein thrombosis in patients with cirrhosis: does sonographic detection of intrathrombus flow allow differentiation of benign and malignant thrombus? *Am J Roentgenol* 1995; **165**: 573-577
- 36 **Wang JH**, Chen TM, Tung HD, Lee CM, Changchien CS, Lu SN. Color Doppler sonography of bile duct tumor thrombi in hepatocellular carcinoma. *J Ultrasound Med* 2002; **21**: 767-772
- 37 **Lee YC**, Wang HP, Huang SP, Chang YT, Wu CT, Yang CS, Wu MS, Lin JT. Obstructive jaundice caused by hepatocellular carcinoma: Detection by endoscopic sonography. *J Clin Ultrasound* 2001; **29**: 363-366
- 38 **Park SJ**, Han JK, Kim TK, Choi BI. Three-dimensional spiral CT cholangiography with minimum intensity projection in patients with suspected obstructive biliary disease: comparison with percutaneous transhepatic cholangiography. *Abdom Imaging* 2001; **26**: 281-286
- 39 **Harbin WP**, Mueller PR, Ferrucci JT. Transhepatic cholangiography: complications and use pattern of the fine needle technique. *Radiology* 1980; **135**: 15-22
- 40 **Zimmon DS**, Falkenstein DB, Riccobono C, Aaron B. Complications of endoscopic retrograde cholangiopancreatography. Analysis of 300 consecutive cases. *Gastroenterology* 1975; **69**: 303-309
- 41 **Wallner BK**, Schumacher KA, Weidenmaier W, Friedrich JM. Dilated biliary tract: evaluation with MR cholangiography with a T2-weighted contrast-enhanced fast sequence. *Radiology* 1991; **181**: 805-808
- 42 **Fulcher AS**, Turner MA, Capps GW, Zfass AM, Baker KM. Half-Fourier RARE MR cholangiopancreatography: experience in 300 subjects. *Radiology* 1998; **207**: 21-32
- 43 **Barish MA**, Yucel EK, Soto JA, Chuttani R, Ferrucci JT. MR cholangiopancreatography: efficacy of three-dimensional turbo spin-echo technique. *Am J Roentgenol* 1995; **165**: 295-300
- 44 **Wu CS**, Wu SS, Chen PC, Chiu CT, Lin SM, Jan YY, Hung CF. Cholangiography of icteric type hepatoma. *Am J Gastroenterol* 1994; **89**: 774-777
- 45 **Lee NW**, Wong KP, Siu KF, Wong J. Cholangiography in hepatocellular carcinoma with obstructive jaundice. *Clin Radiol* 1984; **35**: 119-123
- 46 **Yeh TS**, Jan YY, Tseng JH, Chiu CT, Chen TC, Hwang TL, Chen MF. Malignant perihilar biliary obstruction: magnetic resonance cholangiopancreatographic findings. *Am J Gastroenterol* 2000; **95**: 432-440
- 47 **Chen MF**, Jan YY, Wang CS, Jeng LB, Hwang TL. Intraoperative fiberoptic choledochoscopy for malignant biliary tract obstruction. *Gastrointest Endosc* 1989; **35**: 545-547
- 48 **Dusenbery D**. Biliary stricture due to hepatocellular carcinoma: diagnosis by bile duct brushing cytology. *Diagn Cytopathol* 1997; **16**: 55-56
- 49 **Chen MF**, Jan YY, Jeng LB, Hwang TL, Wang CS, Chen SC. Obstructive jaundice secondary to ruptured hepatocellular carcinoma into the common bile duct. *Cancer* 1994; **73**: 1336-1340
- 50 **Jan YY**, Chen MF, Chen TJ. Long term survival after obstruction of the common bile duct by ductal hepatocellular carcinoma. *Eur J Surg* 1995; **161**: 771-774
- 51 **Tantawi B**, Cherqui D, Tran van Nhieu J, Kracht M, Fagniez PL. Surgery for biliary obstruction by tumour thrombus in primary liver cancer. *Br J Surg* 1996; **83**: 1522-1525
- 52 **Lau W**, Leung K, Leung TW, Liew CT, Chan MS, Yu SC, Li AK. A logical approach to hepatocellular carcinoma presenting with jaundice. *Ann Surg* 1997; **225**: 281-285
- 53 **Wang HJ**, Kim JH, Kim JH, Kim WH, Kim MW. Hepatocellular carcinoma with tumor thrombi in the bile duct. *Hepatogastroenterology* 1999; **46**: 2495-2499
- 54 **Hu J**, Pi Z, Yu MY, Li Y, Xiong S. Obstructive jaundice caused by tumor emboli from hepatocellular carcinoma. *Am Surg* 1999; **65**: 406-410
- 55 **Cherqui D**, Benoist S, Malassagne B, Humeres R, Rodriguez V, Fagniez PL. Major liver resection for carcinoma in jaundiced patients without preoperative biliary drainage. *Arch Surg* 2000; **135**: 302-308
- 56 **Tada K**, Kubota K, Sano K, Noie T, Kosuge T, Takayama T, Makuuchi M. Surgery of icteric-type hepatoma after biliary drainage and transcatheter arterial embolization. *Hepatogastroenterology* 1999; **46**: 843-848
- 57 **Chen CL**, Huang SM, Chien CH, Chang TT, Yu CY, Lee JC. Successful resection of a minute icteric hepatocellular carcinoma-case report. *Hepatogastroenterology* 1994; **41**: 503-505
- 58 **Lee JW**, Han JK, Kim TK, Choi BI, Park SH, Ko YH, Yoon CJ, Yeon KM. Obstructive jaundice in hepatocellular carcinoma: response after percutaneous transhepatic biliary drainage and prognostic factors. *Cardiovasc Intervent Radiol* 2002; **25**: 176-179
- 59 **Takagi H**, Yamada S, Abe T, Uehara M, Takezawa J, Nagamine T, Ichikawa K, Kobayashi S, Katakai S. A case report of transcatheter arterial embolization of cholestatic type of hepatoma. *Gastroenterol Jpn* 1989; **24**: 315-319
- 60 **Chen SC**, Lian SL, Chang WY. The effect of external radiotherapy in treatment of portal vein invasion in hepatocellular carcinoma. *Cancer Chem Pharm* 1994; **33**: S124-127
- 61 **Chen SC**, Lian SL, Chuang WL, Hsieh MY, Wang LY, Chang WY, Ho YH. Radiotherapy in the treatment of hepatocellular carcinoma and its metastases. *Cancer Chemother Pharmacol* 1992; **31**: S103-105
- 62 **Sung KF**, Tsang NM, Tseng JH, Yeh CT. Effective relief of obstructive jaundice in a patient with nonresectable icteric-type hepatocellular carcinoma by external beam radiation therapy: case report. *Chang Gung Med J* 2001; **24**: 114-118
- 63 **Matsueda K**, Yamamoto H, Umeoka F, Ueki T, Matsumura T, Tezen T, Doi I. Effectiveness of endoscopic biliary drainage for unresectable hepatocellular carcinoma associated with obstructive jaundice. *J Gastroenterol* 2001; **36**: 173-180
- 64 **Martin JA**, Slivka A, Rabinovitz M, Carr BI, Wilson J, Silverman WB. ERCP and stent therapy for progressive jaundice in hepatocellular carcinoma: which patients benefit, which patients don't? *Dig Dis Sci* 1999; **44**: 1298-1302
- 65 **Lee BH**, Choe DH, Lee JH, Kim KH, Chin SY. Metallic stents in malignant biliary obstruction: prospective long-term clinical results. *Am J Roentgenol* 1997; **168**: 741-745
- 66 **Okazaki M**, Mizuta A, Hamada N, Kawamura N, Nakao K, Kikuchi T, Osada T. Hepatocellular carcinoma with obstructive jaundice successfully treated with a self-expandable metallic stent. *J Gastroenterol* 1998; **33**: 886-890
- 67 **Yoshioka T**, Uchida H, Kitano S, Makutari S, Maeda M, Taoka T, Ohishi H. Long-term palliative treatment of hepatocellular carcinoma extending into the portal vein and bile duct by chemoembolization and metallic stenting. *Cardiovasc Intervent Radiol* 1997; **20**: 390-393
- 68 **Polydorou AA**, Cairns SR, Dowsett JF, Hatfield ARW, Salmon PR, Cotton PB, Russell RC. Palliation of proximal malignant biliary obstruction by endoscopic endoprosthesis insertion. *Gut* 1991; **32**: 685-689
- 69 **Ducreux M**, Liguory CI, Lefebvre JF, Ink O, Choury A, Fritsch J, Bonnel D, Derhy S, Etienne JP. Management of malignant hilar biliary obstruction by endoscopy: results and prognostic factors. *Dig Dis Sci* 1992; **37**: 778-783
- 70 **Lauffer JM**, Mai G, Berchtold D, Curti CG, Triller J, Baer HU. Multidisciplinary approach to palliation of obstructive jaundice caused by a central hepatocellular carcinoma. *Dig Surg* 1999; **16**: 531-536
- 71 **Ueda M**, Takeuchi T, Takayasu T, Takahashi K, Okamoto S, Tanaka A, Morimoto T, Mori K, Yamaoka Y. Classification and surgical treatment of hepatocellular carcinoma (HCC) with bile duct thrombi. *Hepatogastroenterology* 1994; **41**: 349-354
- 72 **Lau WY**, Leung KL, Leung TW, Ho S, Chan M, Liew CK, Leung N, Johnson P, Li AK. Obstructive jaundice secondary to hepatocellular carcinoma. *Surg Oncol* 1995; **4**: 303-308
- 73 **Huang GT**, Sheu JC, Lee HS, Lai MY, Wang TH, Chen DS. Icteric type hepatocellular carcinoma: revisited 20 years later. *J Gastroenterol* 1998; **33**: 53-56

• ESOPHAGEAL CANCER •

Analysis of gene expression profile induced by EMP-1 in esophageal cancer cells using cDNA Microarray

Hai-Tao Wang, Jian-Ping Kong, Fang Ding, Xiu-Qin Wang, Ming-Rong Wang, Lian-Xin Liu, Min Wu, Zhi-Hua Liu

Hai-Tao Wang, Jian-Ping Kong, Fang Ding, Xiu-Qin Wang, Ming-Rong Wang, Lian-Xin Liu, Min Wu, Zhi-Hua Liu, National Laboratory of Molecular Oncology, Cancer Institute, Chinese Academy of Medical Science and Peking Union Medical College, Beijing 100021, China

Supported by China Key Program on Basic Research (G1998051021) and the Chinese Hi-Tech R&D program (2001AA231310).

Correspondence to: Dr. Zhi-Hua Liu, National Laboratory of Molecular Oncology, Cancer Institute, Chinese Academy of Medical Science and Peking Union Medical College, Beijing 100021, China. liuzh@pubem.cicams.ac.cn

Telephone: +86-10-67723789 **Fax:** +86-10-67715058

Received: 2002-06-20 **Accepted:** 2002-08-09

Abstract

AIM: To obtain human esophageal cancer cell EC9706 stably expressed epithelial membrane protein-1 (EMP-1) with integrated eukaryotic plasmid harboring the open reading frame (ORF) of human EMP-1, and then to study the mechanism by which EMP-1 exerts its diverse cellular action on cell proliferation and altered gene profile by exploring the effect of EMP-1.

METHODS: The authors first constructed pcDNA3.1/myc-his expression vector harboring the ORF of EMP-1 and then transfected it into human esophageal carcinoma cell line EC9706. The positive clones were analyzed by Western blot and RT-PCR. Moreover, the cell growth curve was observed and the cell cycle was checked by FACS technique. Using cDNA microarray technology, the authors compared the gene expression pattern in positive clones with control. To confirm the gene expression profile, semi-quantitative RT-PCR was carried out for 4 of the randomly picked differentially expressed genes. For those differentially expressed genes, classification was performed according to their function and cellular component.

RESULTS: Human EMP-1 gene can be stably expressed in EC9706 cell line transfected with human EMP-1. The authors found the cell growth decreased, among which S phase was arrested and G1 phase was prolonged in the transfected positive clones. By cDNA microarray analysis, 35 genes showed an over 2.0 fold change in expression level after transfection, with 28 genes being consistently up-regulated and 7 genes being down-regulated. Among the classified genes, almost half of the induced genes (13 out of 28 genes) were related to cell signaling, cell communication and particularly to adhesion.

CONCLUSION: Overexpression of human EMP-1 gene can inhibit the proliferation of EC9706 cell with S phase arrested and G1 phase prolonged. The cDNA microarray analysis suggested that EMP-1 may be one of regulators involved in cell signaling, cell communication and adhesion regulators.

Wang HT, Kong JP, Ding F, Wang XQ, Wang MR, Liu LX, Wu M, Liu ZH. Analysis of gene expression profile induced by EMP-1 in esophageal cancer cells using cDNA Microarray. *World J Gastroenterol* 2003; 9(3): 392-398

<http://www.wjgnet.com/1007-9327/9/392.htm>

INTRODUCTION

EMP-1 is a member of the PMP22 family with the similarity in structure. Since EMP-1 was first found by Taylor, it has been isolated independently from human, mouse and rabbit and received many different designations, such as TMP (tumor membrane Protein), PAP (Progression Associated Protein), CL-20 and B4B^[1]. All tissues expressing EMP-1 mRNA contain 2.76-kb EMP-1 transcripts. In some regions of the gastrointestinal tract, including the fundus, ileum, cecum, and colon, however, additional transcripts of approximately 1.7 kb hybridize with the EMP-1 cDNA^[2]. The 2.76-kb EMP-1 cDNA contains five exons about 0.2kb, 0.12kb, 0.1kb, 0.14kb, and 2.2 kb and four introns about 15kb, 1.9kb, 0.1kb, and 0.7 kb in length respectively. EMP-1 has been mapped to chromosome 12p12 by fluorescence in situ hybridization^[3]. EMP-1 is encoded by a single-copy gene with the positions of introns exactly conserved between EMP-1 and PMP22, corroborating the hypothesis that EMP-1 belongs to the PMP22 family^[4]. EMP-1 transcript is expressed at high levels in heart, placenta, lung, skeletal muscle, kidney, spleen, colon prostate, ovary, testicle, small intestine and thymus in human^[5].

EMP-1 was selected from a series of differential expressed genes obtained from cDNA microarray analysis of expression profiles of esophageal cancer in our previous work. EMP-1 expression was 6 fold down-regulated in esophageal cancer lower than in normal tissue. EMP-1 is highly up-regulated during squamous cell differentiation and in certain tumors, and a role in tumorigenesis has been proposed^[6]. Moreover, The overexpression of PMP22 leads to an apoptotic-like phenotype in NIH3T3 growing cells^[7] and delays serum-forskolin-stimulated entry of resting Schwann cells from G1 into the S+G2/M phase in Schwann cell^[8]. Transient expression of EMP-1 specifically inhibited cellular proliferation by more than 50 %^[9]. Preliminary data suggested that EMP-1 was involved in growth control in esophageal cancer cell line EC9706. However, whether there is a similar effect of EMP-1 expression on the cell cycle of epithelial cells remains to be determined and little is known about the function of EMP-1 in growth control in esophageal cancer cell line EC9706.

To elucidate the effect of EMP-1 on EC9706 cell, the open reading frame (ORF) of human EMP-1 was cloned into pcDNA3.1/myc-his, a eukaryotic expression vector. EC9706 was transfected with the integrated plasmid containing EMP-1 to enforce expression of the exogenous EMP-1. Western blotting and RT-PCR were used to analyze positive clones. The cell growth curve was observed and the cell cycle was checked by FACS method. However, the mechanism by which EMP-1 may exert its activity remains unclear. Because the differentiation of mammalian cells is associated with changes in gene expression that is primarily controlled at the level of transcription, we tested the expression alteration with cDNA microarray technology to address the question of which genes are influenced by EMP-1 gene overexpression.

MATERIALS AND METHODS

Sample collection

Fifteen pairs of esophageal tumors and matched adjacent

normal mucosa were obtained at surgery. Samples were frozen in liquid nitrogen until RNA was extracted.

Cell lines and cell culture

Esophageal carcinoma cell line EC9706 was established in our laboratory. The cell lines were maintained in M199 medium with 15 % FBS and cultured at 37 °C in 5 % CO₂.

The eukaryotic plasmid vector pcDNA3.1-myc-his (-) C

An *Xho*I and *Hind*III fragment ORF of EMP-1 was cloned into the pcDNA3.1/myc-his vector. The correct construct sequence was confirmed by DNA sequencing.

Atlas human cancer cDNA expression array

Atlas Human Cancer cDNA Expression Array (Clontech) was used to analyze EMP-1-induced gene expression which included over 588 genes on the nylon membrane.

Isolation of RNA and semi-quantitative RT-PCR

Paired esophageal cancer tissues and adjacent normal mucosa tissues (~100 mg) were homogenized mechanically in 1 ml of TRIzol reagent (Life Technologies, Inc.), and cell pellets were harvested to isolate the total RNA. According to the manufacturer's protocol (Life Technologies, Inc.). First-strand cDNA was synthesized from 5 µg of total RNA using Superscript II reverse transcriptase (Life Technologies, Inc.) and OligodT12-18 primers following the company's protocol. The same amount of cDNAs was subsequently used for PCR amplification. PCR reaction was performed in 25 µl buffer containing 1 µl cDNA, dATP, dCTP, dGTP, dTTP each 0.2 mmol/L, 1×PCR buffer, 1.5 mmol/l MgCl₂ and 1.5U Taq DNA polymerase (GIBCO). The primers for GAPDH are 5' -ACC ACA GTC CAT GCC ATC AC-3' and 5' -TCC ACC ACC CTG TTG CTG TA-3'; EMP-1 5' -GGA TCA GGG CTC CTA GGC TCA-3' and 5' -GGT GGC TTG CCC TCA ACA TT-3'; the primer for the ORF of EMP-1 is 5' -ATC TTT GTG GTC CAC ATC GCT-3' and 5' -CTT CTC CAT GGT GAA GAG CT-3'; Primers for four random selected genes were respectively designed for human CDK inhibitor p19INK4d, 5' -TCC ATG ACG CAG CCC GCA CT-3' and 5' -TCT CTG CAG TGC CAG CTC CA-3'; Human tissue-type plasminogen activator (t-PA), 5' -AGT GCA TTT TCC CAG ATA CT-3' and 5' -TTT GTG GTC CTG TTT CCA AAG-3'; Human interleukin-6, 5' -AGG CACTGG CAG AAA ACA AC-3' and 5' -TCC AAG AAA TGA TCT GGC TC-3'; Human alpha-1 type XI collagen (COL11A1), 5' -TCC TGT TTG TTT TCT TGG CT-3' and 5' -TTA TGA TTT TCA AAG CTT TTG T-3'. The amplification was performed with one denaturing cycle of 5 min at 95 °C, then 94 °C for 40s, 55 °C for 40s, 72 °C for 40s for 25-27 cycles, and one final extension of 7 min at 72 °C. RT-PCR products were analyzed on 1.2 % agarose gel. The number of cycles and melting temperature was adjusted depending on the genes amplified.

In vitro transfection and cell culture

According to the manufacturer's instructions (Invitrogen), the day before transfection, seed 3×10⁶ EC9706 cells in 3 ml of the 15 % serum complete growth medium. Combine diluted DNA with diluted Lipofectamine™ Reagent. For each transfection, add 0.8 ml of medium without serum to the tube containing the complexes. Incubate the cells with the complexes for 5 hours at 37 °C in a CO₂ incubator. Following incubation, add 3 ml of growth medium containing 30 % serum without removing the transfection mixture. Add G418 after 3 days and select monoclonal cell to a fresh bottle and keep on culturing with G418 (1 mg/ml). The positive clones together with the negative parental vector without EMP-1 and EC9706

Cells (3×10⁵ in 2 ml) were seeded and incubated at 37 °C in 5 % CO₂ with G418 (1 mg/ml). Cells were harvested and then quantitated every 24 hours.

Flow cytometry assay

Flow cytometry was performed to assess the cell cycle alteration. Trypsinized adherent and floating cells were collected, washed twice with cold PBS, and resuspended in PBS containing 0.1 % Triton X-100 and 0.1 % RNase for 5 min at room temperature. The samples were then stained with propidium iodide (0.1 mg/ml), filtered through a 300-µm-pore-size nylon mesh, and analyzed in a cell sorter (Coulter, epics® elite ESP)^[10].

Western blotting analysis

Cells were rinsed twice with PBS, and protein preparation was performed according to the manufacturer's instruction (Santa Cruz). Protein concentration in homogenates was determined using a BSA-Protein assay (Hyclone) employing bovine serum albumin as the standard. The extracted proteins (20 µg) were subjected to 15 % polyacrylamide gel electrophoresis in the presence of sodium dodecyl sulfate under reducing conditions, and then transferred onto poly (vinylidene difluoride) (PVDF) membranes (Hybond-P). Mouse monoclonal anti-human hexad-HIS antibodies (Santa Cruz; final dilution 1:1 000) were used as the primary antibody, and horseradish peroxidase-labeled anti-mouse immunoglobulin (Santa Cruz; final dilution 1:1 500) was used as the secondary reagent. Detection was performed using an ECL system (Amersham-Pharmacia).

cDNA microarray analysis

Total RNA was extracted by TRIzol from positive clone 2 cells and the parental vector without cDNA insert pcDNA3.1myc-his (-) C cells as negative control. Poly (A) RNA was purified using an Oligotex-dT30 mRNA purification kit (TAKARA). One µg of highly purified poly (A) RNA from the negative control and cell clone 2 was performed for cDNA microarray analysis. The mRNA was reverse transcribed with ³³P-dATP (Amersham). The paired reactions were purified with a TE-30 column (Clontech, Palo Alto, CA). The radioactive labeled probe was then applied to the array for hybridization at 68 °C for 12 hours. After hybridization, the membrane was washed with buffer of decreasing ionic strength. The X-ray film was scanned at a resolution of 16-bit. AtlasImage software (version1.01a, Clontech) was used for image analysis. The area surrounding each element image was used to calculate a local background, which was then subtracted from the total element signal. Background subtracted element signals are used to calculate intensity ratios. The average of the resulting total intensity signal gives a ratio that is used to balance or normalize the signals. Then semi-quantitative RT-PCR analysis of 4 randomly selected genes confirms the microarray results.

RESULTS

Differential expression of EMP-1 judged by RT-PCR

RT-PCR was used to detect the EMP-1 gene expression in the pair of esophageal cancer (C) and normal mucosa (N). We checked 15 pairs of esophageal cancer and its adjacent normal tissue and found the expression of EMP-1 was higher in normal tissue than that in cancer tissue in 14 pairs, and lower in only 1 pair (Figure 1).

Selection of positive transfectant clone by RT-PCR

Since the expression of EMP-1 should be up-regulated after transfection, RT-PCR was used to analyze the positive clones and the parental vector as negative control. The clones 1, 2, 3,

4, 5, 6, 8 and 10 showed a comparable increased expression of EMP-1 (Figure 2).

Expression of EMP-1 in positive clones detected by western blotting

Since the vector carrying 6xHis peptide as a selective marker, it can be detected by anti-His monoclonal antibody with Western blot. Hexad-His peptide has been expressed in host cell clone 1, clone 2, clone 3, clone 5, clone 6 and clone 8, however, EMP-1 protein was not identified in clone 4 which was highly expressed in transcriptional level for unknown reasons (Figure 3).

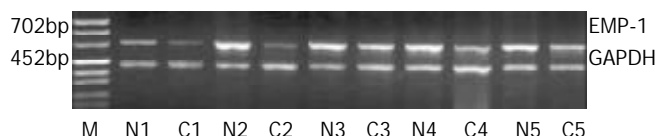


Figure 1 Different expression of EMP-1 detected in matched pairs of esophageal cancer tissue. The upper band represents EMP-1 (702 bp); the lower band represents GAPDH (452 bp). The expression of EMP-1 is higher in normal (N) tissue than its cancer (C) tissue. RT-PCR for GAPDH was used as equal loading control.

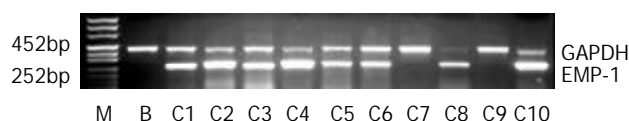


Figure 2 Different expression of EMP-1 cell clones transfected with pcDNA3.1-EMP-1-myc-his (-) C vector and the parental vector without cDNA insert pcDNA3.1myc-his (-) C cells as negative control. Clones 1, 2, 3, 4, 5, 6, 8 and 10 showed the increased expression of EMP-1. RT-PCR for GAPDH was used as equal loading control. B represents the parental vector as negative control.

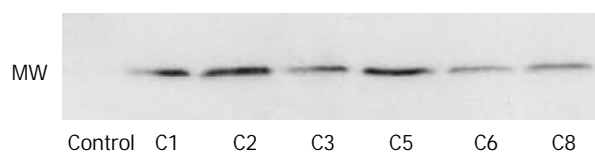


Figure 3 Western blotting check the expression of EMP-1 after transfected into the EC9706 cell with anti-HIS monoclonal antibody. His peptide has been expressed successfully in host cell clones (C1, C2, C3, C5, C6 and C8). Control represents the negative control.

The growth curve of positive clone and the parental vector without the cDNA insert as negative control

The cell proliferation rate had been observed and the cells displayed a decreased proliferation rate in clone 1, clone 2, clone 3, clone 5, clone 6, clone 8 and clone 10, especially in clone 2. The proliferation rates of clone 4, clone 7, and clone 9 are close to that of negative control. The expression of EMP-1 in clone 1, clone 2, clone 3, clone 6 and clone 8 was up-regulated in both RNA and protein levels by RT-PCR and Western blot, respectively, and a reduced ability to proliferate was as shown in these clones (Figure 4).

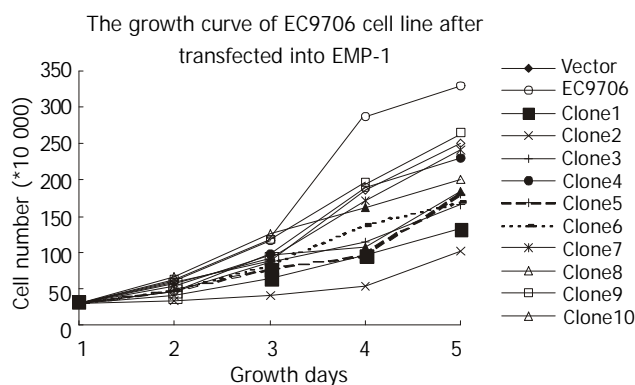


Figure 4 The growth curve of EC9706 cell line after transfected into EMP-1. The clones 1, 2, 3, 5, 6, 8 and 10 slow down obviously, and the clones 4, 7 and 9 are close to the vector control. Vector represents the negative control.

Flow cytometry analysis

Five of ten clones showed similar results after flow cytometry analysis. The percentages of cells in G1 and S phases of clone 1, clone 2, clone 3, clone 6 and clone 8 were 66.6 %, 17.9 %; 64.0 %, 30.2 %; 63.8 %, 29.1 %; 60.9 %, 34.6 %; and 69.5 %, 24.2 %; respectively. The percentage of cells in G1 and S phases of negative control were 52.2 % and 41.7 %, respectively. Comparing the cells transfected with cDNA insert and the negative control, we found that S phase was arrested and G1 phase was prolonged. Then cell clone 2 was used as a representative because its proliferation has been inhibited obviously (Figure 5).

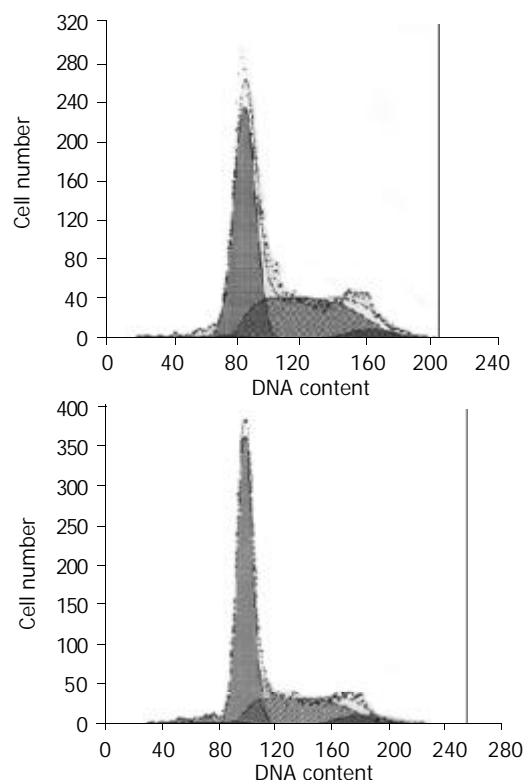


Figure 5 Flow cytometric analysis of cell cycle of negative control (left) and cell clone 2 (right). The percentages of negative cells and the clone 2 cells in G₁, G₂ and S phase are 52.2 %, 6.2 %, 41.7 %; 64 %, 5.8 % and 30.2 %, respectively.

cDNA microarray results of the parental vector pcDNA3.1/myc-his and EMP-1 transfected cell

By cDNA microarray analysis, 35 genes showed an over 2.0-fold change in expression level after transfection, with 28 genes

being consistently up-regulated and 7 genes being down-regulated in clone 2 cells (Figure 6).

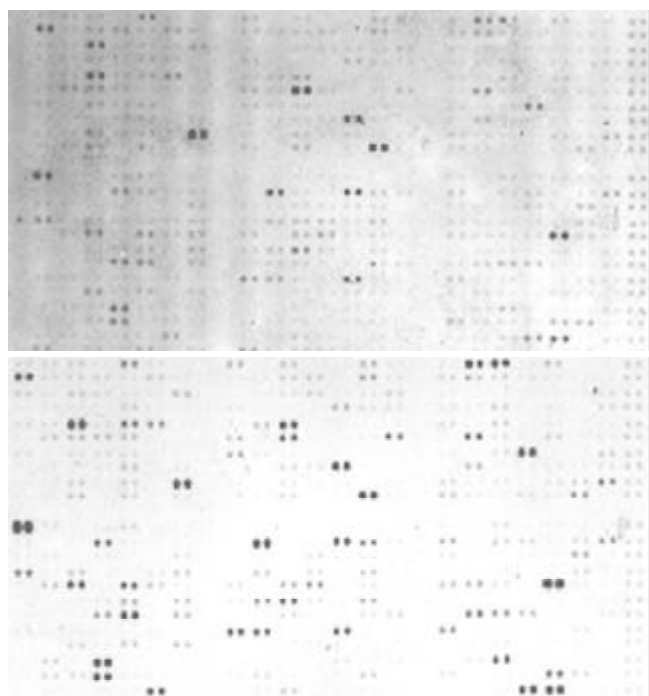


Figure 6 cDNA microarray analysis of parental negative control expression (left) and the EMP-1 transfected cell clone 2 (Right). 35 genes show an over 2.0-fold change in expression level after transfection, with 28 genes being consistently up-regulated and 7 genes being down-regulated.

RT-PCR validation of the microarray results

To confirm the gene expression profile, semi-quantitative RT-PCR was carried out for 4 randomly selected differentially expressed genes. As a result, the expression of these 4 genes was similar with the microarray analysis (Figure 7).

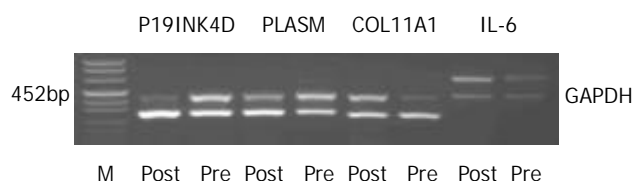


Figure 7 Verification of up-regulated and down-regulated gene expression in EC9706 induced by overexpression of EMP-1. Interleukin-6, plasminogen and P19INK4D increased their expression and COL11A1 decreased its expression. Pre represents the sample not transfected with the vector carried with the ORF of EMP-1, and post represents the sample transfected with EMP-1. RT-PCR for GAPDH was used as equal loading control.

Gene expression profile induced by overexpression of EMP-1

In further analysis of the data from this study provided an insight into the alteration in the EMP-1 induced genes. Because these 588 genes are cancer associated genes and include almost all aspects involved in carcinogenesis and development of tumor and can be the representative of tumor, these data provide an independent and relatively unbiased estimate of the EMP-1 induced expression profile. In general, genes that expression were was more than 2.0-fold were informative and valuable (Table 1).

DISCUSSION

In our previous work on the expression profile of esophageal cancer, we found that the expression of EMP-1 was 6 fold down-regulated in esophageal cancer than that in its adjacent normal mucosa. This study was designed to determine the diverse cellular action of EMP-1 by enforcing its expression in EC9706. Human EMP-1 gene can be stably expressed by EC9706 cell line transfected with human EMP-1. As a result, the cell proliferation was inhibited, S phase was arrested and G1 phase was prolonged after EMP-1 overexpression in EC9706 cells, which is similar to the action of PMP22 in Schwann cells^[8]. We then analyzed EMP-1 induced gene expression using AtlasTM human cancer cDNA expression microarray composed of 588 genes, 35 genes showed an over 2.0- fold change in expression level, in which 28 genes were consistently up-regulated and 7 genes were down-regulated. Among the classified genes, almost half of the induced genes (13 out of 28 genes) were related to cell signaling, communication and adhesion, which indicated that EMP-1 may be one of the cell signaling, communication and adhesion regulators (Table 2).

Table 2 Summary of genes regulated by EMP-1

Major category	Sub category	Up-regulated	Down-regulated
Cell division	General	1	
	DNA synthesis/replication	1	
	Apoptosis	2	
	Cell cycle	1	4
	Chromosome structure	1	
	Total	6	4
Cell signaling or cell communication and adhesion	Cell adhesion		
	Channels/transport protein		
	Effectors/modulators		
	Extracellular Communication	1	
	Hormones/growth factors	4	1
	Intracellular transducers	2	
	Protein modification	3	
	Receptors	3	2
	Total	13	3
Cell structure/ motility	General		
	Cytoskeletal	3	
	Extracellular matrix Proteins	2	
	Microtubule-associated proteins/motors		
	Total	5	
Cell/organism defense	General		
	Homeostasis		
	Immunology	1	
	Total	1	
Gene/protein expression	RNA synthesis	1	
	protein synthesis		
	Total	1	
Metabolism	General		
	Amino acid		
	Cofactors		
	Energy/TCA cycle	2	
	Lipid		
	Nucleotide		
	Protein modification		
	Sugar/glycolysis		
	Transport		
	Total	2	
	Unclassified	1	
	Total	1	

Table 1 Genes whose expression was altered more than 2.0-fold

Genes up-regulated by EMP-1				
Coordinate	Gene Name	Ratio	Category	Sub Category
A3i	Cyclin-dependent kinase 4 inhibitor 2D	2.04	Cell division	Cell-cycle regulators
A7d	Cytokeratin 1	2.26	Cell structure	Intermediate Filament Proteins
B3i	Caspase 9	4.11	Cell division	Cell-apoptosis
B7b	Chromatin assembly factor 1 p48 subunit	2.93	Cell division	Chromosome structure
B7j	Abelson-related gene	4.49	Tumor Suppressors	Oncogenes & Suppressors
C2e	DNA damage-inducible transcript 3	2.80	Cell division	Apoptosis-Associated Proteins
C2j	Ras associated with diabetes protein 1	2.47	Cell signaling	Intracellular transducers
C3e	UV excision repair protein RAD23	5.15	Cell division	DNA synthesis/replication
C4b	Wingless-related MMTV integration 5a	3.09	Cell Adhesion	Extracellular Communication Proteins
C4k	Dishevelled homolog 1-like protein	4.13	Cell signaling	Intracellular Transducers
C7m	Retinoic acid receptor beta	5.47	Cell division	Death Receptors
D3e	Vitronectin (VTN);	2.36	Cell structure	Extracellular Matrix Proteins
D4j	Integrin beta 7 (ITGB7)	2.27	Cell Adhesion	Matrix Adhesion Receptors
D4k	Integrin beta 8 (ITGB8)	2.45	Cell Adhesion	Cell-Cell Adhesion Receptors
D5g	Ezrin; cytovillin 2; villin 2 (VIL2)	3.06	Tumor Suppressors	Oncogenes & Tumor Suppressors
D6l	Caveolin 1	3.29	Metabolism	GTP/GDP Exchangers
E1h	Matrix metalloproteinase 11 (MMP11)	4.64	Cell structure	Extracellular matrix Proteins
E1m	Matrix metalloproteinase 16 (MMP16)	3.06	Protein modification	Metalloproteinases
E2b	Tissue inhibitor of metalloproteinase 1	3.82	Protein modification	Protease Inhibitors
E2h	Tissue-type plasminogen activator	4.39	Protein modification	Serine Proteases
E5b	RHO GDP-dissociation inhibitor 1	2.42	Metabolism	GTP/GDP Exchangers
E5h	Cadherin 5 (CDH5);	2.64	Cell Adhesion	Cell-Cell Adhesion Receptors
F1h	Bone morphogenetic protein 2A (BMP2A)	12.45	Cell communication	Cytokines
F3j	Early growth response protein 1	16.06	RNA synthesis	Transcription Activators & Repressors
F4l	Interleukin 6 (IL6)	4.28	Cell communication	Interleukins & Interferons
F5e	Interleukin 13 (IL13)	2.62	Cell communication	Interleukins & Interferons
F5k	Interferon gamma (IFN-gamma; IFNG)	6.04	Cell communication	Interleukins & Interferons
F5l	Leukocyte interferon-inducible peptide	2.73	Unclassified	Functionally Unclassified Proteins
A1j	Cell division cycle 25 homolog A	0.35	Cell division	Cell-cycle regulators
2m	Cyclin D2 (CCND2)	0.34	Cell division	Cell-cycle regulators
A2n	G1/S-specific cyclin D3 (CCND3)	0.30	Cell division	Cell-cycle regulators
A3k	Polo-like kinase (PLK)	0.47	Cell division	Cell Cycle-Regulating Kinases
D1m	Collagen VI alpha 2 subunit (COL6A2)	0.32	Cell communication	Extracellular Matrix Proteins
D2b	Collagen XI alpha 1 subunit (COL11A1)	0.17	Cell communication	Extracellular Matrix Proteins
D7e	Vascular endothelial growth factor C	0.11	Cell communication	Growth Factors,

cDNA microarray analysis offers the opportunity to monitor changes in gene expression across the entire set of expressed genes in cells. These 588 known genes are classified on the basis of the biological function of the encoded protein, using a modified version of a previously established classification scheme^[11,12]. The classification scheme was composed of six major functional categories and several minor functional categories within the major categories. As shown in Table 2, 34 genes were classified as known function genes, and one gene was categorized as unclassified.

Interestingly, the largest categories (13 out of 28 genes) of EMP-1-induced genes are those involved in cell signaling (Table 1), cell adhesion and cell-cell communication, which included integrin beta 7 (ITGB7), integrin beta 8 (ITGB8) and cadherin 5 (CDH5). These results indicated that EMP-1 might be related with cell adhesion and cell-cell communication.

Cadherin-5 and the alpha E beta 7 integrin mediated heterotypic adhesive interactions between epithelial cells and intraepithelial lymphocytes *in vitro*^[13]. Integrin beta 7 (ITGB7) and integrin beta 8 (ITGB8) are heterodimeric (alpha/beta) transmembrane receptors for extracellular matrix (ECM) ligands. The beta subunit of integrins are considered important for regulation of stimulated cell adhesion and adhesion-dependent signal transduction. Through interactions with molecular partners at cell junctions, they provide a connection between the ECM and the cytoskeleton and regulate many aspects of cell behaviors. Integrins play an important role in lymphocyte adhesion to cellular and extracellular components of their microenvironment^[14]. Cadherin 5 was also induced by EMP-1 in our microarray analysis. It is generally accepted that cadherins are a group of cell adhesion molecules located at intercellular junctions, and they play an important role in

embryogenesis and morphogenesis in animals and humans due to their adhesive and cell-signaling functions. Disturbances of the expression or function of cadherins and their associated proteins are crucial for the initiation and development of many pathological states. Cadherin 5 is an epithelium-specific cadherin that is required for the development and maintenance of the normal function of all epithelial cells in tissues. The loss or down-regulation of cadherin 5 is a key event in the process of tumour invasion and metastasis^[15]. Cadherin 5 has the major role in intercellular adhesion in esophageal mucosa^[16]. Appropriate cadherin expression reflects the differentiation of squamous cell carcinoma^[17]. These results support the putative function of EMP-1, which was a potential maker of differentiation^[18] and was related to cell proliferation, differentiation, regulation and cell death^[3].

In addition, the second largest categories of EMP-1-induced genes were those involved in cell division, Such as cyclin-dependent kinase 4 inhibitor 2D, DNA damage-inducible transcript 3, and retinoic acid receptor beta. The up-regulated cyclin-dependent kinase 4 inhibitor 2D and the down-regulated cyclin-dependent kinase 4 inhibitor 2D and the cyclin D2 (CCND2) and cyclin D3 (CCND3)^[20] affect the cell cycle collaboratively. These support our finding that the inhibition of cell proliferation after overexpression of EMP-1 associates with the induction of S phase arrested and the prolonged G1 phase with flow cytometric assay.

Retinoic acid receptors beta (RAR- β) is another up-regulated gene induced by EMP-1. It is well established that retinoids can modulate epithelial cell growth, differentiation, and apoptosis *in vitro* and *in vivo* by binding to specific nuclear retinoid receptors, which include RAR- β ^[21]. Retinoids can prevent abnormal squamous cell differentiation in nonkeratinizing tissues physiologically. Retinoids can also reverse squamous cell metaplasia, which develops during vitamin A deficiency^[22]. The expression of RAR-beta varied along with the differentiation level of esophageal cancer. RAR-beta mRNA was expressed in 62.7 % (42/67), 55.1 % (43/78) and 29.2 % (7/24) of well, moderated and poorly differentiated SSCs, respectively^[23]. Retinoic acid, which inhibits squamous cell differentiation with RAR-beta involved in, represses EMP-1 expression in normal human bronchial epithelial cells^[4]. EMP-1 is one of down-regulation of a cluster of squamous cell differentiation marker genes^[18] and RAR- β may be involved in this process.

Some genes associated with the intracellular signaling pathway, such as dishevelled homolog 1-like protein and ras associated with diabetes protein 1, were induced by EMP-1 overexpression (Table 1).

A study addressing the relationship between EMP-1 and these cell adhesion and cell-cell communication proteins has not, to our knowledge, previously been reported. The presumed protein structure of EMP-1 also supports its function in cell signaling, cell adhesion and communication. The predicted EMP-1 polypeptide of 157 amino acid residues has a calculated molecular weight of approximately 18 kDa, and bioinformatics analysis reveals that amino acid residues 1-28, 64-89, 95-117, and 134-157 represent four hydrophobic, potentially membrane-spanning domains. Computer-predicted structural domains of EMP-1 are partially mirrored by the exon/intron structure of EMP-1. Most interestingly, exon 4, which covers the potential second transmembrane domain, a small intracellular loop, and half of the third transmembrane domain, encodes the most highly conserved regions between the EMP-1 and PMP22 proteins indicating some shared functional significance for this module in the PMP22 family. Because of the small size of the intracellular loops, it appears unlikely that they are involved in specific interaction with intracellular proteins and therefore in intracellular signaling. In contrast,

the extracellular loops would be able to interact with other molecules and could have functional significance. Furthermore, the first hydrophilic region of PMP22/EMPs, between the first and second hydrophobic domains, forms an extracellular loop that contains one or more consensus sequences that can be N-linked glycosylated *in vitro*, a structure which has been implicated in cell-cell recognition and adhesion processes^[4,24].

In conclusion, the study of the gene expression changes sustains cellular finding that the inhibition of cell proliferation after enforcing expression of EMP-1 associates with the induction of S phase shorten and the prolonged G1 phase. The expression profile and localization of EMP-1 suggests a role in cell signaling, adhesion and communication. This is the first demonstration of global gene expression analysis of esophageal cancer cell line EC9706 transfectant with EMP-1, and these results provides a new insight in the study of the relationship between EMP-1 and esophageal cancer.

REFERENCES

- Gnirke AU**, Weidle UH. Investigation of prevalence and regulation of expression of progression associated protein (PAP). *Anti-cancer Res* 1998; **18**: 4363-4369
- Taylor V**, Welcher AA, Program AEST, Suter U. Epithelial membrane protein-1, peripheral myelin protein 22, and lens membrane protein 20 define a novel gene family. *J Biol Chem* 1995; **270**: 28824-28833
- Chen Y**, Medvedev A, Ruzanov P, Marvin KW, Jetten AM. cDNA cloning, genomic structure, and chromosome mapping of the human epithelial membrane protein CL-20 gene (EMP1), a member of the PMP22 family. *Genomics* 1997; **41**: 40-48
- Lobsiger CS**, Magyar JP, Taylor V, Wulf P, Welcher AA, Program AE, Suter U. Identification and characterization of a cDNA and the structural gene encoding the mouse epithelial membrane protein-1. *Genomics* 1996; **36**: 379-387
- Taylor V**, Suter U. Epithelial membrane protein-2 and epithelial membrane protein-3: two novel members of the peripheral myelin protein 22 gene family. *Gene* 1996; **175**: 115-120
- Jetten AM**, Suter U. The peripheral myelin protein 22 and epithelial membrane protein family. *Prog Nucleic Acid Res Mol Biol* 2000; **64**: 97-129
- Fabbretti E**, Edomi P, Brancolini C, Schneider C. Apoptotic phenotype induced by overexpression of wild-type gas3/PMP22: its relation to the demyelinating peripheral neuropathy CMT1A. *Genes Dev* 1995; **9**: 1846-1856
- Zoidl G**, Blass-Kampmann S, D'Urso D, Schmalenbach C, Muller HW. Retroviral-mediated gene transfer of the peripheral myelin protein PMP22 in Schwann cells: modulation of cell growth. *EMBO J* 1995; **14**: 1122-1128
- Ruegg CL**, Wu HY, Fagnoni FF, Engleman EG, Laus R. B4B, a novel growth-arrest gene, is expressed by a subset of progenitor/pre-B lymphocytes negative for cytoplasmic mu-chain. *J Immunol* 1996; **157**: 72-80
- Kadowaki Y**, Fujiwara T, Fukazawa T, Shao J, Yasuda T, Itoshima T, Kagawa S, Hudson LG, Roth JA, Tanaka N. Induction of differentiation-dependent apoptosis in human esophageal squamous cell carcinoma by adenovirus-mediated p21sdi1 gene transfer. *Clin Cancer Res* 1999; **5**: 4233-4241
- Adams MD**, Kerlavage AR, Fleischmann RD, Fuldner RA, Bult CJ, Lee NH, Kirkness EF, Weinstock KG, Gocayne JD, White O. Initial assessment of human gene diversity and expression patterns based upon 83 million nucleotides of cDNA sequence. *Nature* 1995; **377**: 3-174
- Naiki T**, Nagaki M, Shidoji Y, Kojima H, Imose M, Kato T, Ohishi N, Yagi K, Moriwaki H. Analysis of gene expression profile induced by hepatocyte nuclear factor 4alpha in hepatoma cells using an oligonucleotide microarray. *J Biol Chem* 2002; **277**: 14011-14019
- Ceppek KL**, Shaw SK, Parker CM, Russell GJ, Morrow JS, Rimm DL, Brenner MB. Adhesion between epithelial cells and T lymphocytes mediated by E-cadherin and the alpha E beta 7 integrin. *Nature* 1994; **372**: 190-193
- Poinat P**, De Arcangelis A, Sookhareea S, Zhu X, Hedgcock EM,

- Labouesse M, Georges-Labouesse E. A conserved interaction between beta1 integrin/PAT-3 and nck-interacting kinase/MIG-15 that mediates commissural axon navigation in *C. elegans*. *Curr Biol* 2002; **12**: 622-631
- 15 **Nachtigal P**, Gojova A, Semecky V. The role of epithelial and vascular-endothelial cadherin in the differentiation and maintenance of tissue integrity. *Acta Medica (Hradec Kralove)* 2001; **44**:83-87
- 16 **Bailey T**, Biddlestone L, Shepherd N, Barr H, Warner P, Jankowski J. Altered cadherin and catenin complexes in the Barrett's esophagus-dysplasia-adenocarcinoma sequence: correlation with disease progression and dedifferentiation. *Am J Pathol* 1998; **152**: 135-144
- 17 **Sanders DS**, Bruton R, Darnton SJ, Casson AG, Hanson I, Williams HK, Jankowski J. Sequential changes in cadherin-catenin expression associated with the progression and heterogeneity of primary oesophageal squamous carcinoma. *Int J Cancer* 1998; **79**: 573-579
- 18 **Hippo Y**, Yashiro M, Ishii M, Taniguchi H, Tsutsumi S, Hirakawa K, Kodama T, Aburatani H. Differential gene expression profiles of scirrhous gastric cancer cells with high metastatic potential to peritoneum or lymph nodes. *Cancer Res* 2001; **61**: 889-895
- 19 **Wang Z**, Wang M, Lazo JS, Carr BI. Identification of Epidermal Growth Factor Receptor as a Target of Cdc25A Protein Phosphatase. *J Biol Chem* 2002; **277**: 19470-19475
- 20 **Buschges R**, Weber RG, Actor B, Lichter P, Collins VP, Reifenberger G. Amplification and expression of cyclin D genes (CCND1, CCND2 and CCND3) in human malignant gliomas. *Brain Pathol* 1999; **9**: 435-442
- 21 **De Luca LM**. Retinoids and their receptors in differentiation, embryogenesis, and neoplasia. *FASEB J* 1991; **5**: 2924-2933
- 22 **Chambon P**. A decade of molecular biology of retinoid acid receptors. *FASEB J* 1996; **10**: 940-954
- 23 **Xu M**, Jin YL, Fu J, Huang H, Chen SZ, Qu P, Tian HM, Liu ZY, Zhang W. The abnormal expression of retinoic acid receptor-beta, p 53 and Ki67 protein in normal, premalignant and malignant esophageal tissues. *World J Gastroenterol* 2002; **8**: 200-202
- 24 **Schachner M**, Martini R. Glycans and the modulation of neural-recognition molecule function. *Trends Neurosci* 1995; **18**: 183-191

Edited by Zhang JZ

Peptidergic innervation of human esophageal and cardiac carcinoma

Shuang-Hong Lü, Yan Zhou, Hai-Ping Que, Shao-Jun Liu

Shuang-Hong Lü, Yan Zhou, Hai-Ping Que, Shao-Jun Liu,
Department of Neurobiology, Institute of Basic Medical Sciences,
Academy of Military Medical Sciences, Beijing 100850, China
Supported by the National Natural Science Foundation of China,
No. 39870315

Correspondence to: Dr. Shao-Jun Liu, Department of Neurobiology,
Institute of Basic Medical Sciences, Academy of Military Medical
Sciences, Beijing 100850, China. liusj@nic.bmi.ac.cn
Telephone: +86-10-66932379 **Fax:** +86-10-68213039
Received: 2002-08-15 **Accepted:** 2002-10-18

Abstract

AIM: To investigate the distribution of neuropeptide-immunoreactive nerve fibers in esophageal and cardiac carcinoma as well as their relationship with tumor cells so as to explore if there is nerve innervation in esophageal and cardiac carcinoma.

METHODS: Esophageal and cardiac carcinoma specimens were collected from surgical operation. One part of them were fixed immediately with 4 % paraformaldehyde and then cut with a cryostat into 40- μ m-thick sections to perform immunohistochemical analysis. Antibodies of ten kinds of neuropeptide including calcitonin gene-related peptide (CGRP), galanin (GAL), substance P (SP), etc. were used for immunostaining of nerve fibers. The other part of the tumor specimens were cut into little blocks (1 mm³) and co-cultured with chick embryo dorsal root ganglia (DRG) to investigate if the tumor blocks could induce the neurons of DRG to extend processes, so as to probe into the possible reasons for the nerve fibers growing into tumors.

RESULTS: Substantial amounts of neuropeptide including GAL-, NPY-, SP-immunoreactive nerve bundles and scattered nerve fibers were distributed in esophageal and cardiac carcinomas. The scattered nerve fibers waved their way among tumor cells and contacted with tumor cells closely. Some of them even encircled tumor cells. There were many varicosities aligned on the nerve fibers like beads. They were also closely related to tumor cells. In the co-culture group, about 63 % and 67 % of DRG co-cultured with esophageal and cardiac tumor blocks respectively extended enormous processes, especially on the side adjacent to the tumor, whereas in the control group (without tumor blocks), no processes grew out.

CONCLUSION: Esophageal and cardiac carcinomas may be innervated by peptidergic nerve fibers, and they can induce neurons of DRG to extend processes *in vitro*.

Lü SH, Zhou Y, Que HP, Liu SJ. Peptidergic innervation of human esophageal and cardiac carcinoma. *World J Gastroenterol* 2003; 9(3): 399-403
<http://www.wjgnet.com/1007-9327/9/399.htm>

INTRODUCTION

The problem about the innervation of tumors was noticed as

early as 50 years ago. Though many authors at that time studied this problem and some obtained affirmative results, the ultimate conclusion made by authoritative pathologist^[1] was that there was no innervation in tumor. And this theory was been generally accepted since then.

However, because of the involvement of mental factors in the genesis and development of tumors, the studies on the relationship between nerve and tumor never stopped. Some authors^[2,3] claimed their findings of nerve fibers in tumors, and some others^[4] studied the perineural invasion by carcinoma cells. In our previous investigations, we also observed many scattered nerve fibers in meningioma and cardiac cancer, which was closely related to tumor cells. In addition, accumulated data^[5-7] show that neuropeptides are involved in the regulation of the growth of tumors. Considering these new advancements, we decided to study the distribution of neuropeptide-containing nerve fibers in esophageal and cardiac carcinomas as well as their relationship with tumors so as to find some new proofs about tumor innervation.

MATERIALS AND METHODS

Reagents

Antibodies of ten kinds of neuropeptide were obtained from Sigma, Chemicon or Bohringmanham Companies. Their working dilutions are listed in Table 1. ABC kit was obtained from Vector Company.

Table 1 Antibodies of neuropeptides and their work dilution

Antibody	Working dilution
CGRP	1:8 000
GAL	1:8 000
SP	1:5 000
NT	1:4 000
SOM	1:8 000
CCK	1:4 000
L-ENK	1:5 000
Dyn	1:4 000
NPY	1:6 000
M-ENK	1:6 000

CGRP: Calcitonin gene-related peptide, GAL: Galanin, SP: Substance P, NT: Neurotensin, SOM: Somatostatin, CCK: Cholecystokinin, L-ENK: Leu-enkephalin, Dyn: Dynorphine, NPY: Neuropeptide Y, M-ENK: Met-enkephalin.

Specimens

The surgical tumor specimens were collected from the Affiliated Cancer Hospital of Beijing University and the General Hospital of People's Liberation Army. Clinical and pathological diagnoses confirmed that the esophageal carcinoma specimens were squamous cell carcinomas and cardiac carcinoma specimens were adenocarcinomas. In our preliminary investigations, we found that the probability to find neuropeptide immunoreactive nerve fibers was decreased in large tumors, only tumors with diameter under 3 cm were selected for the present study. Totally, 16 cases of esophageal carcinoma and 13 cardiac carcinoma specimens were used.

After rinsed in saline, one part of the tissue were fixed immediately by immersing in 4 % paraformaldehyde in 0.01 M PBS (pH 7.4) for 10 hrs at 4 °C and then in PBS containing 30 % sucrose to stay overnight. The specimens were then cut with a cryostat (JUNG 2700, America) into 40- μ m-thick sections for immunohistochemical analysis. The other part of the specimens were collected into DMEM containing 1 000U/ml penicillin and streptomycin for co-culture experiment.

Immunohistochemistry

Immunohistochemical reactions were carried out according to the avidin-biotinylated peroxidase complex method (ABC) as previously reported^[8]. Briefly, the tumor sections were incubated at room temperature for 30 min in 1.2 % H₂O₂ (v/v) solution to quench endogenous peroxidase activity. After washed with PBS for 10 min \times 3, they were incubated with 0.3 % Triton X-100 and then moved into antibodies of neuropeptides (diluted by PBS containing 1 % BSA) for 24-48 hrs at 4 °C. The sections were then incubated in biotin-conjugated IgG (diluted in PBS, 1:200) for 2.5hrs at room temperature and washed for 30 min by three changes of PBS, followed by incubation with the streptavidin-peroxidase complex for 2.5 hrs. The reaction product was detected with 3'-diaminobenzidine tetrahydrochloride (DAB, Sigma). Nerve fibers containing the neuropeptides were identified by the presence of dark black color. Thereafter, part of the sections were counterstained with neutral red and dehydrated in graded ethanol before mounted.

Negative controls were made either by omitting the specific neuropeptide antibodies or by replacing them with non-immune goat serum to assess the nonspecific adsorption of secondary antibodies.

Co-culture of tumor blocks with DRG

Tumor blocks were co-cultured with DRG according to the method of reference^[9]. Totally, 10 specimens of the esophageal and cardiac carcinoma respectively were used for co-culture. DRG were isolated from E8-10 chick embryo (obtained from Chinese Academy of Agricultural & Science) and seeded into 24-well plate coated with poly-L-lysine 30 min before co-culture. Tumor specimens were cut into 1 mm³ blocks to co-culture with DRG at a distance of 1.5-2 mm. Each well had one tumor block and one ganglion. Each specimen was co-cultured for 12 wells. They were then incubated at 37 °C with 7.5 % CO₂ for 4hrs to attach. After that, DMEM without any serum was added into the wells. In the control group, DRG were cultured without tumor blocks in the same medium as in the experimental group. There were 10 wells of DRG cultured as control for each case of tumor specimens. The co-cultures were observed under a phase-contrast microscope (IX70, OLYMPUS) 24hrs later and the DRG with processes outgrowth were counted for statistical analysis.

Statistical analysis

The completely randomized design *t* test was used to analyze for statistical significance. The *P* values less than 0.05 were considered as significantly different.

RESULTS

Distribution of neuropeptide-immunoreactive nerve fibers in tumor and their relationship with tumor cells

Under light microscope, substantial amounts of many kinds of neuropeptide-immunoreactive nerve bundles and scattered nerve fibers were observed in both esophageal and cardiac carcinomas. Many of them were distributed around blood vessels and in the connective tissues. But more importantly, a lot of scattered nerve fibers were distributed among tumor cells

(Figures 1-6). In this study, only those areas with neuropeptide immunoreactive nerve fibers scattered among tumor cells were specified as positive. Distribution of positive nerve fibers in tumor was scored as 0 to 3+. The tumor sections with >2/3 positive area were scored as +++, 1/3-2/3 positive area were ++ and <1/3 positive area were + (Table 2). The frequency of neuropeptides-containing nerve fibers varied among individual tumor specimens. In some cases, the positive nerve fibers were numerous around blood vessels and in the parenchyma, while in others there were only a few fibers running along blood vessels. Relatively, in tumors with good differentiation, the frequency of positive nerve fibers was a little higher than in those with poor differentiation. To a great extent, the distribution pattern and frequency were similar in esophageal and cardiac carcinomas. GAL- and NPY-immunoreactive nerve fibers were numerous in the parenchyma in the both carcinomas, whereas CCK- and SOM-immunoreactive nerve fibers were scarce. No NT-immunoreactive nerve fibers could be detected. In the sections of the negative control group, no immunoreactive nerve fibers were observed.

Table 2 Distribution of neuropeptide-immunoreactive nerve fibers in tumors

Antibodies	Cardiac cancer (n=13)			Esophageal cancer (n=16)		
	+++	++	+	+++	++	+
CGRP	0	2	2	0	2	2
GAL	2	6	4	3	7	4
SP	1	5	1	2	5	5
NT	0	0	0	0	0	0
SOM	0	3	3	0	3	6
CCK	0	0	1	0	0	3
L-ENK	1	3	1	0	3	7
Dyn	2	3	5	0	8	1
NPY	2	5	3	1	6	6
M-ENK	3	3	2	0	5	7

The scattered nerve fibers were mainly derived from either the nerve bundles or the connective tissues around (Figure 1). Wherever they came from, they had a common distribution pattern of extending toward the inside of the parenchyma of tumors. Most of the nerve fibers had varicosities aligned on them like beads (Figures 2, 5). Nerve fibers and their varicosities waved their way among tumor cells. Sometimes they were found entering into tumor convergently from the connective tissue around (Figures 3, 4), or extending fine branches into the nest formed by carcinoma cells (Figure 6). They contacted with tumor cells closely; some of them even encircled tumor cells (Figure 2).

Outgrowth of processes of DRG in co-cultured group

After incubation for 24-48hr, most of the DRG in the co-culture group extended their processes longer than their diameter (Table 3, Figure 7). Interestingly, the processes were distributed around DRG asymmetrically (Figure 7). On the sides adjacent to tumor blocks, they were dense and long, whereas on the opposite sides, they were sparse and short, or no processes at all. In the control group, no DRG extended their processes.

Table 3 Outgrowth of processes of DRG co-cultured with tumor blocks

Tumor group	DRG with processes (n)	DRG without processes (n)	Rate of DRG with processes (x \pm s)
Esophageal	49	28	0.63 \pm 0.10 ^a
Cardiac	60	29	0.67 \pm 0.09 ^a
Control	0	63	0

^a*P*<0.0001 vs the control group

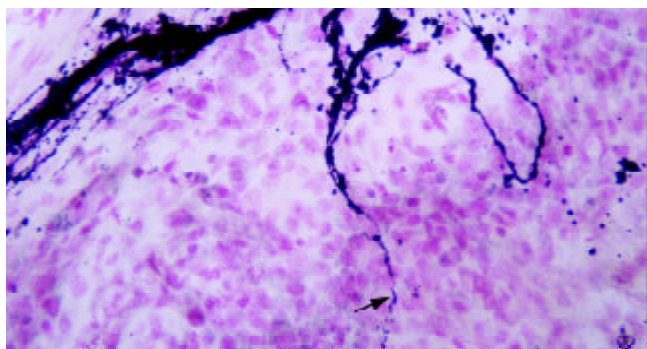


Figure 1 GAL-immunostaining of esophageal carcinoma. Scattered nerve fibers (arrows) branched almost vertically from nerve bundles in connective tissue and entered into tumor parenchyma $\times 250$.

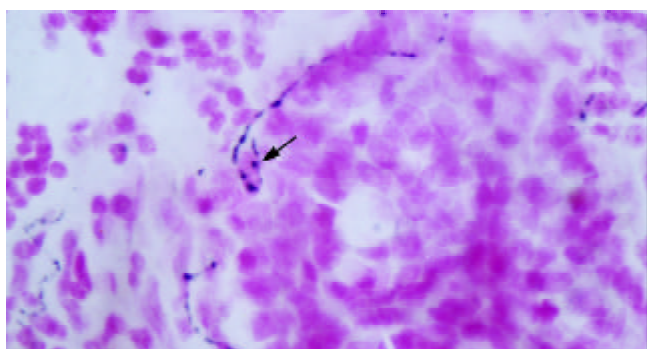


Figure 2 L-ENK-immunoreactive nerve fibers in esophageal carcinoma. The fine nerve fiber (arrow) with varicosities on it encircled a tumor cell and contacted with it closely $\times 500$.

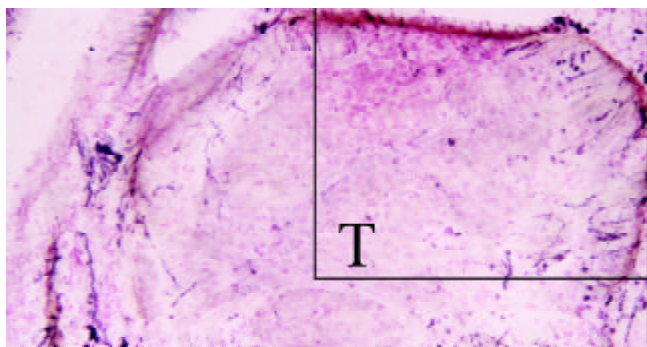


Figure 3 GAL-immunostaining of esophageal carcinoma. Many nerve fibers entered into a nestlike cancerous tissue (T) convergently from collective tissue around it. The structure on the top right corner was amplified in Figure 4 $\times 125$.

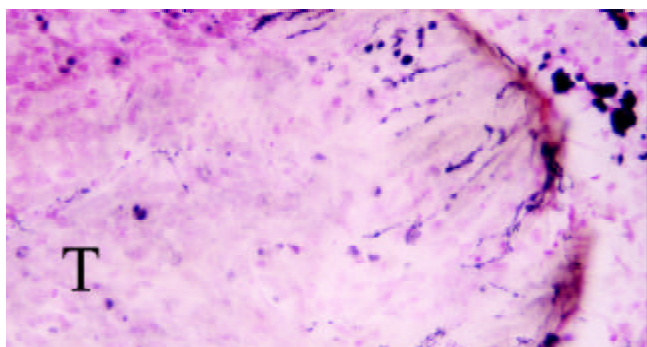


Figure 4 Higher magnification of the part on the top right in Fig.3. GAL-immunoreactive nerve fibers entered into esophageal carcinoma from peripheral areas $\times 250$.

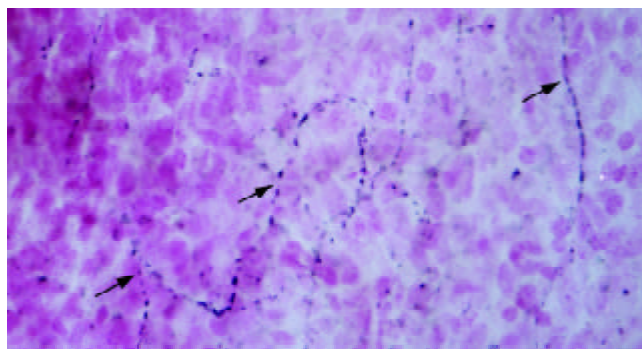


Figure 5 Section of Cardiac adenocarcinoma immunostained for GAL. Many immunoreactive nerve fibers with beads-like varicosities distributed in the parenchyma of tumor $\times 500$.

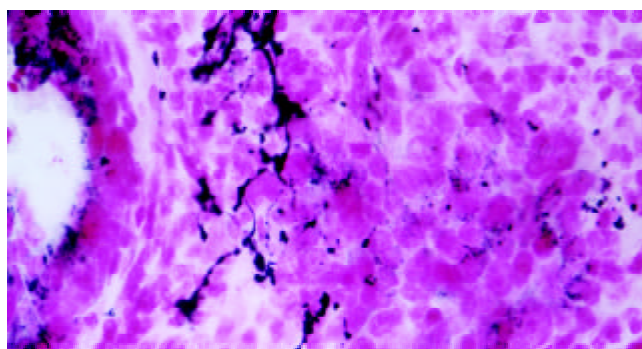


Figure 6 GAL-immunoreactive nerve fibers extended into nestlike cancerous tissue formed by cardiac adenocarcinoma cells. The scattered nerve fibers contacted with tumor cells closely $\times 500$.

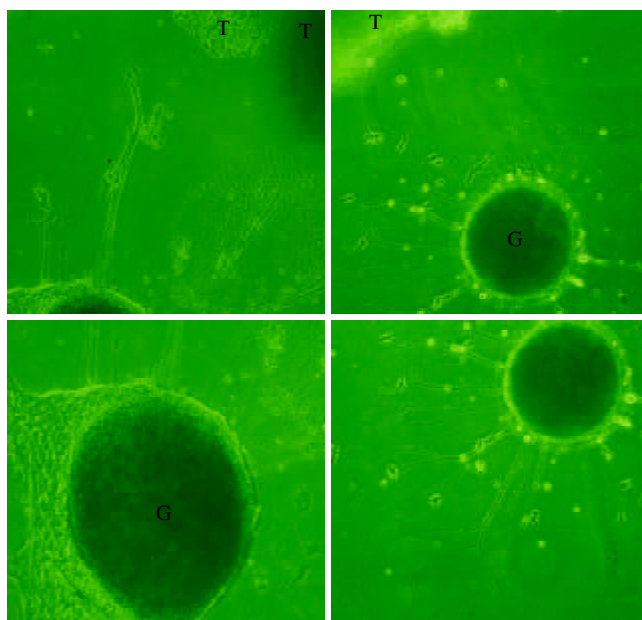


Figure 7 Montage photographs showing the effects of esophageal (a) and cardiac (b) carcinoma tissue block (T) on co-cultured DRG (G). On the side adjacent to tumor, DRG extending long and dense processes whereas on the opposite side, the processes are sparse and short (b), or no processes at all (a) $\times 125$.

DISCUSSION

Previous studies^[10-12] have shown that the esophagus is richly supplied with neuropeptidergic nerves. In the present study, the neuropeptide-immunoreactive nerves fibers in the

esophageal and cardiac carcinomas seem to have roughly the same topographic distribution as those in the normal digestive tract in that GAL-, NPY-, ENK- and SP-containing nerves fibers predominate in esophagus and stomach, whereas SOM-, NT-containing nerves fibers predominate in intestine^[13]. These neuropeptides have very important functions^[14-16] on the physiological activities of digestive system such as the motility, secretion, etc. Recently, there are more and more evidences showing that neuropeptides can also affect the growth and differentiation of tumors^[17-20]. But since there are endocrine cells in gastrointestinal wall, it is difficult to distinguish if the neuropeptides come from endocrine cells or nerve terminals^[21-22]. Therefore, to some extent, the findings of scattered neuropeptides-containing nerve fibers in tumor will help us understand the mechanisms of neuropeptides affecting tumors.

On the other hand, the findings about the distributions of nerve fibers in esophageal and cardiac carcinomas and their close relationship with tumor cells provided a new viewpoint about the innervation of tumors. In a previous report^[2], the single adrenergic and NPY-containing nerve fibers were found distributed in the parenchyma of human parathyroid adenomas, but most of them were located in the perivascular space. And no detailed descriptions of their relationship with tumor cells are available. With regard to the perineural invasion by carcinomas^[3,4], it was usually considered to be one of the important routes of tumor dissemination and could not be called innervation. In 2001, some German researchers^[23] observed nerve fibers within an adenoma of the ciliary body epithelium of the eye. Under a transmission electron microscope, a small number of fine unmyelinated nerve fibers were found containing clear and dense core vesicles in tumors. Recently, they examined the exophytic tumors of the urinary bladder and human choroidal melanoma^[24,25], and also found irregularly distributed fine nerve strands comprised of axons; hence they concluded that tumors may be innervated. In this regard, they happened to have the same view with us. In this study, we found many scattered nerve fibers not only around blood vessels, but also in the parenchyma of tumors and among tumor cells. Although we did not find specific structure of synapse under electron microscope, these scattered nerve fibers with their beads-like varicosities attached with tumor cells so closely that we can reasonably deduce that they must have important effects on tumor cells, because varicosities are considered containing vesicles and can form synapse-like structures, and will release neuropeptides or other neurotransmitters in their vesicles when stimulated properly. These results suggest that esophageal and cardiac carcinomas may be innervated by peptidergic nerve fibers. Together with previous studies, we suggest that it is necessary to investigate the validity of the old theory about the innervation of tumor.

Why do we get the results that the previously published data did not? We think we have the following advantages: (1) we used frozen sections to facilitate the preservation of the antigen; (2) we used immunohistochemical ABC method to examine the immunoreactive nerve fibers, which is more sensitive than old methods. (3) Neuropeptides-containing nerve fibers are widely distributed in digestive tract from esophagus to the anal sphincter, which provide the possibility for nerve fibers to grow into tumors.

In order to understand how the nerve fibers grow into tumors, we performed co-culture experiment to investigate if tumors had the ability to induce neurons to extend their processes. Our results affirmed this possibility. The neurons of DRG extended processes and the processes on the side adjacent to tumor blocks were dense and long, suggesting that the esophageal and cardiac carcinoma tissues may secrete neurotrophic factors, which are important for the extending of neuronal processes. The SDS electrophoresis (data not shown)

of the tumor-conditioned medium confirmed this assumption and demonstrated that one of them was NGF. Many kinds of tumors have been found secrete NGF, BDNF, NT-3, etc.^[26-28]. NGF high-affinity receptor TrkA was also found to exist in esophageal carcinoma^[29]. Therefore, it is possible that these neurotrophic factors in esophageal and cardiac carcinoma tissues act on the neurons in enteric nervous system and induce their fibers to grow into tumors. Or they may exert their neurotrophic functions by helping the injured nerve trunks in tumors regenerate and sprout new nerve fibers. These nerve fibers would extend along with the direction of the diffusion of the neurotrophic factors^[30] and therefore enter into the tumors.

The functional role of these neuropeptide-containing nerve fibers in esophageal and cardiac carcinoma is not clear. The morphological observation indicated that nerve fibers and their varicosities were in close contact with the tumor cells. This would suggest a role of nerve terminals in the regulation of tumor growth and/or differentiation, which is consistent with the function of neuropeptides on tumors. This might partly explain why mental factors could affect the tumorigenesis and tumor development.

REFERENCES

- 1 Willis RA. The spread of the tumors in the human. 3rd ed. London: Butterworths 1973: 121-125
- 2 Luts L, Bergenfelz A, Alumets J, Sundler F. Peptide-containing nerve fibres in normal human parathyroid glands and in human parathyroid adenomas. *Eur J Endocrinol* 1995; **133**: 543-551
- 3 Stack PS. Lymphomatous involvement of peripheral nerves: clinical and pathologic features. *South Med J* 1991; **84**: 512-514
- 4 Takubo K, Takai A, Yamashita K, Yoshimatsu N, Kitano M, Sasajima K, Fujita K. Light and electron microscopic studies of perineural invasion by esophageal carcinoma. *J Natl Cancer Inst* 1985; **74**: 987-993
- 5 Iishi H, Tatsuta M, Baba M, Uehara H, Nakaizumi A. Protection by galanin against gastric carcinogenesis induced by N-Methyl-N'-nitro-N-nitrosoguanidine in wistar rats. *Cancer Res* 1994; **54**: 3167-3170
- 6 Evers BM, Parekh D, Townsend CM Jr, Thompson JC. Somatostatin and analogues in the treatment of cancer. *Ann Surg* 1991; **213**: 190-198
- 7 Tallett A, Chilvers ER, Hannah S, Dransfield I, Lawson MF, Haslett C, Sethi T. Inhibition of neuropeptide-stimulated tyrosine phosphorylation and tyrosine kinase activity stimulates apoptosis in small cell lung cancer cells. *Cancer Res* 1996; **56**: 4255-4263
- 8 Hsu SM, Raine L, Fanger H. Use of avidin-biotin-peroxidase complex (ABC) in immunoperoxidase techniques: a comparison between ABC and unlabeled antibody (PAP) procedures. *J Histochem Cytochem* 1981; **29**: 577-580
- 9 Eranko O, Lahtinen T. Attraction of nerve fiber outgrowth from sympathetic ganglia to heart auricles in tissue culture. *Acta Physiol Scand* 1978; **103**: 394-403
- 10 Uddman R, Alumets J, Hakanson R, Sundler F, Walles B. Peptidergic (enkephalin) innervation of the mammalian esophagus. *Gastroenterology* 1980; **78**: 732-737
- 11 Wattchow DA, Furness JB, Costa M, O'Brien PE, Peacock M. Distributions of neuropeptides in the human esophagus. *Gastroenterology* 1987; **93**: 1363-1371
- 12 Singaram C, Sengupta A, Sweet MA, Sugarbaker DJ, Goyal RK. Nitrinergic and peptidergic innervation of the human oesophagus. *Gut* 1994; **35**: 1690-1696
- 13 Yamashita Y, Pedersen JH, Hansen CP. Distribution of neurotensin-like immunoreactivities in porcine and human gut. *Scand J Gastroenterol* 1990; **25**: 481-488
- 14 Chiba T, Taminato T, Kadowaki S, Inoue Y, Mori K, Seino Y, Abe H, Chihara K, Matsukura S, Fujita T, Goto Y. Effects of various gastrointestinal peptides on gastric release. *Endocrinology* 1980; **106**: 145-149
- 15 Johnson LR. Physiology of the Gastrointestinal Tract. 2nd ed. New York: Raven Press 1987: 41-65
- 16 Aggestrup S, Uddman R, Jensen SL, Hakanson R, Sundler F,

- Schaffalitzky de Muckadell O, Emson P. Regulatory peptides in lower esophageal sphincter of pig and man. *Dig Dis Sci* 1986; **31**: 1370-1375
- 17 **Baldwin GS**, Shulkes A. Gastrin as an autocrine growth factor in colorectal carcinoma: implications for therapy. *World J Gastroenterol* 1998; **4**: 461-463
 - 18 **Camby I**, Salmon I, Bourdel E, Nagy N, Danguy A, Brotchi J, Pasteels JL, Martinez J, Kiss R. Neurotensin-mediated effects on astrocytic tumor cell proliferation. *Neuropeptides* 1996; **30**: 133-139
 - 19 **Nakaizumi A**, Uehara H, Baba M, Iishi H, Tatsuta M. Enhancement by neurotensin of hepatocarcinogenesis by N-nitrosomorpholine in Sprague-Dawley rats. *Cancer Lett* 1996; **110**: 57-61
 - 20 **Seufferlein T**, Rozengurt E. Galanin, neurotensin, and phorbol esters rapidly stimulate activation of mitogen-activated protein kinase in small cell lung cancer cells. *Cancer Res* 1996; **56**: 5758-5764
 - 21 **Johnson LR**. Physiology of the Gastrointestinal Tract. 2nd ed. New York: Raven Press 1987: 111-129
 - 22 **Furness JB**, Young HM, Pompolo S, Bornstein JC, Kunze WA, McConalogue K. Plurichemical transmission and chemical coding of neurons in the digestive tract. *Gastroenterology* 1995; **108**: 554-563
 - 23 **Seifert P**, Spitznas M. Tumours may be innervated. *Virchows Arch* 2001; **438**: 228-231
 - 24 **Seifert P**, Benedic M, Effert P. Nerve fibers in tumors of the human urinary bladder. *Virchows Arch* 2002; **440**: 291-297
 - 25 **Seifert P**, Spitznas M. Axons in human choroidal melanoma suggest the participation of nerves in the control of these tumors. *Am J Ophthalmol* 2002; **133**: 711-713
 - 26 **MacGrogan D**, Saint-Andre JP, Dicou E. Expression of nerve growth factor and nerve growth factor receptor genes in human tissues and in prostatic adenocarcinoma cell lines. *J Neurochem* 1992; **59**: 1381-1391
 - 27 **Ohta T**, Numata M, Tsukioka Y, Futagami F, Kayahara M, Kitagawa H, Nagakawa T, Yamamoto M, Wakayama T, Kitamura Y, Terada T, Nakanuma Y. Neurotrophin-3 expression in human pancreatic cancers. *J Pathol* 1997; **181**: 405-412
 - 28 **Descamps S**, Lebourhis X, Delehedde M, Boilly B, Hondermarck H. Nerve growth factor is mitogenic for cancerous but not normal human breast epithelial cells. *J Biol Chem* 1998; **273**: 16659-16662
 - 29 **Koizumi H**, Morita M, Mikami S, Shibayama E, Uchikoshi T. Immunohistochemical analysis of TrkA neurotrophin receptor expression in human non-neuronal carcinomas. *Pathol Int* 1998; **48**: 93-101
 - 30 **Tessier-Lavigne M**, Goodman CS. The molecular biology of axon guidance. *Science* 1996; **274**: 1123-1133

Edited by Ma JY

Expression of MUC1 in esophageal squamous-cell carcinoma and its relationship with prognosis of patients from Linzhou city, a high incidence area of northern China

Zi-Bo Song, Shan-Shan Gao, Xin-Na Yi, Yan-Jie Li, Qi-Ming Wang, Ze-Hao Zhuang, Li-Dong Wang

Zi-Bo Song, Institute of Medical Genetics, People's Hospital of Henan Province, 450003, Henan Province, China

Shan-Shan Gao, Xin-Na Yi, Yan-Jie Li, Qi-Ming Wang, Ze-Hao Zhuang, Li-Dong Wang, Laboratory for Cancer Research, Medical College of Zhengzhou University, Zhengzhou 450052, Henan Province, China

Supported by National Outstanding Young Scientist Award of China, NO. 30025016; NCI CA65871 (U.S.A.)

Correspondence to: Zi-Bo Song, Institute of Medical Genetics, People's Hospital of Henan Province, 450003, Henan Province, China. zbsong@sohu.com

Telephone: +86-371-5580463

Received: 2002-10-30 **Accepted:** 2002-11-19

Abstract

AIM: To further characterize the possible relationship between the molecular changes and prognosis of ESC and to elucidate the possible mechanisms involved.

METHODS: 114 specimens of ESC were collected from Linzhou city, and all patients were followed up for more than 5 years after resection. Histopathological analysis and immunohistochemical staining (ABC) were employed to detect the alteration of MUC1.

RESULTS: The positive immunostaining rate for MUC1 was 79 % (90/114), and the high-expression rate was 63 % (72/114). The mean survival periods (months) of those with high- and low-expression rates of MUC1 were 41 (95 % CI: 35, 47) and 52 (95 % CI: 45, 59), respectively. Patients in the low-expression group obviously survived longer than those in high-expression group, and the difference was significant ($P < 0.05$). The expression of MUC1 protein in the esophageal carcinoma specimens with metastasis was stronger than those without metastasis, the difference was also significant ($P < 0.05$). The stepwise multivariate analysis showed that "differentiation", "expression of MUC1" and "TNM staging" were the most important factors affecting the prognosis of esophageal carcinoma patients ($P < 0.05$).

CONCLUSION: A good correlation between the alteration of MUC1 and the regional lymph node metastasis was observed. Furthermore, high-expression of MUC1 was associated with poor prognosis for esophageal cancer patients. These results indicated that MUC1 is a promising biomarker for predicting lymph node metastasis and prognosis in esophageal cancer.

Song ZB, Gao SS, Yi XN, Li YJ, Wang QM, Zhuang ZH, Wang LD. Expression of MUC1 in esophageal squamous-cell carcinoma and its relationship with prognosis of patients from Linzhou city, a high incidence area of northern China. *World J Gastroenterol* 2003; 9(3): 404-407

<http://www.wjgnet.com/1007-9327/9/404.htm>

INTRODUCTION

Esophageal squamous-cell carcinoma (ESC) is one of the most common malignant diseases in northern China, and Linzhou city (formerly Linxian) had being the highest incidence area^[1,2]. The five-year survival rate for early esophageal cancer patients is more than 90 %. However, for the patients at late or advanced stage, the five year survival rate is only 10-15 %^[1,2]. So far, the conventional traditional prognostic markers, such as cancer stage based on metastasis and pathological grade are still used to evaluate the prognosis of esophageal cancer patients. But, it has been well recognized that there is discordance between the conventional prognosis biomarkers and the actual prognosis. For example the patients with well differentiated cancer may have a worse prognosis than those with poorly differentiated ones, indicating the limitation of those markers for predicating.

With the development of molecular biotechnology, many new measurements have been applied in cancer prognosis research. Studies on ESC prognosis have been expanded in recent years; however, the molecular mechanisms involved in prognosis of esophageal cancer, especially the survival analysis on whom from high-incidence area of esophageal carcinoma was very limited. We followed up the ESC patients from Linzhou city and determined the alteration of MUC1 expression and its relationship to the prognosis, to further characterize the possible relationship between them so as to elucidate the possible mechanisms of ESC carcinogenesis, and to determine the alteration of MUC1 and prognosis with histopathological and immunohistochemical methods.

MATERIALS AND METHODS

Patients

One hundred and fourteen patients with ESC, who had undergone esophagectomy at the Esophageal Carcinoma Hospital of Linzhou City between 1993 and 1996 were enrolled in this study. All the patients were local residents of Linzhou city and had not received radiation therapy or chemotherapy prior to the surgery. There were 67 men and 49 women. The mean age was 53.5 ± 8.1 (range 37-72) years for males and 53.6 ± 7.8 (range 40-69) years for females, respectively. All specimens were confirmed by pathology as ESC.

Follow-up

All patients were followed up until March 2001, at which the patients had survived for more than 5 years or died within that period after surgical treatment. 57 patients survived less than 5 years died of recurrence or metastasis.

Tissues processing

All tumor specimens were fixed with formalin and embedded with paraffin. Each block was sectioned serially at 5 μ m, one of which was stained with hematoxylin and eosin for histopathological analysis by two pathologists and the others were used for immunostaining.

Histopathological analysis

Histopathological diagnoses were made according to the previously established criteria^[3].

Immunohistochemical staining

Anti-MUC1 antibody was a mouse monoclonal anti-serum directed at a hexapeptide in the tandem repeat region of the protein core of MUC1 (clone Ma552; Novocastra, Burlingame, CA), which was kindly provided by Dr. Yongqin Li (College of Medicine, Harvard University). The avidin-biotin-peroxidase complex (ABC) method was used for MUC1 immunostaining. In brief, after dewaxing, quenching endogenous peroxidase activity with 3 % H₂O₂, and blocking cross-reactivity with normal serum (Vectastain Elite Kit; Vector, Burlingame, CA), the tissues were incubated overnight at 4 °C with primary antibodies (1:400 for MUC1). Location of the primary antibodies was achieved by subsequent use of a biotinylated anti-primary antibody, an avidin-biotin complex conjugated to horseradish peroxidase, and 3',5'-diaminobenzidine (Vectastain Elite Kit). Normal serum blocking and omission of the primary antibody were used as negative controls.

Evaluation of immunostaining

Clear cytoplasm and cell membrane staining was the criterion for a positive reaction. The staining was graded by the percentage of positively stained neoplastic cells as follows: -, <5 %; +, 5-50 %; ++, >50 % of the neoplastic cells stained. For statistical analysis, the examined cases were divided into 2 groups: the low-expression group, composed of the “-” and “+” groups (less than 50 % of neoplastic cells stained) and the high-expression group, the “++” group (over 50 % of the neoplastic cells stained)^[4].

Statistical analysis

Chi-squared test was performed to evaluate the relevance of regional lymph node metastasis and expression of MUC1 protein, Kaplan-Meier was used for survival analysis, and multivariate analysis for screening prognostic factors. The significant difference was considered when the *P* value was less than 0.05.

RESULTS

Results of follow up

Among the follow up of 114 ESC patients followed up, 33 % (33/114) survived 5 years, 50 % (57/114) died within 5 years after surgical treatment and 17 % (20/114) cases were censored during the follow-up.

Expression of MUC1 and its relationship with survival of ESC

Among the 114 surgically resected ESC specimens examined, the positive immunostaining for MUC1 was observed in 90 cases (78.9 %), and high-expression was seen in 72 cases (63.2 %) and low-expression was in 42 cases (36.8 %). The mean survival period (months) and 95 % confidence interval of esophageal carcinoma patients with high- and low-expression of MUC1 were 41(35, 47) and 52(45, 59), respectively. Patients in the low-expression group obviously survived longer than those in high-expression group, and the difference was significant (*P*<0.05, Table 1 and Figure 1).

Relationship between the expression of MUC1 and regional lymph node metastasis

According to the status of the regional lymph nodes with or without metastasis, all specimens were divided into two groups, with metastasis and without metastasis. The expression of

MUC1 protein in the ESC specimens with metastasis was obviously stronger than those without metastasis, and the difference was significant (*P*<0.05, Table 2).

Table 1 Survival analysis of high-expression and low-expression of MUC1 in ESC

Expression of MUC1	No. of specimens examined	No. of death	Mean survival period (month) x (95% CI*)
Low-expression	42	17	52(45, 59)
High-expression	72	40	41(35, 47)
Total	114	57	

*: Confidence Interval; Log-rank: $\chi^2=5.11$, *P*=0.0238.

Table 2 Relationship between the expression of MUC1 and regional lymph node metastasis

Group	No. of specimens examined	Expression of MUC1 protein			
		- n(%)	+ n(%)	++ n(%)	+++ n(%)
Without metastasis	77	19(24.7)	29(37.7)	7(9.1)	22(28.5)
With Metastasis	37	0(0)	4(10.8)	5(13.5)	28(75.7)
Total	114	19	33	12	50

Chi-squared test: $\chi^2=27.4693$, *P*<0.05.

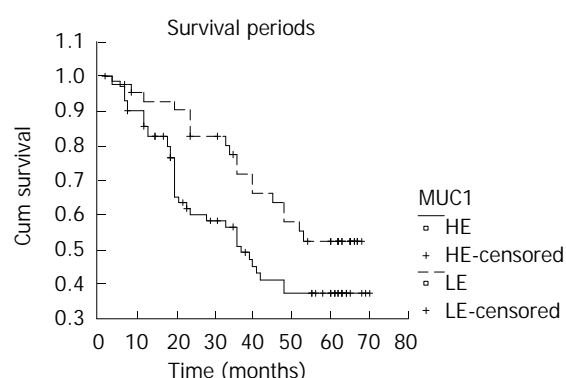


Figure 1 Comparison of survival period between high-expression and low-expression of MUC1 in ESC. HE: High-expression; LE: Low-expression.

Cox model analysis

Ten parameters, including sex, age, invading depth, regional lymph node metastasis, metastasis of other organs, TNM stage, differentiation and MUC1, were used as independent variables, survival periods of ESC patients were used as dependent variables, and all variables were ranked into Cox model analysis (Table 3). The stepwise multivariate analysis showed that “differentiation”, “expression of MUC1” and “TNM staging”, were the most important factors affecting the prognosis of ESC patients (*P*<0.05), RR values for each parameter were 2.2382, 1.9409 and 1.8621, respectively (Table 4).

Table 3 All factors employed by Cox regression model

Factors	Variable
Sex	X1 0=male, 1=female
Age	X2 0=<45 years, 1=45~55 years, 2=>55 years
Invading depth	X3 0=lamina propria or submucosa, 1=muscularis propria, 2=adventitia, 3=adjacent structures
Regional lymph node metastasis	X4 0=no, 1=yes
Distant metastasis	X5 0=no, 1=yes
TNM stage	X6 0=0, 1=I, 2=II, 3=III, 4=IV
Differentiation	X7 0=high, 2=moderate, 3=low
Expression of MUC1	X8 0=low, 1=high

Table 4 Results of Cox model stepwise regression analysis

Variable	Parameter Estimated	Standard error	R	RR
X6	0.6217	0.1549	0.1717	1.8621
X7	0.8057	0.1961	0.1763	2.2382
X8	0.6632	0.3075	0.0311	1.9409

DISCUSSION

Both patients and doctors monitored the patients' survival period after surgery. So far, it is still controversial about evaluating. Our study on the expression of MUC1 in ESC tissues showed that the patients in the low-expression group obviously survived longer than those in high-expression group, and the difference was significant ($P < 0.05$). It is therefore indicated that detection of expression of MUC1 may be of value in assessing the prognosis of ESC patients.

The epithelial mucin coded by the MUC1 gene is a transmembrane molecule, which is expressed in most glandular epithelial cells. The molecule was first identified in human milk, as a large molecular weight glycoprotein rich in serine, threonine and proline carrying a high percentage of *O*-linked carbohydrate^[5]. MUC1 is widely expressed by normal glandular epithelial cells, and the expression is dramatically increased when the cells become malignant^[6,7], and its relationship with the prognosis of several carcinomas have been already reported^[4,8-11]. Changes in the expression levels of MUC1 have also been described in esophageal lesions^[12]. Our finding showed that MUC1 was expressed in all surgical specimens with lymph node metastasis. Its high-expression rate reached 89 %, and was significantly different from the specimens without lymph node metastasis ($P < 0.05$). The lymph node and lymphatic vessel invasion has been reported as poor prognosis factor^[13,14].

Mucins are heavily glycosylated glycoproteins that have protective and lubricating functions^[15,16]. MUC1 expressed in tumors may function as an anti-adhesion molecule, which inhibits cell-cell adhesion, inducing a release of cells from tumor nests. Thus, MUC1 expression may be related to invasion or metastasis of carcinoma cells^[17-19]. MUC1 can down-regulate the expression of E-cadherin, which is a calcium-dependent adhesion molecule, functioning in the cell-cell adhesion, while the low-expression of E-cadherin increased the invading ability of tumor cells^[20-22]. Our previous studies found that MUC1 was expressed in 50 primary ESC cells and the metastasized cancer cells of the matched lymph nodes. In addition, it was found that the coincidence of positive immunostaining between primary tumor and its matching lymph node was observed in 28 cases (56.0 %), while the coincidence of negative immunostaining was observed only in 2 cases (1.0 %)^[23]. It therefore indicated that the expression of MUC1 might play an important role in the invasion or metastasis of ESC cells, which might be one of the mechanisms involving in poor prognosis. But a discordant view was held by Japanese authors who argued that the expression of MUC1 was not significantly associated with metastasis of human esophageal carcinomas^[24]. Further study is still necessary.

Considering the complexity in cancer, it is difficult to define its useful prognostic and predictive factors^[25-28]. In the present study, we use multivariate analytic method for screening the prognostic factors in combination with clinical data. The stepwise multivariate analysis shows that "differentiation", "expression of MUC1" and "TNM staging" are the most important factors affecting the prognosis of ESC patients ($P < 0.05$), our findings also indicate that high expression of MUC1 is related to poor prognosis of ESC.

REFERENCES

- 1 **Yang CS**. Research on esophageal cancer in China: a review. *Cancer Res* 1980; **40**: 2633-2644
- 2 **Lu JB**, Yang WX, Zu SK, Chang QL, Sun XB, Lu WQ, Quan PL, Qin YM. Cancer mortality and mortality trends in Henan, China, 1974-1985. *Cancer Detect Prev* 1988; **13**: 167-173
- 3 **Wang LD**, Shi ST, Zhou Q, Goldstein S, Hong JY, Shao P, Qiu SL, Yang CS. Changes in P53 and cyclin D1 protein levels and cell proliferation in different stages of human esophageal and gastric cardia carcinomas. *Int J Cancer* 1994; **59**: 514-519
- 4 **Sagara M**, Yonezawa S, Nagata K, Tezuka Y, Natsugoe S, Xing PX, McKenzie I FC, Aikou T, Sato E. Expression of MUCIN 1 (MUC1) in esophageal squamous-cell carcinoma: its relationship with prognosis. *Int J Cancer* 1999; **84**: 251-257
- 5 **Taylor-Papadimitriou J**, Burchell J, Miles DW, Dalziel M. MUC1 and cancer. *Biochimica Biophysica Acta* 1999; **1455**: 301-313
- 6 **Hirasawa Y**, Kohno N, Yokoyama A, Kondo K, Hiwada K, Miyake M. Natural autoantibody to MUC1 is a prognostic indicator for non-small cell lung cancer. *Am J Respir Crit Care Med* 2000; **161**: 589-594
- 7 **Baldus SE**, Zirbes TK, Glossmann J, Fromm S, Hanisch FG, Monig SP, Schroder W, Schneider PM, Flucke U, Karsten U, Thiele J, Holscher AH, Dienes HP. Immuneoreactivity of monoclonal antibody BW835 represents a marker of progression and prognosis in early gastric cancer. *Oncology* 2001; **61**: 147-155
- 8 **Xu Y**, Kimura N, Yoshida R, Lin H, Yoshinaga K. Immunohistochemical study of Muc1, Muc2 and human gastric mucin in breast carcinoma: relationship with prognostic factors. *Oncol Rep* 2001; **8**: 1177-1182
- 9 **Lee HS**, Lee HK, Kim HS, Yang HK, Kim YI, Kim WH. MUC1, MUC2, MUC5AC, and MUC6 expressions in gastric carcinoma: their roles as prognostic indicators. *Cancer* 2001; **92**: 1427-1434
- 10 **Kraus S**, Abel PD, Nachtmann C, Linsenmann HJ, Weidner W, Stamp GW, Chaudhary KS, Mitchell SE, Franke FE, Lalani el-N. MUC1 mucin and trefoil factor 1 protein expression in renal cell carcinoma: correlation with prognosis. *Hum Pathol* 2002; **33**: 60-67
- 11 **Kashiwagi H**, Kijima H, Dowaki S, Ohtani Y, Tobita K, Yamazaki H, Nakamura M, Ueyama Y, Tanaka M, Inokuchi S, Makuuchi H. MUC1 and MUC2 expression in human gallbladder carcinoma: a clinicopathological study and relationship with prognosis. *Oncol Rep* 2001; **8**: 485-489
- 12 **Guillem P**, Billeret V, Buisine MP, Flejou JF, Lecomte-Houcke M, Degand P, Aubert JP, Triboulet JP, Porchet N. Mucin gene expression and cell differentiation in human normal, premalignant and malignant esophagus. *Int J Cancer* 2000; **88**: 856-861
- 13 **Brucher BL**, Stein HJ, Werner M, Siewert JR. Lymphatic vessel invasion is an independent prognostic factor in patients with a primary resected tumor with esophageal squamous cell carcinoma. *Cancer* 2001; **92**: 2228-2233
- 14 **Eloubeidi MA**, Desmond R, Arguedas MR, Reed CE, Wilcox CM. Prognostic factors for the survival of patients with esophageal carcinoma in the U.S: the importance of tumor length and lymph node status. *Cancer* 2002; **95**: 1434-1443
- 15 **Jarrard JA**, Linnoila RH, Lee H, Steinberg SM, Witschi H, Szabo E. MUC1 is a novel marker for the type II Pneumocyte lineage during lung carcinogenesis. *Cancer Research* 1998; **58**: 5582-5589
- 16 **Reis CA**, David L, Correa P, Carneiro F, Bolos C, Garcia E, Mandel U, Clausen H, Sobrinho-Simoes M. Intestinal metaplasia of Human stomach displays distinct patterns of mucin (MUC1, MUC2, MUC5AC, and MUC6) expression. *Cancer Research* 1999; **59**: 1003-1007
- 17 **Kam JL**, Regimbald LH, Hilgers JH, Hoffman P, Krantz MJ, Longenecker BM, Hugh JC. MUC1 synthetic peptide inhibition of intercellular adhesion molecule-1 and MUC1 binding requires six tandem repeats. *Cancer Res* 1998; **58**: 5577-5581
- 18 **Takao S**, Uchikura K, Yonezawa S, Shintani H, Aikou T. Mucin core protein expression in extrahepatic bile duct carcinoma is associated with metastases to the liver and poor prognosis. *Cancer* 1999; **86**: 1966-1975
- 19 **Kimura H**, Konishi K, Arakawa H, Oonishi I, Kaji M, Maeda K, Yabushita K, Tsuji M, Miwa A. Number of lymph node metastases influences survival in patients with thoracic esophageal carcinoma: therapeutic value of radiation treatment for

- recurrence. *Dis Esophagus* 1999; **12**: 205-208
- 20 **Kondo K**, Kohno N, Yokoyama A, Hiwada K. Decreased MUC1 expression induces E-cadherin-mediated cell adhesion of breast cancer cell lines. *Cancer Res* 1998; **58**: 2014-2019
 - 21 **Wesseling J**, van der Valk SW, Hilken J. A mechanism for inhibition of E-cadherin-mediated cell-cell adhesion by the membrane-associated mucin episialin/MUC1. *Mol Biol Cell* 1996; **7**: 565-577
 - 22 **Si HX**, Tsao SW, Lam KY, Srivastava G, Liu Y, Wong YC, Shen ZY, Cheung AL. E-cadherin Expression is commonly downregulated by CpG island hypermethylation in esophageal carcinoma cells. *Cancer Lett* 2001; **173**: 71-78
 - 23 **Zhuang ZH**, Wang LD, Gao SS, Fan ZM, Song ZB, Qi YJ, Li YJ, Li JX. Expression of MUC1 in esophageal and gastric cardiac carcinoma tissues from high-incidence area for esophageal cancer in Henan. *Zhenzhou Daxue Xuebao* 2002; **37**: 774-777
 - 24 **Kijima H**, Chino O, Oshiba G, Tanaka H, Kenmochi T, Kise Y, Shimada H, Abe Y, Tokunaga T, Yamazaki H, Nakamura M, Tanaka M, Makuuchi, H, Ueyama Y. Immunohistochemical MUC1 (DF3 Antigen) expression of human esophageal squamous cell carcinoma. *Anticancer Research* 2001; **21**: 1285-1290
 - 25 **Hall PA**, Goings JJ. Predicting the future: a critical appraisal of cancer prognosis studies. *Histopathology* 1999; **35**: 489-494
 - 26 **Song ZB**, Gao SS, Wang LD, Li JL, Fan ZM, Guo HQ, Yi XN. Correlation between p53, PCNA and the prognosis of esophageal carcinoma from the subjects in high-incidence area. *Henan Yixue Yanjiu* 2002; **11**: 97-100
 - 27 **Xiong XD**, Xu LY, Shen ZY, Cai WJ, Luo JM, Han YL, Li EM. Identification of differentially expressed proteins between human esophageal immortalized and carcinomatous cell lines by two-dimensional electrophoresis and MALDI-TOF-mass spectrometry. *World J Gastroenterol* 2002; **8**: 777-781
 - 28 **Zeng WJ**, Liu GY, Xu J, Zhou XD, Zhang YE, Zhang N. Pathological characteristics, PCNA labeling index and DNA index in prognostic evaluation of patients with moderately differentiated hepatocellular carcinoma. *World J Gastroenterol* 2002; **8**: 1040-1044

Edited by Ma JY

Resveratrol induces apoptosis in human esophageal carcinoma cells

Hai-Bo Zhou, Yun Yan, Ya-Ni Sun, Ju-Ren Zhu

Hai-Bo Zhou, Ju-Ren Zhu, Department Of Gastroenterology, Shandong Provincial Hospital, Jinan 250052, Shandong Province, China

Yun Yan, Ya-Ni Sun, People's Hospital of WeiFang, WeiFang 261041, Shandong Province, China

Correspondence to: Dr. Hai-Bo Zhou, Department Of Gastroenterology, Shandong Provincial Hospital, Jinan 250052, Shandong Province, China. zhouhbyy@fm365.com.cn

Telephone: +86-531-2603194

Received: 2002-10-08 **Accepted:** 2002-11-13

Abstract

AIM: To investigate the apoptosis in esophageal cancer cells induced by resveratrol, and the relation between this apoptosis and expression of Bcl-2 and Bax.

METHODS: In *in vitro* experiments, MTT assay was used to determine the cell growth inhibitory rate. Transmission electron microscope and TUNEL staining method were used to quantitatively and qualitatively detect the apoptosis status of esophageal cancer cell line EC-9706 before and after the resveratrol treatment. Immunohistochemical staining was used to detect the expression of apoptosis-regulated gene Bcl-2 and Bax.

RESULTS: Resveratrol inhibited the growth of esophageal cancer cell line EC-9706 in a dose-and time-dependent manner. Resveratrol induced EC-9706 cells to undergo apoptosis with typically apoptotic characteristics, including morphological changes of chromatin condensation, chromatin crescent formation, nucleus fragmentation and apoptotic body formation. TUNEL assay showed that after the treatment of EC-9706 cells with resveratrol ($10 \text{ mmol} \cdot \text{L}^{-1}$) for 24 to 96 hours, the AIs were apparently increased with treated time ($P < 0.05$). Immunohistochemical staining showed that after the treatment of EC-9706 cells with resveratrol ($10 \text{ mmol} \cdot \text{L}^{-1}$) for 24 to 96 hours, the PRs of Bcl-2 proteins were apparently reduced with treated time ($P < 0.05$) and the PRs of Bax proteins were apparently increased with treated time ($P < 0.05$).

CONCLUSION: Resveratrol is able to induce the apoptosis in esophageal cancer. This apoptosis may be mediated by down-regulating the apoptosis-regulated gene Bcl-2 and up-regulating the expression of apoptosis-regulated gene bax.

Zhou HB, Yan Y, Sun YN, Zhu JR. Resveratrol induces apoptosis in human esophageal carcinoma cells. *World J Gastroenterol* 2003; 9(3): 408-411

<http://www.wjgnet.com/1007-9327/9/408.htm>

INTRODUCTION

The Bcl-2 family plays a crucial role in the control of apoptosis. The family includes a number of proteins which have homologous amino acid sequence, including anti-apoptotic members such as Bcl-2 and Bcl-x_L, as well as pro-apoptotic members including Bax and Bad. In *in vitro* experiments, overexpression of Bcl-2 has been shown to inhibit apoptosis,

but overexpression of Bax has been shown to promote apoptosis.

Resveratrol, a phytoalexin found in grapes, fruits, and root extracts of the weed *Polygonum cuspidatum*, is an important constituent of Chinese folk medicine. Indirect evidence suggests that the presence of resveratrol in white and rose wine may be helpful to reduce risks of coronary heart disease which would be achieved by moderate wine consumption. This effect has been attributed to the inhibition of platelet aggregation and coagulation, in addition to the antioxidant and anti-inflammatory activity of resveratrol. Moreover, a recent report shows that resveratrol is a potent cancer chemopreventive agent in three major stages of carcinogenesis. The anti-tumor activity of resveratrol might be related to induce the apoptosis of tumor cells but the precise mechanism of antitumor activity is not well understood.

MATERIALS AND METHODS

Materials

Resveratrol and MTT were obtained from Sigma Chemical Co. Ltd. *In situ* cell detection kit, anti-Bcl-2 monoclonal antibody and anti-Bax monoclonal antibody were purchased from Beijing Zhongshan biotechnology Co. Ltd. Stock solution of resveratrol was made in dimethylsulfoxide (DMSO) at a concentration of $100 \text{ mmol} \cdot \text{L}^{-1}$. Working dilutions were directly made in the cell culture medium. Human esophageal carcinoma cell line EC-9706 was obtained from Professor Ming-Rong Wang in Chinese Scientific Academy.

Methods

Cell culture EC-9706 cells were incubated in RPMI 1640 supplemented with $100 \text{ ml} \cdot \text{L}^{-1}$ fetal bovine serum, $100 \text{ kU} \cdot \text{L}^{-1}$ penicillin, $100 \text{ mg} \cdot \text{L}^{-1}$ streptomycin and $2 \text{ mmol} \cdot \text{L}^{-1}$ L-glutamine under $50 \text{ ml} \cdot \text{L}^{-1}$ CO₂ in a humidified incubator at 37°C . EC-9706 cells were incubated for different time periods in the presence of resveratrol at 0.1, 1, 10 and $100 \text{ mmol} \cdot \text{L}^{-1}$.

MTT assay 1×10^5 cells/well in a 96-well plate after incubation for 24 hours were treated with different concentrations of resveratrol ($0.1, 1, 10, 100 \text{ mmol} \cdot \text{L}^{-1}$) for 24, 48, 72, 96 hours respectively. $10 \mu\text{L}$ of $5 \text{ g} \cdot \text{L}^{-1}$ of MTT was added to the medium in three wells at every dose and incubated for 4 hours at 37°C . Culture media were discarded followed by adding 0.2 ml DMSO and vibrating for 10 minutes. The absorbance (OD) was measured at 570 nm using a microplate reader. The cell growth inhibitory rate was calculated as follows: $[(\text{OD of control group} - \text{OD of experimental group}) / (\text{OD of control group} - \text{OD of blank group})] \times 100 \%$.

Transmission electron microscopy Cells treated with $10 \text{ mmol} \cdot \text{L}^{-1}$ resveratrol were harvested after incubation for 24 hours. Subsequently the cells were fixed in 4% glutaral and immersed with Epon 821, imbedded for 72 hours at 60°C , the cells were prepared into ultrathin section (60 nm) and stained with uranyl acetate and lead citrate. Cell morphology was observed by transmission electron microscopy.

TUNEL assay Apoptosis of EC-9706 cells was evaluated by using an *in situ* cell detection kit. The cells were treated in the presence or absence of $10 \text{ mmol} \cdot \text{L}^{-1}$ resveratrol for 24 to 96 hours and fixed in ice-colded 80% ethanol for up to 24 hours, treated with proteinase K and then 0.3% H₂O₂, labeled with fluorescein dUTP in a humid box for 1 hour at 37°C . The cells

were then combined with POD-Horseradish peroxidase, colorized with DAB and counterstained with methyl green. Controls were received the same management except the labeling of omission of fluorescein dUTP. Cells were visualized with light microscope. The apoptotic index (AI) was calculated as follows: $AI = (\text{Number of apoptotic cells} / \text{Total number}) \times 100\%$.

Immunohistochemical staining Immunohistochemical staining was done by an avidinbiotin technique. EC-9706 cells treated in the presence or absence of $10 \text{ mmol} \cdot \text{L}^{-1}$ resveratrol for 24 to 96 hours were grown six-well glass slides and were fixed by acetone. After washing in PBS, the cells were incubated in 0.3% H_2O_2 solution at room temperature for 5 minutes. The cells were then incubated with anti-Bcl-2 or anti-Bax monoclonal antibody at a $1:300$ dilution at 4°C overnight. After washing in PBS, the second antibody, biotinylated antirat Ig G, was added and the cells were incubated at room temperature for 1 hour. After washing in PBS, ABC compound was added and then incubated at room temperature for 10 minutes. DAB was used as the chromagen. After ten minutes, the brown color signifying the presence of antigen bound to antibodies was detected by light microscopy and photographed at $\times 200$. Controls were managed the same as the experimental group except the incubation of the primary antibody. The positive rate (PR) was calculated as follows: $PR = (\text{Number of positive cells} / \text{Total number}) \times 100\%$.

Statistical analysis

Datas were analyzed by the paired two-tailed Student *t* test, and significance was considered when $P < 0.05$.

RESULTS

MTT assay

EC-9706 cells were exposed to increasing concentrations ($0.1 \text{ mmol} \cdot \text{L}^{-1}$ to $100 \text{ mmol} \cdot \text{L}^{-1}$) of resveratrol for 24 to 96 hours, respectively. EC-9706 cells showed the mortality in a dose- and time-dependent manner. The data were summarised in Table 1.

Table 1 The inhibitory effect of resveratrol on EC-9706 cells

Time(h)	Inhibitory rate(%)				
	RPMI-1640	Resveratrol ($\text{mmol} \cdot \text{L}^{-1}$)			
		0.1	1	10	100
24	0.0	9.2 ^a	18.4 ^b	21.8 ^b	34.4 ^b
48	0.0	17.1 ^b	21.3 ^b	36.7 ^b	45.5 ^b
72	0.0	23.9 ^b	37.5 ^b	48.6 ^b	59.9 ^b
96	0.0	36.6 ^b	45.7 ^b	56.6 ^b	88.8 ^b

^a $P < 0.01$, ^b $P < 0.001$ vs the control group.

Morphological changes

After treatment of EC-9706 cells with resveratrol ($10 \text{ mmol} \cdot \text{L}^{-1}$) for 24 hours, some cells appeared apoptotic characteristics including chromatin condensation, appearance of chromatin crescent, nucleus fragmentation and of formation apoptotic body which could be seen by transmission electron microscope.

TUNEL assay

Apoptotic cell death was determined by TUNEL assay according to the manufacture's instructions. Positive staining located in the nucleus (Figure 1). After treatment with resveratrol ($10 \text{ mmol} \cdot \text{L}^{-1}$) for 24 to 96 hours, AIs were apparently increased with treated time ($P < 0.05$) (Table 2).

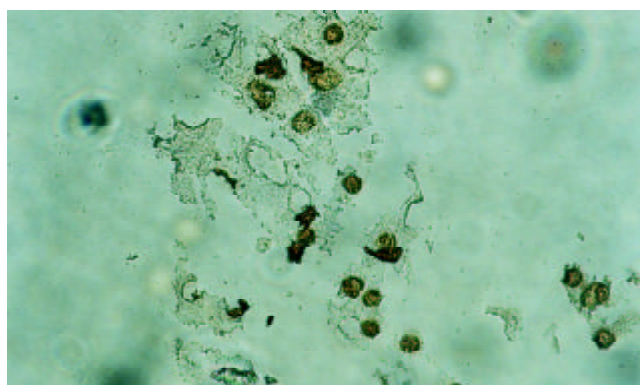


Figure 1 TUNEL assay of apoptotic cells induced by resveratrol with ($\times 200$).

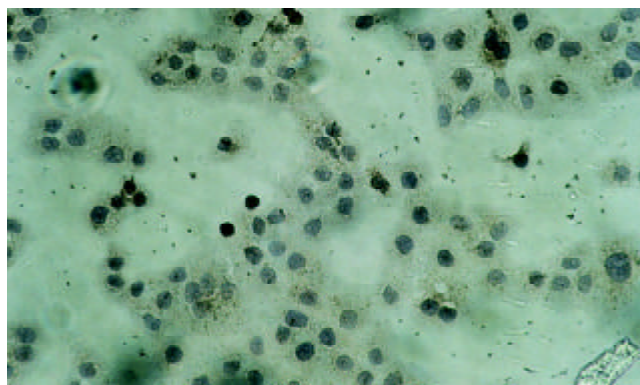


Figure 2 Immunohistochemical staining of the expression of Bcl-2 ($\times 200$).

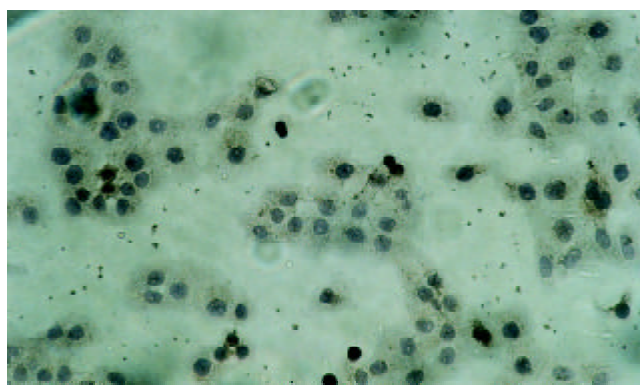


Figure 3 Immunohistochemical staining of the expression of Bax ($\times 200$).

Table 2 Apoptotic Index (AI) of treated EC-9706 cells by resveratrol

Time(h)	AI(%)
0	1.46 ± 2.51
24	4.96 ± 2.67^a
48	16.64 ± 1.87^a
72	27.94 ± 3.32^b
96	37.46 ± 3.96^b

^a $P < 0.05$, ^b $P < 0.01$ vs the control group.

Expression of Bcl-2 proteins

Positive staining located in the cytoplasm (Figure 2). After treatment with resveratrol ($10 \text{ mmol} \cdot \text{L}^{-1}$) for 24 to 96 hours, PRs of Bcl-2 proteins were apparently reduced with treated

time ($P<0.05$) (Table 3). This suggested that resveratrol could down-regulate the expression of Bcl-2.

Expression of bax proteins

Positive staining located in the cytoplasm (Figure 3). After treatment with resveratrol ($10 \text{ mmol} \cdot \text{L}^{-1}$) for 24 to 96 hours, PRs of Bax proteins were apparently increased with treated time ($P<0.05$) (Table 4). This suggested that resveratrol could up-regulate the expression of Bax.

Table 3 Positive rate of Bcl-2 on treated EC-9706 cells by resveratrol

Time (h)	PR(%)
0	35.64±3.95
24	20.50±2.79 ^a
48	10.76±2.46 ^a
72	6.82±1.78 ^b
96	3.88±1.24 ^b

^a $P<0.05$, ^b $P<0.01$ vs the control group.

Table 4 Positive rate of Bax on treated EC-9706 cells by resveratrol

Time(h)	PR(%)
0	10.66±2.26
24	19.68±2.67 ^a
48	30.77±3.76 ^a
72	41.56±6.14 ^a
96	59.96±5.34 ^a

^a $P<0.01$ vs the control group.

DISCUSSION

Currently, only few chemotherapeutic drugs take effect in the treatment of human primary esophageal carcinoma and it clearly need to look for new anti-esophageal carcinoma drugs. Resveratrol, a polyphenol found in various fruits and vegetables and is rich in grapes. The root extracts of the weed *Polygonum cuspidatum*, an important constituent of Chinese folk medicine, is also an ample source of resveratrol^[1,2]. Several studys in last several years have shown that resveratrol have cardiopreptive and chemopreventive effects^[3-5]. This constituent may account for the reduced risk of coronary heart disease in humans which may be achieved by moderate wine consumption^[6]. Resveratrol is able to inhibit the growth of a wide variety of tumor cells, including leukemic, prostate, breast and hepatic cells^[7-11]. The anti-tumor activity of resveratrol might be related to the induction of tumor apoptosis of tumor cells^[12-22].

The Bcl-2 family plays a crucial role in the control of apoptosis. The family includes a number of proteins which have homologous amino acid sequences, including antiapoptotic members such as Bcl-2 and Bcl-x_L, as well as proapoptotic members including Bax and Bad^[23-26]. Overpression of Bax has the effect of promoting the cell death^[27-31]. Conversely, Overpression of antiapoptotic proteins such as Bcl-2 will repress the function of Bax^[32-36]. Thus, the ratio of Bcl-2 / Bax appears to be a critical determinant of a cell's threshold for undergoing apoptosis^[37].

In this study resveratrol could reduce Bcl-2 expression and improve Bcl-2 expression. The ratio of Bcl-2 /Bax was decreased when EC-9706 cells were treated with resveratrol. The decreased ratio could triggered the apoptosis of EC-9706 cells.

Our results demonstrated resveratrol is able to induce the apoptosis in esophageal cancer. This apoptosis may be

mediated by down-regulating the expression of apoptosis-regulated gene Bcl-2 and up-regulating the expression of apoptosis-regulated gene Bax. Resveratrol may be potentially used as a chemotherapeutic drug in the anti-esophageal carcinoma chemphtherapy.

REFERENCES

- 1 **Yoon S**, Kim Y, Ghim S, Song B, Bae Y. Inhibition of protein kinase CKII activity by resveratrol, a natural compound in red wine and grapes. *Life Sci* 2002; **71**: 2145
- 2 **Gao X**, Xu YX, Divine G, Janakiraman N, Chapman RA, Gautam SC. Disparate *in vitro* and *in vivo* antileukemic effects of resveratrol, a natural polyphenolic compound found in grapes. *J Nutr* 2002; **132**: 2076-2081
- 3 **Bhat KP**, Pezzuto JM. Cancer chemopreventive activity of resveratrol. *Ann N Y Acad Sci* 2002; **957**: 210-229
- 4 **Kuwajerwala N**, Cifuentes E, Gautam S, Menon M, Barrack ER, Reddy GP. Resveratrol induces prostate cancer cell entry into s phase and inhibits DNA synthesis. *Cancer Res* 2002; **62**: 2488-2492
- 5 **Joe AK**, Liu H, Suzui M, Vural ME, Xiao D, Weinstein IB. Resveratrol induces growth inhibition, S-phase arrest, apoptosis, and changes in biomarker expression in several human cancer cell lines. *Clin Cancer Res* 2002; **8**: 893-903
- 6 **Wang Z**, Zou J, Huang Y, Cao K, Xu Y, Wu JM. Effect of resveratrol on platelet aggregation *in vivo* and *in vitro*. *Chin Med J (Engl)* 2002; **115**: 378-380
- 7 **Ferry-Dumazet H**, Garnier O, Mamani-Matsuda M, Vercauteren J, Belloc F, Billiard C, Dupouy M, Thiolat D, Kolb JP, Marit G, Reiffers J, Mossalayi MD. Resveratrol inhibits the growth and induces the apoptosis of both normal and leukemic hematopoietic cells. *Carcinogenesis* 2002; **23**: 1327-1333
- 8 **Kampa M**, Hatzoglou A, Notas G, Damianaki A, Bakogeorgou E, Gemetzi C, Kouroumalis E, Martin PM, Castanas E. Wine antioxidant polyphenols inhibit the proferation of human prostate cancer cell lines. *Nutr Cancer* 2000; **37**: 223-233
- 9 **Bove K**, Lincoln DW, Tsan MF. Effect of resveratrol on growth of 4T1 breast cancer cells *in vitro* and *in vivo*. *Biochem Biophys Res Commun* 2002; **291**: 1001-1005
- 10 **Tian XM**, Zhang ZX. The anticancer activity of resveratrol on implanted tumor of HepG2 in nude mice. *Shijie Huaren Xiaohua Zazhi* 2001; **9**: 161-164
- 11 **Sun ZJ**, Pan CE, Liu HS, Wang GJ. Anti-hepatoma activity of resveratrol *in vitro*. *World J Gastroenterol* 2002; **8**: 79-81
- 12 **Pervaiz S**. Resveratrol-from the bottle to the bedside? *Leuk Lymphoma* 2001; **40**: 491-498
- 13 **Dorrie J**, Gerauer H, Wachter Y, Zunino SJ. Resveratrol induces extensive apoptosis by depolarizing mitochondrial membranes and activating caspase-9 in acute lymphoblastic leukemia cells. *Cancer Res* 2001; **61**: 4731-4739
- 14 **She QB**, Bode AM, Ma WY, Chen NY, Dong Z. Resveratrol-induced activation of p53 and apoptosis is mediated by extracellular-signal-regulated protein kinases and p38 kinase. *Cancer Res* 2001; **61**: 1604-1610
- 15 **Tsan MF**, White JE, Maheshwari JG, Bremner TA, Sacco J. Resveratrol induces Fas signaling-independent apoptosis in THP-1 human monocytic leukemia cells. *Br J Haematol* 2000; **109**: 405-412
- 16 **Szende B**, Tyihak E, Kiraly-Veghely Z. Dose-dependent effect of resveratrol on proliferation and apoptosis in endothelial and tumor cell cultures. *Exp Mol Med* 2000; **32**: 88-92
- 17 **Bernhard D**, Tinhofe R, Tonko M, Hubl H, Ausserlechner MJ, Greil R, Kofler R, Csordas A. Resveratrol causes arrest in the S-phase prior to Fas- independent apoptosis in CEM-C7H2 acute leukemia cells. *Cell Death Differ* 2000; **7**: 834-842
- 18 **Mouria M**, Gukovskaya AS, Jung Y, Buechler P, Hines OJ, Reber HA, Pandol SJ. Food-derived polyphenols inhibit pancreatic cancer growth through mitochondrial cytochrome C release and apoptosis. *Int J Cancer* 2002; **98**: 761-769
- 19 **Shih A**, Davis FB, Lin HY, Davis PJ. Resveratrol induces apoptosis in thyroid cancer cell lines via a MAPK- and p53-dependent mechanism. *J Clin Endocrinol Metab* 2002; **87**: 1223-1232
- 20 **Mahyar-Roemer M**, Katsen A, Mestres P, Roemer K. Resveratrol induces colon tumor cell apoptosis independently of p53 and precede by epithelial differentiation, mitochondrial proliferation

- and membrane potential collapse. *Int J Cancer* 2001; **94**: 615-622
- 21 **Lin HY**, Shih A, Davis FB, Tang HY, Martino LJ, Bennett JA, Davis PJ. Resveratrol induced serine phosphorylation of p53 causes apoptosis in a mutant p53 prostate cancer cell line. *J Urol* 2002; **168**: 748-755
 - 22 **She QB**, Huang C, Zhang Y, Dong Z. Involvement of c-jun NH (2)-terminal kinases in resveratrol-induced activation of p53 and apoptosis. *Mol Carcinog* 2002; **33**: 244-250
 - 23 **Konopleva M**, Konoplev S, Hu W, Zaritskey AY, Afanasiev BV, Andreeff M. Stromal cells prevent apoptosis of AML cells by up-regulation of anti-apoptotic proteins. *Leukemia* 2002; **16**: 1713-1724
 - 24 **Van Der Woude CJ**, Jansen PL, Tiebosch AT, Beuving A, Homan M, Kleibeuker JH, Moshage H. Expression of apoptosis-related proteins in Barrett's metaplasia-dysplasia-carcinoma sequence: A switch to a more resistant phenotype. *Hum Pathol* 2002; **33**: 686-692
 - 25 **Panaretakis T**, Pokrovskaja K, Shoshan MC, Grandier D. Activation of Bak, Bax and BH3-only proteins in the apoptotic response to doxorubicin. *J Biol Chem* 2002; [epub ahead of print]
 - 26 **Bellosillo B**, Villamor N, Lopez-Guillermo A, Marce S, Bosch F, Campo E, Montserrat E, Colomer D. Spontaneous and drug-induced apoptosis is mediated by conformational changes of Bax and Bak in B-cell chronic lymphocytic leukemia. *Blood* 2002; **100**: 1810-1816
 - 27 **Matter-Reissmann UB**, Forte P, Schneider MK, Filgueira L, Groscurth P, Seebach JD. Xenogeneic human NK cytotoxicity against porcine endothelial cells is perforin/granzyme B dependent and not inhibited by Bcl-2 overexpression. *Xenotransplantation* 2002; **9**: 325-337
 - 28 **Lanzi C**, Cassinelli G, Cuccuru G, Supino R, Zuco V, Ferlini C, Scambia G, Zunino F. Cell cycle checkpoint efficiency and cellular response to paclitaxel in prostate cancer cells. *Prostate* 2001; **48**: 254-264
 - 29 **Mertens HJ**, Heineman MJ, Evers JL. The expression of apoptosis-related proteins bcl-2 and ki67 in endometrium of ovulatory menstrual cycles. *Gynecol Obstet Invest* 2002; **53**: 224-230
 - 30 **Mehta U**, Kang BP, Bansal G, Bansal MP. Studies of apoptosis and bcl-2 in experimental atherosclerosis in rabbit and influence of selenium supplementation. *Gen Physiol Biophys* 2002; **21**: 15-29
 - 31 **Chang W**, Yang K, Chuang H, Jan J, Shaio M. Glutamine protects activated human T cells from apoptosis by up-regulating glutathione and bcl-2 levels. *Clin Immunol* 2002; **104**: 151
 - 32 **Chen GG**, Lai PB, Hu X, Lam IK, Chak EC, Chun YS, Lau WY. Negative correlation between the ratio of Bax to Bcl-2 and the size of tumor treated by culture supernatants from Kupffer cells. *Clin Exp Metastasis* 2002; **19**: 457-464
 - 33 **Usuda J**, Chiu SM, Azizuddin K, Xue LY, Lam M, Nieminen AL, Oleinick NL. Promotion of photodynamic therapy-induced apoptosis by the mitochondrial protein Smac/DIABLO: dependence on Bax. *Photochem Photobiol* 2002; **76**: 217-223
 - 34 **Sun F**, Akazawa S, Sugahara K, Kamihira S, Kawasaki E, Eguchi K, Koji T. Apoptosis in normal rat embryo tissues during early organogenesis: the possible involvement of Bax and Bcl-2. *Arch Histol Cytol* 2002; **65**: 145-157
 - 35 **Jang M**, Shin M, Shin H, Kim K, Park H, Kim E, Kim C. Alcohol induces apoptosis in TM3 mouse Leydig cells via bax-dependent caspase-3 activation. *Eur J Pharmacol* 2002; **449**: 39
 - 36 **Tilli CM**, Stavast-Koey AJ, Ramaekers FC, Neumann HA. Bax expression and growth behavior of basal cell carcinomas. *J Cutan Pathol* 2002; **29**: 79-87
 - 37 **Pettersson F**, Dalgleish AG, Bissonnette RP, Colston KW. Retinoids cause apoptosis in pancreatic cancer cells via activation of RAR-gamma and altered expression of Bcl-2/Bax. *Br J Cancer* 2002; **87**: 555-561

Edited by Xu XQ

HLA-DRB1 allele polymorphisms in genetic susceptibility to esophageal carcinoma

Jun Lin, Chang-Sheng Deng, Jie Sun, Xian-Gong Zheng, Xing Huang, Yan Zhou, Ping Xiong, Ya-Ping Wang

Jun Lin, Chang-Sheng Deng, Jie Sun, Xian-Gong Zheng, Xing Huang, Yan Zhou, Department of Gastroenterology, Zhongnan Hospital, Wuhan University, Wuhan 430071, Hubei Province, China
Ping Xiong, Department of Immunology, Tongji Medical College of Huazhong University of Science and Technology, Wuhan 430030, Hubei Province, China

Ya-Ping Wang, State Key Lab, Institute of Hydrobiology, The Chinese Academy of Sciences, Wuhan 430077, Hubei Province, China
Correspondence to: Dr Jun Lin, Department of Gastroenterology, Zhongnan Hospital, Wuhan University, Wuhan 430071, Hubei Province, China. linjun64@yahoo.com.cn

Telephone: +86-27-87335914 **Fax:** +86-27-87307622

Received: 2001-07-19 **Accepted:** 2001-08-27

Abstract

AIM: To probe into the genetic susceptibility of HLA-DRB1 alleles to esophageal carcinoma in Han Chinese in Hubei Province.

METHODS: HLA-DRB1 allele polymorphisms were typed by polymerase chain reaction with sequence-specific primers (PCR-SSP) in 42 unrelated patients with esophageal cancer and 136 unrelated normal control subjects and the associated HLA-DRB1 allele was measured by nucleotide sequence analysis with PCR. SAS software was used in statistics.

RESULTS: Allele frequency (AF) of HLA-DRB1*0901 was significantly higher in esophageal carcinoma patients than that in the normal controls (0.2500 vs 0.1397, $P=0.028$, the odds ratio 2.053, etiologic fraction 0.1282). After analyzed the allele nucleotide sequence of HLA-DRB1*0901 which approaches to the corresponded exon 2 sequence of the allele in genebank. There was no association between patients and controls in the rested HLA-DRB1 alleles.

CONCLUSION: HLA-DRB1*0901 allele is more common in the patients with esophageal carcinoma than in the healthy controls, which is positively associated with the patients of Hubei Han Chinese. Individuals carrying HLA-DRB1*0901 may be susceptible to esophageal carcinoma.

Lin J, Deng CS, Sun J, Zheng XG, Huang X, Zhou Y, Xiong P, Wang YP. HLA-DRB1 allele polymorphisms in genetic susceptibility to esophageal carcinoma. *World J Gastroenterol* 2003; 9(3): 412-416

<http://www.wjgnet.com/1007-9327/9/412.htm>

INTRODUCTION

The major histocompatibility complex (MHC) refers to as human leukocyte antigen (HLA). The loss of HLA antigens by neoplastic cells is considered important for tumor growth and metastasis^[1-3]. Since tumor neoantigens on the surface of aberrant cells are recognized by T-cells only in the context of the HLA "self" antigens, loss of the HLA antigens may allow the tumors to escape immunosurveillance^[4]. HLA system is a

kind of genetic marker of human being, and the most complicated human genetic polymorphic system with hereditary features of haplotype inheritance and allele polymorphism and linkage disequilibrium. It played an important role in the event of antigen recognition and presentation, immune response and modulation, destroying foreign antigen targeted cells. The alleles of the HLA system control a variety of immune functions and influence the susceptibility to more than 40 diseases, many of which have an autoimmune component^[5-17], esophageal cancer is a complex, probably multifactorial disease^[18-41]. Association of a particular HLA allele with a disease implies that the frequency of the allele is different in the patient population as compared with that of an ethnically matched control population. However, there has been no report on the association between HLA alleles and esophageal carcinoma.

In this study, we used polymerase chain reaction with sequence-specific primers (PCR-SSP) and DNA sequence analysis techniques on HLA-DRB1 alleles typing to investigate the genetic susceptibility of HLA allele polymorphisms in esophageal carcinoma of Hubei Han Chinese. This may be beneficial to the early prevention and surveillance, thus setting up gene therapy basis for esophageal carcinoma.

MATERIALS AND METHODS

Subjects

Included in our study were healthy controls and patients with esophageal carcinoma. The control group consists of one hundred and thirty-six unrelated donors or healthy individuals by physical examination, including 62 men and 74 women, ranging 22-48 years, in age, with a mean of 36 ± 6 years. The esophageal carcinoma group includes forty-two unrelated patients with esophageal squamous cell carcinoma, 35 men and 7 women, ranging in age 41-80 years, with a mean age of 60 ± 5 years, who were evaluated endoscopically and surgically. And all were tested by histopathology at Zhongnan Hospital of Wuhan University, between August 1998 and June 1999.

DNA extraction

Genomic DNA was isolated from leukocytes obtained from anticoagulated peripheral blood of patients and controls using the salting-out procedure^[5,42,43], or QIAamp Blood Kit (QIAGEN GmbH, Germany) with which DNA was obtained through solid phase affinity columns.

HLA-DRB1 alleles PCR-SSP typing

For HLA-DRB1 "low resolution" typing by PCR-SSP, 23 separate PCR reactions were performed for each sample. PCR-SSP typed system: each PCR reaction mixture contained 2-4 allele- or group-specific -DRB1 primers and the internal positive control primer pair. Allele sequence specific primers (2pmol), designed on the basis of published sequences^[43-45], were used in multiple amplification reaction. HLA-DRB1 alleles PCR-SSP typed system consisted of 60 ng genomic DNA, 0.5 U *Taq* DNA polymerase (Ampli Taq® DNA polymerase, Roche Diagnostic System, Inc. USA), 20 μ mol

each deoxyadenosine triphosphate (dATP), deoxycytidine triphosphate (dCTP), deoxyguanosine triphosphate (dGTP), deoxythymidine triphosphate (dTTP), 10 mmol/L Tris-HCl pH8.3, 50 mmol·L⁻¹ KCl (kalium chloride), 1.5 mmol·L⁻¹ MgCl₂ (magnesium chloride). PCR amplifications were carried out in PTC-100 thermal cycler (MJ Research, Inc, USA) according to the method of Olerup *et al.*^[5,42,43]. Initial denaturation was made at 94 °C for 5 min; with 30 cycles each consisting of denaturation at 94 °C for 30 s, annealing at 65 °C for 1 min and extension at 72 °C for 1 min. The HLA-DRB1 alleles typed vizualization of amplification was observed using medium resolution PCR-SSP products by 20 g·L⁻¹ gels agarose(Boehringer Mannheim GmbH, Germany) electrophoresis. The gels were run for 20 min at 15 V·cm⁻¹ in 0.5xTBE buffer and visualized using UV illumination and keeping file copies in computer.

Positive control, false negative allele

The most common form of individual PCR reaction failure is where random individual reactions fail to produce allele or control bands. This occurred on average in 1 % of all PCR-SSP amplification. In each PCR reaction, a pair primers were included which specifically amplify the exon 2 of HLA-DRB1 alleles. These two primers matched non-allelic sequences and thus functioned as an internal positive amplification control. We used human growth hormone gene as a intra-positive control, in which primer^[5] is 5' -primer, 21 mer, 5' GCC TTC CCA ACC ATT CCC TTA 3', Tm64 °C; 3' -primer, 22 mer, 5' TCA CGG ATT TCT GTT GTG TTT C 3', terminal concentration 0.15 μmol·L⁻¹, product 429 base pair (bp) fragment. Control failure is not a problem if the genotype obtained is heterozygous for all alleles and the type is unequivocal. Homozygous samples, in which the control failed, normally would require typing with a new DNA sample once

again. Individual false negative allele amplifications where the control amplification worked but an expected allele was not amplified, did occur, the same be required repeated typing.

DNA sequence analysis of PCR-SSP products

Specific PCR-SSP products of amplification were obtained from agarose gels electrophoresis, then purified with glassmilk kit (Clontech Laboratories, Inc, USA), and the base sequence was examined by PCR sequence analysis with ABI prism 310 (Perkin-Elmer, USA) with the addition of a terminal deoxytransferase extension step at the end of the chain termination reaction.

Statistical analysis

SAS (6.12 for Win), including χ^2 analysis or Fisher's Exact Test, was used to compare the allele frequency (AF) of HLA-DRB1 between the patients with esophageal carcinoma and the controls.

RESULTS

HLA-DRB1*0901 was present at increased frequency in patients with esophageal squamous cell carcinoma, 0.2500 vs 0.1397, $P=0.028$, odds ratio 2.053, etiologic fraction 0.1282 (Table 1). The rested HLA-DRB1 alleles frequencies showed no significant difference in comparison between patients and the controls, i.e., there was positive association between HLA-DRB1*0901 and the patients of Hubei Hans. The HLA-DRB1*0901 nucleotide sequence, was analyzed in this study, approaches to the corresponded exon 2 of the allele sequence in genebank. Esophageal carcinoma was associated with HLA genotype: individuals carrying HLA-DRB1*0901 may be susceptibilitive to esophageal carcinoma in Hubei Hans.

Table 1 HLA-DRB1 allele frequencies in esophageal cancer patients of Hubei Han Chinese

HLA-DRB1 alleles	Control group			Esophageal cancer group			P
	N1	AF($n_1=272$)	PF($n_2=136$)%	N2	AF($n_1=84$)	PF($n_2=42$)%	
0101-2	13	0.0478	9.5588	2	0.0238	4.7619	>0.05
0103	0	0.0000	0.0000	0	0.0000	0.0000	
150X	46	0.1691	32.3529	9	0.1071	21.4286	>0.05
160X	9	0.0331	6.6176	3	0.0356	7.1429	>0.05
0301	19	0.0699	13.9706	6	0.0714	14.2857	>0.05
0302	2	0.0074	1.4706	0	0.0000	0.0000	>0.05
040X	30	0.1103	20.5882	12	0.1429	26.1905	>0.05
0701-2	13	0.0478	9.5588	3	0.0357	7.1429	>0.05
080X	22	0.0809	15.4412	4	0.0476	9.5238	>0.05
0901	38	0.1397	26.4706	21	0.2500	45.2400	0.028*
1001	11	0.0404	7.3529	2	0.0238	4.7619	>0.05
110X	18	0.0662	12.5000	7	0.0833	16.6667	>0.05
120X	17	0.0625	12.5000	11	0.1310	26.1905	>0.05
1301-2	15	0.0551	11.0294	1	0.0119	2.3810	>0.05
1303-4	4	0.0147	2.9412	0	0.0000	0.0000	>0.05
1305	1	0.0037	0.7353	0	0.0000	0.0000	>0.05
1305-6	0	0.0000	0.0000	0	0.0000	0.0000	
140X	15	0.0551	11.0294	3	0.0357	0.0357	>0.05

AF: allele frequency, PF: phenotype frequency;

P: Fishers exact test (2-tail) or χ^2 , compared with the control with AF;

*Odds ratio=2.053, etiologic fraction=0.12820.

DISCUSSION

Familial aggregation of esophageal cancer is common. There is an approximate increase in abnormal chromosome ratio of this cancerous relatives as compared with the general population, although the inheritance patterns clearly fit no simple Mendelian patterns. However, the illness may exist in the same family at a higher frequency than expected by chance alone^[5,24-27]. This suggests that there may be an internal environment susceptible to malignant and a genetic component in the patients' families, which supports the concept that heredity may play an important role in the pathogenesis of esophageal cancer^[2, 9, 46-53].

Major histocompatibility complex (MHC) is a genetic name describing alleles encoding antigens first discovered because they determine in a major way the fate of a graft, i.e., histocompatibility. In many species, the MHC has an additional name such as HLA for humans, H-2 for mice, SLA for swine, etc. The HLA alleles are located in a 3 500-4 000 kilobase region of chromosome 6; and the allele encoding β 2-microglobulin, a related protein in the system, is on chromosome 15. The major classes of HLA alleles are class I (HLA-A, -B, and -C) and class II (HLA-DR, -DQ, and -DP). Between the class I and II alleles, there are many other alleles, some with immune-related functions that could also be associated with diseases, tumor necrosis factor A and B genes being among them. Class II HLA presents peptides derived from extracellular antigens. The HLA polymorphism appears to be responsible for variations in the immune response of different individuals to different antigens, and may contribute to the susceptibility to diseases and autoimmune disorders^[5,15-17]. The loss of HLA antigens by neoplastic cells is considered important to tumor growth and metastasis, and for tumor escape immune surveillance. HLA class I molecules are required for the presentation of tumor neoantigens to cytotoxic T-lymphocytes. There is evidence that tumor cells with reduced expression or lack of such antigens could evade an immune response and selected for tumor progression. It can be considered that either extensive abnormalities in the regulation of the HLA alleles occurred or substantial chromosomal damage took place in the short arm of chromosome 6, where the human HLA allele complex is located. It was demonstrated that oncogenes may suppress the expression of HLA class I alleles, such as the activation of oncogenes or the inactivation of suppressor-genes^[50,54-56]. The data presented here demonstrate that HLA-DRB1*0901 AF increased in the patients with esophageal cancer compared with that in healthy controls (0.2500 vs 0.1397, $P=0.028$, OR=2.053, EF=0.1282), but none of the rested HLA-DRB1 alleles occurred at markedly altered frequency between the patients and the normal individuals we investigated, indicating that HLA-DRB1*0901 is positively associated with esophageal cancer.

The nucleotide sequence of HLA-DRB1*0901 allele which was measured in our research approaches to the corresponded exon 2 gene sequence of genebank^[44,45]. The AF of HLA-DRB1*0901 was also increased in both Japanese patients with lung cancer and prostate cancer. It is the allele that is associated with genetic susceptibility of various tumors, but why? It was entirely unclear up to now. Pathogenesis of genetic association may be linkage disequilibrium (nonrandom association) and/or changing in the recognized procession of the specific antigen.

It is still controversial whether or not HLA antigen expression in carcinomas correlates with the development of carcinoma and prognosis. The immune responses involving HLA antigens expressed on carcinoma cells are thought to play an important role in eliminating mutated cells or suppressing carcinoma progression^[51-53,57-59]. As reported in some studies, the reduced expression of HLA antigens in malignant tissues

has been proposed as a mechanism whereby tumor-associated proteins cannot be presented in the T cells, therefore the tumor cell proliferates are unperturbed by the immune system and carcinomas protect themselves from hosts' immunosurveillance. There is a possibility that HLA allele genetic association and expression on carcinoma may provide a clue to the understanding of the therapeutic mechanisms of biological response modifiers or immunotherapy which may cut through the induction of HLA antigens on carcinoma cells^[56,60-63]. The cells of a given individual may express HLA alleles, which altered binding to tumor peptides, thereby leading to a modified immune response to the tumor. Identification of the mechanism associating HLA-DRB1*0901 with esophageal cancer could ultimately help target individuals most likely to benefit from cancer screening and prevention programs, and could facilitate novel therapeutic strategies for cancer immunoprevention.

REFERENCES

- 1 **Geertsens R**, Hofbauer G, Kamarashev J, Yue FY, Dummer R. Immune escape mechanisms in malignant melanoma. *Int J Mol Med* 1999; **3**: 49-57
- 2 **Jimenez P**, Canton J, Concha A, Cabrera T, Fernandez M, Real LM, Garcia A, Serrano A, Garrido F, Ruiz-Cabello F. Microsatellite instability analysis in tumors with different mechanisms for total loss of HLA expression. *Cancer Immunol Immunother* 2000; **48**: 684-690
- 3 **Ramal LM**, Maleno I, Cabrera T, Collado A, Ferron A, Lopez-Nevot MA, Garrido F. Molecular strategies to define HLA haplotype loss in microdissected tumor cells. *Hum Immunol* 2000; **61**: 1001-1012
- 4 **Facoetti A**, Capelli E, Nano R. HLA class I molecules expression: evaluation of different immunocytochemical methods in malignant lesions. *Anticancer Res* 2001; **21**: 2435-2440
- 5 **Lin J**, Deng CS, Sun J, Zhou Y, Xiong P, Wang YP. Study on the genetic susceptibility of HLA-DQB1 alleles in esophageal cancer of Hubei Chinese Hans. *Shijie Huaren Xiaohua Zazhi* 2000; **8**: 965-968
- 6 **Noble A**. Review article: molecular signals and genetic reprogramming in peripheral T-cell differentiation. *Immunology* 2000; **101**: 289-299
- 7 **Douek DC**, Altmann DM. T-cell apoptosis and differential human leucocyte antigen class II expression in human thymus. *Immunology* 2000; **99**: 249-256
- 8 **Boyton RJ**, Lohmann T, Londei M, Kalbacher H, Halder T, Frater AJ, Douek DC, Leslie DG, Flavell RA, Altmann DM. Glutamic acid decarboxylase T lymphocyte responses associated with susceptibility or resistance to type I diabetes: analysis in disease discordant human twins, non-obese diabetic mice and HLA-DQ transgenic mice. *Int Immunol* 1998; **10**: 1765-1776
- 9 **Koriyama C**, Shinkura R, Hamasaki Y, Fujiyoshi T, Eizuru Y, Tokunaga M. Human leukocyte antigens related to Epstein-Barr virus-associated gastric carcinoma in Japanese patients. *Eur J Cancer Prev* 2001; **10**: 69-75
- 10 **Chatzipetrou MA**, Tarassi KE, Konstadoulakis MM, Pappas HE, Zafirellis KD, Athanassiades TE, Papadopoulos SA, Panousopoulos DG, Golematas BC, Papasteriades CA. Human leukocyte antigens as genetic markers in colorectal carcinoma. *Dis Colon Rectum* 1999; **42**: 66-70
- 11 **Ishigami S**, Aikou T, Natsugoe S, Hokita S, Iwashige H, Tokushige M, Sonoda S. Prognostic value of HLA-DR expression and dendritic cell infiltration in gastric cancer. *Oncology* 1998; **55**: 65-69
- 12 **Zamani M**, Cassiman JJ. Reevaluation of the importance of polymorphic HLA class II alleles and amino acids in the susceptibility of individuals of different populations to type I diabetes. *Am J Med Genet* 1998; **76**: 183-194
- 13 **Hanifi Moghaddam P**, de Knijf P, Roep BO, Van der Auwera B, Naipal A, Goris F, Schuit F, Giphart MJ. Genetic structure of IDDM1: two separate regions in the major histocompatibility complex contribute to susceptibility or protection. Belgian Diabetes Registry. *Diabetes* 1998; **47**: 263-269
- 14 **Rigby AS**, MacGregor AJ, Thomson G. HLA haplotype sharing

- in rheumatoid arthritis sibships: risk estimates subdivided by proband genotype. *Genet Epidemiol* 1998; **15**: 403-418
- 15 **Azuma T**, Ito S, Sato F, Yamazaki Y, Miyaji H, Ito Y, Suto H, Kuriyama M, Kato T, Kohli Y. The role of the HLA-DQA1 gene in resistance to atrophic gastritis and gastric adenocarcinoma induced by *Helicobacter pylori* infection. *Cancer* 1998; **82**: 1013-1018
 - 16 **Zavaglia C**, Martinetti M, Silini E, Bottelli R, Daielli C, Asti M, Airolidi A, Salvaneschi L, Mondelli MU, Ideo G. Association between HLA class II alleles and protection from or susceptibility to chronic hepatitis C. *J Hepatol* 1998; **28**: 1-7
 - 17 **Weinshenker BG**, Santrach P, Bissonet AS, McDonnell SK, Schaid D, Moore SB, Rodriguez M. Major histocompatibility complex class II alleles and the course and outcome of MS: a population-based study. *Neurology* 1998; **51**: 742-747
 - 18 **Wu MY**, Chen MH, Liang YR, Meng GZ, Yang HX, Zhuang CX. Experimental and clinicopathologic study on the relationship between transcription factor Egr-1 and esophageal carcinoma. *World J Gastroenterol* 2001; **7**: 490-495
 - 19 **Kawaguchi H**, Ohno S, Araki K, Miyazaki M, Saeki H, Watanabe M, Tanaka S, Sugimachi K. p⁵³ polymorphism in human papillomavirus-associated esophageal cancer. *Cancer Res* 2000; **60**: 2753-2755
 - 20 **Wijnhoven BP**, Nollet F, De Both NJ, Tilanus HW, Dinjens WN. Genetic alteration involving exon 3 of the β -catenin gene does not play a role in adenocarcinomas of the esophagus. *Int J Cancer* 2000; **86**: 533-537
 - 21 **Takubo K**, Nakamura K, Sawabe M, Arai T, Esaki Y, Miyashita M, Mafune K, Tanaka Y, Sasajima K. Primary undifferentiated small cell carcinoma of the esophagus. *Hum Pathol* 1999; **30**: 216-221
 - 22 **Fong LY**, Pegg AE, Magee PN. α -difluoromethylornithine inhibits N-nitrosomethylbenzylamine-induced esophageal carcinogenesis in zinc-deficient rats: effects on esophageal cell proliferation and apoptosis. *Cancer Res* 1998; **58**: 5380-5388
 - 23 **Arber N**, Gammon MD, Hibshoosh H, Britton JA, Zhang Y, Schonberg JB, Roterdam H, Fabian I, Holt PR, Weinstein IB. Overexpression of cyclin D1 occurs in both squamous carcinomas and adenocarcinomas of the esophagus and in adenocarcinomas of the stomach. *Hum Pathol* 1999; **30**: 1087-1092
 - 24 **Van Lieshout EM**, Roelofs HM, Dekker S, Mulder CJ, Wobbes T, Jansen JB, Peters WH. Polymorphic expression of the glutathione S-transferase P1 gene and its susceptibility to Barrett's esophagus and esophageal carcinoma. *Cancer Res* 1999; **59**: 586-589
 - 25 **Zou JX**, Wang LD, Shi ST, Yang GY, Xue ZH, Gao SS, Li YX, Yang CS. p53 gene mutations in multifocal esophageal precancerous and cancerous lesions in patients with esophageal cancer in high-risk northern China. *Shijie Huaren Xiaohua Zazhi* 1999; **7**: 280-284
 - 26 **Liu J**, Su Q, Zhang W. Relationship between HPV-E6 p53 protein and esophageal squamous cell carcinoma. *Shijie Huaren Xiaohua Zazhi* 2000; **8**: 494-496
 - 27 **Qin HY**, Shu Q, Wang D, Ma QF. Study on genetic polymorphisms of DDC gene VNTR in esophageal cancer. *Shijie Huaren Xiaohua Zazhi* 2000; **8**: 782-785
 - 28 **Mori M**, Mimori K, Shiraishi T, Alder H, Inoue H, Tanaka Y, Sugimachi K, Huebner K, Croce CM. Altered expression of Fhit in carcinoma and precarcinomatous lesion of the esophagus. *Cancer Res* 2000; **60**: 1177-1182
 - 29 **Dolan K**, Garde J, Walker SJ, Sutton R, Gosney J, Field JK. LOH at the sites of the DCC, APC, and TP53 tumor suppressor genes occurs in Barrett's metaplasia and dysplasia adjacent to adenocarcinoma of the esophagus. *Hum Pathol* 1999; **30**: 1508-1514
 - 30 **Zur Hausen A**, Sarbia M, Heep H, Willers R, Gabbert HE. Retinoblastoma-protein (p16) expression and prognosis in squamous-cell carcinomas of the esophagus. *Int J Cancer* 1999; **84**: 618-622
 - 31 **Shen ZY**, Shen J, Li QS, Chen CY, Chen JY, Zeng Y. Morphological and functional changes of mitochondria in apoptotic esophageal carcinoma cells induced by arsenic trioxide. *World J Gastroenterol* 2002; **8**: 31-35
 - 32 **Xu CT**, Yan XJ. p53 anti-cancer gene and digestive system neoplasms. *Shijie Huaren Xiaohua Zazhi* 1999; **7**: 77-79
 - 33 **Gu HP**, Shang PZ, Su H, Li ZG. Association of CD15 antigen expression with cathepsin D in esophageal carcinoma tissues. *Shijie Huaren Xiaohua Zazhi* 2000; **8**: 259-261
 - 34 **Liu J**, Chen SL, Zhang W, Su Q. P31^{WAF1} gene expression with P53 mutation in esophageal carcinoma. *Shijie Huaren Xiaohua Zazhi* 2000; **8**: 1350-1353
 - 35 **Tan LJ**, Jiang W, Zhang W, Zhang XR, Qiu DH. Fas/FasL expression of esophageal squamous cell carcinoma, dysplasia tissues and normal mucosa. *Shijie Huaren Xiaohua Zazhi* 2001; **9**: 15-19
 - 36 **Wang LD**, Chen H, Guo LM. Alterations of tumor suppressor gene system p53-Rb and human esophageal carcinogenesis. *Shijie Huaren Xiaohua Zazhi* 2001; **9**: 367-371
 - 37 **Gao F**, Yi J, Shi GY, Li H, Shi XG, Tang XM. The sensitivity of digestive tract tumor cells to As₂O₃ is associated with the inherent cellular level of reactive oxygen species. *World J Gastroenterol* 2002; **8**: 36-39
 - 38 **Shen ZY**, Shen WY, Chen MH, Shen J, Cai WJ, Yi Z. Nitric oxide and calcium ions in apoptotic esophageal carcinoma cells induced by arsenite. *World J Gastroenterol* 2002; **8**: 40-43
 - 39 **Gu ZP**, Wang YJ, Li JG, Zhou YA. VEGF₁₆₅ antisense RNA suppresses oncogenic properties of human esophageal squamous cell carcinoma. *World J Gastroenterol* 2002; **8**: 44-48
 - 40 **Wang LD**, Zhou Q, Wei JP, Yang WC, Zhao X, Wang LX, Zou JX, Gao SS, Li YX, Yang CS. Apoptosis and its relationship with cell proliferation, p53, Waf1p21, bcl-2 and c-myc in esophageal carcinogenesis studied with a high-risk population in northern China. *World J Gastroenterol* 1998; **4**: 287-293
 - 41 **Zhang LJ**, Chen KN, Xu GW, Xing HP, Shi XT. Congenital expression of *mdr-1* gene in tissues of carcinoma and its relation with patho-morphology and prognosis. *World J Gastroenterol* 1999; **5**: 53-56
 - 42 **Carter AS**, Bunce M, Cerundolo L, Welsh KI, Morris PJ, Fuggle SV. Detection of microchimerism after allogeneic blood transfusion using nested polymerase chain reaction amplification with sequence-specific primers (PCR-SSP): a cautionary tale. *Blood* 1998; **92**: 683-689
 - 43 **Carter AS**, Cerundolo L, Bunce M, Koo DD, Welsh KI, Morris PJ, Fuggle SV. Nested polymerase chain reaction with sequence-specific primers typing for HLA-A, -B, and -C alleles: detection of microchimerism in DR-matched individuals. *Blood* 1999; **94**: 1471-1477
 - 44 **Schreuder GM**, Hurley CK, Marsh SG, Lau M, Maiers M, Kollman C, Noreen HJ. The HLA Dictionary 2001: a summary of HLA-A, -B, -C, -DRB1/3/4/5, -DQB1 alleles and their association with serologically defined HLA-A, -B, -C, -DR and -DQ antigens. *Tissue Antigens* 2001; **58**: 109-140
 - 45 **Marsh SG**. HLA class II region sequences, 1998. *Tissue Antigens* 1998; **51**: 467-507
 - 46 **Xu M**, Jin YL, Fu J, Huang H, Chen SZ, Qu P, Tian HM, Liu ZY, Zhang W. The abnormal expression of retinoic acid receptor- β , p53 and Ki67 protein in normal, premalignant and malignant esophageal tissues. *World J Gastroenterol* 2002; **8**: 200-202
 - 47 **Zhou Y**, Gao SS, Li YX, Fan ZM, Zhao X, Qi YJ, Wei JP, Zou JX, Liu G, Jiao LH, Bai YM, Wang LD. Tumor suppressor gene p16 and Rb expression in gastric cardia precancerous lesions from subjects at a high incidence area in northern China. *World J Gastroenterol* 2002; **8**: 423-425
 - 48 **Xiong XD**, Xu LY, Shen ZY, Cai WJ, Luo JM, Han YL, Li EM. Identification of differentially expressed proteins between human esophageal immortalized and carcinomatous cell lines by two-dimensional electrophoresis and MALDI-TOF-mass spectrometry. *World J Gastroenterol* 2002; **8**: 777-781
 - 49 **Qin LX**. Chromosomal aberrations related to metastasis of human solid tumors. *World J Gastroenterol* 2002; **8**: 769-776
 - 50 **Wang AH**, Sun CS, Li LS, Huang JY, Chen QS. Relationship of tobacco smoking, CYP1A1, GSTM1 gene polymorphism and esophageal cancer in Xi'an. *World J Gastroenterol* 2002; **8**: 49-53
 - 51 **Bustin SA**, Li SR, Phillips S, Dorudi S. Expression of HLA class II in colorectal cancer: evidence for enhanced immunogenicity of microsatellite-instability-positive tumours. *Tumour Biol* 2001; **22**: 294-298
 - 52 **Hombach A**, Heuser C, Marquardt T, Wiczarkowicz A, Groneck V, Pohl C, Abken H. CD4⁺ T cells engrafted with a recombinant immunoreceptor efficiently lyse target cells in a MHC antigen- and Fas-independent fashion. *J Immunol* 2001; **167**: 1090-1096
 - 53 **Iguchi C**, Nio Y, Takeda H, Yamasawa K, Hirahara N, Toga T,

- Itakura M, Tamura K. Plant polysaccharide PSK: cytostatic effects on growth and invasion; modulating effect on the expression of HLA and adhesion molecules on human gastric and colonic tumor cell surface. *Anticancer Res* 2001; **21**: 1007-1013
- 54 **Kim C**, Matsumura M, Saijo K, Ohno T. *In vitro* induction of HLA-A2402-restricted and carcinoembryonic antigen-specific cytotoxic T lymphocytes on fixed autologous peripheral blood cells. *Cancer Immunol Immunother* 1998; **47**: 90-96
- 55 **Savoie CJ**, Kamikawaji N, Sudo T, Furuse M, Shirasawa S, Tana T, Sasazuki T. MHC class I bound peptides of a colon carcinoma cell line, a Ki-ras gene-targeted progeny cell line and a B cell line. *Cancer Lett* 1998; **123**: 193-197
- 56 **Tanaka H**, Tsunoda T, Nukaya I, Sette A, Matsuda K, Umamo Y, Yamaue H, Takesako K, Tanimura H. Mapping the HLA-A24-restricted T-cell epitope peptide from a tumour-associated antigen HER2/neu: possible immunotherapy for colorectal carcinomas. *Br J Cancer* 2001; **84**: 94-99
- 57 **Wang RF**, Johnston SL, Zeng G, Topalian SL, Schwartzentruber DJ, Rosenberg SA. A breast and melanoma-shared tumor antigen: T cell response to antigenic peptides translated from different open reading frames. *J Immunol* 1998; **161**: 3598-3606
- 58 **Nagorsen D**, Keilholz U, Rivoltini L, Schmittel A, Letsch A, Asemisen AM, Berger G, Buhr HJ, Thiel E, Scheibenbogen C. Natural T-cell response against MHC class I epitopes of epithelial cell adhesion molecule, her-2/neu, and carcinoembryonic antigen in patients with colorectal cancer. *Cancer Res* 2000; **60**: 4850-4854
- 59 **Sato N**, Nabeta Y, Kondo H, Sahara H, Hirohashi Y, Kashiwagi K, Kanaseki T, Sato Y, Rong S, Hirai I, Kamiguchi K, Tamura Y, Matsuura A, Takahashi S, Torigoe T, Ikeda H. Human CD8 and CD4 T cell epitopes of epithelial cancer antigens. *Cancer Chemother Pharmacol* 2000; **46** (Suppl): S86-90
- 60 **Nabeta Y**, Sahara H, Suzuki K, Kondo H, Nagata M, Hirohashi Y, Sato Y, Wada Y, Sato T, Wada T, Yamashita T, Kikuchi K, Sato N. Induction of cytotoxic T lymphocytes from peripheral blood of human histocompatibility antigen (HLA)-A31(+) gastric cancer patients by *in vitro* stimulation with antigenic peptide of signet ring cell carcinoma. *Jpn J Cancer Res* 2000; **91**: 616-621
- 61 **Schirle M**, Keilholz W, Weber B, Gouttefangeas C, Dumrese T, Becker HD, Stevanovic S, Rammensee HG. Identification of tumor-associated MHC class I ligands by a novel T cell-independent approach. *Eur J Immunol* 2000; **30**: 2216-2225
- 62 **Novellino PS**, Trejo YG, Beviacqua M, Bordenave RH, Rumi LS. Regulation of HLA-DR antigen in monocytes from colorectal cancer patients by *in vitro* treatment with human recombinant interferon-gamma. *J Invest Allergol Clin Immunol* 2000; **10**: 90-93
- 63 **Novellino PS**, Trejo YG, Beviacqua M, Bordenave RH, Rumi LS. Cisplatin containing chemotherapy influences HLA-DR expression on monocytes from cancer patients. *J Exp Clin Cancer Res* 1999; **18**: 481-484

Edited by Ma JY

• ESOPHAGEAL CANCER •

Difference of gene expression profiles between esophageal carcinoma and its pericancerous epithelium by gene chip

Shen-Hua Xu, Li-Juan Qian, Han-Zhou Mou, Chi-Hong Zhu, Xing-Ming Zhou, Xiang-Lin Liu, Yong Chen, Wen-Yu Bao

Shen-Hua Xu, Li-Juan Qian, Han-Zhou Mou, Chi-Hong Zhu, Xiang-Lin Liu, Zhejiang Cancer Research Institute, Hangzhou 310022, China

Xing-Ming Zhou, Department of Surgical, Zhejiang Cancer Hospital, Hangzhou 310022, Zhejiang, China

Yong Chen, Wen-Yu Bao, United Gene Scientific Tech. (Group) Company Limited, Shanghai 200092, China

Supported by Zhejiang Medical and Health Science Foundation No. 2002A023

Correspondence to: Dr. Shen-Hua Xu, Zhejiang Cancer Research Institute, No.38 Guangji Road, banshan Hangzhou 310022, Zhejiang, China. xsh1947@LoL365.com

Telephone: +86-571-8144401-263 **Fax:** +86-571-8145807

Received: 2002-07-31 **Accepted:** 2002-09-20

Abstract

AIM: To study the difference of gene expression between esophageal carcinoma and its pericancerous epithelium and to screen novel associated genes in the early stage of esophageal carcinogenesis by cDNA microarray.

METHODS: Total RNA was extracted with the original single step way from esophageal carcinoma, its pericancerous epithelial tissue and normal esophageal epithelium far from the tumor. The cDNA retro-transcribed from equal quantity of mRNA was labeled with Cy5 and Cy3 fluorescence functioning as probes. The mixed probes were hybridized with two pieces of BioDoor 4 096 double dot human whole gene chip. Fluorescence signals were scanned by ScanArray 3 000 laser scanner and farther analyzed by ImaGene 3.0 software with the digital computer.

RESULTS: (1) A total of 135 genes were screened out, in which 85 and 50 genes whose the gene expression levels (fluorescence intensity) in esophageal carcinoma were more than 2 times and less than 0.5 times respectively compared with the normal esophageal epithelium. (2) There were also total 31 genes, among then 27 and 4 whose expressions in pericancerous tissue were 2-fold up-regulated and 0.5-fold down-regulated respectively compared with normal esophageal epithelium. (3) There were 13 genes appeared simultaneously in both pericancerous epithelium and esophageal carcinoma, while another 18 genes existed in pericancerous epithelium only.

CONCLUSION: With the parallel comparison among these three gene profiles, it was shown that (1). A total of 135 genes, Whose expression difference manifested as fluorescence intensity were more than 2 times between esophageal carcinoma and normal esophageal epithelium, were probably related to the occurrence and development of the esophageal carcinoma. (2). The 31 genes showing expression difference more than 2 times between pericancerous and normal esophageal epithelium might be relate to the promotion of esophageal pericancerosis and its progress. The present study illustrated that by using the gene chip to detect the difference of gene expression profiles

might be of benefit to the gene diagnosis, treatment and prevention of esophageal carcinoma.

Xu SH, Qian LJ, Mou HZ, Zhu CH, Zhou XM, Liu XL, Chen Y, Bao WY. Difference of gene expression profiles between esophageal carcinoma and its pericancerous epithelium by gene chip. *World J Gastroenterol* 2003; 9(3): 417-422

<http://www.wjgnet.com/1007-9327/9/417.htm>

INTRODUCTION

The differentially expressed genes in different specimens may be detected with parallel analysis by gene chips which has greatly improved the traditional experiment in that only a single or several genes expression can be observed for each test. More and more cDNA microarray methods are applied nowadays in the study of gene expression. In this paper, gene chip technique was used to analysis the difference of gene expression patterns between the esophageal carcinoma, its pericancerous tissue and normal epithelium of esophagus, in order to explore the tumor-associated gene-clusters and their functions in the process of occurrence and development of esophageal carcinoma, which will be helpful to understand comprehensively the molecular mechanism of cell transformation and provide molecular markers and target genes for clinical diagnosis, prevention, susceptibility forecast and treatment of esophageal carcinoma.

MATERIALS AND METHODS

Materials

All the tissue specimens including esophageal carcinoma, its pericancerous epithelium and normal epithelium of esophagus that serves as control were taken from 11 patients being operated in our hospital from July 17 to September 7, 2000. For each sample, one part was cut to be frozen in liquid nitrogen immediately after surgical resection, and the other part was used for histopathological examination to ensure all the pericancerous and control esophageal epithelia without cancer cells but with their corresponding histological appearance. The clinical and pathological data of these patients were show in Table 1.

Methods

Chip preparation Four thousand and ninety six target cDNA clones used in cDNA chip were provided by United Gene Ltd. and cooperative fellows. These genes were amplified with PCR using universal primers and then purified with standard method. The quality of PCR was monitored by agarose electrophoresis. The obtained genes were dissolved in 3×SSC spotting solution and then spotted on silylated slides (Telechem. Inc) by Cartesian 7 500 spotting Robotics (Cartesian, Inc). Each target gene was dotted twice. After spotting, the slides were hydrated (2 h) and dried (0.5 h, room temperature.). The samples were cross-linked with UV light and treated with 0.2 % SDS, H₂O and 0.2 % NaNBH₄ for 10 min respectively. Then the slides were dried in cold condition and ready for use.

Probe preparation Total sample RNA was extracted by single step method^[1]. Briefly, after taking out from liquid Nitrogen specimens were ground completely into tiny powder while

adding liquid Nitrogen in ceramic mortar and then homogenized in D solution plus 1 % mercaptoethanol. After centrifugation, the supernatant was extracted with phenol: chloroform (1:1), NaAC and acidic phenol: chloroform (5:1) respectively. The aqueous phase was precipitated by equal volume of isopropanol and centrifuged. The precipitate was dissolved with Millie-Q H₂O. After further purification by LiCl precipitating method obtained RNA sample was demonstrated, good in quality with UV analysis and electrophoresis. mRNAs were isolated and purified with Oligotex mRNA Midi Kit (Quagen, Inc.). The fluorescent-labeled cDNA probe was prepared through retro-transcription, referring to the method of Schena^[2]. The probes from normal epithelium were labeled with Cy3-dUTP, while those from cancer tissue and pericancerous epithelium with Cy5-dUTP respectively. The probes were mixed (Cy3-dUTP control + Cy5-dUTP esophageal carcinoma, Cy3-dUTP control + Cy5-dUTP pericancerous epithelium) and precipitated by ethanol, and then resolved in 20 μ l hybridization solution (5 \times SSC + 0.2 % SDS).

Hybridization and washing Probes and chip were denatured respectively in 95 °C bath for 5 min, then the probes were added on the chip. They were hybridized in sealed chamber at 60 °C for 15 - 17 h and washed in turn with solutions of 2 \times SSC + 0.2 % SDS, 0.1 \times SSC + 0.2 % SDS and 0.1 % SSC 10 min each, then dried at room temperature.

Fluorescent scanning and results analysis The chip was read by Scan Array 3 000 Scanner (General Scanning Inc). The overall intensities of Cy3 and Cy5 were normalized and corrected by a coefficient according to the ratios of the located 40 housekeeping genes. The acquired image was further analyzed by ImeGene 3.0 Software with digital computer to obtain the intensities of fluorescent signals and the Cy3/Cy5 ratio. The data were taken on an average of the two repeated spots. The differentially expressed gene were defined as: (1) The absolute value of the Cy5/Cy3 natural logarithm was more than 0.69 (the variation of gene expression was more than 2-fold). (2) Either Cy3 or Cy5 signal value was required for more than 600. (3) The PCR results were satisfactory.

RESULTS

Scatter-plot of hybridization signals on gene chip

The scatter plot that was plotted with Cy3 and Cy5 fluorescent signal values displayed a quite disperses pattern in distribution. Most of spots gathered around a 45° diagonal line, in which blue spots represented the area where the signal intensities varied between 0.5 to 2- fold compared with that of the control. Some red spots distributed beyond or far from 45° diagonal line were indicated the existence of abnormal gene expression in esophageal carcinoma and in pericancerous epithelium. Their signal intensities were 2 times more than that of the control. (Figure 1 A and B).

Results and gene expression pattern by scanning analysis

The fluorescent scanning profile of gene expression was showed in Figure 2 A and B.

cDNA probes that labeled with Cy3 from control epithelium and that labeled with Cy5 from esophageal carcinoma or that labeled with Cy5 from pericancerous epithelium were hybridized through microarray. Hybridization results were obtained in parallel by comparing with these sample gene expression patterns demonstrated. In carcinoma tissues, A total of 41 genes were found having expression variations more than three times from the normal control, the up-and down-regulated genes were 28 and 13 respectively (Table 2). There were also 135 genes that manifested expression variations more than two times from the control and the up-and down-regulated genes were 85 and 50 respectively. Besides, there were nine genes found in the esophageal carcinoma having not been

recorded in genbank. Their functions remain to be studied.

In pericancerous epithelia there were 31 genes found having expression variations more than two times from the control, the up-and down-regulated genes were 27 and 4 respectively. These genes might be divided into 16 groups (Table 3) according to their functions.

There were 13 genes appeared simultaneously in both pericancerous epithelium and esophageal carcinoma, while another 18 genes were found in pericancerous epithelium only (Table 4).

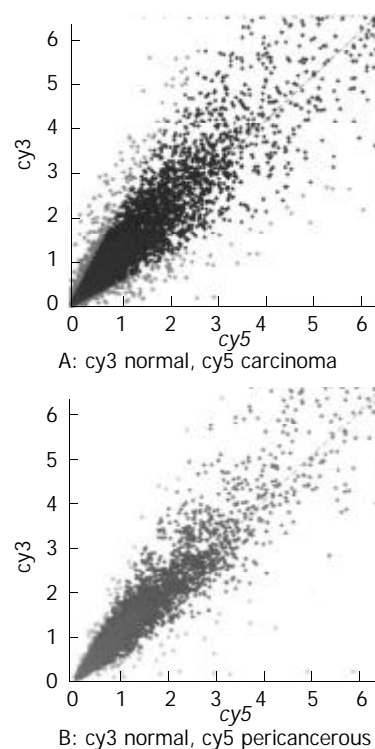


Figure 1 The scatter plots of gene expression pattern. (A) Carcinoma; (B) Pericancerous epithelium.

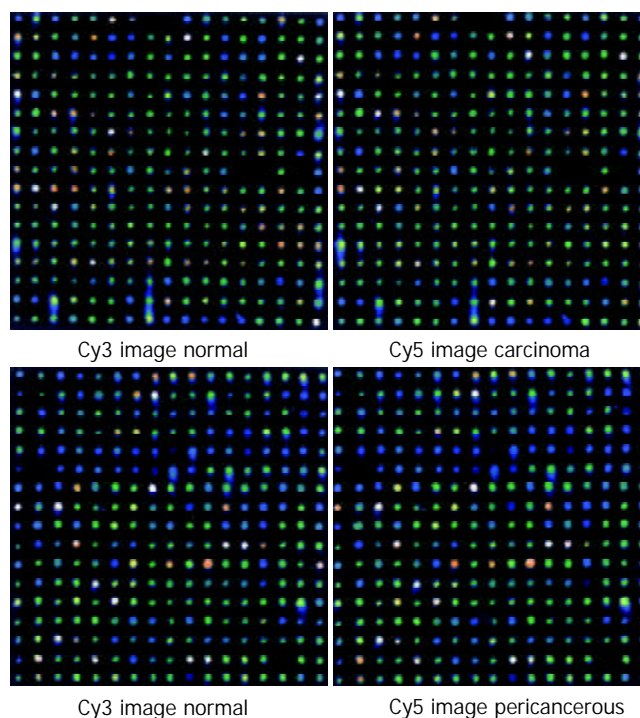


Figure 2 Scanning results of hybridizing signals on gene chip. (A) Carcinoma and the control epithelium; (B) Pericancerous and the control epithelium.

Table 1 Clinical and pathological data of 11 cases with esophageal carcinoma

No. of in-P	Name	Sex	Age	Pathological diagnosis	Lymph metastasis	Clinical stage
106811	Xu_	F	65	Middle esophageal, marrow type, well-middle d. Scc, exterior layer invasion with tumor embolus	0/18	II
106850	Xu _	F	58	Middle esophageal, marrow type, Poor d. Scc with Exterior layer invasion	1/8	III
106839	Yu _	M	60	Middle-inferior esophageal, marrow type, well-middle d. Scc, exterior layer invasion with tumor embolus	0/26	II
107001	Zhou _	M	53	Middle esophageal, ulcer type, middle d. Scc, Exterior layer invasion with tumor embolus	4/19	III
107151	Wang_	M	42	Middle-up esophageal, marrow type, middle d. Scc with exterior layer invasion	0/8	II
107326	Gu _	M	51	Middle- inferior esophageal, marrow type, Middle-Poor d. Scc with exterior layer invasion	2/14	III
107546	Zhao_	F	63	Middle- inferior esophageal, ulcer type, well-Middle d. Scc with shallow muscle layer invasion	0/15	II
107564	Lu_	M	61	Middle- inferior esophageal, marrow type, Middle d. Scc with deep muscle layer invasion	1/32	III
107146	Chen_	F	65	Superior esophageal, ulcer type, well d. Scc with exterior layer invasion	0/17	II
107527	Xu_	M	49	Inferior esophageal, ulcer type, middle d. Scc with shallow muscle layer invasion	1/18	III
107531	Guan_	M	56	Middle esophageal, marrow type, middle d. Scc with deep muscle layer invasion	0/26	II

d.: differentiated Scc: squamous cell carcinoma.

Table 2 Genes with expression difference > 3 or < 0.33 on average ratio between esophageal carcinoma and normal epithelium

Genbank-ID	Fcf	Gene name	R1	R2	AR
hsu67963		Human lysophospholipase homolog(HU-K5)mRNA, complete cds.	0.11	0.16	0.14
Hslimdp	8	H.sapiens mRNA for ZNF185 gene.	0.15	0.23	0.19
4505166			0.13	0.26	0.19
d87451	15	Human mRNA for KIAA0262gene,complete cds	0.13	0.31	0.22
hsy15409	11	Homo sapiens mRNA for putative glucose 6-phosphate translocase.	0.28	0.23	0.25
hsu16996	12	Human protein tyrosine phosphatase mRNA, complete cds.	0.31	0.26	0.29
hsu30255	12	Human phosphogluconate dehydrogenase (hPGDH) gene, complete cds.	0.29	0.30	0.29
4504714			0.47	0.16	0.31
ab002349	15	Human mRNA for KIAA0351 gene, complete cds.	0.14	0.50	0.32
humpai2	13	Human placental plasminogen activator inhibitor mRNA, complete cds.	0.28	0.35	0.32
hsu73824		Human p97 mRNA, complete cds.	0.30	0.34	0.32
hsa132270	2	Homo sapiens mRNA for integral type I protein p24B (p26).	0.31	0.34	0.33
Humorfkg1f	11	Human mRNA for KIAA0058 gene,complete cds.	0.31	0.36	0.33
s74452	3	Cyclin B1[promoter region][human,cervical carcinoma cell line, HeLa cells,Genomic, 351 nt].	3.21	2.79	3.00
hspros27	10	H.sapiens PROS-27 mRNA.	3.29	2.85	3.07
Hstrr	10	Human mRNA for transferrin receptor.	2.70	3.48	3.09
Humprion	15	Homo sapiens mRNA for prion protein, complete cds.	3.07	3.19	3.13
hshr21spa	13	H.sapiens mRNA for protein involved in DNA double-strand break repair.	2.29	4.01	3.15
AB00109S14	11	Homo sapiens gene for H-cadherin, exon 14 and complete cds.	2.95	3.50	3.23
hsranbp1	11	H.sapiens mRNA for RanBP1.	3.98	2.57	3.27
Hsxprf	8	Homo sapiens mRNA for putative transcription factor XPRF.	3.35	3.38	3.37
humcd3621	11	Human antigen CD36 (clone 21) mRNA, complete cds.	3.28	3.54	3.41
Humsparc	5	Human SPARC/osteonectin mRNA, complete cds.	2.87	3.96	3.42
Humhcmap3	5	Human gene for hepatitis C-associated microtubular aggregate protein p44, exon 4.	3.72	3.30	3.51
Humprofii	5	Human profilin II mRNA, complete cds.	3.07	4.07	3.57
5729755			2.35	4.88	3.61
Hsrnasmg	13	H.sapiens mRNA for Sm protein G.	2.91	4.57	3.74
Humpgc	5	Human chondroitin sulfate proteoglycan core protein mRNA, 3' end.	3.67	3.91	3.79
hstop2a10	8	Homo sapiens topoisomerase II alpha (TOP2A) gene,exons 34 and 35,and complete cds.	4.02	3.76	3.89
hsu09559	14	Human Rch1 (RCH1) mRNA, complete cds.	3.75	4.03	3.89
humcol1a42		Human alpha-1 collagen type IV gene, exon 52.	4.37	3.69	4.03
hsinta6r	11	Human mRNA for integrin alpha 6.	3.28	5.43	4.35
d86983	15	Human mRNA for KIAA0230 gene, partial cds.	4.71	4.84	4.78
hsu26555		Human versican V2 core protein precursor splice-variant mRNA, complete cds.	6.93	5.91	6.42
hspgp95	13	Human mRNA for protein gene product (PGP) 9.5.	5.66	7.54	6.60
af052124	15	Homo sapiens clone 23810 osteopontin mRNA, complete cds.	11.77	4.63	8.20
Humcolva		Human alpha-2 type V collagen gene, 3' end.	7.64	10.17	8.91
humca1xia	15	Human alpha-1 type XI collagen (COL11A1) mRNA, complete cds.	6.75	12.07	9.41
Hscalbr11		Human mRNA for 27-kDa calbindin.	6.72	12.17	9.45
hsu50078	8	Human guanine nucleotide exchange factor p532 mRNA, complete cds.	12.28	17.11	14.70
Hsop	5	Human mRNA for osteopontin.	20.23	20.22	20.23

Fcf: function classification average ratio >3: up regulation average ratio <0.33: down regulation; R1: the first ratio; R2: the second ratio; AR: R1+R2 average ratio.

Table 3 Function classification for genes showing expression differences in esophageal carcinoma and pericancerous epithelium that were >2 or <0.5 fold from the control tissue

Gene function classification	Carcinoma/normal			Pericancerous/normal		
	N	>2	<0.5	N	> 2	<0.5
1 Proto-oncogenes and tumor suppression genes	2	1	1	0	0	0
2 Cell signals and transducing proteins	3	2	1	3	3	0
3 Cell cycle proteins	6	5	1	0	0	0
4 Extra-pressure reaction proteins	1	0	1	0	0	0
5 Cell regulatory proteins	7	7	0	3	3	0
6 Cell apoptosis related proteins	1	1	0	1	0	1
7 DNA synthesis, repair and recombinant proteins	3	3	0	0	0	0
8 DNA binding, transcription and its factor	6	4	2	1	1	0
9 Cell receptors	0	0	0	0	0	0
10 Cell surface antigen and adhesion proteins	10	8	2	4	4	0
11 Ion-channel and transporters	24	14	10	2	2	0
12 Metabolism-related proteins	21	10	11	6	4	2
13 Protein synthesis-related genes	14	7	7	2	1	1
14 Development-related genes	1	1	0	2	2	0
15 Other genes	27	18	9	7	7	0
16 New genes	9	4	5	0	0	0
Total	135	85	50	31	27	4

Table 4 Genes showing expression difference between the esophageal carcinoma and pericancerous epithelium

Genbank-ID	Fcf	Gene name	PR	TR
Hscalbr	11	Human mRNA for 27-kDa calbindin.	2.91	9.45
af052124	15	Homo sapiens clone 23810 osteopontin mRNA, complete cds.	5.34	8.20
Hsinta6r	11	Human mRNA for integrin alpha 6.	2.93	4.35
Humprofil	5	Human profilin II mRNA, complete cds.	2.50	3.57
Humhcamap3	5	Human gene for hepatitis C-associated microtubular aggregate protein p44, exon 4.	2.79	3.51
hum927a	10	Human interferon-inducible protein 9-27 mRNA, complete cds.	2.43	2.92
Hstrr	10	Human mRNA for transferrin receptor.	3.76	3.09
hsu50078	8	Human guanine nucleotide exchange factor p532 mRNA, complete cds.	18.7	14.7
Humtfr	10	Human transferrin receptor mRNA, complete cds.	3.51	2.81
hsu30255	12	Human phosphogluconate dehydrogenase(hPGDH)gene, complete cds.	0.48	0.29
hsu05684	2	Homo sapiens dihydrodiol dehydrogenase mRNA, complete cds.	3.75	2.31
Hsop	5	Human mRNA for osteopontin.	37.1	20.2
Hspgp95	13	Human mRNA for protein gene product (PGP) 9.5.	19.4	6.60
hsu46571	13	Human tetratricopeptide repeat protein (tpr2) mRNA, complete cds.	0.41	
Humrsc390	6	Human mRNA for KIAA0018gene, complete cds.	0.44	
hcox4gn	12	Homo sapiens hypothetical protein (COX4AL) gene, partial cds, and cytochrome c oxidase subunit IV precursor (COX4) gene, complete cds.	0.47	
d79997		Human mRNA for KIAA0175 gene, complete cds.	2.05	
ab01755s10	15	Homo sapiens IGSF4 gene, exon 10 and complete cds.	2.06	
Hsnov	15	H.sapiens mRNA for novel gene in Xq28 region.	2.09	
hsifi56r		Human mRNA for 56-KDa protein induced by interferon.	2.1	
af054182	12	Homo sapiens mitochondrial processing peptidase beta-subunit mRNA, complete cds.	2.11	
af131818	15	Homo sapiens clone 25237mRNA sequence.	2.19	
af035301	2	Homo sapiens clone 23876 neuronal olfactomedin-related ER localized protein mRNA, partial cds.	2.28	
Humorfi	14	Homo sapiens (clone S240ii117/zap112) mRNA, complete cds.	2.26	
af038660	12	Homo sapiens chromosome 1p33-p34 beta-1,4-galactosyltransferase mRNA, complete cds.	2.32	
d88687	12	Homo sapiens mRNA for KM-102-derived reductase-like factor,complete cds.	2.51	
hsu05598	12	Human dihydrodiol dehydrogenase mRNA, complete cds.	3.07	
Humalcam	10	Homo sapiens CD6 ligand (ALCAM) mRNA, complete cds.	3.07	
hsu79299	2	Human neuronal olfactomedin-related ER localized protein mRNA,partial cds.	3.33	
ab003476	14	Homo sapiens mRNA for gravin, complete cds. 3.65		
af100757	15	Homo sapiens COP9 complex subunit 4 mRNA, complete cds. 5.96		

Fcf: function classification; TR: esophageal carcinoma average ratio; PR: pericancerous epithelium average ratio.

DISCUSSION

Because of the occult characteristic esophageal carcinoma, one of the most common malignant tumors in China, is difficult to be diagnosed for a size of <2 cm tumor mass by using CT and ultrasound. At present, almost most of the clinical cases are in the late stage, with a five years survival rate of about 30 % only. It is therefore necessary to explore new and efficacious diagnostic method to detect esophageal carcinoma at the early stage.

The carcinogenesis is a process caused by abnormal expression of tumor-associated genes or inactivation of tumor suppression genes or both. Clarifying the gene expression differences between the malignant and normal tissue is therefore the key procedure for the cancer control study. With the advances of molecular biological techniques, gene chip has been used to detect gene expression difference in various specimens by parallel analysis on a large scale^[2-29]. Some papers have also been published about the studying human esophageal carcinoma by using gene chips^[30-35]. However, a investigation on the difference of gene expression profiles between esophageal carcinoma and its paracancerous epithelium by gene chip has not been reported yet.

In the present study the gene chip technique was employed to analyze the difference of gene expression patterns in esophageal carcinoma and its paracancerous epithelium as well as their normal control. The results showed that: (1) There were 135 genes with expression levels marked as fluorescence intensity of more than 2 times or less than 0.5 times in esophageal carcinoma compared with the normal esophageal epithelium. It suggested these genes might well be related to the occurrence and development of the esophageal carcinoma.

Xu *et al*^[2] reported that the protein tyrosine phosphatase (PTPase) the high and low metastatic human ovarian cancer cell lines were down-regulated with a varied degree (0.64 and 0.27 respectively). PTPase was associated with the cell signaling control, energy metabolism, proliferation and the promotion of MHC-I antigen expression, mediated by numerous hormones (such as epidermal growth factor, insulin, insulin-like growth factor 1 and so on). The down-regulated PTPase would decrease the antigen expression on the cell surface, and result in the malignant cell escaping from the immune surveillance. In the present study, the enzyme was also down-regulated (0.29) in the esophageal carcinoma.

We found expression levels that of a variety of adhesion protein genes such as collagen protein type IV (8.9), integrin (4.45), calbindin protein (9.45) were increased, which coincided with Yanagawa *et al*^[16], Mori *et al*^[24], Hippo *et al*^[25] and Kan *et al*^[33] reported papers, inclusive of colorectal, gastric and esophageal carcinomas. The increased adhesion protein expression might associate with the invasiveness and metastasis of cancer cells.

It has been demonstrated that in proliferous cells the activity of topoisomerase II (TopoII) was rapidly increased from S phase to the end of G2/M stage, which meant that the enzyme might relate to the malignant transformation of the tumor cells. Varis *et al*^[22] and Hu *et al*^[34] reported that TopoII expression levels was obviously up-regulated in human gastric cancer and esophageal squamous cell carcinoma. In our study the TopoII expression was up-regulated as well (3.89).

Cell cycle-protein B₁ was also found up-regulated in esophageal carcinoma as Hu *et al*^[34] have reported, which might indicate that the malignant cells were in an abnormal proliferative state.

(2) There were 31 genes with expression levels marked as fluorescence intensity of more than 2 times or less than 0.5 times in pericancerous epithelium compared with normal control. Although an abnormal appearance of pericancerous epithelium was not found in the pathological examination, the

gene expression however indicated that there were thirteen genes expressed both in esophageal carcinoma and in pericancerous epithelium. Among these, the expression levels of 6 up-regulated genes in pericancerous epithelium were less than that of the corresponding genes in esophageal carcinoma and as for the other 6 up-regulated and 1 down-regulated genes, the expression levels in the former was higher than that in the latter. There were 18 genes appeared only in pericancerous epithelium, which suggested that these genes were probable related to the promotion and progression of carcinogenesis at the early stage of esophageal carcinoma.

The application of gene chip technique was a revolution of research method in life science. Our experiment illustrated that the detection of gene expression difference between malignant and normal tissue by gene chip might provide a new direction for diagnosis, therapy and prevention of human esophageal carcinoma.

REFERENCES

- 1 **Peng XL**, Yuan HY, Xie Y, Wang HH. Experimental technique of gene engineering. *HuNa Sci Tech Issue Ag Second* 1998; 197-199
- 2 **Xu SH**, Mou HZ, Lu GQ, Zhu CH, Yang ZY, Gao YL, Lou HK, Liu XL, Chen Y, Yang W. Gene expression profile difference in high and low metastatic human ovarian cancer cell lines by gene chip. *Chin Med J (Engl)* 2002; **115**: 36-41
- 3 **Wang K**, Gan L, Jeffery E, Gayle M, Gown AM, Skelly M, Nelson PS, Ng WV, Schummer M, Hood L, Mulligan J. Monitoring gene expression profile changes in ovarian carcinomas using cDNA microarra. *Gene* 1999; **229**: 101-108
- 4 **Furey TS**, Cristianini N, Duffy N, Bednarski DW, Schummer M, Haussler D. Support vector machine classification and validation of cancer tissue samples using microarray expression data. *Bioinformatics* 2000; **16**: 906-914
- 5 **Ono K**, Tanaka T, Tsunoda T, Kitahara O, Kihara C, Okamoto A, Ochiai K, Takagi T, Nakamura Y. Identification by cDNA microarray of genes involved in ovarian carcinogenesis. *Cancer Res* 2000; **60**: 5007-5011
- 6 **Zou TT**, Selaru FM, Xu Y, Shustova V, Yin J, Mori Y, Shibata D, Sato F, Wang S, Olaru A, Deacu E, Liu TC, Abraham JM, Meltzer SJ. Application of cDNA microarrays to generate a molecular taxonomy capable of distinguishing between colon cancer and normal colon. *Oncogene* 2002; **21**: 4855-4862
- 7 **Lin YM**, Furukawa Y, Tsunoda T, Yue CT, Yang KC, Nakamura Y. Molecular diagnosis of colorectal tumors by expression profiles of 50 genes expressed differentially in adenomas and carcinomas. *Oncogene* 2002; **21**: 4120-4128
- 8 **Sepulveda AR**, Tao H, Carloni E, Sepulveda J, Graham DY, Peterson LE. Screening of gene expression profiles in gastric epithelial cells induced by *Helicobacter pylori* using microarray analysis. *Aliment Pharmacol Ther* 2002; **16** (Suppl 2): 145-157
- 9 **Zhou Y**, Gwadry FG, Reinhold WC, Miller LD, Smith LH, Scherf U, Liu ET, Kohn KW, Pommier Y, Weinstein JN. Transcriptional regulation of mitotic genes by camptothecin-induced DNA damage: microarray analysis of dose- and time-dependent effects. *Cancer Res* 2002; **62**: 1688-1695
- 10 **Iizaka M**, Furukawa Y, Tsunoda T, Akashi H, Ogawa M, Nakamura Y. Expression profile analysis of colon cancer cells in response to sulindac or aspirin. *Biochem Biophys Res Commun* 2002; **292**: 498-512
- 11 **Nguyen DV**, Rocke DM. Tumor classification by partial least squares using microarray gene expression data. *Bioinformatics* 2002; **18**: 39-50
- 12 **Nakeff A**, Sahay N, Pisano M, Subramanian B. Painting with a molecular brush: genomic/proteomic interfacing to define the drug action profile of novel solid-tumor selective anticancer agents. *Cytometry* 2002; **47**: 72-79
- 13 **Takahashi Y**, Nagata T, Ishii Y, Ikarashi M, Ishikawa K, Asai S. Up-regulation of vitamin D3 up-regulated protein 1 gene in response to 5-fluorouracil in colon carcinoma SW620. *Oncol Rep* 2002; **9**: 75-79
- 14 **Hegde P**, Qi R, Gaspard R, Abernathy K, Dharap S, Earle-Hughes

- J, Gay C, Nwokekeh NU, Chen T, Saeed AI, Sharov V, Lee NH, Yeatman TJ, Quackenbush J. Identification of tumor markers in models of human colorectal cancer using a 19,200-element complementary DNA microarray. *Cancer Res* 2001; **61**: 7792-7797
- 15 **Fujita M**, Furukawa Y, Tsunoda T, Tanaka T, Ogawa M, Nakamura Y. Up-regulation of the ectodermal-neural cortex 1 (ENC1) gene, a downstream target of the beta-catenin/T-cell factor complex, in colorectal carcinomas. *Cancer Res* 2001; **61**: 7722-7726
- 16 **Yanagawa R**, Furukawa Y, Tsunoda T, Kitahara O, Kameyama M, Murata K, Ishikawa O, Nakamura Y. Genome-wide screening of genes showing altered expression in liver metastases of human colorectal cancers by cDNA microarray. *Neoplasia* 2001; **3**: 395-401
- 17 **Pinheiro NA**, Caballero OL, Soares F, Reis LF, Simpson AJ. Significant overexpression of oligophrenin-1 in colorectal tumors detected by cDNA microarray analysis. *Cancer Lett* 2001; **172**: 67-73
- 18 **Takemasa I**, Higuchi H, Yamamoto H, Sekimoto M, Tomita N, Nakamori S, Matoba R, Monden M, Matsubara K. Construction of preferential cDNA microarray specialized for human colorectal carcinoma: molecular sketch of colorectal cancer. *Biochem Biophys Res Commun* 2001; **285**: 1244-1249
- 19 **Gupta RA**, Brockman JA, Sarraf P, Willson TM, DuBois RN. Target genes of peroxisome proliferator-activated receptor gamma in colorectal cancer cells. *J Biol Chem* 2001; **276**: 29681-29687
- 20 **Kitahara O**, Furukawa Y, Tanaka T, Kihara C, Ono K, Yanagawa R, Nita ME, Takagi T, Nakamura Y, Tsunoda T. Alterations of gene expression during colorectal carcinogenesis revealed by cDNA microarrays after laser-capture microdissection of tumor tissues and normal epithelia. *Cancer Res* 2001; **61**: 3544-3549
- 21 **Suzuki H**, Gabrielson E, Chen W, Anbazhagan R, van Engeland M, Weijenberg MP, Herman JG, Baylin SB. A genomic screen for genes upregulated by demethylation and histone deacetylase inhibition in human colorectal cancer. *Nat Genet* 2002; **31**: 141-149
- 22 **Varis A**, Wolf M, Monni O, Vakkari ML, Kakkola A, Moskaluk C, Frierson H Jr, Powell SM, Knuutila S, Kallioniemi A, El-Rifai W. Targets of gene amplification and overexpression at 17q in gastric cancer. *Cancer Res* 2002; **62**: 2625-2629
- 23 **Selaru FM**, Xu Y, Yin J, Zou T, Liu TC, Mori Y, Abraham JM, Sato F, Wang S, Twigg C, Olaru A, Shustova V, Leytin A, Hytiroglou P, Shibata D, Harpaz N, Meltzer SJ. Artificial neural networks distinguish among subtypes of neoplastic colorectal lesions. *Gastroenterology* 2002; **122**: 606-613
- 24 **Mori M**, Mimori K, Yoshikawa Y, Shibata K, Utsunomiya T, Sadanaga N, Tanaka F, Matsuyama A, Inoue H, Sugimachi K. Analysis of the gene-expression profile regarding the progression of human gastric carcinoma. *Surgery* 2002; **131**(Suppl 1): S39-47
- 25 **Hippo Y**, Taniguchi H, Tsutsumi S, Machida N, Chong JM, Fukayama M, Kodama T, Aburatani H. Global gene expression analysis of gastric cancer by oligonucleotide microarrays. *Cancer Res* 2002; **62**: 233-240
- 26 **Maeda S**, Otsuka M, Hirata Y, Mitsuno Y, Yoshida H, Shiratori Y, Masuho Y, Muramatsu M, Seki N, Omata M. cDNA microarray analysis of *Helicobacter pylori*-mediated alteration of gene expression in gastric cancer cells. *Biochem Biophys Res Commun* 2001; **284**: 443-449
- 27 **Kudoh K**, Ramanna M, Ravatn R, Elkahoul AG, Bittner ML, Meltzer PS, Trent JM, Dalton WS, Chin KV. Monitoring the expression profiles of doxorubicin-induced and doxorubicin-resistant cancer cells by cDNA microarray. *Cancer Res* 2000; **60**: 4161-4166
- 28 **Sgroi DC**, Teng S, Robinson G, LeVangie R, Hudson JR, Elkahoul AG. *In vivo* gene expression profile analysis of human breast cancer progression. *Cancer Res* 1999; **59**: 5656-5661
- 29 **Pollack JR**, Perou CM, Alizadeh AA, Eisen MB, Pergamenschikov A, Williams CF, Jeffrey SS, Botstein D, Brown PO. Genome-wide analysis of DNA copy-number changes using cDNA microarrays. *Nat Genet* 1999; **23**: 41-46
- 30 **Xu Y**, Selaru FM, Yin J, Zou TT, Shustova V, Mori Y, Sato F, Liu TC, Olaru A, Wang S, Kimos MC, Perry K, Desai K, Greenwald BD, Krasna MJ, Shibata D, Abraham JM, Meltzer SJ. Artificial neural networks and gene filtering distinguish between global gene expression profiles of Barrett's esophagus and esophageal cancer. *Cancer Res* 2002; **62**: 3493-3497
- 31 **Selaru FM**, Zou T, Xu Y, Shustova V, Yin J, Mori Y, Sato F, Wang S, Olaru A, Shibata D, Greenwald BD, Krasna MJ, Abraham JM, Meltzer SJ. Global gene expression profiling in Barrett's esophagus and esophageal cancer: a comparative analysis using cDNA microarrays. *Oncogene* 2002; **21**: 475-478
- 32 **Kihara C**, Tsunoda T, Tanaka T, Yamana H, Furukawa Y, Ono K, Kitahara O, Zembutsu H, Yanagawa R, Hirata K, Takagi T, Nakamura Y. Prediction of sensitivity of esophageal tumors to adjuvant chemotherapy by cDNA microarray analysis of gene-expression profiles. *Cancer Res* 2001; **61**: 6474-6479
- 33 **Kan T**, Shimada Y, Sato F, Maeda M, Kawabe A, Kaganai J, Itami A, Yamasaki S, Imamura M. Gene expression profiling in human esophageal cancers using cDNA microarray. *Biochem Biophys Res Commun* 2001; **286**: 792-801
- 34 **Hu YC**, Lam KY, Law S, Wong J, Srivastava G. Identification of differentially expressed genes in esophageal squamous cell carcinoma (ESCC) by cDNA expression array: overexpression of Fra-1, Neogenin, Id-1, and CDC25B genes in ESCC. *Clin Cancer Res* 2001; **7**: 2213-2221
- 35 **Lu J**, Liu Z, Xiong M, Wang Q, Wang X, Yang G, Zhao L, Qiu Z, Zhou C, Wu M. Gene expression profile changes in initiation and progression of squamous cell carcinoma of esophagus. *Int J Cancer* 2001; **91**: 288-294

Edited by Zhu L

Methylation and mutation analysis of p16 gene in gastric cancer

Yi Ding, Xiao-Ping Le, Qin-Xian Zhang, Peng Du

Yi Ding, Xiao-Ping Le, Qin-Xian Zhang, Molecular Cell Biology Research Center, Medical College of Zhengzhou University; Zhengzhou 450052, Henan Province, China

Peng Du, Henan Key Lab. of Molecular Medicine, Zhengzhou 450052, Henan Province, China

Supported by the National Natural Science Foundation of China, No. 39170440

Correspondence to: Pro. Qin-Xian Zhang, Molecular Cell Biology Research Center, Medical College of Zhengzhou University; 40 Daxue Road, Zhengzhou 450052, Henan Province, China. qxz53@zzu.edu.cn

Telephone: +86-371-6977002 **Fax:** +86-371-6977002

Received: 2002-10-22 **Accepted:** 2002-11-18

Abstract

AIM: To study methylation, frequencies of homozygous deletion and mutation of p16 gene in gastric carcinoma.

METHODS: The methylation pattern in exon 1 and exon 2 of p16 gene was studied with polymerase chain reaction (PCR), using methylation sensitive restriction endonuclease HpaII and methylation insensitive restriction endonuclease MspI. PCR technique was used to detect homozygous deletions of exon 1 and exon 2 of p16 gene and single strand conformation polymorphism (SSCP) technique was used to detect the mutation of the gene.

RESULTS: Hypermethylation changes in exon 1 and exon 2 of p16 gene were observed in 25 % and 45 % of 20 gastric cancer tissues, respectively, while no methylation abnormality was found in normal tissues. The homozygous deletion frequency of exon 1 and exon 2 of p16 gene in 20 gastric cancer tissues was 20 % and 10 %, respectively. No mutation was found in exon 1 of p16 gene, while abnormal single strands were found in 2 (10 %) cases in exon 2 as detected by SSCP.

CONCLUSION: The results suggest that hypermethylation and abnormality of p16 gene may play a key role in the progress of gastric cancer. Hypermethylation of exon 2 of p16 gene may have effects on the carcinogenesis of gastric mucosa and may be a later event.

Ding Y, Le XP, Zhang QX, Du P. Methylation and mutation analysis of p16 gene in gastric cancer. *World J Gastroenterol* 2003; 9(3): 423-426

<http://www.wjgnet.com/1007-9327/9/423.htm>

INTRODUCTION

DNA methylation abnormality could influence gene transcription directly, and it could also cause the abnormal gene expression through the C→T mutation induced by deamination of 5' methyl cytosine (5 mC)^[1]. In the eukaryote, 5 mC mainly appears in the CpG sequence of genome, and it is the site in which p16 gene mutation occurs frequently^[2]. Highly frequent homozygous deletion, mutation and abnormal methylation of p16 gene exhibit in many kinds of carcinoma^[3-9]. In China, studies on p16 gene methylation abnormality and

deletion, mutation in gastric carcinoma have scarcely been reported. In this paper, restriction endonuclease-polymerase chain reaction (PCR) and single strand conformation polymorphism (SSCP) techniques were used to detect the CpG methylation and mutation in exon 1 and 2 of p16 gene. The biological significance of p16 gene and its methylation abnormality in the development and progress of gastric carcinoma were discussed.

MATERIALS AND METHODS

Specimens

20 specimens of gastric carcinoma and their corresponding adjacent normal-appearing gastric tissue were collected from the First and Second Affiliated Hospital of Medical College of Zhengzhou University and frozen in liquid nitrogen in 30 min. All the specimens were pathologically diagnosed and without radio or chemical therapy before operation.

Analysis of methylation

Tissue DNA was extracted by normal phenol-chloroform method. DNA samples were treated with HpaII and MspI. Primers were synthesized by Shanghai Cell Biology Research Institute of China Scientific Institute and purified with PAGE. The primers of p16 exon 1 (E1): 5' -GAA GAA AGA GGA GGG GCT G-3'; 5' -GCG CTA CCT GAT TCC AAT TC-3'; the primers of exon 2 (E2): 5' -CAC AAG CTT CCT TTC CGT CAT G-3', 5' -TCT GAG CTT TGG AAG CTC TCA GG -3'. The length of amplified fragments was 336bp and 424bp respectively. The parameter of PCR cycle was: 92 °C 60 s, 60 °C (renaturing temperature of E2 was 58.5 °C) 60 s, 71 °C 90 s. After 24 cycles, the reaction system was thermal retarded at 71 °C for 10 min. 8 µl of PCR products were electrophoresized on 20 g/L agarose gel. After the electrophoresis, the gel was visualized under ultraviolet and photographed.

PCR-SSCP

The primers were the same as mentioned above. The parameter of PCR cycle was: 91.5 °C 60 s, 61.5 °C (E1) or 59.5 °C (E2) 60 s, 70.5 °C 90 s. After 30 cycles, the reaction system was thermal retarded at 70.5 °C for 10 min. PCR products were electrophoresized on 20 g/L agarose gel and stained with ethidium bromide. SSCP was taken on the 80 g/L undenatured polyacrylamide gel. After denaturing at 95 °C for 5 min, the samples were ice bathed immediately for 5 to 10 min and electrophorized under constant voltage 160 V for 4-6 h. After electrophoresis the gel was removed and silver stained.

Statistic analysis

Data were analyzed using Fisher's exact test of probabilities with SPSS 10.0 statistic software.

RESULTS

Methylation analysis of DNA

HpaII is a methylation sensitive restriction endonuclease, when methylation occurs at the second C in the CCGG target sequence, HpaII can not recognize the target site. However,

Msp I is isoenzyme of HpaII, and can recognize the target site whether or not methylation occurs at the second C in the CCGG target sequence. The exon 1 and 2 of p16 gene include 2 and 4 5' -CCGG-3' sites. If methylation occurs, HpaII can not identify the target sequence, the specific patterns would appear after PCR products are electrophoresed (336bp or 424bp) (Figure 1). If no specific bands were amplified by PCR, then no methylation alteration at second C in 5' -CCGG-3' sequence is indicated (Figure 2).



Figure 1 Methylation analysis of p16 gene exon 1 (abnormality). 1: DNA marker; 2: negative control; 3-5 carcinoma tissue; (3: without enzyme treatment, 4: Hpa II treatment, 5: Msp I treatment); 6-8 normal tissue (6: without enzyme treatment, 7: Hpa II treatment, 8: MspI treatment).

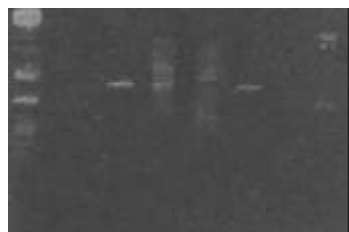


Figure 2 Methylation analysis of p16 gene exon 1 (no abnormality). 1: DNA marker; 2: negative control; 3-5 carcinoma tissue (3: without enzyme treatment, 4: Hpa II treatment, 5: MspI treatment); 6-8 normal tissue (6: without enzyme treatment, 7: Hpa II treatment, 8: MspI treatment).



Figure 3 PCR of p16 gene exon 1 of gastric carcinoma tissue. 1: Marker; 2: negative control; 3-8: 336bp of E1 PCR.



Figure 4 PCR of p16 gene exon 2 of gastric carcinoma tissue. 1: Marker; 2-8: 424bp of E2 PCR; 3: deletion.

Homozygous deletion analysis

After agarose electrophoresis of PCR products, if no amplified products were found at the sites corresponding to 336bp or 424bp, then homozygous deletion of E1 or E2 could be

determined. In gastric carcinoma tissues, 4 cases (20 %) of E1 deletion and 2 cases (10 %) of E2 deletion were found. The 6 cases with homozygous deletion included 1 with well differentiated and 5 with moderately or poorly differentiated gastric carcinoma tissues (Figure 3 and 4).

PCR-SSCP analysis

Mobility shift is defined when abnormal bands appear or the position of bands alter. No abnormal alteration was found at E1 of p16 gene (Figure 5). At E2, abnormal single strand of mobility shift exhibited in 2 (10 %) cases, in 1 of which (IIIa stage, poorly differentiated adenocarcinoma) mobility shift occurred in both carcinoma and adjacent carcinoma tissues (Figure 6).

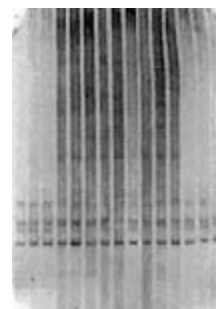


Figure 5 PCR-SSCP of p16 gene exon 1 (no abnormality).

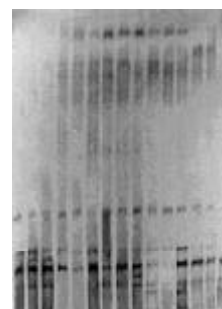


Figure 6 PCR-SSCP of p16 gene exon 1. Abnormal single strand occurred in 2, 3 lane (adjacent carcinoma and carcinoma tissue) and 9 lane (carcinoma tissue).

DISCUSSION

Methylation of p16 gene

In the process of multistage canceration, abnormality of gene expression may be controlled by genetic mechanism and epigenetic mechanism. Epigenetic mechanism is indicated by methylation alteration at 5 mC which cause gene expression abnormality without change in the DNA sequence and product of gene expression, and is a key mechanism causing genomic instability and canceration. Hypermethylation at CpG induces abnormality of DNA conformation stability which may influence the binding of specific protein and DNA regulating sequence, and cause gene silence. Inability to transcribe the tumor suppressor genes resulted in dysfunction of the genes and induced the development of carcinoma^[10, 11].

Regional hypermethylation plays an important role in the alteration of gene expression in human carcinoma and in the progression of carcinoma. In the present paper, methylation at CpG in exons 1 and 2 of p16 gene in gastric carcinoma tissues was detected by treatment of methylation sensitive restriction endonuclease combined with PCR technique. The results showed that abnormal methylation was present in 5 and 9 of 20 cancer tissues, respectively, but no abnormality was found in corresponding adjacent normal gastric mucosa, suggesting

an association between methylation of p16 gene and gastric carcinogenesis. Homozygous deletion of p16 gene occurred, to some extent, in many kinds of human carcinoma cells. However, gene mutation rarely occurred and the frequency of homozygous deletion was low in primary carcinoma. It is interesting that in some human carcinoma without site mutation or homozygous deletion, for example, in the pulmonary cancer cell line in oat cell type, the frequency of remethylation at p16 CpG island is 78 % resulting in the loss of p16 gene transcription activity. The same phenomena exists in mammary, prostate, gastric and colon carcinomas, especially in the colon carcinoma with the frequency of methylation being high as 92 %. In the cells of colon carcinoma without homozygous deletion, methylation occurs at both alleles of p16 gene, and is related to its entire deactivation^[1]. Based on the fact that the alteration of methylation of p16 gene and other genes occur in many kinds of carcinomas lacking of mutation and deletion, methylation might be a key mechanism of deactivation of tumor suppressor genes in primary carcinoma. Expression of p16 gene in gastric carcinoma is decreased significantly^[12-22]. However, the frequency of mutation and deletion of p16 gene is low, suggesting that abnormal methylation might be a key mechanism in alteration of the gene expression in gastric carcinoma.

The results in the present study showed that abnormal methylation mainly appeared in poorly differentiated gastric carcinoma. Two cases with methylation in both exons were poorly differentiated and progressive gastric carcinoma. Hypermethylation of exon 2 mainly exhibited in the cases of late stage of gastric carcinoma, suggesting that hypermethylation of exon 2 is related to the differentiated degree and the clinical progression of gastric carcinoma, and thus might be a late event. Kampster *et al.*^[23] reported in their study on methylation of p16 gene in esophagus carcinoma that alteration of methylation at exon 2 was obviously related to clinical stage and progression of carcinoma, and a correlation existed between hypermethylation of exon 1 and no gene expression. Yi *et al.*^[24] reported that methylation of p16 gene in colorectal cancer was obviously related to the Duke's stage. Methylation of p16 gene was increased gradually with the progression of carcinoma, and could induce detectable alteration and consequence to late stage which may be related to clinical stage of gastric carcinoma.

Deletion and mutation of p16 gene

Deletion and mutation of p16 gene are also important mechanisms responsible for the dysfunction of tumor suppressor genes. Abnormality in 9p21-22 of chromosome has been reported in many kinds of carcinoma cells, and p16 gene is an important gene located in this region. By analysis of the sites adjacent to p16 gene, simultaneous mini-deletions (<200bp) of p16 allele were found in many carcinomas, and homozygous deletion of p16 gene has been testified in many kinds of primary carcinoma^[25-27]. Lu *et al.*^[28] detected that the deletion of E1 of p16 gene in 16.4 % of gastric carcinoma tissues, Wu *et al.*^[29] reported a rate of 10 % (6/60). Different deletion rates of p16 gene in gastric carcinoma were reported by the other investigators^[30-32]. In the present study, deletion of E1 and E2 was detected in 20 % and 10 %, respectively, of 20 cases gastric carcinoma cases, but amplified products appeared in corresponding normal gastric mucosa tissues.

Mutation of p16 gene mainly includes nonsense, missense, and frame shift mutation. The frequency of mutation is significantly lower than deletion with 70-90 % being present on E2^[2]. Mutation of p16 gene in gastric carcinoma is rare, but the frequency is much higher than the natural mutation (10-6~10-4) of general genes, thus, it is conceivable that mutation of p16 gene might be involved in the development and

progression of gastric carcinoma. In the present study, mutation of p16 gene E2 was detected in 2 cases of gastric carcinoma tissues, and no E1 mutation was found. Both the gastric carcinoma cases with mutation were progressive gastric carcinoma. One of them exhibited mobility shift in both carcinoma and adjacent carcinoma tissues, and belonged to IIIa stage and poorly differentiated adenocarcinoma, suggesting that p16 gene mutation might be a late event in the process of gastric carcinoma. It has been reported that the mutation site of p16 gene is the same as that of p53 gene, i.e. at CpG. It is believed that mutation is induced by nucleotide methylation^[2]. It is suggested that mutation of p16 gene might be the consequence of the DNA genomic insatibility, and gradually causes the canceration.

REFERENCES

- 1 **Yskoob J**, Fan XG, Hu GL, Zhang Z. DNA methylation and carcinogenesis in digestive neoplasms. *World J Gastroenterol* 1998; **4**: 174-177
- 2 **Pollock PM**, Pearson JV, Hayward NK. Compilation of somatic mutation of the CDKN2 gene in human cancers: non random distribution of base substitutions. *Genes Chromosomes Cancers* 1996; **15**: 77-88
- 3 **Hayashi K**, Metzger R, Salonga D, Danenberg K, Leichman LP, Fink U, Sendler A, Kelsen D, Schwartz GK, Groshen S, Lenz HJ, Danenberg PV. High frequency of simultaneous loss of p16 and p16 beta gene expression in squamous cell carcinoma of the esophagus but not in adenocarcinoma of the esophagus or stomach. *Oncogene* 1997; **15**: 1481-1488
- 4 **Song ZY**, Xu RZ, Qian KD, Tang XQ, Zhao XY, Lin M. Abnormal expression of p16/CDKN2 gene in human gastric carcinoma. *Xin Xiaohua Bingxue Zazhi* 1997; **5**: 139-140
- 5 **Igaki H**, Sasaki H, Tachimori Y, Kato H, Watanabe H, Kimura T, Harada Y, Sugimura T, Terada M. Mutation frequency of the p16/CDK2 gene in primary cancer in the upper digestive tract. *Cancer Res* 1995; **55**: 3421-3423
- 6 **Okamoto A**, Hussain SP, Hagiwara K, Spillare EA, Rusin MR, Demetrick DJ, Serrano M, Hannon GJ, Shiseki M, Zariwala M. Mutations in the p16INK4/MTS1/CNKN2, p15INK4B/MTS2, and p18 genes in primary and metastatic lung cancer. *Cancer Res* 1995; **55**: 1448-1451
- 7 **Mori T**, Miura K, Aoki T, Nishihira T, Mori S, Nakamura Y. Frequent somatic mutation of the MTS1/CDK4I (multiple tumor suppressor/cyclin-dependent kinase 4 inhibitor) gene in esophageal squamous cell carcinoma. *Cancer Res* 1994; **54**: 3396-3397
- 8 **Gonzalez-Zulueta M**, Bender CM, Yang AS, Nguyen T, Beart RW, Van Tornout JM, Jones PA. Methylation of the 5' CpG island of the p16/CDK2 tumor suppressor gene in normal and transformed human tissues correlates with gene silencing. *Cancer Res* 1995; **55**: 4531-4535
- 9 **Zhang J**, Lai MD, Chen J. Methylation status of p16 gene in colorectal carcinoma and normal colonic mucosa. *World J Gastroenterol* 1999; **5**: 451-454
- 10 **Issa JP**, Ottaviano YL, Celano P, Hamilton SR, Davidson NE, Baylin SB. Methylation of oestrogen receptor CpG island links aging and neoplasia in human colon. *Nat Genet* 1994; **7**: 536-540
- 11 **Zingg JM**, Jones PA. Genetic and epigenetic aspects of DNA methylation on genome expression, evolution, mutation and carcinogenesis. *Carcinogenesis* 1997; **18**: 869-882
- 12 **Wang B**, Shi LC, Zhang WB, Xiao CM, Wu JF, Dong YM. Expression of tumor suppressor gene p16 in gastric cancer and precancerous lesions. *Shijie Huaren Xiaohua Zazhi* 2001; **9**: 39-42
- 13 **Zhou Y**, Gao SS, Li YX, Fang ZM, Zhao X, Qi YJ, Wei JP, Zou JX, Liu G, Jiao LH, Bai YM, Wang LD. Tumor suppressor gene p16 and Rb expression in gastric cardia precancerous lesions from subjects at a high incidence area in northern China. *World J Gastroenterol* 2002; **8**: 423-425
- 14 **He XS**, Su Q, Chen ZC, He XT, Long ZF, Ling H, Zhang LR. Expression, deletion and mutation of p16 gene in human gastric cancer. *World J Gastroenterol* 2001; **7**: 515-521
- 15 **Wei TY**, Wei MX, Yang SM. Expression of cyclin D1 P16 and Rb protein in gastric cancer. *Shijie Huaren Xiaohua Zazhi* 2000; **8**: 234-235

- 16 **Zhu ZY**, Tian X, Wang X, Yang XL. Mutation of p16 and APC gene in gastric cancer. *Shijie Huaren Xiaohua Zazhi* 2000; **8**: 1418-1419
- 17 **Yang SM**, Yang LS, Li L, Deng LY, Wang CY, Yuan XB, Shen XD. Methylation of MTS1/P16 gene and expression of P16 protein in gastric cancer. *Shijie Huaren Xiaohua Zazhi* 2000; **8**: 1427-1429
- 18 **Zhao Y**, Zhang XY, Shi XJ, Hu PZ, Zhang CS, Ma FC. Expression of P16, P53 and proliferating cell nuclear antigen in gastric cancer. *Shijie Huaren Xiaohua Zazhi* 1999; **7**: 246-248
- 19 **Li GX**, Li GQ, Zhao CZ, Xu GL. Relationship between telomerase hTRT and the expression of tumor suppressor gene p53 and p16. *Shijie Huaren Xiaohua Zazhi* 2002; **10**: 591-593
- 20 **Jiang YX**, Zhao MY, Geng M, Chao YC, Wang XY. Expression of P16, cerB-2 protein in gastric tumor. *Shijie Huaren Xiaohua Zazhi* 2002; **10**: 1050-1051
- 21 **Yang ZL**, Li YG, Huang YF, Wang QW. Expression of cyclin D1, CDK4, P16 and Rbin gastric cancer. *Shijie Huaren Xiaohua Zazhi* 2000; **8**: 362-363
- 22 **Wang GT**. Progression in the study on gastric precancerous lesions and its reversion. *Shijie Huaren Xiaohua Zazhi* 2000; **8**: 1-4
- 23 **Kempster S**, Phillips WA, Baindur-Hudson S, Thomas RJ, Dow C, Rockman SP. Methylation of exon 2 of p16 is associated with late stage oesophageal cancer. *Cancer Lett* 2000; **150**: 57-62
- 24 **Yi J**, Wang ZW, Cang H, Chen YY, Zhao R, Yu BM, Tang XM. P16 gene methylation in colorectal cancers associated with Duke's staging. *World J Gastroenterol* 2001; **7**: 722-725
- 25 **Hui AM**, Shi YZ, Li X, Takayama T, Makuuchi M. Loss of p16 (INK4) protein, alone and together with loss of retinoblastoma protein, correlate with hepatocellular carcinoma progression. *Cancer Lett* 2000; **154**: 93-99
- 26 **Lin SC**, Chang KW, Chang CS, Liu TY, Tzeng YS, Yang FS, Wong YK. Alteration s of p16/MTS1 gene in oral squamous cell carcinomas from Taiwanese. *J Oral Pathol Med* 2000; **29**: 159-166
- 27 **Liggett WH Jr**, Sidransky D. Role of the p16 tumor suppressor gene in cancer. *J Clinical Oncol* 1998; **16**: 1197-1206
- 28 **Lu YY**, Gao CF, Cui JQ. Deletion and down-regulation of mts1/p16 gene in humangastric cancer. *Zhonghua Zhongliu Zazhi* 1996; **18**: 189-191
- 29 **Wu MS**, Shun CT, Sheu JC, Wang HP, Wang JT, Lee WJ, Chen CJ, Wang TH, Lin JT. Overexpression of mutant p53 and c-erbB-2 proteins and mutations of the p15 and p16 genes in human gastric carcinoma: with respect to histological subtypes and stages. *J Gastroenterol Hepatol* 1998; **13**: 305-310
- 30 **Jiang HX**, Liu ZM, Zhuang YQ, Yang DH, Jiang YQ, Li JQ. Homologous deletion of p16 gene in human gastric carcinoma. *Huaren Xiaohua Zazhi* 1998; **6**: 934-935
- 31 **Lee YY**, Kang SH, Seo JY, Jung CW, Lee KU, Choe KJ, Kim BK, Kim NK, Koeffler HP, Bang YJ. Alterations of p16INK4A and p15INK4B genes in gastric carcinomas. *Cancer* 1997; **15**: 1889-1896
- 32 **Tang SH**, Luo HS. Aberration of p16 gene and p18 gene in gastric carcinoma. *Shijie Huaren Xiaohua Zazhi* 2001; **9**: 91-92

Edited by Xia HHX

Relationship between the expression of human telomerase reverse transcriptase gene and cell cycle regulators in gastric cancer and its significance

Jin-Chen Shao, Ji-Feng Wu, Dao-Bin Wang, Rong Qin, Hong Zhang

Jin-Chen Shao, Ji-Feng Wu, Dao-Bin Wang, Rong Qin, Hong Zhang, Department of Pathology, Anhui Medical University, Hefei, 230032, Anhui Province, China

Jin-Chen Shao, Department of Pathology, Shanghai Chest Hospital, 241 HuaiHaiXi Rd, Shanghai 200030, China

Supported by Science and Technology Fund, Governmental Department of Education, Anhui Province, No.99j10091

Correspondence to: Professor Ji-Feng Wu, Department of Pathology, Anhui Medical University, Hefei, 230032, Anhui Province, China. jifengwu@mail.hf.ah.cn

Telephone: +86-551-5161130

Received: 2002-09-13 **Accepted:** 2002-10-29

Abstract

AIM: To investigate the expression of human telomerase reverse transcriptase gene (hTERT) in gastric cancer (GC) and its relevance with cell cycle regulators including P16INK4, cyclin and P53.

METHODS: In situ hybridization (ISH) for hTERT mRNA was performed in 53 cases of gastric cancer and adjacent cancerous tissues. Immunohistochemical staining (S-P method) for hTERT protein, P16INK4, cyclinD1 and P53 was performed in 53 cases of GC and adjacent cancerous tissues.

RESULTS: Of 53 cases of GC, the expression of hTERT mRNA and hTERT protein was significantly higher than the expression of hTERT mRNA and hTERT protein in adjacent cancerous tissues ($P < 0.01$), the positive rates of hTERT mRNA and hTERT protein were 79.2 % and 88.6 %. There was a statistical difference of the expression of hTERT protein among well differentiated adenocarcinoma, poorly differentiated adenocarcinoma and mucoid carcinoma. And there was a highly significant positive correlation between the expression of hTERT mRNA and hTERT protein ($r = 0.625$, $P < 0.01$). However, the expression of hTERT mRNA and its protein in GC were not related with other clinicopathological parameters including gender, age, location and size of neoplasm, invasion depth, lymph node metastasis and clinical stage. There was a significant positive correlation between the expression of hTERT mRNA and cyclinD1 protein ($r = 0.350$, $P < 0.01$). There was a significant positive correlation between the expression of cyclinD1 protein and hTERT protein ($r = 0.549$, $P < 0.01$), so was between P53 and hTERT protein ($r = 0.319$, $P < 0.05$).

CONCLUSION: The expression of hTERT gene is correlated significantly to the specific defects of cell cycle on G1/S check point; telomerase activity may depend on cell cycle in gastric cancer and it is available to clarify the molecular mechanism of telomerase activity regulation. The expression of hTERT mRNA and hTERT protein in GC is significantly different from the expression of hTERT mRNA and hTERT protein in adjacent cancerous tissue which indicates that these targets are correlated closely to the occurrence of GC and can provide important morphologic index for diagnosis of GC.

Shao JC, Wu JF, Wang DB, Qin R, Zhang H. Relationship between the expression of human telomerase reverse transcriptase gene and cell cycle regulators in gastric cancer and its significance. *World J Gastroenterol* 2003; 9(3): 427-431

<http://www.wjgnet.com/1007-9327/9/427.htm>

INTRODUCTION

Telomerase activity is absent in most normal somatic cells, but has been detected in the tissues of vast majority of human malignant neoplasm by a highly sensitive method of Trap-PCR assay, and the positive of telomerase activity is 85 %. Currently, it may be the broadest-spectrum molecular marker of malignant neoplasm^[1]. Human telomerase is composed of human telomerase RNA(hTR), human telomerase reverse transcriptase (hTERT/hTERT as well as human telomerase catalytic subunit, hEst2) and human telomerase associated protein (TP) which connects two subunit concerned above^[2-5]. High level hTERT expression has been detected in primary carcinoma, cancer cell lines and tissues which express telomerase activity. There is a consistent correlation between hTERT and telomerase activity. Meanwhile, we can't detect hEst2/hTERT in cell lines whose telomerase activity is negative and in well differentiated tissues^[6-8]. Therefore, Meyerson proposed that the expression of hEst2/hTERT mRNA is a critical step in cell immortalization and tumorigenesis^[3].

It has been reported in telomere-telomerase hypothesis that the senescence process of human cell can be divided into two stages, one is the mortality stage 1(M1), another is the mortality stage 2(M2). When telomerase shortens to a critical length 2kb-4kb, the stability of chromosome will be damaged and the cells enter the senescence stage that is M1. At this stage, DNA breaks with activation of P53-dependent or-independent DNA damage pathways, and the DNA damage can also induce products of CDK3 inhibitors such as p21, p27 and lead to the G1 block and eventual death^[9]. If certain tumor suppressor genes PRb, P53 or P16 are inactivated and are deprived of normal function, cells will prolong their life span, but usually not to immortalization. Then telomere further decreases to M2 stage. Most cells will die at this stage, but rare cells will survive and become immortalized because of the up-regulation or re-activation of telomerase activity which restores the telomere function and the stability of chromosome^[10]. Thus, telomere length and activation of telomerase closely correlate to life span of cells. Zhux *et al* demonstrated that the level of telomerase activity varies with different phases of cell cycle^[11]. In this study, we chose hTERT which could represent telomerase activity and markers around the G1/S check point of cell cycle such as P16, cyclinD1, P53 to reveal the interaction between hTERT gene and regulation of cell cycle and to investigate the role of these indexes in the oncogenesis and development of gastric cancer by in situ hybridization method and immunohistochemistry technique.

MATERIALS AND METHODS

Tissue specimens

Tissue specimens of gastric cancer were obtained from the first affiliated hospital of Anhui Medical University from October 1994 to October 1997. No patient had been treated with anti-neoplasm therapy before surgical removal. 53 patients (42 males, 11 females, from 23 to 73 years old, median age 55 years) were as follows: 22 cases of poorly differentiated adenocarcinoma, 26 cases of well differentiated adenocarcinoma (including 18 cases of tubular adenocarcinoma, 8 papillary adenocarcinoma), 5 cases of mucoid carcinoma (including 4 cases of mucinous adenocarcinoma, 1 case of signet-ring cell carcinoma). 53 cases of adjacent cancerous tissues were taken as controls. All specimens were fixed in 10 % formalin, embedded in paraffin, cut in serial 4 μ m sections and adhered to slides treated by poly-L-Lysine and 0.1 % DEPC.

Reagents

hTERT ISH detection kit was purchased from Boster Biological Technology Ltd. The probe labeled by digoxin is made of three sequences of oligonucleotide of hTERT: (1) 5' -AGTCAGGCTG GGCCT CAGAG AGCTG AGTAG GAAGG-3'; (2) 5' -GCATG TACGG CTGGA GGTCT GTCAA GGTAAGACG-3'; (3) 5' -TGCAC ACCGT CTGGA GGCTG TTCAC CTGCA AATCC-3'.

Rabbit polyclonal antibodies against hTERT and P16INK4, monoclonal mouse antibodies against cyclinD1 and P53, and S-P immunohistochemical kit were purchased from Beijing Zhongshan Biological Technology Ltd.

In situ hybridization

The specimens were deparaffinized and rehydrated through a graded series of ethanol, and endogenous peroxidase was blocked by using 3 % hydrogen peroxide for 10 min. After washed with distilled water treated by 0.1 % DEPC three times at 5 min each, the slides were digested with pepsin diluted by 3 % citric acid at 37 °C for 15-20 min. 20 μ l reagent of pre-hybridization was added to each slide at 37 °C for 2 hours, then 20 μ l of probe was hybridized to each slide at 42 °C for 16-20 hours. After hybridization, each slide was washed with 2 \times SSC twice at 37 °C for 20 min each, then again with 0.2 \times SSC twice at 37 °C for 10 min each. Blocking reagent was dropped to the slides and incubated for 30 min, then the mouse anti-digoxin antibody labeled by biotin was added at 37 °C for 60 min. After washed with 0.5M PBS thrice at 2 min each, the slides were incubated with strept-avidin-biotin complex (SABC) for 20 min at 37 °C, then washed with 0.5M PBS four times at 5 min each. At last, chromogen DAB was added to visualize the reaction products of peroxidase, then the slides were counterstained for nuclei by haematoxylin stain. A negative control was prepared according to the above steps with the probe substituted by 2 \times SSC, a positive control showed positive always in repeated experiments. The positive signals of hTERT mRNA expression were stains with brown-yellow color located in cytoplasm and/or nucleus. The percentage of positive cells was determined by 10 areas at high power fields (\times 400) and graded as follows: negative (-); mildly positive (+), the percentage of positive staining was less than 25 %, moderately positive (++) , the percentage of positive staining was less than 25-50 %; strongly positive (+++), the percentage of positive staining was more than 50 %.

Immunohistochemistry

Immunohistochemical staining was performed by S-P method, anti-hTERT antibody was diluted into 1:100, anti-P16INK4 1:50, anti-cyclinD1 1:50. anti-P53 antibody was the reagent ready to use. A negative control was dyed according to the above

method with the primary antibody substituted by animal serum. The positive standard of hTERT protein expression was stains with the brown-yellow color in cell plasma, P53 positive expression was stains in nucleus, the expression of P16 and cyclinD1 was stains in nucleus and(or) cytoplasm. A semi-quantitative evaluation was used to determine positive expression of positive cell by viewing 10 areas at high power field (\times 400)^[12]: negative(-), cells were stained less than 10 %; mildly positive (+), cells were stained in 11-25 %; moderately positive (++) , cells were stained in 26-50 %; strongly positive (+++), cells were stained over 50 %. And we regarded the last three grades as positive.

Statistical analyses

The data was copied down by Excel and analyzed by SPSS version 10.0. The χ^2 test or Fisher's exact test ($n < 5$) was used for statistical analysis, Spearman rank correlation was performed for correlation analysis.

RESULTS

Expression of hTERTmRNA and hTERT protein

The positive signals of hTERTmRNA were brownish-yellow stains located in cytoplasm and/or nucleus (Figure 1,2). There was barely hTERTmRNA expression in adjacent cancerous tissues, only a few positive cells in dysplasia and intestinal metaplasia of adjacent cancerous tissues. Positive expression of hTERTmRNA was detected in 42 of 53(79.2 %) of GC, but only 8 of 53(15.1 %) of adjacent cancerous tissues. The expression of hTERTmRNA of GC was significantly higher than those of the adjacent cancerous tissues ($P < 0.01$) (Table1).

Table 1 Expression of hTERTmRNA in histologic pattern of gastric cancer and adjacent cancerous tissue

Groups	n	hTERTmRNA				Positive(%)	P
		(-)	(+)	(++)	(+++)		
WD	26	5	12	7	2	80.8	0.067 ^a
PD	22	3	11	8	0	83.4	
Mucoid GC	5	3	1	1	0	40.0	
Adjacent	53	45	6	2	0	15.1	<0.01 ^b

^a: comparison among groups of GC; ^b: comparison between adjacent cancerous tissue and GC. WD: well differentiated adenocarcinoma; PD: poorly differentiated adenocarcinoma.

The positive signals of hTERT protein were brownish-yellow stains located in cytoplasm and the strength of coloration was directly proportional to positive percentage (Figure 3, 4). There was barely hTERT protein expression in adjacent cancerous tissues, but a few positive cells in dysplasia and intestinal metaplasia of adjacent cancerous tissues. Positive expression of hTERT protein was detected in 47 of 43(88.6 %) of GC, but 13 of 53(24.5 %) of adjacent cancerous tissues, so there was significant difference between GC and adjacent cancerous tissues ($P < 0.01$). There was statistical difference of the expression of hTERT protein among groups of different histologic patterns. Further comparison showed no significant difference between well differentiated adenocarcinoma and poorly differentiated adenocarcinoma, but there was statistical difference between mucoid carcinoma and well differentiated adenocarcinoma, so was mucoid carcinoma and poorly differentiated adenocarcinoma (Table2). And there was a highly significant positive correlation between the expression of hTERTmRNA and its protein ($r = 0.625$, $P < 0.01$).

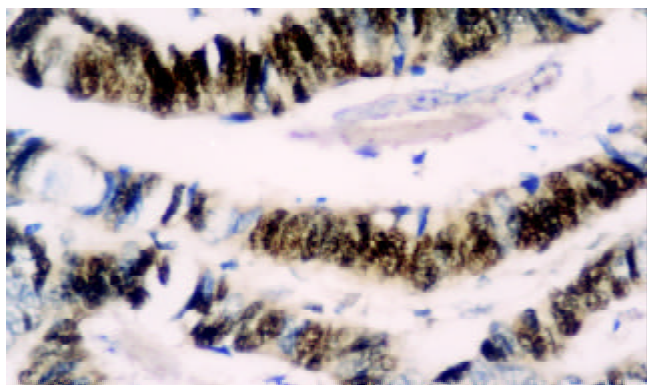


Figure 1 The expression of hTERTmRNA is strongly positive in tubular adenocarcinoma. ISH×400.

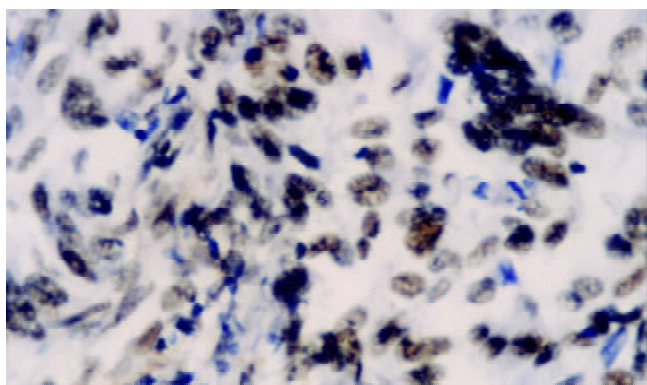


Figure 2 The expression of hTERTmRNA is moderately positive in poorly differentiated adenocarcinoma. ISH×400.

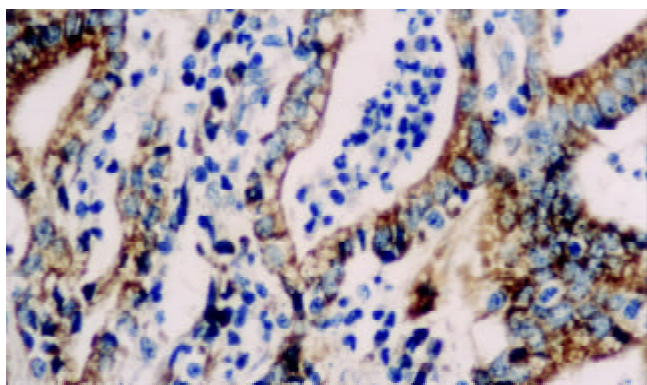


Figure 3 The expression of hTERT protein is strongly positive in papillary adenocarcinoma. S-P×400.

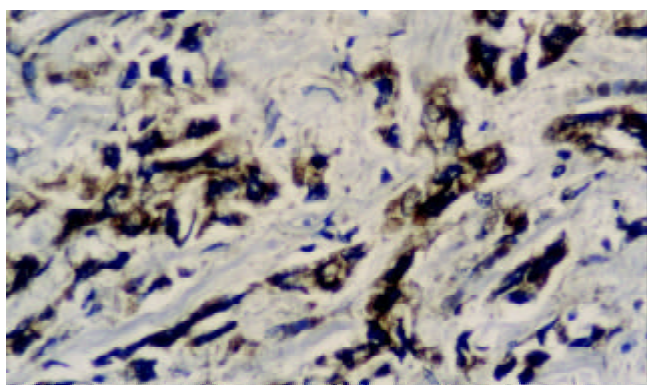


Figure 4 The expression of hTERT protein is moderately positive in poor differentiated adenocarcinoma. S-P×400.

Table 2 Expression of hTERT protein in histologic pattern of gastric cancer and adjacent cancerous tissue

Groups	n	hTERT protein				Positive(%)	P
		(-)	(+)	(++)	(+++)		
WD	26	1	6	15	4	96.2	<0.01 ^a
PD	22	2	9	10	1	90.9	
Mucoid GC	5	3	2	0	0	40.0	<0.01 ^b
Adjacent	53	40	11	2	0	24.5	

^a: comparison among groups of GC; ^b: comparison between adjacent cancerous tissue and GC.

We grouped the 53 cases of cancer patients who had complete clinical data as gender, age, tumor location and size, lymph node metastasis, invasion depth and clinical staging, and found that the expression of hTERTmRNA and its protein in GC was not related with clinicopathological parameters concerned above (Table 3).

Table 3 Relationship between the expression of hTERTmRNA, hTERT protein and clinicopathological parameters in gastric cancer

Parameters	n	hTERTmRNA positive (%)	P	hTERT protein positive(%)	P
Gender					
Male	42	35 (83.3)	0.309	39 (92.9)	0.180
Female	11	7 (63.6)		8 (72.7)	
Age(years)					
<55	25	18 (72.0)	0.219	20 (80.0)	0.147
≥55	28	24 (85.7)		27 (96.4)	
Tumor size(cm)					
< 5	24	20 (83.3)	0.735	22 (91.7)	0.678
≥5	29	22 (75.9)		25 (86.2)	
Tumor location					
Cardia	26	23 (88.5)	0.128	24 (92.3)	0.529
Body	16	10 (62.5)		13 (81.3)	
Antrum	11	9 (81.8)		10 (90.9)	
Lymph node metastasis					
Absent	25	18 (72.0)	0.219	20 (80.0)	0.089
Present	28	24 (85.7)		27 (96.4)	
Invasion depth					
Not invading serosa	8	7 (87.5)	0.879	7 (87.5)	1.000
Invading serosa	45	35 (77.8)		40 (88.9)	
Clinical stage					
I and II	47	37 (78.7)	1.000	41 (87.2)	0.806
III and IV	6	5 (83.3)		6 (100.0)	

Correlation between hTERTmRNA, hTERT protein and cell cycle regulators

The positive percentage of P16INK4 expression was 60.3 % (32/53) of GC, but 88.6 % (47/53) of the adjacent cancerous tissues; the positive percentage of cyclinD1 overexpression was 69.8 % (37/53) of GC, but 5.7 % (3/53) of adjacent cancerous tissues; the positive expression of P53 was 32 of 53 (60.4 %) of GC, but none of adjacent tissues. We analyzed relationship between hTERTmRNA, hTERT protein and cell cycle regulators through Spearman rank correlation. There was a significant positive correlation between the expression of hTERT mRNA and cyclinD1 protein ($r=0.350$, $P<0.01$), and a significant positive correlation between the expression of cyclinD1 protein and hTERT protein ($r=0.549$, $P<0.01$), so was P53 and hTERT protein ($r=0.319$, $P<0.05$). The expression of

P16INK4 didn't correlate with hTERTmRNA and hTERT protein, but the tumor tissues of the group with negative P16INK4 in combination with cyclinD1 overexpression had the strongest positive stains of hTERTmRNA, and the hTERTmRNA overexpression of this group was 79 % (10/13). However, the hTERTmRNA overexpression of the group with positive P16INK4 in combination with low-expression of cyclinD1 was 37.5 % (3/8), but there was no significant difference between the two groups ($P>0.05$).

DISCUSSION

Current studies have proposed that activation of telomerase is a critical step in tumorigenesis of gastric cancer. Jong *et al* observed telomerase activity in 25 of 27 primary GC and found the up-regulation of hTERTmRNA expression in 26 of 26 GC tissues by RT-PCR analysis^[6]. Hiyama *et al* had detected telomerase activity in 66 samples of primary GC and found that the positive percentage was 85 %, but 6 % in the adjacent cancerous tissues^[13]. In our study, we detected the expression of hTERT gene in 53 GC specimens by ISH and immunohistochemistry, and found that positive percentage of hTERTmRNA and hTERT protein was 79.2 % and 88.6 % respectively in GC, and was 15.1 % and 24.5 % in the adjacent cancerous tissues. Meanwhile, the index of hTERT could be located for observation and determined semiquantitatively. So it provided an important morphological marker for detection of GC. It is reported that telomerase activity is associated with histological differentiation and malignant grade of tumor^[14,15]. However, telomerase activity doesn't correlate with age, gender, tumor stage and histological differentiation of gastric cancer^[16-19]. In our present study of GC, the expression of hTERTmRNA and hTERT protein was not associated with clinicopathological parameters including gender, age, tumor size, location, lymph node metastasis, invasion depth and clinical staging. There was statistical difference of hTERT protein only between mucoid carcinoma and well differentiated adenocarcinoma, poorly differentiated adenocarcinoma, but our cases of mucoid carcinoma were few. Therefore, we considered that the expression of hTERT gene might be associated with gastric carcinogenesis, but not involved in differentiation and biological property of the tumor. Mild expression of hTERTmRNA and hTERT protein in dysplasia and intestinal metaplasia of adjacent cancerous tissues showed that the expression of hTERT gene might be presented in precancerous lesions or diseases, and the positive cells may be precancerous cells, but it was needed to do further studies to demonstrate the precise significance of this phenomenon.

There are several checkpoints of different function during cell cycle including G1/S checkpoint, S checkpoint and G2/M checkpoint. G1/S checkpoint that is the PRb pathway is especially important to ensure completion of cell cycle events on schedule and to prevent abnormal cells from proliferation to carcinogenesis^[20]. At the end of G1 stage, cyclinD1 combined with CDK4/6 is responsible for the phosphorylation of PRB to release an important transcription factor -E2F, which initiates DNA synthesis and drives the cells through G1/S checkpoint. There are two vital inhibitory pathways of G1/S checkpoint, one is that P16INK4 competitively combines with CDK4 against cyclinD1 to suppress CDK4 activity^[21,22], the other is that P53 initiates P21 gene to express P21 protein combined with cyclinD1/CDK4 and to inhibit the activity of cyclinD1/CDK4 when DNA is damaged^[23-29]. The two pathways both abolish phosphorylation of PRb, and cell cycle arrests at G1 phase. It is reported at the M1/M2 model of telomere-telomerase hypothesis that a cell can't obtain immortality until it passes through M1/M2 stage. When the activity of tumor suppressor proteins such as P53, PRb,

P16INK4 are absent, the cells can prolong their life by passing through M1 stage, thus there will provide more chances of activating telomerase for those cells to pass through M2 and obtain immortality^[30-33].

There were a few studies about relationship between P16INK4 and telomerase. In the studies of human keratinocytes and mesothelial cells, Dickson *et al* proposed that the expression of hTERT and loss of P16INK4 were two prerequisites for cell immortalization and carcinogenesis^[34]. Landberg *et al* reported that though down-regulation of P16INK4 was not related to telomerase activity, tumors with low P16INK4 had demonstrated to have high activity of telomerase; down-regulation of P16INK4 alone was insufficient to activation of telomerase, and it was necessary in combination with other cell cycle defects such as overexpression of cyclinD1 or cyclinE^[35]. In our study of GC, the expression of P16INK4 was not associated with hTERTmRNA and hTERT protein, but there were two strong positive cases of hTERTmRNA which were absence of P16INK4 expression. So it was coordinate with studies in breast cancer of Landberg. CyclinD1 and P16INK4 locating in up-stream of PRb regulated phosphorylation of PRb and combined with CDK competitively, and the function of the two regulators was just contrary. During the progress of carcinogenesis, the abnormal expression of the two was in cooperation. Absence of P16INK4 and overexpression of cyclinD1 always occurred at the same time in studies of telomerase. In the investigation of development of UVB-induced tumors in SKH-1 hairless mice, Balasubramanian *et al* found that telomerase activity increased persistently after exposure to UVB, meanwhile, the expression of cyclinD1 and cyclinE was up-regulated when combined with CDK4, CDK2, and the expression of P16INK4, P21WAF1 and P27KIP1 all changed significantly between tumor and normal epidermis^[36]. It was reported that the overexpression of cyclinD1 protein was associated with high telomerase level in the studies of breast cancer, and tumors with cyclinD1 or E overexpression in combination with low P16INK4 and normal PRb demonstrated high activity of telomerase^[35]. In our study, there was positive correlation between cyclinD1 protein and hTERTmRNA, hTERT protein, the strongest expression of hTERTmRNA existed in the tumor sample which presented the absence of P16INK4 and overexpression of cyclinD1 at the same time. Our data demonstrated that cyclinD1 protein was highly correlated with the expression of hTERT gene. The mechanism may be that the overexpression of cyclinD1 protein accelerates the phosphorylation of PRb and elevates the proliferation rate of abnormal cells, then cell cycle loses regulation. Activated telomerase drives cells to pass through M2 stage to tumorigenesis. If in combination with inactivation of tumor suppressor genes such as the loss of P16INK4, it is especially helpful for activation of telomerase and quickening the pace of carcinogenesis. Therefore, the overexpression of cyclinD1 represents a cell cycle defect correlated with telomerase activity closely. Li *et al* reported that telomerase activity was inhibited lately in human breast cancer cells after introducing recombinant human P53 to them, and this experiment indicated that activity of telomerase might be regulated by P53 *in vivo* and the down-regulation of P53 might increase the telomerase activity^[37]. In our study, the expression of P53 positively correlated with hTERT protein; the result demonstrated that P53 regulated the telomerase, and it prompted that when the pathway of P53-P21WAF1 was inactive, abnormal cells devoid of braking mechanism and passing through G1/S checkpoint to S stage at which telomerase activity increases giving cells the chance to pass through M2 and achieving immortality that produces specific tumor phenotype.

Our data shows that the expression of hTERT gene is correlated significantly to the specific defects of cell cycle in

G1/S checkpoint, which proposes that telomerase activity may depend on cell cycle in gastric cancer and thus helps to clarify the molecular mechanism of telomerase activity regulation.

REFERENCES

- 1 **Hiyama E**, Kodama T, Shinbara K, Iwao T, Itoh M, Hiyama K, Shay JW, Matsuura Y, Yokoyama T. Telomerase activity is detected in pancreatic cancer but not in benign tumors. *Cancer Res* 1997; **57**: 326-331
- 2 **Feng J**, Funk WD, Wang SS, Weinrich SL, Avilion AA, Chiu CP, Adams RR, Chang E, Allsopp RC, Yu J, Li S, West MD, Harely CB, Andrews WH, Greider CW, Villeponteau B. The RNA component of human telomerase. *Science* 1995; **269**: 1236-1241
- 3 **Meyerson M**, Counter CM, Eaton EN, Ellisen LW, Steiner P, Caddle SD, Ziaugra L, Beijersbergen RL, Davidoff MJ, Liu Q, Bacchetti S, Haber DA, Weinberg RA. hEST2, the putative human telomerase catalytic subunit gene, is up-regulated in tumor cells and during immortalization. *Cell* 1997; **90**: 785-795
- 4 **Smith S**, Gariat I, Schmitt A, de Lange T. Tankyrase, a poly(ADP-ribose) polymerase at human telomerase. *Science* 1998; **282**: 1484-1487
- 5 **Harrington L**, McPhail T, Mar V, Zhou W, Oulton R, Bass MB, Arruda I, Robinson MO. A mammalian telomerase-associated protein. *Science* 1997; **275**: 973-977
- 6 **Jong HS**, Park YI, Kim S, Sohn JH, Kang SH, Song SH, Bang YI, Kim NK. Up-regulation of human telomerase catalytic subunit during gastric carcinogenesis. *Cancer* 1999; **86**: 559-565
- 7 **Meyerson M**. Telomerase enzyme activation and human cell immortalization. *Toxicol Lett* 1998; **102-103**: 41-45
- 8 **Takakura M**, Kyo S, Kanaya T, Tanaka M, Inoue M. Expression of human telomerase subunits and correlation with telomerase activity in cervical cancer. *Cancer Res* 1998; **58**: 1558-1561
- 9 **Vaziri H**, Benchimol S. From telomere loss to P53 induction and activation of a DNA-damage pathway at senescence: the telomere loss/DNA damage model of cell aging. *Exp Gerontol* 1996; **31**: 295-301
- 10 **Rogan EM**, Bryan TM, Hukku B, Maclean K, Chang AC, Moy EL, Englezou A, Warneford SG, Dalla-Pozza L, Reddel RR. Alterations in P53 and P16INK4 expression and telomere length during spontaneous immortalization of Li-Fraumeni syndrome fibroblasts. *Mol Cell Biol* 1995; **15**: 4745-4753
- 11 **Zhu X**, Kumar R, Mandal M, Sharma N, Sharma HW, Dhingra U, Sokoloski JA, Hsiao R, Narayanan R. Cell cycle-dependent modulation of telomerase activity in tumor cells. *Proc Natl Acad Sci USA* 1996; **93**: 6091-6095
- 12 **Barnes DM**, Dublin EA, Fisher CJ, Levison DA, Millis RR. Immunohistochemical detection of p53 protein in mammary carcinoma: an important new independent indicator of prognosis? *Hum Pathol* 1993; **24**: 469-476
- 13 **Hiyama E**, Yokoyama T, Tatsumoto N, Hiyama K, Imamura Y, Murakami Y, Kodama T, Piatyszek MA, Shay JW, Matsuura Y. Telomerase activity in gastric cancer. *Cancer Res* 1995; **55**: 3258-3262
- 14 **Sharma HW**, Sokoloski JA, Perez JR, Maltese JY, Sartorelli AC, Stein CA, Nichols G, Khaled Z, Telang NT, Narayanan R. Differentiation of immortal cells inhibits telomerase activity. *Proc Natl Acad Sci USA* 1995; **92**: 12343-12346
- 15 **Yuan X**, Zhang B, Ying J, Jin Y, Hou L. Expression of telomerase gene in human tumor tissues. *Zhonghua Binglixue Zazhi* 2000; **29**: 16-19
- 16 **Ahn MJ**, Noh YH, Lee YS, Lee JH, Chung TJ, Kim IS, Choi IY, Kim SH, Lee JS, Lee KH. Telomerase activity and its clinicopathological significance in gastric cancer. *Eur J Cancer* 1997; **33**: 1309-1313
- 17 **Yang SM**, Fang DC, Luo YH, Lu R, Yang JL, Liu WW. The Detection of telomerase activity and subunit in different lesions of gastric mucosa. *Aizheng* 2001; **20**: 23-27
- 18 **Zhan WH**, Ma JP, Peng JS, Gao JS, Cai SR, Wang JP, Zheng ZQ, Wang L. Telomerase activity in gastric cancer and its clinical implications. *World J Gastroenterol* 1999; **5**: 316-319
- 19 **Yao XX**, Yin L, Sun ZC. The expression of hTERT mRNA and cellular immunity in gastric cancer and precancerosis. *World J Gastroenterol* 2002; **8**: 586-590
- 20 **Clurman BE**, Roberts JM. Cell cycle and cancer. *J Natl Cancer Inst* 1995; **87**: 1499-1501
- 21 **Kamb A**, Gruis NA, Weaver-Feldhaus J, Liu Q, Harshman K, Tavtigian SV, Stockert E, Day RS 3rd, Johnson BE, Skolnick MH. A cell cycle regulator potentially involved in genesis of many tumor types. *Science* 1994; **264**: 436-440
- 22 **Serrano M**, Hannon GJ, Beach D. A new regulatory motif in cell-cycle control causing specific inhibition of cyclin D/CDK4. *Nature* 1993; **366**: 704-707
- 23 **Harper JW**, Adami GR, Wei N, Keyomarsi K, Elledge SJ. The p21 Cdk-interacting protein Cip1 is a potent inhibitor of G1 cyclin-dependent kinases. *Cell* 1993; **75**: 805-816
- 24 **el-Deiry WS**, Tokino T, Velculescu VE, Levy DB, Parsons R, Trent JM, Lin D, Mercer WE, Kinzler KW, Vogelstein B. WAF1, a potential mediator of p53 tumor suppression. *Cell* 1993; **75**: 817-825
- 25 **Deng C**, Zhang P, Harper JW, Elledge SJ, Leder P. Mice lacking p21CIP1/WAF1 undergo normal development, but are defective in G1 checkpoint control. *Cell* 1995; **82**: 675-684
- 26 **Somasundaram K**, Zhang H, Zeng YX, Houvras Y, Peng Y, Zhang H, Wu GS, Licht JD, Weber BL, El-Deiry WS. Arrest of the cell cycle by the tumour-suppressor BRCA1 requires the CDK-inhibitor p21WAF1/Cip1. *Nature* 1997; **389**: 187-190
- 27 **Liu Y**, Martindale JL, Gorospe M, Holbrook NJ. Regulation of p21WAF1/CIP1 expression through mitogen-activated protein kinase signaling pathway. *Cancer Res* 1996; **56**: 31-35
- 28 **Marchetti A**, Doglioni C, Barbareschi M, Buttitta F, Pellegrini S, Bertacca G, Chella A, Merlo G, Angeletti CA, Dalla Palma P, Bevilacqua G. p21 RNA and protein expression in non-small cell lung carcinomas: evidence of p53-independent expression and association with tumoral differentiation. *Oncogene* 1996; **12**: 1319-1324
- 29 **Greenblatt MS**, Bennett WP, Hollstein M, Harris CC. Mutations in the P53 tumor suppressor gene: clues to cancer etiology and molecular pathogenesis. *Cancer Res* 1994; **54**: 4855-4878
- 30 **Sherr CJ**. Cancer cell cycles. *Science* 1996; **274**: 1672-1677
- 31 **Herman JG**, Merlo A, Mao L, Lapidus RG, Issa JP, Davidson NE, Sidransky D, Baylin SB. Inactivation of the CDKN2/p16/MTS1 gene is frequently associated with aberrant DNA methylation in all common human cancers. *Cancer Res* 1995; **55**: 4525-4530
- 32 **Velculescu VE**, El-Deiry WS. Biological and clinical importance of the p53 tumor suppressor gene. *Clin Chem* 1996; **42**: 858-868
- 33 **Cho Y**, Gorina S, Jeffrey PD, Pavletich NP. Crystal structure of a p53 tumor suppressor-DNA complex: understanding tumorigenic mutations. *Science* 1994; **265**: 346-355
- 34 **Dickson MA**, Hahn WC, Ino Y, Ronfard V, Wu JY, Weinberg RA, Louis DN, Li FP, Rheinwald JG. Human keratinocytes that express hTERT and also bypass a P16(INK4a)-enforced mechanism that limits life span become immortal yet retain normal growth and differentiation characteristics. *Mol Cell Biol* 2000; **20**: 1436-1447
- 35 **Landberg G**, Nielsen NH, Nilsson P, Emdin SO, Cajander J, Roos G. Telomerase activity is associated with cell cycle deregulation in human breast cancer. *Cancer Res* 1997; **57**: 549-554
- 36 **Balasubramanian S**, Kim KH, Ahmad N, Mukhtar H. Activation of telomerase and its association with G1-phase of the cell cycle during UVB-induced skin tumorigenesis in SKH-1 hairless mouse. *Oncogene* 1999; **18**: 1297-1302
- 37 **Li H**, Cao Y, Berndt MC, Funder JW, Liu JP. Molecular interactions between telomerase and the tumor suppressor protein P53 *in vitro*. *Oncogene* 1999; **18**: 6785-6794

• GASTRIC CANCER •

Prospective cohort study of comprehensive prevention to gastric cancer

Hai-Qiang Guo, Peng Guan, Hai-Long Shi, Xuan Zhang, Bao-Sen Zhou, Yuan Yuan

Hai-Qiang Guo, Peng Guan, Hai-Long Shi, Xuan Zhang, Bao-Sen Zhou, Department of Epidemiology, College of Public Health, China Medical University, Shenyang 110001, Liaoning Province, China
Yuan Yuan, Cancer Institute, The First Clinical Hospital, China Medical University, Shenyang 110001, Liaoning Province, China
Supported by National Ninth Five-year Study Program for Taking Key Scientific Problems, No.96-906-01-04, and National Tenth Five-year Study Program for Taking Key Scientific Problems, No. 2001BA703B06(B)

Correspondence to: Prof. Yuan Yuan, Cancer Institute, The First Clinical Hospital, China Medical University, Shenyang 110001, Liaoning Province, China. yyuan@mail.cmu.edu.cn

Telephone: +86-24-23256666-6292

Received: 2002-07-17 **Accepted:** 2002-11-04

Abstract

AIM: To evaluate the preliminary effects of comprehensive prevention of gastric cancer in Zhuanghe County epidemiologically.

METHODS: Stratified sampling and cluster sampling were applied to define the intervention group and the control group. The prospective cohort study was used for evaluating the effect of preventing gastric cancer. The relative risk (RR) and attributable risk percent (AR %) of intervention on gastric cancer death were calculated. Potential years of life lost (PLYL) of the disease was analyzed, and the RR and AR % of PYLL were calculated. Survival analysis was applied among the screened patients.

RESULTS: In the first 4 years after intervening, the relative risk (RR) of intervention on death was 0.5059 (95 % CI: 0.3462~0.7392, $P<0.05$) with significance statistically. AR % of the intervention on death was 49.41 %. The RR of intervention on cumulative PYLL was 0.6778 (95 % CI: 0.5604~0.8198, $P<0.05$) with statistic significance. AR % of the intervention on cumulative PYLL was 30.32 %. The four-year survival rate of the screened patients was 0.6751 (95 % CI: 0.5298~0.9047).

CONCLUSION: The initiative intervention results showed that the intervention approach used in the trial was effective, it reduced mortality and increased survival rate, and alleviated the adverse effect of gastric cancer on the health and life of screened population.

Guo HQ, Guan P, Shi HL, Zhang X, Zhou BS, Yuan Y. Prospective cohort study of comprehensive prevention to gastric cancer. *World J Gastroenterol* 2003; 9(3): 432-436
<http://www.wjgnet.com/1007-9327/9/432.htm>

INTRODUCTION

Gastric cancer is one of the most common malignant tumor, its prevalence in 1999 was 138.60×10^{-5} according to the report of WHO^[1], however, its prevalence (300.87×10^{-5}) and mortality

rate (29.31×10^{-5}) are even higher in China^[1]. The incidence of gastric cancer has been declining globally during the recent decades, but not in China^[2]. It was believed that the main reasons of the declining were prevention and diagnosis, but not therapy^[3]. Most studies show that the incidence of gastric cancer is related to dietary factors, infection of helicobacter pylori(Hp), etc.^[4-9]. If these relative factors were eliminated or decreased, the incidence and mortality of gastric cancer would be lowered., thus gastric cancer could be prevented^[10-13]. So it is very important to find an effective comprehensive preventive method for gastric cancer.

Zhuanghe is a county in Liaoning Province with total population of approximate 900 000, locates along the seaside of the Huanghai Sea. The previous survey showed that the incidence of gastric cancer in this county was higher than the average level of other areas. In 1994, the mortality rate was 49.55×10^{-5} in male, and 22.23×10^{-5} in female. The population in Zhuanghe County has been surveyed in census and studied for 18 years by the Stomach Investigation Group of China Medical University because of higher incidence and mortality of gastric cancer. A series of comprehensive preventive approaches have been applied since 1997, including primary and secondary prevention. The goal was to explore a series of comprehensive preventive approaches to reduce the incidence and the mortality of gastric cancer. The initiative effect of intervention approaches by epidemiological study was evaluated in this paper.

MATERIALS AND METHODS

Definition of sample

Stratified sampling and cluster sampling were applied to define the intervention group and the control group. Each village in this county was stratified into two groups according to location geographically close seaside or not, then the sampled villages were defined by cluster sampling in the two groups, and the number of the sampled villages in each group was proportional to its location stratification. All individuals of the sampled villages were used as the samples.

Sixteen villages were sampled as the intervention group, other 14 villages were used as the control based on location, economic level, and proportion of population in each intervention village. 63 133 persons from 30 villages, 16 870 in the intervention group, and 14 900 in the control group were observed, respectively. The age and sex were proportional in each group.

Intervention approaches

The design of the intervention was as the following (Figure 1).

Common approaches in intervention and control group
Knowledge of prevention and treatment of gastric cancer, especially dietary habits was provided for all residents through broadcasting, video, brochures and face-to-face conversation.
Approaches in intervention groups
Initially 3 033 persons were selected as suspected high risk population from intervention villages according to the epidemiological survey and clinical symptoms. Persons who had the family history of

gastric cancer, and/or were over 35 years old and had history of gastric illness, or had obvious symptoms of gastric illness were grouped as suspected high risk population, from which 1781 persons were further detected and grouped as high risk population of gastric cancer^[16-18], and were treated with antibiotics, Chinese herb medicine, and nutritional therapy, based on X-ray, HP detected, and gastroscopic and pathological examination^[19-21]. Patients with gastric cancer screened from the high risk population were treated promptly.

The whole process of screening and treatment was performed under strict quality control. Twenty five percent of intervened individuals were randomly selected and checked for the compliance to medication by interviewing with individuals and their family and measuring the metabolites of medicine in urine, results showed that the compliance rate was 96.6 %. The screening and surveying were initiated in 1997 and had been processed successfully since then.

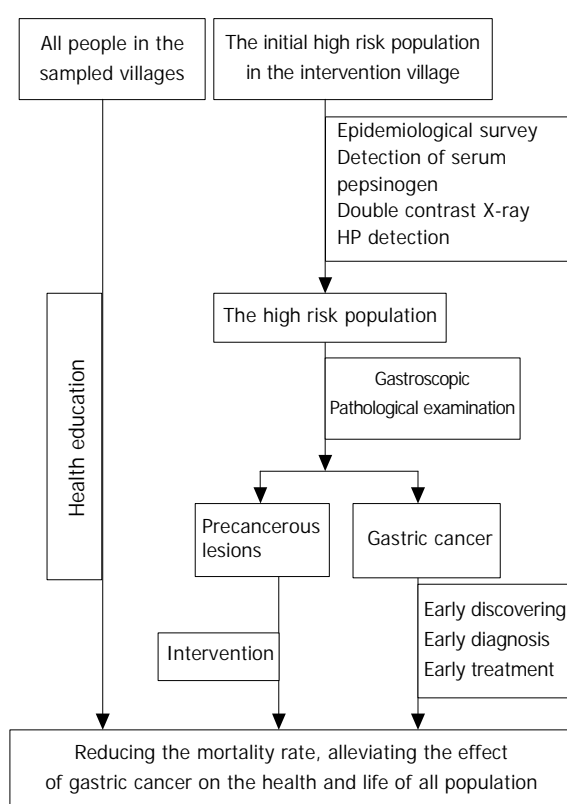


Figure 1 The intervention trial sketch.

Analysis of data

The prospective cohort study was applied to observe the samples. The cause of all death including gastric cancer from 1996 to 2000 were documented in both intervention group and control groups. The screened patients with gastric cancer were observed and reported annually.

The relative risk (RR) and attributable risk percent (AR %) of intervention on death of gastric cancer, potential years of life lost (PLYL) of the disease, and the RR and AR % of PYLL were calculated. The survival rate of all the screened patients with gastric cancer was evaluated.

The maximum expectancy method was adopted to calculate PYLL^[22].

$$PYLL = \sum a_i d_i, a_i = L - x - 0.5$$

L: the upper limit age, evaluated at 70.

x: the middle value of age interval.

a_i : the residual years from age interval ($i \sim i+1$) to the maximum expect age (L).

d_i : the death number of age interval ($i \sim i+1$) from the disease.
 $PYLL = (PYLL/N) * 1000\%$.

N: the number of total observed population or person-years.

Life-table method and product-limit method^[23] were applied to analyze the survival rate of all the screened patients with gastric cancer.

$$S(t) = \prod (1 - d_i/n_i)$$

n_i : the adjusted population at the beginning of the period i .

d_i : the death number of the period i .

RESULT AND ANALYSIS

General

The composition of the sample is shown in Table 1.

Table 1 Composition of the samples

	Male	Female	Total
Intervention group	26 922	26 256	53 178
Control group	23 840	23 924	47 788
Total	50 762	50 204	100 966

During the first screening in 1997, 32 patients with gastric cancer were diagnosed, in which 18 patients were early gastric cancer, and 14 were advanced gastric cancer. The incidence of cancer in the screened group was 1.80 % (32/1781). In addition, 1 306 persons were detected having other gastric diseases. The screening rate of all gastric diseases was 75.13 % (1 338/1 781), therefore the screening method was very effective. From 1998 to 1999, 12 patients with gastric cancer were detected, in which 7 patients were early gastric cancer, and 5 were advanced gastric cancer.

Mortality of gastric cancer

The mortality rate of gastric cancer in Zhuanghe from 1996 to 2000 was between $45.21 \times 10^{-5} \sim 63.29 \times 10^{-5}$, the annual rate was 53.24×10^{-5} (person·year)⁻¹, whose 95 % CI is $44.57 \times 10^{-5} \sim 61.91 \times 10^{-5}$, which is higher than the average rate in China (29.31×10^{-5}). The rate in male was 75.11×10^{-5} (95 % CI: $60.60 \times 10^{-5} \sim 89.61 \times 10^{-5}$), and in female was 30.08×10^{-5} (95 % CI: $20.98 \times 10^{-5} \sim 39.18 \times 10^{-5}$). The death from gastric cancer was 8.25 % of all death from any reasons, and 38.94 % of all carcinoma deaths, which were higher than that of the national average level ($P < 0.05$)^[24-26].

The annual mortality rate of gastric cancer in Zhuanghe was shown in Figure 2. The alterations of mortality from 1996 to 2000 were not statistically significant.

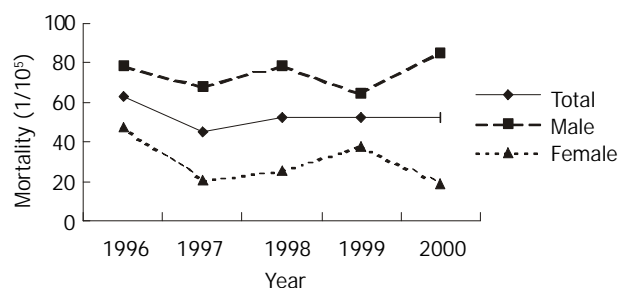


Figure 2 Mortality of gastric cancer in Zhuanghe County from 1996 to 2000.

The annual mortality rates of gastric cancer in intervention groups were shown in Figure 3. The rates in the period from 1997 to 2000 were lower than that in 1996 with no significance by Poison test^[27] ($P > 0.05$ except that in male in 2000. In

contrast, the average mortality rate (34.97×10^{-5}) in intervention groups during post-intervention period (1997-2000) was lower significantly than that (59.31×10^{-5}) in pre-intervention period (1996) (one-sided test, $\chi^2=2.930$, $P<0.05$). However, no statistical decrease of mortality was found in control groups (Figure 4).

The tendency of descending in mortality of gastric cancer was observed (Figure 3). The linear correlation analysis is shown in Table 2. No obvious alteration in the mortality of gastric cancer in control group from 1996 to 2000 was observed.

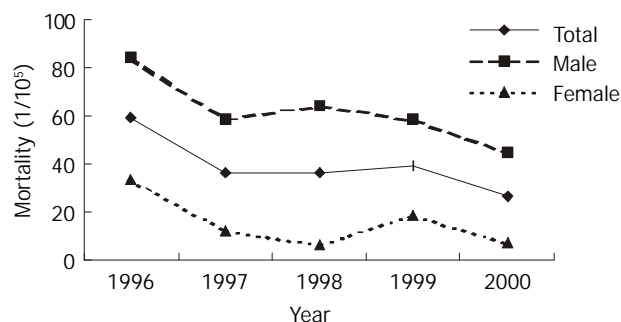


Figure 3 Mortality of gastric cancer in intervention groups from 1996 to 2000.

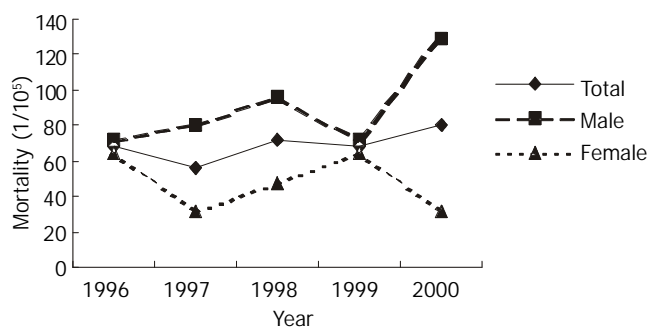


Figure 4 Mortality of gastric cancer in control groups from 1996 to 2000.

Table 2 Linear correlation in gender of gastric cancer mortality in intervention groups

Group	<i>r</i>	<i>F</i>	<i>P</i>
Male	0.8688	9.2369	0.0559
Female	0.6690	2.4308	0.2169
Total	0.8148	5.9256	0.0930

The difference of the mortality rate of gastric cancer between the intervention group and the control group in 1996 was not significant ($\chi^2=0.0283$, $P>0.05$). The annual average rates between the intervention group and the control group from 1997 to 2000 differed significantly ($\chi^2=5.873$, $P<0.05$) (Figure 5).

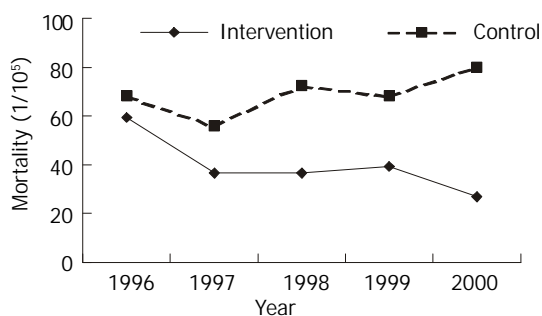


Figure 5 Mortality rate in intervention and control groups from 1996 to 2000.

Relative risk analysis

One hundred and ten patients in both groups had died from gastric cancer since the beginning the trial in 1997. The cumulative mortality rate (CMR) was 34.97×10^{-5} in intervention villages, and 69.13×10^{-5} in control villages. The relative risk (RR) of intervention was 0.5059 (95 % CI: 0.3462~0.7392, $P<0.05$) with statistic significance. The attributable risk percent of the intervention was 49.41 %, which indicated that intervention reduced gastric cancer death by 49.41 % of all population. All these data showed that the intervention approaches can reduce the death of gastric cancer.

Table 3 Cumulative mortality rate and relative risk

	Total person-year	Death No.	CMR (10^{-5})	RR	RR 95%CI	AR%
Control	99 816	69	69.13			
Intervention	117 234	41	34.97	0.5059	0.3462~0.7392	49.41

Potential years of life lost in gastric cancer

From 1996 to 2000, the potential years of life lost (PYLL) of gastric cancer were 731 person-years, and the PYLL was 3.07 ‰ which meant the lost years of 1 000 people from gastric cancer were 3.07 every year. In the intervention group, the PYLL was 300 person-years, and the PYLL was 2.89 ‰. The PYLL of the control group was 431 person-years, and the PYLL was 3.94 ‰ (Figure 6). The PYLL in intervention group in 1996 and 1998 was not significantly different from that in control group ($\chi^2=1.3948$, 0.2074, $P>0.05$), and the differences in 1997, 1999 and 2000 were statistically significant ($\chi^2=5.0603$, 73.2124, 11.4119, $P<0.05$). Difference of the total PYLL from 1997 to 1999 between the intervention group and the control group was significant ($\chi^2=16.1527$, $P<0.01$).

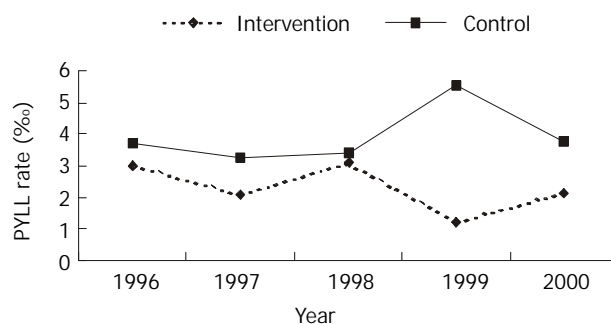


Figure 6 PYLL in intervention group and control group from 1996 to 2000.

The RR of intervention to cumulative PYLL was 0.6778 (95 % CI: 0.5604~0.8198, $P<0.05$), which was statistically significant. The AR % of the intervention to cumulative PYLL was 30.32 %, which showed that the intervention decreased PYLL of gastric cancer by 30.32 % of all population.

Table 4 PYLL and its RR

	Total person-year	PYLL	PYLL (%)	RR	RR 95%CI	AR%
Control	87 757	272	3.10			
Intervention	103 191	223	2.16	0.6778	0.5604~0.8198	30.32

Survival analysis

During the 4-year observation after intervening, 32 patients with gastric cancer were detected by screening, of which 9 patients died. The annual survival rates were shown in Table 5.

Table 5 Annual survival rate and its 95 % CI

Year	Survival rate	Standard error	95 % CI of survival rate
1-	0.8305	0.0691	0.6951, 0.9659
2-	0.7173	0.0852	0.5503, 0.8842
3-	0.7173	0.0852	0.5503, 0.8842
4-	0.6751	0.0956	0.5298, 0.9047

The one-year and three-year survival rate of the screened patients with cancer was 0.8305 (95 % CI: 0.6951~0.9659), and 0.7173 (95 % CI: 0.5503~0.8842), respectively, which are higher than those in Changle County of Fujian Province^[28]. In this study, all screened patients were not operated due to some reasons; otherwise, the survival rate would be higher.

DISCUSSION

All intervention approaches were based on the following studies: (1) Many epidemiological and histological studies showed gastric cancer is related with infection of *Helicobacter pylori*, which cause excessive hyperplasia and reduction of apoptosis of gastric epithelium. These cellular dynamic changes lead to injury of DNA and the generation of gastric cancer cell clone^[29-33]. (2) Garlic oil can inhibit malignant proliferation of cancer cells, and induce their differentiation. The mechanism is likely to adjust the expression of oncogene. Garlic oil can restrain and reverse experimental gastric cancer and precancerous lesions^[34,35]. (3) Surveys showed that cancer is correlated with precancerous lesions. Not all precancerous lesions will develop to cancers, but the generation of cancers may be prevented if the precancerous lesions are cared and cured early^[36,37].

It was reported that gastric cancer was related with high-salt diet and preserved-food diet^[14,15,38,39]. These dietary habits are extremely common in Zhuanghe County, and may be the main cause of gastric cancer^[40]. Accordingly, health education for applying and maintaining right dietary habits was stressed in intervention and control groups.

The analysis of the mortality and PYLLs was focused on all the population instead of a single patient in evaluating the initiative effects of comprehensive preventive approaches. The intervention can reduce the mortality rate of patients with gastric cancer and alleviate the effect of gastric cancer on the health and life of all population. The analysis of PYLL endues the death with weight according to the age of the death, and age standardized mortality rate is applied, so this method reflects the "early death" and the "deferred death". At the initial period of prevention, the decrease of the mortality may not be obvious, but the time on the mortality may be deferred, that is, the survival time of the patients may be prolonged due to early discovering, early diagnosis, and early treatment. It is more suitable to analyze and evaluate the initial effect of comprehensive prevention and treatment of gastric cancer than mortality analysis. Analysis of survival is based on patients with gastric cancer rather than the whole population, and thus it reflects whether the approaches have prolonged the life of patients with gastric cancer.

The results of the survey show that although local mortality rate of gastric cancer in Zhuanghe County is still higher than that of national level in China, the initial outcome of the intervention indicates that the intervention approaches used in the trial are effective, as these approaches have prolonged the screened patients' life, reduced the mortality rate, and alleviated the adverse effect of gastric cancer on the health and life of all population screened. Because effect of chemical intervention effect is behind of the approaches, the initial outcome showed

in this article is mostly due to secondary prevention, that is early discovering, early diagnosis and early treatment.

REFERENCES

- 1 <http://www.who.int/whr/1999/en/report.htm>: The World Health Report 1999 of WHO
- 2 **Li LM.** Epidemiology. 4th ed. Beijing: People's Medical Publishing House, 2000: 86-89
- 3 **Vutuc C,** Waldhoer T, Haidinger G, Ahmad F, Micksche M. The burden of cancer in Austria. *Eur J Cancer Prev* 1999; **8**: 49-55
- 4 **Inoue M,** Tajima K, Kobayashi S, Suzuki T, Matsuura A, Nakamura T, Shirai M, Nakamura S, Inuzuka K, Tominaga S. Protective factor against from atrophic gastritis to gastric cancer -data from a cohort study in Japan. *Int J Cancer* 1996; **66**: 309-314
- 5 **Forman D,** Newell DG, Fullerton F, Yarnell JWG, Stacey AR, Wald N, Sitas F. Association between infection with *Helicobacter pylori* and risk of gastric cancer: evidence from a prospective investigation. *BMJ* 1991; **302**: 1302-1305
- 6 **Correa P.** Human gastric carcinogenesis: a multistep and multifactorial process-First American Cancer Society Award Lecture on Cancer Epidemiology and Prevention. *Cancer Res* 1992; **52**: 6735-6740
- 7 **Chyou PH,** Nomura AM, Hankin JH, Stemmermann GN. A case-cohort study of diet and stomach cancer. *Cancer Res* 1990; **50**: 7501-7504
- 8 **Lee JK,** Park BJ, Yoo KY, Ahn YO. Dietary factors and stomach cancer: a case-control study in Korea. *Int J Epidemiol* 1995; **24**: 33-41
- 9 **Tredaniel J,** Boffetta P, Buiatti E, Saracci R, Hirsch A. Tobacco smoking and gastric cancer: review and meta-analysis. *Int J Cancer* 1997; **72**: 565-573
- 10 **Harris A.** Treatment of *Helicobacter pylori*. *World J Gastroenterol* 2001; **7**: 303-307
- 11 **Wang DX,** Fang DC, Li W, Du QX, Liu WW. A study on relationship between infection of *Helicobacter pylori* and inactivation of antioncogenes in cancer and pre-cancerous lesion. *Shijie Huaren Xiaohua Zazhi* 2001; **9**: 984-987
- 12 **Zhao AG,** Zhao HL, Jin XJ, Yang JK, Tang LD. Effects of Chinese Jianpi herbs on cell apoptosis and related gene expression in human gastric cancer grafted onto nude mice. *World J Gastroenterol* 2002; **8**: 792-796
- 13 **Lao SX,** Chen GX. The traditional Chinese medicine study of precancerous lesions of gastric cancer. *Shijie Huaren Xiaohua Zazhi* 2002; **10**: 1117-1120
- 14 **Kato I,** Tominaga S, Ito Y, Kobayashi S, Yoshii Y, Matsuura A, Kameya A, Kano T. A comparative case-control analysis of stomach cancer and atrophic gastritis. *Cancer Res* 1990; **50**: 6559-6564
- 15 **Beno I,** Sigmundova V. Nitrates and nitrites in gastric juice in chronic gastritis. *Bratisl Lek Listy* 1993; **94**: 531-535
- 16 **Sun LP,** Yuan Y. Determinations of plasma pepsinogen levels and its application to diagnosis and treatment of gastric cancer. *Shijie Huaren Xiaohua Zazhi* 2001; **9**: 1174-1176
- 17 **Hou P,** Tu ZX, Xu GM, Gong YF, Ji XH, Li ZS. *Helicobacter pylori* vacA genotypes and cagA status and their relationship to associated diseases. *World J Gastroenterol* 2000; **6**: 605-607
- 18 **Xiao XD,** Liu WZ. Treatment to infection of *Helicobacter pylori*. *Shijie Huaren Xiaohua Zazhi* 1999; **7**: 3-4
- 19 **Wang W,** Xia T, Zhang ZH. Effects of Yiweicongji Herbs on chronic atrophic gastritis and precancerous conditions. *Shijie Huaren Xiaohua Zazhi* 1999; **7**: 541-542
- 20 **Yao YL,** Zhang WD. Relationship between *Helicobacter pylori* and gastric cancer. *Shijie Huaren Xiaohua Zazhi* 2001; **9**: 1045-1049
- 21 **Shan ZW.** Present situation of study on infection of *Helicobacter pylori* and expectation of its treatment of the traditional Chinese medicine. *Shijie Huaren Xiaohua Zazhi* 1998; **6**: 553-554
- 22 **Ram F,** Dhar M. A modified procedure for calculating person years of life lost. *Janasamkhyā* 1992; **10**: 1-12
- 23 **Zhao ZT.** Research Method and Application of Epidemiology. 1st ed. Beijing: Science Publishing house, 2000:543-545
- 24 **Health Statistical Information Center.** The Annual Data of National Health in 1996. Beijing: Ministry of health China, 1997: 308-310
- 25 **Health Statistical Information Center.** The Annual Data of Na-

- tional Health in 1997. Beijing: Ministry of health China, 1998: 308-310
- 26 **Health Statistical Information Center.** The Annual Data of National Health in 1998. Beijing: Ministry of health China, 1999: 308-310
- 27 **Jin PH.** Medical Statistics. 1st ed. Shanghai: Publishing House of Shanghai Medical University 1993: 349, 203
- 28 **Chen JG,** Li WG, Liu B, Ye BF, Pan HB, Li SK, Chen DL. An epidemiological study on features of the distribution of cancer of some common sites. *Zhonghua Liuxingbingxue Zazhi* 1986; **7**: 193-199
- 29 **McNamara D,** O' Morain C. *Helicobacter pylori* and gastric cancer. *Ital J Gastroenterol Hepatol* 1998; **30** (Suppl): S294-298
- 30 **Sud R,** Wells D, Talbot IC, Delhanty JD. Genetic alterations in gastric cancers from British patients. *Cancer Genet Cytogenet* 2001; **126**: 111-119
- 31 **Chung YJ,** Park SW, Song JM, Lee KY, Seo EJ, Choi SW, Rhyu MG. Evidence of genetic progression in human gastric cancers with microsatellite instability. *Oncogene* 1997; **15**: 1719-1726
- 32 **Xia HX,** Fan XG, Talley NJ. Clarithromycin resistance in *Helicobacter pylori* and its clinical relevance. *World J Gastroenterol* 1999; **5**: 263-266
- 33 **Que FG,** Gores GJ. Cell death by apoptosis: basic concepts and disease relevance for the gastroenterologist. *Gastroenterology* 1996; **110**: 1238-1243
- 34 **Li XG,** Xie JY, Lu YY. Suppressive action of garlic oil on growth and differentiation of human gastric cancer cell line BGC-823. *Shijie Huaren Xiaohua Zazhi* 1998; **6**: 10-12
- 35 **Su Q,** Luo ZY, Teng H, Yin WD, Li YQ, He XE. Effect of garlic and garlic-green tea mixture on serum lipids in MNNG-induced experimental gastric cancer and precancerous lesion. *Shijie Huaren Xiaohua Zazhi* 1998; **6**: 112-113
- 36 **Bajtai A,** Hidvegi J. The role of gastric mucosal dysplasia in the development of gastric cancer. *Pathol Oncol Res* 1998; **4**: 297-300
- 37 **You WC,** Zhang L, Gail MH, Li JY, Chang YS, Blot WJ, Zhao CL, Liu WD, Li HQ, Ma JL, Hu YR, Bravo JC, Correa P, Xu GW, Fraumeni JF Jr. Precancerous lesions in two counties of China with contrasting gastric cancer risk. *Int J Epidemiol* 1998; **27**: 945-948
- 38 **Tominaga K,** Koyama Y, Sasagawa M, Hiroki M, Nagai M. A case-control study of stomach cancer and its genesis in relation to alcohol consumption, smoking, and familial cancer history. *Jpn J Cancer Res* 1991; **82**: 974-979
- 39 **Pisani P,** Oliver WE, Parkin DM, Alvarez N, Vivas J. Case-control study of gastric cancer screening in Venezuela. *Br J Cancer* 1994; **69**: 1102-1105
- 40 **Yuan Y,** Gong W, Xu RT, Wang XJ, Gao H, Dong M, Wu HQ, Wang L, Wang MX, Song XJ, Wang FC, Jiang H, Song LY, Li X, Zhou BS, Zhang YC. Census Report of gastric cancer in Zhuanghe County, a high-risk area of gastric cancer. *Shijie Huaren Xiaohua Zazhi* 1998; **6**(Suppl 7): 478

Edited by Ren SY

Studies on microsatellite instability in p16 gene and expression of hMSH2 mRNA in human gastric cancer tissues

Qin-Xian Zhang, Yi Ding, Xiao-Ping Le, Peng Du

Qin-Xian Zhang, Yi Ding, Xiao-Ping Le, Molecular Cell Biology Research Center, Medical College of Zhengzhou University; Zhengzhou 450052, Henan Province, China

Peng Du, Henan Key Lab. of Molecular Medicine, Zhengzhou 450052, Henan Province, China

Supported by the National Natural Science Foundation of China, No. 39170440

Correspondence to: Pro. Qin-Xian Zhang, Molecular Cell Biology Research Center, Medical College of Zhengzhou University; 40 Daxue Lu, Zhengzhou 450052, Henan Province, China. qxz53@zzu.edu.cn

Telephone: +86-371-6977002 **Fax:** +86-371-6977002

Received: 2002-09-13 **Accepted:** 2002-10-29

Abstract

AIM: To detect the loss of heterozygosity (LOH) frequency of microsatellite sites D9s171, D9s1604 of p16 gene and expression of hMSH2 mRNA in various differentiated types of gastric cancer, adjacent cancer tissues and normal gastric mucosa.

METHODS: LOH was detected by polymerase chain reaction (PCR)-denaturing polyacrylamide gel electrophoresis-silver staining. The expression of hMSH2 mRNA was examined with *in situ* hybridization.

RESULTS: The frequency rate of LOH was significantly higher in gastric cancers than that in adjacent cancer tissues ($P=0.032$). No significant difference was noted among various differentiated types and various clinical stages of gastric cancers. The significantly reduced expression of hMSH2 mRNA positive signal cells exhibited in gastric cancers, in comparison with that in the adjacent cancer tissues and normal gastric mucosa, respectively ($P=0.001$). No significant difference was noted among various clinical stages of gastric cancers ($P>0.05$). The difference of positive signal cells in poorly differentiated cancers and those in well and moderately differentiated cancers were significant ($P<0.001$).

CONCLUSION: The frequencies of LOH in two microsatellite sites, D9s171 and D9s1604, in p16 genome were associated with development of gastric cancer and no significant correlation was demonstrated between the LOH frequency and the cell differentiated types of tumor cells or clinical stages. There was a positive relationship between the expression of hMSH2 mRNA and the differentiated types of gastric cancer.

Zhang QX, Ding Y, Le XP, Du P. Studies on microsatellite instability in p16 gene and expression of hMSH2 mRNA in human gastric cancer tissues. *World J Gastroenterol* 2003; 9(3): 437-441 <http://www.wjgnet.com/1007-9327/9/437.htm>

INTRODUCTION

Microsatellite instability (MI) occurs frequently adjacent to the loci of tumor suppressor genes^[1]. The defects of mismatch

repair (MMR) gene are closely related to the occurrence of MI and abnormality of genes^[2,3]. Expression of p16 gene was significantly reduced in gastric cancer^[4-12] and was associated with the progression and metastasis^[13,14]. The relationship between the MI of p16 gene in the gastric cancer and adjacent cancer tissue and the abnormal expression of MMR gene has rarely been reported. In this paper, two microsatellite loci, D9s171 and D9s1604 located at the upstream of p16 gene, were selected to study the loss of heterozygosity (LOH) of 9p21-22 region in gastric cancer tissues. The expression of hMSH2 mRNA in gastric cancer, adjacent cancer and normal gastric tissues was detected by *in situ* hybridization with hMSH2 oligonucleotide probe.

MATERIALS AND METHODS

Specimens

All the specimens were collected from the First and Second Affiliated Hospital of Medical College of Zhengzhou University and the People Hospital of Henan Province.

Specimens used to extract DNA: Specimens of gastric cancer tissue, adjacent cancer tissue and normal gastric mucosa were from each of 20 patients with gastric cancer. Of 20 patients, there were 4 cases with well differentiated and 16 moderately and poorly differentiated gastric cancer tissue. All specimens were used for isolation of DNA.

Specimens used *in situ* hybridization: gastric cancer specimens in 27 cases (including 20 cases gastric cancer specimens, with no history of radio- or chemotherapy preoperatively), adjacent cancer tissue specimens in 10 cases and normal gastric tissue specimens in 19 cases were used *in situ* hybridization. All the specimens were diagnosed pathologically (well differentiated in 5 cases, moderately 9 and poorly differentiated cancer 13). According to the PTNM of International Alliance of Anticancer in 1987, the specimens were divided into 4 clinical stages, the number in stage I, II, III and IV was 5, 10, 9 and 3, respectively.

Detection of microsatellite instability

The tissue DNA was extracted by routine phenol-chloroform method. The primers were synthesized by Shanghai Cell Biology Research Institute of China Scientific Institute and purified with PAGE. The sequence of primer was as follows, D9s171: 5' AGCTAAGTGAACCTCATCTCTGTCT3', 5' ACCCTAGCACTGATGGTATAGTCT3', and the length of amplified fragment was 159-177bp; D9s1604: 5' CCTGGGTCTCCAAATTTGTCA3', 5' AGCACATGACACTGTGTGTG3', and the length of amplified fragment was 172-196bp. The annealing temperature of PCR was 60 °C and 50 °C, respectively. The PCR products were electrophoresized on 80 g/L denatured polyacrylamide gel under constant voltage of 30 V/cm. The gel was stained with silver staining after electrophoresis.

In situ hybridization

Digoxigenin-labeled hMSH2 oligonucleotide probe and BCIP/NBT staining system were used to demonstrate the expression

of hMSN2 mRNA. Control consisted of specimens pretreated with 0.05 g/L RNase A at 37 °C for 30 min, and specimens hybridized with hybridization buffer without probe.

Analysis of results

Compared with that of normal gastric mucosa removed from the same case, if the band of the identical allele disappeared or its intensity reduced over 50 %, the result was defined as LOH positive. Specimens *in situ* hybridization observed under microscope, the cells with cytoplasm containing bluish violet granules were determined as positive signal cells. Five fields in each specimen was checked randomly.

Statistic analysis

Data of electrophoretic specimens were analyzed using Fisher's exact test of probabilities with SPSS 10.0 statistic software. Correlative analysis were decided by using paired χ^2 test for numerical samples and $P < 0.05$ was considered as significant difference. *In situ* hybridization specimens were treated using one way analysis of variance and $P < 0.05$ was considered as different significantly.

RESULTS

Results of LOH at D9s171 and D9s 1604 of p16 gene in gastric cancer and adjacent cancer tissues (Figure 1 and 2)

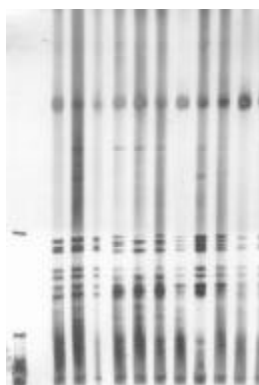


Figure 1 LOH of D9s171 in gastric cancer. Left 1: Marker Left 6: LOH(+).

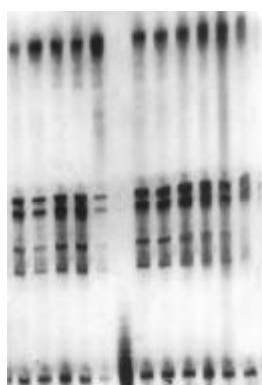


Figure 2 LOH of D9s1604 in gastric cancer. Left 6: LOH(+).

The number of LOH at D9s171 and D9s1604 in cancer tissues in 20 cases was 3 and 10, respectively, and that in adjacent cancer tissues was 2 and 4, respectively. There was no significant difference between the ratio of LOH at the two microsatellite loci. However, the combined ratio of LOH at the two microsatellite loci in gastric cancer tissues was obviously higher than that in adjacent cancer tissue ($P < 0.05$) (Table 1).

Table 1 LOH at D9s171 and D9s 1604 in gastric cancer and adjacent cancer tissue

	LOH(+)	LOH(-)	Total
Gastric cancer tissue	13	7	20
Adjacent cancer tissue	6	14	20
Total	19	21	40

^a $P < 0.05$ vs adjacent cancer tissue.

Relationship between the ratio of LOH and the differentiated type and clinical stage of gastric cancer

The difference of incidence of LOH at D9s1604 in well differentiated adenocarcinoma (1/4) and that in moderately and poorly differentiated cancer (10/16) was not significant ($P > 0.05$). The proportion of LOH in early stage and progressive stage of cancer was 50 % (4/8) and 58.2 (7/12), respectively.

Relationship between the LOH occurred at D9s171 and at D9s1604 in gastric cancer and adjacent cancer tissues

The incidence of LOH at D9s171 and D9s1604 were showed in Table 2. Analysis by paired χ^2 test for numerical sample showed that an intrinsic relation exhibits between them.

Table 2 Relation between LOH occurred at D9s171 and at D9s1604 in gastric cancer

D9s1604	D9s171		Total
	+	-	
+	4	10	14
-	1	25	26
Total	5	35	40

+: LOH (+); -: LOH (-); ^a $P < 0.05$ vs LOH (-).

Expression of hMSH2 mRNA in normal gastric mucosa, gastric cancer and adjacent cancer tissues

The *in situ* hybridization positive signals of hMSH2 mRNA appeared as bluish violet granules distributed in the cytoplasm. No positive signals were found in nucleus. There were round or irregular granules in positive cells in normal gastric tissues. The number of positive signal cells increased from the superficial to deep layer of mucosa. A few positive signal cells scattered in the submucosa and no positive signal cells in muscular layer (Figure 3). Expression of hMSH2 mRNA in gastric cancer and adjacent cancer tissues was significantly decreased than that in normal gastric tissues (Table 3). The positive signal cells mainly scattered in the deep layer of mucosa. No positive signal cells were found in the submucosa and muscular layer (Figure 4, 5).

Table 3 hMSH2 mRNA in the normal gastric mucosa, gastric cancer and adjacent cancer tissue ($\bar{x} \pm s$) (*In situ* hybridization)

	<i>n</i>	No. of positive cases (ratio)	No. of positive cells in each scope
Normal gastric mucosa	19	13(68.4 %)	175.8±26.4 ^a
Adjacent cancer tissue	10	6(60 %)	99.7±16.8 ^b
Gastric cancer tissue	27	20(74.1%)	42.1±25.9 ^c

^a $P < 0.01$ vs adjacent cancer tissue; ^b $P < 0.01$ vs gastric cancer tissue.

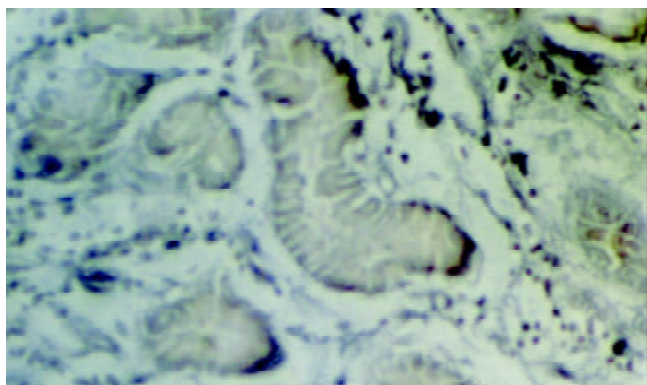


Figure 3 hMSH2 in normal gastric mucosa (×1000).

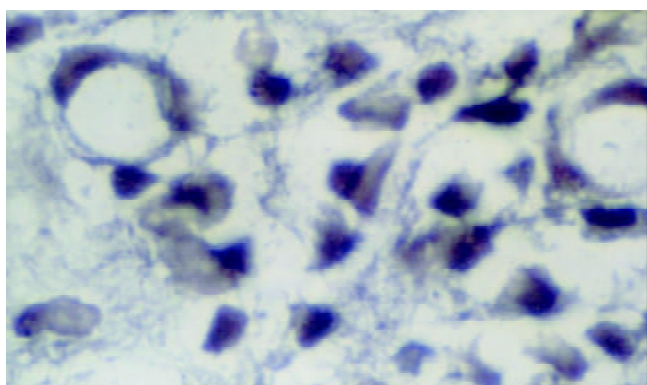


Figure 4 hMSH2 in adjacent gastric cancer tissue (×1000).

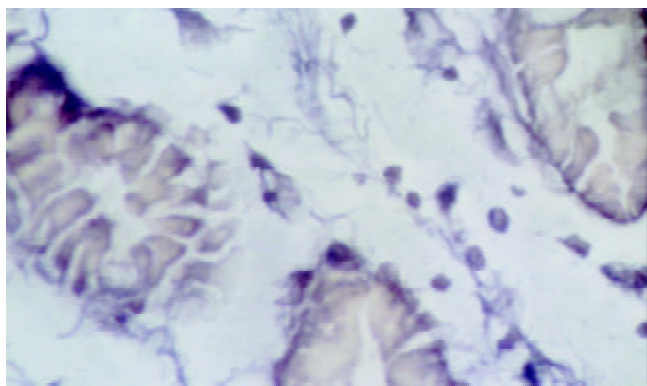


Figure 5 hMSH2 in gastric cancer tissue (×1000).

Expression of hMSH2 mRNA in various clinical stage of gastric cancer

Compared with that in the normal gastric tissue, the expression of hMSH2 mRNA in gastric cancer tissues was reduced significantly. However, there was no obvious difference in the number of positive cells among the various clinical stages of gastric cancer ($P>0.05$) (Table 4).

Table 4 hMSH2 mRNA in various clinical stage gastric cancer (*In situ* hybridization)

Clinical stage	<i>n</i>	No. of positive cases	No. of positive cells	F value	P value
I	5	4	62.8±25.4	2.495	0.097
II	10	8	46.3±24.4		
III	9	6	32.3±22.3		
IV	3	2	13.5±3.5		

Expression of hMSH2 mRNA in various differentiated types of gastric cancer

Compared with that in the normal gastric tissue, the expression of hMSH2 mRNA in gastric cancer tissue was decreased significantly ($P>0.05$). The number of positive signal cells differed among various differentiated types of gastric cancer. In poorly differentiated cancer tissue, the positive signal cells scattered in the middle and lower parts of mucosa, and the number of positive signal cells was smallest (Figure 6). There was a significant difference between the number of positive signal cells in the poorly differentiated gastric cancer tissue and that in the moderately and well differentiated gastric cancer tissue (Figure 7, 8).

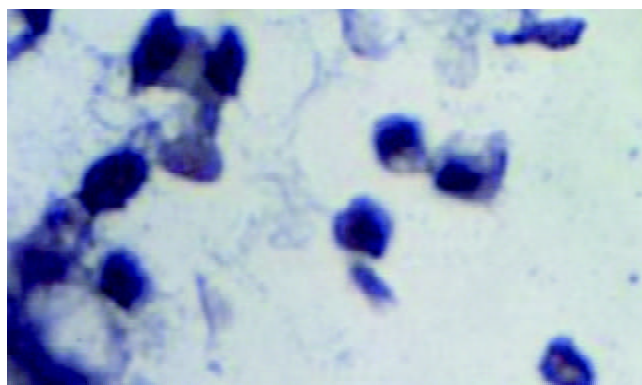


Figure 6 hMSH2 in poorly differentiated gastric cancer (×1000).

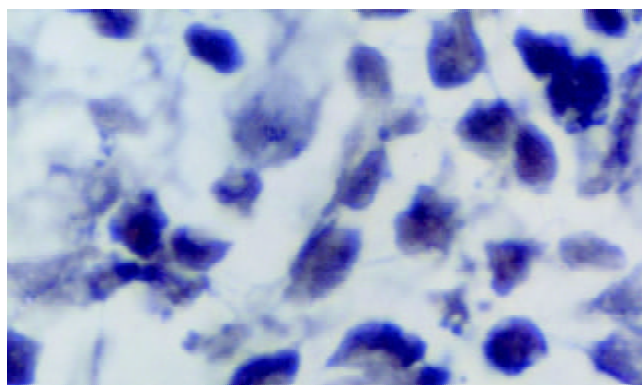


Figure 7 hMSH2 in moderately differentiated gastric cancer (×1000).

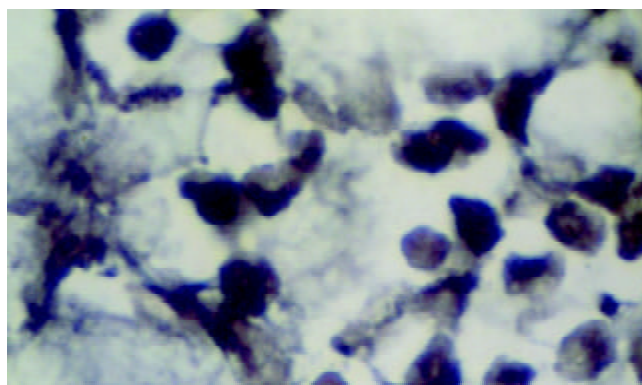


Figure 8 hMSH2 in well differentiated gastric cancer (×1000).

Negative reaction was showed in situ hybridization assay in control specimen.

DISCUSSION

Microsatellite instability of p16 gene

Microsatellite DNA is a genome-wide simple repeat sequence. Its normal length is shorter than 350bp, and the number of repeating is less than 60. The number of repeat unit of MI varied with individuals or tissues even in same body^[15]. MI varied in different kinds of cancer^[16-19]. In the gastric cancer tissues, MI was a frequent event, and the average frequency of MI was reported in different papers to be 33.9 %, 32.1 % and 25 %, respectively^[20-22]. The results showed that the LOH frequency of D9s171 and D9s1604 microsatellite loci, located at upstream of p16 gene, were 15 % and 50 %, respectively. The LOH frequency in well differentiated gastric cancer tissue was lower than that in the moderately and poorly differentiated gastric cancer tissue without significant difference ($P>0.05$). The relation of MI and the differentiation degree of gastric cancer has been not known clearly^[23,24].

It was showed that MI occurred at early stage of malignancy and gradually caused the formation of cancer^[25,26]. The results in this study showed that the LOH of microsatellite loci exhibited 50 % frequency at the early stage of gastric cancer, which suggested that the alteration of these loci might activate specific oncogenes and deactivate tumor suppressor genes, therefore, cause the development and progress of cancer. The alteration of microsatellite DNA normally appears as LOH. If LOH occurs frequently at the same locus of one chromosome in the tumor, the site of occurring LOH usually is the location of tumor suppressor gene^[27]. Through the analysis of the loci adjacent to p16 gene, small losses (<200bp) of p16 gene could be found in many kinds of cancer, which might be one of deactivation mechanisms of p16 gene. In this paper, two microsatellite loci were selected to demonstrate MI, D9s171 located at the site between the upstream of p16 gene and an adjacent tumor suppressor gene p15, D9s1604 located at the site between the exon 1 α and exon 1 β of p16 gene. LOH was detected at both D9s171 and D9s1604, and correlation between the occurrence of MI at the D9s171 and at the D9s1604 was existed, which suggested that occurrence of MI at the two loci might be related molecular event.

Expression of hMSH2 mRNA

Mismatch repair gene superfamily belongs to housekeeping genes, and is able to correct unmatched or mismatched bases in the process of DNA replication and DNA damage repairing, and control the accuracy of replication and recombination. Up to date, 6 human mismatch repair genes have been found, including 3 homologous of bacterial MutS (hMSH2, hMSH6 and hMSH3) and 3 homologous of bacterial MutL (hMSH1, hPMS1 and hPMS2). Loss of hMSH2 protein existed in the colonic and other cancer^[28-33] and genetic alterations in hMSH2 was observed in gastric cancer cell line^[34]. Loss of hMSH2 protein in the cancer tissue indicated that hMSH2 peptide or its coding mRNA was at an instable state. The number of the positive signal cells of hMSH2 mRNA in normal gastric mucosa, in adjacent cancer tissue, and in gastric cancer tissue was 175.8 ± 26.4 , 99.7 ± 16.8 and 42.1 ± 25.9 , respectively. The number of positive signal cells was decreased significantly in adjacent cancer and gastric cancer tissue ($P<0.01$) No significant difference was found in the number of the positive signal cells of hMSH2 mRNA at various clinical stages in gastric cancer. A correlation might exist between the instability of gene expression and the development of gastric cancer. Tumor development is a multi-step process of somatic cell mutation and colonial amplification. With the hMSH2 (or other mismatch repair genes) mutation and the cell proliferation, the instability of genome occurred, and then the mutator acted selectively at the mutated site, caused enlargement of genome

instability in deepness and wideness, the accumulation of oncogene mutation was accelerated and caused the formation of tumor finally^[35].

Expression of hMSH2 protein in 115 bladder cancers was studied with immunohistochemistry^[36] and showed that low expression of hMSH2 protein exhibited in 25 % cases and complete loss in 2 cases. A closely correlation existed between the decrease of hMSH2 mRNA and the recurrence of poorly differentiated cancer. The results in this work showed that expression of hMSH2 mRNA significantly decreased in gastric cancer tissues, especially in moderately and poorly differentiated cancer ($P<0.05$). The results suggested that low expression of hMSH2 mRNA in poorly differentiated cancer might be related to the metastasis and prognosis of cancer. The lower the gastric cancer was differentiated, the more unstable the gene expression was. As the ratio of DNA mismatch increased, the instability of genome enhanced, tumor became more invasive and the prognosis got worse.

REFERENCES

- 1 Yamamoto H, Sawai H, Perucho M. Frameshift somatic mutation in gastrointestinal cancer of the microsatellite mutator phenotype. *Cancer Res* 1997; **57**: 4420-4426
- 2 Fleisher AS, Esteller M, Wang S, Tamura G, Suzuki H, Yin J, Zou TT, Abraham JM, Kong D, Smolinski KN, Shi YQ, Rhyu MG, Powell SM, James SP, Wilson KT, Herman JG, Meltzer SJ. Hypermethylation of the hMLH1 gene promoter in human gastric cancers with microsatellite instability. *Cancer Res* 1999; **59**: 1090-1095
- 3 Kang YJ, Wang LN, Zhang ZK. Microsatellite instability and DNA mismatch repair system. *Shijie Huaren Xiaohua Zazhi* 2000; **8**: 1139-1140
- 4 Wang B, Shi LC, Zhang WB, Xiao CM, Wu JF, Dong YM. Expression of tumor suppressor gene p16 in gastric cancer and precancerous lesions. *Shijie Huaren Xiaohua Zazhi* 2001; **9**: 39-42
- 5 Zhou Y, Gao SS, Li YX, Fan ZM, Zhao X, Qi YJ, Wei JP, Zou JX, Liu G, Jiao LH, Bai YM, Wang LD. Tumor suppressor gene p16 and Rb expression in gastric cardia precancerous lesions from subjects at a high incidence area in northern China. *World J Gastroenterol* 2002; **8**: 423-425
- 6 He XS, Su Q, Chen ZC, He XT, Long ZF, Ling H, Zhang LR. Expression, deletion and mutation of p16 gene in human gastric cancer. *World J Gastroenterol* 2001; **7**: 515-521
- 7 Wei TY, Wei MX, Yang SM. Expression of cyclin D1 P16 and Rb protein in gastric cancer. *Shijie Huaren Xiaohua Zazhi* 2000; **8**: 234-235
- 8 Zhu ZY, Tian X, Wang X, Yang XL. Mutation of p16 and APC gene in gastric cancer. *Shijie Huaren Xiaohua Zazhi* 2000; **8**: 1418-1419
- 9 Yang SM, Yang LS, Li L, Deng LY, Wang CY, Yuan XB, Shen XD. Methylation of MTS1/P16 gene and expression of P16 protein in gastric cancer. *Shijie Huaren Xiaohua Zazhi* 2000; **8**: 1427-1429
- 10 Zhao Y, Zhang XY, Shi XJ, Hu PZ, Zhang CS, Ma FC. Expression of P16, P53 and proliferating cell nuclear antigen in gastric cancer. *Shijie Huaren Xiaohua Zazhi* 1999; **7**: 246-248
- 11 Li GX, Li GQ, Zhao CZ, Xu GL. Relationship between telomerase hTERT and the expression of tumor suppressor gene p53 and p16. *Shijie Huaren Xiaohua Zazhi* 2002; **10**: 591-593
- 12 Jiang YX, Zhao MY, Geng M, Chao YC, Wang XY. Expression of P16, cerB-2 protein in gastric tumor. *Shijie Huaren Xiaohua Zazhi* 2002; **10**: 1050-1051
- 13 Yang ZL, Li YG, Huang YF, Wang QW. Expression of cyclin D1, CDK4, P16 and Rb in gastric cancer. *Shijie Huaren Xiaohua Zazhi* 2000; **8**: 362-363
- 14 Wang GT. Progression in the study on gastric precancerous lesions and its reversion. *Shijie Huaren Xiaohua Zazhi* 2000; **8**: 1-4
- 15 Ji XL. Microsatellite instability: New point in gene study. *Shijie Huaren Xiaohua Zazhi* 1999; **7**: 372-374
- 16 Spanakis NE, Gorgoulis V, Mariatos G, Zacharatos P, Kotsinas A, Garinis G, Trigidou R, Karameris A, Tsimare-Papastamatiou H, Kouloukousa M, Manolis EN, Kittas C. Aberrant p16 expression is correlated with homozygous deletions at the 9p21-23 chro-

- mosome region in non-small cell lung cancers. *Anticancer Res* 1999; **19**: 1893-1899
- 17 **Niederacher D**, Yan HY, An HY, Bender HG, Beckmann MW. CDKN2A gene inactivation in epithelial sporadic ovarian cancer. *Br J Cancer* 1999; **80**: 1920-1926
 - 18 **Li M**, Zhang ZF, Reuter VE, Cordon-Cardo C. Chromosome 3 allelic losses and microsatellite alterations in transitional cell cancer of the urinary bladder. *Am J Pathol* 1996; **149**: 229-235
 - 19 **Ionov Y**, Peinado MA, Malkhosyan S, Shibata D, Perucho M. Ubiquitous somatic mutations in simple repeated sequences reveal a new mechanism for colonic carcinogenesis. *Nature* 1993; **363**: 558-561
 - 20 **Wang Y**, Ke Y, Ning T, Feng L, Lu G, Liu WEZ. Studies of microsatellite instability in Chinese gastric cancer tissue. *Zhonghua Yixue Yichanxue Zazhi* 1998; **15**: 155-157
 - 21 **Fang DC**, Zhou XD, Luo YH, Wang DX, Lu R, Yang SM, Liu WW. Microsatellite instability and the loss of heterologous of tumor suppressor gene in gastric cancer. *Shijie Huaren Xiaohua Zazhi* 1999; **7**: 479-481
 - 22 **Fang DC**, Luo YH, Yang SM, Li XA, Ling XL, Fang L. Mutation analysis of APC gene in gastric cancer with microsatellite instability. *World J Gastroenterol* 2002; **8**: 787-791
 - 23 **Han HJ**, Yanagisawa A, Kato Y, Park JG, Nakamura Y. Genetic instability in pancreatic cancer and poorly differentiated type of gastric cancer. *Cancer Res* 1993; **53**: 5087-5089
 - 24 **Lin JT**, Wu MS, Shun CT, Lee WJ, Wang JT, Wang TH, Sheu JC. Microsatellite instability in gastric cancer with special references to histopathology and cancer stages. *Eur J Cancer* 1995; **31A**: 1879-1882
 - 25 **Wirtz HC**, Muller W, Noguchi T, Scheven M, Ruschoff J, Hommel G, Gabbert HE. Prognostic value and clinicopathological profile of microsatellite instability in gastric cancer. *Clin Cancer Res* 1998; **4**: 1749-1754
 - 26 **Kim JJ**, Baek MJ, Kim L, Kim NG, Lee YC, Song SY, Noh SH, Kim H. Accumulated frameshift mutations at coding nucleotide repeats during the progression of gastric cancer with microsatellite instability. *Lab Invest* 1999; **79**: 1113-1120
 - 27 **Weissenbach J**, Gyapay G, Dib C, Vignal A, Morissette J, Millasseau P, Vaysseix G, Lathrop M. A second generation linkage map of the human genome. *Nature* 1992; **359**: 794-801
 - 28 **Jass JR**, Iino H, Ruzsiewicz A, Painter D, Solomon MJ, Koorey DJ, Cohn D, Furlong KL, Walsh MD, Palazzo J, Edmonston TB, Fishel R, Young J, Leggett BA. Neoplastic progression occurs through mutator pathways in hyperplastic polyposis of colorectum. *Gut* 2000; **47**: 43-49
 - 29 **Borresen AL**, Lothe RA, Meling GI, Lystad S, Morrison P, Lipford J, Kane MF, Rognum TO, Kolodner RD. Somatic mutation in the hMSH2 gene in microsatellite unstable colorectal cancers. *Hum Mol Genet* 1995; **4**: 2065-2072
 - 30 **Bock N**, Meden H, Regenbrecht M, Junemann B, Wangerin J, Marx D. Expression of the mismatch repair protein hMSH2 in cancer in situ and invasive cancer of the breast. *Anticancer Res* 2000; **20**: 119-124
 - 31 **Leach FS**, Hsieh JT, Molberg K, Saboorian MH, McConnell JD, Sagalowsky AI. Expression of the human mismatch repair gene hMSH2: a potential marker for urothelial malignancy. *Cancer* 2000; **88**: 2333-2341
 - 32 **Parc YR**, Halling KC, Burgart LJ, McDonnell SK, Schaid DJ, Thibodeau SN, Halling AC. Microsatellite instability and hMLH1/hMSH2 expression in young endometrial cancer patients: associations with family history and histopathology. *Int J Cancer* 2000; **86**: 60-66
 - 33 **Chen HC**, Bhattacharyya N, Wang L, Recupero AJ, Klein EA, Harter ML, Banerjee S. Defective DNA repair genes in a primary culture of human renal cell cancer. *J Cancer Res Clin Oncol* 2000; **126**: 185-190
 - 34 **Shin KH**, Park JG. Microsatellite instability is associated with genetic alteration but not with low levels of expression of the human mismatch repair proteins hMSH2 and hMLH1. *Eur J Cancer* 2000; **36**: 925-931
 - 35 **Perucho M**. Microsatellite instability: the mutator that mutates the other mutator. *Nat Med* 1996; **2**: 630-631
 - 36 **Jin TX**, Furihata M, Yamasaki I, Kamada M, Liang SB, Ohtsuki Y, Shuin T. Human mismatch repair gene (hMSH2) product expression in relation to recurrence of transitional cell cancer of the urinary bladder. *Cancer* 1999; **85**: 478-484

Edited by Ren SY

Paclitaxel induces apoptosis in human gastric carcinoma cells

Hai-Bo Zhou, Ju-Ren Zhu

Hai-Bo Zhou, Ju-Ren Zhu, Department Of Gastroenterology, Shandong Provincial Hospital, Jinan 250052, Shandong Province, China

Correspondence to: Dr. Hai-Bo Zhou, Department Of Gastroenterology, Shandong Provincial Hospital, Jinan 250052, Shandong Province, China. zhouhbyy@fm365.com.cn

Telephone: +86-531-2603194

Received: 2002-08-03 **Accepted:** 2002-11-21

Abstract

AIM: To investigate the apoptosis in gastric cancer cells induced by paclitaxel, and the relation between this apoptosis and expression of Bcl-2 and Bax.

METHODS: In *in vitro* experiments, MTT assay was used to determine the cell growth inhibitory rate. Transmission electron microscope and TUNEL staining method were used to quantitatively and qualitatively detect the apoptosis status of gastric cancer cell line SGC-7901 before and after the paclitaxel treatment. Immunohistochemical staining was used to detect the expression of apoptosis-regulated gene Bcl-2 and Bax.

RESULTS: Paclitaxel inhibited the growth of gastric cancer cell line SGC-7901 in a dose-and time-dependent manner. Paclitaxel induced SGC-7901 cells to undergo apoptosis with typically apoptotic characteristics, including morphological changes of chromatin condensation, chromatin crescent formation, nucleus fragmentation and apoptotic body formation. Paclitaxel could reduce the expression of apoptosis-regulated gene Bcl-2, and improve the expression of apoptosis-regulated gene Bax.

CONCLUSION: Paclitaxel is able to induce the apoptosis in gastric cancer. This apoptosis may be mediated by down-expression of apoptosis-regulated gene Bcl-2 and up-expression of apoptosis-regulated gene Bax.

Zhou HB, Zhu JR. Paclitaxel induces apoptosis in human gastric carcinoma cells. *World J Gastroenterol* 2003; 9(3): 442-445
<http://www.wjgnet.com/1007-9327/9/442.htm>

INTRODUCTION

Apoptosis is a form of cell death characterized by active cellular suicide during T-cell clonal deletion, embryogenesis, and DNA damage. Apoptotic cell death is often associated with distinctive characteristics, such as nuclear fragmentation, cytoplasmic blebbing, and internucleosomal fragmentation of DNA. Whether a cell committed to apoptosis partly depends upon the balance between proteins that mediate cell death, such as Bax, and proteins that promote cell viability, such as Bcl-2 or Bcl-xl. Overexpression of Bax has been shown to accelerate the cell death. Overexpression of antiapoptotic proteins such as Bcl-2 represses the death function of Bax. Thus, the ratio of Bcl-2 to Bax appears to be a critical determinant of a cell's threshold for undergoing apoptosis.

Microtubule inhibitors such as paclitaxel can increase tubulin polymerization, tubulin bundling, and cell cycle arrest.

Paclitaxel have been proven to induce apoptosis in many cancers. In order to study the mechanism of paclitaxel induces apoptosis of SGC-7901 gastric cancer cells, MTT assay was used to determine the cell growth inhibitory rate. Transmission electron microscope and TUNEL staining method were used to quantitatively and qualitatively detect the apoptosis status of gastric cancer cell line SGC-7901 before and after the paclitaxel treatment. Immunohistochemical staining was used to detect the expression of apoptosis-regulated gene Bcl-2 and Bax.

We report here the results of our findings showing paclitaxel inhibited the growth of gastric cancer cell line SGC-7901 in a dose-and time-dependent manner. Paclitaxel induced SGC-7901 cells to undergo apoptosis with typically apoptotic characteristics, including morphological changes of chromatin condensation, chromatin crescent formation, nucleus fragmentation and apoptotic body formation. Paclitaxel reduces Bcl-2 expression and improves Bax expression on SGC-7901 cells.

MATERIALS AND METHODS

Materials

Paclitaxel was obtained from Xiehe Pharmaceutical Factory in Biejing. MTT was obtained from Sigma Chemical Co. Ltd. Anti-Bcl-2 monoclonal antibody and anti-Bax monoclonal antibody were purchased from Beijing Zhongshan biotechnology Co. Ltd.

Methods

Cell culture Human gastric carcinoma cell line SGC-7901 was obtained from laboratory in Shandong Provincial Hospital and maintained in RPMI 1640 supplemented with 100 ml·L⁻¹ fetal bovine serum, 100 kU·L⁻¹ penicillin, 100 mg·L⁻¹ streptomycin and 2 μmol·L⁻¹ L-glutamine under 50 ml·L⁻¹ CO₂ in a humidified incubator at 37 °C. SGC-7901 cells were incubated for different time periods in the presence of paclitaxel at 0.001, 0.01, 0.1, 1 μmol·L⁻¹.

MTT assay 1×10⁵ cells/well in a 96-well plate after 24 hours incubation were treated with increasing concentrations of paclitaxel (0.001 μmol·L⁻¹ to 1 μmol·L⁻¹) for 24 to 96 hours. 10 μL of 5 g·L⁻¹ of MTT was added to the cells in every well and incubated for 4 hours at 37 °C. Culture media were discarded followed by addition of 0.2 ml of DMSO and vibration for 10 minutes. The absorbance (OD) was measured at 570 nm using a microplate reader. The cell growth inhibitory rate was calculated as follows: (OD of control group - OD of experimental group/OD of control group - OD of blank group) ×100 %.

Transmission electron microscopy The cells treated with 0.1 μmol·L⁻¹ paclitaxel were trypsinized and harvested after 24 hours. Subsequently the cells were fixed in 4 % glutaral and immersed with Epon 821, imbedded in capsules and converged for 72 hours at 60 °C, the cells were prepared into ultrathin section (60 nm) and stained with uranyl acetate and lead citrate. Cell morphology was examined by transmission electron microscopy.

TUNEL assay Apoptosis of SGC-7901 cells was evaluated by using an *in situ* cell detection kit (Beijing Zhongshan biotechnology Co. Ltd). The cells were treated in the presence or absence of 0.1 μmol·L⁻¹ paclitaxel for 24 to 96 hours and fixed in ice-cold 80 % ethanol for up to 24 hours, treated with proteinase K and then 0.3 % H₂O₂, labeled with fluorescein

dUTP in a humid box for 1 hour at 37 °C. The cells were then combined with POD-Horseradish peroxidase, colorized with DAB. Controls consisted of omission of fluorescein dUTP. Cells were visualized with light microscope. The Apoptotic Index (AI) was calculated as follows: $AI = (\text{Number of apoptotic cells} / \text{Total number}) \times 100\%$.

Immunohistochemical staining Immunohistochemical staining was accomplished utilizing an avidinbiotin technique. SGC-7901 cells treated in the presence or absence of 0.1 $\mu\text{mol} \cdot \text{L}^{-1}$ paclitaxel for 24 to 96 hours were grown on six-well glass slides and fixed in acetone. After washing in PBS, the cells were incubated in 0.3 % H_2O_2 solution at room temperature for 5 minutes. The cells then were incubated with anti-Bcl-2 or anti-Bax at a 1:300 dilution at 4 °C overnight. Following washing in PBS, the second antibody, biotinylated antirat Ig G, was added and the cells were incubated at room temperature for 1 hour. After washing in PBS, ABC compound was added and then incubated at room temperature for 10 minutes. DAB was used as the chromagen. After ten minutes, the brown color signifying the presence of antigen bound to antibodies was detected by light microscopy and photographed at $\times 200$. Controls consisted of omission of the primary antibody. The Positive Rate (PR) was calculated as follows: $PR = (\text{Number of positive cells} / \text{Total number}) \times 100\%$.

Statistical analysis

Data were analyzed employing the paired two-tailed Student *t* test, and significance was assumed at $P < 0.05$.

RESULTS

MTT assay

SGC-7901 cells were exposed to increasing concentrations (0.001 $\mu\text{mol} \cdot \text{L}^{-1}$ to 1 $\mu\text{mol} \cdot \text{L}^{-1}$) of commercially available paclitaxel for 24 to 96 hours. Our results show a dose- and time-dependent increase in tumor cell mortality. The data were summarised in Table 1.

Table 1 The inhibitory effect of paclitaxel on SGC-7901 cells (inhibitory rate, %)

Time(h)	RPMI-1640	Paclitaxel (mmol·L ⁻¹)			
		0.1	1	10	100
24	0.0	9.6 ^b	18.8 ^d	22.8 ^d	34.3 ^d
48	0.0	17.5 ^d	21.6 ^d	36.4 ^d	45.4 ^d
72	0.0	23.8 ^d	37.3 ^d	47.6 ^d	58.9 ^d
96	0.0	35.6 ^d	44.7 ^d	57.6 ^d	87.8 ^d

^b $P < 0.01$, ^d $P < 0.001$ vs the control group.

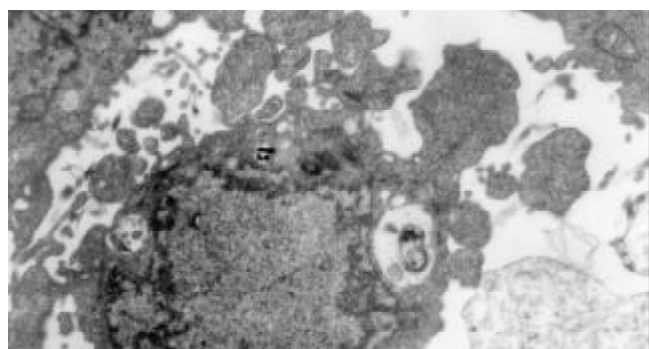


Figure 1 Paclitaxel-induced apoptosis in SGC-7901 cells with Transmission Electron Microscope Apoptotic cell with chromatin condensation, chromatin crescent formation, nucleus fragmentation ($\times 4000$).

Morphological changes

After treatment of SGC-7901 cells with paclitaxel (0.1 $\mu\text{mol} \cdot \text{L}^{-1}$) for 24 hours, some cells appeared apoptotic characteristics including chromatin condensation, chromatin crescent formation, nucleus fragmentation and apoptotic body formation were seen by transmission electron microscope (Figure 1).

TUNEL assay

Positive staining located in the nucleus (Figure 2). The results showed after treatment of SGC-7901 cells with paclitaxel (0.1 $\mu\text{mol} \cdot \text{L}^{-1}$) for 24 to 96 hours, the AIs were apparently increased with treat time ($P < 0.05$) (Table 2).

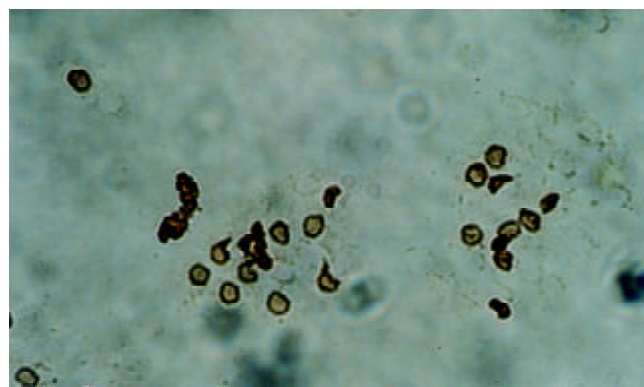


Figure 2 Apoptotic cells induced by paclitaxel with TUNEL assay ($\times 200$)

Table 2 Apoptotic Index (AI) of treated SGC-7901 cells by paclitaxel

Time(h)	AI(%)
0	1.43 \pm 2.42
24	4.89 \pm 2.63 ^b
48	16.34 \pm 1.85 ^b
72	27.86 \pm 3.23 ^d
96	36.49 \pm 3.95 ^d

^b $P < 0.05$, ^d $P < 0.01$ vs the control group.

Expression of Bcl-2 proteins

Positive staining located in the cytoplasm). The results showed after treatment of SGC-7901 cells with paclitaxel (0.1 $\mu\text{mol} \cdot \text{L}^{-1}$) for 24 to 96 hours, the PRs of Bcl-2 proteins were apparently reduced with treat time ($P < 0.05$) (Table 3). This suggested paclitaxel could reduce Bcl-2 expression.

Table 3 Positive Rate of Bcl-2 on treated SGC-7901 cells by paclitaxel

Time(h)	PT(%)
0	35.44 \pm 3.86
24	20.50 \pm 2.71 ^b
48	10.66 \pm 2.36 ^b
72	6.78 \pm 1.65 ^d
96	3.98 \pm 1.34 ^d

^b $P < 0.05$, ^d $P < 0.01$ vs the control group.

Expression of bax proteins

Positive staining located in the cytoplasm. The results showed after treatment of SGC-7901 cells with paclitaxel (0.1 $\mu\text{mol} \cdot \text{L}^{-1}$) for 24 to 96 hours, the PRs of Bax proteins were apparently improved with treat time ($P < 0.05$) (Table 4). This suggested paclitaxel could improve Bcl-2 expression.

Table 4 Positive Rate of Bax on treated SGC-7901 cells by paclitaxel

Time(h)	PT(%)
0	10.27±2.19
24	19.68±2.64 ^b
48	30.57±3.76 ^b
72	41.28±6.14 ^b
96	59.98±6.25 ^b

^b $P < 0.05$ vs the control group.

DISCUSSION

Apoptosis is a form of cell death characterized by active cellular suicide during T-cell clonal deletion, embryogenesis, and DNA damage. Apoptotic cell death is often associated with distinctive characteristics, such as nuclear fragmentation, cytoplasmic blebbing, and internucleosomal fragmentation of DNA^[1-6]. The Bcl-2 family plays a central role in the control of apoptosis. The family includes a number of proteins which have amino acid sequence homology, including anti-apoptotic members such as Bcl-2 and Bcl-x_L, as well as pro-apoptotic members including Bax and Bad^[7-10]. Overexpression of Bax has been shown to accelerate the cell death^[11-15]. Conversely, Overexpression of antiapoptotic proteins such as Bcl-2 represses the death function of Bax^[16-20]. Thus, the ratio of Bcl-2 to Bax appears to be a critical determinant of a cell's threshold for undergoing apoptosis^[21].

Microtubule inhibitors such as paclitaxel can increase tubulin polymerization, tubulin bundling, and cell cycle arrest^[22-24]. Paclitaxel have been proven to induce apoptosis in many cancers^[25-37]. In order to study the mechanism of paclitaxel induces apoptosis of SGC-7901 gastric cancer cells, MTT assay was used to determine the cell growth inhibitory rate. Transmission electron microscope and TUNEL staining method were used to quantitatively and qualitatively detect the apoptosis status of SGC-7901 gastric cancer cell before and after the paclitaxel treatment. Immunohistochemical staining was used to detect the expression of apoptosis-regulated gene Bcl-2 and Bax.

In the present study, MTT assay was used to observe the effect of paclitaxel on the growth of SGC-7901 gastric carcinoma cells *in vitro*, indicating that the drug could inhibit the the growth of gastric carcinoma cells. Our results show a dose- and time-dependent increase in tumor cell mortality. Its concentration- and time-effect relationships were significant. TUNEL assay showed after treatment of SGC-7901 cells with paclitaxel (0.1 $\mu\text{mol} \cdot \text{L}^{-1}$) for 24 to 96 hours, the AIs were apparently increased with treat time ($P < 0.05$). Immunohistochemical staining was used to detect the expression of Bcl-2 proteins and Bax proteins. The results showed after treatment of SGC-7901 cells with paclitaxel (0.1 $\mu\text{mol} \cdot \text{L}^{-1}$) for 24 to 96 hours, the PRs of Bcl-2 proteins were apparently reduced with treat time ($P < 0.05$), but the PRs of Bax proteins were apparently improved with treat time ($P < 0.05$). These suggested paclitaxel could reduce Bcl-2 expression and improve Bcl-2 expression. The ratio of Bcl-2 to Bax was decreased. The decreased ratio could trigger the apoptosis of SGC-7901 cells.

The research in our laboratory demonstrated paclitaxel is able to induce the apoptosis in gastric cancer. This apoptosis may be mediated by down-expression of apoptosis-regulated gene Bcl-2 and up-expression of apoptosis-regulated gene Bax. The mechanism of Paclitaxel as a chemotherapeutic drug in anti-gastric carcinoma chemotherapy should be further studied.

REFERENCES

- 1 **Manygoats KR**, Yazzie M, Stearns DM. Ultrastructural damage in chromium picolinate-treated cells: a TEM study. *J Biol Inorg Chem* 2002; **7**: 791-798
- 2 **Gu Y**, Zeng S, Qiu P, Peng D, Yan G. Apoptosis of bovine trabecular meshwork cells induced by dexamethasone. *Chung Hua Yen Ko Tsa Chih* 2002; **38**: 302-304
- 3 **Fidzianska A**. Suicide muscle cell programme-apoptosis. Ultrastructural study. *Folia Neuropathol* 2002; **40**: 27-32
- 4 **Narayanan S**, Stewart GC, Chengappa MM, Willard L, Shuman W, Wilkerson M, Nagaraja TG. Fusobacterium necrophorum Leukotoxin Induces Activation and Apoptosis of Bovine Leukocytes. *Infect Immun* 2002; **70**: 4609-4620
- 5 **Dini L**, Pagliara P, Carla EC. Phagocytosis of apoptotic cells by liver: a morphological study. *Microsc Res Tech* 2002; **57**: 530-540
- 6 **Mathiasen IS**, Sergeev IN, Bastholm L, Elling F, Norman AW, Jaattela M. Calcium and calpain as key mediators of apoptosis-like death induced by vitamin D compounds in breast cancer cells. *J Biol Chem* 2002; **277**: 30738-30745
- 7 **Konopleva M**, Konoplev S, Hu W, Zaritskey AY, Afanasiev BV, Andreeff M. Stromal cells prevent apoptosis of AML cells by up-regulation of anti-apoptotic proteins. *Leukemia* 2002; **16**: 1713-1724
- 8 **Van Der Woude CJ**, Jansen PL, Tiebosch AT, Beuving A, Homan M, Kleibeuker JH, Moshage H. Expression of apoptosis-related proteins in Barrett's metaplasia-dysplasia-carcinoma sequence: A switch to a more resistant phenotype. *Hum Pathol* 2002; **33**: 686-692
- 9 **Panaretakis T**, Pokrovskaja K, Shoshan MC, Grander D. Activation of Bak, Bax and BH3-only proteins in the apoptotic response to doxorubicin. *J Biol Chem* 2002; [epub ahead of print]
- 10 **Bellosillo B**, Villamor N, Lopez-Guillermo A, Marce S, Bosch F, Campo E, Montserrat E, Colomer D. Spontaneous and drug-induced apoptosis is mediated by conformational changes of Bax and Bak in B-cell chronic lymphocytic leukemia. *Blood* 2002; **100**: 1810-1816
- 11 **Matter-Reissmann UB**, Forte P, Schneider MK, Filgueira L, Groscurth P, Seebach JD. Xenogeneic human NK cytotoxicity against porcine endothelial cells is perforin/granzyme B dependent and not inhibited by Bcl-2 overexpression. *Xenotransplantation* 2002; **9**: 325-337
- 12 **Lanzi C**, Cassinelli G, Cuccuru G, Supino R, Zuco V, Ferlini C, Scambia G, Zunino F. Cell cycle checkpoint efficiency and cellular response to paclitaxel in prostate cancer cells. *Prostate* 2001; **48**: 254-264
- 13 **Mertens HJ**, Heineman MJ, Evers JL. The expression of apoptosis-related proteins bcl-2 and ki67 in endometrium of ovulatory menstrual cycles. *Gynecol Obstet Invest* 2002; **53**: 224-230
- 14 **Mehta U**, Kang BP, Bansal G, Bansal MP. Studies of apoptosis and bcl-2 in experimental atherosclerosis in rabbit and influence of selenium supplementation. *Gen Physiol Biophys* 2002; **21**: 15-29
- 15 **Chang W**, Yang K, Chuang H, Jan J, Shiao M. Glutamine protects activated human T cells from apoptosis by up-regulating glutathione and bcl-2 levels. *Clin Immunol* 2002; **104**: 151
- 16 **Chen GG**, Lai PB, Hu X, Lam IK, Chak EC, Chun YS, Lau WY. Negative correlation between the ratio of Bax to Bcl-2 and the size of tumor treated by culture supernatants from Kupffer cells. *Clin Exp Metastasis* 2002; **19**: 457-464
- 17 **Usuda J**, Chiu SM, Azizuddin K, Xue LY, Lam M, Nieminen AL, Oleinick NL. Promotion of photodynamic therapy-induced apoptosis by the mitochondrial protein Smac/DIABLO: dependence on Bax. *Photochem Photobiol* 2002; **76**: 217-223
- 18 **Sun F**, Akazawa S, Sugahara K, Kamihira S, Kawasaki E, Eguchi K, Koji T. Apoptosis in normal rat embryo tissues during early organogenesis: the possible involvement of Bax and Bcl-2. *Arch Histol Cytol* 2002; **65**: 145-157
- 19 **Jang M**, Shin M, Shin H, Kim K, Park H, Kim E, Kim C. Alcohol induces apoptosis in TM3 mouse Leydig cells via bax-dependent caspase-3 activation. *Eur J Pharmacol* 2002; **449**: 39
- 20 **Tilli CM**, Stavast-Koey AJ, Ramaekers FC, Neumann HA. Bax expression and growth behavior of basal cell carcinomas. *J Cutan Pathol* 2002; **29**: 79-87
- 21 **Pettersson F**, Dalgleish AG, Bissonnette RP, Colston KW. Retinoids cause apoptosis in pancreatic cancer cells via activation of RAR-gamma and altered expression of Bcl-2/Bax. *Br J*

- Cancer* 2002; **87**: 555-561
- 22 **Demaria S**, Volm MD, Shapiro RL, Yee HT, Oratz R, Formenti SC, Muggia F, Symmans WF. Development of tumor-infiltrating lymphocytes in breast cancer after neoadjuvant paclitaxel chemotherapy. *Clin Cancer Res* 2001; **7**: 3025-3030
 - 23 **Oyaizu H**, Adachi Y, Okumura T, Okigaki M, Oyaizu N, Taketani S, Ikebukuro K, Fukuhara S, Ikehara S. Proteasome inhibitor 1 enhances paclitaxel-induced apoptosis in human lung adenocarcinoma cell line. *Oncol Rep* 2001; **8**: 825-829
 - 24 **Charles AG**, Han TY, Liu YY, Hansen N, Giuliano AE, Cabot MC. Taxol-induced ceramide generation and apoptosis in human breast cancer cells. *Cancer Chemother Pharmacol* 2001; **47**: 444-450
 - 25 **Zhou J**, Gupta K, Yao J, Ye K, Panda D, Giannakakou P, Joshi HC. Paclitaxel-resistant human ovarian cancer cells undergo c-Jun NH2-terminal kinase-mediated apoptosis in response to noscaphine. *J Biol Chem* 2002; [epub ahead of print]
 - 26 **Li Y**, Shi T, Zhao W. The mechanism of docetaxel-induced apoptosis in human lung cancer cells. *Zhonghua Zhongliu Zazhi* 2000; **22**: 208-211
 - 27 **Fowler CA**, Perks CM, Newcomb PV, Savage PB, Farndon JR, Holly JM. Insulin-like growth factor binding protein-3 (IGFBP-3) potentiates paclitaxel-induced apoptosis in human breast cancer cells. *Int J Cancer* 2000; **88**: 448-453
 - 28 **Makino K**, Yu D, Hung MC. Transcriptional upregulation and activation of p53Cdc via p34 (cdc2) in Taxol-induced apoptosis. *Oncogene* 2001; **20**: 2537-2543
 - 29 **Yu C**, Wang S, Dent P, Grant S. Sequence-dependent potentiation of paclitaxel-mediated apoptosis in human leukemia cells by inhibitors of the mitogen-activated protein kinase kinase/mitogen-activated protein kinase pathway. *Mol Pharmacol* 2001; **60**: 143-154
 - 30 **Cheng SC**, Luo D, Xie Y. Taxol induced Bcl-2 protein phosphorylation in human hepatocellular carcinoma QGY-7703 cell line. *Cell Biol Int* 2001; **25**: 261-265
 - 31 **Odoux C**, Albers A, Amoscato AA, Lotze MT, Wong MK. TRAIL, FasL and a blocking anti-DR5 antibody augment paclitaxel-induced apoptosis in human non-small-cell lung cancer. *Int J Cancer* 2002; **97**: 458-465
 - 32 **Huisman C**, Ferreira CG, Broker LE, Rodriguez JA, Smit EF, Postmus PE, Kruyt FA, Giaccone G. Paclitaxel triggers cell death primarily via caspase-independent routes in the non-small cell lung cancer cell line NCI-H460. *Clin Cancer Res* 2002; **8**: 596-606
 - 33 **Hu L**, Hofmann J, Lu Y, Mills GB, Jaffe RB. Inhibition of phosphatidylinositol 3'-kinase increases efficacy of paclitaxel in *in vitro* and *in vivo* ovarian cancer models. *Cancer Res* 2002; **62**: 1087-1092
 - 34 **Carre M**, Carles G, Andre N, Douillard S, Ciccolini J, Briand C, Braguer D. Involvement of microtubules and mitochondria in the antagonism of arsenic trioxide on paclitaxel-induced apoptosis. *Biochem Pharmacol* 2002; **63**: 1831-1842
 - 35 **Peng WD**, Zhang J, Hui HX, Xu YM, Zhu F, Yang AG, Wang CJ. Upregulation of bax Gene Expression Promotes Paclitaxel-induced Apoptosis in Esophageal Carcinoma Cells. *Shengwu Huaxue Yusheng Wuwuli Xuebao (Shanghai)* 2000; **32**: 356-358
 - 36 **Bacus SS**, Gudkov AV, Lowe M, Lyass L, Yung Y, Komarov AP, Keyomarsi K, Yarden Y, Seger R. Taxol-induced apoptosis depends on MAP kinase pathways (ERK and p38) and is independent of p53. *Oncogene* 2001; **20**: 147-155
 - 37 **Qin YC**, Qi YQ, Si JL, Lin J, Zhu JR, Liu JY. Paclitaxel induces apoptosis in human gastric cancer cells and influences on the activity of telomerase *in vitro*. *Shijie Huaren Xiaohua Zazhi* 2001; **9**: 1086-1087

Edited by Ren SY

Protective effect of ascorbic acid in experimental gastric cancer: reduction of oxidative stress

Claudia P.M.S.Oliveira, Paulo Kassab, Fabio P. Lopasso, Heraldo P. Souza, Mariano Janiszewski, Francisco R. M. Laurindo, Kioshi Iriya, Antonio A. Laudanna

Claudia P.M.S.Oliveira, Paulo Kassab, Fabio P.Lopasso, Antonio A. Laudanna, Department of Gastroenterology of Medical School of University of São Paulo (USP), São Paulo, Brazil

Heraldo P. Souza, Mariano Janiszewski, Department of Emergency Medicine of Medical School of University of São Paulo (USP), São Paulo, Brazil

Francisco R. M. Laurindo, Heart Institute of Medical School of University of São Paulo (USP), São Paulo, Brazil

Kioshi Iriya, Department of Pathology of Medical School of University of São Paulo (USP), São Paulo, Brazil

Correspondence to: Claudia P.M.S.Oliveira, M.D., Department of Gastroenterology School of Med. of University of São Paulo, Av. Dr Enéas de Carvalho Aguiar n° 255, Instituto Central 9th Floor, 9159, 05403000 São Paulo, Brazil. mauclaud@uol.com.br

Telephone: +55-11-30696447 **Fax:** +55-11-3082-7599

Received: 2002-03-13 **Accepted:** 2002-04-06

Abstract

AIM: Oxidative stress participates in the cell carcinogenesis by inducing DNA mutations. Our aim was to assess whether ascorbic acid, an antioxidant, could have a role in preventing ROS (Reactive Oxygen Species) generation in experimental gastric carcinoma in a rat model.

METHODS: Experimental gastric cancer was induced in twelve Wistar male rats (weighting 250-350 g) by profound duodeno-gastric reflux through split gastrojejunostomy. The rats were allocated to the following groups: Group I ($n=6$) was the control; Group II ($n=6$) which was maintained with daily intake of tape water with Vitamin C (30 mg/Kg). After 6 or 12 months, samples of gastric tumor or non tumor mucosa were taken from the anastomosis of both groups. Oxidative stress was measured by superoxide quantification through lucigenin-amplified chemiluminescence base and by staining with Nitrobluetetrazolium. The histopathologic confirmation of adenocarcinoma was made by eosin-hematoxylin method.

RESULTS: The intestinal type of gastric adenocarcinoma was microscopically identified in all animals of group I whereas only 3 rats of group II showed an adenocarcinoma without macroscopic evidence of them. The cancers were located in the anastomosis in all cases. Basal luminescence from tumor gastric tissue generated 38.4 ± 6.8 count per minute/mg/ $\times 10^6$ (mean \pm SD) and 14.9 ± 4.0 count per minute/mg/ $\times 10^6$, respectively, in group I and II animals ($P < 0.05$). The Nitrobluetetrazolium method showed intense staining in tumor tissues but not in non neoplastic mucosa.

CONCLUSION: Experimental gastric tumors seem to produce more reactive oxygen species than non neoplastic gastric tissue. The reduction of oxidative stress and gastric tumor incidence in rats were induced by the intake of ascorbic acid. Therefore, it may have a role in the prevention of gastric carcinoma.

Oliveira CPMS, Kassab P, Lopasso FP, Souza HP, Janiszewski M, Laurindo FRM, Iriya K, Laudanna AA. Protective effect of ascorbic acid in experimental gastric cancer: reduction of oxidative stress. *World J Gastroenterol* 2003; 9(3): 446-448

<http://www.wjgnet.com/1007-9327/9/446.htm>

INTRODUCTION

The pathogenesis of human gastric cancer is a multistep and multifactorial process^[1]. The complex of cellular and molecular changes can be mediated by a diversity of endogenous and environmental agents that include free radicals, *H. pylori* infection^[2, 3] bile reflux, intake of diets high salt and low consumption of fruits and vegetables^[1]. Free radicals or reactive oxygen species (ROS) are low molecular weight metabolites reactive enough to damage essential biological molecules. The inability of the cell to scavenge ROS, overproduced by failure of the antioxidant systems, induced lesions in macromolecules such as DNA, proteins and lipids of cytosolic membranes. The release of ROS inside the nuclear membranes of the cell can damage the DNA, and there it induces mutations^[8,9] which is one of bases of the carcinogenesis^[4]. There are several mechanisms that could explain the relationships between the cell oxidative stress and the growth of tumors, such as proto-oncogene expression, generation of genotoxic products like 8-hydroxynonenal and conversion of procarcinogens to carcinogens^[4].

Epidemiologic studies has shown that vitamin C dietary intake decreases the risk for gastric tumor development^[5, 6]. Both antioxidant property and the ability to react with nitrite make vitamin C a putative candidate agent in the prevention of N-nitroso compound generation^[5,7,8]. There were a number reports on the role of the ROS as the first step in cancer induction, but there were few on ROS generation in tumor tissue and on the possible properties of vitamin C in protecting the cell against tumor transformation using an intragastric bile reflux rat model. The objectives of this work were to determine what is the oxidative stress involvement in experimental gastric carcinogenesis induced by intragastric bile reflux and what are the effects of the ascorbic acid on ROS generation in this model.

MATERIALS AND METHODS

The animal experiments were carried out in accordance to the Institute of Experimental Animals of School of Medicine, University of São Paulo Guidelines for Care and Use of Laboratory Animals.

Study groups

Wistar male rats (weighting 250-350 g) were submitted to the surgical procedure and were randomly allocated into two groups: Group I ($n=6$) was the control animals; Group II ($n=6$) was animals with daily oral administration (7 days per week) of Vitamin C (30 mg/Kg body weight) tape water solution. The total amount of vitamin C for 4 animals, in each cage, was dissolved in the total minimal volume of water intake that was previously measured for each animal. All rats were maintained in light and dark alternatively each phase for 12 h.

Surgical procedures

Experimental gastric cancer was induced by profound duodeno-gastric reflux in twelve Wistar rats underwent split gastrojejunostomy. The jejunum was divided at 5 cm distant from duodeno-jejunal angle. The afferent loop was anastomosed to the gastric body whereas the efferent jejunal loop was anastomosed in pre-pyloric antrum. The animals were killed at 6th month after the surgical procedure according with the appearance of weight loss, intestinal obstruction, ascites, anemia and visible abdominal mass. When these signs did not appear, the animals were killed at the 12th month after the operation. Just after killing, three fragments of 5 mm² each, were taken from the gastric tumor and from the gastric mucosa without tumor, at the same place on the anastomosis.

Lucigenin-amplified chemiluminescence assays

Each fragment was immersed in Krebs-HEPES buffer composition in mmol/L: NaCl 118.3; KCl 4.69; CaCl₂ 1.87; MgSO₄ 1.20; KH₂PO₄ 1.03; NaHCO₃ 25.0; Glucose 11.1; Na-HEPES 20.0) at 37 °C, strictly maintained at pH 7.40, for at least 15 min. The gastric fragments were rapidly transferred to a counter vial, under light protection, and immersed in 2.0 mL of a solution of Krebs-HEPES buffer and 0.10 mol/L lucigenin (Sigma Chemicals). This lucigenin concentration was chosen because, instead of higher concentration ranges, it has been shown to reflect superoxide generation by tissues. Each fragment was counted for 10 min in a luminometer (Berthold Multi Biolumat). Vials containing the buffer and lucigenin alone were counted and these blank values were subtracted from the signals obtained from the tissue fragments. The counts were normalized for the dry weight of each fragment. The results were expressed as counts per min per mg. In some experiments the gastric fragments were hold for 45 min in a solution of superoxide dismutase (100 kU/L) before and during the counts. NADH (0.1 mol/L) or NADPH (0.1 mol/L) were added to the counter vials in some experiments.

Histochemistry with nitrobluetetrazolium

Nitrobluetetrazolium (NBT) is a yellow dye that, under double reduction, generates insoluble bluish/black diformazan precipitates that are visible by light microscopy. NBT can be reduced directly by superoxide radicals, but it can also work as an electron acceptor during diaphorase enzyme activity. The gastric fragments (tumoral or not) were prepared as above, and immersed in a solution containing NBT (1.25 mg/mL), bovine serum albumin (17 mg/mL), NADH (0.1 mmol/L) and NADPH (0.1 mmol/L) for 30 minutes. The fragments were, then, fixed in 4 % buffered formalin, pH=7.40, for 24 hours. Afterwards, these specimens were then, embedded in paraffin, cut into 10 micra-thick slices and examined by light microscopy, without additional staining.

Hystology

The fragments previously fixed in 100 mL/L formalin, were dehydrated though increasing concentration of alcohol solutions, soaked in paraffin, cut into 5 mm -thick slices, stained with hematoxinilin-eosin (HE) and examined by light microscopy.

Statistical analysis

The data are expressed as mean \pm SEM. The values of differences between groups were compared using the Student test. *P* critical value of 0.05 was chosen to identified significant different means.

RESULTS

Each of the six rats of Group I at 6th month after surgery had

two advanced gastric tumor (Figure 1A), each one on the side of gastric mucosa of both afferent and efferent anastomosis. The rats of Group II had no signs of gastric tumor. However, in three of them, an early well differentiated intestinal adenocarcinoma of the anastomosis was microscopically detected (Figures 1B). The stromal tissue of these tumors had plenty inflammatory cells. The three other rats had epithelial inflammation and intestinal metaplasia in the same place of the macroscopic tumors in the another three animals. The well differentiated patterns of tumors were similar in both groups.

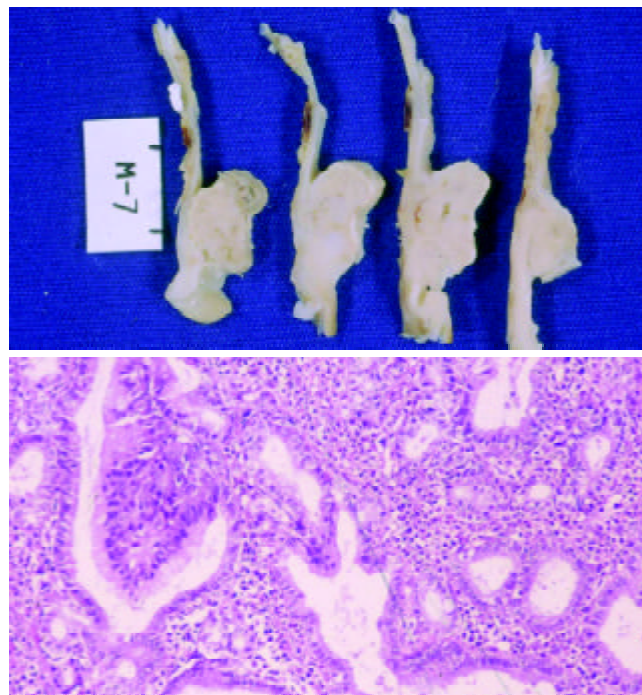


Figure 1 A. Microscopic appearance of the gastric tumor (Note the tubular pattern with variability of glomerular size, rudimentary papillary and nuclear atipia); B. Macroscopic appearance.

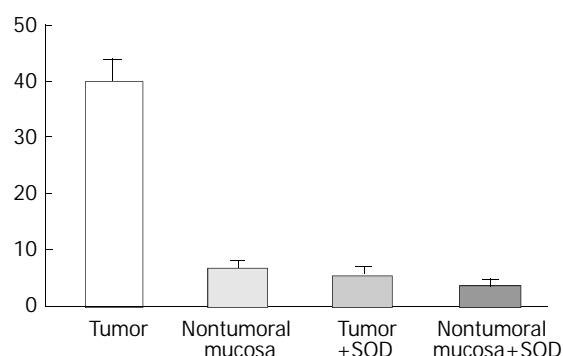


Figure 2 Lucigenin amplified-luminescence (count per minute $\times 10^6$). Basal Luminescence in the tumor and non tumoral mucosa. The addition of SOD (100 kU/L) to the substrate decreases the amplified-luminescence in visible tumoral mucosa and non tumoral gastric mucosa of rats.

The values of basal luminescence were higher in Group I (38.4 ± 6.8 count per minute/per mg $\times 10^6$) than in Group II (14.9 ± 4.0) ($P < 0.05$). The addition of NADPH to the substrate increased the luminescence in the non visible tumor tissue of the rats of Group II more than tumor tissues of Group I. Addition of NADH, however, increased the luminescence production by tumors and non tumorous mucosa. The luminescence generation after addition of superoxide dismutase

(SOD) was reduced in about 80 % and 30 % respectively, is the tumors and in non tumor gastric mucosa (Figure 2). Histochemical features produced by NBT showed insoluble bluish/black diformazan precipitates, visible with light microscopy in tumor tissue but not in the non tumoral tissues.

DISCUSSION

The choice of this experimental design was based on our previous studies which demonstrated that the appearance of gastric cancer was evident in these models at least after the 6th month of the surgical procedure. Gastric carcinogenesis is a multifactorial event. Endogenous and environmental stimuli are involved like *H. pylori* infection and gastric accumulation of N-nitroso compounds^[9-11]. Indeed there are evidences that oxidative stress participates in the carcinogenic cell transformation induced by DNA mutations^[1,4]. Studies on populations at high risk to gastrointestinal cancer have shown that dietary antioxidants are able to reduce the prevalence rates of cancer and, therefore, seem to protect them against the carcinogenesis in the stomach^[12,13]. In our rat model of profound duodeno-gastric reflux induced gastric adenocarcinomas within a 6-12 month period after the surgical procedure without antioxidant therapy. On the contrary, in animals with daily intake of vitamin C during the postoperative period, no obvious signs of gastric tumor were detected after 12 months. Though, in three of them, microscopic early gastric adenocarcinoma was found. Interestingly, the other three rats of this group remained without gastric carcinoma for as long as twelve months after the potential carcinogenetic surgical procedure. So, vitamin C seems to have a breaking role on the carcinogenetic process in the gastric mucosa under chronic and intense duodenal-gastric reflux. Probably this action might be due to the its antioxidant properties and the ability to react with nitrites, preventing the formation of gastric N-nitroso compounds.

The lucigenin-amplified luminescence method showed that the generation of ROS was higher in gastric neoplastic than in non neoplastic tissue. Macroscopic tumor in the rats of group I produced more luminescence than gastric tissue in the rats of group II without any visible tumor. These features suggest that increased ROS activity participates in gastric carcinogenesis during the development to the most advanced stages of the cancer. Indeed, the presence of ROS in non tumorous mucosa during the presence of cancer in the anastomosis suggests that is not possible to preclude the primary effect of the reflux that might induce cancer during the early stage of carcinogenetic process. The use of an antioxidant agent, such as vitamin C, can reduce the ROS generation and, thus tumor cell transformation. Recent studies have suggested that the gastric concentration of ascorbic acid is decreased in *H. pylori* infected patients^[2,3], especially, in patients who had intestinal metaplasia and serious and extensive gastritis. This fact could be associated with the gastric carcinogenic mechanism. On the other hand, intragastric bile reflux seems to induce intestinal metaplasia in humans, but only in the presence of *H. pylori* gastritis^[14]. In our previous studies using rats without *H. pylori* infection, metaplasia had preceeded the appearance of gastric adenocarcinoma. In the present study a relationship between intragastric bile reflux and oxidative stress could be observed. The use of vitamin C reduced the ROS generation that might have had a role in the tumoral cell transformation. The addition of NADPH induces superoxide generation by action of NADPH oxidase produced by activated neutrophils present in inflammatory tissues. The ROS generation in group I seems to be produced by the tumor and not by the inflammatory activity because: (1) there was no increase of luminescence when it was added to phorbol myristate acetate and (2) the luminescent response to NADH addition was higher than NADPH addition.

However, in group II, the addition of NADPH increased the luminescent activity more than it did after the NADH addition. These observations are relevant, because, in gastric tissue with visible tumors, superoxide generation might be related to gastric adenocarcinoma but not to the inflammatory process. Notwithstanding, when the gastric tissue without visible tumors was exposed to NADPH, there was an increase in the luminescence measures, in spite of the inflammation present in the tissue samples. A relationship was also established between histochemical data and superoxide generation. Moreover, the addition of a superoxide blocker (superoxide dismutase) to the substrate of tumor tissues caused a 80 % reduction of the luminescence generation.

As previously reported, the present study confirms the relationship between gastric superoxide anion generation and gastric carcinogenesis of the intestinal type, in rats. Vitamin C also seems to have a protective role in the cell mutagenic factors by a retarding action upon the growth of gastric tumors. This putative protection may be explained by the reduction of oxidative stress in gastric tissue. Consequently, vitamin C could be used in further therapeutic approaches.

REFERENCES

- 1 **Correa P.** A New Paradigm For Human Gastric Carcinogenesis. *J Clin Gastroenterol* 2000; **30**: 381-385
- 2 **Reed PI,** Vitamin C. *Helicobacter pylori* Infection and Gastric Carcinogenesis. *Int J Vitam Nutr Res* 1999; **69**: 220-227
- 3 **Zhang ZW,** Patchett SE, Perrett D, Katelaris PH, Domizio P, Farthing MJG. The relation between gastric vitamin C concentrations, mucosa histology, and Cag A seropositivity in the human stomach. *Gut* 1998; **43**: 322-326
- 4 **Farinati F,** Cardin R, Degan P, Rugge M, Di Mario F. Oxidative DNA damage accumulation in gastric carcinogenesis. *Gut* 1998; **42**: 351-356
- 5 **Correa P,** Malcom G, Schmidt B, Fontham E, Ruiz B, Bravo JC, Bravo LE, Zarama G, Realpe JL. Antioxidants micronutrients and gastric cancer. *Aliment Pharmacol Ther* 1998; **12** (Suppl1): 73-82
- 6 **Tsubono Y,** Tsugane S, Gey KF. Plasma antioxidant vitamins and carotenoid in five Japanese populations with varied mortality from gastric cancer. *Nutr Cancer* 1999; **34**: 56-61
- 7 **Mowat C,** Carswell A, Wirz A, McColl KE. Omeprazole and dietary nitrate independently affect levels of vitamin C and nitrite in gastric juice. *Gastroenterology* 1999; **116**: 813-822
- 8 **Dabrowska-Ufniaz E,** Dzieniszewski J, Jaroż M, Wartnerowicz M. Vitamin C concentration in gastric juice in patients with precancerous lesions of the stomach and gastric cancer. *Med Sci Monit* 2002; **8**: CR96-103
- 9 **You WC,** Zhang L, Gail MH, Chang YS, Liu WD, Ma JL, Li JY, Jin ML, Hu YR, Yang CS, Blaser MJ, Correa P, Blot WJ, Fraumeni JF Jr, Xu GW. Gastric dysplasia and gastric cancer: *Helicobacter pylori*, serum vitamin C, and other risk factors. *J Natl Cancer Inst* 2000; **92**: 1607-1612
- 10 **Yamaguchi N,** Kakizoe T. Synergistic interaction between *Helicobacter pylori* gastritis and diet in gastric cancer. *Lancet Oncol* 2001; **2**: 88-94
- 11 **Zhang ZW,** Abdullahi M, Farthing MJ. Effect of physiological concentrations of vitamin C on gastric cancer cells and *Helicobacter pylori*. *Gut* 2002; **50**: 165-169
- 12 **Jacobs EJ,** Connell CJ, McCullough ML, Chao A, Jonas CR, Rodriguez C, Calle EE, Thun MJ. Vitamin C, vitamin E, and multivitamin supplement use and stomach cancer mortality in the Cancer Prevention Study II cohort. *Cancer Epidemiol Biomarkers Prev* 2002; **11**: 35-41
- 13 **Correa P,** Fontham ET, Bravo JC, Bravo LE, Ruiz B, Zarama G, Realpe JL, Malcom GT, Li D, Johnson WD, Mera R. Chemoprevention of gastric dysplasia: randomized trial of antioxidant supplements and anti-helicobacter pylori therapy. *J Natl Cancer Inst* 2000; **92**: 1881-1888
- 14 **Dixon MF.** Prospects for intervention in gastric carcinogenesis: reversibility of gastric atrophy and intestinal metaplasia. *Gut* 2001; **49**: 2-4

The microcell mediated transfer of human chromosome 8 into highly metastatic rat liver cancer cell line C5F

Hu Liu, Sheng-Long Ye, Jiong Yang, Zhao-You Tang, Yin-Kun Liu, Lun-Xiu Qin, Shuang-Jian Qiu, Rui-Xia Sun

Hu Liu, Sheng-Long Ye, Jiong Yang, Zhao-You Tang, Yin-Kun Liu, Lun-Xiu Qin, Shuang-Jian Qiu, Rui-Xia Sun, Liver Cancer Institute, Zhong Shan Hospital, Fudan University, Shanghai 200032, China

Supported by The State Key Basic Research Program, No.G1998051200 and National Scientific Foundation of China, No. 30271459

Correspondence to: Sheng-Long Ye, Professor, Liver Cancer Institute, Zhong Shan Hospital, Fudan University, Shanghai 200032, China. slye@shmu.edu.cn

Telephone: +86-21-64041990-2150 **Fax:** +86-21-64037181

Received: 2002-10-05 **Accepted:** 2002-11-04

Abstract

AIM: Our previous research on the surgical samples of primary liver cancer with CGH showed that the loss of human chromosome 8p had correlation with the metastatic phenotype of liver cancer. In order to seek the functional evidence that there could be a metastasis suppressor gene (s) for liver cancer on human chromosome 8, we tried to transfer normal human chromosome 8 into rat liver cancer cell line C5F, which had high metastatic potential to lung.

METHODS: Human chromosome 8 randomly marked with neo gene was introduced into C5F cell line by MMCT and positive microcell hybrids were screened by double selections of G418 and HAT. Single cell isolation cloning was applied to clone microcell hybrids. Finally, STS-PCR and WCP-FISH were used to confirm the introduction.

RESULTS: Microcell hybrids resistant to HAT and G418 were obtained and 15 clones were obtained by single-cell isolation cloning. STS-PCR and WCP-FISH proved that human chromosome 8 had been successfully introduced into rat liver cancer cell line C5F. STS-PCR detected a random loss in the chromosome introduced and WCP-FISH found a consistent recombination of the introduced human chromosome with the rat chromosome.

CONCLUSION: The successful introduction of human chromosome 8 into highly metastatic rat liver cancer cell line builds the basis for seeking functional evidence of a metastasis suppressor gene for liver cancer harboring on human chromosome 8 and its subsequent cloning.

Liu H, Ye SL, Yang J, Tang ZY, Liu YK, Qin LX, Qiu SJ, Sun RX. The microcell mediated transfer of human chromosome 8 into highly metastatic rat liver cancer cell line C5F. *World J Gastroenterol* 2003; 9(3): 449-453

<http://www.wjgnet.com/1007-9327/9/449.htm>

INTRODUCTION

With the practice of diagnosis of primary liver cancer at early stage, surgical resection of small hepatocellular carcinoma (HCC) and other improvements in medical diagnosis, imaging, nonsurgical therapies, etc, important progresses have been

made toward the control of liver cancer. For example, surgical resection of small HCC has resulted in a marked increase in 5-year survival rate from 20-30 % to 40-60 %. In our institute, the 5-year survival rate of 963 patients with small HCC (≤ 5 cm) resection was 65.1 %. However, recurrence and metastasis still remain to be major challenges for clinical workers^[1-3]. The main obstacle to control of metastasis for liver cancer is the lack of sensitive predictive biomarkers and novel molecular targets for biotherapies^[4,5]. The discovery of metastasis suppressor genes for liver cancer will undoubtedly be of vital importance to the prognostic diagnosis and intervention therapy for overcoming the metastasis of liver cancer.

Our previous study suggested that there may harbor metastasis suppressor genes on human chromosome 8p^[6]. To seek functional evidence for this possibility, we tried to introduce the normal human chromosome 8 into the highly metastatic rat liver cancer cell line C5F^[7] through microcell mediated chromosome transfer (MMCT). The positive microcell hybrids were screened through drug selection and confirmed by sequence tagged sites- polymerase chain reaction (STS-PCR) and whole chromosome painting-fluorescence in situ hybridization (WCP-FISH).

MATERIALS AND METHODS

Cell lines

The highly metastatic rat liver cancer cell line C5F^[7] was generously provided by Dr.Kumiko Ogawa (the First Department of Pathology, Nagoya City University, Nagoya, Japan). The cells were maintained in Dulbecco's modified Eagle's medium (DMEM) supplemented with 10 % fetal bovine serum (FBS). The human chromosome 8 donor cell line A9 (neo8) was purchased from Japanese Collection of Research Bioresources (JCRB) Cell Bank, Osaka, Japan. A9 (neo8) is a mouse fibroblast cell line that contains a human chromosome 8. The human chromosome 8 was randomly marked with neo resistant gene. The A9 (neo8) cells were cultured in DMEM containing 10 % FBS and 800 μ g·mL⁻¹ geneticin (G418).

Reagents and instruments

Colcemid, cytochalasin B, phytohemagglutinin A (PHA), polyethylene glycol (PEG, MW1 300~1 600, Hybrid-Max[®]) and Dimethylsulfoxide (DMSO, Hybrid-Max[®]) were purchased from Sigma, USA. DMEM high glucose, 100 \times HAT (10 mM hypoxanthin, 40 μ M aminopterin, 1.6 mM thymidine) and G418 were ordered from Life Technologies, GIBCO BRL, USA. Isopore[™] polycarbonate membranes were purchased from Millipore, USA. WCP paint DNA probes for chromosome 8 (SpectrumGreen[™]) were purchased from Vysis Inc, IL, USA. Primers were ordered from Sangon Biotechnology Company, Shanghai, China. Taq polymerase, dNTP and 100bp DNA ladder marker were the products of Sino-America Biotechnology Company, China. Fetal bovine serum (FBS, define) and Bovine Calf Serum (BCS) were purchased from Hyclone, USA. PE-2400 thermocycler was the product of Perkin-Elmer Company, USA. The high speed Hitachi himac CR21G centrifuge was the product of Hitachi, Japan. Cyto

Vision™ Chromosome Analysis System (Cytovision™ Image Analysis Workstations, USA) was the product of Applied Imaging, USA.

MMCT^[8-10]

Micronucleation of A9(neo8) A9(neo8) cells were seeded in six straight-neck T25 flasks respectively. Colcemid was added to the culture to the final concentration of 0.05 $\mu\text{g} \cdot \text{mL}^{-1}$ when the cells reached confluence of 80 %. The cells were subsequently incubated at 37 °C in 50 mL $\cdot \text{L}^{-1}$ CO₂ incubator for 40-48 h.

Enucleation and filtration Media was removed from culture and cells were washed twice with PBS. The flasks were filled to the neck with DMEM containing 20 $\mu\text{g} \cdot \text{mL}^{-1}$ cytochalasin B which had been prewarmed at 37 °C. Flasks were sealed with parafilm, and then put into a R12A3 rotor (fixed-angle 28°) to centrifuge at 7 500 \times g at 36 °C for 75 min. Pellets were collected and resuspended with DMEM. Suspension was serially filtered through 8 μm , 5 μm and 5 μm polycarbonate membranes. Microcells were observed and counted on hemacytometer under microscope. Microcells were collected again by centrifuging at 2 000 \times g at 4 °C for 20 min and thereafter resuspended with 2 mL of DMEM with 100 $\mu\text{g} \cdot \text{mL}^{-1}$ PHA-P.

Microcell fusion & drug selection of microcell hybrids The recipient cell line C5F was trypsinized to make single cell suspension and counted on a hemacytometer for its cell density. C5F cells equivalent to 1/10 of microcells were taken and washed twice with PBS to get rid of remnant serum and thereby collected by centrifugation and resuspended with the PHA-P solution containing the microcells. The mixture was incubated at 37 °C for 15 min and subsequently centrifuged at 2 000 \times g for 15 min. Supernatant was removed as much as possible. Microcells were fused with the recipient cells for 30-60 s with 1 mL of 50 % PEG, 10 % DMSO in DMEM. Fusion reaction were terminated immediately by adding 10 mL of DMEM containing 5 % DMSO to remove the PEG medium. Pellets were resuspended with DMEM supplemented with 10 % FBS. The culture was recovered at 37 °C for 48 h and replaced with selective media of 1 \times HAT and 800 $\mu\text{g} \cdot \text{mL}^{-1}$ G418. The selective medium was refreshed twice per week.

Single cell Isolation cloning^[11]

Viable cells in selective media of G418 and HAT were trypsinized to make single cell suspension. Cell density was examined on a hemacytometer. Fifty to one hundred cells were added into a P100 culture plate with serum free DMEM. Single cells were picked up with a P20 pipette under microscope in laminar flow. It was assured that there was only one cell in view under a low-power objective to exclude the possibility of aspirating more than one cell each time. The opening of tip was pointed by the side of the selected cell and 5 μL media was aspirated each time. The single cell could be seen disappear into the tip under the low magnification microscope. Single cells were added to 96-well cell culture plate containing 0.1 mL of selective media (DMEM supplemented with 20 %FBS containing 1 \times HAT and 800 $\mu\text{g} \cdot \text{mL}^{-1}$ G418) in each well. After about 10 days, clones that are actively proliferating were picked up and transferred to a 24-well plate. After about 7 days, cells were transferred again to T25 flask. When cells reached large quantity, they were freed down in liquid nitrogen to keep in stock.

Genomic DNA extraction from cell lines^[12]

About 1 \times 10⁶ cultured cells were harvested by trypsinization and centrifugation, into which 0.5 mL of cell lysis buffer (100 mmol $\cdot \text{L}^{-1}$ NaCl, 1 mmol $\cdot \text{L}^{-1}$ EDTA, 0.5 % SDS, 50 mmol $\cdot \text{L}^{-1}$ Tris-HCl, pH 8.0) and 10 μL of Proteinase K (2 g $\cdot \text{L}^{-1}$) were

added. The mixture was incubated at 37 °C in water bath for 6 h. Genomic DNA was extracted with phenol and chloroform, precipitated with ethanol, dissolved with 20 μL of sterile dd-H₂O, quantitated by spectrophotometer, diluted to 10 $\mu\text{g} \cdot \mu\text{L}^{-1}$ with sterile dd-H₂O, and finally aliquoted and stored at -20 °C.

STS-PCR^[13,14]

A human STS, D8S277, which located at 8p23.3-p22, was randomly chosen to confirm the result of MMCT. Primers were designed according to the published sequences on NCBI UniSTS database (<http://www.ncbi.nlm.nih.gov/genome/sts/>). Forward primer: CCAGGTGAGTTTATCAATTCCTGAG; reverse primer: TGAGAGGT CTGAGT GAC ATCCG. PCR product size: 148-180 (bp). PCR reaction solution (10 mmol $\cdot \text{L}^{-1}$ Tris, 50 mmol $\cdot \text{L}^{-1}$ KCl, 2 mmol $\cdot \text{L}^{-1}$ MgCl₂, 0.001 % Gelatin, 200 mmol $\cdot \text{L}^{-1}$ dNTPs, 0.5 mmol $\cdot \text{L}^{-1}$ primers and 2U of *Taq* polymerase) was added into 50 ng of DNA template for each sample respectively. PCR program was run as: 94 °C 2 min, 1 cycle; 95 °C 40 s 60 °C 40 s 72 °C 40 s, 35 cycles in all; 72 °C 4 min, 1 cycle; keep at 4 °C. Results were checked on 2 % agarose gel electrophoresis stained with ethidium bromide.

Chromosome slide preparation^[15]

Microcell hybrids at logarithmic phase were treated with colcemid at a final concentration of 0.02 $\mu\text{g} \cdot \text{mL}^{-1}$ for 45 to 60 min at 37 °C and trypsinized subsequently to make single cell suspension. Cells were pelleted and then exposed to 5 mL of hypotonic solution (0.075 M KCl) by incubating for 10 to 15 min at 37 °C in a water bath. Chromosomes were repetitively fixed with methanol: glacial acetic acid (3:1, volume ratio) for 3 times, and finally resuspended with 0.5-1 mL of fixative. Three to four drops were dropped evenly on a cold wet slide, which was allowed to dry later. It was examined under low magnification phase objective (10 \times or 16 \times) to check the cell density and spread of metaphase chromosomes.

WCP-FISH^[16]

WCP-FISH was performed according to the protocol provided by Vysis Inc (IL, USA). Briefly chromosome slides were immersed in denaturation solution (700 mL $\cdot \text{L}^{-1}$ formamide/ 2 \times SSC) at 73 \pm 1 °C in water bath for 5 min and subsequently dehydrated serially in 700 mL $\cdot \text{L}^{-1}$, 850 mL $\cdot \text{L}^{-1}$ and 1 000 mL $\cdot \text{L}^{-1}$ ethanol and dried at 45 °C- 50 °C. The WCP probe mix (7 μL of WCP hybridization buffer, 2 μL of purified H₂O and 1 μL of WCP paint DNA probe for human chromosome 8 Spectrum Green™) was incubated at 73 \pm 1 °C in water bath for 5 min and placed at 45 °C~50 °C ready for use. The probe mix was applied to the target area and coverslip was immediately applied which was sealed with rubber cement. Slides were placed in a prewarmed humidified box, which were put into a 37 °C incubator for 16 h. Coverslips were removed from slides, which were immediately immersed in 0.4 \times SSC/ 3 mL $\cdot \text{L}^{-1}$ NP-40 prewarmed to 73 \pm 1 °C agitating for 1-3 s. Slides were removed after 2 min and immersed into 2 \times SSC/ 1 mL $\cdot \text{L}^{-1}$ NP-40 at ambient temperature agitating for 1-3 s and removed after 5 s to 1 min. Slides were air dried in darkness. 10 μL of DAPI counterstain was applied to the target area of slide and coverslip was applied. Slides were viewed using DAPI/Green Vysis filter set on an optimally performing fluorescence microscope and images were captured using CytoVision™ Chromosome Analysis System (Applied Imaging).

RESULTS

Selective screening of microcell hybrids and single cell isolation cloning

Three to four weeks after MMCT, viable floating cells were

observed among dead cells in selective media containing G418 and HAT. Figure 1. The viable cells had good refraction and round shape while the dead cells had poor refraction and morphologic shrinkage.

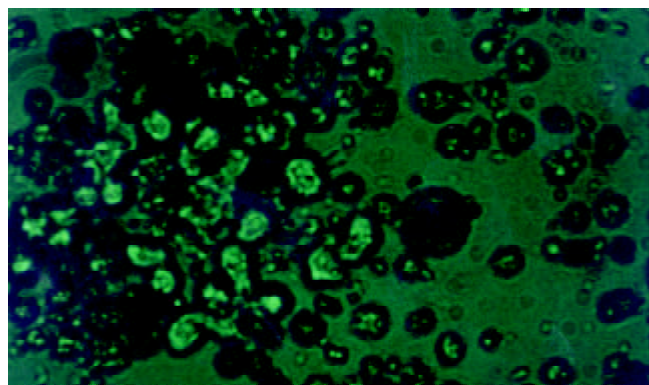


Figure 1 Double selection of microcell hybrids in HAT and G418 (10×25 magnification).

Fifteen microcell hybrid clones were obtained by single cell isolation cloning, which were named neo8/C5F-1~15 respectively. It took about 4 weeks for the progress of enlargement culture serially from 96- to 24-well cell culture plate and finally to T25 flask. Feeder cells are proven unnecessary for the single cell isolation cloning of C5F microcell hybrids. Figure 2 showed the microcell hybrid clone obtained in 96-well plate containing selective media of HAT (1×) and G418 (800 $\mu\text{g} \cdot \text{mL}^{-1}$) one week after single cell isolation.

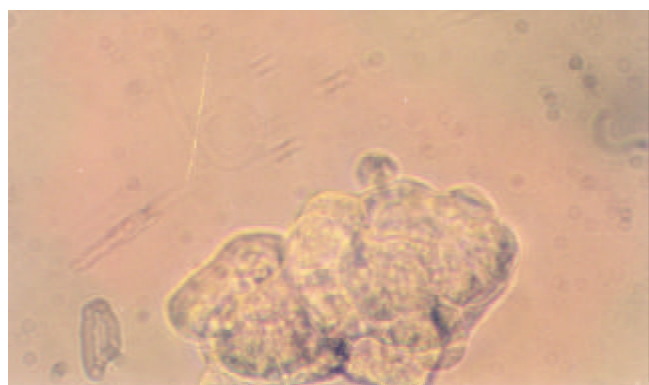


Figure 2 Single-cell isolation cloning in 96-well cell culture plate (10×25 magnification).

STS-PCR

The chromosome donor cell line A9 (neo8) was taken as positive control and the recipient cell line C5F as negative control. DNA extracted from A9 (neo8), C5F and microcell hybrids was used as template. PCR was performed with the primers for D8S277, which is a unique STS located on human chromosome 8p23.3-p22. PCR products, when checked on 2 % agarose gel electrophoresis, were found of the same length with those reported in UniSTS database of NCBI. Figure 3 showed that neo8/C5F-3 had the deletion of D8S277.

WCP-FISH

WCP-FISH was performed using whole chromosome painting DNA probe for human chromosome 8 (WCP 8 probe SpectrumGreen™, Vysis) to confirm its presence. Figure 4 (a and b) showed that the human chromosome 8 had been successfully introduced into rat liver cancer cell line. Meanwhile, the recombination of human chromosome 8 with rat chromosome could be observed clearly by comparing the

probe with its DAPI counterstain image. This recombination was found to be consistent in different metaphase cells.

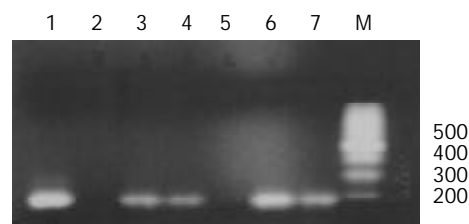


Figure 3 STS-PCR Amplification of D8S277. 1: chromosome donor cell line A9(neo8); 2: recipient cell line C5F; 3-7: microcell hybrids neo8/C5F-1-5; M: 100bp ladders.

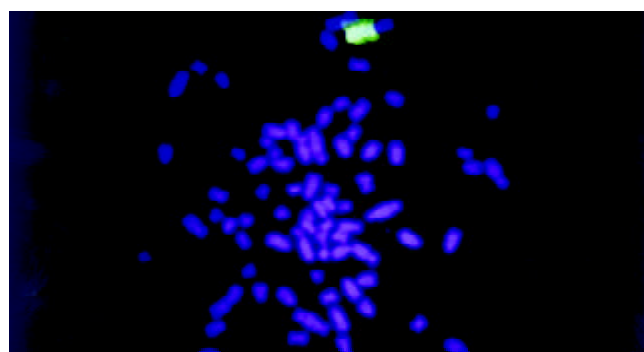


Figure 4a WCP-FISH analysis of neo8/C5F microcell hybrids.



Figure 4b WCP-FISH of neo8/C5F microcell hybrids DAPI counterstain.

DISCUSSION

Metastasis is a major problem puzzling both specialists of cancer biology and of clinical oncology. Thousands of cancer patients die of it each year while clinicians can do little to deal with it. The main reason is that the molecular mechanisms of metastasis have not been totally clarified yet. Researchers fascinated by metastasis hope that the discovery of metastasis suppressor genes could shed light on the solution of this problem, while hitherto few of them have been discovered^[17,18].

Metastasis suppressor genes suppress the formation of spontaneous, macroscopic metastases without affecting the growth rate of the primary cancer. Until presently, only five genes, nm23, KAI1, KISS1, MKK4 and BrMS1, have been proved to meet this criteria^[17,18]. Despite the first metastasis suppressor gene nm23 was discovered by subtractive hybridization, most of encoding regions of metastasis suppressor genes have been discovered with the methodology of MMCT^[18], which is thought to be the methodology particularly suitable for the functional localization of metastasis suppressor genes^[19]. MMCT is established on somatic cell

hybrid. Before MMCT was introduced, researchers had found that somatic cell fusion of metastatic cell line with normal cells could change its metastatic phenotype^[20]. Microcells that contain only one single human chromosome are obtained by the micronucleation and enucleation of human monochromosome donor cells, which include only one intact human chromosome labeled with selective markers such as the neo gene. The target monochromosomes are thereby introduced into recipient cells through the fusion of microcells with recipient cells and the cloning screening of microcell hybrids based on drug resistance conferred. Due to unknown reasons, the introduced chromosome is unstable and random loss or recombination can occur, which result in a series of microcell hybrid clones with different regions of the target chromosome. In this study, the human chromosome 8 introduced into C5F was found to not only have random loss by STS-PCR but also have recombined with rat chromosome by FISH. Those clones in all are called human monochromosome somatic cell panel^[21]. In order to judge which region on the target chromosome harbors the gene of deserved function, spontaneous metastasis assay will be performed with these microcell hybrids. Based on the comparison of changes of metastatic phenotype and different chromosome regions each microcell hybrid contains, the target gene can be narrowed down to specific chromosome region.

Most of current researches for the discovery of metastasis suppressor genes focused on the functional localization of metastasis suppressor genes for prostate cancer, melanoma and breast cancer^[19, 22-31]. However, there hasn't been any report of such work on liver cancer. Our previous study on the surgical samples of primary liver cancer through comparative genomic hybridization (CGH) showed that the loss of the short arm of human chromosome 8 had correlation with metastasis, which suggested that there could be metastasis suppressor gene(s) on chromosome 8p^[6]. This discovery made our present research work imperative. In this study, the highly metastatic rat liver cancer cell line C5F, whose incidence of subcutaneous tumorigenicity is 100 % and that of lung metastasis is 89 %, was chosen as the recipient. The genetic background of rat facilitated STS-PCR screening of the regions remained on the chromosome introduced, as STS is a unique genetic marker different between species. One STS on human chromosome 8p23.3-22, D8S277, was chosen to confirm the introduction of human chromosome with the genomic DNA of microcell hybrids as templates. The results indicated that the microcell hybrids contained the STS specific for human chromosome 8, which could be taken as a proof for the successful chromosome transfer. Meanwhile some clones had deletions of STS, which showed that random losses of regions on human chromosome had occurred. This phenomenon built the basis for construction of human monochromosome panel. The target chromosome was randomly labeled with the G418 resistance gene, neo, which facilitated the selection of positive microcell hybrid clones. In the mean time, the chromosome donor cell line A9 is hypoxanthine-guanine phosphoribosyl transferase (HGPRT) deficient. Therefore A9 can't survive in the media with HAT. Double selections of G418 and HAT were applied in this study to exclude the fake clones from either chromosome donor cell line or recipient cell line. Based on the acquisition of drug resistance, we can reasonably infer that the target chromosome has been transferred into C5F. The results of FISH provide the most direct evidence for the successful chromosome transfer. Recombination between human chromosome and rat chromosome was also observed in different metaphase cells, which showed that the recombination had been stabilized. The introduction of human chromosome can cause transient genetic instability, but with the selection the genetic change will become stable, which is the foundation for further analysis.

All in all, the human chromosome 8 has been successfully transferred into the highly metastatic rat liver cancer cell line C5F, which builds solid basis for future researches on the discovery of metastasis suppressor genes for liver cancer.

ACKNOWLEDGEMENTS

We are much grateful to Dr. Kumiko Ogawa (First Department of Pathology, Nagoaya City University, Japan) for his generous offer of C5F cell line, Prof. Hong-Xuan Lin (Plant Physiology and Ecology Insitute, Chinese Academy of Science, Shanghai, China) for his warmhearted provision and assistance in the usage of Hitachi high speed centrifuge and Dr. M.Z.Zdzienicka and Wouter Wiegant (Leiden Univerity Medical College, Netherland) for kindly providing us the detailed protocol of MMCT.

REFERENCES

- 1 **Tang ZY.** Hepatocellular carcinoma- cause, treatment and metastasis. *World J Gastroenterol* 2001; **7**: 445-454
- 2 **Tang ZY.** Hepatocellular carcinoma. *J Gastroenterol Hepatol* 2000; **15** (Suppl): G1-G7
- 3 **Tang ZY, Yu YQ, Zhou XD, Ma ZC, Wu ZQ.** Progress and prospects in hepatocellular carcinoma surgery. *Ann Chir* 1998; **52**: 558-563
- 4 **Qin LX, Tang ZY.** The prognostic significance of clinical and pathological features in hepatocellular carcinoma. *World J Gastroenterol* 2002; **8**: 193-199
- 5 **Qin LX, Tang ZY.** The prognostic molecular markers in hepatocellular carcinoma. *World J Gastroenterol* 2002; **8**: 385-392
- 6 **Qin LX, Tang ZY, Sham JS, Ma ZC, Ye SL, Zhou XD, Wu ZQ, Trent JM, Guan XY.** The association of chromosome 8p deletion and tumor metastasis in human hepatocellular carcinoma. *Cancer Res* 1999; **59**: 5662-5665
- 7 **Ogawa K, Nakanishi H, Takeshita F, Futakuchi M, Asamoto M, Imaida K, Tatematsu M, Shirai T.** Establishment of rat hepatocellular carcinoma cell lines with differing metastatic potential in nude mice. *Int J Cancer* 2001; **91**: 797-802
- 8 **Fournier RE.** A general high-efficiency procedure for production of microcell hybrids. *Proc Natl Acad Sci U S A* 1981; **78**: 6349-6353
- 9 **McNeill CA, Brown RL.** Genetic manipulation by means of microcell-mediated transfer of normal human chromosomes into recipient mouse cells. *Proc Natl Acad Sci U S A* 1980; **77**: 5394-5398
- 10 **Kraakman-van der Zwet M, Overkamp WJ, Jaspers NG, Natarajan AT, Lohman PH, Zdzienicka MZ.** Complementation of chromosomal aberrations in AT/NBS hybrids: inadequacy of RDS as an endpoint in complementation studies with immortal NBS cells. *Mutation Res* 2001; **485**: 177-185
- 11 **Cowell JK.** Single-cell Isolation Cloning. Human Chromosome Principles and techniques, Verma RS and Babu A eds. 2nded. *McGraw-Hill Inc USA* 1995: 37-38
- 12 **Sambrook J, Russell DW.** Molecular cloning: A laboratory manual. 3rded. *New York: Cold Spring Harbor Laboratory Press* 2000: 542-545
- 13 **Schuler GD.** Electronic PCR: bridging the gap between genome mapping and genome sequencing. *Trends Biotechnol* 1998; **16**: 456-459
- 14 **Nelson DL.** Applications of polymerase chain reaction methods in genome mapping. *Curr Opin Genet Dev* 1991; **1**: 62-68
- 15 **Verma RS, Babu A.** Human Chromosome Principles and techniques. 2nded. *Mc Graw-Hill Inc USA* 1995: 12-13
- 16 **Jenkins RB, Le Beau MM, Kraker WJ, Borell TJ, Stalboerger PG, Davis EM, Penland L, Fernald A, Espinosa R 3rd, Schaid DJ.** Fluorescence *in situ* hybridization: a sensitive method for trisomy 8 detection in bone marrow specimens. *Blood* 1992; **79**: 3307-3315
- 17 **Welch DR, Rinker-Schaeffer CW.** What defines a useful marker of metastasis in human cancer? *J Natl Cancer Inst* 1999; **91**: 1351-1353
- 18 **Yoshida BA, Sokoloff MM, Welch DR, Rinker-Schaeffer CW.** Metastasis-suppressor genes: a review and perspective on an emerging field. *J Natl Cancer Inst* 2000; **92**: 1717-1730

- 19 **Mashimo T**, Watabe M, Cuthbert AP, Newbold RF, Rinker-Schaeffer CW, Helfer E, Watabe K. Human chromosome 16 suppresses metastasis but not tumorigenesis in rat prostatic tumor cells. *Cancer Res* 1998; **58**: 4572-4576
- 20 **Ramshaw IA**, Carlsen S, Wang HC, Badenoch-Jones P. The use of cell fusion to analyze factors involved in tumor cell metastasis. *Int J Cancer* 1983; **32**: 471-478
- 21 **Overhauser J**. Somatic Cell Hybrid Mapping Panels: Resources for Mapping Disease Genes. In: Human Genome Methods, Adolph KW ed. *CRC Press LLC USA* 1998: 258-264
- 22 **Dong JT**, Lamb PW, Rinker-Schaeffer CW, Vukanovic J, Ichikawa T, Issacs JT, Barrett JC. KAI1, a metastasis suppressor gene for prostate cancer on human chromosome 11p11.2. *Science* 1995; **268**: 884-886
- 23 **Chekmareva MA**, Hollowell CM, Smith RC, Davis EM, LeBeau MM, Rinker-Schaeffer CW. Localization of prostate cancer metastasis suppressor activity on human chromosome 17. *Prostate* 1997; **33**: 271-280
- 24 **Nihei N**, Kouprina N, Larionov V, Oshima J, Martin GM, Ichikawa T, Barrett JC. Functional evidence for a metastasis suppressor gene for rat prostate cancer within a 60-kilobase region on human chromosome 8p21-p12. *Cancer Res* 2002; **62**: 367-370
- 25 **Ichikawa T**, Ichikawa Y, Dong J, Hawkins AL, Griffin CA, Isaacs WB, Oshimura M, Barrett JC, Isaacs JT. Localization of metastasis suppressor gene(s) for prostatic cancer to the short arm of human chromosome 11. *Cancer Res* 1992; **52**: 3486-3490
- 26 **Yoshida BA**, Dubauskas Z, Chekmareva MA, Christiano TR, Stadler WM, Rinker-Schaeffer CW. Mitogen-activated protein kinase kinase 4/stress-activated protein/Erk kinase 1 (MKK4/SEK1), a prostate cancer metastasis suppressor gene encoded by human chromosome 17. *Cancer Res* 1999; **59**: 5483-5487
- 27 **Miele ME**, Jewett MD, Goldberg SF, Hyatt DL, Morelli C, Gualandi F, Rimessi P, Hicks DJ, Weissman BE, Barbanti-Brodano G, Welch DR. A human melanoma metastasis-suppressor locus maps to 6q16.3-q23. *Int J Cancer* 2000; **86**: 524-528
- 28 **Lee JH**, Miele ME, Hicks DJ, Phillips KK, Trent JM, Weissman BE, Welch DR. KiSS-1, a novel human malignant melanoma metastasis-suppressor gene. *J Natl Cancer Inst* 1996; **88**: 1731-1737
- 29 **Mashimo T**, Goodarzi G, Watabe M, Cuthbert AP, Newbold RF, Pai SK, Hirota S, Hosobe S, Miura K, Bandyopadhyay S, Gross SC, Watabe K. Localization of a novel tumor metastasis suppressor region on the short arm of human chromosome 2. *Genes Chromosomes Cancer* 2000; **28**: 285-293
- 30 **Goodarzi G**, Mashimo T, Watabe M, Cuthbert AP, Newbold RF, Pai SK, Hirota S, Hosobe S, Miura K, Bandyopadhyay S, Gross SC, Balaji KC, Watabe K. Identification of tumor metastasis suppressor region on the short arm of human chromosome 20. *Genes Chromosomes Cancer* 2001; **32**: 33-42
- 31 **Seraj MJ**, Samant RS, Verderame MF, Welch DR. Functional evidence for a novel human breast carcinoma metastasis suppressor, BRMS1, encoded at chromosome 11q13. *Cancer Res* 2000; **60**: 2764-2769

Edited by Zhang J

Effects of tachyplesin on the regulation of cell cycle in human hepatocarcinoma SMMC-7721 cells

Qi-Fu Li, Gao-Liang Ouyang, Xuan-Xian Peng, Shui-Gen Hong

Qi-Fu Li, Xuan-Xian Peng, The Key Laboratory of China Education Ministry for Cell Biology and Tumor Cell Engineering, School of Life Sciences, Xiamen University, Xiamen 361005, Fujian Province, China
Gao-Liang Ouyang, Shui-Gen Hong, Laboratory of Cell Biology, School of Life Sciences, Xiamen University, Xiamen 361005, Fujian Province, China

Supported by the National Natural Science Foundation of China, No. 30170724

Correspondence to: Dr. Qi-Fu Li, The Key Laboratory of China Education Ministry for Cell Biology and Tumor Cell Engineering, School of Life Sciences, Xiamen University, Xiamen 361005, Fujian Province, China. chifulee@163.net

Telephone: +86-592-2183619 **Fax:** +86-592-2186392

Received: 2002-08-26 **Accepted:** 2002-10-29

Abstract

AIM: To investigate the effects of tachyplesin on the cell cycle regulation in human hepatocarcinoma cells.

METHODS: Effects of tachyplesin on the cell cycle in human hepatocarcinoma SMMC-7721 cells were assayed with flow cytometry. The protein levels of p53, p16, cyclin D1 and CDK4 were assayed by immunocytochemistry. The mRNA levels of p21^{WAF1/CIP1} and c-myc genes were examined with *in situ* hybridization assay.

RESULTS: After tachyplesin treatment, the cell cycle arrested at G₀/G₁ phase, the protein levels of mutant p53, cyclin D1 and CDK4 and the mRNA level of c-myc gene were decreased, whereas the levels of p16 protein and p21^{WAF1/CIP1} mRNA increased.

CONCLUSION: Tachyplesin might arrest the cell at G₀/G₁ phase by upregulating the levels of p16 protein and p21^{WAF1/CIP1} mRNA and downregulating the levels of mutant p53, cyclin D1 and CDK4 proteins and c-myc mRNA, and induce the differentiation of human hepatocarcinoma cells.

Li QF, Ouyang GL, Peng XX, Hong SG. Effects of tachyplesin on the regulation of cell cycle in human hepatocarcinoma SMMC-7721 cells. *World J Gastroenterol* 2003; 9(3): 454-458
<http://www.wjgnet.com/1007-9327/9/454.htm>

INTRODUCTION

A variety of anticancer agents with distinctive effects have been used for treatment of malignant tumors. These agents generally induce tumor cell necrosis and apoptosis as well as differentiation. Today, induction of differentiation is a new strategy in cancer therapy^[1-6]. A number of recent experiments have showed that cell-cycle-arrest may be necessary for cell differentiation. The current knowledge of cell cycle regulation have revealed that the progression of the cell cycle is governed mainly by the activation and deactivation of cyclin-dependent kinases (CDKs). In order for cell cycle arrest to differentiation, it is necessary either to downregulate positive regulation of

CDKs, such as cyclins, or to activate negative regulators of CDKs, such as CDK inhibitors (CKIs)^[7].

It had revealed that tachyplesin, a low molecular weight peptide, could alter the morphological and ultrastructural characteristics, inhibit the proliferation and induce the differentiation of human gastric carcinoma cells and hepatocarcinoma cells^[8,9]. In this paper, we investigate the effects of tachyplesin on the regulation of cell cycle in human hepatocarcinoma SMMC-7721 cells.

MATERIALS AND METHODS

Reagents

Tachyplesin was isolated from acid extracts of Chinese horseshoe crab (*Tachyplesus tridentatus*) hemocytes as described by Nakamura^[10] with minor modification. RPMI-1640 medium were obtained from Gibco. Fetal calf serum was supplied by Si-Ji-Qing Biotechnology Co. (Hangzhou, China). Mouse anti-human p53, p16, cyclin D1 monoclonal antibodies and rabbit anti-human CDK4 antibody were purchased from Santa Cruz. Immunocytochemistry detection kit and *in situ* hybridization kit were provided by Beijing Zhongshan Biotechnology Co.

Cell culture and treatment

SMMC-7721 cells, provided by the Institute of Biochemistry and Cell Biology, Shanghai Institute of Biological Sciences, Chinese Academy of Sciences, were maintained in RPMI-1640 medium supplemented with 20 % heat-inactivated fetal calf serum, 100 units/mL penicillin, 100 mg/L streptomycin and 50 mg/L kanamycin at 37 °C, 5 % CO₂ in air atmosphere. SMMC-7721 cells were treated with culture medium containing 3.0 mg/L tachyplesin after being seeded for 24 hours.

Flow cytometry assay

SMMC-7721 cells and the cells treated with 3.0 mg/L tachyplesin for 2, 4 or 6 days were collected, rinsed in 0.1 M PBS, resuspended and fixed in 70 % ethanol at 4 °C overnight. Cells were centrifuged, resuspended in 100 mg/L RNase A at 37 °C for 30 min and in 50 mg/L propidium iodide at 4 °C for 30 min. Cell cycle was analyzed by flow cytometry.

Immunohistochemistry analysis

SMMC-7721 cells and the cells treated with 3.0 mg/L tachyplesin for 5 days were seeded in little penicillin bottles with coverslips for 48 hours respectively. The cells grown on coverslips were fixed with cold acetone for 10 min, rinsed twice in PBS for 15 min, immersed in 3 % hydrogen peroxide for 10 min, washed with distilled water and PBS for 15 min, blocked with 10 % normal goat serum for 10 min at room temperature, and incubated with primary antibodies at 4 °C overnight. After incubation with primary antibodies, coverslips were rinsed twice in PBS for 15 min, incubated with biotin-labeled secondary antibody at 37 °C for 10 min, rinsed twice in PBS for 15 min, and then incubated in streptavidin-peroxidase at 37 °C for 10 min. The antigen-antibody complex was visualized with diaminobenzidine (DAB) substrate. Negative controls were incubated in the absence of primary antibodies.

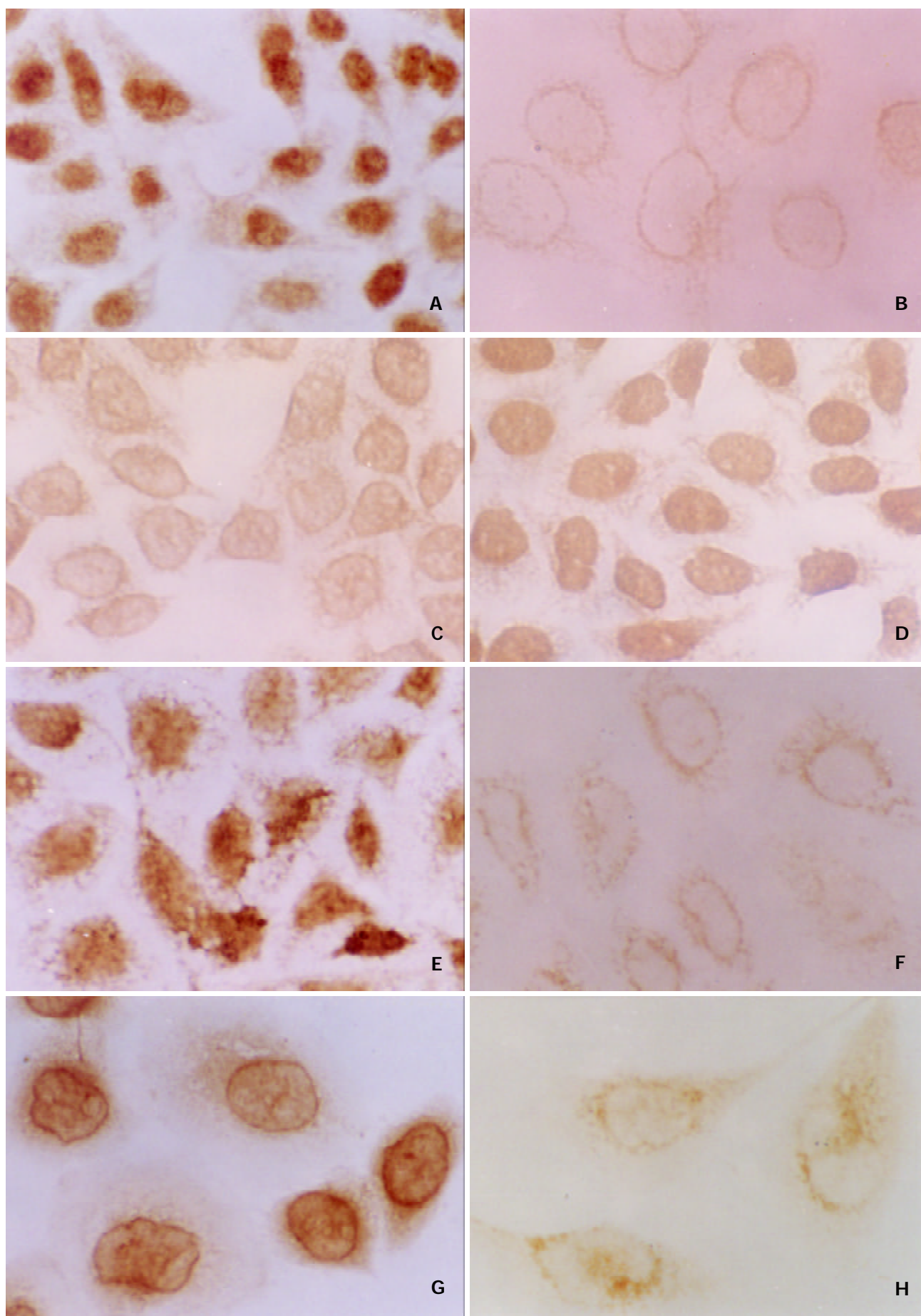


Figure 1 Immunocytochemistry analysis of the effects of tachyplesin on the protein levels of mutant p53, p16, cyclin D1, CDK4 in SMMC-7721 cells ($\times 536$). The protein levels of mutant p53 (A), cyclin D1 (E), CDK4 (G) were high in SMMC-7721 cells while the levels of mutant p53 (B), cyclin D1 (F), CDK4 (H) were decreased by tachyplesin. The level of p16 protein was low in SMMC-7721 cells (C) while high in the tachyplesin-treated cells (D).

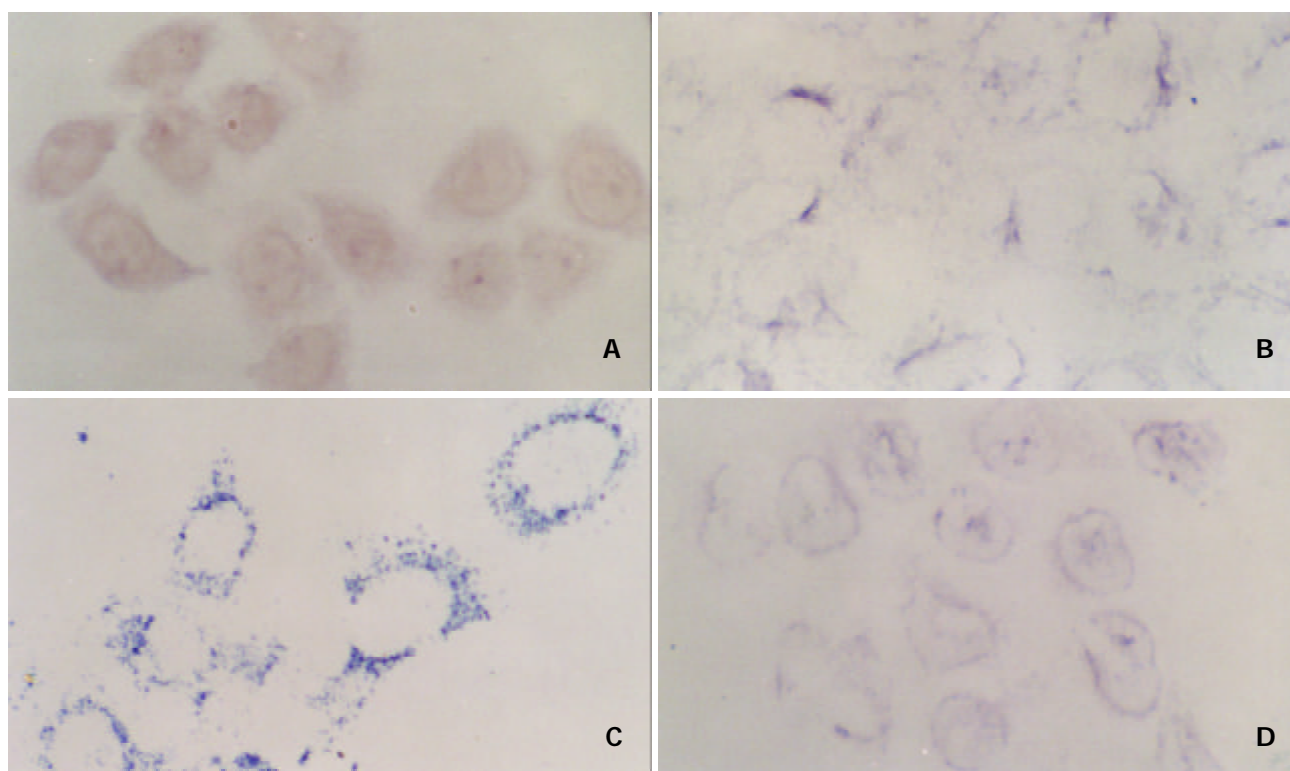


Figure 2 *In situ* hybridization analysis of p21^{WAF1/CIP1} and c-myc mRNA in untreated and tachyplesin-treated SMMC-7721 cells ($\times 536$). The level of p21^{WAF1/CIP1} mRNA was low in SMMC-7721 cells (A) but high in the tachyplesin-treated cells (B). High level of c-myc mRNA was observed in SMMC-7721 cells (C) while the level of c-myc mRNA in the tachyplesin-treated cells down-regulated (D).

In situ hybridization

SMMC-7721 cells and the cells treated with 3.0 mg/L tachyplesin for 5 days were seeded in little penicillin bottles with coverslips for 48 hours respectively. *In situ* hybridization procedure was carried out as described by Spector^[11] with minor modifications. The coverslips were rinsed twice in PBS, prefixed with methanol/acetone (1:1, v/v) for 10 min, incubated in 0.1 M HCl for 10 min, rinsed in 0.01 M PBS for 5 min $\times 2$, and incubated in 25 mg/L proteinase K at 37 °C for 20 min and in 0.2 % glycine in PBS for 5 min $\times 3$. They were postfixed in 4 % paraformaldehyde for 10 min, dehydrated, and air dried. The prehybridization was conducted at room temperature for 1 hour, followed by hybridization in a humid chamber at 42 °C for 16-22 hours. The hybridization solution contained prehybridization solution and 1.0 ug/mL digoxigenin-labeled p21^{WAF1/CIP1} cRNA or c-myc cRNA probe. Coverslips were rinsed in 2 \times SSC at 37 °C for 15 min $\times 2$, in 1 \times SSC for 5 min $\times 2$, in 0.5 \times SSC for 5 min $\times 2$, in 0.2 \times SSC for 5 min $\times 2$, washed with Buffer I (100 mM Tris-HCl buffer, 150 mM NaCl, pH7.5) for 5 min, and incubated with Blocking buffer (2 % horse serum and 0.3 % Triton X-100 in Buffer I) for 1 hour, and then incubated at 37 °C for 1 hour in alkaline phosphatase-conjugated anti-digoxigenin antibody diluted 1:500 in Blocking buffer, then rinsed in Buffer I for 15 min $\times 3$, and equilibrated in Buffer II (100 mM Tris-HCl buffer, 100 mM NaCl, 50 mM MgCl₂, pH9.5). The alkaline phosphatase reaction was conducted by incubation with NBT/BCIP solution for 20-30 min. The reaction was stopped with Buffer III (10 mM Tris-HCl buffer, 1 mM EDTA, pH8.0). The coverslips were then dehydrated in alcohol, cleared in xylene, and mounted on gelatin. The negative controls were processed without labeled probes.

RESULTS

Effects of tachyplesin on the cell cycle distribution of SMMC-7721 cells

Cell cycle kinetics of SMMC-7721 cells was analyzed by flow

cytometry. As demonstrated in Table 1, 3.0 mg/L tachyplesin could induce an accumulation of the cells at G₀/G₁ phase on day 2, 4, 6, respectively. Compared with control group, the amount of cells at G₀/G₁ phase increased from 48.2 % to 65.6 %, while the quantity of cells in S phase decreased from 48.0 % to 24.8 % after being treated with tachyplesin for 6 days. This indicated that tachyplesin could arrest the SMMC-7721 cells at G₀/G₁ phase.

Table 1 Effects of 3.0 mg/L tachyplesin on the cell cycle kinetics of SMMC-7721 cells

	SMMC-7721	Tachyplesin 2 d	Tachyplesin 4 d	Tachyplesin 6 d
G ₀ /G ₁	48.2 %	66.5 %	61.8 %	65.6 %
S	48.0 %	29.7 %	34.8 %	24.8 %
G ₂ /M	3.8 %	3.8 %	3.4 %	9.6 %

Effects of tachyplesin on p53, p16 protein levels in SMMC-7721 cells

It has revealed that p53 protein detected by immunohistochemistry is mutant p53. Immunohistochemistry showed that the level of mutant p53 protein was high in the nucleus and cytoplasm of SMMC-7721 cells. However, very low level of mutant p53 protein in the tachyplesin-treated cells was observed (Figure 1A and B). p16 protein was distributed mainly in the nucleolus of SMMC-7721 cells in low level while the level of immunohistochemical reaction was very high in the tachyplesin-treated cells (Figure 1C and D).

Effects of tachyplesin on cyclin D1, CDK4 protein levels in SMMC-7721 cells

As shown in Figure 1E and F, the level of cyclin D1 protein was high in the nucleolus and cytoplasm of untreated cells while it was very weak in the cells treated with tachyplesin. It also revealed that exposure of SMMC-7721 cells to tachyplesin resulted in an obvious decrease of CDK4 protein level (Figure 1G and H).

Effects of tachyplesin on p21^{WAF1/CIP1}, c-myc mRNA levels in SMMC-7721 cells

To investigate the effects of tachyplesin on the expression of tumor suppressor gene and oncogene associated with the G₀/G₁ arrest, the levels of p21^{WAF1/CIP1} and c-myc mRNA were also detected. *In situ* hybridization assay showed that the level of p21^{WAF1/CIP1} mRNA was low in the nuclear and cytoplasm of the untreated cells while it was high in the cytoplasm around the nucleolus in the cells treated with tachyplesin (Figure 2A and B). And high level of c-myc mRNA was observed in the cytoplasm of SMMC-7721 cells. However, the level of c-myc mRNA was down-regulated in the tachyplesin-treated cells (Figure 2 C and D).

DISCUSSION

In multi-cellular organism, the balance among cell proliferation, cell differentiation and cell death maintains a constant cell number. Cell proliferation depends on the cell's growth and division cycles, which are governed by periodic assembly of the core cell cycle clock, composed of cyclins and cyclin-dependent kinases (CDKs)^[7,12]. Distinct cyclins associate and activate different CDKs throughout the cell cycle. The activity of cyclin/CDK complexes is modulated by both activating and inhibiting phosphorylation of the CDKs, and by binding to cyclin-dependent kinases inhibitors (CKIs). In higher eukaryotic cells, signals that arrest the cycle usually act at a G₁ checkpoint. The G₁ checkpoint can be viewed as a master checkpoint of the mammalian cell cycle^[7,13]. Regulation of the G₁ phase of the cell cycle is extremely complicated and involves many different families of cyclins, CDKs and CKIs. In eukaryotes, D-cyclins (D1, D2, and D3) bind CDK4/6 to wire external signals to the cell cycle and regulate progression through mid-G₁. cyclin E binds CDK2 in late G₁ and its activity is rate-limiting for progression from G₁ to S phase^[14]. The p16 tumor suppressor belongs to the INK4 family of CKIs. p16 specifically inhibit CDK4/6 by preventing binding of the activating cyclin subunits. p21^{WAF1/CIP1}, one CKI of CIP/KIP family, unlike p16, binds to a number of cyclin/CDK complexes such as cyclin D1/CDK4, cyclin E/CDK2 and cyclin A/CDK2, inhibits kinases activities and induces cell cycle arrest and cell differentiation^[7,15-17].

In addition, some other genes are associated with G₁ checkpoint. It is known that wild-type p53 gene has anti-proliferation, anti-transforming and inducing apoptosis activities. Growth arrest induced by wild-type p53 blocks cells prior to or near the checkpoint in late G₁ phase. Mutations of p53 are observed with a high incidence in most cancer^[18,19]. One of the phenotype effects of mutant p53 protein is called dominant-negative effect, which mutant p53 can override the normal inhibitory function of wild-type p53. In the meantime, c-myc gene, an early-response gene necessary for cell cycle progression (G₁-S transition), also plays an essential role in the regulation of the cell cycle and differentiation^[20-24].

As revealed by many experiments, the regulation of G₁/S checkpoint was abnormal in tumor cells. G₀/G₁ arrest was a common phenomenon in the cells undergoing induction of differentiation. And many differentiation inducers could arrest tumor cells in G₀/G₁ phase and alter the expression of cell cycle regulators^[25-31]. Our results showed that tachyplesin could down-regulate the levels of mutant p53, cyclin D1, CDK4 proteins and c-myc mRNA, up-regulate the levels of p16 protein and p21^{WAF1/CIP1} mRNA in SMMC-7721 cells, and arrest the cell in G₀/G₁ phase as other inducers on tumor cells. Taken together, the results indicated that tachyplesin might decrease the kinase activity of cyclin D1/CDK4 complex by decreasing the expression of mutant p53 protein and increasing the levels of p16 and p21^{WAF1/CIP1}, and suppress the phosphorylation of

retinoblastoma (Rb) protein and downregulate the level of c-myc mRNA, which cause a decrease of the cell in S phase significantly and arrest most of the cells at G₀/G₁ phase, and induce the cells to terminal differentiation as other inducers.

REFERENCES

- 1 Yoneda K, Yamamoto T, Ueta E, Osaki T. Induction of cyclin-dependent kinase inhibitor p21 in vesnarinone-induced differentiation of squamous cell carcinoma cells. *Cancer Lett* 1998; **133**: 35-45
- 2 Lo Coco F, Zelent A, Kimchi A, Carducci M, Gore SD, Waxman S. Progress in differentiation induction as a treatment for acute promyelocytic leukemia and beyond. *Cancer Res* 2002; **62**: 5618-5621
- 3 Wang Z, Sun G, Shen Z, Chen S, Chen Z. Differentiation therapy for acute promyelocytic leukemia with all-trans retinoic acid: 10-year experience of its clinical application. *Chin Med J* 1999; **112**: 963-967
- 4 Leszczyniecka M, Roberts T, Dent P, Grant S, Fisher PB. Differentiation therapy of human cancer: basic science and clinical applications. *Pharmacol Ther* 2001; **90**: 105-156
- 5 Hansen LA, Sigman CC, Andreola F, Ross SA, Kelloff GJ, De Luca LM. Retinoids in chemoprevention and differentiation therapy. *Carcinogenesis* 2000; **21**: 1271-1279
- 6 Gali-Muhtasib H, Bakkar N. Modulating cell cycle: current applications and prospects for future drug development. *Curr Cancer Drug Targets* 2002; **2**: 309-336
- 7 Donjerkovic D, Scott DW. Regulation of the G₁ phase of the mammalian cell cycle. *Cell Res* 2000; **10**: 1-16
- 8 Li QF, Ouyang GL, Li CY, Hong SG. Effects of tachyplesin on the morphology and ultrastructure of human gastric carcinoma cell line BGC-823. *World J Gastroenterol* 2000; **6**: 676-680
- 9 Ouyang GL, Li QF, Peng XX, Liu QR, Hong SG. Effects of tachyplesin on proliferation and differentiation of human hepatocellular carcinoma SMMC-7721 cells. *World J Gastroenterol* 2002; **8**: 1053-1058
- 10 Nakamura T, Furunaka H, Miyata T, Tokunaga F, Muta T, Iwanaga S, Niwa M, Takao T, Shimonishi Y. Tachyplesin, a class of antimicrobial peptide from the hemocytes of the horseshoe crab (*Tachypus tridentatus*), isolation and chemical structure. *J Biol Chem* 1988; **263**: 16709-16713
- 11 Spector DL, Goldman RD, Leinwand LA. Cells A Laboratory Manual. Cold Spring Harbor Laboratory Press 1998
- 12 Steinman RA. Cell cycle regulators and hematopoiesis. *Oncogene* 2002; **21**: 3403-3413
- 13 Wang J, Barsky LW, Shum CH, Jong A, Weinberg KI, Collins SJ, Triche TJ, Wu L. Retinoid-induced G₁ arrest and differentiation activation are associated with a switch to cyclin-dependent kinase-activating kinase hypophosphorylation of retinoic acid receptor alpha. *J Biol Chem* 2002; **277**: 43369-43376
- 14 Agami R, Bernards R. Convergence of mitogenic and DNA damage signaling in the G₁ phase of the cell cycle. *Cancer Lett* 2002; **177**: 111-118
- 15 Harada K, Ogden GR. An overview of the cell cycle arrest protein, p21^{WAF1}. *Oral Oncol* 2000; **36**: 3-7
- 16 Garte AL, Tyner AL. The growth-regulatory role of p21 (WAF1/CIP1). *Prog Mol Subcell Biol* 1998; **20**: 43-71
- 17 Boulaire J, Fotedar A, Fotedar R. The functions of the cdk-cyclin kinase inhibitor p21WAF1. *Pathol Biol* 2000; **48**: 190-202
- 18 Lin D, Shields MT, Ullrich SJ, Appella E, Mercer WE. Growth arrest induced by wild-type p53 protein blocks cells prior to or near the restriction point in late G₁ phase. *Proc Natl Acad Sci USA* 1992; **89**: 9210-9214
- 19 Liu MC, Gelmann EP. P53 gene mutations: case study of a clinical marker for solid tumors. *Semin Oncol* 2002; **29**: 246-257
- 20 Bartova E, Kozubek S, Kozubek M, Jirsova P, Lukasova E, Skalnikova M, Cafourkova A, Koutna I. Nuclear topography of the c-myc gene in human leukemic cells. *Gene* 2000; **244**: 1-11
- 21 He Y, Zhang J, Zhang J, Yuan Y. The role of c-myc in regulating mdr-1 gene expression in tumor cell line KB. *Chin Med J* 2000; **113**: 848-851
- 22 Jiang N, Zhan F, Cao L, Yao K, Li G. c-myc gene inactivation during inducing of nasopharyngeal carcinoma cells with retinoic

- acid. *Chin Med J* 2000; **113**: 823-826
- 23 **Obaya AJ**, Kottenko I, Cole MD, Sedivy JM. The proto-oncogene c-myc acts through the cyclin-dependent kinase (Cdk) inhibitor p27(Kip1) to facilitate the activation of Cdk4/6 and early G(1) phase progression. *J Biol Chem* 2002; **277**: 31263-31269
- 24 **Boxer LM**, Dang CV. Translocations involving c-myc and c-myc function. *Oncogene* 2001; **20**: 5595-5610
- 25 **Chen RC**, Su JH, Ouyang GL, Cai KX, Li JQ, Xie XG. Induction of differentiation in human hepatocarcinoma cells by Isoverbascoside. *Planta Med* 2002; **68**: 370-372
- 26 **Yuan SL**, Huang RM, Wang XI, Song Y, Huang GQ. Reversing effect of Tanshinone on malignant phenotypes of human hepatocarcinoma cell line. *World J Gastroenterol* 1998; **4**: 317-319
- 27 **Kiyokama H**, Richon VM, Rifkind RA, Marks PA. Suppression of cyclin-dependent kinase 4 during induced differentiation of erythroleukemia cells. *Mol Cell Biol* 1994; **14**: 7195-7203
- 28 **Spinella MJ**, Freemantle SJ, Sekula D, Chang JH, Christie AJ, Dmitrovsky E. Retinoic acid promotes ubiquitination and proteolysis of cyclin D1 during induced tumor cell differentiation. *J Biol Chem* 1999; **274**: 22013-22018
- 29 **Bergh G**, Telleus A, Fritzson A, Kornfalt S, Johnson E, Gullberg U. Forced expression of the cyclin-dependent kinase inhibitor p16^{INK4A} in leukemic U-937 cells reveals dissociation between cell cycle and differentiation. *Exp Hematol* 2001; **29**: 1382-1391
- 30 **Hyman T**, Rothmann C, Heller A, Malik Z, Salzberg S. Structural characterization of erythroid and megakaryocytic differentiation in Friend erythroleukemia cells. *Exp Hematol* 2001; **29**: 563-571
- 31 **Zhang LP**, Jiang JK, Tam JW, Zhang Y, Liu XS, Xu XR, Liu BZ, He YJ. Effects of matrine on proliferation and differentiation in K-562 cells. *Leuk Res* 2001; **25**: 793-800

Edited by Ren SY

Detection of HBV, PCNA and GST-p in hepatocellular carcinoma and chronic liver diseases

Li-Juan Shen, Hua-Xian Zhang, Zong-Ji Zhang, Jin-Yun Li, Ming-Qin Chen, Wei-Bo Yang, Run Huang

Li-Juan Shen, Hua-Xian Zhang, Zong-Ji Zhang, Run Huang,
Department of Pathology, Kunming Medical College, Kunming 650031, Yunnan Province, China

Jin-Yun Li, Department of Pathology, the Second Affiliated Hospital, Kunming Medical College, Kunming 650032, Yunnan Province, China

Ming-Qin Chen, the Third Affiliated Hospital, Kunming Medical College, Kunming 650032, Yunnan Province, China

Wei-Bo Yang, Department of infectious diseases, the First Affiliated Hospital, Kunming Medical College, Kunming 650032, Yunnan Province, China

Supported by Natural Science Foundation of Yunnan Province, China, NO.2000C0058M and Scientific Research Foundation of the Education Department of Yunnan Province, NO.0011010

Correspondence to: Li-Juan Shen, Department of Pathology, Kunming Medical College, Kunming 650031, Yunnan Province, China. wycslj@public.km.yn.cn

Telephone: +86-871-5338845 **Fax:** +86-871-5173299

Received: 2002-07-27 **Accepted:** 2002-08-23

Abstract

AIM: To investigate the change of HBV DNA, PCNA and GST- π in chronic liver disease and hepatocellular carcinoma (HCC).

METHODS: Hepatitis B surface antigen (HBsAg), proliferating cell nuclear antigen (PCNA) and glutathione S-transferases (GST- π) were detected by immunohistochemical staining and HBV DNA was detected by *in situ* hybridization (ISH) in formalin-fixed and paraffin-embedded sections with a total of 111 specimens of chronic hepatitis, liver cirrhosis, paratumorous tissue, HCC and normal liver tissue.

RESULTS: The positive rates of HBsAg and HBVDNA were 62.5 % (15/24) and 75.0 % (12/16) in chronic hepatitis, 64.0 % (16/25) and 83.3 % (15/18) in liver cirrhosis, 72.7 % (16/22) and 85.7 % (12/14) in the paratumorous tissue and 45.0 % (14/31) and 64.3 % (9/14) in HCC. The positive HBVDNA granules in chronic hepatitis, liver cirrhosis and the paratumorous tissue were more intense than that in HCC. The positive rates of PCNA and GST- π were 34.8 % (8/23) and 25.0 % (4/16) in chronic hepatitis, 73.7 % (14/19) and 17.6 % (3/17) in liver cirrhosis, 86.7 % (13/15) and 53.3 % (8/15) in the paratumorous tissue, 100 % (15/15) and 60.0 % (9/15) in HCC, respectively, and the positive rate of GST- π in the paratumorous tissue was significantly higher than that in the liver cirrhosis without tumor ($P < 0.05$), but same as that in HCC ($P > 0.05$).

CONCLUSION: The HBV infection may increase expression of PCNA and GST- π . The paratumorous cirrhosis may be a sequential lesion of precancerous cirrhosis around HCC.

Shen LJ, Zhang HX, Zhang ZJ, Li JY, Chen MQ, Yang WB, Huang R. Detection of HBV, PCNA and GST- π in hepatocellular carcinoma and chronic liver diseases. *World J Gastroenterol* 2003; 9(3): 459-462

<http://www.wjgnet.com/1007-9327/9/459.htm>

INTRODUCTION

Proliferating cell nuclear antigen (PCNA) is an auxiliary protein of DNA polymerase and is thought to play an important role in the elongation or replication of the DNA chain. It accumulated in the nucleus during the G-1 and S stages of the cell cycle and the percentage of PCNA-positive cell is correlated with the proliferative activity and the prognosis of various malignant tumors^[1-5]. Glutathione S-transferases (GST- π) is closely related with cancer and is increased in blood and tissues of cancer patients, it is now recognized as a tumor marker^[6, 7]. We have detected hepatitis B surface antigen (HBsAg), PCNA and GST- π by immunohistochemical staining and hepatitis B virus DNA (HBV DNA) by *in situ* hybridization (ISH) in patients with chronic hepatitis, liver cirrhosis, the paratumorous tissue, hepatocellular carcinoma (HCC) and normal liver tissue, to see whether there are any changes of HBV, PCNA and GST- π in the above diseases.

MATERIALS AND METHODS

Materials

Specimens obtained from surgical resection, autopsy and needle aspiration biopsy of livers from 1965 to 2001 were fixed in 10 % formalin, embedded in paraffin sections, and stained by routine HE. They were divided into 5 groups: Normal liver tissues used as controls ($n=9$); Chronic hepatitis ($n=24$); liver cirrhosis ($n=25$); The paratumorous tissue ($n=22$); HCC ($n=31$). All specimens were examined by two pathologists. The diagnosis of hepatitis was according to the standard of Xi'an Conference in 2000^[8].

Immunohistochemical staining

Immunohistochemistry S-P method was used to detect HBsAg, PCNA and GST- π . Mouse monoclonal antibody to human HBsAg (ZMHB5), PCNA (PC10), GST- π (353-10) and Immunostaining S-P Kit were purchased from Fuzhou Maxim Biotechnical Company. The main steps were as follows: (1) The tissues were treated with endogenous peroxidase blocking solution at room temperature for 10 minutes and then incubated in normal nonimmune serum at room temperature for 10 minutes. (2) The mouse anti HBsAg, PCNA or GST- π antibody were added to adjacent tissue sections respectively and incubated overnight at 4 °C. (3) Biotin-conjugated second antibody was added to the sections and incubated at room temperature for 10 minutes. (4) S-P complex was added at room temperature for 10 minutes and then DAB was used for the color reaction. The tissue sections were washed with PBS (0.01M, pH 7.4) between each step. Positive and negative controls were simultaneously used to ensure specificity and reliability of the staining process. A positive section was taken as positive control. In negative control, PBS was used to replace the first antibody. The positive result showed brown coloration in the cytoplasm or /and the nucleus and was graded as follows: $<10\%$ -, $10-30\%$ +, $31-50\%$ ++, $>50\%$ +++^[9].

In situ hybridization (ISH)

In situ hybridization was used for detection of HBV DNA.

The HBV DNA probed with biotin-labeled and ISH-kit were purchased from Fuzhou Maxim Biotechnical Company. The main steps were as follows: (1) Baked the slides at 60-80 °C for 1 hour till overnight. (2) Deparaffinized by xylene and graded alcohols. (3) Dried at 37 °C for 5 min. (4) Added proteinase K at 37 °C for 10-15 min. (5) Enhancer wash buffer for 5 min. (6) Dehydrated the slides by graded alcohols. (7) Dried at 37 °C for 5 min. (8) Added biotin-labeled probe with coverslip. (9) Denatured at 95 °C for 8-10 min. (10) Hybridized at 37 °C for 1-2 hours in humidity chamber. (11) Soaked off coverslips in PBS. (12) Hybridization wash at 37 °C for 10 min. (13) Protein block at 37 °C for 20 min. (14) Conjugated at 37 °C for 20 min. (15) PBS rinsed enhancer wash buffer for 5 min. (16) The substrate (NBT/BCIP) showed coloration at room temperature for 10-40 min, or till the coloration developed became complete. (17) Distilled water washed for 2-3 times. (18) The slides were counterstained using nuclear fast red. The positive and negative controls were concomitantly used to ensure the specificity and reliability of the staining with a known HBVDNA positive tissue section, the normal liver tissues and hybridization liquids without probe were served as controls. The positive result showed blue coloration in the cytoplasm or/and in the nucleus.

RESULTS

Detection of HBsAg and HBV DNA

HBsAg and HBVDNA were widely expressed in chronic hepatitis, liver cirrhosis, paratumorous tissue cirrhosis and HCC (Table 1). The positive rates of HBsAg and HBVDNA were highest in the paratumorous tissue.

Table 1 Detection of hepatitis B virus, PCNA and GST- π in hepatocellular carcinoma and chronic liver diseases

Group	HBsAg ^a	HBVDNA ^b	PCNA ^c	GST- π ^d
1. Normal liver tissue	0/9 (0)	0/9 (0)	0/5 (0)	0/5 (0)
2. Chronic hepatitis	15/24 (62.5)	12/16 (75.0)	8/23 (34.8)	4/16 (25.0)
3. Liver cirrhosis	16/25 (64.0)	15/18 (83.3)	14/19 (73.7)	3/17 (17.6)
4. Paratumorous tissue	16/22 (72.7)	12/14 (85.7)	13/15 (86.7)	8/15 (53.3)
5. HCC	14/31 (45.2)	9/14 (64.3)	15/15 (100)	9/15 (60.0)

HCC: hepatocellular carcinoma; HBsAg: Hepatitis B surface antigen; HBVDNA: hepatitis B virus DNA; PCNA: proliferating cell nuclear antigen; GST- π : glutathione S-transferases.

^a $P < 0.05$, 5 vs 4; ^b $P < 0.01$, 1 vs 4; ^c $P < 0.01$, 1 vs 4; ^d $P < 0.05$, 3 vs 4, $P < 0.01$, 1 vs 4.

The expression of HBsAg was seen in the cytoplasm (Figure 1). HBVDNA was detected in the cytoplasm and in the nucleus. HBVDNA positive granules in chronic hepatitis, liver cirrhosis and the paratumorous tissue were more intense than that in HCC. HBVDNA positive granules in HCC was mainly expressed in the nucleus but the signals were much weaker (Figure 2).

Detection of PCNA and GST- π

PCNA and GST- π were widely expressed in chronic hepatitis, liver cirrhosis, paratumorous tissue and HCC, the positive rates of PCNA and GST- π increased evidently in the paratumorous tissue and HCC (Figure 3-4). The positive rate of GST- π in paratumorous tissue (53.3 %) was significantly higher than that in cirrhosis without tumor (17.6 %) ($P < 0.05$, $\chi^2 = 6.58$).

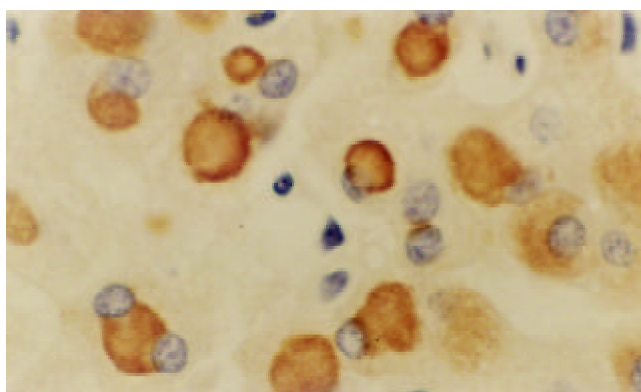


Figure 1 HBsAg was expressed at cytoplasm in chronic hepatitis. $\times 400$.

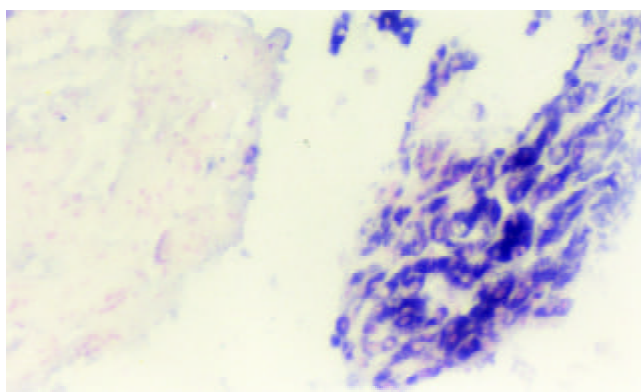


Figure 2 HBV DNA was rich in paratumorous tissue (right) and less in HCC (left). $\times 100$.

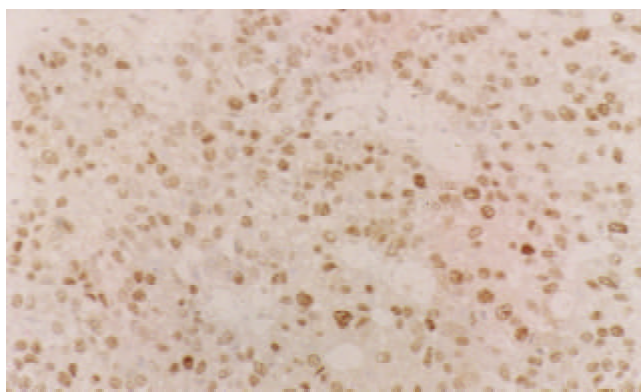


Figure 3 PCNA was expressed in nuclei of HCC. $\times 100$.

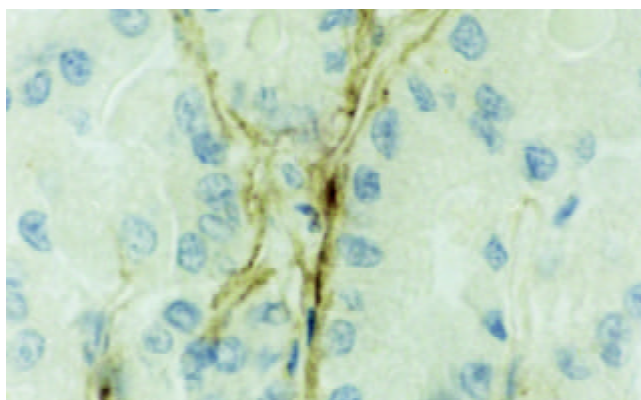


Figure 4 GST- π was expressed on cell membranes of HCC. $\times 400$.

DISCUSSION

HCC is one of the most common malignant tumors in China. In recent decades, the incidence of HCC has been found to be increasing and HCC came ranks the second in cancer mortality since 1990s^[10]. Most of patients with HCC were associated with HBV^[11-15]. The relative risk of HBV carrier developing HCC approaches 200:1, which is the highest relative risks known for HCC^[16]. we have found that there are higher positive rates of HBsAg and HBV DNA in chronic hepatitis, liver cirrhosis, paratumorous tissue and HCC, but the highest positive rate in the paratumorous tissue, supports the view of HBV as the main cause of HCC in China. The positive rate of HBV DNA in HCC was 64.3 %, mainly expressed in nuclei, HBV DNA positive granules were less and weakly stained, perhaps because most of the HBV DNA had been integrated into the genome of HCC tissue. The positive rates of HBV DNA were 85.7 % in the paratumorous tissue, which was mainly expressed in the cytoplasm, HBV DNA positive granules were more intense, because HBV DNA was mainly in the free form and in an active replicative state. Our results were similar to those of most researchers^[17]. The carcinogenesis of HCC was related to integration of HBV DNA into the genome with rearrangement of the chromosome. The integration of viral gene often occurred in the earlier stage of HCC. The integration of HBV might lead to the structural abnormality of the chromosome, which enhanced the transcription of oncogene and lost the its suppressor function, resulting in malignant transformation of hepatic cells by reverse activation of the X gene of HBV^[18]. HBV DNA was integrated into the genome randomly. The integrated HVB DNA was not complete, there were some defect in the virus genome which caused the weakening of HBV DNA hybridization signal in the nuclei of HCC^[19]. The integrated HVB DNA in the hepatic cells could bring about abnormal expression of the gene and abnormal synthesis of protein so that the growth of HCC and the differentiation and regulation of the hepatic cells became out of control. PCNA is a better marker for assessment of cellular proliferative activity, the poorer the differentiation of the cancer, the stronger the proliferative activity and the higher positive rate of PCNA^[20-21]. When the carcinogenesis initiated, the shape and structure of the cells did not have much changes, but the function and the metabolism enzymes had already been abnormal. The expression of GST- π might increase abnormally in the course of the carcinogenesis of many tumors. This change occurred much more earlier than that of the morphology^[22,23]. Our study demonstrated that PCNA and GST- π were all expressed in chronic hepatitis (34.8 % and 25.0 %), liver cirrhosis (73.7 % and 17.6 %), the paratumorous tissue (86.7 % and 53.3 %) and HCC (100 % and 60.0 %). But the positive rates of PCNA and GST- π increased significantly in the paratumorous tissue and in the HCC. These results demonstrated that repeated degeneration, necrosis and hyperplasia occurred in the chronic HBV hepatitis, because of the increase of cell proliferation and the integration of viral genome, caused disturbed proteins synthesis abnormality in metabolism enzymes. It might be a gradual developmental process from quantitation to qualitation change. The paratumorous tissue differs essentially from cirrhosis without tumor, it is rather a precancerous lesion^[24-28], which already has some characteristics of fetal liver or HCC with earlier expression AFP and AFPmRNA^[29,30], also with increased expression of PCNA and GST- π ^[31-39].

REFERENCES

- Zeng WJ**, Liu GY, Xu J, Zhou XD, Zhang YE, Zhang N. Pathological characteristics, PCNA labeling index and DNA index in prognostic evaluation of patients with moderately differentiated hepatocellular carcinoma. *World J Gastroenterol* 2002; **8**: 1040-1044
- Kong XB**, Liang LJ, Huang JF. A Study of correlation between apoptosis, expression of p21 protein and PCNA and the clinical prognosis in hepatocellular carcinoma. *Aizheng J* 1999; **18**: 426-429
- Huang Y**, Cai SM, Yu SY, Shi DR, Zhang GL, Wang HY, Lu HF. Significance of c-erbB-2 and PCNA expression in adenocarcinoma of uterine cervix. *Zhonghua Zhongliu Zazhi* 1997; **19**: 150-152
- Wang D**, Shi JQ. Immunohistochemical detection of proliferating cell nuclear antigen in hepatocellular carcinoma. *Aizheng J* 1996; **15**: 112-114
- Zhang XL**, Shi JQ, Wang XD, Wang D. Quantitative study of proliferative activity of human hepatocellular cancerous cells and cancer-adjacent hepatocytes. *Dishan Junyi Daxue Xuebao* 1996; **18**: 36-39
- Li CH**, Guo YJ, Ye XS, Tang XF. Advances in study of molecular biology of tumors. The first edition. *Beijing, Milit Med Publ House* 1996: 103-115
- Chen LY**, Zhang S, Lin H, Wang XY. Significance of expression of GST- π in gastric carcinomas. *Linchuang Yu Shiyan Binglixue Zazhi* 1999; **15**: 221-223
- Branch association of infectious disease, parasitic disease and hepatic disease under Chinese Medical Association. The prevention and treatment regime of virus hepatitis. *Zhonghua Ganzhangbing Zazhi* 2000; **8**: 324-329
- Qin LX**, Tang ZY, Ma ZC, Wu ZQ, Zhou XD, Ye QH, Ji Y, Huang LW, Jia HL, Sun HC, Wang L. P53 immunohistochemical scoring: an independent prognostic marker for patients after hepatocellular carcinoma resection. *World J Gastroenterol* 2002; **8**: 459-463
- Tang ZY**. Hepatocellular carcinoma—cause, treatment and metastasis. *World J Gastroenterol* 2001; **7**: 445-454
- Kao JH**. Hepatitis B viral genotypes: clinical relevance and molecular characteristics. *J Gastroenterol Hepatol* 2002; **17**: 643-650
- Okuda K**. Hepatocellular carcinoma. *J Hepatol* 2000; **32** (Suppl 1): 225-237
- Jin Y**, Abe K, Sato Y, Aita K, Irie H, Shiga J. Hepatitis B and C virus infection and p53 mutation in human hepatocellular carcinoma in Harbin, Heilongjiang Province, China. *Hepatol Res* 2002; **24**: 379-384
- Evans AA**, Chen G, Ross EA, Shen FM, Lin WY, London WT. Eight-year follow-up of the 90,000-person Haimen cohort: I. Hepatocellular carcinoma mortality, risk factors, and gender differences. *Cancer Epidemiol Biomarkers Prev* 2002; **11**: 369-376
- Ding X**, Mizokami M, Yao G, Xu B, Orito E, Ueda R, Nakanishi M. Hepatitis B virus genotype distribution among chronic hepatitis B virus carriers in Shanghai, China. *Intervirology* 2001; **44**: 43-47
- Yu MC**, Yuan JM, Govindarajan S, Ross RK. Epidemiology of hepatocellular carcinoma. *Can J Gastroenterol* 2000; **14**: 703-709
- Yuan FP**, Huang PS, Gao MQ, Gong HS. Expression of transforming growth factor α and its relationship with HBV infection in hepatocellular carcinoma. *Zhonghua Binglixue Zazhi* 1999; **28**: 35-38
- Wang XZ**, Chen XC, Yang YH, Chen ZX, Huang YH, Tao QM. Expression of HbxAg and Fas/FasL in patients with hepatocellular carcinoma. *Aizheng J* 2001; **20**: 41-44
- Zhang LN**, Cao YL, Song J, Ma CH, Liou SX, Suen WS. The correlation between integration of HBV X, S, Pre-S, C gene and the expression of oncogenes/tumor suppressor gene in primary hepatocellular carcinoma. *Zhonghua Ganzhangbing Zazhi* 1999; **7**: 138-139
- Hino N**, Higashi T, Nouse K, Nakatsukasa H, Urabe Y, Kinugasa N, Yoshida K, Ashida K, Ohguchi S, Tsuji T. Proliferating cell nuclear antigen and grade of malignancy in small hepatocellular carcinoma—evaluation in US-guided specimens. *Hepatology* 1997; **44**: 245-250
- Ikeguchi M**, Sato N, Hirooka Y, Kaibara N. Computerized nuclear morphometry of hepatocellular carcinoma and its relation to proliferative activity. *J Surg Oncol* 1998; **68**: 225-230
- Qi CH**, Guo SC, Li H, Li CH. Expression of GST- π in gastric carcinoma and precancerous lesions. *Zhonghua Binglixue Zazhi* 1995; **24**: 53-54
- Nie KR**, Li CH, Zhu YJ, Zhang XM, Huang GJ, Zhang DW, Zhang RG. Immunohistochemical study of GST- π in lung cancer.

- Zhonghua Jiehe He Huxi Zazhi* 1993; **16**: 141-143
- 24 **Shen LJ**, Zhang ZJ, Ou YM, Zhang HX, Huang R, He Y, Wang MJ, Xu GS. Computer morphometric analysis of human hepatocellular carcinoma and the related lesion. *Zhongguo Zuzhihuaxue Yu Xibaohuaxue Zazhi* 1997; **6**: 53-56
- 25 **Shen LJ**, Zhang ZJ, Ou YM, Zhang HX, Huang R, He Y, Wang MJ, Xu GS. Computed morphometric analysis and expression of alpha fetoprotein in hepatocellular carcinoma and its related lesion. *World J Gastroenterol* 2000; **6**: 415-416
- 26 **Shen LJ**, Zhang ZJ, Zhang HX, Ou YM, Huang R, Yang WB. Computer morphometric analysis and detection by immunohistochemistry and in situ hybridization in hepatocellular carcinoma and the related lesion. *Zhonghua Ganzangbing Zazhi* 2001; **9**: 278, 290
- 27 **Shen LJ**, Zhang ZJ, Zhang HX, Yang WB, Huang R. Expression of GST- π and HBV infection in hepatocellular carcinoma. *Aizheng J* 2002; **21**: 29-32
- 28 **Shen LJ**, Zhang ZJ, Zhang HX, Yang WB, Huang R. Expression of Alpha fetoprotein and its relationship with HBV infection. *Shiyong Aizheng Zazhi* 2002; **17**: 162-163,166
- 29 **Zhang JZ**. Carcinogenesis and expression of alpha fetoprotein in experimental hepatocarcinoma. *Linchuang Yu Shiyang Binglixue Zazhi* 1999; **15**: 224-226
- 30 **He P**, Liu BB, Ye SL, Tang ZY. Analysis of AFPmRNA in human hepatoma and paratumorous tissue. *Zhongguo Zhongliu Shengwu Zhiliao Zazhi* 1998; **5**: 163-166
- 31 **Su Q**, Benner A, Hofmann WJ, Otto G, Pichlmayr R, Bannasch P. Human hepatic preneoplasia: phenotypes and proliferation kinetics of foci and nodules of altered hepatocytes and their relationship to liver cell dysplasia. *Virchows Arch* 1997; **431**: 391-406
- 32 **Zhong S**, Tang MW, Yeo W, Liu C, Lo YM, Johnson PJ. Silencing of GSTP1 gene by CpG island DNA hypermethylation in HBV-associated hepatocellular carcinomas. *Clin Cancer Res* 2002; **8**: 1087-1092
- 33 **Nishikawa T**, Wanibuchi H, Ogawa M, Kinoshita A, Hiroi T, Funae Y, Kishida H, Nakae D, Fukushima S. Promoting effects of monomethylarsonic acid, dimethylarsinic acid and trimethylarsine oxide on induction of rat liver preneoplastic glutathione s-transferase placental form positive foci: a possible reactive oxygen species mechanism. *Int J Cancer* 2002; **100**: 136-139
- 34 **Sawaki M**, Hattori A, Tsuzuki N, Sugawara N, Enomoto K, Sawada N, Mori M. Chronic liver injury promotes hepatocarcinogenesis of the LEC rat. *Carcinogenesis* 1998; **19**: 331-335
- 35 **Marwoto W**, Miskad UA, Siregar NC, Gani RA, Boedihusodo U, Nurdjanah S, Suwarso, Watadianto Boedi P, Hasan HA, Akbar N, Noer HM, Hayashi Y. Immunohistochemical study of p53 and AFP in hepatocellular carcinomas, a comparison between Indonesian and Japanese cases. *Kobe J Med Sci* 2000; **46**: 217-229
- 36 **Feng Z**, He R, Lu Z, Ling Y. Expression of ras oncogene p21 product and proliferating cell nuclear antigen in liver cirrhosis and the correlation with liver cell dysplasia. *Zhonghua Ganzangbing Zazhi* 2000; **8**: 343-345
- 37 **Zhao M**, Zimmermann A. Liver cell dysplasia: reactivities for c-met protein, Rb protein, E-cadherin and transforming growth factor-beta 1 in comparison with hepatocellular carcinomas. *Histol Histopathol* 1998; **13**: 657-670
- 38 **Tiniakos DG**, Brunt EM. Proliferating cell nuclear antigen and Ki-67 labeling in hepatocellular nodules: a comparative study. *Liver* 1999; **19**: 58-68
- 39 **Mise K**, Tashiro S, Yogita S, Wada D, Harada M, Fukuda Y, Miyake H, Isikawa M, Izumi K, Sano N. Assessment of the biological malignancy of hepatocellular carcinomas: relationship to clinicopathological factors and prognosis. *Clin Cancer Res* 1998; **4**: 1475-1482

Edited by Wu XN

A novel HBV antisense RNA gene delivery system targeting hepatocellular carcinoma

Chun-Hong Ma, Wen-Sheng Sun, Pei-Kun Tian, Li-Fen Gao, Su-Xia Liu, Xiao-Yan Wang, Li-Ning Zhang, Ying-Lin Cao, Li-Hui Han, Xiao-Hong Liang

Chun-Hong Ma, Wen-Sheng Sun, Li-Fen Gao, Su-Xia Liu, Xiao-Yan Wang, Li-Ning Zhang, Ying-Lin Cao, Li-Hui Han, Xiao-Hong Liang, Institute of Immunology, Medical College of Shandong University, Jinan 250012, Shandong Province, China

Pei-Kun Tian, National Laboratory for Oncogenes and Related Genes, Shanghai Cancer Institute, Shanghai 200032, China

Supported by the National Natural Science Foundation Community, No. 39970333

Correspondence to: Prof Wen-Sheng Sun, Institute of Immunology, Medical College of Shandong University, Jinan 250012, Shandong Province, China. sunwenshengsws@yahoo.com

Telephone: +86-531-8382038

Received: 2002-07-18 **Accepted:** 2002-09-04

Abstract

AIM: To construct a novel HBV antisense RNA delivery system targeting hepatocellular carcinoma and study its inhibitory effect *in vitro* and *in vivo*.

METHODS: GE7, a 16-peptide specific to EGFR, and HA20, a homologue of N-terminus of haemagglutinin of influenza viral envelope protein, were synthesized and conjugated with polylysine. The above conjugates were organized into the pEBAF-as-preS2, a hepatocarcinoma specific HBV antisense expression vector, to construct a novel HBV antisense RNA delivery system, named AFP-enhancing 4-element complex. Hepatocellular carcinoma HepG2.2.15 cells was used to assay the *in vitro* inhibition of the complex on HBV. Expression of HBV antigen was assayed by ELISA. BALB/c nude mice bearing HepG2.2.15 cells were injected with AFP-enhancing 4-element complex. The expression of HBV antisense RNA was examined by RT-PCR and the size of tumor in nude mice were measured.

RESULTS: The AFP-enhancing 4-element complex was constructed and DNA was completely trapped at the slot with no DNA migration when the ratio of polypeptide to plasmid was 1:1. The expression of HBsAg and HBeAg of HepG2.2.15 cells was greatly decreased after being transfected by AFP-enhancing 4-element complex. The inhibitory rates were 33.4 % and 58.5 % respectively. RT-PCR showed HBV antisense RNA expressed specifically in liver tumor cells of tumor-bearing nude mice. After 4 injections of AFP-enhancing 4-element complex containing 0.2 µg DNA, the diameter of the tumor was 0.995 cm±0.35, which was significantly smaller than that of the control groups (2.215 cm±0.25, $P < 0.05$).

CONCLUSION: AFP-enhancing 4-element complex could deliver HBV antisense RNA targeting on hepatocarcinoma and inhibit both HBV and liver tumor cells *in vitro* and *in vivo*.

Ma CH, Sun WS, Tian PK, Gao LF, Liu SX, Wang XY, Zhang LN, Cao YL, Han LH, Liang XH. A novel HBV antisense RNA gene delivery system targeting hepatocellular carcinoma. *World J Gastroenterol* 2003; 9(3): 463-467

<http://www.wjgnet.com/1007-9327/9/463.htm>

INTRODUCTION

A major hurdle in most current gene therapy lies in how to transfer genes to target tissues efficiently and how to obtain therapeutic expression of target genes. The targeting efficacy of gene transfection and expression directly determines whether the gene therapy has high efficiency and whether it is harmful to normal tissues. Therefore, how to enhance the targeting efficacy of gene delivery has become a problem to be solved urgently^[1-4].

At present, various gene delivery methods have been used in gene therapy^[5-8]. Among them, there are two important methods to achieve tumor-targeting gene therapy: one is receptor-mediated gene delivery; another is the construction of tumor-targeting gene expression vector which utilizes tumor-specific transcription regulatory sequence^[9-12]. However, either of them, if used singly, can not really accomplish the tumor-targeting gene therapy.

This paper reported a novel HBV antisense RNA delivery system targeting on hepatocarcinoma cells, named AFP enhancing 4-element complex. This complex includes four elements: (1) recombinant EB virus vector, pEBAF-as-preS2, in which antisense preS2 gene was cloned under the control of human α -fetoprotein (AFP) promoter and enhancer, enabled preS2 antisense RNA to be expressed specifically in AFP-positive cells; (2) ligand oligopeptide GE7, synthesized according to the putative binding region of epidermal growth factor (EGF) to its receptor (EGFR), could transfer DNA specifically to EGFR positive cells; (3) HA20, a homologue of N-terminus of haemagglutinin of Influenza envelope protein, was synthesized as endosome-releasing oligopeptide (EROP); (4) polylysine was polycation peptides (PCP) which could interact with pEBAF-as-preS2 DNA to form a complex after conjugation with GE7 and HA20. Both *in vitro* and *in vivo* studies indicated that preS2 antisense RNA could be expressed strictly and specifically in hepatocarcinoma cells after being transfected by this complex. This study implicated the great therapeutic potential of AFP-enhancing 4-element complex for HBV-associated hepatocellular carcinoma.

MATERIALS AND METHODS

Cells and cultures

Hepatocellular carcinoma cell line HepG2.2.15 integrated with whole HBV gene not only can accomplish the transcription and translation of HBV, but also may produce Dane's particles. This cell line, provided by BeiJing Institute of Medicine and Biology, was cultured in the MEM medium containing 10 % FCS and 380 µg/ml G418. The human hepatocellular carcinoma cell line BEL7402 was cultured in the DMEM medium with 10 % FCS. The human umbilical vein endothelial cell line ECV304 contributed by Chinese Academy of Military Medical science was cultured in the DMEM medium, containing 10 % FCS and antibiotics. The medium mentioned above were purchased from Hyclone Co. American, serum from GIBCO Co.

Animals

BALB/C nude mice, male, 5-6 weeks of age, were purchased

from experimental animal center of Tongji medical college, Central China Science and Technology University, Wuhan. 1×10^7 HepG2.2.15 cells were transplanted subcutaneously into nude mice and were ready for use when the tumor size reached about 0.5 cm in diameter.

Plasmid

HBV preS2 gene (3 203-3 340) was cloned reversely downward 5.5 kb of AFP promoter and enhancer to construct hepatocarcinoma specific preS2 antisense RNA expression vector, pEBAF-as-preS2 (Figure 1) which could express antisense RNA against preS2 in AFP-positive cells. (published elsewhere).

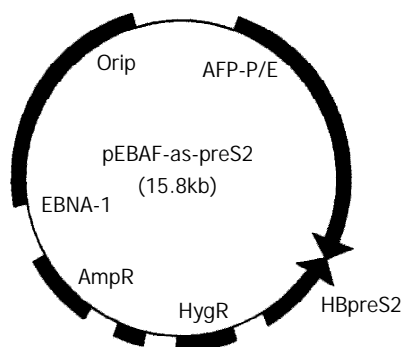


Figure 1 Physical map of pEBAF-as-preS2. hepatocarcinoma specific preS2 antisense RNA expression vector, pEBAF-as-preS2 was constructed by inserting HBV preS2 gene (3203-3340) reversely downward the AFP promoter and enhancer (AFP-P/E) of plasmid pEBAF which contains the key element of EB virus duplication (Ori P and EBNA-1).

Synthesis of GE7-PL and HA20-PL^[13]

GE7, a 16-peptide specific to EGFR, and HA20, a homologue of N-terminus of haemagglutinin of influenza viral envelope protein, were synthesized by National Laboratory for Oncogene and Related Genes, Shanghai Cancer Institute. GE7 and HA20 were conjugated with polylysine (PL) respectively (GE7-PL and HA20-PL).

Preparation of AFP-enhancing 4-element complex

pEBAF-as-preS2 DNA, GE7-PL and HA20-PL conjugates were respectively mixed dropwise into 10 μ l of deionized water in different ratios. The mixture was incubated at 25 $^{\circ}$ C for 30 min. A mixture containing 0.2 μ g plasmid DNA was analyzed on 1 % agarose gel electrophoresis to examine the retardation of DNA migration, in order to determine the optimal ratio. According to the optimal ratio of DNA to conjugates based on above experiment, the plasmid DNA was mixed dropwise to the conjugates of GE7-PL and HA20-PL and reacted at 25 $^{\circ}$ C for 30 min. Examine the retardation of DNA by 1 % agarose gel electrophoresis. Then the complex could be used for gene transfection.

In vitro gene transfer by 4-element complex

5×10^4 cells were seeded into 0.5 ml medium in each well of a 24 well plate. After cell density reached a confluence of 60 %, the medium was removed and replaced with 0.5 ml of complete medium containing 4-element complex in a quantity equivalent to 0.2 μ g DNA. Cells were cultured at 37 $^{\circ}$ C and incubated with 5 % CO₂ overnight, then replaced with fresh complete MEM medium without 4-element complex and cultured at 37 $^{\circ}$ C with 5 % CO₂. 3 days after, the supernatant was collected to detect the HBV antigen. Non-transfected HepG2.2.15 cells were used as negative control.

Detection of virus antigens

According to the protocol of antigen detection kit (Lizhu Co. ShenZhen, China), the concentration of HBsAg and HBeAg in the supernatant were detected by ELISA. The results were illustrated with P/N value (P/N=sample A/negative control A; A stands for the amount of light absorbent).

In vivo gene transfection by AFP-enhancing 4-element complex

AFP-enhancing 4-element complex containing 0.2 μ g DNA were injected into a tail vein of nude mice bearing 0.5 cm tumor. Animals were sacrificed 3 days after injection, then the tumor, liver, spleen, kidney, stomach were dissected and used for extracting the total RNA.

Extraction of total RNA

Total RNA was extracted from 5 mm³ fresh mice tissues according to the protocol of TRIZOL kit. Products were quantitated by Biophotometer (Eppendorf Co.).

Primer design

According to the sequence described by Ono *et al* in 1986^[14], the primers were designed to amplify HBpreS2 gene: forward (S2P1): 5' GCTCTAGACTCAGGCCATGCATG3'; reverse (S2P2): 5' GCTCTAGATGGTGAGTGATTGGAGGT3'. The primers for β -actin, a housekeeping gene, were designed simultaneously (forward: 5' AACTGTGCCCA 3'; reverse: 5' ATGATGGAGTTGAAGGTAGTTTCGTGGAT3'). All of these oligonucleotide primers were synthesized by Shanghai Biology and Engineering Company.

RT-PCR

Reverse transcription was performed in 20 μ l volume including: 1 μ g of total RNA, 4 μ l of 5 \times buffer, 20 nmol dNTP, 20 Units of RNase inhibitor and 200 Units of Moloney murine leukemia virus (M-MLV) reverse transcriptase. The reverse transcription reaction was performed at 42 $^{\circ}$ C for 1 hr. The products were denatured at 70 $^{\circ}$ C for 10 min and then preserved at 4 $^{\circ}$ C. cDNA was used as templates for the amplification of preS2 with primers S2P1 and S2P2. PCR was carried out in 25 μ l volume with 1 μ l of cDNA, 2.5 μ l of 10 \times buffer, 0.3 mmol Mg⁺⁺, 5nmol/L dNTP, 3 Units of *Taq* polymerase, 10 nmol/L primers (forward and reverse). Reaction conditions were: 94 $^{\circ}$ C for 5 min, then 35 cycles at 94 $^{\circ}$ C for 40 sec, 50 $^{\circ}$ C for 40 sec, 72 $^{\circ}$ C for 50 sec, followed by a final extension period of 7 min at 72 $^{\circ}$ C.

In vivo tumor-inhibitory experiments

100 μ l AFP-enhancing 4-element complex containing 0.2 μ g pEBAF-as-preS2 DNA were injected into tumors of nude mice bearing hepatocarcinoma cells HepG2.2.15, once each week for 4 weeks and physiological salt solution was injected likewise in the control group. The diameters of tumors were measured every 3 days. Animals were sacrificed 1 week after the final injection. Tumor tissues were dissected and their diameters were measured.

RESULTS

Construction of AFP-enhancing 4-element complex

Polypeptide and plasmid were mixed in different ratios. According to the results of 1 % agarose gel electrophoresis, DNA was completely trapped at the slot with no DNA migration when the ratio was 1:1 (Figure 2). This is the optimal ratio of polypeptide to pEBAF-as-preS2 plasmid DNA.

Extraction of total RNA

Total RNA from all biopsies were analysed by Biophotometer

(Eppendorf Co.). The ratios of A260 to A280 were all between 1.8 to 2.0. Using above total RNA as templates, RT-PCR were performed with primers for β -actin gene. A band of about 300bp in size was obtained in agarose gel electrophoresis (Figure 3A), proving that RNA was qualified for RT-PCR.

Hepatocarcinoma directed expression of antisense RNA mediated by AFP-enhancing 4-element complex

RT-PCR was carried out with specific primers (S2P1, S2P2) for HBpreS2 gene. 2 % gel electrophoresis demonstrated that the products of amplification could be detected only in tumor tissues of animals injected with AFP-enhancing 4-element complex. No specific bands could be tested in other tissues, especially in the epithelial cells of stomach mucosa and spermatiduct. (Figure 3B).

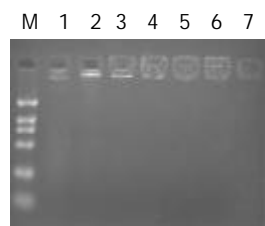


Figure 2 Construction of AFP-enhancing 4-element complex. 0.2 μ g plasmid DNA was independently mixed dropwise with various quantity of polypeptide conjugation for 30 min at room temperature, and then the mixture was analyzed with 1 % agarose gel electrophoresis. Fig 2 showed the DNA retardation of different complex mixed with DNA and peptide in different ratios. The ratio of DNA and peptide in Lane 1 to 7 is 0, 1/1, 1/2, 1/2.5, 1/3, 1/3.5, 1/4. M indicates DNA marker.

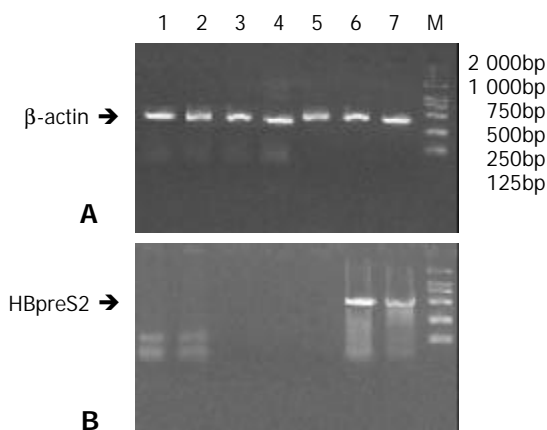


Figure 3 RT-PCR of tissues in nude mice treated AFP-enhancing 4-element complex. Total RNAs of different tissues of Nude mice bearing hepatocarcinoma were extracted 3 days after treatment with AFP-enhancing 4-element complex and then RT-PCR was performed; the expression of HBV preS2 gene was analyzed. A. RT-PCR of beta-actin. (bands 1 to 7 stand for the PCR products of spermatiduct, stomach, liver, spleen, heart, and tumors, M stands for the DNA marker); B. RT-PCR of HBV preS2 gene.

Inhibitory effects of AFP-enhancing 4-element complex on expression of HBV antigen in hepatocarcinoma cells

In order to correct the results, the supernatants of cell cultures in all groups were collected before transfection, marked as P/N-0hr. The final results were calculated according to the following formula: antigen secretion of cells transfected with AFP-enhancing 4-element (tested)=[P/N of tested]/([P/N-0hr of tested] \times [P/N-0hr of control]). HBsAg and HBeAg expressions of

HepG2.2.15 were lowered prominently after transfection with AFP-enhancing 4-element complex. The inhibitory rates were 33.4 % and 58.5 % respectively (Figure 4).

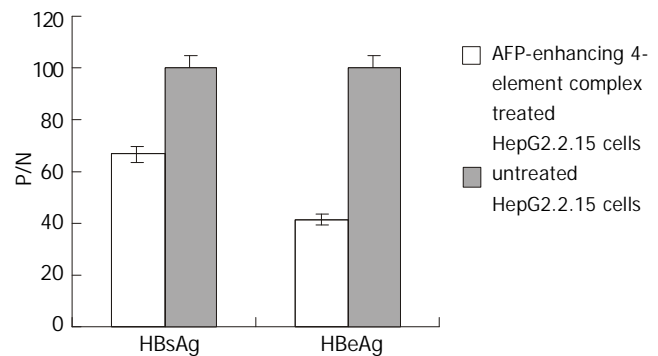


Figure 4 Effect of AFP-enhancing 4-element complex on HBV gene expression in HepG2.2.15 cells.

In vivo inhibitory effects of AFP-enhancing 4-element complex on growth of hepatocellular carcinoma in nude mice

After 4 injections of AFP-enhancing 4-element complex containing 0.2 μ g DNA, the diameter of tumor tissue was $0.995 \text{ cm} \pm 0.35$, which was significantly smaller than that of the control groups ($2.215 \text{ cm} \pm 0.25$, $P < 0.05$).

DISCUSSION

Hepatocellular carcinoma (HCC), especially HBV-associated HCC, is one of the most common malignant tumor in China. At present, there's still no efficient therapy methods^[15-26]. Antisense nucleic acid, blocking the target gene and inhibiting its expression at the molecular level, has potential antiviral and antitumor effects^[27-31]. In recent years, great interests have been focusing on such novel gene therapy. Compared with synthesized antisense DNA, antisense RNA could be expressed constantly *in vivo*, so that it has long-term antiviral effects. Thus, antisense RNA is an ideal choice in gene therapy for HBV^[32-34].

There are three crucial factors to determine the efficacy of antisense gene therapy^[35]: whether the target gene plays a crucial role in tumorigenesis, whether it could be transfected uniquely to target cells, and whether it could be expressed efficiently and specifically in those target cells. In this research, according to the characteristics of HBV-associated HCC, we selected preS2 which might play an important role in the pathogenetic target site to be blocked. Moreover, in order to express preS2 antisense RNA strictly targeting on liver tumor cells, virus expression vector containing hepatocarcinoma-specific regulatory sequences (AFP promoter and enhancer) and ERGP (HA20) combined with receptor mediated gene delivery system was prepared.

The protein encoded by preS2 gene plays an important role in the infection as well as malignant transformation of HBV^[36,37]. In a previous research, we have proved that synthesized antisense oligodeoxynucleotides (asON) against translation initiation region (3' 203-3' 219) of HBpreS2 has the strongest inhibitory effect on the expression of HBV antigen in HepG2.2.15 cells *in vitro*^[38]. In addition, AS5, designed by Putlitz^[33] in this region, could efficiently inhibit the viral replication and the expression of HBV antigen. In this paper, preS2 gene (3' 203-3' 240nt) was selected as target site for blocking by antisense RNA. Inhibitory experiments *in vitro* had demonstrated that a block of preS2 gene (3' 203-3' 240) could efficiently inhibited the expression of HBV antigen in HepG 2.2.15 cells. The inhibitory rates of the expression of HBsAg and HBeAg were 33.4 % and 58.5 % respectively.

The receptor-mediated gene delivery system transfers genes into the target cells by endocytosis via specific receptor. In 1998, Tian, Gu *et al* (Shanghai Cancer Institute)^[13] established a novel high-efficiency receptor-mediated gene delivery system in which GE7 targeted on EGFR were used to transfer genes to tumor cells, and HA20 was synthesized as an EROP to enable the exogenous genes to escape from the lysosome. These properties guaranteed this system to have a significant potential in gene therapy.

However, the expression of EGFR is not limited to tumor cells. We have demonstrated that green fluorescence protein (GFP) reporter gene could be also expressed in the epithelial cells of stomach mucosa and spermaduct after being transfected with 4-element complex *in vivo* (published elsewhere).

For this reason, hepatocarcinoma tissue-specific antisense RNA expression vector under the control of AFP promoter was used to conjugate with GE7-PL and HA20-PL to construct an AFP-enhancing 4-element complex. As a specific marker for primary hepatocellular carcinoma, alpha fetal protein (AFP) possesses a high-targetable transcription-regulatory sequence which could be regulated precisely^[39]. Therefore, it could direct the therapeutic gene to be specifically expressed in AFP-positive hepatocellular carcinoma cells. Using human AFP incis element (promoter and enhancer) to control the expression of antisense RNA could not only enhance the high efficacy, but also possesses the targetability to hepatocellular carcinoma cells. Results showed that preS2 antisense RNA was only examined in tumor tissues of nude mice injected with AFP-enhancing 4-element complex but could not be examined in the epithelial cells of stomach mucosa and spermaduct either. Moreover, the growth of hepatocellular carcinoma in nude mice could be thwarted distinctively by being injected with AFP-enhancing 4-element complex at a dose equivalent of 0.2 µg DNA per mouse each time for 4 times.

In summary, this experiment showed that AFP-enhancing 4-element complex could deliver preS2 antisense RNA targeted on hepatoma cells and inhibited both HBV gene expression *in vitro* and tumor growth *in vivo*. All these results indicated the therapeutic potential of AFP-enhancing 4-element complex for HBV related HCC.

REFERENCES

- Mah C, Fraites TJ Jr, Zolotukhin I, Song S, Flotte TR, Dobson J, Batich C, Byrne BJ. Improved Method of Recombinant AAV2 Delivery for Systemic Targeted Gene Therapy. *Mol Ther* 2002; **6**: 106-112
- Zhang Y, Zhu C, Pardridge WM. Antisense gene therapy of brain cancer with an artificial virus gene delivery system. *Mol Ther* 2002; **6**: 67-72
- Ghosh SS, Takahashi M, Thummala NR, Parashar B, Roy Chowdhury N, Roy Chowdhury J. Liver-directed gene therapy: Promises, problems and prospects at the turn of the century. *J Hepatol* 2000; **32** (Suppl 1): 238-252
- Lalwani AK, Jero J, Mhatre AN. Current issues in cochlear gene transfer. *Audiol Neurotol* 2002; **7**: 146-151
- Walther W, Stein U, Fichtner I, Voss C, Schmidt T, Schleef M, Nellessen T, Schlag PM. Intratumoral low-volume jet-injection for efficient nonviral gene transfer. *Mol Biotechnol* 2002; **21**: 105-115
- Oupicky D, Ogris M, Seymour LW. Development of long-circulating polyelectrolyte complexes for systemic delivery of genes. *J Drug Target* 2002; **10**: 93-98
- Richardso P, Kren BT, Steer CJ. *In vivo* application of non-viral vectors to the liver. *J Drug Target* 2002; **10**: 123-131
- Yaghamai R, Cutting GR. Optimized regulation of gene expression using artificial transcription factors. *Mol Ther* 2002; **5**: 685-694
- Wu GY, Wilson JM, Shalaby F, Grossman M, Shafritz DA, Wu CH. Receptor mediated gene delivery in vivo. partial correction of genetic analbuminemia in nagase rats. *J Biol Chem* 1991; **266**: 14338-14342
- Huber BE, Richards CA, Krenitsky TA. Retroviral mediated gene therapy for the treatment of hepatocellular carcinoma: an innovative approach for cancer therapy. *Proc Natl Acad Sci USA* 1991; **88**: 8039-8043
- Sato Y, Tanaka K, Lee G, Kanegae Y, Sakai Y, Kaneko S, Nakabayashi H, Tamaoki T, Saito I. Enhanced and specific gene expression via tissue-specific production of crecrecombinase using adenovirus vector. *Biochem Biophys Res Commun* 1998; **244**: 455-462
- Brand K, Loser P, Arnold W, Bartels T, Strauss M. Tumor cell-specific transgene expression prevents liver toxicity of the adenoviral HSVtk/GCV approach. *Gene Ther* 1998; **5**: 1363-1371
- Tian PK, Ren SJ, Ren CC, Teng QS, Qu SM, Yao M, Gu JR. A novel receptor-targeted gene delivery system for gene therapy. *Zhongguo Kexue (Series C)* 1998; **28**: 554-558
- Ono Y, Onda H, Sasaada R, Igarashi K, Sugino Y, Nishioka K. The complete nucleotide sequences of the cloned hepatitis B virus DNA; subtype adr and adw. *Nucleic Acids Research* 1983; **11**: 1747-1757
- Maddrey WC. Hepatitis B: an important public health issue. *J Med Virol* 2000; **61**: 362-366
- Lau GK. Hepatitis B infection in China. *Clin Liver Dis* 2001; **5**: 361-379
- Merican I, Guan R, Amarapuka D, Alexander MJ, Chutaputti A, Chien RN, Hasnain SS, Leung N, Lesmana L, Phiet PH, Sjalfoellah Noer HM, Sollano J, Sun HS, Xu DZ. Chronic hepatitis B virus infection in Asian countries. *J Gastroenterol Hepatol* 2000; **15**: 1356-1361
- Zhuang L, You J, Tang BZ, Ding SY, Yan KH, Peng D, Zhang YM, Zhang L. Preliminary results of Thymosin-α1 versus interferon-α-treatment in patient with HBeAg negative and serum HBV DNA positive chronic hepatitis B. *World J Gastroenterol* 2001; **7**: 407-410
- Xie Q, Guo Q, Zhou XQ, Gu RY. Effect of adenine arabinoside monophosphate coupled to lactosaminated human serum albumin on duck hepatitis B virus. *Shijie Huaren Xiaohua Zazhi* 1999; **7**: 125-126
- Li J, Tang B. Effect on replication of hepatitis B virus by Chinese traditional medicine. *Shijie Huaren Xiaohua Zazhi* 2000; **8**: 945-946
- Xu CT, Pan BR. Current status of gene therapy in gastroenterology. *World J Gastroenterol* 1998; **4**: 85-89
- Xu KC, Wei BH, Yao XX, Zhang WD. Recently therapy for chronic hepatitis B virus by combined traditional Chinese and Western medicine. *Shijie Huaren Xiaohua Zazhi* 1999; **7**: 970-974
- Lau GK. Use of immunomodulatory therapy (other than interferon) for the treatment of chronic hepatitis B virus infection. *J Gastroenterol Hepatol* 2000; **15** (Suppl): E46-52
- Guan R. Interferon monotherapy in chronic hepatitis B. *J Gastroenterol Hepatol* 2000; **15** (Suppl): E34-40
- Torres J, Locarnini S. Antiviral chemotherapy for the treatment of hepatitis B virus infections. *Gastroenterology* 2000; **118** (2 Suppl 1): S83-103
- Doo E, Liang TJ. Molecular anatomy and pathophysiologic implications of drug resistance in hepatitis B virus infection. *Gastroenterology* 2001; **120**: 1000-1008
- Feng RH, Zhu ZG, Li JF, Liu BY, Yan M, Yin HR, Lin YZ. Inhibition of human telomerase in MKN-45 cell line by antisense hTR expression vector induces cell apoptosis and growth arrest. *World J Gastroenterol* 2002; **8**: 436-440
- Nie QH, Cheng YQ, Xie YM, Zhou YX, Cao YZ. Inhibiting effect of antisense oligonucleotides phosphorothioate on gene expression of TIMP-1 in rat liver fibrosis. *World J Gastroenterol* 2001; **7**: 363-369
- Wang XW, Yuan JH, Zhang RG, Guo LX, Xie Y, Xie H. Antihepatoma effect of alpha-fetoprotein antisense phosphorothioate oligodeoxynucleotides in vitro and in mice. *World J Gastroenterol* 2001; **7**: 345-351
- Yatabe N, Kyo S, Kondo S, Kanaya T, Wang Z, Maida Y, Takakura M, Nakamura M, Tanaka M, Inoue M. 2-5A antisense therapy directed against human telomerase RNA inhibits telomerase activity and induces apoptosis without telomere impairment in cervical cancer cells. *Cancer Gene Ther* 2002; **9**: 624-630
- Yang S, Fang D, Liu A, Yang J, Luo Y, Lu R, Liu W. Reversing malignant phenotypes of liver cancer cell lines with antisense gene to human telomerase reverse transcriptase. *Zhonghua*

- Ganzangbing Zazhi* 2002; **10**: 97-99
- 32 **Wu J**, Gerber MA. Gerber. The inhibitory effects of antisense RNA on hepatitis B virus surface antigen synthesis. *J General Virol* 1997; **78**: 641-647
- 33 **zu Putlitz J**, Wieland S, Blum HE, Wands JR. Antisense RNA complementary to hepatitis B virus specifically inhibits viral replication. *Gastroenterology* 1998; **115**: 702-713
- 34 **Arteaga CL**, Holt JT. Tissue-targeted antisense c-fos retroviral vector inhibits established breast cancer xenografts in nude mice. *Cancer Res* 1996; **56**: 1098-1103
- 35 **Wang S**, Dolnick BJ. Quantitative evaluation of intracellular sense: antisense RNA hybrid duplexes. *Nucleic Acids Res* 1993; **21**: 4383-4391
- 36 **Neurath AR**, Strick N, Sproul P. Search for hepatitis B virus cell receptors reveals binding sites for interleukin 6 on the virus envelope protein. *J Exe Med* 1992; **175**: 461-469
- 37 **Alka S**, Hemlata D, Vaishali C, Shahid J, Kumar PS. Hepatitis B virus surface (S) transactivator with DNA-binding properties. *J Med Virol* 2000; **61**: 1-10
- 38 **Ma CH**, Sun WS, Liu SX, Ding PF, Zhang LN, Cao YL, Song J. Comparison of the anti-HBV effect of various antisense oligodeoxynucleotides. *Zhonghua Weisheng Wuxue Yu Mianyixue Zazhi* 2000; **20**: 12-14
- 39 **Watanabe K**, Saito A, Tamaoki T. Cell-specific enhances activity in far upstream region of the human alpha-fetoprotein gene. *J Biol Chem* 1987; **262**: 4812-4818

Edited by Lu HM

Is the expression of γ -glutamyl transpeptidase messenger RNA an indicator of biological behavior in recurrent hepatocellular carcinoma?

I-Shyan Sheen, Kuo-Shyang Jeng, Yi-Chun Tsai

I-Shyan Sheen, Liver Research Unit, Chang Gung Memorial Hospital, Taipei, Taiwan, China

Kuo-Shyang Jeng, Departments of Surgery, Mackay Memorial Hospital, Taipei, Taiwan and Mackay Junior School of Nursing, Taipei, Taiwan, China

Yi-Chun Tsai, Medical Research, Mackay Memorial Hospital, Taipei, Taiwan, China

Supported by grants from the Department of Health, National Science Council, Executive Yuan, Taiwan. NSC 87-2314-B-195-003

Correspondence to: Kuo-Shyang Jeng, M.D., F.A.C.S. Department of Surgery, Mackay Memorial Hospital, No. 92, Sec 2, Chung-San North Road, Taipei, Taiwan, China. issheen.jks@msa.hinet.net

Telephone: +886-2-25433535 **Fax:** +886-2-27065704

Received: 2002-10-04 **Accepted:** 2002-11-04

Abstract

AIM: To investigate the correlation between gamma-glutamyl transpeptidase (γ -GTP) expression in the primary HCC and post-resection recurrence and its biological behaviors.

METHODS: Forty consecutive patients having curative resection for HCC were included in this study. The primers for reverse-transcription polymerase chain reaction (RT-PCR) were corresponding to the 5'-noncoding human γ -GTP mRNA of fetal liver (type A), HepG2 cells (type B), and placenta (type C). Both the cancer and non-cancerous tissues of the resected liver were analyzed. The correlations between the expression of γ -GTP and the clinicopathological variables and outcomes (recurrence and survival) were studied.

RESULTS: Those with type B γ -GTP mRNA in cancer had significant higher recurrence rate than those without it (63.6 % vs 14.3 %). Both those with type B in cancer and in non-cancer died significantly more than those without it (45.5 % vs 0 % and 53.6 % vs 0 %, respectively). By multivariate analysis, the significant predictors of recurrence included high serum AFP ($P=0.0108$), vascular permeation ($P=0.0084$), and type B γ -GTP mRNA in non-cancerous liver ($P=0.0107$). The significant predictors of post-recurrence death included high serum AFP ($P=0.0141$), vascular permeation ($P=0.0130$), and daughter nodules ($P=0.0053$). As to the manifestations (recurrent number, recurrent extent, segments, extra-hepatic metastasis, and death) in recurrent patients, there were no statistical significant differences between those with type B in the primary tumor and those without it. The difference between those with type B in non-cancerous liver and those without it also was not significant.

CONCLUSION: Patients of HCC with type B γ -GTP mRNA both in cancer and in non-cancerous tissue had a worse outcome, earlier recurrence, and more post-recurrence death.

Sheen IS, Jeng KS, Tsai YC. Is the expression of γ -glutamyl transpeptidase messenger RNA an indicator of biological behavior in recurrent hepatocellular carcinoma? *World J Gastroenterol* 2003; 9(3): 468-473

<http://www.wjgnet.com/1007-9327/9/468.htm>

INTRODUCTION

Hepatocellular carcinoma (HCC) is one of the leading malignant tumors with a poor prognosis in areas of high hepatitis B and C prevalence. During the last 10 years, efforts have been made worldwide toward earlier detection and safer surgical resection of HCC. However, despite these recent diagnostic and therapeutic advances, postoperative recurrence is still common^[1-4]. How to predict recurrence before resection is a challenging problem for surgeons. Certain characteristics related to HCC recurrence have been reported widely and variably in the literatures^[1-14]. γ -glutamyl transpeptidase (γ -GTP) is an important enzyme catalyzing hydrolysis of glutathione and transfer of the γ -glutamyl residue and is widely distributed in mammalian tissues^[15-23]. The enzyme has been used as an important marker enzyme for some neoplasms, HCC and preneoplastic lesions of the liver^[24-31]. According to Tsutumi's study, changes in the expression of hepatic γ -GTP mRNA may be related to the development of HCC^[24]. The aim of this study is to elucidate the role of the expression of γ -GTP in both cancerous and non-cancerous liver tissues of primary lesion in the prediction of HCC recurrence.

MATERIALS AND METHODS

Patients and tumor samples

Forty patients with HCC who underwent curative hepatectomy at the Department of Surgery, Mackay Memorial Hospital from January 1997 to June 1998, whose tissue specimens histopathologically found to have no degeneration or necrosis, were included in this study. Freshly resected specimens were used. Clinical details were available from medical records on all patients (Table 1). The mean age of patients was 52.4 ± 16.6 years (range 16-82) with a male to female ratio of 26:14. The operations included major resections (12 partial lobectomies, 18 lobectomies and 5 extended lobectomies) and minor resections (4 segmentectomies and 1 subsegmentectomy). After the resection, all patients were followed up at out-patient-clinic receiving regular clinical assessment, periodic abdominal ultrasonography (every 2 to 3 months during the first 5 years, then every 4 to 6 months thereafter) to detect tumor recurrence, serum alpha-fetoprotein (AFP) and liver biochemistry (every 2 months during the first 2 years, then every 4 months during the following 3 years, and every 6 months thereafter). Abdominal computed tomography was also done (every 6 months during the first year, then every year). Liver specimens were stored at -80°C until RNA extraction.

Patients in the control group included 5 healthy volunteers, 5 individuals with chronic active hepatitis without HCC and 5

individuals with liver cirrhosis without HCC. All received liver biopsies for γ -GTP mRNA study during exploratory laparotomy.

Table 1 Demography

Characteristics	Total (n=40)
Age (years)	52.4 \pm 16.6 [16-78]
Male:female (65%)	
Liver cirrhosis	33 (82.5%)
Child-Pugh class A:B	32:8 (80%:20%)
Tumor size	
Small (<3 cm)	6 (15.0%)
Median (3-10 cm)	23 (57.5%)
Large (>10 cm)	11 (27.5%)
HBsAg (+)	22 (55.0%)
Anti-HCV (+)	15 (37.5%)
AFP	
Below 20 μ g /L	17 (42.5%)
Over 1000 μ g/L	14 (35.0%)
Capsule	
Complete	18 (45.0%)
Incomplete or absent	22 (55.0%)
Edmondson-Steiner grade	
I & II	19 (47.5%)
III & IV	21 (52.5%)
Vascular permeation	17 (42.5%)
Satellite formation	19 (47.5%)
Multiple HCC	13 (32.5%)
Major resection	32 (80.0%)
Minor resection	8 (20.0%)

Reverse transcription-polymerase chain reaction

For HCC liver specimens, both nucleotide probes to each type of γ -GTP mRNA were shown in Table 2. To rule out any false positive, cancerous and non-cancerous tissue were studied for the expression of γ -GTP mRNA, respectively. For the resected specimens, the non-cancerous tissue was taken at least 1.0 cm far from HCC. For control group, only non-cancerous liver tissue was studied.

Table 2 Nucleotide sequences of the primer sets and specific oligonucleotide probes to each type of γ -GTP 5'-noncoding mRNA

Type of γ -GTP mRNA or	Primers or probes	Nucleotide sequences
Primer sets		
A type	Sense	5'-CAC AGG GGA CAT ACA GTG AG-3'
	Antisense	5'-GAA ATA GCT GAA GCA CGC GC-3'
B type	Sense	5'-GGA TTC TCC CAG AGA TTG CC-3'
	Antisense	5'-GAA GGT CAA GGG AGG TTA CC-3'
C type	Sense	5'-GCC CAG AAG TGA GAG CAG TT-3'
	Antisense	5'-TCC AGA AAG CAG CTA GAG GG-3'
Oligonucleotide probes		
A type		5'-GGG CAG GGC TTG GTG AAT GGT AGC TGT GAT TAT CAT CAT G-3'
B type		5'-CGC AGG ATG GTG TGC GAG GAC CCC GAG CTG GTG TTC CAG GC-3'
C type		5'-ATA GAG ACA CCG ATT CCT GGA GGT CCA AAG AGC CTC AGG A-3'

Total RNA was extracted from the homogenized liver specimens by the method of Chomocynsky *et al.*^[32]. cDNA of γ -GTP mRNAs were amplified by reverse-transcription polymerase chain reaction (RT-PCR) using three different primer sets, which were specific for the three types. Six oligonucleotides, designed from cDNA sequences of γ -GTP at the 5'-noncoding region of human fetal liver, human placenta, and HepG2 cells were synthesized for use as the primers in PCR. The expected size of each PCR product was 308 bp in fetal liver (type A), 300 bp in Hep G2 (type B), and 386 bp in placenta (type C). The existence of intron sequences between each PCR primer set was confirmed by human γ -GTP genomic cloning and partial sequencing. The primer sets for type A, type B, and type C were corresponded to the sequences on γ -GTP cDNA from fetal liver, Hep G2 cells and placenta, respectively. An aliquot of the amplified γ -GTP cDNA fragments was analyzed on a 1 % agarose gel and transferred onto a Hybond-N membrane. The amplified γ -GTP cDNA were hybridized on Southern blots with oligonucleotide probes which were specific for each type of γ -GTP mRNA.

As the probes for type A, type B, and type C, 3 oligonucleotides were synthesized and were labeled at their 3' end using fluorescein d-UTR. The hybridized bands were reacted with HRP-labeled anti-fluorescein antibody and visualized on film using the ECL 3'-oligolabelling and detection systems of Amersham Life Science (Buckinghamshire, England), according to the instruction manual.

Parameters

The difference of γ -GTP expression in diverse clinicopathologic parameters were evaluated. Parameters included the presence of liver cirrhosis (confirmed by the operative findings and also by the pathology examination of the specimen), hepatitis B surface antigen (HBsAg), hepatitis C virus infection (anti-HCV), Child-Pugh classification of liver reverse (class A vs B), serum alpha-fetoprotein (AFP, <20 ng/ml vs 20-1 000 ng/ml vs >1 000 ng/ml) titer, tumor size (<3 cm, 3-10 cm, >10 cm), cell differentiation grade (Edmondson-Steiner grade I-II vs III-IV), encapsulation (complete, infiltration by HCC or absent) and vascular permeation (including vascular invasion and/or tumor thrombi within the portal vein or hepatic vein), daughter nodules or satellite nodules, multi-centric HCC and clinical evidence of recurrence, recurrence free interval, survival and death. The expression of γ -GTP mRNA of both cancerous tissue and non-cancerous tissue of the liver from resected specimens were compared with the above parameters by both univariate (UV) and multivariate (MV) analysis, respectively.

Statistical analysis

Statistical program (BMDP), Student's *t*-test or Mann-Whitney U test for continuous variables, χ^2 test of Fisher's exact test for categorical variables, and logistic regression and COX proportional hazards model for multivariate analysis were used. *P* value <0.05 was considered as a significant difference.

RESULTS

The types of γ -GTP mRNAs in livers obtained from 15 control patients were shown in Table 3. The γ -GTP mRNA expression was monogenic in 13 patients and polygenic in 2 patients. Type A was found in all patients (100 %), type B was found in one patient (6.7 %) and type C was found in one patient (6.7 %). In those with HCC, from the cancerous portion of the livers, the distribution of the type of γ -GTP mRNA was one (2.5 %) case of type A (monogenic), 24 (60.0 %) cases of type B (monogenic), 15 (37.5 %) cases of both type A and B (polygenic), and none of type C. From their non-cancerous portion of the livers, the distribution of the type of γ -GTP

mRNA was 12 (30.0 %) cases of type A (monogenic), 16 (40 %) cases of type B (monogenic), 12 (30 %) cases of type A and type B (polygenic) and none of type C (Table 3). Among those with HCC, the frequency of type A with type B (polygenic) or type B (monogenic) was 97.5 % in cancerous tissues and 70.0 % in non-cancerous tissues.

Table 3 Frequency of γ -GTP mRNA in liver

Tissues	mRNA types (%)				
	A	A+B	B	A+B or B	C
HCC					
Cancerous	1 (2.5)	15 (37.5)	24 (60.0)	39 (97.5)	0 (0)
Non-Cancerous	12 (30.0)	12 (30.0)	16 (40.0)	28 (70.0)	0 (0)
Control					
	A	B	C		
Control	15 (100.0)	1 (6.7)	1 (6.7)		

The correlation between those with type B and type B with type A in cancerous tissue and non-cancerous tissue and patients' characteristics were shown in Table 4. Gender, positivity of HBsAg, and Child-Pugh class A or B showed no statistically significant differences between the presence and the absence of type B and type B with type A γ -GTP mRNA.

Table 4 Correlation between type B γ -GTP mRNA and clinical parameters

Parameters	Cases	Type B/A+B(%)	
		HCC liver	Non HCC liver
Male	26	23 (88.5)	20 (76.9)
Female	14	10 (71.4)	8 (43.9)
HBsAg (+)	22	19 (86.4)	17 (60.7)
(-)	18	14 (77.8)	11 (39.3)
HCV (+)	15	14 (93.3)	14 (93.3) ^b
(-)	25	19 (76.0)	14 (56.0) ^b
Child A	32	25 (75.8)	21 (65.6)
Child B	8	8 (100.0)	7 (87.5)
AFP (ng/ml) <20	17	11 (64.7) ^a	9 (32.1) ^c
=20	23	22 (95.6) ^a	19 (82.6) ^c

Denotes: ^a $P=0.0295$; ^b $P=0.0151$; ^c $P=0.0430$.

From the univariate analysis, in cancerous portion of HCC livers, a significant correlation was found between type B and type B with type A expression of γ -GTP mRNA and high serum AFP level ($P=0.0295$). In non-cancerous portion of HCC livers, a significant correlation was found between type B and type B with A expression of γ -GTP mRNA and positivity of HCV antibody ($P=0.0151$) and high serum AFP level ($P=0.0430$).

The correlations between the types of γ -GTP mRNA expression and pathological parameters were shown in Table 5. From the univariate analysis, in cancerous portion of HCC livers, a significant correlation was found between type B and type B with type A γ -GTP mRNA and the presence of daughter nodules ($P=0.0089$).

In non-cancerous portion of HCC livers, a significant correlation was found between type B and type B with type A and the Edmondson-Steiner grade I and II vs III and IV ($P=0.0226$), the absence of tumor capsule ($P=0.0014$), the presence of vascular permeation ($P=0.0042$) and the presence of daughter nodules ($P=0.0012$). In both cancerous and non-cancerous livers, no statistically significant difference was

shown between type B and type B with type A and the presence of liver cirrhosis, tumor size and multi-centric HCC.

From outcome point of view, among those 39 patients whose cancerous liver with type B or type B with A γ -GTP mRNA, 21 patients (53.8 %) had recurrence (Table 6). As for the other patients without type B and B with A did not have had recurrence. The difference was statistically significant ($P=0.0328$). Among the former, 15 patients (38.5) died. Among the latter, no patient died. The difference was also statistically significant ($P=0.0328$). The death was related to tumor recurrence.

Table 5 Correlation between types of γ -GTP mRNA and pathological parameters

Parameters	Cases	Type B/A+B(%)	
		HCC liver	Non HCC liver
Cirrhosis (+)	33	27 (81.8)	22 (66.7)
(-)	7	6 (85.7)	6 (85.7)
Size < 3 cm	6	6 (100.0)	4 (66.7)
3-10 cm	11	7 (63.6)	5 (45.4)
=10 cm	23	20 (86.9)	19 (82.6)
Differentiated grade I/II	19	14 (73.7)	10 (52.6) ^b
III/IV	21	19 (90.5)	18 (85.7) ^b
Complete capsule (+)	18	13 (72.2)	8 (44.4) ^c
(-)	22	20 (90.9)	20 (90.9) ^c
Vascular permeation (+)	17	16 (94.1)	16 (94.1) ^d
(-)	23	17 (73.9)	12 (52.2) ^d
Daughter nodules (+)	19	19 (100.0) ^a	18 (94.7) ^e
(-)	21	14 (66.7) ^a	10 (47.6) ^e
Multi-centric (+)	13	12 (92.3)	12 (92.3)
(-)	27	21 (77.8)	16 (59.2)

Denotes: ^a $P=0.0089$; ^b $P=0.0226$; ^c $P=0.0014$; ^d $P=0.0042$; ^e $P=0.0012$.

Table 6 Correlation between γ -GTP mRNA and their outcome

γ -GTP mRNA	Cases	Recurrence (%)	Death (%)
Type B in HCC liver (+)	33	21 (63.6) ^a	15 (45.5) ^b
(-)	7	1 (14.3) ^a	0 (0) ^b
Type B in non-HCC liver (+)	28	22 (78.6) ^c	15 (53.6) ^d
(-)	12	0 (0) ^c	0 (0) ^d

Denotes: ^a $P=0.0328$; ^b $P=0.0328$; ^c $P<0.0001$; ^d $P=0.0011$

Among 28 patients whose non-cancerous liver tissue was type B or type B with type A, 22 patients (78.6 %) had recurrence. Among the other 12 patients without type B or type B with type A, no patient had recurrence. The difference had statistical significance ($P<0.0001$). Among the former, 15 patients (53.6 %) died, while among the latter, no patient died. The difference had statistical significance ($P=0.0011$).

The correlations between the parameters and recurrence were shown in Table 7. In UV analysis, statistically significant difference was found in high serum AFP ($P=0.0001$), large size ($P=0.0213$), differentiation grade (III and IV) ($P=0.0049$), absence of complete capsule ($P=0.001$), vascular permeation ($P<0.0001$), presence of daughter nodules ($P=0.0003$), type B (including type B and type B with type A) in cancerous liver ($P=0.0094$) and type B in non-cancerous (including type B and type B with type A) liver ($P=0.0003$). In MV analysis, only AFP ($P=0.0108$), vascular permeation ($P=0.0048$), and type B γ -GTP mRNA in non-cancerous liver had significant difference ($P=0.0107$).

Table 7 Significant factors in recurrence and death

Parameters	Recurrence		Death	
	UV	MV	UV	MV
Sex	n.s.	n.s.	n.s.	n.s.
Age	n.s.	n.s.	n.s.	n.s.
Child-Pugh's classification: A vs. B	n.s.	n.s.	n.s.	n.s.
HBsAg (+)	n.s.	n.s.	0.0166	n.s.
HCV (+)	n.s.	n.s.	n.s.	n.s.
AFP<20 vs. 20-1000	0.0001	0.0108	0.0006	0.0141
γ -GTP mRNA (+)	n.s.	n.s.	n.s.	n.s.
Pathology of HCC:				
Size: <3 cm vs. 3-10 cm	0.0213	n.s.	0.0080	n.s.
Cirrhosis	n.s.	n.s.	n.s.	n.s.
Edmondson-Steiner grade				
Complete capsule (+)	0.0001	n.s.	0.0007	n.s.
Vascular permeation (+)	<0.0001	0.0084	<0.0001	0.0130
Daughter nodules (+)	0.0003	n.s.	0.0001	0.0053
Multicentric (+)	0.0549	n.s.	0.0550	n.s.
Type B γ -GTP mRNA in HCC liver	0.0094	n.s.	0.0119	n.s.
Type B γ -GTP mRNA in non-HCC liver	0.0003	0.0107	0.0046	n.s.

Denotes: n.s.=not significant.

Significant factors relevant to post-recurrence survival in univariate analysis included negative HBsAg ($P=0.0166$), low serum AFP level ($P=0.0006$), small tumor size ($P=0.0080$), complete capsule ($P=0.0007$), absence of vascular permeation ($P<0.0001$), absence of daughter nodules ($P=0.0001$), absence of multi-centric HCC ($P=0.550$), absence of type B γ -GTP mRNA in cancerous tissue ($P=0.0119$) or non-cancerous tissue of HCC liver ($P=0.0046$). However, in MV analysis, only serum AFP ($P=0.0141$), vascular permeation ($P=0.0130$) and daughter nodules ($P=0.0053$) had significant difference.

DISCUSSION

γ -glutamyl transpeptidase (γ -GTP) is a plasma membrane-bound enzyme which has major importance in the metabolism of glutathione^[33,34]. Stark *et al* mentioned that metabolism of glutathione by γ -GTP in pre-neoplastic liver foci may initiate an oxidative process leading to a radical-rich environment and result in oxidative damage^[25]. Such damage may contribute to foci progress to malignancy. It has been reported that HCC of rat and human both expresses γ -GTP enzymes with unique carbohydrate moieties compared with normal liver enzymes^[20,24,28,35]. The presence of the unique γ -GTP isoform for HCC in patient serum had been used as a marker for the diagnosis of HCC^[28]. γ -GTP was used as an important marker enzyme for chemically induced HCC, because it is present in both primary HCC and pre-neoplastic lesions of the liver or some other liver diseases^[24-27,30,31,36-40]. It has been recently used as a response indicator in the treatment of hepatitis^[41].

Experimentally, Mallory bodies develop in mice treated chronically with griseofulvin, and HCC is also found in these animals^[42]. In hepatocytes developing Mallory bodies, histologically detectable γ -GTP activity was observed from the early stage of development. These results strongly suggested that changes in γ -GTP in livers may be closely related to the phenotypical expression of carcinogenesis of hepatocytes.

Furthermore, many previous studies concerning γ -GTP in HCC strongly suggest that changes in hepatic γ -GTP expression may closely related to the development of HCC. However, its mechanisms are not well known, and the reports of genomic analysis on the specific γ -GTP to HCC is not common.

Recently, human γ -GTP complementary DNA (cDNA) sequences from fetal liver, placenta, and HepG2 cells have been published. These cDNA sequences showed identical GGT protein structure. The most significant difference among these cDNAs exists in the 5'-noncoding region, suggesting that (1) human γ -GTP mRNA might be regulated by alternative-splicing mechanisms in this region, or (2) they are derived from different γ -GTP genes. Pawlak *et al* reported that at least four different γ -GTP genes or pseudogenes are present in human genome^[16]. However, pathophysiological roles of the genetic polymorphisms of γ -GTP genes are not well known. In Tsutsumi's study, polymorphisms of γ -GTP mRNAs at the 5'-noncoding region were analyzed.

The results obtained in placenta, fetal liver and Hep G2 cells indicate that the system used in the study is specific to define three types of γ -GTP mRNA^[24]. Differences of γ -GTP in tissues have been attributed to sialic acid contents^[15]. In normal liver, the main type of γ -GTP mRNA was type A^[24]. The expression was monogenic in most cases and polygenic in some cases. In the polygenic cases, type C was found commonly and type B was found occasionally. According to Tsutsumi's report, in cases with liver diseases but not HCC, the distribution of the of γ -GTP mRNA was nearly the same as in normal livers^[24]. Our results are similar with the above. On the other hand, the main type of γ -GTP mRNA in cancerous tissue was type B. In Tsutsumi's series, type B was found in all cases, and in more than half of the cases, only type B was detected^[24]. In our series, type B was found in 60 % of patients and the combination of type A with type B and only type B are detected in 97.5 %. Tsutsumi reported that in non-cancerous tissues from livers with HCC, the main types of γ -GTP mRNA were type A and B^[24]. Both types were found in all cases, except for one case in which type B was not detected. In this study, type B was found in 40 % of patients and both type B with Type A and type B were detected in 70 % of patients. The prevalence of type B was significantly higher in both cancerous and non-cancerous tissues of liver with HCC than that in livers without HCC. The prevalence of type A in cancerous tissues, but not in non-cancerous tissues, was significantly lower than that in livers without HCC. These results strongly suggested that the γ -GTP mRNA expression in the human liver may shift from type A to type B during the development of HCC. The high prevalence of type B in non-cancerous tissues of livers with HCC suggested that the shift of the γ -GTP mRNA may occur from the preneoplastic stage of hepatocytes. The shift of mRNA expression may occur early in the development of recurrence or even in pre-neoplastic stage. Based on that, we used the shift of the γ -GTP mRNA as a tool to predict the recurrence of HCC during the follow-up after resection of primary lesion of HCC.

The high recurrence rate after resection is one of the main factors in the poor outcome for HCC patients^[1-6]. Tumor recurrence limits the long-term survival. However, tumor recurrence is well correlated with tumor invasiveness. From the literatures, tumor invasiveness may be determined from high serum AFP, hepatitis vascular permeation, the grade of cell differentiation, infiltration or absence of capsule, size, coexisting cirrhosis, presence of daughter nodules, and multiple lesions^[1-14]. Our study suggested that the presence of type B (Hepa G cells) in both HCC tissue and non-cancerous liver tissue of resected HCC specimens was closely related to some invasiveness parameters of HCC. The presence of type B γ -GTP mRNA in cancerous tissue was correlated statistically with high serum level of AFP, daughter nodules, post-resection recurrence and post-recurrence survival. Whereas, the presence of type B γ -GTP mRNA in non-cancerous liver tissue was correlated significantly with hepatitis C infection, high serum level of AFP, Edmondson-Steiner grade III and IV of cellular

differentiation, absence of infiltration of capsule, vascular permeation, daughter nodules, post-resection recurrence and postrecurrence survival.

The presence of type B γ -GTP mRNA which is detected from non-cancerous portion of liver tissue of the resected HCC specimens may be considered as its presence in the remnant liver of the patients who had receiver resection. High level of serum AFP had been considered as a poor prognostic index^[5]. According to our study, it was correlated well with the presence of type B γ -GTP mRNA in both cancerous tissue and non-cancerous tissue. It was also correlated statistically significantly with tumor recurrence and survival.

More hepatitis C infection, but not hepatitis B infection was found in the presence of type γ -GTP mRNA in the remnant live. It was also corresponded with a higher recurrence and less survival. Some literature has also mentioned that the prognosis of hepatitis C infection is worse^[1,11]. Vascular permeation, indicating tumor invasiveness, consists of either tumor invasion of the hepatic vein, portal vein and/or hepatic artery, or tumor thrombi within the vessels. It may be detected preoperatively by ultrasonography, arteriography or portography, intraoperatively by ultrasonography or direct observation, or postoperatively by pathological examination of surgical specimens. Vascular permeation is the most consistent significant prognostic factor of postoperative tumor recurrence^[2, 3, 8-10, 11-13]. In univariate analysis, the presence of type B the prognosis in the remnant liver is significantly related to vascular permeation and in the COX model, patients with vascular permeation had significantly more recurrence and less survival.

Whether the grade of differentiation of HCC is a determinant of recurrence after resection has been debated for a long time^[1, 2, 9, 11]. The histological differentiation of the HCCs in this study correlated significantly with γ -GTP, and the presence of type B γ -GTP mRNA increased with increasing dedifferentiation. Our findings are consistent with that shift to type B γ -GTP mRNA in the remnant liver may be associated with the progression of HCC as an event in hepatocarcinogenesis.

The exact mechanism of capsular formation is not known. A tumor capsule may act as a barricade preventing the spread of cancer cells and has a positive role in the prognosis of HCC^[2, 5, 7, 8, 10, 13]. The invaded capsule was regarded as incomplete in our series. We found that the expression of type B γ -GTP mRNA in the remnant liver was higher in patients with no capsule and incomplete capsule. Multifocal HCCs are also a controversial issue. Some consider them an early metastasis via the portal vein but some consider them multicentric. The former is a poor prognostic factor but the latter might not be. Without the aid of molecular biology, it is difficult to differentiate daughter nodules, intrahepatic metastatic nodules and multicentric HCC^[14]. In the present study, we selected daughter or satellite nodules according to the criteria of the Liver Cancer Study Group of Japan. As for the evaluation of prognosis after recurrence, some authors reported that the most significant factor affecting the survival time of patients with intrahepatic recurrence was the number of tumor nodules at the time of recurrence^[1, 2, 4, 8, 9, 12]. In our study, those with the presence of daughter nodules showed a higher presence of type B γ -GTP mRNA in both remnant liver and the original resected HCC tissues.

Tumor size has been emphasized as one of the significant prognostic factors because vascular invasion and daughter lesions may increasingly develop as the tumor grows^[2-5, 8, 11-13]. In our study, no correlation between the presence of type B γ -GTP mRNA and tumor size was found. In addition, tumor size also had no correlation with recurrence or survival in our patients. From our experience, some large HCCs were the result

of expansive growth and had slow intraportal or distant spread. Our studies showed tumor invasiveness and prognosis was correlated with the presence of HCV infection, high serum level of AFP, vascular permeation, the grade of cell differentiation, infiltration or absence of capsule and daughter nodules. They were also all associated with the expression of type level mRNA in the remnant liver. Among them, serum AFP level and daughter nodules were associated with the presence of type B in HCC tissues. It suggested that the shift of type A to type B of γ -GTP mRNA in the liver tissues were strongly related to the development of HCC, including the progression of preneoplastic tissue and the potential of post-resection recurrence, the invasiveness of HCC and less survival of the patients. It was recommended that the expression of γ -GTP mRNA in both cancerous tissue and non-cancerous tissue of the resected HCC specimens may play a significant role in predicting the prognosis of HCC in patients after resection.

REFERENCES

- 1 Ikeda K, Saitoh S, Tsubota A, Arase Y, Chayama K, Kumada H, Watanabe G, Tsurumaru M. Risk factors for tumor recurrence and prognosis after curative resection of hepatocellular carcinoma. *Cancer* 1993; **71**: 19-25
- 2 Arii S, Tanaka J, Yamazoe Y, Minematsu S, Morino T, Fujita K, Maetani S, Tobe T. Predictive factors for intrahepatic recurrence of hepatocellular carcinoma after partial hepatectomy. *Cancer* 1992; **69**: 913-919
- 3 Shirabe K, Kanematsut T, Matsumata T, Adachi E, Akazawa K, Sugimachi K. Factors linked to early recurrence of small hepatocellular carcinoma after hepatectomy: univariate and multivariate analysis. *Hepatology* 1991; **14**: 802-805
- 4 Jow SC, Chiu JH, Chau GY, Loong CC, Lui WY. Risk factors linked to tumor recurrence of human hepatocellular carcinoma after hepatic resection. *Hepatology* 1992; **16**: 1367-1371
- 5 Nagao T, Inoue S, Goto S, Mizuta T, Omori Y, Kawano N, Morioka Y. Hepatic resection for hepatocellular carcinoma. *Ann Surg* 1987; **205**: 33-40
- 6 Sasaki Y, Imaoka S, Masutani S, Ohashi I, Ishikawa O, Koyama H, Iwanaga T. Influence of coexisting cirrhosis on long-term prognosis after surgery in patients with hepatocellular carcinoma. *Surgery* 1992; **112**: 515-521
- 7 Lai EC, Ng IO, Ng MM, Lok AS, Tam PC, Fan ST, Choi TK, Wong J. Long-term results of resection for large hepatocellular carcinoma: a multivariate analysis of clinicopathological features. *Hepatology* 1990; **11**: 815-818
- 8 Anonymous. Primary liver cancer in apan-clinicopathologic features and results of surgical treatment. Liver cancer study group of Japan. *Ann Surg* 1990; **211**: 277-287
- 9 Hsu HC, Sheu JC, Lin YH, Chen DS, Lee CS, Hwang LY, Beasley RP. Prognostic histologic features of resected small hepatocellular carcinoma (HCC) in Taiwan. *Cancer* 1985; **56**: 672-680
- 10 el-Assal ON, Yamanoi A, Soda Y, Yamaguchi M, Yu L, Nagasue N. Proposal of invasiveness score to predict recurrence and survival after curative hepatic resection for hepatocellular carcinoma. *Surgery* 1997; **122**: 571-572
- 11 Haratake J, Takeda S, Kasai T, Nakano S, Tokui N. Predictable factors for estimating prognosis of patients after resection of hepatocellular carcinoma. *Cancer* 1993; **72**: 1178-1183
- 12 Yamanaka N, Okamoto E. Conditions favoring long-term survival after hepatectomy for hepatocellular carcinomas. *Cancer Chem Pharm* 1989; **23** (Suppl): S83-S86
- 13 Vauthey JN, Vauthey JN, Klimstra D, Franceschi D, Tao Y, Fortner J, Blumgart L, Brennan M. Factors affecting long-term outcome after hepatic resection for hepatocellular carcinoma. *Am J Surg* 1995; **169**: 28-35
- 14 Nakano S, Haratake J, Okamoto K, Takeda S. Investigation of resected multinodular hepatocellular carcinoma: assessment of unicentric or multicentric genesis from histological and prognosis viewpoint. *Am J Gastroenterol* 1994; **9**: 189-193
- 15 Pawlak A, Cohen EH, Octave JN, Schweickhardt R, Wu SJ, Bulle F, Chikhi N, Baik JH, Siegrist S, Guellaen G. An alternatively processed mRNA specific for gamma-glutamyl transpeptidase

- in human tissues. *J Biol* 1990; **265**: 3256-3262
- 16 **Pawlak A**, Wu SJ, Bulle F, Suzuki A, Chikhi N, Ferry N, Baik JH, Siegrist S, Guellaen G. Different gamma-glutamyl transpeptidase mRNAs are expressed in human liver and kidney. *Biochem Biophys Res Communications* 1989; **164**: 912-918
 - 17 **Das ND**, Shichi H. Tissue difference in gamma-glutamyl transpeptidase attributed to sialic acid content. *Life Sciences* 1979; **25**: 1821-1827
 - 18 **Kottgen E**, Reutter W, Gerok W. Two different gamma-glutamyl transpeptidase during development of liver and small intestine: a fetal and an adult glycoprotein. *Biochem Biophys Res Communications* 1976; **72**: 61-66
 - 19 **Rajpert-De Meyts E**, Heisterkamp N, Groffen J. Cloning and nucleotide sequence of human gamma-glutamyl transpeptidase. *Proc Natl Acad Sci USA* 1988; **85**: 8840-8844
 - 20 **Hudson EA**, Munks RJ, Manson MM. Characterization of transcriptional regulation of gamma-glutamyl transpeptidase in rat liver involving both positive and negative regulatory elements. *Mol Carcinog* 1997; **20**: 376-388
 - 21 **Brouillet A**, Holic N, Chobert MN, Laperche Y. The gamma-glutamyl transpeptidase gene is transcribed from a different promoter in rat hepatocytes and biliary cells. *AM J Pathol* 1998; **152**: 1039-1048
 - 22 **Hanigan MH**, Frierson HF Jr, Brown JE, Lovell MA, Taylor PT. Human ovarian tumors express gamma-glutamyl transpeptidase. *Cancer Res* 1994; **54**: 286-290
 - 23 **Wetmore LA**, Gerard C, Drazen JM. Human lung expresses unique gamma-glutamyl transpeptidase transcripts. *Proc Natl Acad Sci USA* 1993; **90**: 7461-7465
 - 24 **Tsutsumi M**, Sakamuro D, Takada A, Zang SC, Furukawa T, Taniguchi N. Detection of a unique gamma-glutamyl transpeptidase messenger RNA species closely related to the development of hepatocellular carcinoma in humans: a new candidate for early diagnosis of hepatocellular carcinoma. *Hepatology* 1996; **23**: 1093-1097
 - 25 **Stark AA**, Russell JJ, Langenbach R, Pagano DA, Zeiger E, Huberman E. Localization of oxidative damage by a glutathione-gamma-glutamyl transpeptidase system in preneoplastic lesions in sections of livers from carcinogen-treated rats. *Carcinogenesis* 1994; **15**: 343-348
 - 26 **Tsuchiya S**, Yamazaki T, Camba EM, Morita T, Matsue H, Yoshida Y, Sato K. Comparison of the peptide and saccharide moieties of gamma-glutamyl transpeptidase isolated from neoplastic and non-neoplastic human liver tissue. *Clin Chem Acta* 1985; **152**: 17-26
 - 27 **Toya D**, Sawabu N, Ozaki K, Wakabayashi T, Nakagen M, Hattori N. Purification of gamma-glutamyltranspeptidase (gamma-GTP) from human hepatocellular carcinoma (HCC), and comparison of gamma-GTP with the enzyme from human kidney. *Ann N Y Acad Sci* 1983; **417**: 86-96
 - 28 **Taniguchi N**, House S, Kuzumaki N, Yokosawa N, Yamagiwa S, Iizuka S, Makita A, Sekiya C. A monoclonal antibody against gamma-glutamyltransferase from human primary hepatoma: its use in enzyme-linked immunosorbent assay of sera of cancer patients. *JNCI* 1985; **75**: 841-847
 - 29 **Doodspeed DC**, Dunn TJ, Miller CD, Pitot HC. Gamma-glutamyl transpeptidase transpeptidase cDNA: comparison of hepatoma and kidney mRNA in the human and rat. *Gene* 1989; **76**: 1-9
 - 30 **Carter JH**, Richmond RE, Carter HW, Potter CL, Daniel FB, DeAngelo AB. Quantitative image cytometry of hepatocytes expressing gamma-glutamyl transpeptidase and glutathione S-transferase in diethylnitrosamine-initiated rats treated with phenobarbital and/or phthalate esters. *J Histochem Cytochem* 1992; **40**: 1105-1115
 - 31 **Gallagher BC**, Rudolph DB, Hinton BT, Hanigan MH. Differential induction of gamma-glutamyl transpeptidase in primary cultures of rat and mouse hepatocytes parallels induction during hepatocarcinogenesis. *Carcinogenesis* 1998; **19**: 1251-1255
 - 32 **Chomczynski P**, Sacchi N. Single-step method of RNA isolation by acid guanidinium thiocyanate-phenol-chloroform extraction. *Ann Biochem* 1987; **162**: 156-159
 - 33 **Sakamuro D**, Yamazoe M, Matsuda Y, Kangawa K, Taniguchi N, Matsuo H, Yoshikawa H, Ogasawara N. The primary structure of human gamma-glutamyl transpeptidase. *Gene* 1988; **73**: 1-9
 - 34 **Hochwald SN**, Harriossn LE, Rose DM, Anderson M, Burt ME. Gamma-glutamyl transpeptidase mediation of tumor glutathione utilization *in vivo*. *J Natl Cancer Inst* 1996; **88**: 193-197
 - 35 **Habib GM**, Rajagopalan S, Godwin AK, Lebovitz RM, Lieberman MW. The same gamma-glutamyl transpeptidase RNA species is expressed in fetal liver, hepatic carcinomas, and rasT24-transformed rat liver epithelial cells. *Mol Carcinog* 1992; **5**: 75-80
 - 36 **Okuyama K**. Separation and identification of serum gamma-glutamyl transpeptidase isoenzymes by wheat germ agglutinin affinity electrophoresis: a basic analysis and its clinical application to various liver diseases. *Keio J Med* 1993; **42**: 149-156
 - 37 **Seckin P**, Alptekin N, Kocak-Toker N, Uysal M, Aykac-Toker G. Hepatic gamma-glutamyl cysteine synthetase and gamma-glutamyl transpeptidase activities in galactosamine-treated rats. *Res Commun Mol pathol Pharmacol* 1995; **87**: 237-240
 - 38 **Kitten O**, Ferry N. Mature hepatocytes actively divide and express gamma-glutamyl transpeptidase after D-galactosamine liver injury. *Liver* 1998; **18**: 398-404
 - 39 **Colombatto P**, Randone A, Civitico G, Monti Gorin J, Dolci L, Medaina N, Oliveri F, Verme G, Marchiaro G, Pagni R, Karayiannis P, Thomas HC, Hess G, Bonino F, Brunetto MR. Hepatitis G virus RNA in the serum of patients with elevated gamma-glutamyl transpeptidase and alkaline phosphatase-a specific liver disease. *J Viral Hepatitis* 1996; **3**: 301-306
 - 40 **Griffiths SA**, Good VM, Gordon LA, Hudson EA, Barrett MC, Munks RJ, Manson MM. Characterization of a promoter for gamma-glutamyl transpeptidase activated in rat liver in response to aflatoxin b1 and ethoxyquin. *Mol Carcinog* 1995; **14**: 251-262
 - 41 **Van Thiel DH**, Friedlander L, Malloy P, Wright HI, Gurakar A, Fagiuoli S, Irish W. gamma-Glutamyl transpeptidase as a response predictor when using alpha-interferon to treat hepatitis C. *Hepato Gastroenterol* 1995; **42**: 888-892
 - 42 **French SW**. The Mallory body: Structure, composition, and pathogenesis. *Hepatology* 1981; **1**: 76-83

Hepatocyte transformation and tumor development induced by hepatitis C virus NS3 c-terminal deleted protein

Qiong-Qiong He, Rui-Xue Cheng, Yi Sun, De-Yun Feng, Zhu-Chu Chen, Hui Zheng

Qiong-Qiong He, Rui-Xue Cheng, Yi Sun, De-Yun Feng, Hui Zheng, Department of Pathology, Xiangya School of Medicine, Central South University, Changsha 410078, Hunan Province, China
Zhu-Chu Chen, Cancer Research Institute, Central South University, Changsha 410078, Hunan Province, China

Supported by the Health Ministry Science Foundation of China, No.98-1-110

Correspondence to: Pro. Rui-Xue Cheng, Department of Pathology, Xiangya School of Medicine, Central South University, Changsha 410078, Hunan Province, China. chengrx@cs.hn.cn

Telephone: +86-731-2650410

Received: 2002-06-24 **Accepted:** 2002-07-11

Abstract

AIM: To study the effect of hepatitis C virus nonstructural protein 3 c-terminal deleted protein (HCV NS3-5') on hepatocyte transformation and tumor development.

METHODS: QSG7701 cells were transfected with plasmid pRcHCNS3-5' (expressing HCV NS3 c-terminal deleted protein) by lipofectamine and selected in G418. The expression of HCV NS3 gene and protein was determined by PCR and immunohistochemistry respectively. Biological behavior of transfected cells was observed through cell proliferation assay, anchorage-independent growth and tumor development in nude mice. The expression of HCV NS3 and *c-myc* proteins in the induced tumor was evaluated by immunohistochemistry.

RESULTS: HCV NS3 was strongly expressed in QSG7701 cells transfected with plasmid pRcHCNS3-5' and the positive signal was located in cytoplasm. Cell proliferation assay showed that the population doubling time in pRcHCNS3-5' transfected cells was much shorter than that in pRcCMV and non-transfected cells (24 h, 26 h, 28 h respectively). The cloning ratio of cells transfected with pRcHCNS3-5', pRcCMV and non-transfected cells was 33 %, 1.46 %, 1.11 %, respectively, the former one was higher than that in the rest two groups ($P < 0.01$). Tumor development was seen in nude mice inoculated with pRcHCNS3-5' transfected cells after 15 days. HE staining showed its feature of hepatocarcinoma, and immunohistochemistry confirmed the expressions of HCV NS3 and *c-myc* proteins in tumor tissue. The positive control group inoculated with HepG2 also showed tumor development, while no tumor developed in the nude mice injected with pRcCMV and non-transfected cells after 40 days.

CONCLUSION: 1. HCV NS3 c-terminal deleted protein has transforming and oncogenic potential. 2. Human liver cell line QSG7701 may be used as a good model to study HCV NS3 pathogenesis.

He QQ, Cheng RX, Sun Y, Feng DY, Chen ZC, Zheng H. Hepatocyte transformation and tumor development induced by hepatitis C virus NS3 c-terminal deleted protein. *World J Gastroenterol* 2003; 9(3): 474-478

<http://www.wjgnet.com/1007-9327/9/474.htm>

INTRODUCTION

HCV infection is a major worldwide health problem. Persistent infection with HCV is a critical risk for the development of hepatocellular carcinoma (HCC)^[1-3]. It has been reported that the Core protein, NS3, NS4B, and NS5A have oncogenic potential^[2, 4-6]. HCV NS3 protein (nucleotide 3 420 to 5 312 with 631 amino acid residues) is a multi-functional viral protein. In addition to serine proteinase activity, which is located in the one-third of the NS3 protein at the N-terminal end, helicase and nucleotide triphosphatase activities are identified in the c-terminal half of the NS3 protein^[7]. HCV NS3 that plays a key role in the life cycle of virus and interacts with host cellular protein has been one of hot spots in recent research. We found that the NIH3T3 cell has stronger telomerase activity after transfected with HCV NS3 plasmid, indicating that HCV NS3 may be an important part in the hepatocarcinogenesis^[8]. Most studies on NS proteins have been carried out by expression of single or multiple NS proteins in cultured none hepatocyte, despite the fact that HCV is a hepacivirus. In order to reflect the relation between HCV NS3 and host cell transformation more clearly, here we tried to transfect human liver cell line QSG7701 with eukaryotic cell plasmid pRcHCNS3-5' (expressing NS3 c-terminal deleted protein), and then inoculated nude mice with transfected cells to investigate its biological behaviors and carcinogenesis.

MATERIALS AND METHODS

Materials

Hepatocyte cell line QSG7701 was got from Shanghai Institute of Cell Biology, Chinese Academe of Sciences (CAS) and HepG2 cell line was got from Cell Center of Central South University. Nude mice (BALB/cA-nude) were got from Shanghai Laboratorial Animal Center, CAS. The plasmid pRcHCNS3-5' (expressing HCV NS3 c-terminal deleted protein) was the kind gift from professor Takegami^[9]. Non-expressive plasmid pRcCMV was purchased from Sigma Com USA. LipofectaminTM reagent, G418 and Dulbecco's modified Eagle medium (DMEM) were products of GIBCO BRL (Germany). *Xba*I, buffer and PCR kit, marker were bought from Sino-American Biotechnology INC (Shanghai, P.R.China). Anti-HCV NS3 protein MAb, anti-c-myc protein MAb and S-P detection kit were purchased from Boshide Com (Wuhan, P. R.China) and Maxim Biotech INC (Fuzhou, P.R.China), respectively. New-born calf serum was got from Sijiqing Bioengineering Ltd. (Hangzhou, P.R.China). PCR primers for amplifying HCVNS3-5' gene were synthesized at Shanghai Sangon Com (Shanghai, P.R.China).

Methods

Experimental groups Group 1: QSG7701 parental cells; Group 2: QSG7701 transfected with blank plasmid pRcCMV; Group 3: QSG7701 transfected with plasmid pRcHCNS3-5'; Group 4: HepG2 cell line used as positive control.

Cell culture Cell lines were maintained in DMEM with 10 % heat-inactivated new-born calf serum, 100 unit/ml penicillin and 100 unit/ml streptomycin at 37 °C in a humidified atmosphere of 5 % CO₂.

Preparation, purification and identification of plasmids pRcHCNS3-5' and pRcCMV Plasmids pRcCMV and pRcHCNS3-5' were transferred into competent *E. coli* JM109 respectively. JM109 was cultured to amplify the two plasmids. Little plasmids were prepared from JM109 to identify the specificity of the plasmids. The plasmid pRcHCNS3-5' was digested with *Xba*I, resolved with agarose gel electrophoresis, and stained with ethidium bromide (EB). As shown in Figure 1, the electrophoresis analysis revealed the major 886bp fragment of the plasmid pRcHCNS3-5' as being expected. Then the plasmids were massively extracted and purified for transfecting QSG7701 cells.

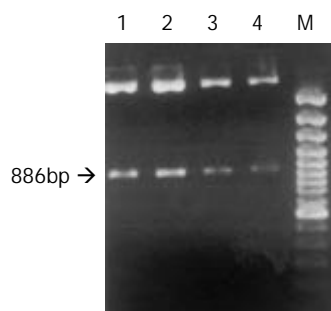


Figure 1 pRcHCNS3-5' digested with *Xba*I. Lane M: DNA marker (Generuler™ 100bpDNA). Lane: 1, 2, 3, 4 plasmid pRcHCNS3-5' with 886bp fragment. (×100).

Transfection of QSG7701 cells with plasmids pRcHCNS3-5' and pRcCMV QSG7701 cells were transfected with the plasmids pRcHCNS3-5' and pRcCMV, respectively according to the instruction of Lipofectamine reagent. Cells were seeded into selection medium containing 400 µg/ml G418 until G418-resistant clones were obtained, and then cells were maintained in G418 with concentration of 200 µg/ml (Figure 2). QSG7701 parental cells were used for the parallel control. To detect cDNA in stable transfectants, total genomic DNA was extracted according to standard methods and subjected to PCR and agarose gel electrophoresis analysis. The primers for amplifying HCVNS3-5' gene were based on published sequences^[9]. PCR conditions were 35 cycles of three steps (94 °C 30 sec, 57 °C 30 sec, 72 °C 40 sec) and then 72 °C 5 min in a 50 µl reaction mixture containing 5 µl 10×buffer, 5 µl 2 mM dNTPs, 0.5 µl of each primer (25 pmol/µl), 1 µl (100 ng)DNA, 0.5 µl 5U/µl Taq DNA polymerase, and 37.5 µl distilled water. PCR products were subjected to electrophoresis on a 0.8 % agarose gel, visualized by EB staining. As shown in Figure 3, 257bp fragment was specifically amplified from DNA of the QSG7701 cells transfected with plasmid pRcHCNS3-5', but no fragment was amplified from DNA of the pRcCMV transfected cells and parental cells.



Figure 2 Colony formation of pRcHCNS3-5' transfected QSG7701 cells in G418 (×100).

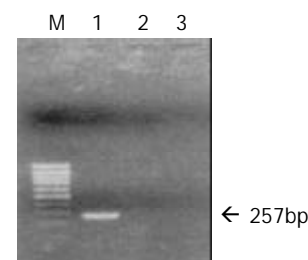


Figure 3 PCR analysis of DNA from QSG7701 transfected with pRcHCNS3-5' and pRcCMV; Lane M: 100bp marker; Lane 1: pRcHCNS3-5' transfected cells; Lane 2: pRcCMV transfected cells; Lane 3: QSG parental cells.

Immunohistochemistry S-P method was used to detect the expression of HCV NS3 protein in parental QSG7701 cells and QSG7701 cells transfected with plasmid pRcHCNS3-5', pRcCMV. PBS substituting Mabs was used as blank control. HCC expressing HCV NS3 protein was used as positive control.

Cell proliferation assay QSG parental cells and cells transfected with pRcHCNS3-5', pRcCMV (6×10^4 cells per well) were seeded in 24-well plates and counted daily with a haemocytometer respectively. Experiment was lasted for 7 days and was repeated three times.

Anchorage-independent growth Cells were suspended at a density of 2×10^3 /ml containing 0.3 % granulated agar. The mixture was added over a layer of 0.7 % agar in medium. After 4 weeks, the morphology of transfected cells was analysed microscopically. Colonies including more than 50 cells were scored. Experiment was repeated three times.

Tumor development in athymic nude mice 12 nude mice (BALB/cA-nude, females, 4-6 weeks, 18-22 g) were divided into 4 groups of 3 nude mice each and inoculated subcutaneously in the right flank with pRcHCNS3-5', pRcCMV and parental cells (1×10^7 cells in 0.2 ml of phosphate-buffered saline) and monitored for tumor development. HepG2 cells were used as the positive control. Tumor size and animal weight were measured weekly. The nude mice were sacrificed and the tumors were removed 40 days after inoculating. Tumor tissue was fixed by 10 % formalin, embedded with paraffin wax, sliced successively 5 µm per section and stained by HE. Immunohistochemistry S-P method was used to detect the expressions of HCV NS3 protein and *c-myc* protein in tumor tissue.

Statistical analysis

F test was used. *P* value of less than 0.05 was considered as statistically significant.

RESULTS

HCV NS3 protein expression in QSG7701 cells transfected with plasmid pRcHCNS3-5'

Immunohistochemical staining showed that QSG7701 cells transfected with pRcHCNS3-5' strongly expressed HCV NS3 protein. The positive signal was in cytoplasm (Figure 4). The positive signal was also found in the positive control group, but not in the blank and negative control groups.

Cell proliferation assay

The population doubling time in cells transfected with pRcHCNS3-5' (12 h) was much shorter than that in those transfected with pRcCMV and parental QSG7701 cells (26 h, 28 h respectively). (Figure 5).

Anchorage-independent growth

The cloning efficiencies in pRcHCNS3-5', pRcCMV

transfected cells and parental cells were 33 %, 1.46 %, 1.11 %, respectively ($P < 0.01$, the former vs the rest two).

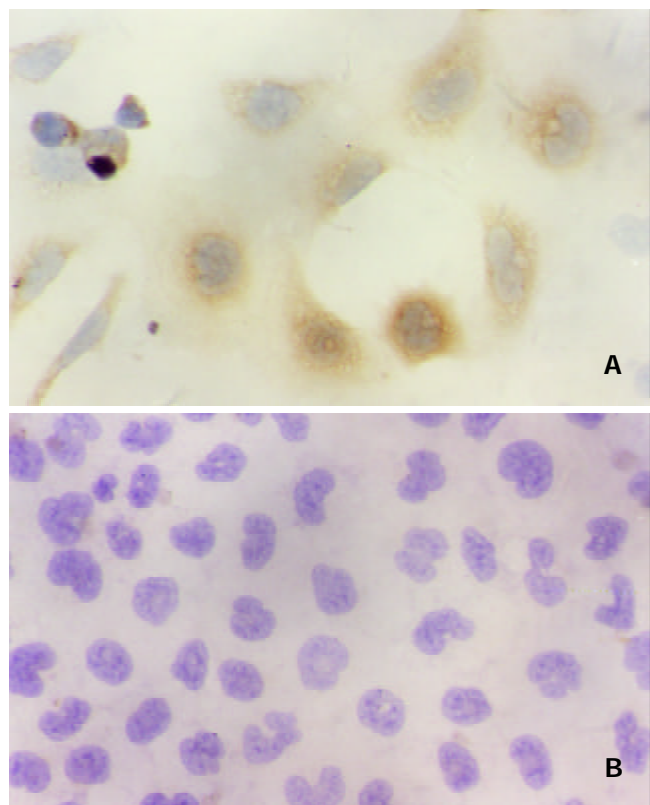


Figure 4 Immunohistochemistry analysis (S-P) of HCV NS3 protein expression in pRcHCNS3-5' transfected cells (up) and the negative control without positive signal (down) ($\times 400$).

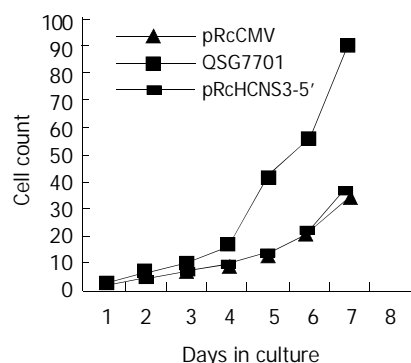


Figure 5 Proliferation rate of cells transfected with pRcHCNS3-5', pRcCMV and parental QSG7701 cells.

Tumor development in nude mice

In the nude mice inoculated with pRcHCNS3-5' transfected cells, the first evidence of well-defined and distinct subcutaneous tumors appeared on day 15. The mean tumor size and weight on day 40 were 3.08 cm³ and 3.13 g, respectively. The HepG2 cells, as positive control, also induced tumor in the nude mice. But no tumor developed in the mice inoculated with pRcCMV and none-transfected QSG7701 cells until 40 days after inoculating (Figure 6). Macroscopically, the tumors induced by pRcHCNS3-5' showed irregular yellow-brown node and appeared to be encapsulated. Central necrosis could be seen on the cut surface. Microscopically, the tumor cells exhibited similarity to hepatocyte except for heterogenesis and they arranged as trabecular with intervening sinusoids. Cancer cell nests with abundance granular necrosis were separated by fibrous tissue (Figure 7a, 7b). They showed the

histologically feature of hepatocellular carcinoma. Immunohistochemical staining showed that tumor tissue expressed HCV NS3 protein and *c-myc* protein. The positive signal was located in cytoplasm (Figure 7c, 7d).

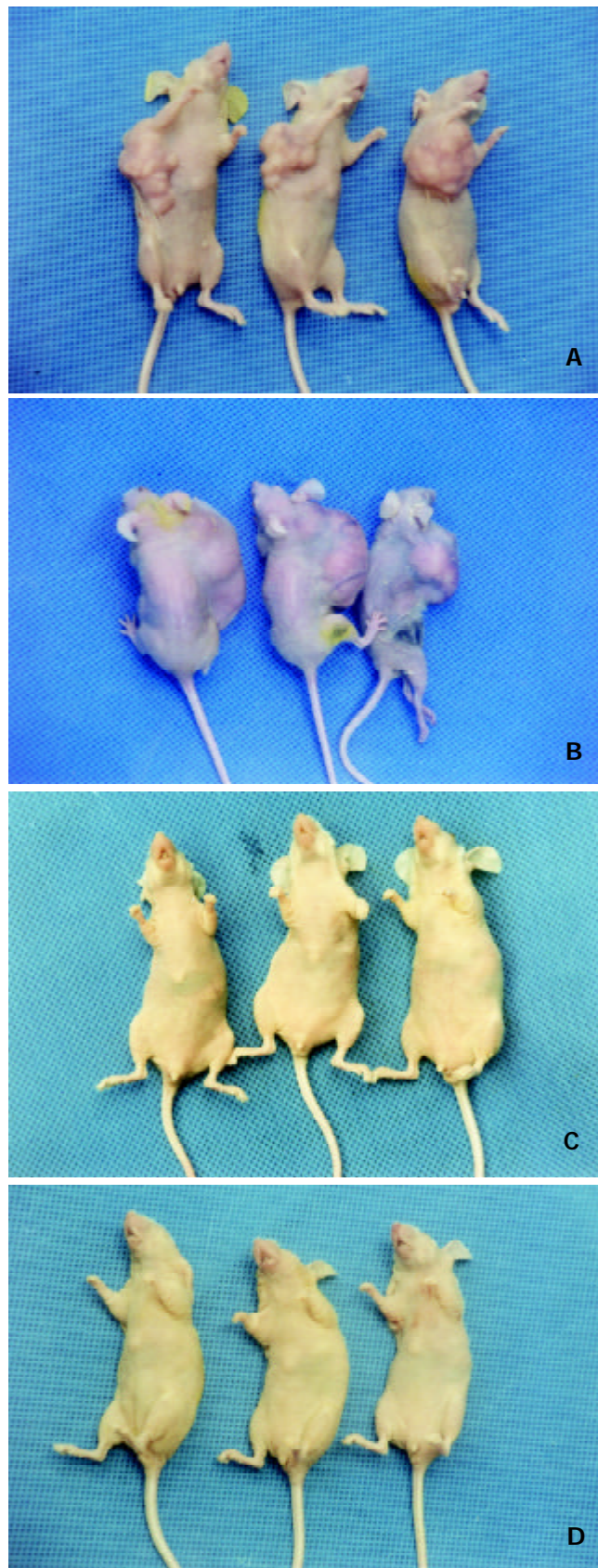


Figure 6 Tumor development in nude mice, 6a, 6b, 6c and 6d show inoculated with pRcHCNS3-5' transfecting QSG7701 cells, HepG2 cells, QSG7701 cells transfected with pRcCMV and parental QSG7701 cells, respectively.

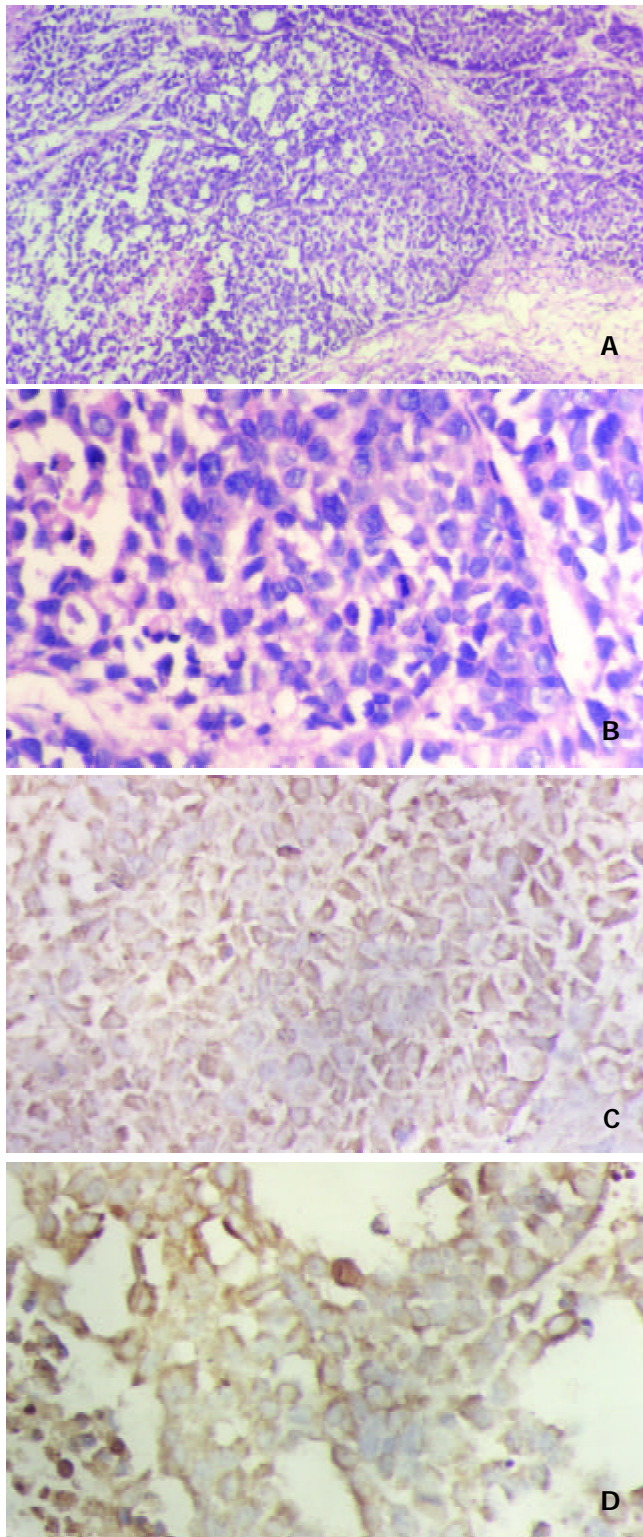


Figure 7 pRcHCNS3-5' induced hepatocellular carcinoma (7a HE×100, 7b HE×400), HCV NS3 (7c) and *c-myc* (7d) protein expressing in the tumor tissue by immunohistochemistry (S-P), the positive signals are both in cytoplasm (×400).

DISCUSSION

It has been reported that persistent infection with HCV is associated with HCC, and HCV replication and protein expression can be observed in HCC tissue^[1, 10-11], although the pathogenesis of HCV infection-associated HCC is still unknown. HCV, as a RNA virus without any RT activity, is replicated in the cytoplasm and does not integrate with host genome like HBV. Furthermore, unlike EBV or HPV, the HCV genome itself, does not contain any known oncogene. Most

studies indicate that the interaction between the HCV protein and liver cell gene/protein has been involved in hepatocarcinogenesis. Zemel *et al* reported significant mutations of amino acids that occur at the catalytic domain of the NS3 serine protease gene isolated from HCC tissue will affect the activity and substrate specificity of serine protease^[12]. Sakamuro^[9] and Zemel^[2] *et al* founded that HCV NS3 could transform NIH3T3 cell and non-tumorigenic rat fibroblast (RF) cell respectively. HCV NS3 can suppress actinomycin D induced apoptosis^[13], inhibit cAMP-dependent protein kinase^[14] and repress P53 function^[15-17]. But the cell lines used by most researchers were not based on HCV natural host cell-hepatocyte. Here non-tumorigenic human liver cell line QSG7701 was used in our study. QSG7701 cells that were immortally normal hepatocytes came from liver tissue 6 cm far from HCC and their karyotype number was 57^[18]. QSG7701 cells with normal hepatocyte phenotype were stably transfected with an expression vector containing cDNA for NS3 proteinase activity. The transfected cells grew rapidly, showed anchorage -independent growth in soft agar and induced significant tumor formation in nude mice. Our study firstly showed that the protease-coding gene of HCV induced malignant transformation of nontumorigenic human liver cells. Moreover injecting pRcHCNS3-5' transfected cells into nude mice led to significant tumor formation. The tumor obtained from the nude mice showed the histologically feature of hepatocellular carcinoma. The results suggest the involvement of proteinase activity of HCV NS3 N terminal peptide in cellular transforming and oncogenic potential.

Current studies show that HCV NS3 may be directly involved in hepatocarcinogenesis by disturbing the regulation of cell proliferation. But the mechanism of carcinogenesis is still perplexing. Carcinogenesis, including HCC, is the result of the abnormal proliferation of cancer cells. It is reported that various oncogenic products are related to functional abnormalities of intracellular signal transduction pathway, which have been proved to be one of the proliferative mechanism of cancer cells. Great progress has been made that HCV proteins regulate signal transduction in the recent studies. Ras/Raf/MAPK pathway is regarded to have close relation to HCV associated HCC.

Constitutive activation of the Ras/Raf/MAPK pathway is important for the transformation of mammalian cells^[19,20]. Indeed, studies have demonstrated that HCC development and progression is associated with the activation of Ras/Raf/MAPK pathway in humans and rodents^[21,22]. Our lab also found that MAPK activity is higher in HCC than that in the adjacent noncancerous lesions, suggesting a progression of HCC through Ras/Raf/MAPK activation^[23]. Recently, the development of anticancer drugs that target signaling proteins of MAPK pathway has been a major goal in the cancer treatment^[24,25]. There are several reports concerning the relationship between HCV protein and Ras/Raf/MAPK signal transduction pathway. For example, some evidences suggest that HCV C protein directly or indirectly activates Ras/Raf/MAPK signal transduction pathway elements (including Raf-1, ERK, MEK, Elk, SRE, AP-1) in different cells such as HepG2, CCL13, COS7, MCF-7, BALB/3T3 and NIH3T3^[26-31]. Borowski *et al* reported an arginine-rich domain located in the NS3 region (residues1487 to 1500 of HCV polyprotein) which strongly resembles the autoinhibitory sequence of the PKA R subunit. It binds to the C subunit of PKA and inhibits the translocation of C subunit into nucleus. Consequently, PKA functions are arrested^[32]. Marshall identified that specific sites between Ras and Raf-1 are essential to plasma membrane localization and Raf activation. The formation of Ras/Raf-1 complex is negatively regulated by PKA through phosphorylation of Raf-1 N terminal serine 43, which is believed to cause an N-terminal cap structure to cover the Ras docking site which ultimately leads to inhibit Raf-1 activation^[33, 34]. HCV NS3 may activate Raf-1 by interfering the function of PKA. We

previously demonstrated that HCV NS3 N-terminal peptide (residues 1020-1295) positively regulates ERK1/2 phosphorylation. Because the N terminal peptide of HCV NS3 used in our study does not include the arginine-rich domain. We preclude that either HCV NS3 interacts with PKA through other domain or HCV NS3 involves in Ras/Raf/MAPK signal transduction pathway through other targets. Nuclear transcriptional factors *c-myc* as a target factor regulated by downstream of the MAPK cascade may increased when MAPK is activated. Overexpression of *c-myc* in tumor tissue of nude mice was detected which was consistent with other's report^[35]. It is supposed that HCV NS3 may be involved in hepatocarcinogenesis through Ras/Raf/MAPK/*c-myc* signal transduction.

ACKNOWLEDGEMENT

We thank professor Takegami for his generous gift of plasmid pRcHCNS3-5'.

REFERENCES

- 1 **Li L**, Wang WL, Yu XX, Zhen JY. Detection of hepatitis C virus RNA in the tissue of hepatocellular carcinoma by multiple detection system. *Zhonghua Shiyen He Linchuangbing Duxue Zazhi* 2000; **14**: 47-52
- 2 **Zemel R**, Gerechet S, Greif H, Bachmatove L, Birk Y, Golan-Goldhirsh A, Kunin M, Berdichevsky Y, Benhar I, Tur-Kaspa R. Cell transformation induced by hepatitis C virus NS3 serine protease. *J Viral Hepat* 2001; **8**: 96-102
- 3 **Koike K**, Tsutsumi T, Fujie H, Shintani Y, Kyoji M. Molecular mechanism of viral hepatocarcinogenesis. *Oncology* 2002; **62**(Suppl 1): 29-37
- 4 **Park JS**, Yang JM, Min MK. Hepatitis C virus nonstructural protein NS4B transforms NIH3T3 cells in cooperation with the Haras oncogene. *Biochem Biophys Res Commun* 2000; **267**: 581-587
- 5 **Ghosh AK**, Steele R, Meyer K, Ray R, Ray RB. Hepatitis C virus NS5A protein modulates cell cycle regulatory genes and promotes cell growth. *J Gen Virol* 1999; **80**: 1179-1183
- 6 **Moriya K**, Fujie H, Shintani Y, Yotsuyanagi H, Tsutsumi T, Ishibashi K, Matsuura Y, Kimura S, Miyamura T, Koike K. The core protein of hepatitis C virus induces hepatocellular carcinoma in transgenic mice. *Nat Med* 1998; **4**: 1065-1067
- 7 **Kato N**. Molecular virology of hepatitis C virus. *Acta Med Okayama* 2001; **55**: 133-159
- 8 **Feng D**, Cheng R, Ouyang X, Zheng H, Tsutomu T. Hepatitis C virus nonstructural protein NS (3) and telomerase activity. *Chin Med J* 2002; **115**: 597-602
- 9 **Sakamuro D**, Furukawa T, Takegami T. Hepatitis C virus nonstructural protein NS3 transforms NIH 3T3 cells. *J Virol* 1995; **69**: 3893-3896
- 10 **Yang JM**, Wang RQ, Bu BG, Zhou ZC, Fang DC, Luo YH. Effect of HCV infection on expression of several cancer-associated gene products in HCC. *World J Gastroenterol* 1999; **5**: 25-27
- 11 **Ohishi M**, Sakisaka S, Harada M, Koga H, Taniguchi E, Kawaguchi T, Sasatomi K, Sata M, Kurohiji T, Tanikawa K. Detection of hepatitis-C virus and hepatitis-C virus replication in hepatocellular carcinoma by *in situ* hybridization. *Scand J Gastroenterol* 1999; **34**: 432-438
- 12 **Zemel R**, Kazatsker A, Greif F, Ben-Ari Z, Greif H, Almog O, Tur-Kaspa R. Mutations at vicinity of catalytic sites of hepatitis C virus NS3 serine protease gene isolated from hepatocellular carcinoma tissue. *Dig Dis Sci* 2000; **45**: 2199-2202
- 13 **Fujita T**, Ishido S, Muramatsu S, Itoh M, Hotta H. Suppression of actinomycin D-induced apoptosis by the NS3 protein of hepatitis C virus. *Biochem Biophys Res Commun* 1996; **229**: 825-831
- 14 **Borowski P**, Heiland M, Oehlmann K, Becker B, Kornetzky L, Feucht H, Laufs R. Non-structural protein 3 of hepatitis C virus inhibits phosphorylation mediated by cAMP-dependent protein kinase. *Eur J Biochem* 1996; **237**: 611-618
- 15 **Okada F**, Shiraki T, Maekawa M, Sato S. A p53 polymorphism associated with increased risk of hepatitis C virus infection. *Cancer Lett* 2001; **172**: 137-142
- 16 **Kwon HJ**, Jung EY, Ahn JY, Lee MN, Jang KL. P53-dependent transcriptional repression of p21(waf1) by hepatitis C virus NS3. *J Gen Virol* 2001; **82**: 2235-2241
- 17 **Feng DY**, Chen RX, Peng Y, Zheng H, Yan YH. Effect of HCV NS (3) protein on p53 protein expression in hep atocarcinogenesis. *World J Gastroenterol* 1999; **5**: 45-46
- 18 **Zhu DH**, Wang JB. The culture of HCC host hepatocyte QSG7701 cell line and as compared with hepatocarcinoma cell. *Zhongliu Fangzhi Yanjiu* 1979; **5**: 7-9
- 19 **Pinkas J**, Leder P. MEK1 signaling mediates transformation and metastasis of EpH4 mammary epithelial cells independent of an epithelial to mesenchymal transition. *Cancer Res* 2002; **62**: 4781-4790
- 20 **Hamad NM**, Elconin JH, Karnoub AE, Bai W, Rich JN, Abraham RT, Der CJ, Counter CM. Distinct requirements for Ras oncogenesis in human versus mouse cells. *Genes Dev* 2002; **16**: 2045-2057
- 21 **Zhu J**, Leng X, Dong N, Liu Y, Li G, Du R. Expression of mitogen-activated protein kinase and its upstream regulated signal in human hepatocellular carcinoma. *Zhonghua Waikexue Zazhi* 2002; **40**: 1-16
- 22 **Ostrowski J**, Woszczynski M, Kowalczyk P, Wocial T, Hennig E, Trzeciak L, Janik P, Bomsztyk K. Increased activity of MAP, p70S6 and p90rS kinases is associated with AP-1 activation in spontaneous liver tumours, but not in adjacent tissue in mice. *Br J Cancer* 2000; **82**: 1041-1050
- 23 **Feng DY**, Zheng H, Tan Y, Cheng RX. Effect of phosphorylation of MAPK and Stat3 and expression of c-fos and c-jun proteins on hepatocarcinogenesis and their clinical significance. *World J Gastroenterol* 2001; **7**: 33-36
- 24 **Shapiro P**. Ras-MAP kinase signaling pathways and control of cell proliferation: relevance to cancer therapy. *Crit Rev Clin Lab Sci* 2002; **39**: 285-330
- 25 **Sebolt-Leopold JS**. Development of anticancer drugs targeting the MAP kinase pathway. *Oncogene* 2000; **19**: 6594-6599
- 26 **Aoki H**, Hayashi J, Moriyama M, Arakawa Y, Hino O. Hepatitis C virus core protein interacts with 14-3-3 protein and activates the kinase Raf-1. *J Virol* 2000; **74**: 1736-1741
- 27 **Giambartolomei S**, Covone F, Levrero M, Balsano C. Sustained activation of the Raf/MEK/Erk pathway in response to EGF in stable cell lines expressing the Hepatitis C Virus (HCV) core protein. *Oncogene* 2001; **20**: 2606-2610
- 28 **Tsuchihara K**, Hijikata M, Fukuda K, Kuroki T, Yamamoto N, Shimotohno K. Hepatitis C virus core protein regulates cell growth and signal transduction pathway transmitting growth stimuli. *Virology* 1999; **258**: 100-107
- 29 **Fukuda K**, Tsuchihara K, Hijikata M, Nishiguchi S, Kuroki T, Shimotohno K. Hepatitis C virus core protein enhances the activation of the transcription factor, Elk1, in response to mitogenic stimuli. *Hepatology* 2001; **33**: 159-165
- 30 **Kato N**, Yoshida H, Kioko Ono-Nita S, Kato J, Goto T, Otsuka M, Lan K, Matsushima K, Shiratori Y, Omata M. Activation of intracellular signaling by hepatitis B and C viruses: C-viral core is the most potent signal inducer. *Hepatology* 2000; **32**: 405-412
- 31 **Shrivastava A**, Manna SK, Ray R, Aggarwal BB. Ectopic expression of hepatitis C virus core protein differentially regulates nuclear transcription factors. *J Virol* 1998; **72**: 9722-9728
- 32 **Borowski P**, Heiland M, Feucht H, Laufs R. Characterisation of non-structural protein 3 of hepatitis C virus as modulator of protein phosphorylation mediated by PKA and PKC: evidences for action on the level of substrate and enzyme. *Arch Virol* 1999; **144**: 687-701
- 33 **Marshall M**. Interactions between Ras and Raf: key regulatory proteins in cellular transformation. *Mol Reprod Dev* 1995; **42**: 493-499
- 34 **Hafner S**, Adler HS, Mischak H, Janosch P, Heidecker G, Wolfman A, Pippig S, Lohse M, Ueffing M, Kolch W. Mechanism of inhibition of Raf-1 by protein kinase A. *Mol Cell Biol* 1994; **14**: 6696-6703
- 35 **Fang Y**, Huang B, Liang Q, Li H, Huang C. Clinical significance of *c-myc* oncogene amplification in primary hepatocellular carcinoma by interphase fluorescence *in situ* hybridization. *Zhonghua Binglixue Zazhi* 2001; **30**: 180-182

Antitumor immunopreventive and immunotherapeutic effect in mice induced by hybrid vaccine of dendritic cells and hepatocarcinoma *in vivo*

Jin-Kun Zhang, Jun Li, Juan Zhang, Hai-Bin Chen, Su-Biao Chen

Jin-Kun Zhang, Jun Li, Juan Zhang, Hai-Bin Chen, Su-Biao Chen, Cancer Pathology Laboratory, Shantou University Medical College, Shantou 515031, Guangdong Province, China

Supported by the Natural Science Foundation of Guangdong Province, China, No. 980180; the Woman Science and Technology Workers Association of Guangdong Province, China, No.2001001

Correspondence to: Prof. Jin Kun Zhang, Tutor of Doctor, Cancer Pathology Laboratory, Shantou University Medical College, 22 Xinlinglu, Shantou 515031, Guangdong Province, China. jkzhang@stu.edu.cn

Telephone: +86-754-8900443 **Fax:** +86-754-8557562

Received: 2002-07-20 **Accepted:** 2002-10-12

Abstract

AIM: To develop a tumor vaccine by fusion of H22 hepatocarcinoma cells and DC, and to study its protective and therapeutic effect against H22 cell.

METHODS: H22-DC vaccine was produced by PEG fusion of H22 and DC induced by cytokine released from splenic mononuclear cells, sorted by CD11c magnetic microbead marker. It was injected through the tail vein of the mice and the H22-DC oncogenesis was detected in the liver, spleen and lung. In order to study the therapeutic and protective effect of H22-DC against tumor H22, two groups were divided: immune group and therapeutic group. Immune group was further divided into P, D, HD and H subgroups, immunized by PBS, DC, H22-DC and inactivated H22, respectively, and attacked by H22 cell. The tumor size, tumor weight, mice survival time and tumor latent period were recorded and statistically analyzed; Therapeutic group was divided into three subgroups of P, D and HD, and attacked by H22, then treated with PBS, DC, and H22-DC, respectively. Pathology and flow cytometry were also applied to study the mechanism how the H22-DC vaccine attacked on the H22 cell.

RESULTS: 1. No oncogenesis was found in spleen, lung and liver after H22-DC injection. 2. Hybrid vaccine immunized mice had strongest CTL activity. 3. In the immune group, latent period was longer in HD subgroup than that in P, H and D subgroup; and tumor size and weight were smaller in HD subgroup than that in P, H and D subgroup. 4. In therapeutic group, tumor size was smaller in HD subgroup than that in P, D subgroup.

CONCLUSION: 1. H22-DC tumor vaccine is safe without oncogenesis *in vivo*. 2. Hybrid vaccine can stimulate potent specific CTL activity against H22. 3. H22-DC vaccine has distinctive prophylactic effect on tumor H22 and can inhibit the tumor growth.

Zhang JK, Li J, Zhang J, Chen HB, Chen SB. Antitumor immunopreventive and immunotherapeutic effect in mice induced by hybrid vaccine of dendritic cells and hepatocarcinoma *in vivo*. *World J Gastroenterol* 2003; 9(3): 479-484
<http://www.wjgnet.com/1007-9327/9/479.htm>

INTRODUCTION

Tumor cells have low antigenicity and high antigen modulatory ability, by which tumor associated antigen or tumor specific antigen can't be efficiently presented to T cells and tumor specific killing T cell can't be efficiently activated^[1-5]. Furthermore, as one of antigen presenting cells (APC), tumor cells are anergy to T cells because of their deficiency of costimulator. Dendritic cells (DC), as a potent professional APC, not only express MHC molecules and costimulators to present tumor antigen and activate tumor specific T cells, but also can directly activate NK cell to kill MHC molecule negative tumor cell in nonspecific immunity. So much attention was paid to DC for its potential application in antitumor immunity^[6-10]. Hepatocarcinoma is a high malignant tumor, so it is an important assignment to find a suitable way to kill the hepatocarcinoma. Our previous work showed that hybrid vaccine could kill tumor cell *in vitro*^[11-16]. In this report, we tried to find a way to apply the DC in the prevention and therapy of hepatocarcinoma.

MATERIALS AND METHODS

Materials

Tumor cell line H₂₂ cell line, constructed by Dalian medical university from the mouse ascite, was heterogeneous cells with higher declination to spread by lymph vessel.

Animal BALB/c mice were bought from laboratory animal center of antibiotic industrial institute in Sichuan china. All mice were male, specific pathogen free animals, with age of 6-8 weeks and weight of 15-20 g.

Main reagents Metrizamide was product of Amresco Company. Mini MACS cell sorter and CD11c MicroBeads marked antibody were products of Miltenyi Biotec GmbH Company. rmGM-CSF (granulocyte-macrophage colony-stimulating factor) was a product of R & D company. Polyethylene glycol (PEG) was purchased from Sigma Chemical Company. MTT solution was a product of Amresco Company.

Methods

Culture of tumor cells H₂₂ cell was incubated in double-layer agarose culture medium (upper layer 0.3 %, base layer 0.6 %) with concentration of $5 \times 10^5/L$ and cultured for 10 days. Single colony was selected and transferred to culture flask for expanding culture. Cells of the logarithmic stage were collected and conserved in frozen conditions for later use. $0.1 \text{ ml } 1 \times 10^7$ H₂₂ cells were incubated subcutaneously at the right armpit, carcinogenesis *in vivo* was observed.

Isolation of DC from spleen Spleen of mice was grinded it into cell suspension, they were lysed by NH_4Cl , centrifugated by metrizamide gradient solution. Cells in the interface were collected, and cultured routinely by complete culture medium RPMI 1640 at 100 % humidity, 37°C , $50 \text{ mL} \cdot \text{L}^{-1} \text{ CO}_2$ for 3 hours, then the suspended cells were removed and continued to be cultured for another 16 hours, the non-adherent cells were collected, and adjusted to the concentration of $1 \times 10^9/L$, then

cultured in the complete medium with $200 \text{ mL} \cdot \text{L}^{-1}$ NCS and rmGM-CSF (500 ng/L) for 5-7 days^[17].

Fusion of DCs and H₂₂ DCs and H₂₂ were washed by PBS for 3 times, then the mixture of these two kinds of cells (DCs: H₂₂=1:1) were centrifugated to remove the upper liquid gently and completely, the cell droplet was loosen by shaking, $500 \text{ mL} \cdot \text{L}^{-1}$ PEG was added in the droplet in 37°C water bath to fuse for 1 min, and simultaneously the tube was shook gently. D-hanks solution was added to terminate the fusion process for 5 min in 37°C water bath, the upper liquid was removed by centrifugation, and the cell droplet was collected. the cell availability and number of fusion cells was detected by trypan blue staining.

Screening and determination of hybrid cell The fusion cells were marked by CD11c antibody, and sorted by Mini MACS to remove the CD11c⁻ cells and the CD11c⁺ cells were collected and they were cultured in RPMI complete medium with rmGM-CSF (500 ng/L) and $200 \text{ mL} \cdot \text{L}^{-1}$ NCS for 2-3 weeks^[18].

Carcinogenic effect of hybrid vacciney in vivo Mice were divided into five groups of HD1group, HD2 group, D group, H group and P group. 0.1 ml hybrid vaccine was injected into tail veil of mice in the HD1group, mice in the other group were injected at right armpit subcutaneously with $0.1 \text{ mL} \cdot 1-2 \times 10^7/\text{ml}$ vaccine, H₂₂ cells+DC, H₂₂ cells and PBS, respectively. And, 14 days later, tissues of the injection site, spleen, liver and lung were isolated, the tumor weight was compared.

Analysis of the CTL activity 20 mice were classified to four groups of HD group, D group, H group and P group, each group had 5 mice. Mice were injected with 0.1 ml hybrid vaccine, DC, heat inactivated H₂₂ and PBS at the concentration of $1 \times 10^{10}-2 \times 10^{10}/\text{L}$, twice every three days. All the mice were killed at 10 days after the last immunization and the spleen lymphocytes were separated and cultured under condition of complete medium with IL-2 ($1 \times 10^5 \text{ u/L}$) and $100 \text{ mL} \cdot \text{L}^{-1}$ FCS at saturated humidity, 37°C , $50 \text{ mL} \cdot \text{L}^{-1} \text{CO}_2$ to induce the CTL. CTL and H₂₂ was mixed at 5:1 and 10:1 effector/target rate, respectively. In addition, there were a CTL control group, a H₂₂ control group and a culture medium control group. All specimens had 3 parallel wells on a 96-well culture plate. All were cultured under conditions of saturated humidity 37°C , $50 \text{ mL} \cdot \text{L}^{-1} \text{CO}_2$ for 48 hours. MTT method was used to detect the CTL cytotoxicity against H₂₂. Chief process was as below: adding 5 g/L MTT solution 20 ul in each well for 4 hour before the detection, then it was centrifugated to remove the free MTT; 150 ul DMSO was added to the cell droplet for 10 min to solve the MTT. Bio-Rad 350-uv automatic enzyme linker detector is used to detect the OD value at 570 wavelength^[19]. All were repeated for 4 times.

Protective effect of hybrid vaccine against H₂₂ 40 BALB/c mice were randomly divided into HD, D, H and P subgroups, ten mice in each subgroup, immunized by 0.1 mL hybrid vaccine, DC, heat inactivated H₂₂ and PBS, respectively, at concentration of $1 \times 10^9/\text{L}$, two times every three days by tail veil. Three days after the last immunization, all mice were injected by 1×10^6 H₂₂ at the right armpit subcutaneously. The mice weight, tumor formation, tumor size and day of mice death were recorded. 5 mice were randomly chose and killed on day 14, tumor tissue, lung tissue, liver tissue and lymph node of neck and armpit were sampled for routine paraffin embedded slice and HE staining. Other mice were kept observation for 50 days.

Therapeutic effect of hybrid vaccine against H₂₂ 30 BALB/c mice were randomly divided into HD, D and P subgroups, ten mice in each subgroup. All mice was injected with H₂₂ tumor cell 1×10^6 subcutaneously at right armpit. 3 days later, tumor was formed in all mice which demonstrated the successful construction of tumor model. Mice in different

groups were treated with 0.1 mL hybrid vaccine, DC, and PBS, respectively, at the concentration of $1 \times 10^9/\text{L}$, two times every three days, by the tail veil. The tumor weight and size were recorded each day. 5 mice were randomly chose and killed on day 14; pathological changes were observed in tumor tissue. The other mice were kept on feeding for 50 days.

Statistical analysis

Data were analyzed by the method of ANOVA (SPSS 10.0 software).

RESULTS

Culture of tumor cell

H₂₂ grew *in vitro* in a suspended manner, single or integrated, its double proliferation time was 24 hours. H₂₂ cell can grow to form colony composed of hundreds of cells in 5-6 days, thousands cells in ten days on agarose cultured medium.

Incubation of 1×10^6 H₂₂ at right armpit subcutaneously *in vivo* can successfully induce tumor in all mice. Tumor grew aggressively to invade the surrounding tissue, tumor appeared necrosis when tissue bulk were big enough, even gangrenous impairment appeared on skin when tissue diameter was beyond 30 mm. Tumor tissue had integrated cell with few intercellular materials, had no funicular structure of normal liver. Tumor cells had distinctive cellular pleomorphism, nuclear pleomorphism, nuclear hyperchromatism and increased nuclear: cytoplasmic ratio (Figure 1).

Morphology of spleen DC

DC was round and irregular with sharp and long, or blunt cell extension. Induced by rmGM-CSF for 5-7 days, DC grew into a colony; outer cell of it had much extension. Sorted by Microbead marked CD11c, most of them were CD11c⁺.

Carcinogenesis of Hybrid vaccine in vivo

No carcinogenesis appeared after hybrid vaccine was injected subcutaneously for 60 days, while H₂₂ was injected, tumor appeared in 100 % mice at site of injection. There was significant in tumor weight between the HD and H₂₂ subgroup ($P < 0.01$). 1×10^6 hybrid vaccine was injected by tail veil, the mice's spleen, lung and liver were sampled after 14 days, three slices were sectioned for each organ, no carcinogenesis appeared (Figure 2-3).

Activity of spleen CTL

CTL activity of mice in HD subgroup was significantly higher than that of D, H and P subgroup (Figure 4).

The protective effect in vivo hybrid vaccine against H₂₂ in different subgroup

Observation of carcinogenesis Mice of different subgroups in protective group were injected with H₂₂ cells, the tumor latent time ranked as $P < H < D < HD$ subgroup ($P < 0.05$). This demonstrated that the HD subgroup had delayed tumor latent time (Figure 5A); tumor size and tumor weight ranked as $HD < D < H < P$ subgroup ($P < 0.05$) (Figure 5B, C), which showed that mice in the HD subgroup had the lowest tumor size and tumor weight, and the D subgroup had secondly lowest tumor size and tumor weight. Survival time among different subgroups had no significant difference ($P > 0.05$) (Figure 5D).

Pathology of different subgroups Macroscopic structure showed the tumor tissue was hard and adherenced to the surrounding tissue. Cutting face of tumor tissue was gray and diffused dot-like brown. Microscopic structure showed that tumor had dot like or sheet like necrosis (Figure 6A, B, C, D).

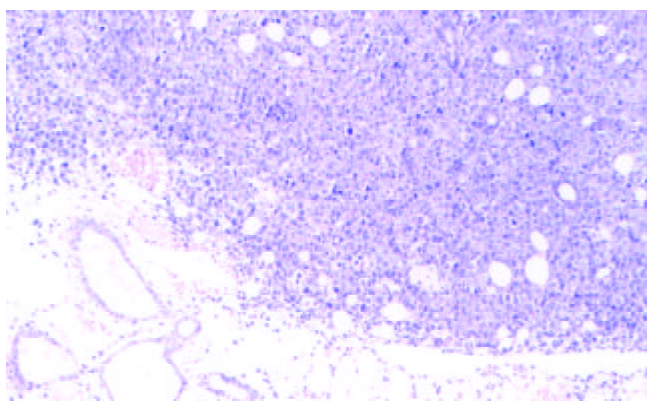


Figure 1 Tumor tissue after 14 d subcutaneous incubation. HE, 3.3×10.

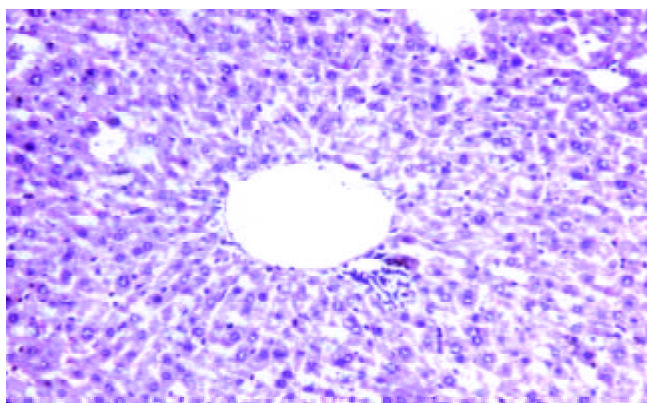


Figure 2 Liver tissue of 14 d after hybrid vaccine injection by tail vein HE, 3.3×20.

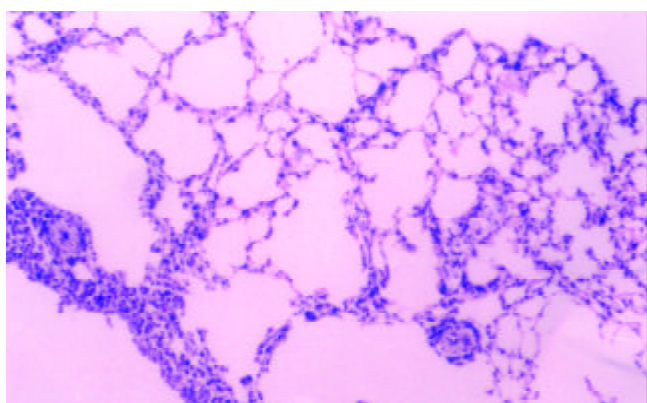


Figure 3 Lung tissue of 14 d after hybrid vaccine injection by tail vein HE, 3.3×20.

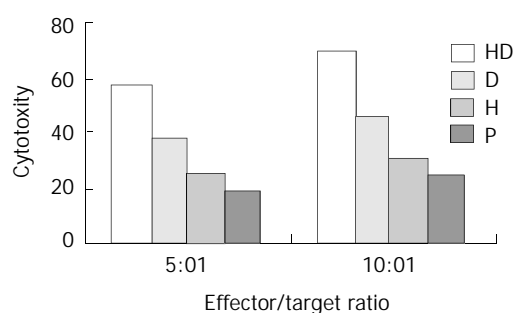


Figure 4 CTL activity of different subgroup at different effector/target ratio.

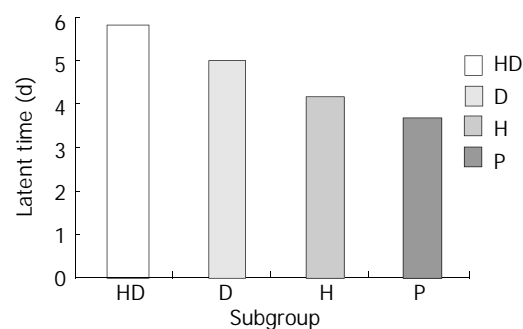


Figure 5A Comparison of latent time among different subgroups.

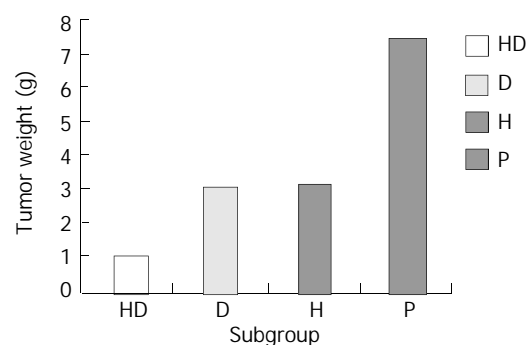


Figure 5B Comparison of tumor weight among different subgroups.

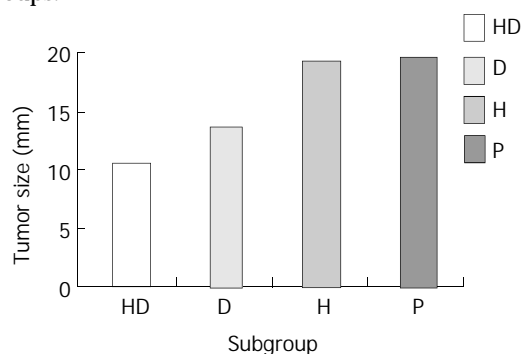


Figure 5C Comparison of tumor size among different subgroups.

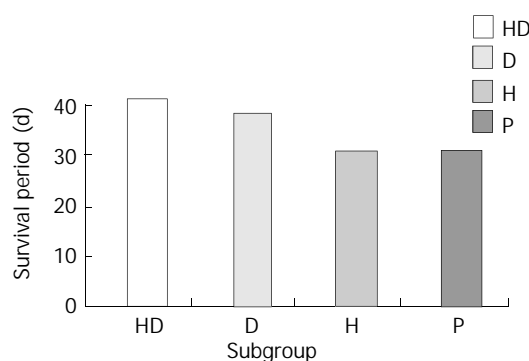


Figure 5D Comparison of survival period among different subgroups.

Therapeutic effect of hybrid vaccine against H_{22}

Inhibitory effect of hybrid vaccine in carcinogenesis Treated with hybrid vaccine, DC and PBS, tumor size in different subgroups ranked as $HD < D < P$ ($P < 0.05$) (Figure 7). Survival time and tumor weight had no significant difference among the different subgroups in therapeutic group.

Pathology of different subgroups Macroscopic structure

showed the tumor tissue was hard and can't separate with surrounding tissue easily. Cutting face of tumor tissue is gray and diffuse dot-like brown. Microscopic structure showed tumor has dot like or sheet like necrosis (Figure 8A, B, C).

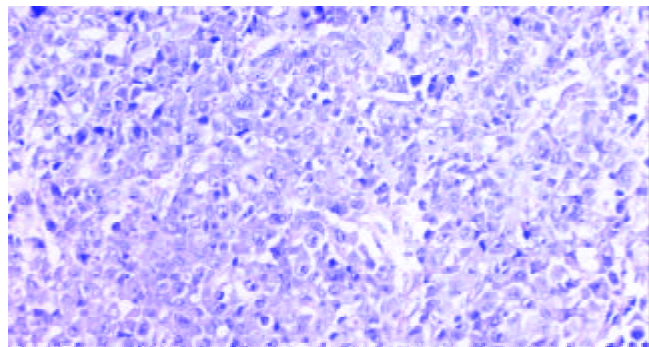


Figure 6A There isn't obvious necrosis in tumor tissue of 14 d in protective group P subgroup. HE, 3.3×20.

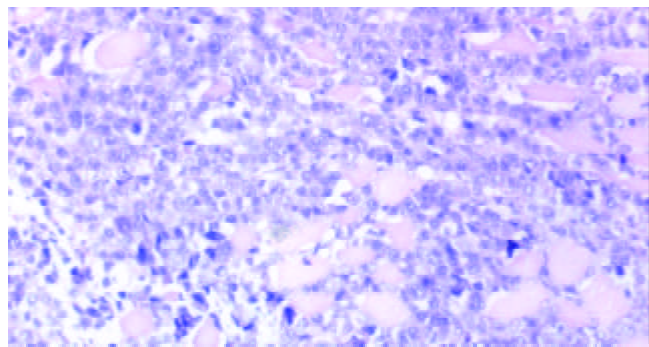


Figure 6B There is dot like necrosis in tumor tissue of 14 d in protective group H subgroup. HE, 3.3×20.

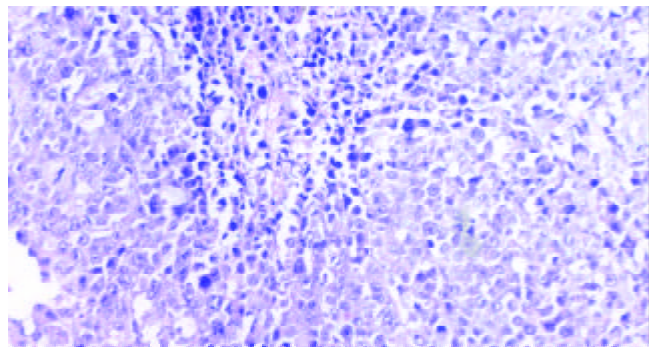


Figure 6C There is sheet like necrosis in tumor tissue of 14 d in protective group D subgroup. HE, 3.3×20.

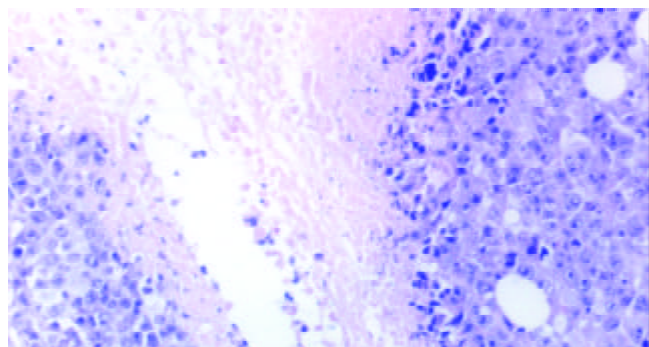


Figure 6D There is extensive necrosis in tumor tissue of 14 d in protective group HD subgroup. HE, 3.3×20.

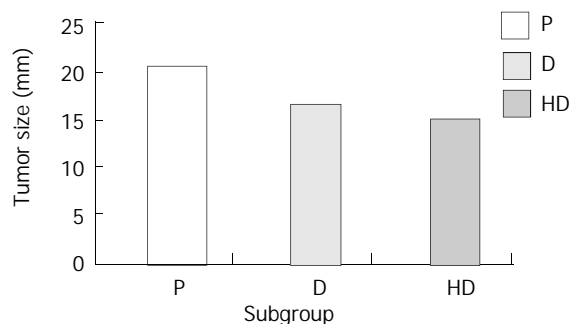


Figure 7 Comparison of tumor size on day 14 among different subgroups of therapeutic group.

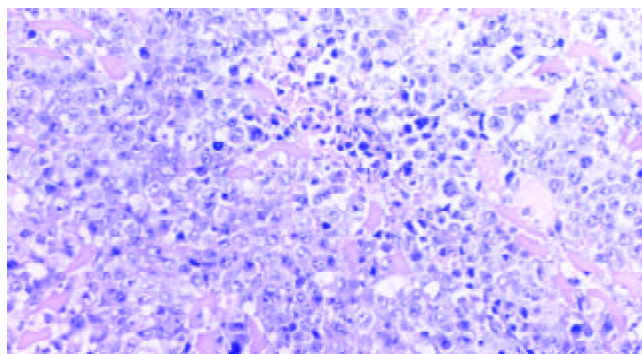


Figure 8A There is dot or sheet like necrosis in tumor tissue of 14d in therapeutic group P subgroup. HE, 20×3.3.

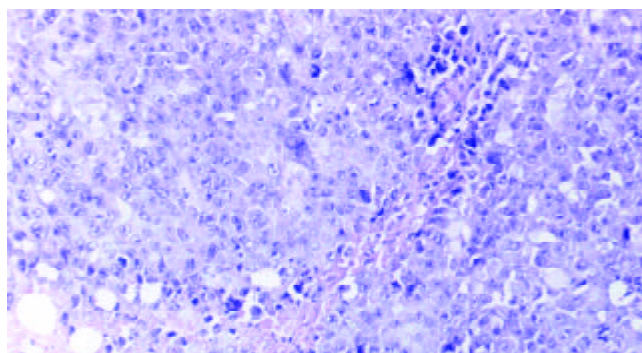


Figure 8B There is sheet like necrosis in tumor tissue of 14 d in therapeutic group D subgroup. HE, 20×3.3.

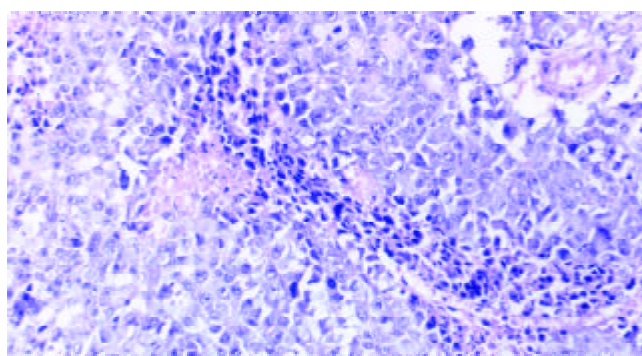


Figure 8C There is sheet like necrosis in tumor tissue of 14 d in therapeutic group HD subgroup. HE, 20×3.3.

DISCUSSION

H₂₂ ascite hepatocarcinoma has strong invasion and spreading declination by lymph vessel. In this report, H₂₂ cells had 100 %

carcinogenesis effect on BALB/c mice, which was consistent with other report^[19]. H₂₂ cells grow quickly *in vitro*, which can be easily used to construct the tumor animal model, and express low level of MHC molecule. So H₂₂ cells are suitable for DC antitumor research.

In this report, DC was separated through centrifugation by metrizamide; the maturation of DC was induced by cytokine of rmGM-CSF; DC and H₂₂ were fused through PEG, they were marked by CD11c, and sorted by Mini MACS. By above process, the hybrid vaccine was successfully constructed^[15,17,19,20]. The methods were simple and easily operated. Hybrid Vaccine, injected subcutaneously, has no tumor formation at local tissue, and injected by tail vein, it also has no carcinogenesis in the liver, lung and spleen, so it loses the carcinogenic effect of H₂₂ cells, and is safe to develop tumor vaccine *in vivo*.

In the protective group, different subgroups had different tumor latent time, and different interval between the H₂₂ incubation and tumor formation. The HD subgroup had the longest tumor latent time; the D subgroup had the second longest tumor latent time. The results showed that the hybrid vaccine and DC could delay the tumor carcinogenesis. The HD subgroup had the lowest tumor size and tumor weight, the D subgroup had the second lowest tumor size and tumor weight. The results showed that hybrid vaccine had the strongest anti-tumor effect. Hybrid vaccine could express some DC characteristics such as membrane molecule MHC-I, II molecule and costimulator, secrete some cell factors which can stimulate the T cell expansion, capture and present endogenous tumor associated antigens derived from parents H₂₂ cells, so it can efficiently stimulate the immune response^[21-25]. There were similar results in other research reports on hybrid vaccines of DC with MC38, NS1, B16 melanoma, RMA-s lymphoma and renal carcinoma^[26-35].

Mice immunized by hybrid vaccine could induce the tumor specific memory T cells, which could quickly be activated and expanded when they contact with tumor antigen again. When CD40 which was expressed by memory T cell integrated with CD40L of DC, it could stimulate DC to secrete high level of IL-12, and to enhance the expression of ICAM-1, CD80 and CD86. The activated DC could stimulate the proliferation of T cells and secretion of IFN- γ of T cells^[36-39]. It was reported that IFN- γ gene modified H₂₂ cells could enhance the antigenicity and the expression of MHC-II molecule from 10 % to 19 %; TNF gene modified H₂₂ cell also could enhance the MHC-I molecule expression in different clones with different transfection methods which was enhanced to 28.39 % and 35.78 % in two clones which had the highest expression of MHC-I; GM-CSF gene modified H₂₂ had lower oncogenicity *in vivo*, the possible mechanism attributed to the enhanced MHC expression^[40-44].

Hybrid vaccine also takes part in nonspecific immunity; it can directly activate NK cells to kill MHC-tumor cells. Some reports demonstrated DC could produce large number of INF- γ , which can inhibit the virus replication and stimulate the NK and macrophages^[45-47]. In this report, the hybrid vaccine antitumor function perhaps attributed to both adaptive and inborn immunity.

In the therapeutic group, tumor size in the HD subgroup was significantly lower than that in other subgroups after treated for 14 days, which showed that H₂₂-DC could inhibit the tumor growth. Some reported the similar effect. For example, after breast cancer cells hybridised with CD14⁺ derived DC, ³H incorporation assay showed that hybrid cell can stimulate the proliferation T cells, while only tumor cell, DC and mixture of DC and tumor cell have no such effect^[48-55].

From above, it is concluded that hybrid vaccine acquired the function of parents cell such as antigen presenting function of DC and T stimulating ability and capture the tumor derived

antigen. Hybrid vaccine has the protective and therapeutic effect against H₂₂. This research can provide some evidence for the clinical application of tumor vaccine.

REFERENCES

- 1 **Cohen PA**, Peng L, Kjaergaard J, Plautz GE, Finke JH, Koski GK, Czerniecki BJ, Shu S. T cell adoptive therapy of tumors: mechanisms of improved therapeutic performance. *Crit Rev Immunol* 2001; **21**: 215-248
- 2 **Nawrocki S**, Wysocki PJ, Mackiewicz A. Genetically modified tumour vaccines: an obstacle race to break host tolerance to cancer. *Expert Opin Biol Ther* 2001; **1**: 193-204
- 3 **Azuma I**, Seya T. Development of immunoadjuvants for immunotherapy of cancer. *Int Immunopharmacol* 2001; **1**: 1249-1259
- 4 **Smyth MJ**, Godfrey DI, Trapani JA. A fresh look at tumor immunosurveillance and immunotherapy. *Nat Immunol* 2001; **2**: 293-299
- 5 **Renner C**, Kubuschok B, Trumper L, Pfreundschuh M. Clinical approaches to vaccination in oncology. *Ann Hematol* 2001; **80**: 255-266
- 6 **Nishioka Y**, Hua W, Nishimura N, Sone S. Genetic modification of dendritic cells and its application for cancer immunotherapy. *J Med Invest* 2002; **49**: 7-17
- 7 **Gunzer M**, Grabbe S. Dendritic cells in cancer immunotherapy. *Crit Rev Immunol* 2001; **21**: 133-145
- 8 **Brossart P**, Wirths S, Brugger W, Kanz L. Dendritic cells in cancer vaccines. *Exp Hematol* 2001; **29**: 1247-1255
- 9 **Meidenbauer N**, Andreesen R, Mackensen A. Dendritic cells for specific cancer immunotherapy. *Biol Chem* 2001; **382**: 507-520
- 10 **Bhardwaj N**. Processing and presentation of antigens by dendritic cells: implications for vaccines. *Trends Mol Med* 2001; **7**: 388-394
- 11 **Sun JL**, Zhang JK, Chen HB, Chen JD, Qiu YQ. Promoting effects of dendritic cells on LPAK cells killing human hepatoma cells. *Zhongguo Zhongliu Lingchuang yu Kangfu* 1998; **5**: 16-18
- 12 **Zhang JK**, Chen HB, Sun JL, Zhou YQ. Effect of dendritic cells on LPAK cells induced at different times in killing hepatoma cells. *Shijie Huaren Xiaohua Zazhi* 1999; **7**: 673-675
- 13 **Zhang JK**, Sun JL, Chen HB, Zhou YQ. Influence of granulocyte macrophage colony stimulating factor and tumor necrosis factor upon the anti hepatoma activities of human dendritic cells. *World J Gastroenterol* 2000; **6**: 718-720
- 14 **Sun JL**, Zhang JK, Chen JD, Chen HB, Chew YQ, Chen JX. *In vitro* study on the morphology of human blood dendritic cells and LPAK cells inducing apoptosis of the hepatoma cell line. *Chinese Medical Journal* 2001; **114**: 600-605
- 15 **Zhang J**, Zhang JK, Zhuo SH, Chen HB. Effect of a cancer vaccine prepared by fusions of hepatocarcinoma cells with dendritic cells. *World J Gastroenterol* 2001; **7**: 690-694
- 16 **Zhang JK**, Li J, Chen HB, Sun JL, Qu YJ, Lu JJ. Antitumor activities of human dendritic cells derived from peripheral and cord blood. *World J Gastroenterol* 2002; **8**: 87-90
- 17 **Chen HB**, Zhang JK, Huang ZL, Sun JL, Zhou YQ. Effects of cytokines on dendritic cells against human hepatoma cells. *Shijie Huaren Xiaohua Zazhi* 1999; **7**: 191-193
- 18 **Sun JL**, Zhang JK, Chen HB, Zhou YQ. Morphology of cultured human peripheral blood dendritic cells and their antitumor activity. *Zhongguo Zuzhihuaxue Yu Xibaoxue Zazhi* 1999; **8**: 28-31
- 19 **Zhang JK**, Chen HB, Sun JL, Zhou YQ. Effect of dendritic cells on LPAK cells induced at different times in killing hepatoma cells. *Shijie Huaren Xiaohua Zazhi* 1999; **7**: 673-675
- 20 **Zhang JK**, Sun JL, Chen HB, Zhou YQ. Ultrastructural comparison of apoptosis of human hepatoma cells and lak cells. *Huaren Xiaohua Zazhi* 1998; **6**: 877-879
- 21 **Hart I**, Colaco C. Fusion induces tumor or rejection. *Nature* 1997; **388**: 626-627
- 22 **van Schooten WC**, Strang G, Palathumpat V. Biological properties of dendritic cells: implications for their use in the treatment of cancer. *Mol Med Today* 1997; **3**: 254-260
- 23 **Kolb HJ**, Holler E. Adoptive immunotherapy with donor lymphocyte transfusions. *Curr Opin Oncol* 1997; **9**: 139-145
- 24 **Mayordomo JI**, Zorina T, Storkus WJ, Zitvogel L, Garcia Prats

- MD, DeLeo AB, Lotze MT. Bone marrow derived dendritic cells serve as potent adjuvants for peptide based antitumor vaccines. *Stem Cells* 1997; **15**: 94-103
- 25 **Slingluff CL Jr.** Tumor antigens and tumor vaccines: peptides as immunogens. *Semin Surg Oncol* 1996; **12**: 446-453
- 26 **Scott Taylor TH.** Pettengell R, Clarke I, Stuhler G, La Barthe MC, Walden P, Dalglish AG. Human tumour and dendritic cell hybrids generated by electrofusion: potential for cancer vaccines. *Biochim Biophys Acta* 2000; **1500**: 265-279
- 27 **Gong J,** Avigan D, Chen D, Wu Z, Koido S, Kashiwaba M, Kufe D. Activation of antitumor cytotoxic T lymphocytes by fusions of human dendritic cells and breast carcinoma cells. *Proc Natl Acad Sci USA* 2000; **97**: 2715-2718
- 28 **Cao X,** Zhang W, Wang J, Zhang M, Huang X, Hamada H, Chen W. Therapy of established tumour with a hybrid cellular vaccine generated by using granulocyte macrophage colony stimulating factor genetically modified dendritic cells. *Immunology* 1999; **97**: 616-625
- 29 **Wang J,** Saffold S, Cao X, Krauss J, Chen W. Eliciting T cell immunity against poorly immunogenic tumors by immunization with dendritic cell tumor fusion vaccines. *J Immunol* 1998; **161**: 5516-5524
- 30 **Celluzzi CM,** Falo LD Jr. Physical interaction between dendritic cells and tumor cells results in an immunogen that induces protective and therapeutic tumor rejection. *J Immunol* 1998; **160**: 3081-3085
- 31 **Lespagnard L,** Mettens P, Verheyden AM, Tasiaux N, Thielemans K, van Meirvenne S, Geldhof A, De Baetselier P, Urbain J, Leo O, Moser M. Dendritic cells fused with mastocytoma cells elicit therapeutic antitumor immunity. *Int J Cancer* 1998; **76**: 250-258
- 32 **Grosjean I,** Caux C, Bella C, Berger I, Wild F, Banchereau J, Kaiserlian D. Measles virus infects human dendritic cells and blocks their allostimulatory properties for CD4+ T cells. *J Exp Med* 1997; **186**: 801-812
- 33 **Gong J,** Apostolopoulos V, Chen D, Chen H, Koido S, Gendler SJ, McKenzie IF, Kufe D. Selection and characterization of MUC1 specific CD8+ T cells from MUC1 transgenic mice immunized with dendritic carcinoma fusion cells. *Immunology* 2000; **101**: 316-324
- 34 **Gong J,** Nikrui N, Chen D, Koido S, Wu Z, Tanaka Y, Cannistra S, Avigan D, Kufe D. Fusions of human ovarian carcinoma cells with autologous or allogeneic dendritic cells induce antitumor immunity. *J Immunol* 2000; **165**: 1705-1711
- 35 **Holmes LM,** Li J, Sticca RP, Wagner TE, Wei Y. A rapid, novel strategy to induce tumor cell specific cytotoxic T lymphocyte responses using instant dendritomas. *J Immunother* 2001; **24**: 122-129
- 36 **Akasaki Y,** Kikuchi T, Homma S, Abe T, Kofe D, Ohno T. Antitumor effect of immunizations with fusions of dendritic and glioma cells in a mouse brain tumor model. *J Immunother Antitumor* 2001; **24**: 106-113
- 37 **Tuting T,** Storkus WJ, Lotze MT. Gene based strategies for the immunotherapy of cancer. *J Mol Med* 1997; **75**: 478-491
- 38 **Gong J,** Chen D, Kashiwaba M, Kufe D. Induction of antitumor activity by immunization with fusions of dendritic and carcinoma cells. *Nat Med* 1997; **3**: 558-561
- 39 **Gluckman JC,** Canque B, Chapuis F, Rosenzweig M. *In vitro* generation of human dendritic cells and cell therapy. *Cytokines Cell Mol Ther* 1997; **3**: 187-196
- 40 **Asher AL,** Mule JJ, Kasid A, Restifo NP, Salo JC, Reichert CM, Jaffe G, Fendly B, Kriegler M, Rosenberg SA. Murine tumor cells transduced with the gene for tumor necrosis factor alpha. Evidence for paracrine immune effects of tumor necrosis factor against tumors. *J Immunol* 1991; **146**: 3227-3234
- 41 **Porgador A,** Tzehoval E, Vadai E, Feldman M, Eisenbach L. Immunotherapy via gene therapy: comparison of the effects of tumor cells transduced with the interleukin 2, interleukin 6, or interferon gamma genes. *J Immunother* 1993; **14**: 191-201
- 42 **Zhang LH,** Pan JP, Yao HP, Sun WJ, Xia DJ, Wang QQ, He L, Wang J, Cao X. Intrasplenic transplantation of IL 18 gene modified hepatocytes: an effective approach to reverse hepatic fibrosis in schistosomiasis through induction of dominant Th1 response. *Gene Ther* 2001; **8**: 1333-1342
- 43 **Lu Y,** Yamauchi N, Koshita Y, Fujiwara H, Sato Y, Fujii S, Takahashi M, Sato T, Kato J, Yamagishi H, Niitsu Y. Administration of sub tumor regression dosage of TNF alpha to mice with pre existing parental tumors augments the vaccination effect of TNF gene modified tumor through the induction of MHC class I molecule. *Gene Ther* 2001; **8**: 499-507
- 44 **van Slooten ML,** Storm G, Zoephel A, Kupcu Z, Boerman O, Crommelin DJ, Wagner E, Kircheis R. Liposomes containing interferon gamma as adjuvant in tumor cell vaccines. *Pharm Res* 2000; **17**: 42-48
- 45 **Homma S,** Toda G, Gong J, Kufe D, Ohno T. Preventive antitumor activity against hepatocellular carcinoma (HCC) induced by immunization with fusions of dendritic cells and HCC cells in mice. *J Gastroenterol* 2001; **36**: 764-771
- 46 **Treon SP,** Raje N, Anderson KC. Immunotherapeutic strategies for the treatment of plasma cell malignancies. *Semin Oncol* 2000; **27**: 598-613
- 47 **Orentas RJ,** Schauer D, Bin Q, Johnson BD. Electrofusion of a weakly immunogenic neuroblastoma with dendritic cells produces a tumor vaccine. *Cell Immunol* 2001; **213**: 4-13
- 48 **Tanaka Y,** Koido S, Chen D, Gendler SJ, Kufe D, Gong J. Vaccination with allogeneic dendritic cells fused to carcinoma cells induces antitumor immunity in MUC1 transgenic mice. *Clin Immunol* 2001; **101**: 192-200
- 49 **Scanlan MJ,** Jager D. Challenges to the development of antigen specific breast cancer vaccines. *Breast Cancer Res* 2001; **3**: 95-98
- 50 **Brugger W,** Brossart P, Scheding S, Stuhler G, Heinrich K, Reichardt V, Grunebach F, Buhring HJ, Kanz L. Approaches to dendritic cell based immunotherapy after peripheral blood stem cell transplantation. *Ann NY Acad Sci* 1999; **872**: 363-371
- 51 **Jager E,** Jager D, Knuth A. Strategies for the development of vaccines to treat breast cancer. *Recent Results Cancer Res* 1998; **152**: 94-102
- 52 **Steinman RM.** Dendritic cells and immune based therapies. *Exp Hematol* 1996; **24**: 859-862
- 53 **Chen CH,** Wu TC. Experimental vaccine strategies for cancer immunotherapy. *J Biomed Sci* 1998; **5**: 231-252
- 54 **Hermans IF,** Moroni-Rawson P, Ronchese F, Ritchie DS. The emerging role of the dendritic cell in novel cancer therapies. *N Z Med J* 1998; **111**: 111-113
- 55 **Engleman EG.** Dendritic cells: potential role in cancer therapy. *Cytotechnology* 1997; **25**: 1-8

Edited by Xu XQ

Photodynamic inhibitory effects of three perylenequinones on human colorectal carcinoma cell line and primate embryonic stem cell line

Lan Ma, Hong Tai, Cong Li, Yu Zhang, Ze-Hua Wang, Wei-Zhi Ji

Lan Ma, Tai Hong, Graduate School of the Chinese Academy of Sciences, Beijing 100871, China

Lan Ma, Yu Zhang, Ze-Hua Wang, Monoclonal Antibody Biotechnology Center, Yunnan University, Kunming 650091, Yunnan Province, China

Tai Hong, The First People's Hospital of Yunnan Province, Kunming 650032, Yunnan, China

Cong Li, Chemistry, Yunnan University, Kunming 650091, Yunnan Province, China

Lan Ma, Tai Hong, Wei-Zhi Ji, Kunming Institute of Zoology, Chinese Academy of Science, Kunming 650223, Yunnan Province, China

Supported by National Natural Science Foundation of China, No. 980174, Natural Scientific Foundation of Yunnan Province, No. C0106M

Correspondence to: Wei-Zhi Ji, Kunming Institute of Zoology, Chinese Academy of Science, Kunming 650223, Yunnan, China. wji@mail.kiz.ac.cn

Telephone: +86-871-5139413 **Fax:** +86-871-5139413

Received: 2002-07-04 **Accepted:** 2002-07-27

Abstract

AIM: To investigate the photodynamic inhibitory effects of Elsinochrome A (EA), Hypocrellin A (HA) and Hypocrellin B (HB) on human colorectal carcinoma Hce-8693 cells and rhesus monkey embryonic stem R366.4 cells, via inducing apoptosis.

METHODS: EA, HA and HB were extracted from metabolites of *Hypomyces* (Fr) Tul.Sp. R366.4 cells or Hce-8693 cells were cultured with different concentrations of EA, HA or HB respectively, irradiated and incubated with fresh medium for 2 h. Cell cycle analysis was performed by flow cytometry (FCM). Data were expressed as means \pm SD and analysis of variance and Student's *t*-test for individual comparisons.

RESULTS: The photodynamic bioactivity of EA was first reported in this study. After irradiation for 5 min, 6 min, 10 min or 20 min, photoactivated EA at lower concentrations, which were 10^{-7} Mol/L, 10^{-6} Mol/L, 10^{-5} Mol/L respectively, had no cytotoxic effects on R366.4 ES cells. Whereas, all of the three perylenequinones could induce apoptosis with a dose-dependent manner when Hce-8693 cells were incubated with photoactivated EA, HA and HB respectively. When Hce-8693 cells were incubated with EA at 10^{-6} Mol/L and irradiated 5 min, 6 min, 10 min and 20 min respectively, the rates of EA-induced apoptosis were 0, 0, 13.4 % and 40.5 %. While the rates of HA-induced apoptosis were 29.5 %, 32.0 %, 40.2 % and 22.6 %. And the rates of HB-induced apoptosis were 0, 0, 0 and 13.7 % respectively. Meanwhile, after 10^{-5} Mol/L treatment, the rates of EA-induced apoptosis were 32.7 %, 19.3 %, 26.4 % and 52.7 %, the rates of HA-induced apoptosis were 47.2 %, 39.1 %, 45.2 % and 56.6 %, and the rates of HB-induced apoptosis were 0, 0, 20.0 % and 13.9 % respectively.

CONCLUSION: EA, HA and HB have significant anti-cancer activity. The order of photodynamic inhibitory effects on tumor cells would be approximately HA>EA>HB. The molecular mechanisms of apoptosis may not be induced by reactive oxygen species and are worth further investigation.

Ma L, Tai H, Li C, Zhang Y, Wang ZH, Ji WZ. Photodynamic inhibitory effects of three perylenequinones on human colorectal carcinoma cell line and primate embryonic stem cell line. *World J Gastroenterol* 2003; 9(3): 485-490

<http://www.wjgnet.com/1007-9327/9/485.htm>

INTRODUCTION

Perylenequinones are a type of photosensitive pigments widespread in nature, which have been isolated from fungi, as well as other organisms^[1-5]. These lipid-soluble 4,9-dihydroxy-3, 10-perylenequinone derivatives are efficient producers of singlet oxygen (1O_2) in visible light^[6-11]. Due to their excellent photosensitive properties, they are expected to be developed as new phototherapeutic medicines^[8,12-17]. Among them, Elsinochrome A (EA) was first reported in 1966 by Chen CT *et al.*, who isolated EA from *Elsinoe* spp. I^[1-2]. And Meille SV *et al.* reported the structure of EA^[18]. Since then, there are no more related reports about EA. Hypocrellins are well-known photosensitizers, including hypocrellin A (HA) and hypocrellin B (HB), isolated from natural fungus sacs of *Hypocrella bambusae* growing in north western region of Yunnan Province in China^[19]. Hypocrellins were potent inhibitors of protein kinase C (PKC)^[20], and could inactivate some types of viruses in the presence of visible light and oxygen. These processes appeared to be mediated predominately by 1O_2 . This was further supported by the extremely high quantum yield of 1O_2 generation by hypocrellin^[21-23]s. Many investigations demonstrated that hypocrellins had a strong photodynamic effect on tumours^[24] and impressive antiviral activity against human immunodeficiency virus type 1 (HIV-1)^[25]. Recently, it has been reported that hypocrellin can photosensitize apoptotic cell death^[26]. The above investigations collectively provide a compelling rationale for the development of hypocrellin and its derivatives as PDT photosensitizers.

Our group has recently isolated a filamentous fungal strain from western region of Yunnan Province in China and identified it as *Ascomycetes Hypocreales Hypocreaceae Hypomyces* (Fr) Tul.sp based on the taxonomic study. *Hypomyces* (Fr) Tul.Sp. was found for the first time to produce Elsinochrome A (EA), Hypocrellin A (HA) and Hypocrellin B (HB), under solid-phase fermentation conditions. Colorectal cancer is common in China. Since EA and Hypocrellins could be a potential tumor photopreventive and phototherapeutic agents, it is worthwhile to investigate the photodynamic effects of these photosensitizers. In this study, we examined the relative potency of EA, HA and HB against two cell lines, human colorectal carcinoma Hce-8693 cells and rhesus monkey embryonic stem (ES) R366.4 cells, and attempted to correlate anticancer activity with chemical structure and quantum yield of 1O_2 .

MATERIALS AND METHODS

Synthesis

The fungal metabolites were isolated from solid-substrate fermentation cultures of *Hypomyces* (Fr) Tul.Sp. and evaporated to dryness. The powder of *Hypomyces* (Fr) Tul.Sp. was extracted with acetone at room temperature and then evaporated to dryness in vacuo. The recrystallized crude product was purified by silica gel column chromatography with a mixed solvent of petroleum ether:EtOAc:EtOH (4:2:1). The purified crystallized products were characterized with element analysis measurement (PE 2 400), UV-visible spectrophotometry (PE UV/V is Lambda Bio), fluorescence spectra instruments (Hitachi-850), FT-IR (PE 1 000), ^1H , ^{13}C -nuclear magnetic resonance (Bruker AM-400). The results were consistent with literature data.

Each of the above products was dissolved respectively in dimethylsulfoxide (DMSO) at 1 M and stored at 4 °C in dark conditions. Under these conditions the solutions were stable for 2 months. The stock solutions were diluted 10^3 to 10^7 fold and in the final experimental conditions, the final DMSO concentration (0.1 %) did not affect the viability of the culture cells, as demonstrated in control experiments.

Cell lines

Rhesus monkey embryonic stem cell line R366.4 was kindly provided by Dr James A Thomson (The Wisconsin Regional Primate Research Center, University of Wisconsin, US). Cells were plated in mouse embryonic fibroblasts (previously exposed to 3 000 rads γ -radiation) in medium consisting of 85 % Dulbecco's Modified Eagle medium (4 500 mg of glucose per liter, with L-glutamine, without sodium pyruvate; GIBCO) with 15 % fetal bovine serum (HyClone), 1×10^{-7} Mol/L 2-mercaptoethanol (Sigma) and 1 % nonessential amino acid stock (GIBCO). Human colorectal carcinoma Hce-8693 cells were obtained from ATCC. The cell lines Hce-8693 were maintained in Dulbecco's Modified Eagle medium (GIBCO) supplemented with 10 % new born calf serum (HyClone). All cell lines were grown at 37 °C under a water-saturated sterile atmosphere containing 5 % CO_2 (Forma Scientific Incubator). All cell manipulations in the presence of EA, HA and HB were performed under subdued light conditions.

Light irradiation

Cells incubated with EA, HA and HB were irradiated with a water-cooled 1 300 W tungsten-bromine lamp. All cells proliferated as monolayers attached to the plastic bottom of the plate which was completely transparent for the excitation light. Temperature recorded in tissue culture plate did not exceed room temperature during the irradiation period. Immediately after irradiation, cells were rinsed three times with PBS and grown in a fresh medium for 2 hours.

Flow cytometry

Cells were incubated with various doses of EA, HA or HB, irradiated, incubated for additional 2 h and then harvested, washed with phosphate-buffered saline (PBS) three times and fixed with 700 mL \cdot L $^{-1}$ ethanol at 4 °C overnight. Fixed cells were washed three times with PBS and stained with 800 μL propidium iodide and 200 μL deoxyribonuclease-free ribonuclease A in PBS. The fluorescence intensity of propidium iodide-stained nuclei was detected with flow cytometer (EPICS-XL, Coulter, USA) and 10 000 cells were analyzed with Multicycle software.

Photocytotoxicity studies in R366.4 cell lines

R366.4 cells growing in sub-confluent culture were used to assess photocytotoxic effects of EA via flow cytometric assays. Graded doses of EA (1×10^{-7} Mol/L, 1×10^{-6} Mol/L, 1×10^{-5} Mol/L, 1×10^{-4} Mol/L, 1×10^{-3} Mol/L) dissolved in DMSO were mixed

into the medium overlying 5.0×10^4 cells in 6-well plates. Following 2 h incubation, the cells were irradiated for 5 min, 6 min, 10 min and 20 min respectively (or not in case of darkness). After the drug-containing medium was removed, the cells were washed with phosphate-buffered saline (PBS) three times and the fresh ES culture medium was put on the cells prior to incubation for 2 h at 37 °C in saturated humidified air with 5 % CO_2 . Finally, the cell proliferation was determined by flow cytometric assay.

Inhibitory effect of EA, HA and HB on the proliferation of Hce-8693 cells by inducing apoptosis

Hce-8693 cells growing in confluent culture were used to assess inhibitory effects of EA, HA and HB via flow cytometric assays. For each compound, graded doses (1×10^{-6} Mol/L, 1×10^{-5} Mol/L, 1×10^{-4} Mol/L, 1×10^{-3} Mol/L) dissolved in DMSO were mixed into the medium overlying 5.0×10^4 cells in 6-well plates. Following 2 h incubation, the cells were irradiated for 5 min, 6 min, 10 min and 20 min respectively (or not in case of darkness). After the drug-containing medium was removed, the cells were washed with phosphate-buffered saline (PBS) three times and the fresh culture medium was put on the cells prior to an incubation for 2 h at 37 °C in saturated humidified air with 5 % CO_2 . Finally, the cell proliferation was determined by flow cytometric assay.

Statistical analysis

Student's *t* test was used to assess statistical significance of differences. If $P < 0.01$, the difference was considered very significant.

RESULTS

Synthesis

The structures of the compounds are shown in Figure 1, and their relevant photochemical properties are summarized in Table 1.

Table 1 The photochemical properties of the perylenequinones

Structure	UV λ_{max} (log ϵ)*	λ_{max} (log ϵ)*	$\phi \cdot ^1\text{O}_2$
EA	459(1.60), 528(0.84), 568(1.04)	460(3.78), 531(3.13), 571(3.60)	0.94
HA	468(1.88), 542(0.83), 582(0.90)	417(5.51), 542(1.02), 582(7.70)	0.83
HB	470(0.27), 540(0.12), 583(0.13)	471(4.39), 543(3.01), 583(3.36)	0.76

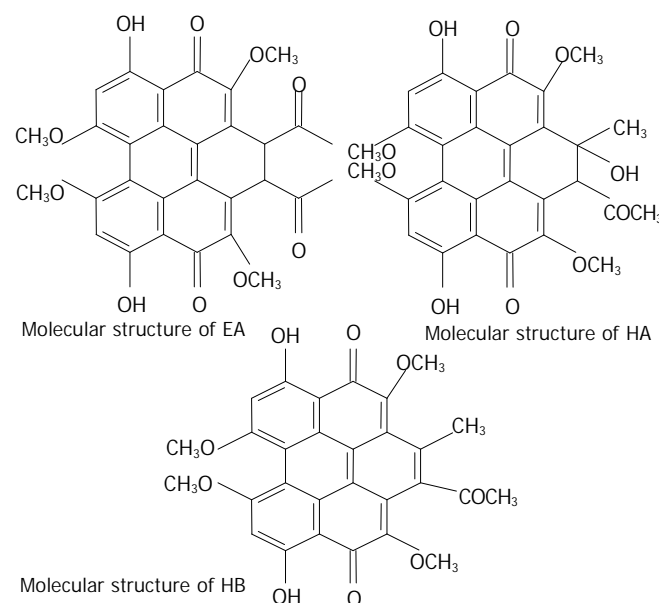


Figure 1 Structures of the three perylenequinones for photo-dynamic activity.

Photodependent cytotoxicity studies in R366.4 cell lines

Embryonic stem (ES) cells are derived from preimplantation embryos, have a normal karyotype, and are capable of indefinite, undifferentiated proliferation^[27]. Recently, *in vitro* mouse ES cell culture method has been used to test mutagenic, cytotoxic and embryotoxic effects of chemical substances^[28-30]. In this study, rhesus monkey ES R366.4 cells were first used to measure the photocytotoxicity of EA by judging the apoptosis of ES cells. After treated the R366.4 ES cells with EA at various concentrations, with or without light irradiation, the rate of apoptosis obtained by FCM were shown in Table 2 and Figure 2. The data illustrated that photoactivated EA had no cytotoxic effects on the R366.4 ES cells at low concentrations, which were 10^{-7} Mol/L, 10^{-6} Mol/L, 10^{-5} Mol/L respectively. Whereas, all of photoactivated EA at higher concentrations (10^{-4} Mol/L and 10^{-3} Mol/L respectively) exhibited a potent cytotoxic effects on R366.4 cells. In general, no large differences in the photodependent cytotoxic effects of EA were found between the different irradiation time. In the case of the photocytotoxic EA no cytotoxic effect was observed in dark conditions.

Table 2 EA-induced apoptosis in R366.4 ES cells with FCM assay (means \pm SD, $n=3$)

Group	Rate of apoptosis/%			
	5 min	6 min	10 min	20 min
Control	0	0	0	0
10^{-7} Mol/L	0	0	0	0
10^{-6} Mol/L	0	0	0	0
10^{-5} Mol/L	0	0	0	0
10^{-4} Mol/L	48.8 \pm 4.50 ^b	50.3 \pm 4.14 ^b	52.1 \pm 2.35 ^b	50.5 \pm 3.68 ^b
10^{-3} Mol/L	54.9 \pm 2.99 ^b	53.4 \pm 4.01 ^b	52.4 \pm 3.50 ^b	50.2 \pm 4.93 ^b

^b $P<0.01$, vs EA control.

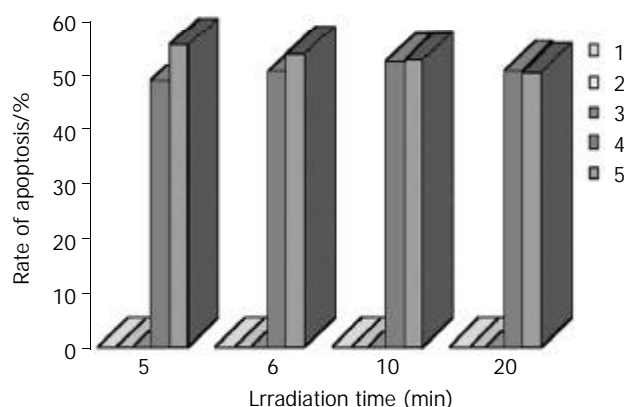


Figure 2 Photodependent cytotoxic effects of EA on R366.4 ES cells at various concentrations: (1) 10^{-7} Mol/L, (2) 10^{-6} Mol/L, (3) 10^{-5} Mol/L, (4) 10^{-4} Mol/L, (5) 10^{-3} Mol/L respectively. Results are means \pm SD of three independent experiments.

Inhibitory effect of EA on the proliferation of Hce-8693 cells by inducing apoptosis

In order to investigate the antiproliferative effect of EA, Hce-8693 cells were incubated with different concentrations of EA under dark conditions and subjected 2 hours to different irradiation time (5, 6, 10 and 20 min respectively). The cells were then further incubated for an additional 2 hours in the dark without photosensitizer and measured via FCM assay. The rates of apoptosis induced by EA are shown in Table 3 and Figure 3. For each irradiation time, the data showed that there was dose-dependent relationship between EA doses and

rate of Hce-8693 cell apoptosis. On the contrary, no large differences in the antiproliferative effect of the photoactivated EA was found between the different irradiation time.

Table 3 Hce-8693 cell apoptosis induced by photoactivated EA (means \pm SD, $n=3$)

Group	Rate of apoptosis/%			
	10^{-6} Mol/L	10^{-5} Mol/L	10^{-4} Mol/L	10^{-3} Mol/L
Control	0	0	0	0
5 min	0	32.7 \pm 7.56 ^b	53.6 \pm 6.62 ^b	63.4 \pm 10.24 ^b
6 min	0	19.3 \pm 4.16 ^b	32.8 \pm 7.38 ^b	55.5 \pm 7.00 ^b
10 min	13.4 \pm 3.25 ^b	26.4 \pm 4.89 ^b	31.3 \pm 5.39 ^b	44.9 \pm 5.46 ^b
20 min	40.5 \pm 8.58 ^b	52.7 \pm 11.82 ^b	65.2 \pm 11.22 ^b	68.0 \pm 5.93 ^b

^b $P<0.01$, vs EA control.

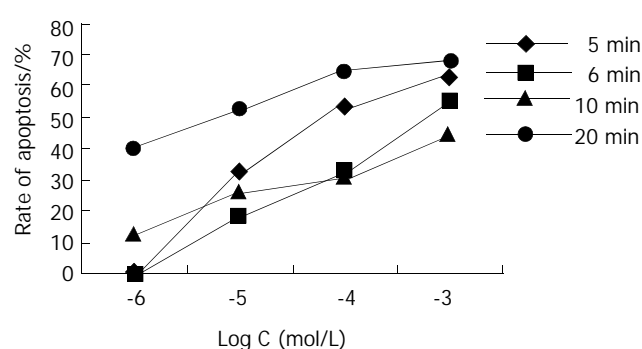


Figure 3 Dose-dependent relationship between EA doses and rate of Hce-8693 cell apoptosis. Cells were incubated for 2 h with 1×10^{-6} Mol/L, 1×10^{-5} Mol/L, 1×10^{-4} Mol/L, 1×10^{-3} Mol/L EA photosensitizer respectively and then irradiated. Results are means \pm SD of three independent experiments.

Inhibitory effect of HA on the proliferation of Hce-8693 cells by inducing apoptosis

In order to investigate the antiproliferative effect of HA, Hce-8693 cells were incubated with different concentrations of HA under dark conditions and subjected 2 hours to different irradiation time (5, 6, 10 and 20 min respectively). The cells were then further incubated for additional 2 hours in the dark without photosensitizer and measured via FCM assay. The rates of apoptosis induced by HA were shown in Table 4 and Figure 4. For each irradiation time, the data showed that there was dose-dependent relationship between HA doses and rates of Hce-8693 cell apoptosis. On the contrary, no large differences in the antiproliferative effect of the photoactivated HA was found between the different irradiation time.

Table 4 Hce-8693 cell apoptosis induced by photoactivated HA (means \pm SD, $n=3$)

Ggroup	Rate of apoptosis/%			
	10^{-6} Mol/L	10^{-5} Mol/L	10^{-4} Mol/L	10^{-3} Mol/L
Control	0	0	0	0
5 min	29.5 \pm 2.29 ^b	47.2 \pm 8.79 ^b	48.4 \pm 4.66 ^b	58.8 \pm 8.40 ^b
6 min	32.0 \pm 5.64 ^b	39.1 \pm 6.41 ^b	43.2 \pm 8.84 ^b	66.4 \pm 8.02 ^b
10 min	40.2 \pm 6.23 ^b	45.2 \pm 8.40 ^b	45.5 \pm 8.38 ^b	53.4 \pm 8.77 ^b
20 min	22.6 \pm 3.39 ^b	56.6 \pm 3.86 ^b	62.8 \pm 4.23 ^b	68.4 \pm 8.85 ^b

^b $P<0.01$, vs HA control.

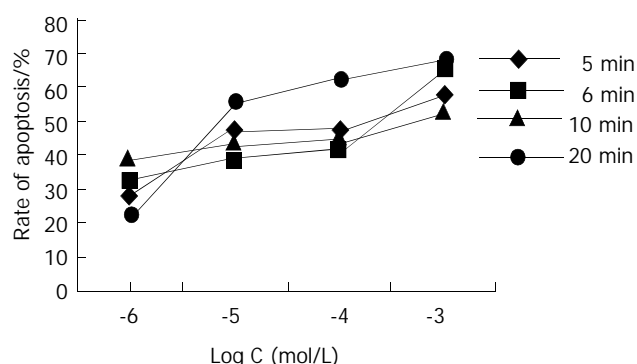


Figure 4 Dose-dependent relationship between HA doses and rate of Hce-8693 cell apoptosis. Cells were incubated for 2 h with 1×10^{-6} Mol/L, 1×10^{-5} Mol/L, 1×10^{-4} Mol/L, 1×10^{-3} Mol/L HA photosensitizer respectively and then irradiated. Results are means \pm SD of three independent experiments.

Inhibitory effect of HB on the proliferation of Hce-8693 cells by inducing apoptosis

In order to investigate the antiproliferative effect of HB, Hce-8693 cells were incubated with different concentrations of HB under dark conditions and subjected 2 hours to different irradiation time (5, 6, 10 and 20 min respectively). The cells were then further incubated for additional 2 hours in the dark without photosensitizer and measured via FCM assay. The rates of apoptosis induced by HB were shown in Table 5 and Figure 5. For each irradiation time, the data showed that there was dose-dependent relationship between HB doses and rate of Hce-8693 cell apoptosis. On the contrary, no large differences in the antiproliferative effect of the photoactivated HB was found between the different irradiation time.

Table 5 Hce-8693 cell apoptosis induced by photoactivated HB (means \pm SD, $n=3$)

Group	Rate of apoptosis/%			
	10^{-6} Mol/L	10^{-5} Mol/L	10^{-4} Mol/L	10^{-3} Mol/L
Control	0	0	0	0
5 min	0	0	28.1 ± 6.21^b	64.8 ± 11.78^b
6 min	0	0	17.3 ± 3.68^b	32.0 ± 7.57^b
10 min	0	20.0 ± 4.21^b	20.5 ± 4.57^b	71.0 ± 10.57^b
20 min	13.7 ± 3.02^b	13.9 ± 2.87^b	19.1 ± 4.06^b	29.4 ± 6.56^b

^b $P < 0.01$, vs HB control.

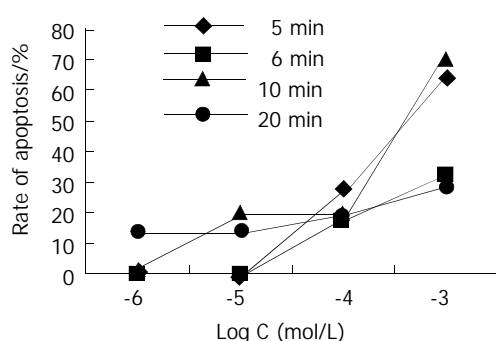


Figure 5 Dose-dependent relationship between HB doses and rate of Hce-8693 cell apoptosis. Cells were incubated for 2 h with 1×10^{-6} Mol/L, 1×10^{-5} Mol/L, 1×10^{-4} Mol/L, 1×10^{-3} Mol/L HB photosensitizer respectively and then irradiated. Results were means \pm SD of three independent experiments.

Inhibitory effect of EA, HA and HB on the proliferation of Hce-8693 cells by inducing apoptosis

From the results of photodependent cytotoxicity studies in R366.4 cell lines, it seemed that photoactivated EA had no cytotoxic effects at 10^{-6} Mol/L and 10^{-5} Mol/L concentrations. On the contrary, EA, HA and HB exhibited more or less antiproliferative effects on human Hce-8693 cells at this range of concentrations. Thus, the photodynamic effects of the photosensitizers could be compared from the rate of apoptosis (Table 6). The order of efficiency would be approximately $HA > EA > HB$ (Figure 6).

Table 6 Comparison of antiproliferative effects of EA, HA and HB

Group	Rate of apoptosis/%					
	10^{-6} Mol/L			10^{-5} Mol/L		
	HA	EA	HB	HA	EA	HB
5 min	0	0	0	47.2 ± 8.79	32.7 ± 7.56	0
6 min	32.0 ± 5.64	0	0	39.1 ± 6.41	19.3 ± 4.16	0
10 min	40.2 ± 6.23	13.4 ± 3.25	0	45.2 ± 8.40	26.4 ± 4.89	20.0 ± 4.21
20 min	22.6 ± 3.39	40.5 ± 8.58	13.7 ± 3.02	56.6 ± 3.86	52.7 ± 11.82	13.9 ± 2.87

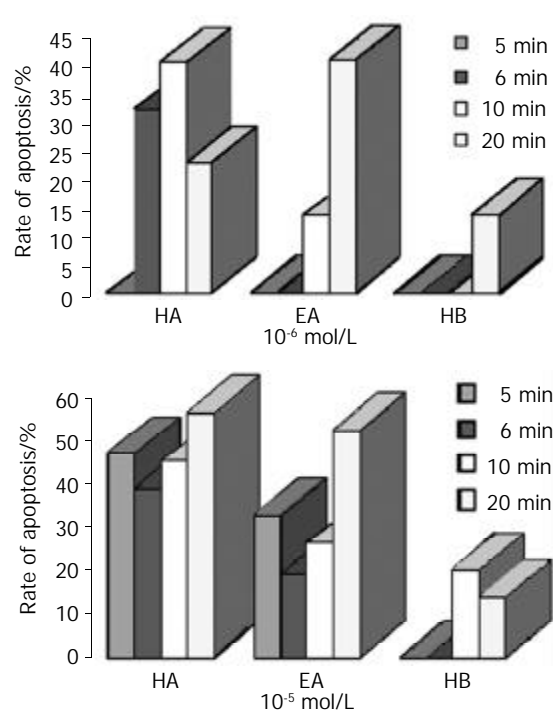


Figure 6 (a)-(b) illustrated the different antiproliferative effects of photoactivated HA, EA and HB on human Hce-8693 cells.

DISCUSSION

Photodynamic therapy (PDT) is a medical treatment based on the use of a sensitizer to promote photoinduced damage to biological molecules including lipids, proteins and DNA^[31,32]. It can be used to eradicate early localized tumours and for palliation of more advanced disease when metastasis has occurred. This treatment modality involves the use of light in combination with a photosensitizing compound. Following excitation of photosensitizers to long-lived excited singlet and/or triplet states, the tumour is destroyed either by reactive oxygen species (Type II mechanism) and/or by radical products (Type I mechanism)^[33-37].

Hypocrellins are efficient singlet oxygen generators during

photochemical reactions and may also exert photosensitization via radical mechanisms, which may confer a degree of independence from classical oxygen-dependent photochemical mechanisms. This feature is important in the context of impaired radiosensitivity and chemosensitivity of hypoxic human tumour cells. However, the precise mode of action of these molecules at the cellular level is not clear and seems to go far beyond Type I and Type II photoprocesses^[38-42]. An additional mechanism involving protons released in the excited state and leading to cellular pH drop has also been proposed for the related pigments hypocrellin and hypericin^[43].

Apoptosis is a complex and programmed process which is regulated by a variety of factors. Recently, it has been reported that hypocrellins and their derivatives can photosensitize apoptotic cell death^[44,45]. However, the molecular mechanisms of tumor cell apoptosis induction by Hypocrellin A and B are poorly understood. The antiproliferative actions of hypocrellin may be due, in part, to the ability of hypocrellin A to induce reactive oxygen species (Type II mechanism)^[46,47]. In addition, hypocrellin A-mediated apoptosis is increased when antisense bcl-2 retrovirus vector is transfected into human gastric adenocarcinoma MGC803 cells^[48]. And also, Ali *et al.* reported that caspase-3 and hydrogen peroxide may play an important role in HA and HB-induced apoptosis^[49, 50].

According to the photochemical properties, the quantum yields of EA, HA and HB are 0.94, 0.83, 0.76 respectively. From the results of inhibitory effect of EA, HA and HB on the proliferation of Hce-8693 cells, it seems that the order of efficiency would be approximately HA>EA>HB. In this way, the molecular mechanisms of Hce-8693 cell apoptosis induction by EA, HA and HB may not be induced by reactive oxygen species (Type II mechanism). It is also noteworthy that photoactivated EA, HA and HB can selectively inhibit the growth of human colorectal carcinoma cells but not rhesus monkey embryonic stem R366.4 cells at lower concentrations. Thus, the molecular mechanisms of apoptosis induced by photoactivated EA, HA and HB are worth further investigation.

REFERENCES

- 1 **Chen CT**, Nakanishi K, Natori S. Biosynthesis of elsinochrome A, the perylenequinone from *Elsinoe* spp. I. *Chem Pharm Bull (Tokyo)* 1966; **14**: 1434-1437
- 2 **Weisgraber KH**, Weiss U. Pigments of *Elsinoe* species. VI. A simple synthesis of a related perylenequinone. *J Chem Soc [Perkin 1]* 1972; **1**: 83-88
- 3 **Stack ME**, Mazzola EP, Page SW, Pohland AE, Highet RJ, Tempesta MS, Corley DG. Mutagenic perylenequinone metabolites of *Alternaria alternata*: altertoxins I, II, and III. *J Nat Prod* 1986; **49**: 866-871
- 4 **Davis VM**, Stack ME. Mutagenicity of stemphytoxin III, a metabolite of *Alternaria alternata*. *Appl Environ Microbiol* 1991; **57**: 180-182
- 5 **Xu S**, Chen S, Zhang M, Shen T. A novel method for the preparation of amino-substituted hypocrellin B. *Bioorg Med Chem Lett* 2001; **11**: 2045-2047
- 6 **Ma JS**, Yan F, Wang CQ, An JY. Hypocrellin-A sensitized photo-oxidation of bilirubin. *Photochem Photobiol* 1989; **50**: 827-830
- 7 **Miller GG**, Brown K, Ballangrud AM, Barajas O, Xiao Z, Tulip J, Lown JW, Leithoff JM, Allalunis-Turner MJ, Mehta RD, Moore RB. Preclinical assessment of hypocrellin B and hypocrellin B derivatives as sensitizers for photodynamic therapy of cancer: progress update. *Photochem Photobiol* 1997; **65**: 714-722
- 8 **He YY**, An JY, Jiang LJ. Glycoconjugated hypocrellin: synthesis of [(beta-D-glucosyl)ethylthyl]hypocrellins and photosensitized generation of singlet oxygen. *Biochim Biophys Acta* 1999; **1472**: 232-239
- 9 **Daub ME**, Ehrenshaft M. The photoactivated cercospora toxin: contributions to plant disease and fundamental biology. *Annu Rev Phytopathol* 2000; **38**: 461-490
- 10 **Yu C**, Chen S, Zhang M, Shen T. Spectroscopic studies and photodynamic actions of hypocrellin B in liposomes. *Photochem Photobiol* 2001; **73**: 482-488
- 11 **Ververidis P**, Davrazou F, Dailianas G, Georgakopoulos D, Kanellis AK, Panopoulos N. A novel putative reductase (Cpd1p) and the multidrug exporter Snq2p are involved in resistance to cercosporin and other singlet oxygen-generating photosensitizers in *Saccharomyces cerevisiae*. *Curr Genet* 2001; **39**: 127-136
- 12 **Wang SS**, Mathes C, Thompson SH. Membrane toxicity of the protein kinase C inhibitor calphostin A by a free-radical mechanism. *Neurosci Lett* 1993; **157**: 25-28
- 13 **Gamou S**, Shimizu N. Calphostin-C stimulates epidermal growth factor receptor phosphorylation and internalization via light-dependent mechanism. *J Cell Physiol* 1994; **158**: 151-159
- 14 **Pedron T**, Girard R, Inoue K, Charon D, Chaby R. Lipopolysaccharide and the glycoside ring of staurosporine induce CD14 expression on bone marrow granulocytes by different mechanisms. *Mol Pharmacol* 1997; **52**: 692-700
- 15 **Dubauskas Z**, Beck TP, Chmura SJ, Kovar DA, Kadkhodai MM, Shrivastav M, Chung T, Stadler WM, Rinker-Schaeffer CW. Activated calphostin C cytotoxicity is independent of p53 status and *in vivo* metastatic potential. *Clin Cancer Res* 1998; **4**: 2391-2398
- 16 **Chen CL**, Chen H, Zhu DM, Uckun FM. Quantitative high-performance liquid chromatography-based detection method for calphostin C, a naturally occurring perylenequinone with potent antileukemic activity. *J Chromatogr B Biomed Sci Appl* 1999; **724**: 157-162
- 17 **Chen CL**, Tai HL, Zhu DM, Uckun FM. Pharmacokinetic features and metabolism of calphostin C, a naturally occurring perylenequinone with antileukemic activity. *Pharm Res* 1999; **16**: 1003-1009
- 18 **Meille SV**, Malpezzi L, Allegra G, Nasini G, Weiss U. Structure of elsinochrome A: a perylenequinone metabolite. *Acta Crystallogr C* 1989; **45**: 628-632
- 19 **Ma JS**, Yan F, Wang CQ, An JY. Hypocrellin-A sensitized photo-oxidation of bilirubin. *Photochem Photobiol* 1989; **50**: 827-830
- 20 **Diwu Z**, Zimmermann J, Meyer T, Lown JW. Design, synthesis and investigation of mechanisms of action of novel protein kinase C inhibitors: perylenequinonoid pigments. *Biochem Pharmacol* 1994; **47**: 373-385
- 21 **Fehr MJ**, Carpenter SL, Wannemuehler Y, Petrich JW. Roles of oxygen and photoinduced acidification in the light-dependent antiviral activity of hypocrellin A. *Biochemistry* 1995; **34**: 15845-15848
- 22 **Hirayama J**, Ikebuchi K, Abe H, Kwon KW, Ohnishi Y, Horiuchi M, Shinagawa M, Ikuta K, Kamo N, Sekiguchi S. Photoinactivation of virus infectivity by hypocrellin A. *Photochem Photobiol* 1997; **66**: 697-700
- 23 **Park J**, English DS, Wannemuehler Y, Carpenter S, Petrich JW. The role of oxygen in the antiviral activity of hypericin and hypocrellin. *Photochem Photobiol* 1998; **68**: 593-597
- 24 **Diwu Z**. Novel therapeutic and diagnostic applications of hypocrellins and hypericins. *Photochem Photobiol* 1995; **61**: 529-539
- 25 **Hudson JB**, Zhou J, Chen J, Harris L, Yip L, Towers GH. Hypocrellin, from *Hypocrella bambusa*, is phototoxic to human immunodeficiency virus. *Photochem Photobiol* 1994; **60**: 253-255
- 26 **Zhang J**, Cao EH, Li JF, Zhang TC, Ma WJ. Photodynamic effects of hypocrellin A on three human malignant cell lines by inducing apoptotic cell death. *J Photochem Photobiol B* 1998; **43**: 106-111
- 27 **Thomson JA**, Kalishman J, Golos TG, Durning M, Harris CP, Becker RA, Hearn JP. Isolation of a primate embryonic stem cell line. *PNAS* 1995; **92**: 7844-7848
- 28 **Schleger C**, Krebsfaenger N, Kalkuhl A, Bader R, Singer T. Innovative cell culture methods in drug development. *ALTEX* 2001; **18**: 5-8
- 29 **Rohwedel J**, Guan K, Hegert C, Wobus AM. Embryonic stem cells as an *in vitro* model for mutagenicity, cytotoxicity and embryotoxicity studies: present state and future prospects. *Toxicol in vitro* 2001; **15**: 741-753
- 30 **Genschow E**, Spielmann H, Scholz G, Seiler A, Brown N, Piersma A, Brady M, Clemann N, Huuskonen H, Paillard F, Bremer S, Becker K. The ECVAM international validation study on *in vitro* embryotoxicity tests: results of the definitive phase and evaluation of prediction models. *Altern Lab Anim* 2002; **30**: 151-176

- 31 **Xu Y**, Zhao H, Zhang Z. Raman spectroscopic study of microcosmic and photosensitive damage on the liposomes of the mixed phospholipids sensitized by hypocrellin and its derivatives. *J Photochem Photobiol B* 1998; **43**: 41-46
- 32 **He YY**, Jiang LJ. Photosensitized damage to calf thymus DNA by a hypocrellin derivative: mechanisms under aerobic and anaerobic conditions. *Biochim Biophys Acta* 2000; **1523**: 29-36
- 33 **Fu NW**. Advances in research on photosensitizers. *Shengli Kexue Jinzhan* 1992; **23**: 36-40
- 34 **Estey EP**, Brown K, Diwu Z, Liu J, Lown JW, Miller GG, Moore RB, Tulip J, McPhee MS. Hypocrellins as photosensitizers for photodynamic therapy: a screening evaluation and pharmacokinetic study. *Cancer Chemother Pharmacol* 1996; **37**: 343-350
- 35 **Diwu ZJ**, Haugland RP, Liu J, Lown JW, Miller GG, Moore RB, Brown K, Tulip J, McPhee MS. Photosensitization by anticancer agents 21: new perylene- and aminonaphthoquinones. *Free Radic Biol Med* 1996; **20**: 589-593
- 36 **Wang ZJ**, He YY, Huang CG, Huang JS, Huang YC, An JY, Gu Y, Jiang LJ. Pharmacokinetics, tissue distribution and photodynamic therapy efficacy of liposomal-delivered hypocrellin A, a potential photosensitizer for tumor therapy. *Photochem Photobiol* 1999; **70**: 773-780
- 37 **Wu T**, Xu S, Shen J, Song A, Chen S, Zhang M, Shen T. New potential photodynamic therapeutic anti-cancer agents: synthesis and characterization of demethoxy amino-substituted hypocrellins. *Anticancer Drug Des* 2000; **15**: 287-293
- 38 **Nenghui W**, Zhiyi Z. Relationship between photosensitizing activities and chemical structure of hypocrellin A and B. *J Photochem Photobiol B* 1992; **14**: 207-217
- 39 Yuying H, Jingyi A, Lijin J. Effect of structural modifications on photosensitizing activities of hypocrellin dyes: EPR and spectrophotometric studies. *Free Radic Biol Med* 1999; **26**: 1146-1157
- 40 **Datta A**, Smirnov AV, Wen J, Chumanov G, Petrich JW. Multidimensional reaction coordinate for the excited-state H-atom transfer in perylene quinones: importance of the 7-membered ring in hypocrellins A and B. *Photochem Photobiol* 2000; **71**: 166-172
- 41 **Wu T**, Shen J, Song A, Chen S, Zhang M, Shen T. Photodynamic action of amino substituted hypocrellins: EPR studies on the photogenerations of active oxygen and free radical species. *J Photochem Photobiol B* 2000; **57**: 14-21
- 42 **Xu S**, Shen J, Chen S, Zhang M, Shen T. Active oxygen species ($^1\text{O}_2$, $\text{O}_2^{\cdot-}$) generation in the system of TiO_2 colloid sensitized by hypocrellin B. *J Photochem Photobiol B* 2002; **67**: 64-70
- 43 **Chaloupka R**, Sureau F, Kocisova E, Petrich JW. Hypocrellin A photosensitization involves an intracellular pH decrease in 3T3 cells. *Photochem Photobiol* 1998; **68**: 44-50
- 44 **Ali SM**, Chee SK, Yuen GY, Olivo M. Hypericin and hypocrellin induced apoptosis in human mucosal carcinoma cells. *J Photochem Photobiol B* 2001; **65**: 59-73
- 45 **Ali SM**, Olivo M, Yuen GY, Chee SK. Photodynamic-induced apoptosis of human nasopharyngeal carcinoma cells using Hypocrellins. *Int J Oncol* 2001; **19**: 633-643
- 46 **Ma J**, Jiang L. Photogeneration of singlet oxygen ($^1\text{O}_2$) and free radicals ($\text{Sens}^{\cdot-}$, $\text{O}_2^{\cdot-}$) by tetra-brominated hypocrellin B derivative. *Free Radic Res* 2001; **35**: 767-777
- 47 **Wu T**, Xu S, Shen J, Chen S, Zhang M, Shen T. EPR investigation of the free radicals generated during the photosensitization of TiO_2 colloid by hypocrellin B. *Free Radic Res* 2001; **35**: 137-143
- 48 **Zhang WG**, Ma LP, Wang SW, Zhang ZY, Cao GD. Antisense bcl-2 retrovirus vector increases the sensitivity of a human gastric adenocarcinoma cell line to photodynamic therapy. *Photochem Photobiol* 1999; **69**: 582-586
- 49 **Ali SM**, Chee SK, Yuen GY, Olivo M. Hypocrellins and Hypericin induced apoptosis in human tumor cells: A possible role of hydrogen peroxide. *Int J Mol Med* 2002; **9**: 461-472
- 50 **Ali SM**, Chee SK, Yuen GY, Olivo M. Photodynamic therapy induced Fas-mediated apoptosis in human carcinoma cells. *Int J Mol Med* 2002; **9**: 257-270

Edited by Xu JY

• COLORECTAL CANCER •

Expression and significance of PTEN, hypoxia-inducible factor-1 alpha in colorectal adenoma and adenocarcinoma

Ying-An Jiang, Li-Fang Fan, Chong-Qing Jiang, You-Yuan Zhang, He-Sheng Luo, Zhi-Jiao Tang, Dong Xia, Ming Wang

Ying-An Jiang, He-Sheng Luo, Department of Gastroenterology, Renming Hospital of Wuhan University, Wuhan 430060, Hubei Province, China

Li-Fang Fan, Zhi-Jiao Tang, Dong Xia, Ming Wang, Department of Pathology, Medical College of Wuhan University, Wuhan 430071, Hubei Province, China

Chong-Qing Jiang, Department of Surgery, Zhongnan Hospital of Wuhan University, Wuhan 430071, Hubei Province, China

You-Yuan Zhang, Department of Pathology, Central Hospital of Huangshi City, Huangshi 435000, Hubei Province, China

Correspondence to: Ying-An Jiang, Central Hospital of Huangshi City, 43 Wuhan Road, Huangshi 435000, Hubei Province, China. hszxyy@public.hs.hb.cn

Telephone: +86-714-6283783 **Fax:** +86-714-6233931

Received: 2002-11-12 **Accepted:** 2003-01-09

Abstract

AIM: To investigate the expression and significance of PTEN, hypoxia-inducible factor-1 alpha (HIF-1 α), and targeting gene VEGF during colorectal carcinogenesis.

METHODS: Total 71 cases colorectal neoplasms (9 cases of colorectal adenoma and 62 colorectal adenocarcinoma) were formalin fixed and paraffin-embedded, and all specimens were evaluated for PTEN mRNA, HIF-1 α mRNA and VEGF protein expression. PTEN mRNA, HIF-1 α mRNA were detected by in situ hybridization. VEGF protein was identified by citrate-microwave SP immunohistochemical method.

RESULTS: There were significant differences in PTEN, HIF-1 α and VEGF expression between colorectal adenomas and colorectal adenocarcinoma ($P < 0.05$). The level of PTEN expression decreased as the pathologic stage increased. Conversely, HIF-1 α and VEGF expression increased with the Dukes stage as follows: stage A (0.1029 ± 0.0457 ; 0.1207 ± 0.0436), stage B (0.1656 ± 0.0329 ; 0.1572 ± 0.0514), and stage C+D (0.2335 ± 0.0748 ; 0.2219 ± 0.0803). For PTEN expression, there was a significant difference among Dukes stage A, B, and C+D, and the level of PTEN expression was found to be significant higher in Dukes stage A or B than that of Dukes stage C or D. For HIF-1 α expression, there was a significant difference between Dukes stage A and B, and the level of HIF-1 α expression was found to be significantly higher in Dukes stage C+D than that of Dukes stage A or B. The VEGF expression had similar results as HIF-1 α expression. In colorectal adenocarcinoma, decreased levels of PTEN were significantly associated with increased expression of HIF-1 α mRNA ($r = -0.36$, $P < 0.05$) and VEGF protein ($r = -0.48$, $P < 0.05$) respectively. The levels of HIF-1 were positively correlated with VEGF expression ($r = 0.71$, $P < 0.01$).

CONCLUSION: Loss of PTEN expression and increased levels of HIF-1 α and VEGF may play an important role in carcinogenesis and progression of colorectal adenocarcinoma.

Jiang YA, Fan LF, Jiang CQ, Zhang YY, Luo HS, Tang ZJ, Xia D, Wang M. Expression and significance of PTEN, hypoxia-inducible factor-1 alpha in colorectal adenoma and adenocarcinoma. *World J Gastroenterol* 2003; 9(3): 491-494

<http://www.wjgnet.com/1007-9327/9/491.htm>

INTRODUCTION

So far, the mechanism of colorectal oncogenesis is not fully understood. Recent studies^[1-6] have reported on the association of a tumor suppressor gene PTEN with the oncogeneses of several type cancer and cancer cell lines and on PTEN playing an important role in the tumor progression and metastases. Moreover, hypoxia-inducible Factor-1 alpha (HIF-1 α) is a transcription factor identified as being activated by hypoxia, and plays a central role in tumor angiogenesis^[7-19]. Therefore, this study was undertaken to investigate the expression and relationship between PTEN and HIF-1 α and VEGF in colorectal carcinogenesis.

MATERIALS AND METHODS

Materials

The specimens of colorectal cancer were surgically obtained from 71 patients at the Hospital of Wuhan University between 1996 and 1997, and 71 patients were catalogued by histological subtypes as follows: 62 cases of colorectal adenocarcinoma (17 cases in Dukes stage A, 18 stage B, 20 stage C and 7 stage D) and 9 patients of colorectal adenoma (5 cases of tubulovillous adenoma, 2 tubular adenoma and 2 villous adenoma).

Antibodies and reagents

A rabbit VEGF polyclonal antibody was purchased from Neomark International Corporation (Taipei, Taiwan), PTEN mRNA, HIF-1 α mRNA *in situ* hybridization and immunohistochemical reagents were purchased from Boster Corporation (Wuhan, China), and S-P reagent was purchased from Maixin Corporation (Fuzhou, China).

Immunohistochemical technique

Sections were dewaxed in xylene, taken thorough ethanol, and then incubated with 3 % hydrogen peroxide to block endogenous peroxidase activity. Sections then were repaired by reagent for 10 minutes, and the procedure of immunohistochemical determination was performed according to the manufacturer's instruction. A rabbit polyclonal antibody was a dilution of 1:50.

In situ hybridization

Frozen sections were cut onto slides, briefly air-dried, and stored at -80 °C. Prior to use they were fixed in 4 % paraformaldehyde in PBS for 20 min, washed in PBS, and treated with proteinase K (0.0005 %) in 0.1 M Tris/0.05 M EDTA, pH 8.0 for 5 min at 37 °C. Slides were rinsed in 0.2 M glycine in water, postfixed in 4 % paraformaldehyde/0.1 M NaOH/0.1 M NaAc for 5 min, rinsed in 0.1 M triethanolamine

(TEA), pH 8.0 for 3 min, acetylated for 10 min in 0.25 % acetic anhydride/0.1 M TEA, pH 8.8, washed in $2\times$ SSC, and dehydrated. RNA probe was then hybridized to the sections at 60 °C for 16 hrs in 50 % formamide/10 % dextran sulfate/0.15 M NaCl/1 \times Denhardt's solution/0.01 M Tris·Cl, pH 8.0/0.01 M DTT with 0.5 mg/ml tRNA. Sections from each tumor were always hybridized to sense probes as a control for specificity. The slides were next rinsed in $4\times$ SSC and incubated at 37 °C for 30 min with 0.1 mg/ml RNaseA in 0.5 M NaCl/0.01 M Tris·Cl, pH 8.0/1 mM EDTA. They were then desalted, dehydrated through graded ethanols, and coated with emulsion. Following exposure at 4 °C for 5 days, emulsion was developed and fixed, and sections were stained with hematoxylin and eosin. To analyse image scanning, we obtained value of absorbance.

Statistical analysis

All results were expressed as the means \pm SD. Statistical analyses, including the Chi-square test and correlated Spearman test, were carried out with the software package SPSS10.0. A *P* value of <0.05 was considered statistically significant.

RESULTS

Characteristics of PTEN and HIF-1 α expression in colorectal adenoma and adenocarcinoma

PTEN mRNA and HIF-1 α mRNA expression was brown granular, and localized in cytoplasm of tumor cells (Figures 1, 2). HIF-1 α mRNA expression was mainly localized in cytoplasm of tumor cells, frequently observed in margin of tumor necrotic zones. VEGF expression was mainly localized in cytoplasm of tumor cells, also observed in endothelial cell of blood vessel (Figure 3). Expression of PTEN mRNA, HIF-1 α mRNA and VEGF protein was detected in 7, 4 and 3 cases of 9 colorectal adenomas respectively. PTEN mRNA expression was significantly higher ($P<0.05$) in adenomas than that in adenocarcinoma, but HIF-1 α mRNA expression was significantly lower ($P<0.05$) in adenomas than that in adenocarcinoma. There was a significant difference ($P<0.05$) in VEGF expression between colorectal adenomas and adenocarcinoma.

Correlation between PTEN, HIF-1 α , VEGF expressions and dukes stages of colorectal adenocarcinoma

Table 1 shows the correlation between PTEN, HIF-1 α , VEGF expression and Dukes stages of colorectal adenocarcinoma. For PTEN expression, there was a significant difference among Dukes stage A, B, C and D, and the level of PTEN expression was found to be significant higher in Dukes stage A or B than that in Dukes stage C+D. For HIF-1 α expression, there was a significant difference between Dukes stage A and Dukes stage B, and the level of HIF-1 α expression was found to be significantly higher in Dukes stage C+D than that in Dukes stage A or B. VEGF expression had same results as HIF-1 α expression.

Table 1 Correlation between expressions of PTEN, HIF-1 α , VEGF and Dukes stages of colorectal adenocarcinoma

Dukes stage	<i>n</i>	PTEN($\bar{x}\pm s$)	HIF-1 ($\bar{x}\pm s$)	VEGF($\bar{x}\pm s$)
A	17	0.1782 \pm 0.0271 ^{ab}	0.1029 \pm 0.0457 ^{ac}	0.1207 \pm 0.0436 ^{ac}
B	18	0.1583 \pm 0.0397 ^b	0.1656 \pm 0.0329 ^c	0.1772 \pm 0.0514 ^c
C+D	27	0.1470 \pm 0.0524	0.2335 \pm 0.0748	0.2219 \pm 0.0803

^a $P<0.05$, vs Dukes stage B; ^b $P<0.05$, vs Dukes stage C+D; ^c $P<0.01$, vs Dukes stage C+D.

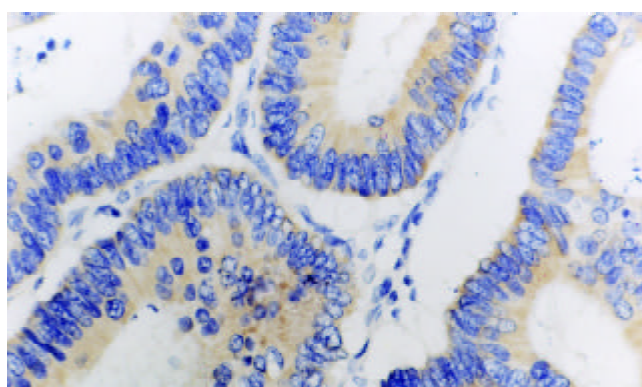


Figure 1 PTEN expression was observed in the cytoplasm of rectal tubular adenoma. Immunostaining, S-P method. $\times 400$.

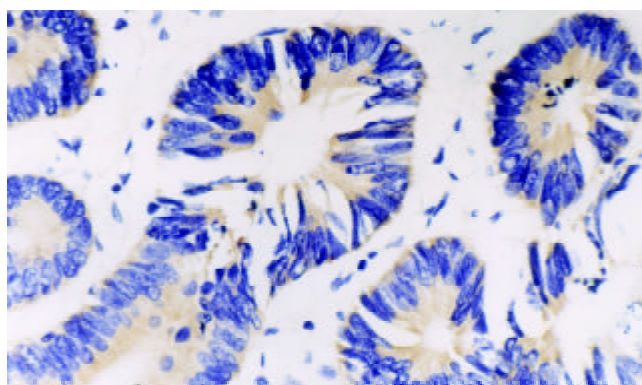


Figure 2 HIF-1 α expression was observed in rectal tubular adenoma. Immunostaining, S-P method. $\times 400$.

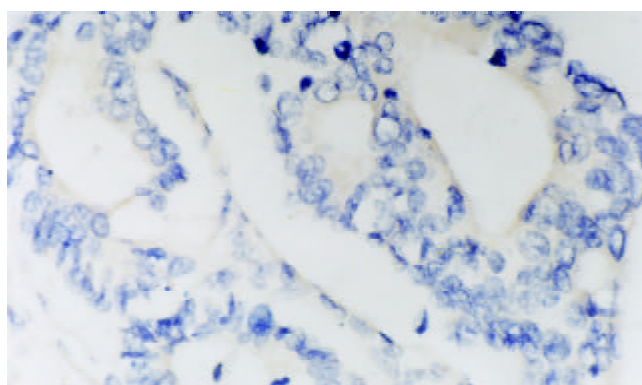


Figure 3 Sigmoid carcinoma shows infiltration into the deep muscular layer, intermediated differentiation, in which VEGF expression was observed. Immunostaining, S-P method. $\times 400$.

Correlation between colorectal adenoma and adenocarcinoma in PTEN, HIF-1 α and VEGF expression

The Spearman analysis showed that the level of PTEN was significantly associated with HIF-1 α expression ($r=-0.36$, $P<0.05$) and with VEGF protein expression ($r=-0.68$, $P<0.05$) respectively. The level of HIF-1 α was correlated with VEGF expression ($r=0.72$, $P<0.01$).

DISCUSSION

PTEN (phosphatase and Tensin homologue deleted on chromosome 10) or MMAC1 (mutated in multiple advanced cancers 1) was recently reported to undergo frequent genetic alterations, including mutations and deletions in multiple advanced cancers^[20-22]. PTEN located at chromosome 10q23.3

encodes a dual-specificity phosphatase that negatively regulates the phosphoinositol-3-kinase (PI3K)/Akt (protein kinase B) pathway and mediates cell cycle arrest and apoptosis^[23]. PTEN protein contains sequence motifs with significant homology to the catalytic domain of protein phosphatases and to the cytoskeletal protein, tensin, and auxilin^[24]. PTEN mutations and deletions were observed in a number of glioma, prostate, kidney and breast carcinoma cell lines or tumor specimens^[25-27]. Recently, Shin *et al.*^[28] screened the PTEN gene in 32 colorectal cancers (8 cell lines and 24 tissues), displaying microsatellite instability (MSI) and six frameshift mutations. We observed that PTEN mRNA decreased as the pathological stage increased, and was significantly associated with VEGF protein expression ($r=-0.68$, $P<0.05$) in colorectal adenoma and adenocarcinoma. These findings suggested that PTEN alteration was possibly involved in the tumor progression and formation of metastasis, and the roles of PTEN in tumor progression and metastasis may be correlated with VEGF expression. Hwang *et al.*^[29] observed that PTEN inhibited the tumorigenicity of B16F10 melanoma cells, and their results suggested that PTEN inhibited tumorigenicity and metastasis through regulating VEGF expression. Jiang *et al.*^[30] found that the overexpression of PTEN inhibited angiogenesis in chicken embryos, and that the PTEN overexpression inhibited the VEGF expression through the PI 3-kinase or Akt dependent pathway. Our results also indicated that PTEN played an important role by inhibiting VEGF expression in colorectal oncogenesis.

HIF-1 is a BHLH-PAS transcription factor that plays an essential role in O₂ homeostasis^[31-34]. HIF-1 is a heterodimer composed of HIF-1 α and HIF-1 β subunits^[31]. HIF-1 β (also known as the aryl hydrocarbon receptor nuclear translocator) is a common subunit of multiple BHLH-PAS proteins, whereas HIF-1 α is the unique, O₂-regulated subunit that determines HIF-1 activity^[35,36]. HIF-1 α activates the transcription of genes encoding transferrin, VEGF, endothelin-1 and inducible nitric oxide synthase, which are implicated in vasodilation, neovascularization, and tumor metastasis^[36,37]. Many studies had identified that HIF-1 α protein was overexpressed in multiple types of human cancer including lung, prostate, breast, and colon carcinomas, even in preneoplastic and premalignant lesions^[38-42]. More importantly, Birner *et al.*^[43] found that the overexpression of HIF-1 α is an important marker in precancerous lesion such as early-stage cervical cancer, cervical intra-epithelial neoplasia III, early stage lymph node-negative breast cancer. We also found that the levels of HIF-1 α mRNA increased gradually as the pathologic stage increased, and were statistically significantly associated with VEGF expression. The same alterations were observed in other tumor tissues. Our findings further identified that HIF-1 α and VEGF played an important role in the tumor angiogenesis and formations of metastases. In this study, we found that HIF-1 α mRNA and VEGF were overexpressed in 4 and 3 cases of colorectal adenomas respectively, and suggested that cell hypoxia occurred prior to carcinogenesis, and persisted to subsequent progression. Generally, these data suggested that HIF-1 α overexpression may be an early stage of carcinogenesis and it occurred prior to angiogenesis or invasion which morphologically confirmed. In this study, the expression of HIF-1 α mRNA and VEGF was significantly higher in the tissues of Dukes stage C/D of colorectal adenocarcinoma than those in Dukes stage A/B, indicating that HIF was involved in the tumor invasion and formation of metastasis. Thus, we believe that the HIF-1 α mRNA and VEGF overexpression is a strong independent prognostic marker in colorectal tumor.

That HIF-1 expression was activated and regulated by EGFR, HER2, and IGFR through PI3K/Akt/FRAP (FKBP-rapamycin-associated protein) pathway had been identified, and a tumor suppressor gene PTEN regulated the HIF-1 α

expression and transcription activation by inhibiting PI3K/Akt/FRAP pathway^[44,45]. The loss of wild-type PTEN resulted in HIF-1 α overexpression, and contributed to the formations of tumor angiogenesis in human prostate cancer and glioma. Our findings that the levels of HIF-1 α were negatively correlated with VEGF expression and the level of PTEN were positively correlated with VEGF expression had further identified that loss of PTEN expression and increased levels of HIF-1 α and VEGF may play an important role in carcinogenesis and progression of colorectal carcinoma.

REFERENCES

- 1 **Teng DH**, Hu R, Lin H, Davis T, Iliev D, Frye C, Swedlund B, Hansen KL, Vinson VL, Gumpert KL, Ellis L, El-Naggar A, Frazier M, Jasser S, Langford LA, Lee J, Mills GB, Pershouse MA, Pollack RE, Tornos C, Troncoso P, Yung WK, Fujii G, Berson A, Steck PA. MMAC1/PTEN mutations in primary tumor specimens and tumor cell lines. *Cancer Res* 1997; **57**: 5221-5225
- 2 **Tsuchiya KD**, Wiesner G, Cassidy SB, Limwongse C, Boyle JT, Schwartz S. Deletion 10q23.2-q23.33 in a patient with gastrointestinal juvenile polyposis and other features of a Cowden-like syndrome. *Genes Chromosomes Cancer* 1998; **21**: 113-118
- 3 **Tsao H**, Zhang X, Benoit E, Haluska FG. Identification of PTEN/MMAC1 alterations in uncultured melanomas and melanoma cell lines. *Oncogene* 1998; **16**: 3397-3402
- 4 **Yang L**, Kuang LG, Zheng HC, Li JY, Wu DY, Zhang SM, Xin Y. PTEN encoding product: a marker for tumorigenesis in progression of gastric carcinoma. *World J Gastroenterol* 2003; **9**: 35-39
- 5 **Wen S**, Stolarov J, Myers MP, Su JD, Wigler MH, Tonks NK, Durden DL. PTEN controls tumor-induced angiogenesis. *Proc Natl Acad Sci U S A* 2001; **98**: 4622-4627
- 6 **Poetsch M**, Dittberner T, Woenckhans C. PTEN/MMAC1 in malignant melanoma and its importance for tumor progression. *Cancer Genet Cytogenet* 2001; **125**: 21-26
- 7 **Semenza GL**, Agani F, Booth G, Forsythe J, Iyer N, Jiang BH, Leung S, Roe R, Wiener C, Yu A. Structural and functional analysis of hypoxia-inducible factor 1. *Kidney Int* 1997; **51**: 553-555
- 8 **Maxwell PH**, Dachs GU, Gleadle JM, Nicholls LG, Harris AL, Stratford IJ, Hankinson O, Pugh CW, Ratcliffe PJ. Hypoxia-inducible factor-1 modulates gene expression in solid tumors and influences both angiogenesis and tumor growth. *Proc Natl Acad Sci U S A* 1997; **94**: 8104-8109
- 9 **Minet E**, Michel G, Remacle J, Michiels C. Role of HIF-1 as a transcription factor involved in embryonic development, cancer progression and apoptosis (review). *Int J Mol Med* 2000; **5**: 253-259
- 10 **Zagzag D**, Zhong H, Scalzitti JM, Laughner E, Simons JW, Semenza GL. Expression of hypoxia-inducible factor 1 α in brain tumors: association with angiogenesis, invasion, and progression. *Cancer* 2000; **88**: 2606-2618
- 11 **Sondergaard KL**, Hilton DA, Penney M, Ollerenshaw M, Demaine AG. Expression of hypoxia-inducible factor 1 α in tumours of patients with glioblastoma. *Neuropathol Appl Neurobiol* 2002; **28**: 210-217
- 12 **Talks KL**, Turley H, Gatter KC, Maxwell PH, Pugh CW, Ratcliffe PJ, Harris AL. The expression and distribution of the hypoxia-inducible factors HIF-1 α and HIF-2 α in normal human tissues, cancers, and tumor-associated macrophages. *Am J Pathol* 2000; **157**: 411-421
- 13 **Bos R**, Zhong H, Hanrahan CF, Mommers EC, Semenza GL, Pinedo HM, Abeloff MD, Simons JW, van Diest PJ, van der Wall E. Levels of hypoxia-inducible factor-1 α during breast carcinogenesis. *J Natl Cancer Inst* 2001; **93**: 309-314
- 14 **Zhong H**, Hanrahan C, van der Poel H, Simons JW. Hypoxia-inducible factor 1 α and 1 β proteins share common signaling pathways in human prostate cancer cells. *Biochem Biophys Res Commun* 2001; **284**: 352-356
- 15 **Nakayama K**, Kanzaki A, Hata K, Katabuchi H, Okamura H, Miyazaki K, Fukumoto M, Takebayashi Y. Hypoxia-inducible factor 1 α (HIF-1 α) gene expression in human ovarian carcinoma. *Cancer Lett* 2002; **176**: 215-223
- 16 **Semenza GL**. Involvement of hypoxia-inducible factor 1 in human cancer. *Intern Med* 2002; **41**: 79-83

- 17 **Koukourakis MI**, Giatromanolaki A, Sivridis E, Simopoulos C, Turley H, Talks K, Gatter KC, Harris AL. Hypoxia-inducible factor (HIF1A and HIF2A), angiogenesis, and chemoradiotherapy outcome of squamous cell head-and-neck cancer. *Int J Radiat Oncol Biol Phys* 2002; **53**: 1192-1202
- 18 **Ryan HE**, Poloni M, McNulty W, Elson D, Gassmann M, Arbeit JM, Johnson RS. Hypoxia-inducible factor-1 α is a positive factor in solid tumor growth. *Cancer Res* 2000; **60**: 4010-4015
- 19 **Semenza GL**. HIF-1 and tumor progression: pathophysiology and therapeutics. *Trends Mol Med* 2002; **8** (Suppl): S62-67
- 20 **Chang JG**, Chen YJ, Perng LI, Wang NM, Kao MC, Yang TY, Chang CP, Tsai CH. Mutation analysis of the PTEN/MMAC1 gene in cancers of the digestive tract. *Eur J Cancer* 1999; **35**: 647-651
- 21 **Guanti G**, Resta N, Simone C, Cariola F, Demma I, Fiorente P, Gentile M. Involvement of PTEN mutations in the genetic pathways of colorectal cancerogenesis. *Hum Mol Genet* 2000; **9**: 283-287
- 22 **Steck PA**, Pershouse MA, Jasser SA, Yung WK, Lin H, Ligon AH, Langford LA, Baumgard ML, Hattier T, Davis T, Frye C, Hu R, Swedlund B, Teng DH, Tavtigian SV. Identification of a candidate tumour suppressor gene, MMAC1, at chromosome 10q23.3 that is mutated in multiple advanced cancers. *Nat Genet* 1997; **15**: 356-362
- 23 **Zhou XP**, Loukola A, Salovaara R, Nystrom-Lahti M, Peltomaki P, de la Chapelle A, Aaltonen LA, Eng C. PTEN mutational spectra, expression levels, and subcellular localization in microsatellite stable and unstable colorectal cancers. *Am J Pathol* 2002; **161**: 439-447
- 24 **Steck PA**, Pershouse MA, Jasser SA, Yung WK, Lin H, Ligon AH, Langford LA, Baumgard ML, Hattier T, Davis T, Frye C, Hu R, Swedlund B, Teng DH, Tavtigian SV. Identification of a candidate tumour suppressor gene, MMAC1, at chromosome 10q23.3 that is mutated in multiple advanced cancers. *Nat Genet* 1997; **15**: 356-362
- 25 **Koul D**, Shen R, Garyali A, Ke LD, Liu TJ, Yung WK. MMAC/PTEN tumor suppressor gene regulates vascular endothelial growth factor-mediated angiogenesis in prostate cancer. *Int J Oncol* 2002; **21**: 469-475
- 26 **Velickovic M**, Delahunt B, McIver B, Grebe SK. Intragenic PTEN/MMAC1 loss of heterozygosity in conventional (clear-cell) renal cell carcinoma is associated with poor patient prognosis. *Mod Pathol* 2002; **15**: 479-485
- 27 **Harima Y**, Sawada S, Nagata K, Sougawa M, Ostapenko V, Ohnishi T. Mutation of the PTEN gene in advanced cervical cancer correlated with tumor progression and poor outcome after radiotherapy. *Int J Oncol* 2001; **18**: 493-497
- 28 **Shin KH**, Park YJ, Park JG. PTEN gene mutations in colorectal cancers displaying microsatellite instability. *Cancer Lett* 2001; **174**: 189-194
- 29 **Hwang PH**, Yi HK, Kim DS, Nam SY, Kim JS, Lee DY. Suppression of tumorigenicity and metastasis in B16F10 cells by PTEN/MMAC1/TEP1 gene. *Cancer Lett* 2001; **172**: 83-91
- 30 **Jiang BH**, Zheng JZ, Aoki M, Vogt PK. Phosphatidylinositol 3-kinase signaling mediates angiogenesis and expression of vascular endothelial growth factor in endothelial cells. *Proc Natl Acad Sci U S A* 2000; **97**: 1749-1753
- 31 **Wang GL**, Jiang BH, Rue EA, Semenza GL. Hypoxia-inducible factor 1 is a basic-helix-loop-helix-PAS heterodimer regulated by cellular O₂ tension. *Proc Natl Acad Sci U S A* 1995; **92**: 5510-5514
- 32 **Iyer NV**, Kotch LE, Agani F, Leung SW, Laughner E, Wenger RH, Gassmann M, Gearhart JD, Lawler AM, Yu AY, Semenza GL. Cellular and developmental control of O₂ homeostasis by hypoxia-inducible factor 1 α . *Genes Dev* 1998; **12**: 149-162
- 33 **Ryan HE**, Lo J, Johnson RS. HIF-1 α is required for solid tumor formation and embryonic vascularization. *EMBO J* 1998; **17**: 3005-3015
- 34 **Carmeliet P**, Dor Y, Herbert JM, Fukumura D, Brusselmans K, Dewerchin M, Neeman M, Bono F, Abramovitch R, Maxwell P, Koch CJ, Ratcliffe P, Moons L, Jain RK, Collen D, Keshet E. Role of HIF-1 α in hypoxia-mediated apoptosis, cell proliferation and tumour angiogenesis. *Nature* 1998; **394**: 485-490
- 35 **Jiang BH**, Semenza GL, Bauer C, Marti HH. Hypoxia-inducible factor 1 levels vary exponentially over a physiologically relevant range of O₂ tension. *Am J Physiol* 1996; **271**: C1172-1180
- 36 **Semenza GL**. Regulation of mammalian O₂ homeostasis by hypoxia-inducible factor 1. *Annu Rev Cell Dev Biol* 1999; **15**: 551-578
- 37 **Kerb R**. New targets, drugs, and approaches for the treatment cancer: an overview. *Cancer Metastasis Rev* 1998; **17**: 145-147
- 38 **Giatromanolaki A**, Koukourakis MI, Sivridis E, Turley H, Talks K, Pezzella F, Gatter KC, Harris AL. Relation of hypoxia inducible factor 1 α and 2 α in operable non-small cell lung cancer to angiogenic/molecular profile of tumours and survival. *Br J Cancer* 2001; **85**: 881-890
- 39 **Saramaki OR**, Savinainen KJ, Nupponen NN, Bratt O, Visakorpi T. Amplification of hypoxia-inducible factor 1 α gene in prostate cancer. *Cancer Genet Cytogenet* 2001; **128**: 31-34
- 40 **Schindl M**, Schoppmann SF, Samonigg H, Hausmaninger H, Kwasny W, Gnant M, Jakesz R, Kubista E, Birner P, Oberhuber G. Overexpression of Hypoxia-inducible Factor 1 α is Associated with an Unfavorable Prognosis in Lymph Node-positive Breast Cancer. *Clin Cancer Res* 2002; **8**: 1831-1837
- 41 **Welsh SJ**, Bellamy WT, Briehl MM, Powis G. The redox protein thioredoxin-1 (Trx-1) increases hypoxia-inducible factor 1 α protein expression: Trx-1 overexpression results in increased vascular endothelial growth factor production and enhanced tumor angiogenesis. *Cancer Res* 2002; **62**: 5089-5095
- 42 **Zhong H**, De Marzo AM, Laughner E, Lim M, Hilton DA, Zagzag D, Buechler P, Isaacs WB, Semenza GL, Simons JW. Overexpression of hypoxia-inducible factor 1 α in common human cancers and their metastases. *Cancer Res* 1999; **59**: 5830-5835
- 43 **Birner P**, Schindl M, Obermair A, Plank C, Breitenacker G, Oberhuber G. Overexpression of hypoxia-inducible factor 1 α is a marker for an unfavorable prognosis in early-stage invasive cervical cancer. *Cancer Res* 2000; **60**: 4693-4696
- 44 **Laughner E**, Taghavi P, Chiles K, Mahon PC, Semenza GL. HER2 (neu) signaling increase the rate of hypoxia-inducible factor 1 α (HIF-1 α) synthesis: novel mechanism for HIF-1-mediated vascular endothelial growth factor expression. *Mol Cell Biol* 2001; **21**: 3995-4004
- 45 **Zhong H**, Chiles K, Feldser D, Laughner E, Hanrahan C, Georgescu MM, Simons JW, Semenza GL. Modulation of hypoxia-inducible factor 1 α expression by the epidermal growth factor/phosphatidylinositol 3-kinase/PTEN/AKT/FRAP pathway in human prostate cancer cells: implications for tumor angiogenesis and therapeutics. *Cancer Res* 2000; **60**: 1541-1545

Edited by Zhang JZ

• COLORECTAL CANCER •

Application of autologous tumor cell vaccine and NDV vaccine in treatment of tumors of digestive tract

Wei Liang, Hui Wang, Tie-Mie Sun, Wen-Qing Yao, Li-Li Chen, Yu Jin, Chun-Ling Li, Fan-Juan Meng

Wei Liang, Tie-Mie Sun, Wen-Qing Yao, Li-Li Chen, Yu Jin, Chun-Ling Li, Fan-Juan Meng, Liaoning Provincial Tumor Research Institute, Shenyang 110042, Liaoning Province, China

Hui Wang, Department of Coloproctology Surgery of Liaoning Tumor Hospital, Shenyang 110042, Liaoning Province, China

Supported by Scientific Foundation of Liaoning Province, No. 895215

Correspondence to: Wen-Qing Yao, Liaoning Provincial Tumor Research Institute, 44 xiaohelan Road, Dadong District, Shenyang 110042, Liaoning Province, China. yaowenq@mail.sy.ln.cn

Telephone: +86-24-24324202

Received: 2002-08-03 **Accepted:** 2002-09-12

Abstract

AIM: To treat patients with stage I-IV malignant tumors of digestive tract using autologous tumor cell vaccine and NDV (Newcastle disease virus) vaccine, and observe the survival period and curative effect.

METHODS: 335 patients with malignant tumors of digestive tract were treated with autologous tumor cell vaccine and NDV vaccine. The autologous tumor cell vaccine received were assigned for long-term survival observation. While these failed to obtain the autologous tumor tissue were given with NDV vaccine for a received short-term observation on curative effect.

RESULTS: The colorectal cancer patients treated with autologous tumor cell vaccine were divided into two groups: the controlled group (subjected to resection alone) ($n=257$), the vaccine group (subjected to both resection and immunotherapy) ($n=310$). 25 patients treated with NDV immunotherapy were all at stage IV without having resection. In postoperation adjuvant therapy patients, the 5, 6 and 7-year survival rates were 66.51 %, 60.52 %, 56.50 % respectively; whereas in patients with resection alone, only 45.57 %, 44.76 % and 43.42 % respectively. The average survival period was 5.13 years (resection alone group 4.15 years), the median survival period was over 7 years (resection alone group 4.46 years). There were significant differences between the two groups. The patients treated with resection plus vaccine were measured delayed-type hypersensitivity (DTH) reactions after vaccination, (indurative scope >5 mm). The magnitude of DTH was related to the prognosis. The 5-year survival rate was 80 % for those with indurations greater than 5 mm, compared with 30 % for those with indurations less than 5 mm. The 1-year survival rate was 96 % for 25 patients treated with NDV immunotherapy. The total effective rate (CR+PR) was 24.00 % in NDV immunotherapy; complete remission (CR) in 1 case (4.00 %), partial remission (PR) in 5 cases (20.00 %), stabilized in 16 cases (64.00 %), progression (PD) in 1 case (4.00 %). After NDV vaccine immunotherapy, the number of NK cell increased and immune function improved obviously.

CONCLUSION: The autologous tumor cell vaccine and NDV vaccine can prolong the patients' life. NDV vaccine is notably

effective for short-term with promotion of quality of life and can be used whenever necessary with good prospects.

Liang W, Wang H, Sun TM, Yao WQ, Chen LL, Jin Y, Li CL, Meng FJ. Application of autologous tumor cell vaccine and NDV vaccine in treatment of tumors of digestive tract. *World J Gastroenterol* 2003; 9(3): 495-498

<http://www.wjgnet.com/1007-9327/9/495.htm>

INTRODUCTION

Malignant tumors of digestive tract is common. It is difficult to improve the survival rate only by resection plus radiotherapy and chemotherapy. This study reported 335 patients treated with autologous tumor cell vaccine and NDV vaccine. 310 of 335 patients with colorectal cancer of stages I-IV received autologous tumor cell vaccine postoperatively and the controlled group (resection alone) constituted 257 patients. The duration of follow-up was 7 years. There were statistically significant differences in the survival rate, the median survival period and the mean survival period between the two groups and the controlled group. The 1-year survival rate was 96 % for 25 late cancer patients treated with NDV vaccine. This study provided a basis for the clinical application of autologous tumor cell vaccine and NDV vaccine^[1,2,5,6,24,25,26,30].

MATERIALS AND METHODS

Clinical data

Those receiving autologous tumor cell vaccine consisted of 567 patients with colorectal cancer in 1993-1995 with a further follow-up of 7-year. 25 patients with late cancer were given NDV vaccine from June, 2001 to June, 2002: 15 men, 10 women; 41 to 83-year-old, mean age 62.3 years, they were all at stage IV patients and were followed up for 1-year. 310 postoperative patients treated with autologous tumor cell vaccine consisted of 204 men and 106 women range from 19 to 79 years, mean age 55.8 years: 136 patients having Miles operation, 98 colonic operation, including 74 anterior resection and 2 partial resection. The resection alone group (controlled group) consisted of 257 patients: 155 men, 102 women; age ranged 18 to 77 years of age, mean age 55.1 years; among these, 120 patients had Miles operation, 78 colonic operation, 59 anterior resection. The DTH reactions were observed in 20 patients treated with immunotherapy after resections. Among these 20 all were stage II, III colorectal cancer among them 10 were male and 10 female age ranged 35 to 65 years, mean age 52.7 years. The follow-up results were shown in Table 1, 2 and 4. The TNM stages were shown in Table 3.

Preparation of autologous tumor cell vaccine

Material and reagent Tumor tissue specimen ($\phi \geq 1$ cm), element for injection (Da Lian Jin Gang Pharmaceutical Factory), mitomycin C, 25 % glutaraldehyde (E merk), RPMI 1640 complete culture media.

Method The tumor tissue obtained under sterile conditions was placed in a sterile container and sent to the lab in two

hours. Prepare the suspended tumor cell solution by routine methods. Then add mitomycin C and elemene 0.3 mg/ml. placed in 37 °C incubator (0.5 h). heated at 42 °C for 30 min. centrifuged, washed, and fixed in 0.0625 % glutaraldehyde (10 min). After washing out the fixation solution, the sterile suspended autologous tumor cell solution ($\geq 10^7$ /ml) was then prepared for use.

Immune procedure First Vaccination: The Patients treated received first vaccination a week after surgical resection, once a week for four weeks.

Intensive immunotherapy: Began at 1 to 2 months intervals after the first vaccination.

Method of injection: The vaccine was injected in three adjacent sites each 3-5 an apact on the anterior arm or deltoid region. one 0.2 ml intradermally and two 0.4 ml hypodamically. DTH

test: Prior to the vaccination and two weeks after vaccination, skin test was performed. For the controlls distilled water was used. DTH reaction was concided position when the indenation was at 72 hours >5 mm (+) , 6-10 mm (++) .

Table 1 Follow-up results of survival status for colorectal cancer patients with resection plus autelogous tumor cell vaccine from 1993 to 2000

Year	n	Survival period							
		0	1	2	3	4	5	6	7
1993-2000	50	50	50	44	39	35	31	31	29
1994-2000	133	133	125	104	94	90	85	75	
1995-2000	127	127	126	116	106	98	93		
Total	310	310	301	264	239	223	209	106	

Table 2 Follow-up results of survival status for colorectal cancer patients with resection alone from 1993 to 2000

Year	n	Survival period							
		0	1	2	3	4	5	6	7
1993-2000	73	73	71	60	54	41	35	34	33
1994-2000	94	94	85	68	56	47	43	43	
1995-2000	90	90	84	69	57	50	47		
Total	257	257	240	197	167	138	125	77	33

Table 3 TNF staging in colorectal cancer patients with resection plus vaccine group and resection alone group

Treatment	n	TNF stages			
		I	II	III	IV
Resection plus vaccine	310	46(14.8%)	121(39%)	80(25.8%)	63(20.3%)
Resection alone	257	55(21.4%)	94(36.6%)	66(25.7%)	42(16.3%)
Total	567	101	215	146	105

Statistical analysis

Using SPSS computer program, analyses were performed by *t*-test for the mean value between the two groups by life table and logrank test for survival rate, by graphical method and linear inner insert method for the median survival period and by Kaplan-Meier method for the mean survival period.

Preparation of NDV vaccine

Primary fluid of NDV La Sota IV weak toxicant stem was vaccinated in chick embryo chorioallantoic cavity. SPF fertilized egg was placed in the 37 °C incubator. On day 10, injecting 0.2 ml NDV diluted with 0.5 % LH into the

chorioallantoic cavity in sterile conditions, sealed it with wax, and obtained the virus after 72 hours in 37 °C incubator. Before getting the virus, placed the chick embryo overnight at 4 °C refrigerator. Then removed the eggshell in air champer, opened the egg membrance and aspirated the chorioallantoic fluid containing virus by sterile technique. The fluid was centrifuged for 30 minutes at low speed (2 800 r/min, 800 g) to get rid of the sediment. The supernatants of NDV was centrifuged 60 minutes at low temperature and high speed (4 °C, 30 000 r/min, 90 000 g) and the viruses were precipitated. Resuspended the virus sediment by pH7.2, 0.1 mol/L PBS, assayed the hemagglutinin unit (Hu) of NDV by 0.5 % fresh chick erythrocyte suspended solution and then diluted to 1:1 280 Hu/ml. The solution was packed into ampoules separately and stored at -20 °C. Unfreeze it before using.

Immune procedure

Injected 1-2 ml in three sites intradermally at deltoid muscle region, once every three days. Three times constituted one course, and the injections also could be given continually.

Immune function assay

Prior to and after the immunotherapy, assayed the NK, CD₃⁺, CD₄⁺, CD₈⁺, CD₄⁺/CD₈⁺ by flow cytometry.

RESULTS

Table 4 Comparison of yearly survival rates of resected colorectal cancer patients in vaccination group and controll group

Treatment method	n	Yearly survival rates (%±s \bar{x})						
		1	2	3	4	5	6	7
Vaccination group	310	97.05 ±0.97	84.35 ±2.10	76.42 ±3.23	71.12 ±3.43	66.51 ±3.84	60.52 ±4.57	56.50 ±6.52
Controll group	257	93.16 ±1.60	74.83 ±2.51	62.50 ±2.06	50.58 ±1.99	45.57 ±1.32	44.76 ±0.81	43.42 ±1.32

^aLife table χ^2 test $P < 0.005$ of the two groups.

By life table method, the 7-year survival rate of the vaccination group was 56.5 % and the median survival period was approximately 50 %. Hence by graphical method the median survival period was over 7 years, whereas by linear inner insert method, the median survival period of the controll group was 4.46 years. The average survival period of vaccination group was 5.13±0.60 years where that of the controlled group 4.15±0.60 years (Table 5).

Table 5 Comparison of median survival period, mean survival period of resected colorectal cancer patients of vaccination group and controlled group

Treatment method	n	Median survival period (year)	Mean survival period (year)
Resection plus vaccination group	310	>7 ^a	5.13±0.60 ^b
Resection alone group	257	4.46	4.15±0.60

^b $P < 0.01$ vs resection alone group.

The positive rate of DTH reactions in resection plus vaccine group was over 90 % whereas in resection alone group all negative. Most active immunotherapy for patients succeeded (Table 6). The remission rate of late digestive tract carcinoma treated with NDV vaccine (Table 7,9). The charge of immune function pre- and post-NDV vaccine therapy (Table 8).

Table 6 Comparison of five-year survival rate, survival period of resected colorectal cancer patients in vaccination group with positive and negative DTH reaction

DTH reactions	<i>n</i>	5-year survival cases	Survival rate ^b	^a Survival period ($\bar{x}\pm s$)
Positive group	10	8	80 %	4.7 \pm 0.67
Negative group	10	3	30 %	3.5 \pm 1.80

χ^2 test ^a $P<0.05$, ^b $P<0.01$ vs negative group.

Table 7 The remission rate of late cancer of digestive tract carcinoma treated with NDV vaccine

Types of disease	<i>n</i>	CR(%)	PR(%)	SD(%)	PD(%)	CR+PR(%)
Colorectal cancer	13	1	3	8	0	4
Stomach cancer	6	0	0	5	0	0
Liver cancer	4	0	2	1	0	2
Pancreatic head cancer	1	0	0	1	1	0
Gall bladder cancer	1	0	0	1	0	0
Total	25	1(4.00%)	5(20.00%)	16(64.00%)	1(4.00%)	6(24.00%)

Table 8 Immunobgice function prior to and after NDV vaccination therapy

Item	<i>n</i>	Before therapy ($\bar{x}\pm s$)	After therapy ($\bar{x}\pm s$)	<i>P</i>
NK	10	24.65 \pm 7.21	36.58 \pm 11.87	<0.05
CD ₃ ⁺	10	67.15 \pm 2.43	71.12 \pm 2.86	<0.01
CD ₄ ⁺	10	38.23 \pm 3.01	41.62 \pm 2.71	<0.01
CD ₈ ⁺	10	30.55 \pm 1.21	29.84 \pm 2.43	>0.05
CD ₄ ⁺ /CD ₈ ⁺	10	1.23 \pm 0.12	1.41 \pm 0.13	<0.05

Table 9 Comparison of treatment courses and therapeutic effect of colorectal cancer patients with NDV immunotherapy

Group	<i>n</i>	CR	PR	SD	PD	CR+PR
1 Course	6	0	0	5	1	0
>2 Courses	7	1	3	3	0	4

$\chi^2=10$, $P<0.01$.

DISCUSSION

The major treatments of malignant tumors of digestive tract malignant tumor postoperatively are radiotherapy and chemotherapy. However, it is very difficult to improve the 5-year survival rate. We treated these patients with autologous tumor cell vaccine and NDV vaccine and made a 7-year follow-up survey of postoperative patients with autologous tumor cell vaccine. The 5, 6, 7-year survival rate are 66.51 %, 60.52 %, 56.50 %, respectively, whereas they were only 45.57 %, 44.76 % and 43.42 % respectively in resection plus radiotherapy or chemotherapy group. The survival rate increased by 20.94 %, 15.76 %, 13.08 %. The increase of amplitude arrived at 46.00 %, 35.20 % and 30.12 % respectively. This indicated autologous tumor cell vaccine could really increase the long-term survival rate of colorectal cancer patients^[7,9,10].

The median survival period increased more obviously: for over 7-year in vaccination group but only 4.46 years in resection alone group, it increased by over 2.5 years. The amplitude of increase was 57 %. The mean survival period was 5.13 years in vaccination group yet only 4.15 years in

resection alone group, an increase of 1 year in average.

The DTH reaction in postoperative colorectal cancer patients showed positive reaction two weeks after the immunotherapy in over 90 %, but negative before therapy. The 5-year survival rate was 80 % in the positive response group, and the 30 % in negative response group, the difference was significant. It demonstrated that active specific immunotherapy by autologous tumor cell vaccine could yield positive DTH reaction in resected colorectal cancer patients. The 5-year survival rate increased obviously as a result of augmented antitumor immunity after immunotherapy^[2,3,7]. We conclude that most of the patients who are treated with active specific immunization lead to a specific antitumor effect. Our vaccine is effective in prevention of tumor progression. The protection achieved can be augmented by serial vaccinations and can be maintained for a long period of time^[4-20].

With booming of biotherapy lately, more attention have been paid to NDV vaccine. Many reports from abroad showed some effectiveness of NDV in malignant tumor of digestive tract and malignant melanoma^[21-23, 27-29] with few adverse effects. After transfection NDV, immune response could be induced with production of cytokines and triggering of active tumor vaccine reaction. In the 1950s, people tried to treat malignant tumor with virus and discovered that much virus had greater killing effect on tumor cells than on normal cells. For example, NDV-73-T could infect all kinds of human tumor cells, with intracellular replication, elicit cell fusion and multinuclear body, and the tumor cells die eventually. NDV had selective killing effect on tumor cells, but not the normal cells. Despite there were many reports about the antitumor effect of NDV^[27-36], yet long-term observation on the use of NDV was scarce, especially about its side effects. The NDV vaccine given to 25 patients in our study were 2-6 courses, some of them 8 courses. The duration of continuous injection was over 3 months, no significant side effects were found. We compared the effectiveness of one course and two course in 13 colorectal cancer patients. See Table 9, the curative effect of the latter was superior to that of the former. A few patients had flu-like symptoms, such as fatigue, lowgrade-fever, soreness of joints. which disappeared in 1-2 days. Now we had treated 80 patients bearing all kinds of late malignant tumor with NDV vaccine. We found that the curative effects on urinary bladder cancer and colorectal cancer were notable. Take for instance, one bladder cancer patient developed a 2.0 \times 2.0 cm tumor in the right wall of his bladder, having hematuria and 2.5 \times 2.7 cm hypodermic metastatic nodule over his left thigh. After four courses of NDV immunotherapy, the mass in the bladder wall and the metastate nodule over his left thigh regressed, hematuria also ceased. One colon cancer patient had a 3.0 \times 3.5 cm cauliflower-like tumor on the left wall of the rectum, about 4 cm away from the anus, having hematochezia. After four courses of NDV vaccine, the mass in the rectum regressed and hematochezia ceased. Another patient with primary liver cancer, measuring 5.5 \times 7.2 cm before the NDV therapy, after three courses, the mass decreased somewhat to 5.5 \times 5.3 cm and the backache ameliorated. NDV injection can remit patients in a late gastric cancer impending to death with extensive peritoneal and pelvic metastasis, anuria, comatous and maintained his life only by intravenous nutrients and renal dialysis. After 12 days of large doses of NDV vaccination, the patient became conscious and could urinate by himself, with stoppage of dialysis, and could eat a little, the survival period prolonged to 30 days. As from Table 8, we could see that NDV could improve the immune functions by activating the lymphocytes. The preliminary use of NDV showed a new therapeutic approach to the treatment of on late malignant tumors, especially for those who were unable to obtain the autologous tumor tissue. After NDV vaccination, the curative efficacy

occures rapidly and long-term observation is undertaking. From this study we can expect that the NDV vaccine has a good prospect.

REFERENCES

- Mimori K, Mori M. Recent advances in the diagnosis and treatment of colorectal cancers. *Nippon Geka Gakkai Zasshi* 2002; **103**: 468-471
- Indar A, Maxwell-Armstrong CA, Durrant LG, Carmichael J, Scholefield JH. Current concepts in immunotherapy for the treatment of colorectal cancer. *J R Coll Surg Edinb* 2002; **47**: 458-474
- de Kleijn EM, Punt CJ. Biological therapy of colorectal cancer. *Eur J Cancer* 2002; **38**: 1016-1022
- Miyagi Y, Imai N, Sasatomi T, Yamada A, Mine T, Katagiri K, Nakagawa M, Muto A, Okouchi S, Isomoto H, Shirouzu K, Yamana H, Itoh K. Induction of cellular immune responses to tumor cells and peptides in colorectal cancer patients by vaccination with SART3 peptides. *Clin Cancer Res* 2001; **7**: 3950-3962
- Bartnes K. Tumor antigens presented to T helper lymphocytes-critical components of the cancer vaccine. *Tidsskr Nor Laegeforen* 2001; **121**: 2941-2945
- Zou SC, Qiu HS, Zhang CW, Tao HQ. A clinical and long-term follow-up study of peri-operative sequential triple therapy for gastric cancer. *World J Gastroenterol* 2000; **6**: 284-286
- Saeterdal I, Bjorheim J, Lislud K, Gjertsen MK, Bukholm IK, Olsen OC, Nesland JM, Eriksen JA, Moller M, Lindblom A, Gaudernack G. Frameshift-mutation-derived peptides as tumor-specific antigens in inherited and spontaneous colorectal cancer. *Proc Natl Acad Sci U S A* 2001; **98**: 13255-13260
- Harris JE, Ryan L, Hoover HC Jr, Stuart RK, Oken MM, Benson AB 3rd, Mansour E, Haller D G, Manola J, Hanna MG Jr. Adjuvant active specific immunotherapy for stage II and III colon cancer with an autologous tumor cell vaccine: Eastern Cooperative Oncology Group Study E5283. *J Clin Oncol* 2000; **18**: 148-157
- Zeh HJ, Stavely-O'Carroll K, Choti MA. Vaccines for colorectal cancer. *Trends Mol Med* 2001; **7**: 307-313
- Habal N, Gupta RK, Bilchik AJ, Yee R, Leopoldo Z, Ye W, Elashoff RM, Morton DL. CancerVax, an allogeneic tumor cell vaccine, induces specific humoral and cellular immune responses in advanced colon cancer. *Ann Surg Oncol* 2001; **8**: 389-401
- Maxwell-Armstrong CA, Durrant LG, Buckley TJ, Scholefield JH, Robins RA, Fielding K, Monson JR, Guillou P, Calvert H, Carmichael J, Hardcastle JD. Randomized double-blind phase II survival study comparing immunization with the anti-idiotypic monoclonal antibody 105AD7 against placebo in advanced colorectal cancer. *Br J Cancer* 2001; **84**: 1433-1436
- Tartaglia J, Bonnet MC, Berinstein N, Barber B, Klein M, Moingeon P. Therapeutic vaccines against melanoma and colorectal cancer. *Vaccine* 2001; **19**: 2571-2575
- Safa MM, Foon KA. Adjuvant immunotherapy for melanoma and colorectal cancers. *Semin Oncol* 2001; **28**: 68-92
- Foon KA. Immunotherapy for colorectal cancer. *Curr Oncol Rep* 2001; **3**: 116-126
- Smith AM, Justin T, Michaeli D, Watson SA. Phase I/II study of G17-DT, an anti-gastrin immunogen in advanced colorectal cancer. *Clin Cancer Res* 2000; **6**: 4719-4724
- Rains N, Cannan RJ, Chen W, Stubbs RS. Development of a dendritic cell (DC)-based vaccine for patients with advanced colorectal cancer. *Hepatogastroenterology* 2001; **48**: 347-351
- Woodlock TJ, Sahasrabudhe DM, Marquis DM, Greene D, Pandya KJ, McCune CS. Active specific immunotherapy for metastatic colorectal carcinoma: phase I study of an allogeneic cell vaccine plus low-dose interleukin-1 alpha. *J Immunother* 1999; **22**: 251-259
- Suh KW, Piantadosi S, Yazdi HA, Pardoll DM, Brem H, Choti MA. Treatment of liver metastases from colon carcinoma with autologous tumor vaccine expressing granulocyte-macrophage colony-stimulating factor. *J Surg Oncol* 1999; **72**: 218-224
- Yamana H, Itoh K. Specific immunotherapy with cancer vaccines. *Gann To Kagaku Ryoho* 2000; **27**: 1477-1488
- Chen W, Rains N, Young D, Stubbs RS. Dendritic cell-based cancer immunotherapy: potential for treatment of colorectal cancer? *J Gastroenterol Hepatol* 2000; **15**: 698-705
- Yip D, Strickland AH, Karapetis CS, Hawkins CA, Harper PG. Immunomodulation therapy in colorectal carcinoma. *Cancer Treat Rev* 2000; **26**: 169-190
- Pecora AL, Rizvi N, Cohen GI, Meropol NJ, Serman D, Marshall JL, Goldberg S, Gross P, O'Neil JD, Groene WS, Roberts MS, Rabin H, Bamat MK, Lorence RM. Phase I trial of intravenous administration of PV701, an oncolytic virus in patients with advanced solid cancers. *J Clin Oncol* 2002; **20**: 2251-2266
- Schneider T, Gerhards R, Kirches E, Firsching R. Preliminary results of active specific immunization with modified tumor cell vaccine in glioblastoma multiforme. *J Neurooncol* 2001; **53**: 39-46
- Schirmacher V. Anti-tumor vaccination. *Zentralbl Chir* 2000; **125** (Suppl 1): 33-36
- Zorn U, Duensing S, Langkopf F, Anastassiou G, Kirchner H, Hadam M, Knuver-Hopf J, Atzpodien J. Active specific immunotherapy of renal cell carcinoma: cellular and humoral immune responses. *Cancer Biother Radiopharm* 1997; **12**: 157-165
- Sonoda K, Sakaguchi M, Okamura H, Yokogawa K, Tokunaga E, Tokiyoshi S, Kawaguchi Y, Hirai K. Development of an effective polyvalent vaccine against both Marek's and Newcastle diseases based on recombinant Marek's disease virus type 1 in commercial chickens with maternal antibodies. *J Virol* 2000; **74**: 3217-3226
- Schirmacher V, Haas C, Bonifer R, Ahlert T, Gerhards R, Ertel C. Human tumor cell modification by virus infection: an efficient and safe way to produce cancer vaccine with pleiotropic immune stimulatory properties when using Newcastle disease virus. *Gene Ther* 1999; **6**: 63-73
- Csatary LK, Moss RW, Beuth J, Torocsik B, Szeberenyi J, Bakacs T. Beneficial treatment of patients with advanced cancer using a Newcastle disease virus vaccine (MTH-68/H). *Anticancer Res* 1999; **19**: 635-638
- Batliwalla FM, Bateman BA, Serrano D, Murray D, Macphail S, Maino VC, Ansel JC, Gregersen PK, Armstrong CA. A 15-year follow-up of AJCC stage III malignant melanoma patients treated postsurgically with Newcastle disease virus (NDV) oncolysate and determination of alterations in the CD8 T cell repertoire. *Mol Med* 1998; **4**: 783-794
- Phuangsab A, Lorence RM, Reichard KW, Peeples ME, Walter RJ. Newcastle disease virus therapy of human tumor xenografts: antitumor effects of local or systemic administration. *Cancer Lett* 2001; **172**: 27-36
- Schirmacher V, Griesbach A, Ahlert T. Antitumor effects of Newcastle disease virus in vivo: local versus systemic effects. *Int J Oncol* 2001; **18**: 945-952
- Zhang JK, Sun JL, Chen HB, Zeng Y, Qu YJ. Influence of granulocyte macrophage colony stimulating factor and tumor necrosis factor on anti-hepatoma activities of human dendritic cells. *World J Gastroenterol* 2000; **6**: 718-720
- Termeer CC, Schirmacher V, Brocker EB, Becker JC. Newcastle disease virus infection induces B7-1/B7-2-independent T-cell costimulatory activity in human melanoma cells. *Cancer Gene Ther* 2000; **7**: 316-323
- Schirmacher V, Bai L, Umansky V, Yu L, Xing Y, Qian Z. Newcastle disease virus activates macrophages for anti-tumor activity. *Int J Oncol* 2000; **16**: 363-373
- Haas C, Ertel C, Gerhards R, Schirmacher V. Introduction of adhesive and costimulatory immune functions into tumor cells by infection with Newcastle Disease Virus. *Int J Oncol* 1998; **13**: 1105-1115
- King DJ. A comparison of the onset of protection induced by Newcastle disease virus strain B1 and a fowl poxvirus recombinant Newcastle disease vaccine to a viscerotropic velogenic Newcastle disease virus challenge. *Avian Dis* 1999; **43**: 745-755

Full-length genome of wild-type hepatitis A virus (DL3) isolated in China

Guo-Dong Liu, Ning-Zhu Hu, Yun-Zhang Hu

Guo-Dong Liu, Ning-Zhu Hu, Yun-Zhang Hu, Department of Vaccine Research, Institute of Medical Biology, Chinese Academy of Medical Sciences, Peking Union of Medical College, Kunming 650118, Yunnan Province, China

Correspondence to: Yun-Zhang Hu, Department of Vaccine Research, Institute of Medical Biology, Chinese Academy of Medical Sciences, 379 Jiaoling Road, Kunming 650118, Yunnan Province, China. huyunz@21cn.com

Telephone: +86-871-8335334 **Fax:** +86-871-8334483

Received: 2002-10-09 **Accepted:** 2002-11-08

Abstract

AIM: To characterize the genome of an wild-type HAV isolate (DL3) in China.

METHODS: A stool specimen was collected from hepatitis A patient from Dalian, China. HAV (DL3) was isolated and viral RNA was extracted. The genome of DL3 was amplified by reverse transcription and polymerase chain reaction (RT-PCR), followed by cloning into pGEM-T vector. The positive colonies were selected and sequenced. The full-length genome of DL3 was analyzed and compared with other wild-type HAV isolates.

RESULTS: The genome of DL3 was 7 476 nucleotides (nt) in size, containing 732-nt 5' untranslated region (UTR), 6 681-nt open reading frame (ORF) which encoded a polyprotein of 2 227 amino acids (aa), and 63-nt 3' UTR. The base composition was 28.96 % A (2 165), 16.08 % C (1 202), 22.11 % G (1 653) and 32.85 % U (2 456). Genomic comparisons with wild-type HAV isolates revealed that DL3 had the highest identity of 97.5 % for nt (185 differences) with AH1, the lowest identity of 85.7 % (1 066 differences) with SLF88. The highest identity of 99.2 % for amino acid (18 differences) appeared among DL3, AH2 and FH3, and the lowest identity of 96.8 % (72 differences) between DL3 and SLF88. Based upon comparisons of the VP1/2A junction and the VP1 amino terminus, DL3 was classified as subgenotype IA. Phylogenetic analysis showed that DL3 was closest to the isolates in Japan.

CONCLUSION: The sequence comparison and phylogenetic analysis revealed that DL3 is most similar to the isolates in Japan, suggesting the epidemiological link of hepatitis A happened in China and Japan.

Liu GD, Hu NZ, Hu YZ. Full-length genome of wild-type hepatitis A virus (DL3) isolated in China. *World J Gastroenterol* 2003; 9 (3): 499-504

<http://www.wjgnet.com/1007-9327/9/499.htm>

INTRODUCTION

Hepatitis A virus (HAV) is an important human pathogen causing hepatitis, with a higher incidence in developing countries than that in developed countries. Direct person-to-person spread by the fecal/oral route is the most important means of transmission of hepatitis A, and infection with HAV

can cause sporadic and epidemic acute hepatitis in humans^[1,2]. Although improvements in sanitation have led to a significant reduction in the endemicity of hepatitis A virus infection, hepatitis A is still the most common viral hepatitis infection and a cause of substantial morbidity in China.

HAV is classified as one of two members of the genus *Hepatovirus* within the family *Picornaviridae*^[3,4]. HAV virion is a naked, spherical particle with a diameter of 27-32 nm. The virion consists of a genome of a linear, single-stranded, 7.5-kb positive-sense RNA and of a protein shell made up of three major proteins, VP1-VP3^[1,5]. The genome can be divided into a long 5' terminal untranslated region (5' UTR) of about 735 nucleotides, a large open reading frame encoding a polyprotein of 2 227 amino acids, a short 3' UTR with a polyA tail. The HAV polyprotein is co- and posttranslationally cleaved into smaller structural proteins (VP1, VP2, VP3 and a putative VP4) and nonstructural proteins (2A, 2B, 2C, 3A, 3B, 3C and 3D) by the virus-encoding proteinase^[6].

Human isolates of HAV possess a single serotype, and monoclonal antibodies raised to various isolates of human HAV have failed to distinguish between individual isolates. However, the nucleotide sequencing of selected genome regions that encode the putative VP1/2A junction region of wild-type HAV isolates present in human specimens has demonstrated significant sequence heterogeneity^[7]. Using this approach, HAV isolates could be differentiated into seven unique genotypes based upon the sequence of the VP1/2A junction region. A genotype is defined as a group of viruses that differed from each other by no more than 15 %, and a subgenotype as a group of viruses with >92.5 % nucleotide sequence identity^[7].

Until now, complete nucleotide sequences of eleven different human wild-type HAV isolates and partial nucleotide sequences of wild-type isolates or cell-adaptative variants of HAV have been reported^[8-19]. These isolates were isolated from hepatitis A epidemic of diverse geographic origin, including partial sequence of the isolates from fulminant hepatitis A in Shanghai in 1988^[7]. But the complete nucleotide sequence of genome of the isolate from China remains unknown. In order to elucidate the genetic characteristics and molecular epidemiology and evolution of wild-type HAV in China, we determined the complete nucleotide sequence of genome of an acute HAV isolate (DL3) from Dalian, and compared the complete genome sequences and deduced amino acid sequence of isolate DL3 with those of other eleven wild-type HAV isolates. There are significant differences and identities among the twelve independent isolates.

MATERIALS AND METHODS

Virus sample

Wild-type human HAV isolate DL3 was recovered from stool specimens stored at -70 °C from an patient with acute hepatitis A, infected during an outbreak at Dalian, Liaoning Province, and was named as DL3. HAV contained in stool were identified by ELISA, immune precipitation and immune electron microscopy. The concentrated and purified HAV for RT-PCR were prepared by chloroform extraction for three times from 10 % of stool supernatant, followed by discontinuous sucrose/glycerol density gradient ultracentrifugation^[20].

cDNA synthesis and cloning

Antigen-capture RT-PCR was used to prepare cDNA of DL3 genome^[21], with some modifications. Sterile 0.5-ml conical tube (Eppendorf) was coated with 100 µl of human anti-HAV IgG diluted 1:1 000 in 50 mM sodium carbonate buffer (pH 9.6). After 4 h of incubation at 37 °C, the unbound IgG was removed, and 150 µl of 1 % bovine serum albumin (Sigma) diluted in the buffer was added. After 1 h at 37 °C, the tube was washed three times with 300 µl of PBS (pH 7.4) containing 0.05 % Tween 80. Purified HAV (100 µl) was added, and the preparation was incubated overnight at 4 °C. The tube was washed six times with 500 µl of a 40 mM Tris (pH 8.4) -40 mM KCL-7 mM MgCl₂ solution. Then 100 µl of water was added and tube was heated to 95 °C for 5 min to disrupt captured viruses and melt any secondary structures within the viral RNA. The first strand cDNA was synthesized using Superscript™ First-Strand Synthesis System for RT-PCR kit (Gibco, Life Technologies), following the instruction by manufacturer. Oligo (dT)₁₈ was used as primer. The partial sequencing showed that subgenotype of isolate from Shanghai in 1988 was IA^[7], the oligonucleotide primers (Table 1) corresponding to the nucleotide sequence of wild-type HAV isolate GBM^[16] were designed to produce subgenomic overlapping HAV fragments with an average length of about 1 000bp which cover the entire HAV genome. The clones of different fragments were performed by PCR in a mixture (50 µl) including 5 µl 10×LA PCR buffer, 8 µl 2.5mM dNTPs, 2 µl template of RT-PCR products, 300 nM positive-sense primer, 300 nM negative-sense primer and 2.5U *Taq* DNA polymerase (TaKaRa). The reaction mixture was subjected to 95 °C for 5 min, then 30 automated cycles of denaturation at 95 °C for 30 sec, annealing at 50 °C for 30 sec, and extension at 72 °C for 1 min or 1 min 30 sec. After the PCR products were recovered and purified, the fragments were ligated into pGEM®-T Vector (Promega). The resulting products were transformed into competent *E. coli* DH5α cells. Three ampicillin-resistant clones were picked out for each fragment. The size of inserts in positive clones was estimated with restriction enzyme site at either side of the inserted fragment. Rapid plasmid preparations were made with the Wizard plasmid purification kit (Promega).

Table 1 The primers used for amplification of DL3 genomic RNA

Clones	Primers	Sequences
A (0.8kb)	5' RACE RT-primer	5-(P)GCAGAATGAATC-3
	5' RACE A1	5-AGTCCGTTGATAGGACTGAG-3
	5' RACE S1	5-TGTTCTTCCTCAATATCTGCC-3
	5' RACE A2	5-TTCTAAGAAGACTCAGGGGG-3
	5' RACE S2	5-CTGGAAAATTCCTTGTGTTGGCC-3
B (0.5kb)	B1	5-GCTGAGGTACTCAGGGGC-3
	B2	5-AGGATAAACAGTCAAGGATGC-3
C (1.1kb)	C1	5-ACATATGCAAGATTTGGCATTG-3
	C2	5-ATCCATAGCATGATAAAGAGG-3
D (1.0kb)	D1	5-CCTGGATTCTGACACTCC-3
	D2	5-CAGTGGATAACATGGCATTG-3
E (1.1kb)	E1	5-TCTGTACAGACAATCAGAG-3
	E2	5-AATCCCTGAACAAATGTCTCC-3
F (1.2kb)	F1	5-TCCAGAATGATGGAGCTGAG-3
	F2	5-CTTCGACAAGCACTCCAAG-3
G (1.2kb)	G1	5-AGTTCCTTAGTAATGACAGTTG-3
	G2	5-GCCATTGGATCAATCTCAGC-3
H (1.1kb)	H1	5-AAGTGAATTTTCTCAGTGTTC-3
	H2	5-GTCCAATCAAGTCAAGATTATC-3
I (0.5kb)	I1	5-GATTCTCTGTTATGGAGATG-3
	I2	5-TTTTTTTTTTTTTTTTTTTTATTT-3

DNA sequencing and analysis

Sequencing strategy of genome of DL3 was showed in Figure 1. Oligonucleotide primers specific for HAV and primers corresponding to the T7/SP6 promoter region of pGEM®-T Vector were used to sequence the inserted and identified HAV fragment. A *Taq* DyeDeoxy Terminator Cycle sequencing kit and a 377 DNA sequencer (Perkin Elmer) were used to determine nucleotide sequences. To eliminate the possibility of errors in the sequence due to *Taq* polymerase for PCR, at least three clones of each amplified fragment, derived from two individual PCR products, were sequenced. Also to correctly determine the sequence of extreme 5' terminus of HAV genome, a 5' RACE reaction^[22] was used to obtain the a cDNA fragment from 5' UTR of genome with 5' -Full RACE Core Set (TaKaRa). Analysis, alignment and translation in the amino acids of the obtained nucleotide sequences were done using the sequence analysis program OMEGA2.0 (Oxford Molecular).

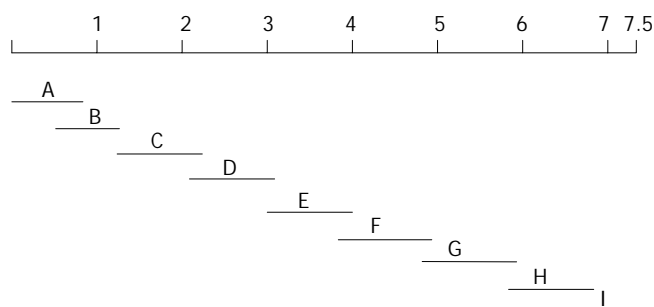


Figure 1 Sequencing strategy of genome of DL3.

Phylogenetic analysis

Multiple alignments of genome sequences of twelve HAV isolates were done using the Clustal W Program^[23]. Phylogenetic tree was calculated from genomes to determine the association of DL3 with other eleven wild-type HAV isolates with Vector NTI Suite6.0 software using the Neighbor Joining method^[24].

Reference isolates

The accession numbers of the sequences included in the analysis were as follows: LA, K02990; HM175, M14707; MBB, M20273; GBM, X75215; AH1: AB020564; AH2: AB020564 AB020565; AH3: AB020564 AB020566; FH1: AB020567; FH2: AB020568; FH3: AB020569; SLF88, AY032861.

RESULTS

Complete nucleotide sequence of DL3 genome and deduced amino acids

The Complete nucleotide sequence of DL3 has been deposited into GenBank under the accession no. AF512536.

The genome was 7 476-nucleotide long and encoded a polyprotein of 2 227 amino acids. The genome contained a 5' UTR of 732 nucleotides that was two nucleotides shorter than that of HAV HM175/WT. The long open reading frame coding for polyprotein was started at base 733 by codon AUG and terminated at base 7 416 by codon UGA followed by a second stop codon (UAA) 7 nucleotides downstream. The 3' UTR consisted of 63 nucleotides. The base composition was 28.96 % A (2165), 16.08 % C (1 202), 22.11 % G (1 653) and 32.85 % U (2 456). The G+C content is 38.19 %.

The 5' UTR contained three main pyrimidine-rich tracts. The first region, near the 5' terminus (nucleotide99- 138), had

a 92.3 % pyrimidine content. The second region (nucleotide 204- 250) had a 83 % pyrimidine content. The third tract (nucleotide 711- 725) with a 93.9 % pyrimidine content lay immediately before the initiation codon. The 5' UTR had a G+C content of 46.29 % which is higher than that of the genome.

Comparisons with other isolates

The complete nucleotide sequence and deduced amino acid

sequences of HAV DL3 have been compared with those of reported wild-type isolates (Table 2, Table3). DL3 had the highest identity of 97.5 % for nt (185 differences) with AH1, but the highest identity of 99.2 % for amino acid (18 differences) with AH2 and FH3. DL3 shared the lowest identities of 85.7 % for nucleotide (1 066 differences) and 96.8 % for amino acid (72 differences) with SLF88. Most of the changes were nucleotide transitions.

Table 2 Nucleotide identities of full-length genomes between DL3 and reference isolates

	Numbers of nucleotide differences/identity										
	AH1	AH2	AH3	FH1	FH2	FH3	GBM	LA	HM175	MBB	SLF88
Full	185/97.5	263/96.5	307/95.9	282/96.2	200/97.3	199/97.3	323/95.7	344/95.4	642/91.4	659/91.2	1066/85.7
5' NTR	15/98.0	29/96.0	25/96.6	16/97.8	13/98.2	13/98.2	18/97.4	14/98.1	38/94.8	50/93.1	84/88.5
VP4	1/98.6	2/97.1	4/94.2	2/97.1	2/97.1	2/97.1	3/95.7	2/97.1	7/89.9	7/89.9	8/88.4
VP2	15/97.7	25/96.2	28/95.8	24/96.4	18/97.3	24/96.4	39/94.1	28/95.8	58/91.3	58/91.3	98/85.3
VP3	15/98.0	25/96.6	28/96.2	27/96.3	13/98.2	23/96.9	35/95.3	40/94.6	67/90.9	63/91.5	114/84.6
VP1	23/97.2	27/96.7	25/97.0	23/97.2	22/97.3	13/98.4	30/96.4	44/94.6	76/90.8	78/90.5	124/84.9
2A	5/97.7	10/95.3	11/94.8	9/95.8	3/98.6	9/95.8	9/95.8	12/94.4	17/92.0	14/93.4	27/87.3
2B	13/98.3	26/96.5	29/96.1	46/93.9	18/97.6	28/96.3	33/95.6	37/95.1	75/90.0	73/90.3	99/86.9
2C	30/97.0	42/95.8	42/95.8	44/95.6	35/96.5	35/96.5	52/94.8	55/94.5	114/88.7	120/88.1	152/84.9
3A	1/99.5	4/98.2	4/98.2	9/95.9	4/98.2	3/98.6	13/94.1	8/96.4	14/93.7	18/91.9	23/89.6
3B	1/98.6	1/98.6	2/97.1	3/95.7	3/95.7	0	2/97.1	3/95.7	6/91.3	7/89.9	12/82.6
3C	14/97.9	20/97.0	24/96.3	25/96.2	16/97.6	21/96.8	30/95.4	27/95.9	56/91.5	50/92.4	98/85.1
3D	51/96.5	51/96.5	84/94.3	53/96.4	52/96.5	27/98.2	57/96.1	64/95.6	113/92.3	114/92.2	209/85.8
3' NTR	1/98.4	1/98.4	1/98.4	1/98.4	1/98.4	1/98.4	2/96.8	10/84.4	1/98.4	7/88.9	18/71.4

Table 3 Amino acid identities of full-length genomes between DL3 and reference isolates

	Numbers of amino acid differences/identity										
	AH1	AH2	AH3	FH1	FH2	FH3	GBM	LA	HM175	MBB	SLF88
Full	21/99.1	18/99.2	36/98.4	28/98.7	21/99.1	18/99.2	36/98.4	34/98.5	35/98.4	49/97.8	72/96.8
VP4	1/95.7	1/95.7	1/95.7	1/95.7	1/95.7	1/95.7	1/95.7	1/95.7	1/95.7	1/95.7	2/91.3
VP2	0	0	0	1/99.5	0	0	1/99.5	0	2/99.1	2/99.1	1/99.5
VP3	1/99.6	1/99.6	1/99.6	2/99.2	1/99.6	1/99.6	1/99.6	1/99.6	2/99.2	2/99.2	4/98.4
VP1	0	0	0	1/99.6	0	1/99.6	2/99.3	13/95.3	1/99.6	2/99.3	2/99.3
2A	1/98.6	1/98.6	1/98.6	1/98.6	1/98.6	0	1/98.6	0	1/98.6	2/97.2	1/98.6
2B	2/99.2	2/99.2	3/98.8	5/98.0	5/98.0	5/98.0	3/98.8	4/98.4	4/98.4	6/97.6	6/97.6
2C	6/98.2	5/98.5	4/98.8	6/98.2	5/98.5	4/98.8	7/97.9	5/98.5	11/96.7	17/94.9	14/95.8
3A	0	1/98.6	1/98.6	1/98.6	0	0	5/93.2	1/98.6	1/98.6	3/95.9	1/98.6
3B	0	0	0	0	0	0	1/95.7	0	0	0	0
3C	2/99.1	2/99.1	3/98.6	2/99.1	2/99.1	2/99.1	3/98.6	2/99.1	2/99.1	2/99.1	8/96.3
3D	8/98.4	5/99.0	22/95.5	8/98.4	6/98.8	4/99.2	11/97.8	7/98.6	10/98.0	12/97.5	33/93.3

5' Untranslated region

The 5' UTR of HAV forms conserved and highly ordered secondary structure and plays an important role in controlling viral translation^[25, 26]. Comparisons with eleven other isolates in 5' UTR showed that DL3 shared the lowest identity of 88.5 % (84 nucleotide changes) with SLF88, the highest identity of 98.2 % (13 nucleotide changes) with FH2 and FH3. There were a G deletion at position 28 and a T deletion at position 102 compared with HM175 and MBB. In contrast to the comparison with complete nucleotide sequence, identities of 5' UTR for DL3 with other isolates were higher than that of complete genomes except the identity with AH2, which suggested that the 5' UTR of HAV was conserved. In contrast to ribosomes scanning from the capped 5' ends of the majority of cellular mRNA, the long and highly structured 5' UTR of HAV mediated the binding of ribosomal subunits internally at internal ribosome entry site (IRES) of nucleotide 324 to nucleotide 692 (base position was corresponding to HM175/WT) that directed cap-independent initiation of viral translation at correct AUG codon^[25, 26]. In this region DL3 shared higher identities of 97.9 %, 98.4 %, 99.2 %, 98.6 %, 98.6 %, 95.9 %, 95.4 % and 94.9 % with AH2, FH1, FH2, FH3, LA, HM175, MBB and SLF88 than that in whole 5' UTR. But DL3 was identical to SLF88 between nucleotide 223 to nucleotide 371 (base position is corresponding to HM175/WT). The result suggested higher conservative and importance of common secondary structure of IRES in initiation of viral translation.

Coding region

The open reading frame of HAV RNA encoding a large polyprotein with 2 227 amino acids was divided into P1, P2 and P3 region. The P1 region encodes structural or capsid proteins, VP4, VP2, VP3 and VP1. The P2 and P3 region encoded nonstructural proteins, 2A, 2B, and 2C, and 3A, 3B, 3C and 3D, respectively. In coding region, the amino acid differences for the structural and nonstructural proteins of twelve isolates are showed in Table 3. In contrast to the high heterogeneous of nucleotide sequences, the amino acid sequences were highly conserved among twelve wild-type isolates. Comparisons within the coding region (6 681 nucleotides) of DL3 and SLF88 yielded 964 nucleotide changes (14.4 % difference), resulting in only 72 amino acid substitutions (3.2 % difference). In comparison with eleven isolates, DL3 had the highest identity (99.2 %) of amino acids with AH2 and FH3, lowest identity (96.8 %) with SLF88.

P1 region, the structural protein region of HAV, consisted of 2 295 nucleotides and encodes 765-amino acid polypeptide which was processed into four structural proteins, VP4, VP2, VP3 and VP1. The capsid protein of HAV consisted of VP1, VP2 and VP3. The presence of a fourth protein VP4 has been described repeatedly, but the reported apparent molecular weights (7- 14kD) contrasted sharply with those predicted from nucleic acid sequence data (1.5 or 2.3kD). Conclusive physical identification of VP4 was still unavailable. The alignment of amino acid sequence indicated that no amino acid mutation of polyprotein of DL3 occurred at cleavage site of VP4/VP2, VP2/VP3, VP3/VP1, implying the importance of conserved cleavage sites in entire viral structure. In VP4 DL3 shared lowest amino acid sequence identities with other isolates in structural region, 91.3 % identity with SLF88, 95.7 % identity with other ten wild-type isolates. DL3 had a unique amino acid mutation (S to A) at position 4 different from all the other isolates. In VP2 region amino acid sequences were highly conserved. There was 100 % identity between DL3 and AH1, AH2, AH3, FH2, FH3 and LA. And even for DL3 and SLF88, the identity was also up to 99.5 %. In VP3 region DL3 had another unique amino acid mutation (K to R) at position 47 different from all the other isolates. It had been reported that

VP1 had the most amino acid diversity of the capsid proteins^[16]. But it was not the case for DL3. In VP1 region there was 100 % amino acid sequence identity between DL3 and AH1, AH2, AH3 and FH2. The highest difference was between DL3 and LA (13 amino acid differences, 95.3 % identity), just because one amino acid was inserted into the LA between amino acids 540-548, at which a cluster of 8 amino acids was altered due to 3 changes in the open reading frame resulting from the insertion of 3 nucleotides.

The HAV P2 region encoded nonstructural proteins 2A, 2B and 2C. The proposed 2A region encoded for 71 amino acids, but the exact function of 2A was not yet determined. Recent study revealed that 2A protein might participate in virion morphogenesis^[27]. 2B and 2C proteins were found to have 251 and 335 amino acids residues, respectively. Both proteins playing important roles in the replication of viral RNA were considered significant in host-dependent adaptation since many mutations had been detected in both regions of adapted variants^[28]. HAV 2C protein was considered to have helicase and NTPase activities. With some variants, multiple mutations in P2 contributed to enhance viral replication with 5' UTR and P3 proteins and to express the cytopathic phenotype^[29]. In 2A, 2B and 2C proteins, 2C protein was the most variable between twelve isolates, DL3 shared the lowest identity of 94.9 % (17 amino acid differences) with MBB and the highest identity of 98.8 % with AH3 and FH3 (only 4 amino acid differences). In contrast, 2B was more conservable. The 99.2 % identities of DL3 with AH1 and AH2 and the 98.8 % identities of DL3 with AH3 and GBM revealed high conservation of 2B protein among wild-type viruses. It has been reported that a little more amino acid substitutions seemed to be found in FH than in AH in 2B region^[18]. This research also showed that more amino acid substitutions were found in FH than that in AH when compared with DL3, suggesting the possible association between the severity of hepatitis A and amino acid substitutions in 2B region.

The HAV P3 region encoded 3A, 3B, 3C and 3D proteins with 74, 23, 219 and 489 amino acids, respectively. 3A functioned as pre-Vpg, 3B was a genome-linked viral protein (Vpg), 3C was the sole protease for HAV protein processing. The recombinant HAV 3C prepared in *E. coli* catalyzed the putative cleavage sites and released mature or intermediate proteins, VP0, VP3, VP1-2A, VP1, 2A, 2B, 2BC, 2C, 3ABC, 3AB, 3C and 3D^[30-34]. 3D was an RNA-dependent RNA polymerase. By comparison, 3B protein showed highest amino acid sequence homology, with 100 % identities among eleven isolates except 95.7 % identity between DL3 and GBM. Compared with 3D proteins, 3C protein showed higher amino acid sequence identities in all twelve isolates. In this protein, DL3 shared the 96.3 % identity with SLF88, 98.6 % with AH3 and GBM, and the highest identity 99.1 % with the other eight isolates. The comparison indicated that high conservation of 3C protein in wild-type HAV played an important role in the replication of virus. 3D among isolates of genotype I showed no significant variation. But the 3D polymerase of SLF88 showed low identity with that of DL3, with only 93.3 % identity (33 amino acid differences). GBM showed a little higher variability among the eleven reference isolates in P3 region, especially for 3A and 3D. The identities for these two proteins between DL3 and GBM were 93.2 % (5 amino acid differences) and 97.8 % (11 amino acid differences), respectively. Even for 3B, GBM had 1 amino acid difference with DL3.

3' Untranslated region

The 3' UTR of DL3 was 63-nucleotide long, the same as those of 9 isolates, 1 nucleotide less than that of LA, and 14 nucleotides more than that of SLF88. All twelve isolates had two stop codons, separated by 6 nucleotides. The 3' UTR

exhibited the great identity in nucleotide sequence between DL3 and isolates from Japan, GBM and HM175, with only 1 or 2 nucleotide difference. But for DL3 and the other 3 isolates, identities were lower, especially 71.4% between DL3 and SLF88.

Subgenotype classification

Alignment analysis of 168 nucleotides in VP1/2A (nucleotide 3 024- 3 191) of DL3 with other eleven wild-type isolates revealed that DL3 had >92.5 % identities with six Japanese isolates, LA and GBM (IA subgenotype), <92.5 % identity with HM175 (IB subgenotype), and only 83.9 % identity with SLF88 (the newly determined isolate of genotype VII). According to these comparison, DL3 was classified as subgenotype IA. Something strange was that comparison of the same region between DL3 and MBB showed 94 % identity, suggesting DL3 to be subgenotype IB. To solve this paradox, the VP1 amino terminus (nucleotide 2 208- 2 468) of DL3 was compared with isolate MBB. The result showed DL3 belonged to subgenotype IA.

Phylogenetic relationships

Phylogenetic relations of various HAV wild-type isolates were analyzed on the genomes of twelve isolates (Figure 2). The result showed that twelve wild-type isolates formed four main subclusters, subcluster I contained DL3, AH1, FH2 and FH3, subcluster II contained AH2 and AH3, subcluster III contained LA and GBM, and subcluster IV contained MBB and HM175. Subcluster I, II, III and FH1 composed of subgenotype IA cluster. SLF88 located near this cluster. By this phylogenetic analysis DL3 isolate showed closer phylogenetic affiliation to AH1 and FH2. Besides, the comparison of full-length genome of nine isolates showed DL3 had higher identity with AH1 and FH2 than those with GBM, LA, HM175, MBB and SLF88. The analysis suggested that phylogenetic relations of various HAV wild-type isolates correlated with geographical region.

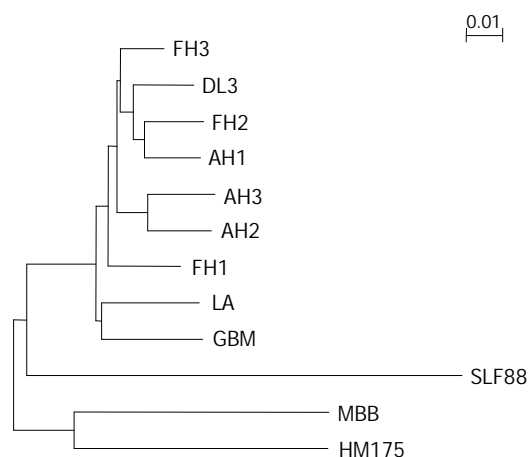


Figure 2 Phylogenetic relations of DL3 full-length genome to those of other HAV.

DISCUSSION

Although hepatitis A remains a disease of major public health importance in China, the study on the genome of wild-type HAV isolate in China has not been reported. Here, we analyzed the full-length genome of a wild-type HAV isolate DL3 in China. The genome sequence of DL3 contained 7 476 nucleotides, dividing into three regions, 732-nucleotide 5' UTR, 6 681-nucleotide ORF coding for a polyprotein of 2 227 amino acid, 63-nucleotide 3' UTR.

Sequence comparisons of genomes showed DL3 shared the highest nucleotide identity (97.5 %) with AH1 and amino

acid identity (99.2 %) with AH2 and FH3, and lowest nucleotide identity (85.7 %) and amino acid identity (96.8 %) with SLF88. But the nucleotide sequence and amino acid sequence differences were not evenly distributed along the genome in all isolates. The 5' UTR region showed high conservatism, and even SLF88 is 88.5 % identical to DL3, an identity higher than that of full-length genome. This suggests the importance of this region for HAV. The 3' UTR region showed high identities between DL3 and other isolates of genotype I. When compared with SLF88, DL3 had high divergence of 28.6 % with SLF88, which lead to 18 nucleotide changes, including 14 deletions and 4 mutations. Although the exact function of 3' UTR is unknown, several studies have revealed that sequence elements within the 3' UTR are expected to play an important role in initiation and regulation of synthesis of HAV RNA^[35, 36]. The high heterogeneity between DL3 and SLF88 in the 3' UTR may suggest the difference of the replicating characteristics between DL3 and SLF88.

In structural region, the highest difference (13 amino acid differences, between DL3 and LA) existed in VP1. But this high divergence was due to 1 amino acid insertion into LA. For DL3 and other eleven isolates, high homology was observed, and the high variability of VP1 reported early was not observed. In nonstructural region the majority of amino acid identities between DL3 and other eleven isolates appeared in 3B and 3C proteins, implying that both proteins play important roles in the replication of virus and the processing of polyprotein. Differences between DL3 and other isolates of subgenotype IA in 2C region were a little more than those in 2B region. But differences between DL3 and other isolates of subgenotype IB or SLF88 in 2C region were much more than those in 2B region. SLF88 had 33 amino acid mutations with DL3 in 3D, suggesting the polymerase of SLF88 may have different efficiency compared with DL3.

Based on the higher nucleotide sequence identities of DL3 with AH1 and FH2 in the whole 7 476-nucleotide genome (97.5 % and 97.3 %, respectively), 732-nucleotide 5' UTR region (98.0 % and 98.2 %, respectively), 63-nucleotide 3' UTR region (98.4 % for both), 168-nucleotide region of subgenotype classification (98.2 %), 6681-nucleotide ORF (97.5 % and 97.2 %, respectively), DL3 is found to be in phylogenesis closest to AH1 and FH2. So we proposed that DL3, AH1 and FH2 probably represent different isolates of the same strain. Moreover, it is noteworthy that Japan where AH1 and FH2 were isolated geographically close to China, where DL3 was isolated. The phylogenetic affiliation and geographical closure suggested the epidemiological link of hepatitis A happened in Dalian and Japan.

By comparison of VP1/2A junction, genotypes were defined by at least 15 %, and subgenotypes differed by at least 7.5 %. According to this, we defined DL3 as subgenotype IA by comparisons with isolates HM175, AH1, AH2, AH3, FH1, FH2 and FH3. Interestingly, comparisons of this region with isolate MBB showed DL3 to be subgenotype IB. To solve this paradox, the VP1 amino terminus of DL3 was compared with isolate MBB. The comparison showed DL3 belonged to subgenotype IA. This suggests that it may not be so accurate to define a genotype only by comparison of VP1/2A junction. And the more accurate result may be achieved by comparison of more nucleic acid fragments.

REFERENCES

- 1 **Lemon SM.** Type A hepatitis: new developments in an old disease. *N Engl J Med* 1985; **313**: 1059-1067
- 2 **Cuthbert JA.** Hepatitis A: old and new. *Clin Microbiol Rev* 2001; **14**: 38-58
- 3 **Minor PD.** Picornaviridae. In Francki RIB, Fauquet CM, Kundson

- DL, Brown F, eds. Archives of Virology, Supplement 2. New York: Springer-Verlag 1991: 320-326
- 4 **Marvil P**, Knowles NJ, Mockett APA, Britton P, Brown TDK, Cavanagh D. Avian encephalomyelitis virus is a picornavirus and is most closely related to hepatitis A virus. *J Gen Virol* 1999; **80**: 653-662
- 5 **Weitz M**, Siegl G. Hepatitis A virus: structure and molecular virology. In: Zuckerman AJ, Thomas HC. Viral hepatitis. 2nd edition. London: Churchill Livingstone 2001: 15-27
- 6 **Totsuka A**, Moritsugu Y. Hepatitis A virus proteins. *Intervirology* 1999; **42**: 63-68
- 7 **Robertson BH**, Jansen RW, Khanna B, Totsuka A, Nainan OV, Siegl G, Widell A, Margolis HS, Isomura S, Ito K, Ishizu T, Moritsugu Y, Lemon SM. Genetic relatedness of hepatitis A virus strains recovered from different geographical regions. *J Gen Virol* 1992; **73**: 1365-1377
- 8 **Ticehurst JR**, Racaniello VR, Baroudy BM, Baltimore D, Purcell RH, Feinstone SM. Molecular cloning and characterization of hepatitis A virus cDNA. *Proc Natl Acad Sci USA* 1983; **80**: 5885-5889
- 9 **Linemeyer DL**, Menke JG, Martin-Gallardo A, Hughes JV, Young A, Mitra SW. Molecular cloning and partial sequencing of hepatitis A viral cDNA. *J Virol* 1985; **54**: 247-255
- 10 **Najarian R**, Caput D, Gee W, Potter SJ, Renard A, Merryweather J, Van Nest G, Dina D. Primary structure and gene organization of human hepatitis A virus. *Proc Natl Acad Sci USA* 1985; **82**: 2627-2631
- 11 **Venuti A**, Di Russo C, Del Grosso N, Patti A-M, Ruggeri F, Stasio RP, Martiniello GM, Pagnotti P, Degener AM, Midulla M, Pana A, Perez-Bercoff R. Isolation and molecular cloning of a fast-growing isolate of human hepatitis A virus from its double-stranded replicative form. *J Virol* 1985; **56**: 579-588
- 12 **Robertson BH**, Brown VK, Bradley DW. Nucleic acid sequence of the VP1 region of attenuated MS-1 hepatitis A virus. *Virus Res* 1987; **8**: 309-316
- 13 **Cohen JJ**, Ticehurst JR, Purcell RH, Buckler-White A, Baroudy BM. Complete nucleotide sequence of wild-type hepatitis A virus: Comparison of different isolates of hepatitis A virus and other picornaviruses. *J Virol* 1987; **61**: 50-59
- 14 **Paul AV**, Tada H, von der Helm K, Wissel T, Kiehn R, Wimmer E, Deinhardt F. The entire nucleotide sequence of the genome of human hepatitis A virus (isolate MBB). *Virus Res* 1987; **8**: 153-171
- 15 **Khanna B**, Spelbring JE, Innis BL, Robertson BH. Characterization of a genetic variant of human hepatitis A virus. *J Med Virol* 1992; **36**: 118-124
- 16 **Graff J**, Normann A, Feinstone SM, Flehmig B. Nucleotide sequence of wild-type hepatitis A virus GBM in comparison with two cell culture-adapted variants. *J Virol* 1994; **68**: 548-554
- 17 **Beneduce F**, Pisani G, Divizia M, Pana A, Morace G. Complete nucleotide sequence of a cytopathic hepatitis A virus isolate isolated in Italy. *Virus Res* 1995; **36**: 299-309
- 18 **Fujiwara K**, Yokosuka O, Fukai K, Imazeki F, Saisho H, Omata M. Analysis of full-length hepatitis A virus genome in sera from patients with fulminant and self-limited acute type A hepatitis. *J Hepatol* 2001; **35**: 112-119
- 19 **Ching KZ**, Nakano T, Chapman LE, Demby A, Robertson BH. Genetic characterization of wild-type genotype VII hepatitis A virus. *J Gen Virol* 2002; **83**: 53-60
- 20 **Bishop NE**, Hugo DL, Borovec SV, Anderson DA. Rapid and efficient purification of hepatitis A virus from cell culture. *J Virol Med* 1994; **47**: 203-216
- 21 **Jansen RW**, Siegl G, Lemon SM. Molecular epidemiology of human hepatitis A virus defined by an antigen-capture polymerase chain reaction method. *Proc Natl Acad Sci USA* 1990; **87**: 2867-2871
- 22 **Frohman MA**, Dush MK, Martin GR. Rapid production of full-length cDNAs from rare transcripts: amplification using a single gene-specific oligonucleotide primer. *Proc Natl Acad Sci USA* 1988; **85**: 8998-9002
- 23 **Thompson JD**, Higgins DG, Gibson TJ. Clustal W: improving the sensitivity of progressive multiple sequence alignment through sequence weighting, position-specific gap penalties and weight matrix choice. *Nucleic Acids Res* 1994; **22**: 4673-4680
- 24 **Saitou N**, Nei M. The neighbor-joining method: a new method for reconstructing phylogenetic trees. *Mol Biol Evol* 1987; **4**: 406-425
- 25 **Brown EA**, Day SP, Jansen RW, Lemon SM. The 5' nontranslated region of hepatitis A virus RNA: secondary structure and elements required for translation *in vitro*. *J Virol* 1991; **65**: 5828-5838
- 26 **Brown EA**, Zajac AJ, Lemon SM. *In vitro* characterization of an internal ribosome entry site (IRES) present within the 5' nontranslated region of hepatitis A virus RNA: comparison with the IRES of encephalomyocarditis virus. *J Virol* 1994; **68**: 1066-1074
- 27 **Cohen L**, Benichou D, Martin A. Analysis of deletion mutants indicated that the 2A polypeptide of hepatitis A virus participates in virion morphogenesis. *J Virol* 2002; **76**: 7495-7505
- 28 **Emerson SU**, Huang YK, Purcell RH. 2B and 2C mutations are essential but mutations throughout the genome of HAV contribute to adaptation to cell culture. *Virol* 1993; **194**: 475-480
- 29 **Zhang H**, Chao SF, Ping LH, Grace K, Clarke B, Lemon SM. An infectious cDNA clone of a cytopathic hepatitis A virus: genomic regions associated with rapid replication and cytopathic effect. *Virol* 1995; **212**: 686-697
- 30 **Schultheiss T**, Kusov YY, Gauss-Muller V. Proteinase 3C of hepatitis A virus (HAV) cleaves the HAV polypeptide P2-P3 at all sites including VP1/2A and 2A/2B. *Virol* 1994; **198**: 275-281
- 31 **Schultheiss T**, Sommergruber W, Kusov Y, Gauss-Muller V. Cleavage specificity of purified recombinant hepatitis A virus 3C proteinase on natural substrates. *J Virol* 1995; **69**: 1727-1733
- 32 **Probst C**, Jecht M, Gauss-Muller V. Processing of proteinase precursors and their effect on hepatitis A virus particle formation. *J Virol* 1998; **72**: 8013-8020
- 33 **Harmon SA**, Updike W, Jia XY, Summers DF, Ehrenfeld E. Polyprotein processing in cis and in trans by hepatitis A virus 3C protease cloned and expressed in Escherichia coli. *J Virol* 1992; **66**: 5242-5247
- 34 **Malcolm BA**, Chin SM, Jewell DA, Stratton-Thomas JR, Thudium KB, Ralston R, Rosenberg S. Expression and characterization of recombinant hepatitis A virus 3C proteinase. *Biochemistry* 1992; **31**: 3358-3363
- 35 **Nuesch JP**, Weitz M, Siegl G. Proteins specifically binding to the 3' untranslated region of hepatitis A virus RNA in persistently infected cells. *Arch Virol* 1993; **128**: 65-79
- 36 **Kusov Y**, Weitz M, Dollenmeier G, Gauss-Muller V, Siegl G. RNA-protein interactions at the 3' end of the hepatitis A virus RNA. *J Virol* 1996; **70**: 1890-1897

Edited by Zhang ZJ

Glucose intolerance in Chinese patients with chronic hepatitis C

Liang-Kung Chen, Shinn-Jang Hwang, Shih-Tzer Tsai, Jiing-Chyuan Luo, Shou-Dong Lee, Full-Young Chang

Liang-Kung Chen, Shinn-Jang Hwang, Department of Family Medicine, Department of Medicine, Taipei Veterans General Hospital and National Yang-Ming University School of Medicine, Taipei, Taiwan, China

Shinn-Jang Hwang, Jiing-Chyuan Luo, Shou-Dong Lee, Full-Young Chang, Division of Gastroenterology, Department of Medicine, Taipei Veterans General Hospital and National Yang-Ming University School of Medicine, Taipei, Taiwan, China

Shih-Tzer Tsai, Division of Endocrinology and Metabolism, Department of Medicine, Taipei Veterans General Hospital and National Yang-Ming University School of Medicine, Taipei, Taiwan, China

Correspondence to: Shinn-Jang Hwang, M.D., F.A.C.G., Department of Family Medicine, Taipei Veterans General Hospital, No. 201, Shih-Pai Road Sec 2, Taipei, 11217, Taiwan, China. sjhwang@vghtpe.gov.tw
Telephone: +886-2-28757460 **Fax:** +886-2-28737901

Received: 2002-07-31 **Accepted:** 2002-11-04

Abstract

AIM: To investigate the prevalence and the risk factors of glucose intolerance in Chinese patients with chronic hepatitis C and to evaluate the relationship between interferon (IFN) treatment and glucose intolerance in these patients.

METHODS: Prospective cross-sectional study was done to evaluate the prevalence of glucose intolerance in Chinese patients with chronic hepatitis C virus (HCV) infection from the outpatient clinic of Department of Family Medicine, Taipei Veterans General Hospital. Chronic hepatitis C was defined as persistent presence of anti-HCV and persistent elevation of liver transaminase for at least 1.5 folds for at least 6 months. Moreover, patients were further categorized into normal fasting glucose and glucose intolerance (diabetes mellitus (DM) and impaired fasting glucose) according to the diagnostic criteria of American Diabetic Association.

RESULTS: Totally, 359 Chinese patients with chronic hepatitis C were enrolled (212 males and 147 females, mean age = 58.1 ± 13.0 years). One hundred and twenty-three patients (34.3 %) had received various forms of IFN treatment. One hundred and twenty-five patients (34.6 %) had glucose intolerance, including 99 patients (27.6 %) with DM and 26 patients (7.0 %) with impaired fasting glucose. In comparison with those with normal fasting glucose levels, patients with chronic hepatitis C with glucose intolerance were significantly older, had a significantly higher body mass index, and they were more likely to suffer from obesity, to have family history of diabetes and to have had previous IFN treatment. Stepwise multivariate logistic regression revealed significantly that age ≥ 57 years, obesity, previous history of IFN treatment and the presence of family history of diabetes were independent risk factors associated with the presence of glucose intolerance in chronic hepatitis C patients.

CONCLUSION: In conclusion, 34.6 % of Chinese patients with chronic hepatitis C had glucose intolerance. Chronic hepatitis C patients who were older in age, obese, had previous IFN treatment history and had family history of

diabetes were prone to develop glucose intolerance. To our knowledge, this is the first population-based report to confirm that interferon treatment to be an independent risk factor to develop glucose intolerance.

Chen LK, Hwang SJ, Tsai ST, Luo JC, Lee SD, Chang FY. Glucose intolerance in Chinese patients with chronic hepatitis C. *World J Gastroenterol* 2003; 9(3): 505-508

<http://www.wjgnet.com/1007-9327/9/505.htm>

INTRODUCTION

Hepatitis C virus (HCV) infection has become a common worldwide medical problem. Patients with chronic HCV infection may develop various extrahepatic manifestations including cryoglobulinemia, the presence of serum autoantibodies, glomerulonephritis, sialoadenitis and porphyria cutanea tarda^[1-3]. The association of chronic HCV infection and diabetes mellitus (DM) was first reported by Alison *et al.* in 1994^[4]. Based on case-control studies, the prevalence of DM had been reported in 21 % to 50 % of patients with chronic HCV infection, which was significantly higher than that in the general population or among patients with other diseases^[4-7]. Population surveys from western countries also demonstrated that chronic HCV infection was associated with a high incidence of DM^[5,7]. In addition, the prevalence of anti-HCV was significantly higher in patients with DM than in the general population^[8,9].

The cause of a higher prevalence of DM in patients with chronic HCV infection remains unclear. Altered glucose metabolism has been well documented in patients with chronic liver diseases, especially in patients with liver cirrhosis^[10]. However, patients with HCV-related liver cirrhosis is associated with a significantly higher prevalence of DM than those cirrhotic patients with other etiologies^[1]. Furthermore, recipients of HCV-related liver transplantation were more likely to develop post-transplantation DM when compared to recipients with other etiologies^[6,11]. Therefore, HCV infection *per se* plays an important role in the pathogenesis of DM in patients with chronic HCV infection. Yet, analysis in previous studies rarely considered the confounding factors associated with DM development such as age, obesity and diabetic family history.

Interferon (IFN) has been widely used in the treatment of patients with chronic hepatitis C^[12-16]. Development of DM has also been reported as an adverse effect of IFN- α treatment in patients with chronic hepatitis C^[17,18]. In addition, exacerbation of previous diabetic control has been reported in chronic hepatitis B patients who received IFN- α treatment^[19]. The mechanism of IFN-related DM development or exacerbation of glycemic control remains unclear.

According to the American Diabetic Association (ADA) criteria, DM is diagnosed as repeated fasting plasma glucose ≥ 126 mg/dL, and impaired fasting glucose (IFG) is defined as the fasting plasma glucose >110 mg/dL and <126 mg/dL^[20]. Patients with IFG were reported to be prone to develop DM^[21]. Previous studies focused on the relationship of chronic HCV infection and DM. Patients with IFG were rarely evaluated. The purpose of this study was to evaluate the prevalence of

glucose intolerance (DM and IFG) in Chinese patients with chronic hepatitis C in Taiwan. In addition, risk factors associated with DM development such as age, body mass index (BMI), diabetic family history in first-degree relatives and previous IFN treatment were also evaluated to clarify the possible role of chronic HCV infection in association with the development of DM.

MATERIALS AND METHODS

Demographic data

From July 1999 to June 2001, we conducted a cross-sectional study by enrolling and following patients who were previously or newly diagnosed as chronic hepatitis C in the Office Clinics of Taipei Veterans General Hospital in Taipei, Taiwan. The diagnosis of chronic hepatitis C was based on the presence of serum anti-HCV with or without histological confirmation. At least twice for more than 6 months, all patients had elevated serum alanine aminotransferase levels 1.5-fold above the upper limit of the normal value (>60 U/L). Patients who had positive serum hepatitis B surface antigens and chronic liver diseases were excluded.

According to the ADA diagnostic criterias, diagnosis of DM was established according to the documentation of DM in previous medical records and/or repeated fasting plasma glucose ≥ 7 mmol/L (126 mg/dL), and IFG was diagnosed with a FPG >110 mg/dL and <126 mg/dL^[20]. In this study, both patients with DM and IFG were categorized together as having glucose intolerance to compare them with patients with normal glucose tolerance.

The BMI and family history of DM were recorded for each patient during enrollment. The BMI was expressed as the body weight (in kilograms) divided by the square of the body length (in meter). The family history of diabetes was obtained from the patients themselves and was recorded as positive if their first-degree relatives had DM. Obesity was defined when BMI was >27 Kg/m² in males and >25 Kg/m² in females^[22]. Liver cirrhosis was diagnosed by either liver histology or by characteristic findings in abdominal sonography, computed tomography, celiac angiography and/or the presence of esophageal varices and ascites.

IFN treatment

We recorded details of patients who received IFN treatment, including various regimens of IFN α -2a, IFN α -2b, consensus IFN, subcutaneous injections three times a week, and long-acting pegylated IFN α -2a subcutaneous injections once a week with or without oral ribavirin for either 24 weeks or 48 weeks^[23-26].

Biochemical data

Series of biochemical tests including serum alanine aminotransferase and fasting plasma glucose were measured by using an autoanalyzer (Hitachi sequential multiple autoanalyzer; Model 736, Tokyo, Japan). Antibodies to HCV were measured by using a second-generation enzyme immunoassay containing both structural and non-structural antigens (EverNew, Taipei, Taiwan). Hepatitis B surface antigens were measured by using a radioimmunoassay (Abbott Laboratories, Chicago, IL, USA).

Statistical analysis

Data in the text and tables are expressed as mean \pm standard deviation (mean \pm S.D.). Results were compared between groups depending on the type of data analyzed using the Chi-squared test, Student *t*-test or Mann-Whitney *U*-test. Stepwise multivariate logistic regression (SPSS 10.0, Chicago, IL, USA)

was performed to evaluate the predictive variables associated with the presence of glucose intolerance in patients with chronic hepatitis C. For all tests, results with *P* values less than 0.05 were considered statistically significant.

RESULTS

General data of patients

Totally, 359 patients (212 males and 147 females) were enrolled in this study and completed their follow-up investigations in the Office Clinic for more than six months. The mean age of all patients was 58.1 ± 13.0 years old (ranging from 22 to 85 years old). Among these patients, 112 (31.2 %) had a previous history of blood transfusion. Patients without a transfusion history had a past history of undisposable needle injections. None of these patients were intravenous drug abusers or under regular hemodialysis. Among all patients, 66 (18.4 %) of them had a family history of diabetes. The mean BMI of all patients was 24.0 ± 3.5 Kg/m². Eighty-seven (24.2 %) patients were obese. One hundred and fifty patients had received a percutaneous liver biopsy. Clinical and histology-diagnosed liver cirrhosis was identified in 75 patients (20.9 %). One hundred and twenty-three patients (34.3 %) had a prior history of IFN treatment with a mean duration of 3.3 years (ranging from 0.5 to 7 years) from completion of IFN treatment till enrollment.

Results of glucose intolerance

Among the 359 patients, 125 patients (34.6 %) had glucose intolerance, including 99 patients (27.6 %) with DM, and 26 patients (7.0 %) with IFG. The remaining 234 patients had normal fasting glucose. None of the 125 patients with glucose intolerance were diagnosed as type 1 DM. The mean age of chronic hepatitis C patients with glucose intolerance was significantly older than the age of those with normal fasting glucose (61.1 ± 11.2 vs 56.6 ± 13.6 years; $P=0.001$). The mean BMI of chronic hepatitis C patients with glucose intolerance was significantly higher than that of those with normal fasting glucose (24.5 ± 3.7 vs 23.7 ± 3.2 Kg/m², $P=0.024$). Thirty-eight of the 125 (30.4 %) patients with glucose intolerance were obese, which was significantly higher than those with normal fasting glucose (53/235, 22.6 %, $P=0.02$). Chronic hepatitis C patients with glucose intolerance had a significantly higher rate of diabetic family history than those with normal fasting glucose (29.6 % vs 12.8 %, $P<0.001$, Table 1).

Table 1 Comparisons of demographic data between chronic hepatitis C patients with glucose intolerance* and normal fasting glucose

	Patients with glucose intolerance (<i>n</i> =125)	Patients with normal fasting glucose (<i>n</i> =234)	<i>P</i> value
Age	61.1 \pm 11.2	56.6 \pm 13.6	0.001
Sex (male:female)	47:78	99:135	0.452
Body mass index (Kg/m ²)	24.5 \pm 3.7	23.7 \pm 3.2	0.024
Family history of DM (+/-)	37:88	30:204	<0.001
Obesity (+/-)	38:87	49:185	0.046
Liver cirrhosis (+/-)	28:97	47:187	0.706
Previous interferon treatment (+/-)	51:74	66:168	0.021

Denotes: Data were expressed as mean \pm S.D. * Patients with glucose intolerance included patients with diabetes mellitus and impaired fasting glucose by the diagnostic criteria of the American Diabetic Association.

Data of IFN treatment

One hundred and seventeen patients (32.6 %) had a previous history of IFN treatment. Among these 117 patients, 44 patients were treated with consensus IFN 3 µg ($n=14$), 9 µg ($n=17$) or 15 µg ($n=13$) for 24 weeks, 29 patients were treated with IFN α -2b 3 million units (MU) three times a week for 24 weeks, 4 patients were treated with IFN α -2a 6 MU three times a week for 12 weeks followed by 3 MU three times a week for 36 weeks, and 7 patients were treated with IFN α -2b 3 MU three times a week for 48 weeks along with oral ribavirin (1 000 mg/day for patients who weighed less than 75 Kg, and 1 200 mg/day for those who weighed more than 75 Kg).

Twenty-seven patients were treated with pegylated IFN α -2a 180 µg once a week for 48 weeks, and 19 of them also received oral ribavirin treatment. Six patients received pegylated IFN α -2a 180 µg once a week and oral ribavirin for 24 weeks. In patients who had a previous history of IFN treatment, 42.7 % (50/117) were glucose intolerant, which was significantly higher than the 30.2 % (73/242) of those without a history of IFN treatment ($P=0.021$). Fifty-one patients out of a total of 125 patients (40.8 %) with glucose intolerance had a past history of IFN treatment, which was significantly higher than the 66 patients out of 234 patients (28.2 %) with normal fasting glucose ($P=0.021$). There was no significant difference in gender and in relation to the presence of cirrhosis between the two groups (Table 1).

Dependent variable associated with glucose intolerance

Age, gender, BMI, family history of diabetes, the presence of liver cirrhosis and previous IFN treatment were identified as independent variables in a logistic regression analysis with the glucose intolerance as the dependent variable. Continuous variables were transformed into categorical variables with the cut-off determined by the Receiver Operating Characteristic curve. Stepwise multivariate logistic regression analysis revealed that age ≥ 57 years, the presence of family history of diabetes, obesity and previous IFN treatment were significant as independent predictive variables associated with the presence of glucose intolerance in patients with chronic hepatitis C (Table 2).

Table 2 Significant predictive variables of glucose intolerance in chronic hepatitis C patients using stepwise multivariate logistic regression analysis

	Coefficient	Odds ratio	95% CI	Pvalue
Age ≥ 57 years	1.251	3.50	2.06-5.92	<0.001
Diabetic family history	1.289	3.64	2.00-6.57	<0.001
Obesity	0.576	1.78	1.05-3.03	0.034
Previous interferon treatment	0.803	2.23	1.34-3.72	0.002

Denotes: CI: confidence interval.

DISCUSSION

The close relationship between DM and chronic HCV infection had been reported in several previous studies although the exact pathogenesis remains unclear^[4-11]. The age-adjusted population-based prevalence of type 2 DM and IFG in Taiwan was 5.9 % and 15.7 %, respectively^[27-30]. According to our results, the prevalence of DM and IFG in patients with chronic hepatitis C was 27.6 % and 7.0 %, respectively. The prevalence of glucose intolerance (DM and IFG) was significantly higher than the age-matched normal population in Taiwan.

An altered glucose metabolism had been reported in patients with chronic liver diseases and liver cirrhosis^[11]. However,

patients with HCV-related chronic hepatitis and liver cirrhosis demonstrated a stronger correlation than those patients with other etiologies^[5,6,11]. Patients with a viral infection alone such as cytomegalovirus, Coxsackie virus and mumps were reported to develop DM, but most of the reported cases were type 1 DM^[31-33]. The pathogenesis of HCV-related DM remains mysterious.

Although the close relationship between DM and chronic HCV infection has been noted, the risk factors of DM including age, sex, the presence of family history of diabetes, BMI, liver cirrhosis, and previous history of IFN treatment has not been well investigated in previous case-control studies. In the general population, male gender, older age, obesity and the presence of family history of diabetes were well recognized as significant risk factors for the development of DM. According to our results, all these risk factors except the male gender remained independent risk factors associated with the presence of DM in chronic hepatitis C patients. These findings indicated that multiple factors may contribute to the development of DM in patients with chronic hepatitis C.

Of particular interest, our results showed significantly that previous IFN treatment was an independent risk factor for the development of glucose intolerance in patients with chronic hepatitis C. IFN had been widely used in the treatment of patients with chronic hepatitis C^[12-16]. Development of DM or the exacerbation of previously stable glycemic control in diabetic patients had been reported as drug side effects in chronic hepatitis C patients who were receiving IFN treatment, but the mechanism of this phenomenon remains unknown^[17-19]. The presence of islet cell autoantibodies had ever been reported in a chronic hepatitis C patient during IFN treatment^[34]. Fabris *et al* reported that the development of DM during IFN treatment was resulted from the amplification of previously existing autoimmunity against pancreatic β cells^[35]. However, a report contradicting these findings was published later^[36].

Koivisto *et al* also postulated that impaired glucose tolerance was found in healthy volunteers who received IFN treatment, and this phenomenon may have resulted from the development of insulin resistance through the complex interaction between insulin and its counter-regulatory hormones^[37]. However, by using a minimal model, IFN- α injection was reported to ameliorate the glucose tolerance in diabetic and non-diabetic patients with chronic HCV infection^[38]. Our results showed that previous IFN therapy can be used significantly as an independent variable to predict the development of glucose intolerance in patients with chronic hepatitis C. Patients enrolled in our study received various forms of IFN with different dosages and durations. Therefore, further evaluations are needed to clarify the enigmatic association between IFN treatment and DM development in patients with chronic hepatitis C.

In conclusion, 34.6 % of patients with chronic hepatitis C were glucose intolerant. Chronic hepatitis C patients who were older in age, were obese, and had a previous history of IFN treatment as well as a family history of diabetes were prone to develop glucose intolerance. To our best knowledge, this is the first population-based report to confirm that interferon treatment to be an independent risk factor to develop glucose intolerance.

ACKNOWLEDGEMENTS

This study was supported by a grant (NSC) from National Science Council, Taiwan. The authors wish to thank Miss Wei-Lin Chen for her assistance in blood collection, and Miss Rei-Hwa Lu for her laboratory assistance.

REFERENCES

- 1 Gumber SC, Chopra S. Hepatitis C: a multifaceted disease. *Ann Intern Med* 1995; **123**: 615-620

- 2 **Hwang SJ**, Lee SD, Li CP, Lu RH, Chan CY, Wu JC. Clinical study of cryoglobulinemia in Chinese patients with chronic hepatitis C. *J Gastroenterol Hepatol* 1997; **12**: 513-517
- 3 **Luo JC**, Hwang SJ, Li CP, Lu RH, Chan CY, Wu JC, Chang FY, Lee SD. Clinical significance of serum auto-antibodies in Chinese patients with chronic hepatitis C: negative role of serum viral titre and genotype. *J Gastroenterol Hepatol* 1998; **13**: 475-479
- 4 **Allison ME**, Wreghitt T, Palmer CR, Alexander GJ. Evidence for a link between hepatitis C virus infection and diabetes mellitus in a cirrhotic population. *J Hepatol* 1994; **21**: 1135-1139
- 5 **Caronia S**, Taylor K, Pagliaro L, Carr C, Palazzo U, Petrik J, O'Rahilly S, Shore S, Tom BD, Alexander GJ. Further evidence for an association between non-insulin-dependent diabetes mellitus and chronic hepatitis C virus infection. *Hepatology* 1999; **30**: 1059-1063
- 6 **Knobler H**, Stagnaro-Green A, Wallenstein S, Schwartz M, Roman SH. Higher incidence of diabetes in liver transplant recipients with hepatitis C. *J Clin Gastroenterol* 1998; **26**: 30-33
- 7 **Mason AL**, Lau JY, Hoang N, Qian K, Alexander GJ, Xu L, Guo L, Jacob S, Regenstein FG, Zimmerman R, Everhart JE, Wasserfall C, Maclaren NK, Perrillo RP. Association of diabetes mellitus and chronic hepatitis C virus infection. *Hepatology* 1999; **29**: 328-333
- 8 **Ozyilkan E**, Erbas T, Simsek H, Telatar F, Kayhan B, Telatar H. Increased prevalence of hepatitis C virus antibodies in patients with diabetes mellitus. *J Intern Med* 1994; **235**: 283-284
- 9 **Simo R**, Jardi R, Hernandez C, Mesa J, Genesca J. High prevalence of hepatitis C virus infection in diabetic patients. *Diabetes Care* 1996; **19**: 998-1000
- 10 **Kingston ME**, Ali MA, Atiyeh M, Donnelly RJ. Diabetes mellitus in chronic active hepatitis and cirrhosis. *Gastroenterology* 1984; **87**: 688-694
- 11 **Bigam DL**, Pennington JJ, Carpentier A, Wanless IR, Hemming AW, Croxford R, Greig PD, Lilly LB, Heathcote JE, Levy GA, Catral MS. Hepatitis C-related cirrhosis: a predictor of diabetes after liver transplantation. *Hepatology* 2000; **32**: 87-90
- 12 **Carithers RL Jr**, Emerson SS. Therapy of hepatitis C: meta-analysis of interferon alfa-2b trials. *Hepatology* 1997; **26** (Suppl 1): 83S-88S
- 13 **Poynard T**, Leroy V, Cohard M, Thevenot T, Mathurin P, Opolon P, Zarski JP. Meta-analysis of interferon randomized trials in the treatment of viral hepatitis C: effects of dose and duration. *Hepatology* 1996; **24**: 778-789
- 14 **Farrell GC**. Therapy of hepatitis C: interferon alfa-nl trials. *Hepatology* 1997; **26** (Suppl 1): 96S-100S
- 15 **Poynard T**, Marcellin P, Lee SS, Niederau C, Minuk GS, Ideo G, Bain V, Heathcote J, Zeuzem S, Trepo C, Albrecht J. Randomized trial of interferon alfa-2b plus ribavirin for 48 weeks or 24 weeks versus alfa-2b plus placebo for 48 weeks for treatment of chronic hepatitis C virus. *Lancet* 1998; **352**: 1426-1432
- 16 **McHutchison JG**, Gordon SC, Schiff ER, Shiffman ML, Lee WM, Rustgi VK, Goodman ZD, Ling MH, Cort S, Albrecht JK. Interferon alfa-2b alone or in combination with ribavirin as initial treatment for chronic hepatitis C. *N Engl J Med* 1998; **339**: 1485-1492
- 17 **Okanoue T**, Sakamoto S, Itoh Y, Minami M, Yasui K, Sakamoto M, Nishioji K, Katagishi T, Nakagawa Y, Tada H, Sawa Y, Mizuno M, Kagawa K, Kashima K. Side effects of high-dose interferon therapy for chronic hepatitis C. *J Hepatol* 1996; **25**: 383-391
- 18 **Fattovich G**, Giustina G, Favarato S, Ruol A. A survey of adverse events in 11,241 patients with chronic viral hepatitis treated with alpha interferon. *J Hepatol* 1996; **24**: 38-47
- 19 **Lopes EP**, Oliveira PM, Silva AE, Ferraz ML, Costa CH, Miranda W, Dib SA. Exacerbation of type 2 diabetes mellitus during interferon alfa therapy for chronic hepatitis B. *Lancet* 1994; **343**: 224
- 20 **The Expert Committee of the Diagnosis and Classification of Diabetes Mellitus**. Report of the expert committee on the diagnosis and classification of diabetes mellitus. *Diabetes Care* 1997; **20**: 1183-1197
- 21 **Tsai ST**, Li CL, Chen CH, Chou P. Community-based epidemiological study of glucose tolerance in Kin-Chen, Kinmen: support for a new intermediate classification. *J Clin Epidemiol* 2000; **53**: 505-510
- 22 **National Diabetes Data Group**. Classification and diagnosis of diabetes mellitus and other categories of glucose intolerance. *Diabetes* 1979; **28**: 1039-1057
- 23 **Hwang SJ**, Chan CY, Lu RH, Wu JC, Lee SD. Randomized controlled trial of recombinant interferon-alpha 2b in the treatment of Chinese patients with chronic hepatitis C. *J Interferon Cytokine Res* 1995; **15**: 611-666
- 24 **Hwang SJ**, Lee SD, Chan CY, Lu RH, Chang FY. A randomized, double-blind controlled trial of consensus interferon in the treatment of Chinese patients with chronic hepatitis C. *Am J Gastroenterol* 1999; **94**: 2496-2500
- 25 **Hwang S**, Lee S, Chu C, Lu R, Chang F. An open-label trial of consensus interferon 15 microg in the treatment of Chinese patients with chronic hepatitis C. *Hepatol Res* 2001; **19**: 284-293
- 26 **Zeuzem S**, Feinman SV, Rasenack J, Heathcote EJ, Lai MY, Gane E, O'Grady J, Reichen J, Diago M, Lin A, Hoffman J, Brunda MJ. Peginterferon alfa-2a in patients with chronic hepatitis C. *N Engl J Med* 2000; **343**: 1666-1672
- 27 **Tai TY**, Yang CL, Chang CJ. Epidemiology of diabetes mellitus among adults in Taiwan, ROC. *J Med Assoc Thailand* 1987; **70** (Suppl 2): 42-48
- 28 **Lin JD**, Shieh WB, Huang MJ, Huang HS. Diabetes mellitus and hypertension based on the family history and 2-h postprandial blood sugar in the Ann-Lo district (northern Taiwan). *Diabetes Res Clin Pract* 1993; **20**: 75-85
- 29 **Lu FH**, Yang YC, Wu JS, Wu CH, Chang CJ. A population-based study of the prevalence and associated factors of diabetes in southern Taiwan. *Diabet Med* 1998; **15**: 564-572
- 30 **Chang C**, Lu F, Yang YC, Wu JS, Wu TJ, Chen MS, Chuang LM, Tai TY. Epidemiologic study of type 2 diabetes in Taiwan. *Diabetes Res Clin Pract* 2000; **50** (Suppl 2): S49-S59
- 31 **Forrest JM**, Menser MA, Burgess JA. High frequency of diabetes mellitus in young adults with congenital rubella. *Lancet* 1971; **2**: 332-334
- 32 **King ML**, Shaikh A, Bidwell D, Voller A, Banatvala JE. Coxsackie-B-virus-specific IgM responses in children with insulin-dependent (juvenile onset; type I) diabetes mellitus. *Lancet* 1983; **1**: 1397-1399
- 33 **Pak CY**, Eun HM, McArthur RG, Yoon JW. Association of cytomegalovirus infection with autoimmune type 1 diabetes. *Lancet* 1988; **2**: 1-4
- 34 **Campbell S**, McLaren EH, Danesh BJ. Rapidly reversible increase in insulin requirement with interferon. *Brit Med J* 1996; **313**: 92
- 35 **Fabris P**, Betterle C, Greggio NA, Zanchetta R, Bosi E, Biasin MR, de Lalla F. Insulin-dependent diabetes mellitus during alpha-interferon therapy for chronic viral hepatitis. *J Hepatol* 1998; **28**: 514-517
- 36 **Betterle C**, Fabris P, Zanchetta R, Pedini B, Tositti G, Bosi E, de Lalla F. Autoimmunity against pancreatic islets and other tissues before and after interferon- α therapy in patients with hepatitis C virus chronic infection. *Diabetes Care* 2000; **23**: 1177-1181
- 37 **Koivisto VA**, Cantell K, Pelkonen R. Effect of interferon on glucose tolerance and insulin sensitivity. *Diabetes* 1989; **38**: 641-647
- 38 **Konrad T**, Vicini P, Zeuzem S, Toffolo G, Breim D, Lormann J, Herrmann G, Wittmann D, Lenz T, Kusterer K, Teuber G, Cobelli C, Usadel KH. Interferon- α improves glucose tolerance in diabetic and non-diabetic patients with HCV-infected liver disease. *Exp Clin Endocrinol Diabetes* 1999; **107**: 343-349

A mutation specific polymerase chain reaction for detecting hepatitis B virus genome mutations at nt551

Chun-Ling Ma, De-Xing Fang, Hua-Biao Chen, Fa-Qing Li, Hui-Ying Jin, Su-Qin Li, Wei-Guo Tan

Chun-Ling Ma, De-Xing Fang, Hua-Biao Chen, Fa-Qing Li, Hui-Ying Jin, Su-Qin Li, Wei-Guo Tan, Huadong Research Institute for Medical Biotechnics, Nanjing 210002, Jiangsu Province, China
Supported by the Natural Science Foundation of Jiangsu Province, No. BJ2000039

Correspondence to: Chun-Ling Ma, Huadong Research Institute for Medical Biotechnics, Nanjing 210002, China. mchunling@hotmail.com

Telephone: +86-25-4542419 **Fax:** +86-25-4541183

Received: 2002-06-08 **Accepted:** 2002-07-11

Abstract

AIM: The hepatitis B surface antigen (HBsAg) is considered to be one of the best markers for the diagnosis of acute and chronic HBV infection. But in some patients, this antigen cannot be detected by routine serological assays despite the presence of virus. One of the most important explanations for the lack of detectable HBsAg is that mutations which occur within the "a" determinant of HBV S gene can alter expression of HBsAg and lead to changes of antigenicity and immunogenicity of HBsAg accordingly. As a result, these mutants cannot be detected by diagnosis assays. Thus, it is essential to find out specific and sensitive methods to test the new mutants and further investigate their distribution. This study is to establish a method to investigate the distribution of the HBsAg mutant at nt551.

METHODS: A mutation specific polymerase chain reaction (msPCR) was established for amplifying HBV DNA with a mutation at nt551. Four sets of primer pairs, P551A-PPS, P551G-PPS, P551C-PPS and P551T-PPS, with the same sequences except for one base at 3' terminus were designed and synthesized according to the known HBV genome sequences and the popular HBV subtypes, adr and adw, in China. At the basis of regular PCR method, we explored the specific conditions for amplifying HBV DNAs with a mutation at nt551 by regulating annealing temperature and the concentration of these primers. 126 serum samples from patients of hepatitis B were collected, among which 16 were positive for HBV S DNA in the nested PCR amplification. These 16 HBV S DNAs were detected by using the msPCR method.

RESULTS: When the annealing temperature was raised to 71 °C, nt551A and nt551G were amplified specifically by P551A-PPS and P551G-PPS; At 72 °C and 5 pmole of the primers (each) in reaction of 25 µl volume, nt551C and nt551T were amplified specifically by P551C-PPS and P551T-PPS. 16 of HBV S gene fragments were characterized by using this method. 14 of them were positive for nt551A, one was positive for nt551G, and the other one was positive for nt551T. The results were confirmed by nucleotide sequencing.

CONCLUSION: The mutation specific polymerase chain reaction is a specific and sensitive method for detecting the mutations of HBV genome at nt551.

Ma CL, Fang DX, Chen HB, Li FQ, Jin HY, Li SQ, Tan WG. A mutation specific polymerase chain reaction for detecting hepatitis B virus genome mutations at nt551. *World J Gastroenterol* 2003; 9(3): 509-512

<http://www.wjgnet.com/1007-9327/9/509.htm>

INTRODUCTION

Hepatitis B virus (HBV) is a hepatotropic DNA virus, in the reverse transcription process of DNA replication, the HBV DNA template is transcribed by cellular RNA polymerase to pregenomic RNA, which is reverse transcribed to DNA by viral polymerase, and a consequence of the unique way of HBV replication is a significant tendency of mutation^[1-3]. Substitution, deletion and frame-shift by insertion or deletion of short sequence were found in four open reading frames^[4-7]. The diversity is also shown in different serological subtypes such as adr, adw, ayr and ayw, which have a common "a" determinant. It is well known that "a" determinant is the common antigenic epitopes of all subtypes of HBsAg. A large antigenic area of "a" determinant is now called the major hydrophilic region (MHR). Mutations within MHR of HBsAg have been considered to be associated with vaccine failure and chronic infection^[1,2,6,8]. These mutations have been reported repeatedly since Carman found the first case of immune escape mutants in 1990^[9]. The point mutation reported most commonly in immunized children causes a substitution of Arg for Gly at position 145 of HBsAg^[1,3,8,9]. Other reports about substitutions in HBsAg such as 120, 121, 126, 129, 131, 133, 141, 144 were found repeatedly^[8-12]. These findings of HBV immune escape mutants have caused attention from scientists all over the world in recent years. Immune escape of HBV mutants was best known to be associated with HBV genome itself, but the immune pressure was considered to be one of the most important factors that result in escape mutants^[13-17].

The immune escape variants could influence the effect of HBV vaccine, it was argued that the components of mutant HBsAg should be considered to be added in the HBV vaccine in the future^[3,13,17,18]. However, in order to achieve this aim, it is needed to confirm first the mutants that are the big problems among hepatitis B patients. At present, it is very important to find out new escape mutants and further investigate their distribution. Specific and sensitive assays are essential for investigating the distribution of mutants. To detect the mutant HBV DNA, mutation specific polymerase chain reaction (msPCR) is a potential method. Our lab had discovered a mutation at nt551 A-to-G of HBV genome, resulting in the alteration at aa133 Met to Val of HBsAg, from a four-year-old hepatitis B patient^[123]. To investigate the distribution of mutants with a mutation at nt551 among the hepatitis B patients in China, a msPCR method was established according to HBV DNA sequences and the main popular subtypes, adr and adw.

MATERIALS AND METHODS

Materials

Collection of serum samples 126 of serum samples were

provided by Department of Laboratory Diagnosis, Nanjing Jinling Hospital. The viral markers were tested by using the enzyme immune assay (EIA) methodology. All of the samples were positive for anti-HBs and negative for HBsAg. The ALT level was considered to be abnormal to all of them.

Methods

Extraction of HBV genome DNAs DNAs was isolated and purified from 100 μ L of serum samples. Proteinase K (20 mg/ml) and SDS (10 %) were added into 100 μ L of sera and their concentrations in reaction were 2.5 mg/ml and 0.5 %, respectively. After a brief vortex, the mixture was heated at 70 °C for 3 hours. Then the same volume of phenol: chloroform was added to the mixture to extract DNA. The DNA pellet was obtained with 100 % ethanol precipitation, and was washed with 70 % ethanol. The dried DNA pellet was then resuspended in 20 μ L of H₂O and stored at -20 °C. All of 126 sera were prepared in this way.

Amplification of HBV S DNAs The amplification of HBV S gene was carried out by using the nested PCR method. In the first-round PCR, the 50 μ L reaction solution including 5 μ L DNA template and 40 pmole (each) of the first-round primers. The mixture was heated to 94 °C for 5 min, followed by 30 PCR cycles consisting of 94 °C for 30 s, 55 °C for 30 s and 72 °C for 60 s in a thermal cycler. And then 1.25 μ L of the first-round PCR product served as the template for the second-round of PCR amplification which consisting of the same cycles except that the annealing temperature was raised to 65 °C. Positive PCR product, a DNA band of 1.2kb as expected, was detected on agarose gel electrophoresis. After amplification, we achieved 16 HBV S DNAs.

The primers for the nested PCR were designed according to the known HBV genome sequences and the main popular subtypes, adr and adw, in China, as follows:

The primers for first-round:

P1': 5' ACATCATCTGTGGAAGGC 3', nt2756-nt2773, the upstream primer;

P6': 5' TATCCCATGAAGTTAAGG 3', nt884-nt867, the downstream primer;

The primers for second-round:

PEC: 5' CGGAATTCACCATATTCTTGGGAACAAG 3', nt2 823-nt2 844, the upstream primer;

PPS: 5' GCTGCAGGTTTAAATGTATACCCAAAGAC 3', nt838-nt816, the downstream primer;

An EcoRI or a Pst I sites was originally added at 5' -end respectively for cloning purpose.

Amplification of HBV DNA fragments for control To achieve the HBV DNA fragment with an A at nt551, the wild-type HBV S DNA as template was amplified by using the primer pair P551A-PPS under the condition of regular PCR. The HBsAg mutant with a G at nt551 as template was amplified by using the primer pair P551G-PPS to achieve the HBV DNA fragment with a G at nt551. The HBV DNA fragment with a C or T at nt551 was achieved by using introducing mutation in a PCR. The PCR primer sequences were as follows:

P551A: 5' TCCTGCTCAAGGAACCTCTA 3', nt532-nt551, upstream primer;

P551G: 5' TCCTGCTCAAGGAACCTCTG 3', nt532-nt551, upstream primer;

P551C: 5' TCCTGCTCAAGGAACCTCTC 3', nt532-nt551, upstream primer;

P551T: 5' TCCTGCTCAAGGAACCTCTT 3', nt532-nt551, upstream primer;

PPS: See the above.

P551C-PPS and P551T-PPS were used respectively to amplify HBV DNA fragments with a C or T at nt551, which are 314 bp long. Additionally, two upstream primers had been designed respectively by introducing mutation in order to

achieve the controls of HBV DNA with a C or T at nt551.

P551CM: TCCTGCTCAAGGAACCTCTCTGTTTC, nt532-nt557; P551TM: TCCTGCTCAAGGAACCTCTTTGTTTC, nt532-nt557.

Establishment of msPCR In order to amplify HBV DNA specifically, the annealing temperature of PCR was regulated according to the T_m. The reaction volume of PCR was 25 μ L. The PCR reaction was carried out by using P551A-PPS, P551G-PPS, P551C-PPS and P551T-PPS as primer pairs to amplify HBV S DNA templates with an A, G, C, or T at nt551, respectively.

Application of msPCR Under the condition of the msPCR method, the 16 of samples which were positive for HBV S DNA as templates were amplified by using P551A-PPS, P551G-PPS, P551C-PPS and P551T-PPS as primer pairs respectively.

HBV S DNA sequencing In order to confirm the validity of the msPCR, the purified PCR products of HBV S gene fragments from selected samples according to the results of msPCR, NO.2, NO.5, NO.8 and NO.57 were sequenced by using the primer PPS.

RESULTS

HBV DNA fragments for control

The HBV S DNA with an A, G, C or T at nt551 was amplified respectively for control. This result is shown in Figure 1.

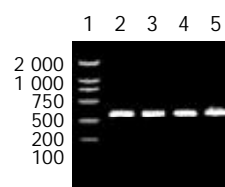


Figure 1 Amplification of Control HBV DNA. Lane 1: DNA Marker; Lane 2: HBV DNA with an A at nt551 amplified by P551A-PPS; Lane 3: HBV DNA with a G at nt551 amplified by P551G-PPS; Lane 4: HBV DNA with a C at nt551 amplified by P551CM-PPS; Lane 5: HBV DNA with a T at nt551 amplified by P551TM-PPS. The amplified DNA fragments are 314 bp long.



Figure 2 Establishment of the msPCR for nt551A and nt551G. Lane 1: DNA Marker; Lane 2-5: P551A-PPS amplified HBV DNAs of control (nt551A in Lane 2, nt551G in Lane 3, nt551C in Lane 4, nt551T in Lane 5). Lane 6-9: P551G-PPS amplified HBV DNAs of control (nt551A in Lane 6, nt551G in Lane 7, nt551C in Lane 8, nt551T in Lane 9).

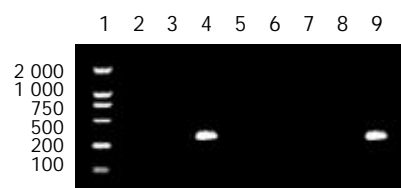


Figure 3 Establishment of the msPCR for nt551C and nt551T. Lane 1: DNA Marker; Lane 2-5: P551C-PPS amplified HBV DNAs of control (nt551A in Lane 2, nt551G in Lane 3, nt551C in Lane 4, nt551T in Lane 5). Lane 6-9: P551T-PPS amplified HBV DNAs of control (nt551A in Lane 6, nt551G in Lane 7, nt551C in Lane 8, nt551T in Lane 9).

Table 1 Application of the msPCR for detecting HBV DNA

Primerpairs	HBV DNA samples															
	2	5	8	13	17	31	32	33	34	46	47	50	53	57	67	85
P551A-PPS	-	+	+	+	+	+	+	+	+	+	+	+	+	-	+	+
P551G-PPS	-	-	-	-	-	-	-	-	-	-	-	-	-	+	-	-
P551C-PPS	-	-	-	-	-	-	-	-	-	-	-	-	-	-	-	-
P551T-PPS	+	-	-	-	-	-	-	-	-	-	-	-	-	-	-	-

	124		133		147
HBV(adr)	TGCACGATTCTCTGCTCAAGGCAACTCTATGTTTCCCTCATGTTGCTGTACAAAACCTTCGGACGGAAACTGC				
NO.2	-----T-----				
NO.5	-----A-----				
NO.8	-----A-----				
NO.57	-----G-----				

Figure 4 NO.2, NO.5, NO.8 and NO.57 are compared with the know adr subtype HBV genome. The sequence from nt524 to nt595 code for aa124 to aa147 of HBsAg (The first T in the single EcoRI cleavage site of HBV genome is nt1).

Establishment of msPCR

When the annealing temperature was set from 65 °C to 70 °C, the results of amplification were not specific to the four primer pairs. In other words, the templates were amplified by non-matching primers. Then the annealing temperature was raised to 71 °C, the specific amplified results were found for P551A-PPS and P551G-PPS; When the annealing temperature was raised to 72 °C and the concentration of the primers (each) were at 5 pmole in reaction of 25 µl volume, P551C-PPS and P551T-PPS amplified HBV DNAs with C or T at nt551 specifically. The specific results to establish msPCR method are shown in Figure 2 and Figure 3.

Application of msPCR

16 samples were tested by using the msPCR method. This result is shown in Table 1.

HBV S DNA sequencing

According to the results of msPCR, four DNA samples, No.2, No.5, No.8 and No.57 were selected to sequence. The sequencing results showed that No.2 was a T at nt551, both No.5 and No.8 were an A at nt551, and No.57 was a G at nt551, confirming the results of the msPCR. The sequencing results are shown in Figure 4.

DISCUSSION

In the recent years, mutant HBsAg have caused great academic interest^[19,20], and many analyses and researches have been made for the emergence of HBV mutants with mutations in the “a” determinant of HBsAg which result in immune escape^[13-16,21]. According to these research results, it is very important to further investigate mutant distributions and clarify mutations in HBV S gene which could cause the changes of antigenicity and immunogenicity of HBsAg^[3,12,22-24]. It is well known that the mutants of HBsAg were able to cause infection and horizontal transmission despite the presence of anti-HBs^[25-29]. The increasing use of HBV vaccine has had overwhelming positive influence on the prevention of hepatitis B viral infection, but have no effective impact to those mutants^[30]. The mutations in the coding region of “a” determinant of HBsAg could not be detected in some routine assays^[31,32].

This study was to obtain a specific and sensitive method for monitoring the HBsAg mutant with a mutation at nt551. The method of msPCR is different from immunoassays that are

based on the antigen-antibody reaction^[33,34]. To detect mutant HBsAg, the unique specific monoclonal antibodies are required. But these kinds of antibodies are limited or not available commercially. Because HBV is a double-stranded DNA virus, its genome is fairly stable in the blood and tissue, the PCR amplification of HBV DNA is relatively easy^[35]. The msPCR is actually a method to detect the specific site mutation. This method was firstly developed to detect site mutation of allele-special genes of β-globin genome DNA for sickle cell anemia^[36]. And then it was used in virological studies. This mechanism was used in our study.

The msPCR was established at the basis of the known HBV DNA. The primers were only one-base different from each other at 3' terminus, thus the non-specific DNA should not be amplified at regular value of T_m. However, we considered the variability of annealing temperature and set it as high as possible. When it was 71 °C and 72 °C, the ideal result was found respectively for different primer pairs. The process confirmed that the annealing temperature is the key factor to establish msPCR method of nt551. Additionally, the concentration of the primers is also an important factor for this msPCR. In short, different primers amplify HBV DNA specifically with different conditions.

The aim of this study was to detect the mutation of the known HBV S gene at nt551. All of 126 serum samples were collected from hepatitis B patients in hospital. After the nested PCR amplification, 16 samples were positive for HBV S gene. The msPCR detection showed that 14 of them were an A at nt551, one was a G at nt551, and the other was a T at nt551. The reliability of msPCR was confirmed by sequencing analysis of four samples. A special attention should be paid to No.2. It is a T at nt551, resulting in a Met (ATG) to Leu (TTG) change at aa133 of HBsAg. Whether this mutation caused the change of antigenicity need further identification. In addition to these mutations in HBsAg “a” determinant, there were several other mutations in S gene. These results further confirmed the diversity and popularity of HBV S gene mutation.

In conclusion, this msPCR is a sensitive and specific approach for the detection of mutations in HBV S gene, and will have tremendous potential in screening HBsAg mutants and further investigating their distribution in patients of hepatitis B.

REFERENCES

- 1 **Koyanagi T**, Nakamuta M, Sakai H, Sugimoto R, Enjoji M, Koto K, Iwamoto H, Kumazawa T, Mukaide M, Nawata H. Analysis

- of HBs antigen negative variant of hepatitis B virus: unique substitutions, Glu129 to Asp and Gly145 to Ala in the surface antigen gene. *Med Sci Monit* 2000; **6**: 1165-1169
- 2 **Brunetto MR**, Rodriguez UA, Bonino F. Hepatitis B virus mutants. *Intervirology* 1999; **42**: 69-80
 - 3 **Kfoury Baz EM**, Zheng J, Mazuruk K, Van Le A, Peterson DL. Characterization of a novel hepatitis B virus mutants demonstration of mutation-induced hepatitis B virus surface antigen group specific "a" determinant conformation change and its application in diagnosis assays. *Transfus Med* 2001; **11**: 355-362
 - 4 **Dong J**, Cheng J, Wang Q, Huangfu J, Shi S, Zhang G, Li L, Si C. The study on heterogeneity of hepatitis B virus. *Zhonghua Yixue Zazhi* 2002; **82**: 81-85
 - 5 **Kreutz C**. Molecular, immunological and clinical properties mutated hepatitis B viruses. *J Cell Mol Med* 2002; **6**: 113-143
 - 6 **Zhong S**, Chan JY, Yeo W, Tam JS, Johnson PJ. Hepatitis B envelope protein mutants in human hepatocellular carcinoma tissues. *J Viral Hepat* 1999; **6**: 195-202
 - 7 **Weinberger KM**, Zoulek G, Bauer T, Bohm S, Jilg W. A novel deletion mutant of hepatitis B virus surface antigen. *J Med Virol* 1999; **58**: 105-110
 - 8 **Roznovsky L**, Harrison TJ, Fang ZL, Ling R, Lochman I, Orsagova I, Pliskova L. Unusual hepatitis B surface antigen variation in a child immunised against hepatitis B. *J Med Virol* 2000; **61**: 11-14
 - 9 **Carman WF**, Zanetti AR, Karayiannis P, Waters J, Tanzi E, Zuckerman AJ, Thomas HC. Vaccine-induced escape mutant of hepatitis B virus. *Lancet* 1990; **336**: 325-329
 - 10 **Yang X**, Lei J, Zhang Y, Luo H, Huang L, Zheng Y, Tang X. A novel stop codon mutation in S gene: the molecular basis of a patient with cryptogenic cirrhosis. *Zhonghua Yixue Zazhi* 2002; **82**: 400-402
 - 11 **Zhu Q**, Lu Q, Xiong S, Yu H, Duan S. Hepatitis B virus S gene mutants in infants infection despite immunoprophylaxis. *Chin Med J* 2001; **114**: 352-354
 - 12 **Fang DX**, Li FQ, Tan WG, Chen HB, Jin HY, Li SQ, Lin HJ, Zhou ZX. Transient expression and antigenic characterization of HBsAg of HBV nt551 A to G mutant. *World J Gastroenterol* 1999; **5**: 73-74
 - 13 **Santantonio T**, Gunther S, Sterneck M, Rendina M, Messner M, Launois B, Francavilla A, Pastore G, Will H. Liver graft infection by HBV S-gene mutants in transplant patients receiving long-term HBIG prophylaxis. *Hepatogastroenterology* 1999; **46**: 1848-1854
 - 14 **Rodriguez-Frias F**, Buti M, Jardi R, Vargas V, Quer J, Cotrina M, Martell M, Esteban R, Guardia J. Genetic alterations in the S gene of hepatitis B virus in patients with acute hepatitis B, chronic hepatitis B and hepatitis B liver cirrhosis before and after liver transplantation. *Liver* 1999; **19**: 177-182
 - 15 **He C**, Nomura F, Itoga S, Isobe K, Nakai T. Prevalence of vaccine-induced escape mutants of hepatitis B virus in the adult population in Chinese prospective study in 176 restaurant employees. *J Gastroenterol Hepatol* 2001; **16**: 1373-1377
 - 16 **Cooreman MP**, Leroux-Roels G, Paulij WP. Vaccine-and hepatitis B immune globulin-induced escape mutations of hepatitis B virus surface antigen. *J Biomed Sci* 2001; **8**: 237-247
 - 17 **Komatsu H**, Fujisawa T, Sogo T, Isozaki A, Inui A, Kobata M, Ogawa Y. Acute self-limiting hepatitis B after immunoprophylaxis failure in an infant. *J Med Virol* 2002; **66**: 28-33
 - 18 **Heijttink RA**, Van Bergen P, Van Roosmalen MH, Paulij WP, Schalm SW, Osterhaus AD. Anti-HBs after hepatitis B immunization with plasma-derived and recombinant DNA-derived vaccines: binding to mutant HBsAg. *Vaccine* 2001; **19**: 3671-3680
 - 19 **Francois G**, Kew M, van Damme P, Mphahlele MJ, Meheus A. Mutants hepatitis B viruses: a matter of academic interest only or a problem with far-reaching implications? *Vaccine* 2001; **19**: 3799-3815
 - 20 **Burda MR**, Gunther S, Dandri M, Will H, Petersen J. Structural and functional heterogeneity of nature occurring hepatitis B virus variants. *Antiviral Res* 2001; **52**: 125-138
 - 21 **Coleman PE**, Chen YC, Mushahwar IK. Immunoassay detection of hepatitis B surface antigen mutants. *J Med Virol* 1999; **59**: 19-24
 - 22 **Torresi J**, Earnest-Silveira L, Civitico G, Walters TE, Lewin SR, Fyfe J, Locarnini SA, Manns M, Trautwein C, Bock TC. Restoration of replication phenotype of lamivudine-resistant hepatitis B virus mutants by compensatory changes in the "fingers" subdomain of the viral polymerase selected as a consequence of mutations in the overlapping S gene. *Virology* 2002; **299**: 88
 - 23 **Cooreman MP**, van Roosmalen MH, te Morsche R, Sunnen CM, Ven EM, Jansen JB, Tytgat GN, de Wit PL, Paulij WP. Characterization of the reactivity pattern of monoclonal antibodies against wild-type hepatitis surface antigen to G145R and other naturally occurring a loop escape mutations. *Hepatology* 1999; **30**: 1287-1292
 - 24 **Wu L**, Yuan ZH, Liu F, Waters JA, Wen YM. Comparing the immunogenicity of hepatitis B virus gene variants by DNA immunization. *Viral Immunol* 2001; **14**: 359-367
 - 25 **Owiredu WK**, Kramvis A, Kew MC. Molecular analysis of hepatitis B virus genomes isolated from black African patients with fulminant hepatitis B. *J Med Virol* 2001; **65**: 485-492
 - 26 **Banerjee K**, Guptan RC, Bisht R, Sarin SK, Khandekar P. Identification of a novel surface mutant of hepatitis B virus in a seronegative chronic liver disease patient. *Virus Res* 1999; **65**: 103-109
 - 27 **Chen WN**, Oon CJ. Hepatitis B virus surface antigen (HBsAg) mutants in Singapore adults and vaccinated children with high anti-hepatitis B virus antibody levels but negative for HBsAg. *J Clin Microbiol* 2000; **38**: 2793-2794
 - 28 **Oon CJ**, Chen WN, Goo KS, Goh KT. Intra-familial evidence of horizontal transmission hepatitis B virus surface antigen mutant G145R. *J Infect* 2000; **41**: 260-264
 - 29 **Chen WN**, Oon CJ, Koh S. Horizontal transmission of a hepatitis B virus surface antigen mutant. *J Clin Microbiol* 2000; **38**: 938-939
 - 30 **Schorries M**, Peter T, Rasenack J. Isolation, characterization and biological significance of hepatitis B virus mutants from some of a patient with immunologically negative HBV infection. *J Hepatol* 2000; **33**: 799-811
 - 31 **Weinberger KM**, Bauer T, Bohm S, Jilg W. High genetic variability of the group-specific adeterminant of hepatitis B virus surface antigen (HBsAg) and the corresponding fragment of the viral polymerase in chronic virus carriers lacking detectable HBsAg in serum. *J Gen Virol* 2000; **81**(Pt 5): 1165-1174
 - 32 **Chen WN**, Oon CJ, Moh MC. Detection of hepatitis B virus surface antigen mutants in paraffin-embedded hepatocellular carcinoma tissues. *Virus Genes* 2000; **20**: 263-267
 - 33 **Ijaz S**, Torre F, Tedder RS, Williams R, Naoumov NV. Novel immunoassay for the detection of hepatitis surface escape mutants and its application in transplant recipients. *J Med Virol* 2001; **63**: 210-216
 - 34 **Jolivet-Reynaud C**, Lesenechal M, O'Donnell B, Becquart L, Foussadier A, Forge F, Battail-Poirot N, Carman W, Jolivet M. Localization of hepatitis B surface antigen epitopes present on variants and specifically recognised by anti-hepatitis B surface antigen monoclonal antibodies. *J Med Virol* 2001; **65**: 241-249
 - 35 **Worman HJ**, Feng L, Mamiya N. Molecular biology and the diagnosis and treatment of liver diseases. *World J Gastroenterol* 1998; **4**: 185-191
 - 36 **Wu DY**, Ugozzoli L, Pal BK, Wallace RB. Allele-specific enzymatic amplification of β -globin genomic DNA for diagnosis of sickle cell anemia. *Proc Natl Acad Sci USA* 1989; **86**: 2757-2760

Expression of RNase H of human hepatitis B virus polymerase in *Escherichia coli*

Hong Cheng, Hui-Zhong Zhang, Wan-An Shen, Yan-Fang Liu, Fu-Cheng Ma

Hong Cheng, Yan-Fang Liu, Fu-Cheng Ma, Department of Pathology, Xijing Hospital, Fourth Military Medical University, Xi'an 710033, Shaanxi Province, China

Hui-Zhong Zhang, Wan-An Shen, Orthopedics Oncology Institute of Chinese PLA, Fourth Military Medical University, Tangdu Hospital, Xi'an 710038, Shaanxi Province, China

Correspondence to: Dr. Hong Cheng, Department of Pathology, Xijing Hospital, Fourth Military Medical University, Xi'an 710033, Shaanxi Province, China. nelson@fmmu.edu.cn

Telephone: +86-29-3375497

Received: 2002-10-17 **Accepted:** 2002-11-16

Abstract

AIM: To amplify HBV-RNase H gene fragment and expression of RNase H for further use in the studies of HBV associated liver diseases.

METHODS: The encoding gene of HBV-RNase H was separately amplified for the first half and second half (H1 and H2) by PCR from full length HBV gene and cloned into pT7Blue-T vector. Clones were first screened by digestion with *Xba*I and *Hind*III enzyme for the correct size, and analyzed further by DNA sequencing. The RNase H1 and H2 fragments isolated from *Xba*I and *Hind*III digestion products of pT7 Blue-RNase H plasmid were ligated to the GSTag expressing vectors separately, and expressed in *E. coli* BL21. The expressed proteins were checked by PAGE gel and Western blot.

RESULTS: Both H1 and H2 nucleotide sequences consisting of known genes and proteins, in correct size, were further confirmed by Western blot to be the GST and RNase H1 or H2 fusion proteins.

CONCLUSION: The successful cloning and expression of HBV-RNase H will contribute to further research and application in HBV-associated diseases.

Cheng H, Zhang HZ, Shen WA, Liu YF, Ma FC. Expression of RNase H of human hepatitis B virus polymerase in *Escherichia coli*. *World J Gastroenterol* 2003; 9(3): 513-515
<http://www.wjgnet.com/1007-9327/9/513.htm>

INTRODUCTION

Human hepatitis B virus (HBV) infection has a wide range of clinical outcomes, from self-limited silent or acute infection to fulminant hepatitis. It has been estimated that over 300 million cases of chronic HBV infection exist globally^[1]. In China, nearly 100 million people have a persistent infection with HBV, who are at risk of developing chronic hepatitis leading to liver cirrhosis and hepatocellular carcinoma^[2-6]. Significant advances have been made during the last few years in the treatment of chronic hepatitis B^[7-13]. Several new antiviral agents have been shown to be safe and effective in inhibiting HBV replication^[14-20]. However, it has remained refractory to

the treatment since not all patients respond properly and still there is no breakthrough results in therapeutic vaccine^[21-23]. The increase of chronic hepatitis and hepatocellular carcinoma associated with the HBV infection has become a worldwide medical problem.

HBV replication is accomplished by its own polymerase. Hepadnavirus polymerases are multifunctional enzymes that play critical roles during the viral life cycle^[24]. Ribonuclease H (RNase H), the HBV RNaseH domain of HBV polymerase, is one of the four domains (Terminal, Spacer, Reverse Transcriptase and RNase H) encoded by HBV polymerase gene. With 480 bp in full length and encoding a 16ku protein which is responsible for degrading RNA from RNA-DNA intermediate, HBV-RNase H plays a pivotal role in the HBV life cycle. Although the rest of HBV encoded antigen rather than RNase H has been studied in detail^[25-30], there is less paper about HBV-RNase H which is intimately related with HBV replication. To explore the potential use of HBV-RNase H in the diagnosis and treatment of HBV associated liver diseases, we cloned and expressed RNase H of the HBV polymerase.

MATERIALS AND METHODS

Materials

pTKHH2 plasmid containing the full length HBV genomic DNA of subtype adw2 was kindly provided by Dr. Lingxun Duan in Thomas Jefferson University (Philadelphia PA). The primers with restriction enzyme site *Xba*I at 5' end and *Hind*III at 3' end used to amplify HBV-RNase H gene was synthesized in Gibco Inc. pT7Blue cloning vector, DH5 α competent cells, GSTag expression vector and anti-GST antibody were products of Novagen Inc.

Plasmid construction^[31,32]

Two pairs of primers were used in PCR reactions to amplify the first half (H1 1-240) and the second half (H2 241-480) fragments of RNase H gene from pTKHH2 plasmid (P1: 5' - TTCTAGACCGCCAGGTCTGTGCCAAGTG-3', P2: 5' - AAG CTTACCAGTTGGCAGCACAGCCTAG-3' for H1; and P3: 5' - TTCTAGACA TCCTGCGCGGGACGTCCTTTG-3', P4: 5' -AAGCTTAATGCGGTGGTCTCCA TGCG-3' for H2). The amplified H1 and H2 fragments were purified on a 15 g/L low-melting agarose gel, utilizing the PCR purification system (Promega Inc). The purified PCR products were directly ligated into the pT7 Blue-T vector respectively. After transformation of the *Escherichia coli* strain DH5 α , recombinants were selected on x-Gal plates. Ten white colonies were selected for miniprep and the insert evaluation was by enzyme digestion and DNA sequencing. The plasmids with proper inserts were recut with *Xba*I and *Hind*III enzyme and ligated into pGSTag vector. The pGSTag containing H1 or H2 fragment were transformed into BL21 *Escherichia coli* strain and propagated in LB medium.

Expression^[33] and identification of HBV-RNaseH

Picked the recombinant colonies and grew them overnight at 37 °C in 3 mL of LB medium. Removed 1 mL culture and

inoculated into 100 mL of fresh LB medium and grew at 37 °C to an A600 of 0.6. Added 100 mmol/L IPTG to the bacterial culture to a final concentration of 0.3 mmol/L and incubated the culture for an additional 3–4 h. Pelletized the cells by centrifuging at 12 000 g for 3 min and resuspending the bacterial pellet in 3 mL lysis buffer. After the bacteria lysed by ultrasonic machine, the fusion proteins were purified with glutathione Sepharose 4B column and identified by PAGE gel stained with Coomassie blue and further confirmed by Western blot.

RESULTS

Recombinant expression vectors of pGSTag containing Cloned HBV RNase H1 and H2 fragments were identified by restriction enzyme digestion and DNA sequencing and the results showed that the inserted DNA fragment were expected known sequences. The expressed proteins could be seen in Coomassie blue stained PAGE gel with 34 ku band (Figure 1) which were further confirmed by Western blot as GST and HBV RNase H fusion protein.

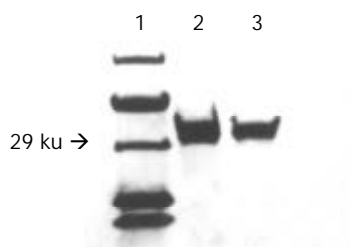


Figure 1 PAGE Electrophoresis stained with Coomassie brilliant blue light. 1: Protein MW standards; 2: RNaseH1 protein (34 ku); 3: RNaseH2 protein (34 ku).

DISCUSSION

Genome replication of hepadnavirus proceeds by reverse transcription from a viral pregenomic RNA template by a virally encoded polymerase, a polypeptide of 90 to 97 ku^[34]. The genome of all hepadnaviruses has the open reading frame, the polymerase gene, and the product or products of this polymerase gene are involved in multiple functions of the viral life cycle. These functions include a priming activity which initiates minus-strand DNA synthesis, a polymerase activity which synthesizes DNA by using either RNA or DNA templates (reverse transcriptase), a nuclease activity which degrades the RNA strand of RNA-DNA hybrids (RNase H), and involvement in packaging the RNA pregenome into nucleocapsids^[35].

Molecular genetic studies have revealed that the human HBV polymerase protein, a polypeptide of about 94 ku, which plays a critical role in the HBV life cycle, contains four domains. These are the 5' -terminal protein (TP), spacer, RNA reverse transcriptase (RT)/DNA polymerase, and RNase H, respectively, from the amino (N) to carboxy (C) terminus^[36-42]. All of the TP and RT and RNase H, rather than spacer protein, play an important role in the process of HBV replication. The RNase H, as it functions in all other retrovirus, can degrade the RNA of DNA-RNA hybrid which plays a role in optimizing the priming of minus-strand DNA synthesis^[43]. We had constructed an expression vector containing full length of HBV RNase H DNA and we failed to propagate the transformed bacteria, which might be caused by the toxic effect of RNase H activation as Lee Yi reported^[44] earlier. So we redesigned two pairs of primers to clone and expressed with two separate fragments of the RNase H. The successfully expressed RNase H and its function which will be performed in our next experiment will

contribute to further generating anti-RNase H antibody producing hybridoma cells for the purpose of HBV related liver diseases gene therapy. It has been confirmed that RNase H can be used as a marker to reflect the low level virus replication without other positive markers^[45], so to investigate and analyze the results of anti-HBV RNase H might be able to provide a new marker for the early diagnosis of HBV infection and to assess the effects of clinical therapy of HBV infection diseases.

REFERENCES

- 1 **Pramoolsinsup C.** Management of viral hepatitis B. *J Gastroenterol Hepatol* 2002; **17** (Suppl): S125-145
- 2 **Wang PZ,** Zhang ZW, Zhou YX, Bai XF. Quantitative PCR detection of HBV-DNA in patients with chronic hepatitis B and its significance. *Shijie Huaren Xiaohua Zazhi* 2000; **8**: 755-758
- 3 **Shi H,** Wang FS. Host factors in chronicity of hepatitis B virus infection and their significances clinic alh. *Shijie Huaren Xiaohua Zazhi* 2001; **9**: 66-69
- 4 **Wang Y,** Liu H, Zhou Q, Li X. Analysis of point mutation in site 1896 of HBV precore and its detection in the tissues and serum of HCC patients. *World J Gastroenterol* 2000; **6**: 395-397
- 5 **Li Y,** Su JJ, Qin LL, Yang C, Luo D, Ban KC, Kensler TW, Roe-buck BD. Chemopreventive effect of oltipraz on AFB1-induced hepatocarcino- genesis in tree shrew model. *World J Gastroenterol* 2000; **6**: 647-650
- 6 **De Clercq E.** Highlights in the development of new antiviral agents. *Mini Rev Med Chem* 2002; **2**: 163-175
- 7 **Du DW,** Zhou YX, Feng ZH, Li GY, Yao ZQ. Study on immunization of anti-subcutaneous transplanting tumor induced by gene vaccine. *Shijie Huaren Xiaohua Zazhi* 1999; **7**: 955-957
- 8 **Du DW,** Zhou YX, Feng ZH, Yao ZQ, Li GY. Immune responses to interleukin 12 and hepatitis B gene vaccine in H2 d mice. *Shijie Huaren Xiaohua Zazhi* 2000; **8**: 128-130
- 9 **Wang QC,** Zhou YX, Yao ZQ, Feng ZH. Effects of DNA vector constructs and different genes on the induction of immune responses by HBV DNA based vaccine. *Shijie Huaren Xiaohua Zazhi* 2000; **8**: 289-291
- 10 **Huang ZH,** Zhuang H, Lu S, Guo RH, Xu GM, Cai J, Zhu WF. Humoral and cellular immunogenicity of DNA vaccine based on hepatitis B core gene in rhesus monkeys. *World J Gastroenterol* 2001; **7**: 102-106
- 11 **Liu HB,** Meng ZD, Ma JC, Han CQ, Zhang YL, Xing ZC, Zhang YW, Liu YZ, Cao HL. A 12-year cohort study on the efficacy of plasma-derived hepatitis B vaccine in rural newborns. *World J Gastroenterol* 2000; **6**: 381-383
- 12 **Li H,** Wang L, Wang SS, Gong J, Zeng XJ, Li RC, Nong Y, Huang YK, Chen XR, Huang ZN. Research on optimal immunization strategies for hepatitis B in different endemic areas in China. *World J Gastroenterol* 2000; **6**: 392-394
- 13 **Zeng XJ,** Yang GH, Liao SS, Chen AP, Tan J, Huang ZJ, Li H. Survey of coverage, strategy and cost of hepatitis B vaccination in rural and urban areas of China. *World J Gastroenterol* 1999; **5**: 320-323
- 14 **Liu P,** Hu YY, Liu C, Zhu DY, Xue HM, Xu ZQ, Xu LM, Liu CH, Gu HT, Zhang ZQ. Clinical observation of salvianolic acid B in treatment of liver fibrosis in chronic hepatitis B. *World J Gastroenterol* 2002; **8**: 679-685
- 15 **Jin J,** Yang JY, Liu J, Kong YY, Wang Y, Li GD. DNA immunization with fusion genes encoding different regions of hepatitis C virus E2 fused to the gene for hepatitis B surface antigen elicited immune responses to both HCV and HBV. *World J Gastroenterol* 2002; **8**: 505-510
- 16 **Guan XJ,** Guan XJ, Wu YZ, Jia ZC, Shi TD, Tang Y. Construction and characterization of an experimental ISCOMS-based hepatitis B polypeptide vaccine. *World J Gastroenterol* 2002; **8**: 294-297
- 17 **Hussain M,** Lok AS. Mutations in the hepatitis B virus polymerase gene associated with antiviral treatment for hepatitis B. *J Viral Hepat* 1999; **6**: 183-194
- 18 **Stuyver L,** Van Geyt C, De Gendt S, Van Reybroeck G, Zoulim F, Leroux-Roels G, Rossau R. Line probe assay for monitoring drug resistance in hepatitis B virus-infected patients during antiviral therapy. *J Clin Microbiol* 2000; **8**: 702-707

- 19 **Liu P**, Liu C, Xu LM, Xue HM, Liu CH, Zhang ZQ. Effects of Fuzheng Huayu 319 recipe on liver fibrosis in chronic hepatitis B. *World J Gastroenterol* 1998; **4**: 348-353
- 20 **Zoulim F**. Detection of hepatitis B virus resistance to antivirals. *J Clin Virol* 2001; **21**: 243-253
- 21 **Honorati MC**, Facchini A. Immune response against HBsAg vaccine. *World J Gastroenterol* 1998; **4**: 464-466
- 22 **Li H**, Li RC, Liao SS, Yang JY, Zeng XJ, Wang SS. Persistence of hepatitis B vaccine immune protection and response to hepatitis B booster immunization. *World J Gastroenterol* 1998; **4**: 493-496
- 23 **Gao FG**, Sun WS, Cao YL, Zhang LN, Song J, Li HF, Yan SK. HBx DNA probe preparation and its application in study of hepatocarcinogenesis. *World J Gastroenterol* 1998; **4**: 320-322
- 24 **Zu Pudlitz J**, Lanford RE, Carlson RI, Notvall L, de la Monte SM, Wands JR. Properties of monoclonal antibodies directed against hepatitis B virus polymerase protein. *J Virol* 1999; **73**: 4188-4196
- 25 **Lin X**, Yuan ZH, Wu L, Ding JP, Wen YM. A single amino acid in the reverse transcriptase domain of hepatitis B virus affects virus replication efficiency. *J Virol* 2001; **75**: 11827-11833
- 26 **Lott L**, Beames B, Notvall L, Lanford RE. Interaction between hepatitis B virus core protein and reverse transcriptase. *J Virol* 2000; **74**: 11479-11489
- 27 **Laras A**, Koskinas J, Hadziyannis SJ. *In vivo* suppression of precore mRNA synthesis is associated with mutations in the hepatitis B virus core promoter. *Virology* 2002; **295**: 86-96
- 28 **Laras A**, Koskinas J, Avgidis K, Hadziyannis SJ. Incidence and clinical significance of hepatitis B virus precore gene translation initiation mutations in e antigen-negative patients. *J Viral Hepat* 1998; **5**: 241-248
- 29 **Stuyver LJ**, Locarnini SA, Lok A, Richman DD, Carman WF, Dienstag JL, Schinazi RF. Nomenclature for antiviral-resistant human hepatitis B virus mutations in the polymerase region. *Hepatology* 2001; **33**: 751-757
- 30 **Kim Y**, Hong YB, Jung G. Hepatitis B virus: DNA polymerase activity of deletion mutants. *Biochem Mol Biol Int* 1999; **47**: 301-308
- 31 **Cheng H**, Liu YF, Zhang HZ, Zhang SZ. Construction and expression of anti-HCC immunotoxin of sFv-TNF- α and GFP fusion proteins. *Shijie Huaren Xiaohua Zazhi* 2001; **9**: 640-644
- 32 **Cheng H**, Liu YF, Zhang HZ, Shen WA. Construction of the recombinant retroviral vector encoding anti-HCC single-chain bi-functional antibody and establishment of a stable virus producing PA317 cell line. *Shijie Huaren Xiaohua Zazhi* 2000; **8**: 708-709
- 33 **Lee YI**, Hong YB, Kim Y, Rho HM, Jung G. RNase H activity of human hepatitis B virus polymerase expressed in *Escherichia coli*. *Biochem Biophys Res Commun* 1997; **233**: 401-407
- 34 **Li Z**, Tyrrell DL. Expression of an enzymatically active polymerase of human hepatitis B virus in an coupled transcription-translation system. *Biochem Cell Biol* 1999; **77**: 119-126
- 35 **Chen KL**, Chen CM, Shih CM, Huang HL, Lee YH, Chang C, Lo SJ. Hepatitis B viral polymerase fusion proteins are biologically active and can interact with the hepatitis C virus core protein *in vivo*. *J Biomed Sci* 2001; **8**: 492-503
- 36 **Villamil FG**. Hepatitis B: Progress in the last 15 years. *Liver Transpl* 2002; **8**(10 Suppl 1): S59-66
- 37 **Chen Y**, Marion PL. Amino acids essential for RNaseH activity of hepadnaviruses are also required for efficient elongation of minus-strand viral DNA. *J Virol* 1996; **70**: 6151-6156
- 38 **Lok AS**, Hussain M, Cursano C, Margotti M, Gramenzi A, Grazi GL, Jovine E, Benardi M, Andreone P. Evolution of hepatitis B virus polymerase gene mutations in hepatitis B e antigen-negative patients receiving lamivudine therapy. *Hepatology* 2000; **32**: 1145-1153
- 39 **Torresi J**. The virological and clinical significance of mutations in the overlapping envelope and polymerase genes of hepatitis B virus. *J Clin Virol* 2002; **25**: 97
- 40 **Cerritelli SM**, Fedoroff OY, Reid BR, Crouch RJ. A common 40 amino acid motif in eukaryotic Rnases H1 and caulimovirus ORF VI proteins binds to duplex RNAs. *Nucleic Acids Res* 1998; **26**: 1834-1840
- 41 **Wakil SM**, Kazim SN, Khan LA, Raisuddin S, Parvez MK, Guptan RC, Thakur V, Hasnain SE, Sarin SK. Prevalence and profile of mutations associated with lamivudine therapy in Indian patients with chronic hepatitis B in the surface and polymerase genes of hepatitis B virus. *J Med Virol* 2002; **68**: 311-318
- 42 **Kim Y**, Hong YB, Jung G. Hepatitis B virus: DNA polymerase activity of deletion mutants. *Biochem Mol Biol Int* 1999; **47**: 301-308
- 43 **Li Z**, Tyrrell DL. Expression of an enzymatically active polymerase of human hepatitis B virus in an coupled transcription-translation system. *Biochem Cell Biol* 1999; **77**: 119-126
- 44 **Kim Y**, Jung G. Active human hepatitis B viral polymerase expressed in rabbit reticulocyte lysate system. *Virus Genes* 1999; **19**: 123-130
- 45 **Yuki N**, Hayashi N, Kasahara A, Katayama K, Ueda K, Fusamoto H, Kamada T. Detection of antibodies against the polymerase gene product in hepatitis B virus infection. *Hepatology* 1990; **12**: 193-198

Edited by Wu XN

Virulence of water-induced coccoid *Helicobacter pylori* and its experimental infection in mice

Fei-Fei She, Jian-Yin Lin, Jun-Yan Liu, Cheng Huang, Dong-Hui Su

Fei-Fei She, Department of Microbiology, Medical College of Wuhan University, Wuhan 234007, Hubei Province, China & Department of Microbiology, Fujian Medical University, Fuzhou 350004, Fujian Province, China

Jian-Yin Lin, Department of Molecular Medicine, Fujian Medical University, Fuzhou 350004, Fujian Province, China

Jun-Yan Liu, Department of Microbiology, Medical College of Wuhan University, Wuhan 234007, Hubei Province, China

Cheng Huang, Department of Microbiology, Fujian Medical University, Fuzhou 350004, Fujian Province, China

Dong-Hui Su, Department of Immunology, Fujian Medical University, Fuzhou 350004, Fujian Province, China

Supported by the Natural Science Foundation of Fujian Province, China, No. C95031

Correspondence to: Fei-Fei She, Department of Microbiology, Fujian Medical University, Fuzhou 350004, Fujian Province, China. cyslff@163.net

Telephone: +86-591-3569309

Received: 2002-09-14 **Accepted:** 2002-10-17

Abstract

AIM: To explore the virulence and the infectivity of coccoid *Helicobacter pylori* (*H. pylori*) transformed from spiral form by exposure to sterile tap water.

METHODS: Three strains of *H. pylori*, isolated from gastric biopsy specimens of confirmed peptic ulcer, were converted from spiral into coccoid form by exposure to sterile tap water. Both spiral and coccoid forms of *H. pylori* were tested for the urease activity, and the adherence to Hep-2 cells. The presence of flagella was examined under electron microscopy. In the experimental animal infection, the spiral and coccoid forms of *H. pylori* originated from the same strain F49 were inoculated intragastrically into BALB/c mice respectively four times at a 3-day interval. Half of the mice from each group were sacrificed at Day 21 and Day 28 after the last inoculation. Histology and *H. pylori* colonization were detected by urease test of gastric mucosa, cultures of *H. pylori*, and electron microscopy and so on.

RESULTS: The urease activity and the ability of adherence to Hep-2 cells were found to be lower in coccoid *H. pylori* than that in its spiral form. For example, the transformation in strain F₄₄ led to a significant decrease of the adherence rate and adherence index from 70.0±5.3 % to 30.2±3.5 % ($P<0.01$), and from 2.6±0.4 to 0.86±0.3 ($P<0.01$), respectively. The flagella of coccoid *H. pylori* were observed under electron microscope. In the experimental infection in mice, the positive rate of gastric mucosa urease test was 93.8 % (15/16) in the group infected by spiral *H. pylori* and 50 % (8/16) in the group infected by coccoid *H. pylori*, and the estimated coccoid *H. pylori* colony number was 1.75 vs 0.56. The positive rates of *H. pylori* culture were 87.5 % (14/16) in spiral *H. pylori* group and 68.8 % (11/16) in coccoid *H. pylori* group. There was no significant difference in either urease test or bacterial culture rate between the groups examined at Day 21 and Day 28 after inoculation.

Electron microscopic examination of the samples taken from both groups showed the adherence of *H. pylori* in spiral, bacillary and coccoid shapes to the epithelial cells of gastric wall. Histological examination showed the occurrence of gastric mucosal injury as indicated by various degrees of erosion, ulcer, and inflammatory cell infiltration. Mucosal injury was slighter in the mice infected by coccoid *H. pylori*. No positive result was obtained in the control group that received intragastrical administration of sterile tap water.

CONCLUSION: Although the virulence of coccoid *H. pylori* induced by water decrease, coccoid *H. pylori* still remains a considerable urease activity and the adhering ability to epithelial cells. Furthermore, the flagella, an important component responsible for bacterial movement and infection, were still observed as a cellular structure of coccoid *H. pylori* under electron microscope. The coccoid *H. pylori* induced by water is capable of colonizing in gastric mucosa and causing gastritis in mice.

She FF, Lin JY, Liu JY, Huang C, Su DH. Virulence of water-induced coccoid *Helicobacter pylori* and its experimental infection in mice. *World J Gastroenterol* 2003; 9(3): 516-520
<http://www.wjgnet.com/1007-9327/9/516.htm>

INTRODUCTION

Helicobacter pylori has been recognized as an important pathogen that causes chronic gastritis and peptic ulcer and likely as a risk factor associated with gastric carcinoma^[1-9]. *H. pylori* infection is endemic. In despite of more than 10 years of intensive research, the precise mode and route of *H. pylori* transmission remain elusive. Four routes including fecal-oral, oral-oral, gastro-oral and iatrogenic transmission have been postulated^[10-13]. The association between water consumption and *H. pylori* infection indicates that *H. pylori* may be transmitted through a waterborne route^[14-16]. *H. pylori* exists in two forms: the spiral form and the coccoid form. Coccoid *H. pylori* is non-culturable but alive^[17-20]. Some researches have shown that *H. pylori* can survive water microcosms in coccoid form^[20,21]. The coccoid *H. pylori* in water has therefore been suspected to contribute an important part to the transmission of the bacteria. However, the virulence and infectivity of coccoid *H. pylori* in water has not been studied. To explore the pathogenicity of the coccoid *H. pylori* in water, three strains of spiral *H. pylori* were treated by prolonged exposure to sterile tap water and examined for the presence of flagella under electron microscopy and tested for their urease activity and their adherence to Hep-2 cells. A strain was inoculated into the BABL/C mice. The gastric mucosal samples were taken to assess the bacterial *in vivo* colonization and pathological effects by means of urease test, bacterial culture, electron microscopy, and light microscopy.

MATERIALS AND METHODS

Animals

Female BALB/c mice were purchased from Shanghai

Experimental Animal Center, Chinese Academy of Sciences and raised under SPF conditions. Those of 8 weeks old, weighing 20-22 g were used for bacterial inoculation. Sterile food and tap water were given ad libitum.

Cells

Human epithelial cell line Hep-2 cells were maintained in 1 640 medium supplemented with 10 % fetal calf serum, 200 IU/ml penicillin and 50 µg/ml streptomycin at 37 °C in 5 % CO₂-95 % air, and re-cultivated twice a week.

Bacterial strains

Three strains (F44, F45 and F49) of *H. pylori* were isolated in this laboratory from gastric biopsy specimens of confirmed peptic ulcer patients. The isolates were spiral in shape, positive for catalase, oxidase, urease, and *cagA* and *vacA* gene. Stock cultures were maintained in defatted milk at -80 °C.

H. pylori cultivation and coccoid form induction

The stored strains of *H. pylori* were cultured on Brucella agar with 5 % sheep blood at 37 °C for 2-3 d under microaerophilic conditions (5 % O₂; 10 % CO₂; 85 % N₂). After being subcultured, the bacteria were harvested and suspended in sterile tap water and the suspensions were incubated at 4 °C for a few days (about 3-4 d) until 100 % transformation to coccoid form was achieved and confirmed under light microscopy. The transformed bacteria were inoculated on the Brucella agar media supplemented with 5 % sheep blood for reversion trial culture. The stock suspensions were stored at 4 °C until use.

Electron microscopy

H. pylori flagella were examined under A Hu-12A transmission electron microscope. To prepare the bacterial samples, *H. pylori* suspensions were centrifuged, and the pellets were embedded in Epoxy 618. The ultra-thin sections were cut and negatively stained by 1 % phosphotungstic acid.

Assessment of cell adherence

Hep-2 cells were grown to confluence on glass coverslips in culture flask, and 0.5 ml of the suspension of *H. pylori* (10⁸ cfu/ml) was added to culture medium (5 ml) for an additional 3.5 h culture at 37 °C in 5 % CO₂-95 % air. Cultures on the coverslips were washed and stained with Wright-Giemsa. One hundred Hep-2 cells were examined under light microscope for the counts of both the cells adhered by bacteria and the bacteria adhering to each cell. The adherence rate and adherence index were then calculated by the formula (described in the Results).

Animal infection experiment

Forty-two BALB/c mice were randomly divided into 3 groups. By oral gavage, groups 1 and 2 (16 mice each) were given 0.4 ml (10⁹ cfu/ml) of suspensions of F49 strain spiral *H. pylori* and coccoid *H. pylori* (in water for 40 days), respectively, four times at a 3-day interval. The control group (10 mice) received 0.4 ml sterile tap water. At Day 21 and 28 after inoculation, half of the mice from each group were sacrificed, respectively. Before killing, the mice were fasted for 36 hours with free access to water. At sacrifice, stomachs were removed, opened and washed with sterile saline and longitudinally divided into 3 sections in same size, which were used respectively for fast urease test and bacterial culture, electron microscopy, and histological examination.

Urease activity assay

Urease activity fast assay kit was purchased from Sanqiang

Company (Sanming, Fujian). The assays were made according to the manufacturer's instructions. Diluted *H. pylori* cultures (10¹⁰ cfu/ml, 5 µl), or tissue fragments (3×3 mm) obtained from the pylorus part of one-third of the mouse gastric mucosa were added to the test wells to react with the commercial reagents. To evaluate the urease activity, the colors developed in the assay were scored into five grades (++++, +++, ++, + and -) for bacterial cultures and four grades (+++ , ++, + and -) for tissue fragments.

Bacterial examination

After collected for urease assay, the remaining one-third gastric mucosa samples were grounded into homogenate, daubed on Brucella agar with 5 % sheep blood, and incubated at 37 °C for 3-4 d under microaerophilic conditions. Colonies were taken and identified under light microscopy, urease activity test and *cagA* gene amplification by PCR. In addition, two samples from groups 1 and 2 respectively, which were bacteriologic positive and trimmed to 1 mm³, were embedded in Epoxy 618, then the ultra-thin sections were cut, stained by uranyl acetate and lead citrate and examined under a Hu-12A transmission electron microscope.

Light microscopic histological examination

The gastric mucosal samples were embedded in paraffin, cut in 5 µm sections, stained with hematoxylin-eosin, and examined under light microscope.

Statistical analysis

Data was analyzed using the Student *t* test. The statistically significant difference was suggested by a value of *P*<0.05, and the very significant difference by *P*<0.01.

RESULTS

In vitro virulence of water-induced coccoid *H. pylori*

Flagella Three strains (F44, F45 and F49) of *H. pylori* were seen under light microscope in a typical spiral shape before their exposure to water. After 3-4 d incubation in sterile tap water at 4 °C, no spiral but only coccoid shaped bacteria were observed. Reversion trial showed that water-induced coccoid *H. pylori* failed to grow on Brucella agar supplemented with 5 % sheep blood. Electron microscopy showed that the flagella remained a part of the bacterial cell structure (Figure 1).

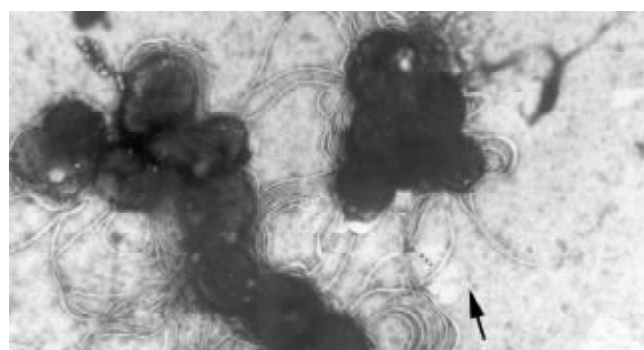


Figure 1 The flagella of coccoid *H. pylori* under transmission electron microscope ×6 000.

Urease activity Table 1 shows the urease activity assayed for three strains (F44, F45 and F49) of *H. pylori* both in spiral form (normal culture) and the respective coccoid form (subjected to water treatment). Strong urease activity (++++) was confirmed in the spiral *H. pylori* of all the three strains tested. The urease activity of the water-induced *H. pylori*, i.e., the

coccoid form of these three strains, significantly reduced, but still existed on a detective level (+ to ++).

Table 1 Urease activity of *H. pylori*

Strain	Urease activity	
	Spiral form	Coccoid form
F44	++++	+
F45	++++	++
F49	++++	+

Adhering ability All the three strains of *H. pylori* in both spiral form and water-induced coccoid form were tested for their adhering ability to Hep-2 cells. According to the following formula, the rate and the index of adherence were calculated. The rate of adherence=the amount of cell adherenced by bacteria/100×100 %;

The index of adherence=the amount of bacteria adhering to cells/100;

Five groups of each 100 Hep-2 cells were counted for the number of cells adhered by bacteria and the total number of bacteria adhering to the cells. The percentages of cells adhered by bacteria (adherence rate) and the average bacteria number (adherence index) adhered to each cell are presented in Table 2. The adherence was observed in all groups tested. Student *t* test showed a very significant difference between the spiral and coccoid forms of *H. pylori* in either adherence rate or adherence index.

Table 2 Adherence of *H. pylori* to Hep-2 cells

	Adherence rate (%) ^a			Adherence index ^b (Bacteria numbers per cell)		
	F44	F45	F49	F44	F45	F49
Spiral form	70.0±5.3	73.0±5.1	72.6±4.5	2.6±0.4	3.1±0.5	2.9±0.4
Coccoid form	30.2±3.5	35.7±4.1	31.4±4.0	0.86±0.3	0.91±0.3	0.88±0.4
<i>t</i> value	12.3	11.2	12.8	7.2	7.8	7.4
<i>P</i>	<0.01	<0.01	<0.01	<0.01	<0.01	<0.01

^aAdherence rate=amount of cells adhered by bacteria/100×100 %; ^bAdherence index=total amount of bacteria adhering to 100 cells/100; Five groups of 100 cells on the same coverslip were counted for the bacteria adhered. Data are presented as mean ±SD. *t* and *P* values were obtained using Student *t* test.

Coccoid *H. pylori* infection in mice

Bacterial colonization *H. pylori* colonization in the gastric mucosa of inoculated mice was determined by the urease assay and bacterial culture of the of tissue samples. The bacterial cultures were found to be characteristic of spiral *H. pylori* as proved by the spiral shaped structure under light microscope, the positive urease activity, and the positive amplification of cagA gene fragments (data not shown). Data shown in Table 3 were the rates of positive findings in each group of mice. The positive rates of urease test of gastric mucosa, which was infected by spiral *H. pylori* and coccoid *H. pylori*, were 93.8 % (15/16) and 50 % (8/16), respectively. The positive rates of cultures of *H. pylori* were 87.5 % (14/16) and 68.8 % (11/16) respectively. Neither urease assay nor bacterial culture was found positive in the mice of the control group. Sampling at Day 21 and Day 28 after inoculation found almost no difference in both tests. In the semi-quantitative study, the color development in fast urease assay was scored. The colors distinguished at grades -, +, ++, and +++, which were associated with the existence of the *H. pylori* in 0, 1-10, 11-30, and >30 per microscope field, respectively, according to the guide of

test kit, were accordingly assigned by 0, 1, 2, and 3 point(s). Table 4 presents the number of mice scored at the same points in this assay and the average points of each group. Again, the score in group 1 was much higher than in group 2 (1.75 vs 0.56), while the score in control group was zero. In addition, electron microscopy showed the adherence of bacteria to the gastric mucosal samples taken from both group 1 and group 2 (Figure 2A and B). These bacteria were in spiral, bacillary or coccoid shapes, and some of them had invaded into the gastric epithelial cells. No similar bacterium adherence and invasion was observed in the samples from control group.

Table 3 Tests of bacteria in gastric mucosa samples

Group	Total no.	Fast urease test			Culture of bacterial		
		Positive/total		Positive rate(%)	Positive/total		Positive rate(%)
		D21	D28		D21	D28	
1	16	7/8	8/8	93.8	7/8	7/8	87.5
2	16	4/8	4/8	50.0	5/8	6/8	68.8
Control	10	0/5	0/5	0	0/5	0/5	0

Group 1 was inoculated with spiral *H. pylori*, group 2 was inoculated with water-induced coccoid *H. pylori*, and control group received sterile tap water.

Table 4 Scores for urease tests of tissue samples

Groups	Color development				Urease activity (mean score)
	-	+	++	+++	
1	1 ^a	5	7	3	1.75 ^b
2	8	7	1	0	0.56
Control	10	0	0	0	0

^aNumbers of mice; ^bRefers to text for scoring and calculation.

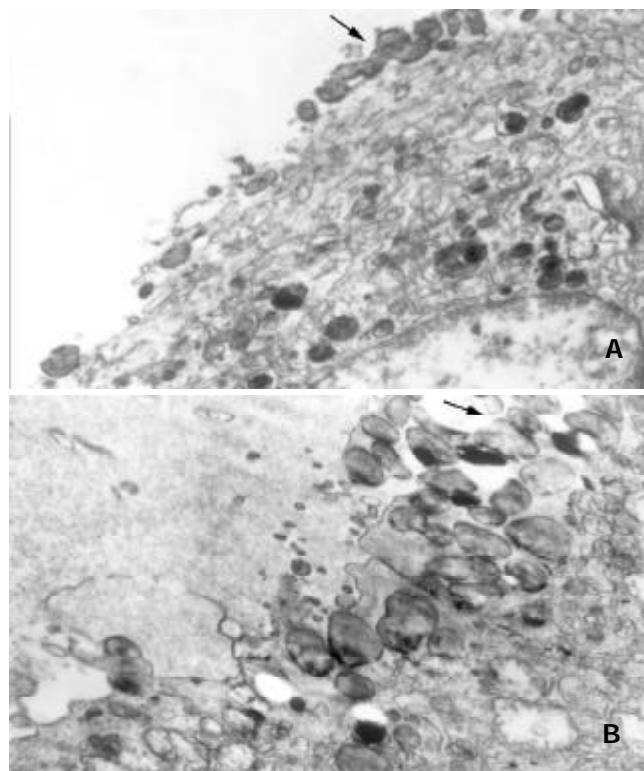


Figure 2 *H. pylori* colonization in mouse stomach under transmission electron microscope. A. infection of spiral *Hp.* ×7 000; B. infection of coccoid *Hp.* ×9 000.

Histopathological alteration Inflammatory pathological features were observed in both group 1 and group 2 samples under light microscope (Table 5 and Figure 3). Fifteen mice of group 1 and ten mice of group 2 developed inflammatory cell infiltration and different degrees of erosion or ulcer. The frequency and intensity of the erosion in group 1 was higher than in group 2. Two out of sixteen mice in group 1 even developed mucosal ulcers. Mucosal injury was slighter in the mice infected by coccoid *H.pylori*. None of these features was found in the control group.

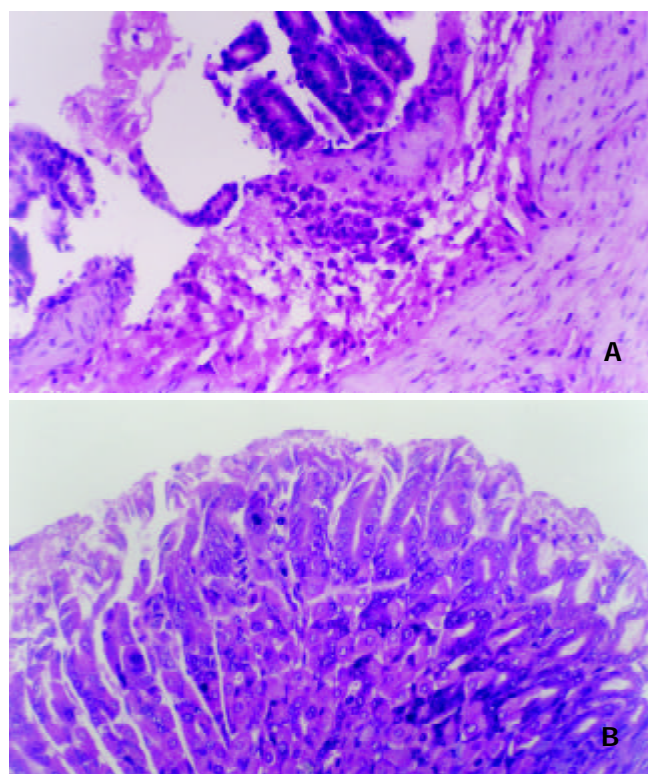


Figure 3 Light microscopy for gastric mucosa of mice. H&E×200. A. infection of spiral *Hp*; B. infection of coccoid *Hp*.

Table 5 Pathological alterations of gastric mucosa from mice

Groupe	Histopathological event (no. of mice)				
	Normal	Gentle erosion	Deep erosion	Ulcer	Total
1	1	7	6	2	16
2	6	9	1	0	16
Control	10	0	0	0	10

DISCUSSION

Increasing reports showed that *H. pylori* had been detected from water by immunomagnetic separation, bacterial culture or polymerase chain reaction (PCR) technique^[22-27] and that consumption of water was closely related to *H.pylori* infection^[14-16]. Water borne route is therefore thought to be an important route of *H. pylori* transmission. *H.pylori* has been found to be able to convert from spiral form to coccoid form under certain adverse circumstances such as increased oxygen tension, extended incubation and exposure to antibiotics or water^[17,28-32]. Some researches suggested that *H. pylori* in coccoid form can survive the water for a long time. However, it remains unknown whether coccoid *H. pylori* can attack and colonize in stomach., resulting in the diseases of digestive system. Going deep inside to the behavior of coccoid *H. pylori*

will thus be very beneficial to our understandings on the transmission of *H. pylori* infection and its association with many severe human diseases like gastritis, ulcer and peptic carcinomas.

The putative pathogenic determinants of *H.pylori* have been divided into two major groups^[35]: maintenance factors, which allow the bacterium to colonize and remain within the host, and virulence factors, which contribute to the pathogenetic effects of the bacterium. Flagella, urease activity and adherence to epithelial cells of *H.pylori* are important maintenance factors^[34-37]. If coccoid *H.pylori* in water remains infective, they must possess maintenance factors in order to colonize and remain in stomach. In this study, it is shown that both urease activity and adherence to Hep-2 cells of coccoid *H. pylori* decreased as compared with the spiral forms, suggesting a reduction of virulence related to colonization of *H.pylori* when the transformation to coccoid form occurs. However, as shown by the microbial assays, coccoid *H.pylori* induced by water still remains a considerable urease activity and the adhering ability to epithelial cells. Furthermore, the flagella, an important component responsible for bacterial movement and infection, were still observed as a cellular structure of coccoid *H.pylori* under electron microscope. This adds to the potential of *in vivo* infection of the coccoid *H.pylori* induced by water.

In the animal experiments described here, some mice (10/16) inoculated with water-induced coccoid *H.pylori* developed significant pathological changes such as mucosal erosion and inflammatory cell infiltration in gastric mucosa, as were shown by histopathological examinations. The evidences of the coccoid *H.pylori* being the pathogen of the mucosal injury were further provided by bacteriological examinations. In this aspect, a 50 % positive rate and a considerable intensity of urease test were detected in the mucosal samples of mice inoculated with water-induced coccoid *H.pylori*, and the positive *H.pylori* cultures of these samples reached a percentage of 68.8 %. In addition, electron microscopy for these samples showed the presence of spiral bacteria in gastric mucosa. All these findings reveal the ability of water-induced coccoid *H. pylori* in their colonization on mouse gastric wall and their injury to the mucosal tissues.

It might be reasonably queried whether there still exists an undetectable trace amount of spiral *H.pylori* among the huge quantity of their coccoid variance, which could be intrinsically responsible for the virulence and infectivity of the bacteria in some studies including ours. The facts that the bacteria were kept in in-nutritious water for up to 40 days and that the water-treated bacteria were assayed for *in vitro* virulence in real time, eliminated the possibility of an expansion of the spiral population or in-water reversion of the coccoid variance to its spiral origins. The failure of the trial reversion in supplemented Brucella medium further supported the concept of a direct virulence of the coccoid *H. pylori*. Now that the spiral shaped bacteria were observed in the mucosal tissues of mice inoculated with coccoid *H. pylori*, it seemed that the reversion took place *in vivo*. However, whether the reversion is a key precondition for the infection remains unclear. In despite of our ignorance in the process and mechanisms of the inter-transformation of *H.pylori*, conclusions can be drawn from our current study that water-induced coccoid form of *H.pylori* remains virulent and infective to gastric wall in mice. Water borne route transmission of *H.pylori* needs more attention.

REFERENCES

- Gao GL, Pan BR, Yang SF, SongG, Xu XQ, Liu Y. The value of *Helicobacter pylori* in gastro-duodenal diseases. *Xin Xiaohuabingxue Zazhi* 1994; 2: 232-233

- 2 **Li ZX**, Zhang WD, Zhou DY, Zhang YL, Guo XP, Yang HT. Relationship between *Helicobacter pylori* and duodenal ulcer. *Xin Xiaohuabingxue Zazhi* 1996; **4**: 153-155
- 3 **Liu WZ**, Zheng X, Shi Y, Dong QJ, Xiao SD. Effect of *Helicobacter pylori* infection on gastric epithelial proliferation in progression from normal mucosa to gastric carcinoma. *World J Gastroenterol* 1998; **4**: 246-248
- 4 **Blaser MJ**, Perez-Perez GI, Kleanthous H, Cover TL, Peek RM, Chyou PH, Stemmermann GN, Nomura A. Infection with *Helicobacter pylori* strains possessing cagA is associated with an increased risk of developing adenocarcinoma of the stomach. *Cancer* 1995; **55**: 2111-2115
- 5 **Lu XL**, Qian KD, Tang XQ, Zhu YL, Du Q. Detection of *H.pylori* DNA in gastric epithelial cells by in situ hybridization. *World J Gastroenterol* 2002; **8**: 305-307
- 6 **Liu WZ**, Zheng X, Shi Y, Dong QJ, Xiao SD. Effect of *Helicobacter pylori* infection on gastric epithelial proliferation in progression from normal mucosa to gastric carcinoma. *World J Gastroenterol* 1998; **4**: 246-248
- 7 **Wang RT**, Wang T, Chen K, Wang JY, Zhang JP, Lin SR, Zhu YM, Zhang WM, Cao YX, Zhu CW, Yu H, Cong YJ, Zheng S, Wu BQ. *Helicobacter pylori* infection and gastric cancer: evidence from a retrospective cohort study and nested case-control study in China. *World J Gastroenterol* 2002; **8**: 1103-1107
- 8 **Xue FB**, Xu YY, Wan Y, Pan BR, Ren J, Fan DM. Association of *H. pylori* infection with gastric carcinoma: a Meta analysis. *World J Gastroenterol* 2001; **7**: 801-804
- 9 **Cai L**, Yu SZ, Zhang ZF. *Helicobacter pylori* infection and risk of gastric cancer in Changde County, Fujian Province, China. *World J Gastroenterol* 2000; **6**: 374-376
- 10 **Song Q**, Spahr A, Schmid RM, Adler G, Bode G. *Helicobacter pylori* in the oral cavity: high prevalence and great DNA diversity. *Dig Dis Sci* 2000; **45**: 2162-2167
- 11 **Yoshimatsu T**, Shirai M, Nagata K, Okita K, Nakazawa T. Transmission of *Helicobacter pylori* from challenged to nonchallenged nude mice kept in a single cage. *Dig Dis Sci* 2000; **45**: 1747-1753
- 12 **Leung WK**, Siu KL, Kwok CK, Chan SY, Sung R, Sung JJ. Isolation of *Helicobacter pylori* from vomitus in children and its implication in gastro-oral transmission. *Am J Gastroenterol* 1999; **94**: 2881-2884
- 13 **Liu WZ**, Xiao SD, Jiang SJ, Li RR, Pang ZJ. Seroprevalence of *Helicobacter pylori* infection in medical staff in Shanghai. *Scand J Gastroenterol* 1996; **31**: 749-752
- 14 **Baker KH**, Hegarty JP. Presence of *Helicobacter pylori* in drinking water is associated with clinical infection. *Scand J Infect Dis* 2001; **33**: 744-746
- 15 **Klein PD**, Graham DY, Gaillour A, Opekun AR, Smith EO. Water source as risk factor for *H.pylori* infection in Peruvian children. *Lancet* 1991; **337**: 1503-1506
- 16 **Bunn JE**, MacKay WG, Thomas JE, Reid DC, Weaver LT. Detection of *Helicobacter pylori* DNA in drinking water biofilms: implications for transmission in early life. *Lett Appl Microbiol* 2002; **34**: 450-454
- 17 **Bode G**, Mauch F, Malfertheiner P. The coccoid forms of *Helicobacter pylori*. Criteria for their viability. *Epidemiol Infect* 1993; **111**: 483-490
- 18 **Cellini L**, Allocati N, Di Campli E, Dainelli B. *Helicobacter pylori*: A fickle germ. *Microbiol Immunol* 1994; **38**: 25-30
- 19 **Benaissa M**, Babin P, Quellard N, Pezennec L, Cenatiempo Y, Fauchere JL. Changes in *Helicobacter pylori* ultrastructure and antigens during conversion from the bacillary to the coccoid form. *Infect Immun* 1996; **64**: 2331-2335
- 20 **Shahamat M**, Mai U, Paszko-Kolva C, Kessel M, Colwell RR. Use of autoradiography to assess viability of *Helicobacter pylori* in water. *Appl Environ Microbiol* 1993; **59**: 1231-1235
- 21 **Mizoguchi H**, Fujioka T, Nasu M. Evidence for viability of coccoid forms of *Helicobacter pylori*. *J Gastroenterol* 1999; **34** (Suppl 11): 32-36
- 22 **Winiecka-Krusnell J**, Wreiber K, von Euler A, Engstrand L, Linder E. Free-living amoebae promote growth and survival of *Helicobacter pylori*. *Scand J Infect Dis* 2002; **34**: 253-256
- 23 **Lu Y**, Redlinger TE, Avitia R, Galindo A, Goodman K. Isolation and genotyping of *Helicobacter pylori* from untreated municipal wastewater. *Appl Environ Microbiol* 2002; **68**: 1436-1439
- 24 **Mazari-Hiriart M**, Lopez-Vidal Y, Castillo-Rojas G, Ponce de Leon S, Cravioto A. *Helicobacter pylori* and other enteric bacteria in freshwater environments in Mexico City. *Arch Med Res* 2001; **32**: 458-467
- 25 **Horiuchi T**, Ohkusa T, Watanabe M, Kobayashi D, Miwa H, Eishi Y. *Helicobacter pylori* DNA in drinking water in Japan. *Microbiol Immunol* 2001; **45**: 515-519
- 26 **Mazari-Hiriart M**, Lopez-Vidal Y, Calva JJ. *Helicobacter pylori* in water systems for human use in Mexico City. *Water Sci Technol* 2001; **43**: 93-98
- 27 **Hegarty JP**, Dowd MT, Baker KH. Occurrence of *Helicobacter pylori* in surface water in the United States. *J Appl Microbiol* 1999; **87**: 697-701
- 28 **Catrenich CE**, Makin KM. Characterization of the morphologic conversion of *Helicobacter pylori* from bacillary to coccoid forms. *Scand J Gastroenterol* 1991; **181** (Suppl): 58-64
- 29 **Cellini L**, Allocati N, Angelucci D, Iezzi T, Di Campli E, Marzio L, Dainelli B. Coccoid *Helicobacter pylori* not culturable *in vitro* reverts in mice. *Microbiol Immunol* 1994; **38**: 843-850
- 30 **Costa K**, Bacher G, Allmaier G, Dominguez-Bello MG, Engstrand L, Falk P, de Pedro MA, Garcia-del Portillo F. The morphological transition of *Helicobacter pylori* cells from spiral to coccoid is preceded by a substantial modification of the cell wall. *J Bacteriol* 1999; **181**: 3710-3715
- 31 **Xu ZM**, Zhou DY, Pan LJ, Song S. Transformation and reversion of *Helicobacter pylori* *in vitro*. *Shijie Huaren Xiaohua Zazhi* 1999; **7**: 215-217
- 32 **Shirai M**, Kakada J, Shibata K, Morshed MG, Matsushita T, Nakazawa T. Accumulation of polyphosphate granules in *Helicobacter pylori* cell under anaerobic conditions. *J Med Microbiol* 2000; **49**: 513-519
- 33 **Dunn BE**, Cohen H, Blaser MJ. *Helicobacter pylori*. *Clin Microbiol Rev* 1997; **10**: 720-741
- 34 **Eaton KA**, Brooks CL, Morgan DR, Krakowka S. Essential role of urease in pathogenesis of gastritis induced by *Helicobacter pylori* in gnotobiotic piglets. *Infect Immun* 1991; **59**: 2470-2475
- 35 **Smoot DT**, Mobley HL, Chippendale GR, Lewison JF, Resau JH. *Helicobacter pylori* urease activity is toxic to human gastric epithelial cells. *Infect Immun* 1990; **58**: 1992-1994
- 36 **Boren T**, Falk P, Roth KA, Larson G, Normark S. Attachment of *Helicobacter pylori* to human gastric epithelium mediated by blood group antigens. *Science* 1993; **262**: 1892-1895
- 37 **Ottmann KM**, Lowenthal AC. *Helicobacter pylori* uses motility for initial colonization and to attain robust infection. *Infect Immun* 2002; **70**: 1984-1990

Edited by Ma JY

• *H. pylori* •

Overexpression of c-fos in *Helicobacter pylori*-induced gastric precancerosis of Mongolian gerbil

Yong-Li Yang, Bo Xu, Yu-Gang Song, Wan-Dai Zhang

Yong-Li Yang, Yu-Gang Song, Wan-Dai Zhang, Institute of Gastrointestinal Diseases, Nanfang Hospital, First Military Medical University, Guangzhou 510515, Guangdong Province, China

Bo Xu, Department of Orthopedics, Nanfang Hospital, First Military Medical University, Guangzhou 510515, Guangdong Province, China

Correspondence to: Dr. Yong-Li Yao, Institute of Gastrointestinal Diseases, Nanfang Hospital, First Military Medical University, Guangzhou 510515, Guangdong Province, China. xbyyl@fimmu.edu.cn

Telephone: +86-20-85141547 **Fax:** +86-20-87208770

Received: 2001-09-26 **Accepted:** 2001-11-06

Abstract

AIM: To explore dysregulation of *c-fos* in several human malignancies, and to further investigate the role of *c-fos* in *Helicobacter pylori* (*H. pylori*)-induced gastric precancerosis.

METHODS: Four-week-old male Mongolian gerbils were employed in the study. 0.5 mL 1×10^8 cfu \cdot L⁻¹ suspension of *H. pylori* NCTC 11 637 in Brucella broth were inoculated orally into 20 Mongolian gerbils. Another 20 gerbils were inoculated with Brucella broth as controls. 10 of the infected gerbils and 10 of the non-infected control gerbils were sacrificed at 25 and 45 weeks after infection. The stomach of each gerbil was removed and opened for macroscopic observation. The expression of *c-fos* was analyzed by RT-PCR and immunohistochemical studies in *H. pylori*-induced gastric precancerosis of Mongolian gerbil. Half of each gastric antrum mucosa was dissected for RNA isolation and RT-PCR. β -actin was used as the housekeeping gene and amplified with *c-fos* as contrast. PCR products of *c-fos* were analyzed by gel image system and the level of *c-fos* was reflected with the ratio of *c-fos*/ β -actin. The immunostaining for *c-fos* was conducted using monoclonal antibody of *c-fos* and the StreptAvidin-Biotin-enzyme Complex kit.

RESULTS: *H. pylori* was constantly found in all infected animals in this study. After infection of *H. Pylori* for 25 weeks, ulcers were observed in the antral and the body of stomach of 60 % infected animals (6/10). Histological examination showed that all animals developed severe inflammation, especially in the area close to ulcers, and multifocal lymphoid follicles appeared in the lamina propria and submucosa. After infection of *H. Pylori* for 45 weeks, severe atrophic gastritis in all infected animals, intestinal metaplasia in 80 % infected animals (8/10) and dysplasia in 60 % infected animals (6/10) could be observed. *C-fos* mRNA levels were significantly higher after infection of *H. pylori* for 25 weeks (1.84 ± 0.79), and for 45 weeks (1.59 ± 0.37) than those in control-animals (0.74 ± 0.22 , $P < 0.01$). *C-fos* mRNA levels were increased 2.5-fold by 25th week ($P < 0.01$) and 2.1-fold by 45th week ($P < 0.01$) in precancerosis induced by *H. pylori*, when compared with normal gastric epithelium of Mongolian gerbil. Immunohistochemical staining revealed exclusive nuclear staining of *c-fos*. Furthermore, there was a sequential increase in *c-fos* positive cells from normal epithelium to precancerosis.

CONCLUSION: The study suggested that overexpression of *c-fos* occurs relatively early in gastric tumorigenesis in this precancerosis model induced by *H. pylori*.

Yang YL, Xu B, Song YG, Zhang WD. Overexpression of *c-fos* in *Helicobacter pylori*-induced gastric precancerosis of Mongolian gerbil. *World J Gastroenterol* 2003; 9(3): 521-524
<http://www.wjgnet.com/1007-9327/9/521.htm>

INTRODUCTION

H. pylori, a gram-negative spiral bacterium first isolated in 1982 from a patient with chronic active gastritis, is responsible for a large portion of chronic gastritis and nearly all duodenal ulcers, most gastric ulcers, and probably an increased risk of gastric adenocarcinoma^[1-9]. More than 50 % of the adult population are infected with *H. pylori* in developing countries as well as in developed countries. Gastric cancer is a major health problem^[10] and remains the second most common cancer in the world^[11]. Although epidemiological studies have indicated that *H. pylori* infection plays a crucial role in human gastric carcinogenesis^[12-25], there is no direct proof that *H. pylori* is actually associated with gastric carcinogenesis^[26]. The purpose of this study was to elucidate the relationship between *H. pylori* infection and gastric carcinogenesis by using an animal model of long-term *H. pylori* infection, and to explore the role played by *c-fos* in gastric tumorigenesis.

MATERIALS AND METHODS

Animals treatment

Four-week-old specific pathogen-free male Mongolian gerbils weighing 20 ± 5 g were employed in this study. They were housed in individual metabolic cages in a temperature conditioned room 23 ± 2 °C with a 12 h light-dark cycle, allowed to access to standard rat chow (provided by Experimental Animal Center, First Military Medical University) and water ad libitum, and acclimatized to the surrounding for 7 days prior to the experiments. *H. pylori* (NCTC 11 637) was obtained from American Type Culture Collection and cultured on Brucella agar plates containing 70 mL \cdot L⁻¹ goat blood in a microaerobic condition (volume fraction, N₂: 85 %, O₂: 5 %, CO₂: 10 %, in aerobic globe box) at 37 °C for 3 days. The strain was identified by morphology, Gram's stain, urease production and so on.

Experimental protocol

0.5 mL 1×10^8 cfu \cdot L⁻¹ suspension of *H. pylori* NCTC 11 637 in Brucella broth were inoculated orally into 20 Mongolian gerbils for 14 days continuously which had been fasted overnight. Another 20 gerbils were inoculated with Brucella broth as controls. 10 of the infected gerbils and 10 of the non-infected control gerbils were sacrificed after infection for 25 and 45 weeks, respectively. The stomach of each animal was removed and opened for macroscopic observation. Half of each gastric antrum mucosa were dissected for RNA isolation. The rest of the stomach samples were used for histological examination,

which were fixed with neutral-buffered 100 mL·L⁻¹ formalin and processed by standard methods that embedded in paraffin, sectioned and attained with haematoxylin for analyzing histological changes. Giemsa stain for detecting for *H. pylori* and Alcian blue (AB)/PAS stain for examining intestinal metaplasia.

RNA isolation and RT-PCR analysis

Using Tripure isolation reagent (Boehringer Mannheim, Germany), total cellular RNA was isolated from previously frozen tissues according to the manufacturer's instruction. All RNA samples were analyzed for integrity of 18s and 28s rRNA by ethidium bromide staining of 0.5 µg RNA resolved by electrophoresis on 12 g·L⁻¹ agarose-formaldehyde gels. RT-PCR analysis was performed as follows. RNA was incubated at 60 °C for 10 min and chilled to 4 °C immediately before being reverse transcribed. 1 µg of total RNA was reversely transcribed using antisense primers in a volume of 20 µl for 40 min at 50 °C, containing 200 U MMLV reverse transcriptase, 1×buffer RT, 1 MU·L⁻¹ Rnasin, 0.5 mmol·L⁻¹ dNTPs of dATP, dGTP, dCTP and dTTP and each antisense primers including *c-fos* and β -actin at 0.2 µmol·L⁻¹. The samples were heated to 99 °C for 5 min to terminate the reverse transcription reaction. By using a Perkin-Elmer DNA Thermocycler 4 800 (Perkin-Elmer, Norwalk, CT), 5 µl cDNA mixture obtained from the reverse transcription reaction was then amplified for *c-fos* and β -actin. β -actin was used as the housekeeping gene and amplified with *c-fos* as control. The amplification reaction mixture consisted of 10×buffer 5 µl, 0.2 mmol·L⁻¹ dNTPs of dATP, dGTP, dCTP and dTTP, 2.5 U Taq DNA polymerase, and sense and antisense primers at 0.2 µmol·L⁻¹ in a final volume of 50 µl. The reaction mixture was first heated at 94 °C for 2 min and amplification was carried out for 29 cycles at 94 °C for 0.5 min, 58 °C for 1 min, 70 °C for 1.5 min, followed by an incubation for 7 min at 70 °C. The amplification cycles was previously determined to keep amplification in the linear range to avoid the "plateau effect" associated with increased PCR cycles. The PCR primers were as following: *c-fos*, sense 5'-CAC GAC CAT GAT GTT CTC GG-3' and antisense 5'-AGT AGA TTG GCA ATC TCG GT-3'; β -actin, sense 5'-CCA AGG CCA ACC GCG AGA AGA TGA C-3' and antisense 5'-AGG GTA CAT GGT GGT GCC GCC AGA C-3'. PCR products of *c-fos* and β -actin had 348 bp and 587 bp, respectively. PCR products were run on a 15 g·L⁻¹ agarose gel in 0.5×TBE buffer and then analyzed by gel image analysis system. The level of *c-fos* was reflected with the ratio of *c-fos*/ β -actin.

Immunohistochemical staining

Four micrometers paraffin-embedded tissue sections were deparaffinized and rehydrated. Endogenous peroxidase activity was ablated with 10 mL·L⁻¹ hydrogen peroxide in methanol. The immunostaining for *c-fos* was conducted using the StreptAvidin-Biotin-enzyme Complex kit (Boster, Wuhan). Immunostaining by replacing primary antibody with PBS was also conducted as a negative control. The staining was evaluated semiquantitatively on the basis of the percentage of positive cells, and classified as follows^[27]: diffusely positive (+++) when positive cells accounted for more than 70 % of the total cells, partially positive (++) when positive cells were 35-70 %, partially positive (+) when positive cells accounted for 5-35 %, and negative (-) when positive cells accounted for less than 5 %.

Statistical analysis

Experimental results were analyzed with Chi-square Tests and K-Related Samples Test by SPSS software. Statistical significance was determined at $P < 0.05$.

RESULTS

Histopathological findings

H. pylori was detected in gastric antrum and gastric body of all infected animals in this study, and more in gastric antrum than that in gastric body. After infection of *H. Pylori* for 25 weeks, ulcers were observed in the gastric antrum and gastric body in 60 % infected animals (6/10). Histological examination showed that all infected animals developed severe inflammation, especially in the area close to ulcers; multifocal lymphoid follicles appeared in the lamina propria and submucosa; and there were mild atrophic gastritis in all infected animals. After infection of *H. Pylori* for 45 weeks, severe atrophic gastritis in all infected animals, intestinal metaplasia in 80 % infected animals (8/10) and dysplasia in 60 % infected animals (6/10) could be observed. Those metaplastic glands appeared more atypical than the surrounding nonmetaplastic and hyperplastic glands. Severe atrophic gastritis, intestinal metaplasia and dysplasia were gastric precancerosis. In the uninfected animals, there were no significant changes throughout the study.

Analysis of *c-fos* mRNA expression

There was *c-fos* mRNA expression in gastric antrum mucosa of control-animals. *C-fos* mRNA levels were significantly higher after infection of *H. pylori* for 25 weeks (1.84 ± 0.79), and for 45 weeks (1.59 ± 0.37) than that in control-animals (0.74 ± 0.22 , $P < 0.01$); *C-fos* mRNA levels were increased 2.5-fold in 25 weeks ($P < 0.01$) and 2.1-fold in 45 weeks ($P < 0.01$) in precancerosis induced by *H. pylori*, when compared with control gastric epithelium of Mongolian gerbil (Figure 1-4).

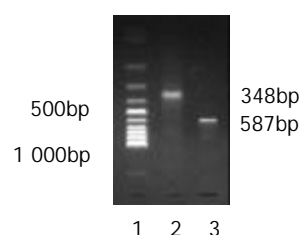


Figure 1 RT-PCR products. Lane 1 PCR marker; Lane 2 *c-fos*; Lane 3 β -actin.

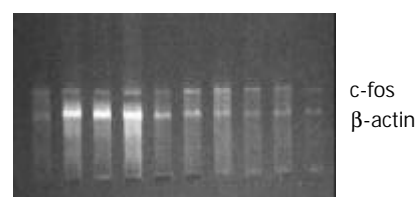


Figure 2 RT-PCR analysis of *c-fos* mRNA levels using β -actin as internal control. Total RNA was first reverse transcribed into cDNA and then amplified by PCR in control.

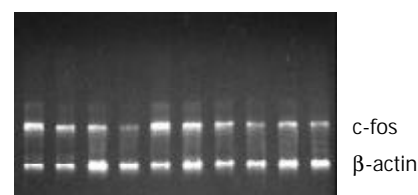


Figure 3 RT-PCR analysis of *c-fos* mRNA levels using β -actin as internal control after *H. pylori* infection for 25 weeks.

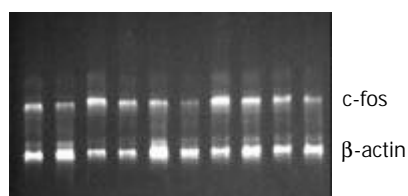


Figure 4 RT-PCR analysis of *c-fos* mRNA levels using β -actin as internal control after *H. pylori* infection for 45 weeks.

Immunohistochemical analysis of *c-fos* protein expression

Immunohistochemical analysis was performed to examine whether increased *c-fos* mRNA expression were accompanied by increased expression of *c-fos* protein. *C-fos* protein expression lied in nuclei (Figure 5). *C-fos* protein expression was evaluated significantly ($P < 0.01$) in precancerosis induced by *H. pylori* for 45 weeks, when compared with control gastric epithelium of Mongolian gerbil (Table 1).

Table 1 Expression of *c-fos* by Immunohistochemical staining

Group	<i>n</i>	c-fos				Positive/%
		-	+	++	+++	
Control	10	10	0	0	0	0
Inf 25 weeks	10	8	2	0	0	20
Time 45 weeks	10	6	4	0	0	40 ^a

^a $P < 0.01$, vs Control.

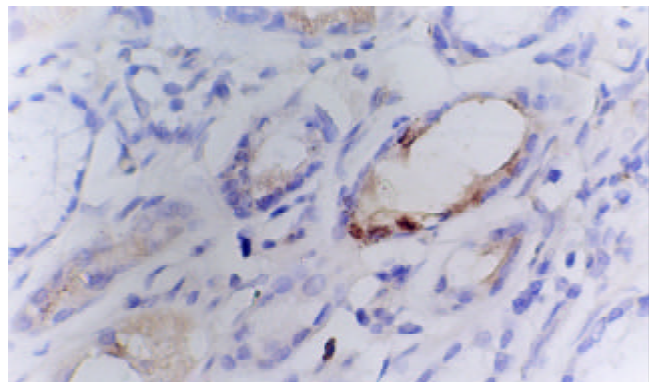


Figure 5 Expression of *c-fos* after *H. pylori* infection for 25 weeks, immunohistochemistry staining ($\times 400$).

DISCUSSION

H. pylori infection is now known as a major cause of acute and chronic active gastritis, peptic ulcer disease and atrophic gastritis and is also considered as a risk factor in the incidence of gastric adenocarcinoma and mucosa-associated lymphoma^[1-8]. Chronic colonization of the human stomach by the gram-negative spiral bacterium *H. pylori* is associated with the development of cancer in the distal portion of the stomach. Although there is no direct proof that *H. pylori* is actually associated with gastric carcinogenesis, epidemiological studies have indicated that *H. pylori* infection plays an important role in human gastric carcinogenesis. Because of this strong epidemiological association, *H. pylori* is classified as a definite carcinogen (group I) by the International Agency for Research on Cancer (IARC), a branch of the World Health Organization (WHO). Many animals infected with human *H. pylori* have already been studied to determine the pathogenetic background, but none

of the models studied mimics human *H. pylori* infection and subsequent pathology. Recently, two experiments were conducted in Japan that demonstrated that chronic *H. pylori*-infection models of Mongolian gerbils would develop gastric carcinoma. These results will be extremely helpful to elucidate the mechanism of gastric carcinogenesis due to *H. pylori* infection^[9-26]. Apoptosis, a programmed cell death, was ignored, just like *H. pylori*, only to reappear recently. However, the number of current publications dealing with apoptosis of *H. pylori* has increased exponentially. Although gastric epithelial apoptosis is a programmed physiological event in the superficial aspect of the mucosa and is important for healthy cell turnover, *H. pylori* infection reportedly promotes such a cell death sequence^[27,28]. Because apoptosis regulates the cycle of cell turnover in balance with proliferation, dysregulation of apoptosis or proliferation evoked by *H. pylori* colonization would be linked to the gastric carcinogenesis^[29-31].

C-fos is an immediate early response gene, and *c-fos* protein is an important transcription-factor of nuclei^[32-39]. Oncogene *c-fos* is also a kind of effect protein of the karyomitos signal, which can trigger and regulate the transcription of the genes related with proliferation. Besides, *c-fos* can also regulate its own gene expression with a positive feedback and promote the mitosis and proliferation of the cells. Because *c-fos* can regulate cell proliferation and cell apoptosis, its abnormal expression might induce cell turnover and carcinogenesis^[40-46]. Previous studies have showed that the expression of oncogene *c-fos* is closely related to cellular multiplication and differentiation. The amplification and over-expression of *c-fos* gene are associated with malignancy and tumorigenicity of cells. Recently, some studies suggested that oncogene *c-fos* was amplified in the primary tumor DNA^[47-49]. Shirin *et al* tested the hypothesis that *H. pylori* might inhibit cell growth and cell cycle progression by inhibiting signaling pathways that mediate the transactivation of the serum-response element in the *c-fos* promoter^[27].

In this study, mRNA level of *c-fos* was measured by quantitative RT-PCR analysis in Mongolian gerbil gastric antrum mucosa to explore dysregulation of *c-fos* in malignancies and to further investigate the role of *c-fos* in *H. pylori*-induced gastric precancerosis. In addition, the expression and localization of its protein product was analyzed by immunohistochemical staining. *C-fos* mRNA levels were significantly increased in precancerosis induced by *H. pylori*, when compared with normal gastric epithelium of Mongolian gerbil. Immunohistochemical staining revealed exclusive nuclear staining of *c-fos*. Furthermore, there was a sequential increase in *c-fos* positive cells from normal epithelium to precancerosis. This study indicates that the expression of *c-fos* mRNA and protein is increased from normal epithelium to precancerosis. The dysregulation of *c-fos* expression occurs relatively early in gastric tumorigenesis in this model and may participate in tumor progression. These findings suggest that *H. pylori*-induced gastric precancerosis is associated with dysregulation of gastric epithelial cell cycle. Further studies are needed to delineate the mechanism of those alterations.

REFERENCES

1. **Tabata H**, Fuchigami T, Kobayashi H, Sakai Y, Nakanshi M, Tomioka K, Nakamura S, Fujishima M. *Helicobacter pylori* and mucosal atrophy in patients with gastric cancer: a special study regarding the methods for detecting *Helicobacter pylori*. *Dig Dis Sci* 1999; **44**: 2027-2034
2. **Meining AG**, Bayerdorffer E, Stolte M. *Helicobacter pylori* gastritis of the gastric cancer phenotype in relatives of gastric carcinoma patients. *Eur J Gastroenterol Hepatol* 1999; **11**: 717-720
3. **Yamaoka Y**, Kodama T, Kashima K, Graham DY. Antibody against *Helicobacter pylori* Cag A and Vac A and the risk for gas-

- tric cancer. *J Clin Pathol* 1999; **52**: 215-218
- 4 **Danesh J**. *Helicobacter pylori* infection and gastric cancer: systematic review of the epidemiological studies. *Aliment Pharmacol Ther* 1999; **13**: 851-885
- 5 **Harris RA**, Owens DK, Witherell H, Parsonnet J. *Helicobacter pylori* and gastric cancer: what are the benefits of screening only for the Cag A phenotype of *H. pylori*? *Helicobacter* 1999; **4**: 69-76
- 6 **Hansen S**, Melby KK, Aase S, Jellum E, Vollset SE. *Helicobacter pylori* infection and risk of cardia cancer and non-cardia gastric cancer. A nested case-control study. *Scand J Gastroenterol* 1999; **34**: 353-360
- 7 **Scheiman JM**, Cutler AF. *Helicobacter pylori* and gastric cancer. *Am J Med* 1999; **106**: 222-226
- 8 **Kuipers EJ**. Review article: exploring the link between *Helicobacter pylori* and gastric cancer. *Aliment Pharmacol Ther* 1999; **13**: 3-11
- 9 **Alexander GA**, Arng MC. Association of *Helicobacter pylori* infection with gastric cancer. *Mil Med* 2000; **165**: 21-27
- 10 **Zhuang XQ**, Lin SR. Study on the relationship between *Helicobacter pylori* and gastric cancer. *Shijie Huaren Xiaohua Zazhi* 2000; **9**: 206-207
- 11 **Vandenplas Y**. *Helicobacter pylori* infection. *World J Gastroenterol* 2000; **6**: 20-31
- 12 **Pan KF**, Liu WD, Ma JL, Zhou T, Zhang L, Chang YS, You WC. Infection of *Helicobacter pylori* in children and mode of transmission in a high-risk area of gastric cancer. *Shijie Huaren Xiaohua Zazhi* 1998; **6**: 42-44
- 13 **Zhang L**, Jiang J, Pan KF, Liu WD, Ma JL, Zhou T, Perez GT, Blaser MJ, Chang YS, You WC. Infection of *Helicobacter pylori* with cag A strain in a high-risk area of gastric cancer. *Shijie Huaren Xiaohua Zazhi* 1998; **6**: 40-41
- 14 **Zhuang XQ**, Lin SR. Study on *Helicobacter pylori* infection in gastric cancer and precancerosis. *Shijie Huaren Xiaohua Zazhi* 2000; **8**: 710-711
- 15 **Hu PJ**. *Helicobacter pylori* and gastric cancer. *Shijie Huaren Xiaohua Zazhi* 1999; **7**: 1-2
- 16 **Huang XQ**. *Helicobacter pylori* infection and gastrointestinal hormones: a review. *World J Gastroenterol* 2000; **6**: 783-788
- 17 **Shang SH**, Zheng JW. Treatment on *Helicobacter pylori*-induced diseases. *Shijie Huaren Xiaohua Zazhi* 2000; **8**: 556-557
- 18 **Wang XH**, Zhang WD, Zhang YL, Zeng JZ, Sun Y. Relationship between *Hp* infection and oncogene and tumor suppressor gene expression in gastric cancer and precancerosis. *Shijie Huaren Xiaohua Zazhi* 1998; **6**: 516-518
- 19 **Ye GA**, Zhang WD, Liu LM, Shi L, Xu ZM, Chen Y, Zhou DY. *Hp vac A* gene and chronic gastritis. *Shijie Huaren Xiaohua Zazhi* 2001; **9**: 593-594
- 20 **Quan J**, Fan XG. Experimental studies on *Helicobacter pylori* and gastric cancer. *Shijie Huaren Xiaohua Zazhi* 1999; **7**: 1068-1069
- 21 **Lu SY**, Pan XZ, Peng XW, Shi ZL, Lin L, Chen MH. Effect of *Hp* infection on gastric epithelial cell kinetics in stomach diseases. *Shijie Huaren Xiaohua Zazhi* 2000; **8**: 386-388
- 22 **Xiao SD**. *Helicobacter pylori* and gastric cancer. *Shijie Huaren Xiaohua Zazhi* 1998; **6**: 4
- 23 **Harry XH**. Association between *Helicobacter pylori* and gastric cancer: current knowledge and future research. *World J Gastroenterol* 1998; **4**: 93-96
- 24 **Zu Y**, Shu J, Yang CM, Zhong ZF, Dai HY, Wang X, Qin GM. Study on *Helicobacter pylori* infection and risk of gastric cancer. *Shijie Huaren Xiaohua Zazhi* 1998; **6**: 367-368
- 25 **Cai L**, Yu SZ, Zhang ZF. *Helicobacter pylori* infection and risk of gastric cancer in Changle County, Fujian Province, China. *World J Gastroenterol* 2000; **6**: 374-376
- 26 **Shimizu M**, Nikaido T, Toki T, Shiozawa T, Fujii S. Clear cell carcinoma has an expression pattern of cell cycle regulatory molecules that is unique among ovarian adenocarcinomas. *Cancer* 1999; **85**: 669-677
- 27 **Shirin H**, Sordillo EM, Oh SH, Yamamoto H, Delohery T, Weinstein B, Moss SF. *Helicobacter pylori* inhibits the G1 to S transition in AGS gastric epithelial cell. *Cancer Res* 1999; **59**: 2277-2281
- 28 **Gao H**, Wang JY, Shen XZ, Liu JJ. Effect of *Helicobacter pylori* infection on gastric epithelial cell proliferation. *World J Gastroenterol* 2000; **6**: 442-444
- 29 **Hidekazu SU**, Hiromasa IS. Role of apoptosis in *Helicobacter pylori*-associated gastric mucosal injury. *J Gastroenterol Hepatol* 2000; **15**: D46-D54
- 30 **Zhuang XQ**, Lin SR. Research of *Helicobacter pylori* infection in precancerous gastric lesions. *World J Gastroenterol* 2000; **6**: 428-429
- 31 **Gu JZ**, Hou TW, Wang XX. Study on precancerous gastric lesions induced by *Helicobacter pylori*. *Shijie Huaren Xiaohua Zazhi* 2001; **9**: 111
- 32 **Tischmeyer W**, Grimm R. Activation of immediate early genes and memory formation. *Cell Mol Life Sci* 1999; **55**: 564-574
- 33 **Lennartsson J**, Blume Jensen P, Hermanson M, Ponten E, Carlberg M, Ronnstrand L. Phosphorylation of Shc by Src family kinases is necessary for stem cell factor receptor/c-kit mediated activation of the Ras/MAP kinase pathway and c-fos induction. *Oncogene* 1999; **18**: 5546-5553
- 34 **Trauth JA**, Seidler FJ, McCook EC, Slotkin TA. Persistent c-fos induction by nicotine in developing rat brain regions: interaction with hypoxia. *Pediatr Res* 1999; **45**: 38-45
- 35 **Duan R**, Porter W, Samudio I, Vyhidal C, Kladde M, Safe S. Transcriptional activation of c-fos protooncogene by 17beta-estradiol: mechanism of aryl hydrocarbon receptor-mediated inhibition. *Mol Endocrinol* 1999; **13**: 1511-1521
- 36 **Morrissey JJ**, Raney S, Heasley E, Rathinavelu P, Dauphinee M, Fallon JH. IRIDIUM exposure increase c-fos expression in the mouse brain only at levels which likely result in tissue heating. *Neuroscience* 1999; **92**: 1539-1546
- 37 **Hasebe T**, Imoto S, Sasaki S, Tsubono Y, Mukai K. Proliferative activity and tumor angiogenesis is closely correlated to stromal cellularity of fibroadenoma: proposal fibroadenoma, cellular variant. *Pathol Int* 1999; **49**: 435-443
- 38 **Whong WZ**, Gao HG, Zhou G, Ong T. Genetic alterations of cancer-related genes in glass fiber-induced transformed cells. *J Toxicol Environ Health* 1999; **56**: 397-404
- 39 **Chen W**, Dong Z, Valcic S, Timmermann BN, Bowden GT. Inhibition of ultraviolet B-induced c-fos gene expression and p38 mitogen-activated protein kinase activation by (-)-epigallocatechin gallate in a human keratinocyte cell line. *Mol Carcinog* 1999; **24**: 79-84
- 40 **Aigner A**, Juhl H, Malerczyk C, Tkybusch A, Benz CC, Czubyko F. Expression of a truncated 100 kDa HER2 splice variant acts as an endogenous inhibitor of tumor cell proliferation. *Oncogene* 2001; **20**: 2101-2111
- 41 **Mitsuno Y**, Yoshida H, Maeda S, Ogura K, Hirata Y, Kawabe T, Shiratori Y, Omata M. *Helicobacter pylori* induced transactivation of SRE and AP-1 through the ERK signaling pathway in gastric cancer cells. *Gut* 2001; **49**: 18-22
- 42 **He SW**, Shen KQ, He YJ, Xie B, Zhao YM. Regulatory effect and mechanism of gastrin and antagonists on colorectal carcinoma. *World J Gastroenterol* 1999; **5**: 408-416
- 43 **Yuan SL**, Huang RM, Wang XJ, Song Y, Huang GQ. Reversing effect of Tanshinone on malignant phenotypes of human hepatocarcinoma cell line. *World J Gastroenterol* 1998; **4**: 317-319
- 44 **YH**, Hu DR, Nie QH, Liu GD, Tan ZX. Study on activation and c-fos, c-jun expression of in vitro cultured human hepatic stellate cells. *Shijie Huaren Xiaohua Zazhi* 2000; **8**: 299-301
- 45 **Jiang LX**, Fu XB, Sun TZ, Yang YH, Gu XM. Relationship between oncogene c-jun activation and fibrobl. *Shijie Huaren Xiaohua Zazhi* 1999; **7**: 498-500
- 46 **Chen BW**, Wang HT, Liu ZX, Jia BQ, Ma QJ. Effect of exogenous EGF on proto-oncogene expression in experimental gastric ulcers. *Shijie Huaren Xiaohua Zazhi* 1999; **7**: 504-506
- 47 **Chai Y**, Chipitsyna G, Cui J, Liao B, Liu S, Aysola K, Yezdani M, Reddy ES, Rao VN. C-fos oncogene regulator Elk-1 interacts with BRCA1 splice variants BRCA1a/1b and enhances BRCA1a/1b-mediated growth suppression in breast cancer cells. *Oncogene* 2001; **20**: 1357-1367
- 48 **Ma KS**, Zhang FS, He ZP, Wanf SG, Zhong JH. Effect of CCK on cell apoptosis of bile duct neoplasms. *Shijie Huaren Xiaohua Zazhi* 2000; **8**: 1312-1313
- 49 **Salmi A**, Carpen O, Rutanen E. The association between c-fos and c-jun expression and estrogen and progesterone receptors is lost in human endometrial cancer. *Tumour Biol* 1999; **20**: 202-211

L-forms of *H. pylori*

Ke-Xia Wang, Chao-Pin Li, Yu-Bao Cui, Ye Tian, Qing-Gui Yang

Ke-Xia Wang, Chao-Pin Li, Yu-Bao Cui, Ye Tian, Qing-Gui Yang,
School of Medicine, Anhui University of Science & Technology
Huainan 232001, Anhui Province, China

Correspondence to: Dr. Chao-Pin Li, Department of Etiology and Immunology, School of Medicine, Anhui University of Science and Technology Huainan 232001, Anhui Province, China. cpli@aust.edu.cn
Telephone: +86-554-6658770 **Fax:** +86-554-6662469

Received: 2002-09-14 **Accepted:** 2002-10-17

Abstract

AIM: To study the occurrence of L-forms of *H. pylori* infection in patients with peptic ulcers and its association with possible changes of cellular immune function in the patients.

METHODS: Endoscopic biopsy specimens of gastric antrum and gastric corpus were taken from 228 patients with peptic ulcers and inoculated into Skirrow selective medium for *H. pylori* vegetative forms and special medium for *H. pylori* L-forms, followed by bacterial isolation and identification. And peripheral venous blood of the patients was taken to detect the percentage of CD3⁺, CD4⁺ and CD8⁺ with biotin-streptavidin (BSA) and the level of IL-2, IL-6 and IL-8 with ELISA.

RESULTS: (1) The detection rates of *H. pylori* L-forms and vegetative forms in the patients were 50.88 % (116/228) and 64.91 % (148/228) respectively, and the co-infection rate of *H. pylori* L-forms and vegetative forms was 78.38 % (116/148). To be more exact, the detection rates of *H. pylori* L-forms in male and female patients were 57.04 % (77/135) and 41.94 % (39/93) respectively, and statistics found significant difference between them ($P < 0.05$). Furthermore, the detection rates of *H. pylori* L-forms in patients aged 14 years-, 30 years-, 40 years- and 50 years- were 31.91 % (15/47), 42.86 % (24/56), 56.94 % (41/72) and 67.92 % (36/53) respectively, and there was significant difference between them ($P < 0.01$). (2) The percentages of CD3⁺, CD4⁺, CD8⁺, the ratio of CD4⁺/CD8⁺, and the level of IL-2, IL-6, IL-8 in *H. pylori*-positive patients were (52.59±5.44) %, (35.51±5.74) %, (27.77±8.64) %, (1.56±0.51), (2.66±0.47) mg/L, (108.62±5.85) ng/L and (115.79±7.18) ng/L respectively, compared with those in *H. pylori*-negative patients, the percentages of CD3⁺, CD4⁺ and the ratio of CD4⁺/CD8⁺ decreased, but the level of IL-2, IL-6 increased, and the difference was significant ($P < 0.001$ - $P < 0.01$). Moreover, the percentages of CD3⁺, CD4⁺, CD8⁺, the ratio of CD4⁺/CD8⁺, and the level of IL-2, IL-6, IL-8 in the patients with mixed infection of both *H. pylori* L-forms and vegetative forms were (51.69±5.28) %, (34.75±5.89) %, (27.15±7.45) %, (1.48±0.47), (2.16±0.38) mg/L, (119.45±5.44) ng/L and (123.64±6.24) ng/L respectively, compared with those in patients with simple infection of *H. pylori* vegetative forms, the percentage of CD4⁺, the ratio of CD4⁺/CD8⁺ and the level of IL-2 increased, but the level of IL-6 and IL-8 decreased, statistical difference was found between them ($P < 0.001$ - $P < 0.05$).

CONCLUSION: L-forms variation often occurs in patients with peptic ulcers who are infected by *H. pylori*, which is

commonly found in male patients and related to ages. The L-forms variation of *H. pylori* can be an important factor causing disorder of cellular immune function in the patients with peptic ulcers who are infected by *H. pylori*.

Wang KX, Li CP, Cui YB, Tian Y, Yang QG. L-forms of *H. pylori*. *World J Gastroenterol* 2003; 9(3): 525-528
<http://www.wjgnet.com/1007-9327/9/525.htm>

INTRODUCTION

Helicobacter pylori (*H. pylori*) is one of the commonest bacteria causing chronic infection, which infects more than 50 % of the human population, and is associated with a range of pathology, such as chronic gastritis, peptic ulcer and gastric cancer^[1-5]. And infection of *Helicobacter pylori* is life-long that elicits a marked host inflammatory response. However, natural infection fails to yield protective immunity^[6].

H. pylori is a gram-negative, spiral and microaerophilic bacterium that colonizes the gastric epithelium of humans^[7]. It causes chronic gastritis and, together with non-steroidal anti-inflammatory drugs, is considered as the most frequent etiologic agent of peptic ulcer^[8-10]. After long-term treatment with antibiotic, cell walls deficiency of *H. pylori* vegetative forms occurs and *H. pylori* L-forms comes into being^[11,12]. Whether in animal experiments or clinical studies, damages induced by *H. pylori* were reported to be associated with Th1 cell-mediated immune response^[13-15].

In order to confirm the occurrence of L-forms variation of *H. pylori* vegetative forms and its association with possible changes of cellular immune function in the patients, gastric mucosa biopsy specimens were taken from 228 patients with peptic ulcers randomly enrolled in this study to isolate and identify *H. pylori* vegetative forms and L-forms, and T lymphocyte subsets and the level of IL-2, IL-6 and IL-8 of the patients were detected at the same time.

MATERIALS AND METHODS

Materials

Patients A total of 228 patients with peptic ulcer (gastric ulcers 66, duodenal ulcers 132, and complex ulcers of gastric and duodenal 30) diagnosed in our affiliated hospital from August, 2000 to April 2002 were involved in this study. All of them were except aged from 14 to 67 years, 135 male and 93 female, other were eliminated for presence of other diseases.

Reagents *H. pylori* L-forms solid medium designed by Jia JH was served in this study. Based on broth culture medium, the medium consisted of peptone 1 %, tryptone 1 %, glucose 0.1 %, yeast powder 0.2 %, D-methionine 0.02 %, NaCl 1.5 %, MgSO₄·7H₂O, 15mM, agar 0.8 % and Caprine plasma 15 % with the inducer of carbenicillin and made into pour plate. BSA reagent for T lymphocyte subsets was provided by Jin' an Medical Laboratory Institute in Shanghai, Separating medium for Lymphocyte was supplied by The Second Biochemical Reagent Factory in Shanghai (batch No. 011215), and the test kit for IL-6 (batch No. 1006-32), IL8 (batch No.1008-25), IL-2 (batch No.1002-21) was offered by Besancon Company in France.

Methods

We used gastric antral and corporal biopsies for bacterial culture, blood samples for detection of T lymphocyte subsets and IL-2, IL-6, IL-8.

Bacteriological examination Endoscopic biopsies of gastric antrum and gastric corpus were taken from 228 patients with peptic ulcers and inoculated into Skirrow selective medium for *H. pylori* vegetative forms and special medium for *H. pylori* L-forms. Then the plates were incubated at 37 °C under microaerobic conditions (5 % O₂, 8 % H₂, 7 % CO₂ and 80 % N₂) for 72 hours. Based on the results of Gram staining, cell morphology and positive reaction for urease, oxidase and immunoenzyme staining, the identification was carried out.

Detection of cellular immune function To investigate the possible changes of cellular immune function in *H. pylori*-infected individuals, including the patients infected by *H. pylori* L-forms and vegetative forms, the level of CD3+, CD4+, CD8+, CD4+/CD8+ and IL-2, IL-6, IL-8 in peripheral blood of *H. pylori*-positive individuals were tested with biotin-streptavidin (BSA) method. Firstly, the peripheral venous blood of the subjects was taken, anticoagulated with heparin, and diluted with fluid free of Ca²⁺, Mg²⁺. Secondly, peripheral blood mononuclear cells were separated with lymphocytes separating medium, cleaned, and the number of cells was adjusted to (1-3)×10⁹/L of which 10 µl was taken and smeared in an acid-proof varnish circle on the surface of the slides. When it dried naturally, McAb of anti-CD3+, anti-CD4+ and anti-CD8+ and sheep anti-guinea pig IgG, SA-HRP was added into the circle. After development with DAB, the slides were observed under microscope. Only brown cytomembrane staining was regarded as positive, otherwise, as negative specimen. A total of 200 cells were counted, and the positive percentages of cells were analyzed respectively. In addition, the level of IL-2, IL-6 and IL-8 were detected by ELLISA following the procedure detailed in the product description.

Statistical analysis

Data were expressed as mean ± standard deviation. And multiple comparison tests were performed with χ^2 test and *t*-test.

RESULTS

Bacteriological examination By endoscopic biopsy of gastric mucosa, 116 out of all the 228 patients were detected to be positive for both *H. pylori* vegetative forms and L-forms, and 32 (14.04 %) to be positive for vegetative forms only. The detection rates of *H. pylori* L-forms and vegetative forms were 50.88 % (116/228) and 64.91 % (148/228) respectively. "Fried Egg" colonies grew in the special medium for *H. pylori* L-forms after induction with carbenicillin. And the morphology of *H. pylori* L-forms was highly variably seen on the smears under microscopy, such as spheroid, coccoid form, big body, elementary body, long filament body.

Relationship between infection of *H. pylori* L-forms and gender as well as age of the patients with peptic ulcer The detection rates of *H. pylori* L-forms and vegetative forms in the patients were 50.88 % (116/228) and 64.91 % (148/228) respectively, and among the vegetative forms of *H. pylori*-positive patients, it was 78.38 % (116/148) which was the co-infection rate of L-forms of *H. pylori*. To be more exact, the detection rates of *H. pylori* L-forms in male and female patients were 57.04 % (77/135) and 41.94 % (39/93) respectively, and with statistically significant difference between them (*P*<0.05). In addition, the detection rate of *H. pylori* L-forms was associated with age. The detailed results were shown in Table 1.

Detection of cellular immune function Compared with the percentages of CD3+, CD4+, CD8+, the ratio of CD4+/CD8+, and the level of IL-2, IL-6, IL-8 in *H. pylori*-negative patients,

the percentages of CD3+, CD4+ and the ratio of CD4+/CD8+ decreased in *H. pylori*-positive patients, but the level of IL-2, IL-6 increased. And compared with the percentages of CD3+, CD4+, CD8+, the ratio of CD4+/CD8+, and the level of IL-2, IL-6, IL-8 in the patients only infected by vegetative forms of *H. pylori*, the percentage of CD4+, the ratio of CD4+/CD8+ and the level of IL-2 increased in the patients not only infected by L-forms of *H. pylori* but also the vegetative forms, but the level of IL-6 and IL-8 decreased, statistical difference was found between them (*P*<0.001-*P*<0.05). All of these were shown in Table 2 and Table 3.

Table 1 Relationship between *H. pylori* L-forms and gender as well as ages of the patients with peptic ulcer (n, %)

Age	Male		Female		Total	
	n	Detection Rate (%)	n	Detection Rate (%)	n	Detection Rate (%)
14~	28	9 (32.14)	19	6 (31.58)	47	15 (31.91) ^b
30 ~	36	13 (36.11)	20	11 (55.00)	56	24 (42.86) ^b
40~	42	28 (66.67)	30	13 (43.33)	72	41 (56.94) ^b
50~	29	27 (93.10)	24	9 (37.50)	53	36 (67.92) ^b
Total	135	77 (57.04) ^a	93	39 (41.94) ^a	228	116 (50.88)

^a*P*<0.05, $\chi^2=5.02$; ^b*P*<0.01, $\chi^2=15.43$.

Table 2 Detection of the T lymphocyte subsets in 228 patients with peptic ulcers

Group	n	CD3+ (%)	CD4+ (%)	CD8+ (%)	CD4+/CD8+ (%)
Hp(-)	80	65.72±9.38 ^c	46.33±4.86 ^d	29.83±7.39	1.74±0.34 ^e
Hp(+)	148	52.59±5.44 ^c	35.51±5.74 ^d	27.77±8.64	1.56±0.51 ^e
Hp(+)&Hp-L(-)	32	55.87±6.23	38.27±6.43 ^f	30.04±11.84	1.86±0.58
Hp(+)&Hp-L(+)	116	51.69±5.28	34.75±5.89 ^f	27.15±7.45	1.48±0.47 [*]
Total	228	57.20±6.43	39.31±5.18	28.49±7.86	1.61±0.466

^c*P*<0.001, *t*=13.38; ^d*P*<0.001, *t*=14.31; ^e*P*<0.01, *t*=2.82; ^f*P*<0.01, *t*=2.93; ^{*}*P*<0.05, *t*=2.65.

Table 3 Detection of IL-2, IL-6, IL-8 in patients with peptic ulcers

Group	n	IL-2 (mg/L)	IL-6 (ng/L)	IL-8 (ng/L)
Hp(-)	80	7.24±0.65 ^h	40.82±3.15 ⁱ	52.35±3.63 ^j
Hp(+)	148	2.66±0.47 ^h	108.62±5.85 ⁱ	115.79±7.18 ^j
Hp(+)&Hp-L(-)	32	4.49±0.57 ^k	69.35±6.51 ⁱ	87.33±8.45 ^m
Hp(+)&Hp-L(+)	116	2.16±0.38 ^k	119.45±5.44 ⁱ	123.64±6.24 ^m
Total	228	4.27±0.52	84.83±4.73	93.53±5.68

^h*P*<0.001, *t*=61.14; ⁱ*P*<0.001, *t*=96.32; ^j*P*<0.001, *t*=74.03; ^k*P*<0.001, *t*=27.30; ^l*P*<0.001, *t*=43.95; ^m*P*<0.001, *t*=26.86.

DISCUSSION

Helicobacter pylori is a gram-negative, spiral-shaped, microaerophilic bacterium that colonizes the human gastric epithelium but not cleared by the host immune response, which can be found in approximately 50 % of the world's population, and which plays a causative role in peptic ulcer and perhaps gastric cancer. As a matter of fact, it results in a release of various bacterial and host dependent cytotoxic substances including ammonia, platelet activating factor, cytotoxins and lipopolysaccharides as well as cytokines such as interleukins (IL)-1-12, tumor necrosis factor alpha (TNF-alpha), interferon

gamma (INF-gamma) and reactive oxygen species^[16-22]. Although the mucus layer is the major reservoir of *H. pylori* *in vivo*, a growing body of evidence suggests that *H. pylori* can persist in multiple intracellular sites^[23]. And primary gastritis, duodenitis, peptic ulcer are no longer considered to be disorders of the balance of secretion of acid and immune responses of the gastric mucosa, but it is thought to be caused by *Helicobacter pylori* infection. Moreover, the chronic inflammatory response associated with natural infection can contribute to tissue damage and the pathogenesis of gastroduodenal disease^[24-27]. In 1994, the connection of *H. pylori* to stomach cancer became so certain that the World Health Organization International Agency for Research in Cancer (IARC) classified it as a class I carcinogen. So *H. pylori* became the first bacteria to be connected with carcinogenesis^[28-30].

Recurrence of *H. pylori* infection after successful dual or triple therapy is fairly common, and gastroduodenal disease, gender, and gastritis activity seem to affect relapse of infection^[31,32]. Many scholars believed that pleomorphic variation of the *H. pylori* is a crucial factor to the occurrence and development of gastric malignant tumor, and some detailed it to L-forms variation of *H. pylori* that played an important role in prolongation and relapse of peptic ulcer as well as chronic gastritis.

In this study, gastric mucosal biopsy specimens from 228 patients with peptic ulcers were inoculated into Skirrow selective blood plate for *H. pylori* vegetative forms and special plate for *H. pylori* L-forms. The experimental results showed that 116 patients were infected with both *H. pylori* L-forms and vegetative forms, but 32 patients were infected with *H. pylori* only. This indicated that L-form variation of *H. pylori* is common in patients with peptic ulcers related to *H. pylori*. Under circumstances of gastric juice, bile, antibiotic and other factors either *in vitro* or *in vivo*, many bacteria could come into pleomorphic variation^[33-36]. For example, in penicillin-susceptible bacteria, penicillin causes growth of a small fraction of cells as wall-deficient forms if an appropriate osmo protection is provided (unstable L-forms). According to some scholar's reports, *H. pylori* vegetative forms could turn into *H. pylori* L-forms in the treatment of peptic ulcer with antibacterial, so co-infection of *H. pylori* L-forms and vegetative forms yields in some patients with *H. pylori*. Following the loss of cell walls, the L-forms lose certain components of antigen and become less antigenic, and with increase of charge of the bacteria surface, which make it more adhesive when cultivating in a liquid L-form medium. Moreover, when condition is available, L-forms can revert to typical vegetative forms, which may be an important factor leading to deterioration and relapse of infection^[33]. That is to say *H. pylori* L-forms possess more adhesiveness, invasiveness and risky. Therefore, co-infection of *H. pylori* vegetative forms in extracellular and L-forms in intracellular can result in chronic damage to the host cells.

In this study, the detection rates of *H. pylori* L-forms in male and female were 57.04 % (77/135) and 41.94 % (39/93), which were significantly different. This may be related to some male habits, such as smoking, drinking, irregular diet, which might damage gastric mucosa and change the gastric internal environment^[37-39]. In addition, *H. pylori* L-forms infection could occur in different age groups and the positive rate of *H. pylori* L-forms seemed to be related to the patients' ages, as opportunities of infection increase with time due to age, smoking, exposure to antibacterial agents, eating habit, etc.

In recent years, cellular immune function of the patients with *H. pylori* has been discussed very frequently. Rather than providing protection, the chronic inflammatory response associated with natural infection can contribute to tissue damages and pathogenesis of gastroduodenal disease, including atrophic gastritis, peptic ulcer, and gastric cancer. These

immune responses are likely to attribute to a subset of T helper lymphocyte, so-called Th1 cells, that enhance cell-mediated immunity and induce damage to the gastric epithelium^[13-15]. To investigate the reason for Th1 immune response caused by *H. pylori* based on the variation of L forms, detection of T lymphocyte subsets and the level of IL-2, IL-6, IL-8 in peripheral blood of the patients were performed. The results showed that in 148 *H. pylori*-positive patients, CD3+, CD4+, CD4+/CD8 and IL-2 decreased, IL-6 and IL-8 increased, which were significantly different from those in *H. pylori*-negative ($P < 0.001$, $P < 0.01$). It indicated that *H. pylori* infection might weaken the immune function of the host and cause a predominant Th1 cellular response.

The results showed that among the 148 patients with *H. pylori* vegetative forms, 116 were co-infected with *H. pylori* L-forms. That is to say, only 32 patients were found with *H. pylori* vegetative forms only. Therefore, the roles of *H. pylori* L-forms in the change of immune function of the patients with peptic ulcers are worthy of great awareness. Compared the T lymphocyte subsets and the levels of IL-2, IL-6, IL-8 in patients with *H. pylori* vegetative forms only and co-infection of *H. pylori* vegetative forms and L-forms, the percentage of CD4+, CD4+/CD8 and the level of IL-2 in the patients with co-infection were lower than those with vegetative forms infection only, but the level of IL-6 and IL-8 was higher. As a conclusion, *H. pylori* L-forms infection is related to disorder of the immune function of the host, and may be one of the crucial factors causing Th1 immune response. When infesting in the host cell, *H. pylori* L-forms may be a pronounced inducer for Th1-type CD4 (+) T cell response and decrease the percentage of CD4+ and the ratio of CD4+/CD8. Active CD4+-T cell may also inhibit the activation of Th1 cells cytokine, and the outcome of IL-2 is a risk factor of cellular immune response.

In addition, in this study, the levels of IL-6 and IL-8 in peripheral blood of the patients increased significantly, which is likely to be associated with ulceration inflammation, blood macrophage stimulation and active secretion by the neutrophils and vascular endothelial cells. Once attached to the gastric epithelial cells, *H. pylori* incites an immune response characterized by the increased pro-inflammatory cytokine of IL-8, IL-12 and TNF-alpha. Activated inflammatory and immunologically competent cells as neutrophils, lymphocytes, monocytes, could release cytokine as IL-6, IL-8 and IFN-gamma. As a result, the level of IL-6 and IL-8 in serum of the patients increased^[40].

To sum up, vegetative forms of *H. pylori*'s susceptibility turning into L-forms is because of antibacterial agent and alteration of gastric environment in patients with peptic ulcers, and it is common for patients to be co-infected by both *H. pylori* vegetative forms and L-forms. Once *H. pylori* L-forms occurs, the morphology and microstructure of the organisms change, to be exact, the cell walls of the L-forms are partly or completely lost, the charge of the bacteria surface increases, and the adherence and invasiveness of the bacteria become more powerful. All of these make the pathogen invading into intracellular compartment Mac easily, which can be an important factor causing disordered cellular immune function in the patients with peptic ulcers infected by *H. pylori*.

REFERENCES

- 1 **Vandenplas Y.** *Helicobacter pylori* infection. *World J Gastroenterol* 2000; **6**: 20-31
- 2 **Pineros DM,** Riveros SC, Marin JD, Ricardo O, Diaz OO. *Helicobacter pylori* in gastric cancer and peptic ulcer disease in a Colombian population. Strain heterogeneity and antibody profiles. *Helicobacter* 2001; **6**: 199-206
- 3 **Kotloff KL,** Sztein MB, Wasserman SS, Losonsky GA, DiLorenzo SC, Walker RI. Safety and immunogenicity of oral inactivated

- whole-cell *Helicobacter pylori* vaccine with adjuvant among volunteers with or without subclinical infection. *Infect Immun* 2001; **69**: 3581-3590
- 4 **Brigic E**, Hodzic L, Zildzic M. *Helicobacter pylori* and gastroduodenal disease in our patients: 2-year experience. *Med Arh* 2000; **54**: 313-316
 - 5 **Nguyen TN**, Barkun AN, Fallone CA. Host determinants of *Helicobacter pylori* infection and its clinical outcome. *Helicobacter* 1999; **4**: 185-197
 - 6 **Ernst PB**, Pappo J. T-cell-mediated mucosal immunity in the absence of antibody: lessons from *Helicobacter pylori* infection. *Acta Odontol Scand* 2001; **59**: 216-221
 - 7 **Oyedeji KS**, Smith SI, Arigbabu AO, Coker AO, Ndububa DA, Agbakwuru EA, Atoyebe OA. Use of direct Gram stain of stomach biopsy as a rapid screening method for detection of *Helicobacter pylori* from peptic ulcer and gastritis patients. *J Basic Microbiol* 2002; **42**: 121-125
 - 8 **Ballesteros-Amozurrutia MA**. Peptic ulcer and *Helicobacter pylori*. Results and consequences of its eradication. *Rev Gastroenterol Mex* 2000; **65**: 41-49
 - 9 **McColl KE**, Gillen D, El-Omar E. The role of gastrin in ulcer pathogenesis. *Baillieres Best Pract Res Clin Gastroenterol* 2000; **14**: 13-26
 - 10 **Vergara M**, Calvet X, Roque M. *Helicobacter pylori* is a risk factor for peptic ulcer disease in cirrhotic patients. A meta-analysis. *Eur J Gastroenterol Hepatol* 2002; **14**: 717-722
 - 11 **Schmidtke LM**, Carson J. Induction, characterization and pathogenicity in rainbow trout *Oncorhynchus mykiss* (Walbaum) of *Lactococcus garvieae* L-forms. *Vet Microbiol* 1999; **69**: 287-300
 - 12 **Rakovskaia IV**. Role of works of S. V. Prozorovskii in solving problems of persistence of wall-free forms of microorganisms. *Vestn Ross Akad Med Nauk* 2001; **11**: 5-8
 - 13 **Ihan A**, Tepes B, Gubina M. Diminished Th1-type cytokine production in gastric mucosa T-lymphocytes after *H. pylori* eradication in duodenal ulcer patients. *Pflugers Arch* 2000; **440**: 89-90
 - 14 **Londono-Arcila P**, Freeman D, Kleanthous H, O'Dowd AM, Lewis S, Turner AK, Rees EL, Tibbitts TJ, Greenwood J, Monath TP, Darsley MJ. Attenuated *Salmonella enterica* Serovar Typhi expressing urease effectively immunizes mice against *Helicobacter pylori* challenge as part of a heterologous mucosal priming-parenteral boosting vaccination regimen. *Infect Immun* 2002; **70**: 5096-5106
 - 15 **Kusters JG**, Scand J. Recent developments in *Helicobacter pylori* vaccination. *Gastroenterol Suppl* 2001; **234**: 15-21
 - 16 **Stassi G**, Arena A, Speranza A, Iannello D, Mastroeni P. Different modulation by live or killed *Helicobacter pylori* on cytokine production from peripheral blood mononuclear cells. *New Microbiol* 2002; **25**: 247-252
 - 17 **Amjad M**, Kazmi SU, Qureshi SM, Reza-ul Karim M. Inhibitory effect of IL-4 on the production of IL-1 beta and TNF-alpha by gastric mononuclear cells of *Helicobacter pylori* infected patients. *Ir J Med Sci* 2001; **170**: 112-116
 - 18 **Han FC**, Yan XJ, Su CZ. Expression of the CagA gene of *H. pylori* and application of its product. *World J Gastroenterol* 2000; **6**: 122-124
 - 19 **Olbe L**, Fandriks L, Thoreson AC, Svennerholm AM, Hamlet A. When is *H. pylori* a cause of duodenal ulcer? Hypersecretion of gastric acid, active duodenitis and reduced bicarbonate secretion are links in the chain. *Lakartidningen* 2000; **97**: 5910-5913
 - 20 **Konturek PC**, Bielanski W, Konturek SJ, Hahn EG. *Helicobacter pylori* associated gastric pathology. *J Physiol Pharmacol* 1999; **50**: 695-710
 - 21 **Ji KY**, Hu FL. Progress on *Helicobacter pylori* and cytokine. *Shijie Huaren Xiaohua Zazhi* 2002; **10**: 503-508
 - 22 **Guillemin K**, Salama NR, Tompkins LS, Falkow S. Cag pathogenicity island-specific responses of gastric epithelial cells to *Helicobacter pylori* infection. *Proc Natl Acad Sci* 2002; **99**: 15136-15141
 - 23 **Allen LA**. Intracellular niches for extracellular bacteria: lessons from *Helicobacter pylori*. *J Leukoc Biol* 1999; **66**: 753-756
 - 24 **Innocenti M**, Thoreson AC, Ferrero RL, Stromberg E, Bolin I, Eriksson L, Svennerholm AM, Quiding-Jarbrink M. *Helicobacter pylori*-induced activation of human endothelial cells. *Infect Immun* 2002; **70**: 4581-4590
 - 25 **Al-Muhtaseb MH**, Abu-Khalaf AM, Aughsteen AA. Ultrastructural study of the gastric mucosa and *Helicobacter pylori* in duodenal ulcer patients. *Saudi Med J* 2000; **21**: 569-573
 - 26 **Di Leo A**, Messa C, Russo F, Linsalata M, Amati L, Caradonna L, Pece S, Pellegrino NM, Caccavo D, Antonaci S, Jirillo E. *Helicobacter pylori* infection and host cell responses. *Immunopharmacol Immunotoxicol* 1999; **21**: 803-846
 - 27 **Naito Y**, Yoshikawa T. Molecular and cellular mechanisms involved in *Helicobacter pylori*-induced inflammation and oxidative stress (1,2). *Free Radic Biol Med* 2002; **33**: 323-326
 - 28 **Zhang WD**, Xu ZM. Status and cognition of studies on *Helicobacter pylori*. *Shijie Huaren Xiaohua Zazhi* 2000; **8**: 1084-1088
 - 29 **Pineros DM**, Riveros SC, Marin JD, Ricardo O, Diaz OO. *Helicobacter pylori* in gastric cancer and peptic ulcer disease in a Colombian population. Strain heterogeneity and antibody profiles. *Helicobacter* 2001; **6**: 199-206
 - 30 **Miehke S**, Kirsch C, Dragosics B, Gschwandler M, Oberhuber G, Antos D, Dite P, Lauter J, Labenz J, Leodolter A, Malfertheiner P, Neubauer A, Ehninger G, Stolte M, Bayerdorffer E. *Helicobacter pylori* and gastric cancer: current status of the Austrian Czech German gastric cancer prevention trial (PRISMA Study). *World J Gastroenterol* 2001; **7**: 243-247
 - 31 **Zullo A**, Rinaldi V, Hassan C, Taggi F, Giustini M, Winn S, Castagna G, Attili AF. Clinical and histologic predictors of *Helicobacter pylori* infection recurrence. *J Clin Gastroenterol* 2000; **31**: 38-41
 - 32 **Ihan A**, Tepez B, Gubina M, Malovrh T, Kopitar A. Diminished interferon-gamma production in gastric mucosa T lymphocytes after *H. pylori* eradication in duodenal ulcer patients. *Hepatogastroenterology* 1999; **46**: 1740-1745
 - 33 **Xu ZM**, Zhou DY, Pan LJ, Song S. Transformation and reversion of *Helicobacter pylori* in vitro. *Shijie Huaren Xiaohua Zazhi* 1999; **7**: 215-217
 - 34 **Wen M**, Zhang Y, Yamada N, Matsuhisa T, Matsukura N, Sugisaki Y. An evaluative system for the response of antibacterial therapy: based on the morphological change of *Helicobacter pylori* and mucosal inflammation. *Pathol Int* 1999; **49**: 332-337
 - 35 **Khin MM**, Hua JS, Ng HC, Wadstrom T, Bow H. Agglutination of *Helicobacter pylori* coccoids by lectins. *World J Gastroenterol* 2000; **6**: 202-209
 - 36 **She FF**, Su DH, Lin JY, Zhou LY. Virulence and potential pathogenicity of coccoid *Helicobacter pylori* induced by antibiotics. *World J Gastroenterol* 2001; **7**: 254-258
 - 37 **Brenner H**, Bode G, Adler G, Hoffmeister A, Koenig W, Rothenbacher D. Alcohol as a gastric disinfectant? The complex relationship between alcohol consumption and current *Helicobacter pylori* infection. *Epidemiology* 2001; **12**: 209-214
 - 38 **Parasher G**, Eastwood GL. Smoking and peptic ulcer in the *Helicobacter pylori* era. *Eur J Gastroenterol Hepatol* 2000; **12**: 843-853
 - 39 **Guarner J**, Mohar A. The association between *Helicobacter pylori* and gastric neoplasia. Epidemiologic evidence. *Rev Gastroenterol Mex* 2000; **65**: 20-24
 - 40 **Ohara T**, Arakawa T, Higuchi K, Kaneda K. Overexpression of co-stimulatory molecules in peripheral mononuclear cells of *Helicobacter pylori*-positive peptic ulcer patients. *Eur J Gastroenterol Hepatol* 2001; **13**: 11-18

Inhibitive effect of cordyceps sinensis on experimental hepatic fibrosis and its possible mechanism

Yu-Kan Liu, Wei Shen

Yu-Kan Liu, Wei Shen, Department of Gastroenterology, the Second affiliated hospital, Chongqing University of Medical Sciences, Chongqing 400010, China

Correspondence to: Wei Shen, Department of Gastroenterology, the Second affiliated hospital, Chongqing University of Medical Sciences, Chongqing 400010, China. shenwei2002932@sohu.com
Telephone: +86-23-63849076-2323 **Fax:** +86-23-63849076

Received: 2002-07-08 **Accepted:** 2002-10-21

Abstract

AIM: To investigate the inhibitive effect and its possible mechanism of Cordyceps Sinensis (CS) on CCl₄-plus ethanol-induced hepatic fibrogenesis in experimental rats.

METHODS: Rats were randomly allocated into a normal control group, a model control group and a CS group. The latter two groups were administered with CCl₄ and ethanol solution at the beginning of the experiment to induce hepatic fibrosis. The CS group was also treated with CS 10 days after the beginning of CCl₄ and ethanol administration. All control groups were given corresponding placebo at the same time. At the end of the 9th week, rats in each group were humanely sacrificed. Blood and tissue specimens were taken. Biochemical, radioimmunological, immunohistochemical and molecular biological examinations were used to determine the level change of ALT, AST, HA, LN content in serum and TGFβ₁, PDGF, collagen I and III expression in tissue at either protein or mRNA level or both of them.

RESULTS: As compared with the model control group, serum ALT, AST, HA, and LN content levels were markedly dropped in CS group (86.0±34.4 vs 224.3±178.9, 146.7±60.2 vs 272.6±130.1, 202.0±79.3 vs 316.5±94.1 and 50.4±3.0 vs 59.7±9.8, respectively, $P<0.05$). Tissue expression of TGFβ₁ and its mRNA, collagen I mRNA were also markedly decreased (0.2±0.14 vs 1.73±1.40, 1.68±0.47 vs 3.17±1.17, 1.10±0.84 vs 2.64±1.40, respectively, $P<0.05$). More dramatic drop could be seen in PDGF expression (0.87±0.43 vs 1.91±0.74, $P<0.01$). Although there was no statistical significance, it was still strongly suggested that collagen III mRNA expression was also decreased in CS group as compared with model control group (0.36±0.27 vs 0.95±0.65, $P=0.0615$). In this experiment, no significant change could be found in PDGF mRNA expression between two groups (0.35±0.34 vs 0.70±0.46, $P>0.05$).

CONCLUSION: Cordyceps sinensis could inhibit hepatic fibrogenesis derived from chronic liver injury, retard the development of cirrhosis, and notably ameliorate the liver function. Its possible mechanism involves inhibiting TGFβ₁ expression, and thereby, down regulating PDGF expression, preventing HSC activation and deposition of procollagen I and III.

Liu YK, Shen W. Inhibitive effect of cordyceps sinensis on experimental hepatic fibrosis and its possible mechanism. *World J Gastroenterol* 2003; 9(3): 529-533
<http://www.wjgnet.com/1007-9327/9/529.htm>

INTRODUCTION

The incidence rate of chronic in China is high, which afflicts the patients by progressively developing into irreversible cirrhosis^[1,2]. Hepatic fibrosis is the intermediate and crucial stage of this process, characterized by reversibility. If treated properly in this stage, cirrhosis could be successfully prevented^[3].

Clinical observation and experimental data suggested that liver fibrosis could be reabsorbed under certain conditions. Chinese herbs, well known for their definite effectiveness, cheap prices and negligible side effects, have particular advantages in therapeutic research of hepatic fibrogenesis. Several herbs were suggested recently by some reports to have preventive effect on hepatic fibrosis^[4-12], and cordyceps sinensis (CS) is one of them^[4,5]. However, its exact effectiveness and detailed mechanisms have not been elaborated. In this study, we established the animal model of chronic liver injury-hepatic fibrosis-cirrhosis, intervened with CS, and observed its inhibitive effect. An array of indexes in protein and mRNA levels was established in order to thoroughly investigate its possible mechanism.

MATERIALS AND METHODS

Animals

Male Wistar rats weighing between 200 g and 300 g were obtained from Experimental Animal Center of ChongQing University of Medical Science, China. The rats were housed 3 or 4 per cage and subjected to 12-day/12-night cycle with unrestricted access to basic food. All animals were treated humanely according to the national guideline for the care of animals in the country.

Preparation for CS suspension

CS was purchased from Bao Ding Pharmaceutical Company, China.

The CS and double-distilled water were mixed in proportion of 1:3 and subject to full vibration.

Reagents

TGFβ₁, PDGF, procollagen I and III RNA probe and detection kit for *in-situ* hybridization were purchased from Boster Biologic Technology Company, China. Anti-TGFβ₁ monoclonal antibody, anti-PDGF multiclonal antibody and its detection kit for immunohistochemical assay were purchased from Santa Cruz biologic technology Company, USA. Serum ALT, AST, HA, and LN examinations were performed by the Laboratory Department of Chong Qing University of Medical Sciences, China.

Establishment of animal model: carbon tetrachloride (CCL₄)-plus-ethanol induced hepatic fibrosis

Sixty-six male Wista rats were randomly assigned to a normal control group, a model control group and a CS group. At the beginning of the experiment, rats in model control group and CS group were subjected to hypodermic injection of (40 % in bean oil) at a dose of 0.3 ml/100 g of body weight twice a week. Besides, rats in these two groups also received 5 %

ethanol solution as the only fluid to drink. Rats in normal control group received hypodermic injection of bean oil at the same dose and frequency as the other two groups and received water ad libitum. Ten days after the CCL₄ administration (for 3 times), CS group was given CS suspension orally at a dose of 1 ml/100 g body weight daily. In the meantime, three rats in model control group were randomly sacrificed to evaluate the liver histological change at this moment while other rats along with rats in normal control group were given saline orally at a dose of 1 ml/100 g body weight daily. All the administrations lasted 9 weeks.

Collection of specimens

At the end of the 9th week, rats in each group were humanely sacrificed by amobarbital sodium anesthesia. Midline laparotomy was performed. Livers were excised and blood was collected through cardiopuncture.

Histological grading

Liver tissues were fixed in formalin and embedded in paraffin blocks according to standard procedures (glass slide was cleaned with 95 % ethanol, treated with APES solution and air dried.) four to six micron thick tissue sections were cut using microtome and applied to slides; And deparafinized in xylenes using three changes for 5 minutes each. Hydrate sections gradually passed through graded alcohols: washing in 100 % ethanol twice, then 95 % ethanol twice for 10 minutes each; and washing in deodorized water for 1 minute. Hemotoxylin and eosin (HE) staining was performed according to the standard procedure.

Fibro-proliferation degree of liver sections were graded numerically based on the criterion described below: grade 0: normal liver; grade 1: few collagen fibrils extend from the central vein and portal tract; grade 2: collagen fibrils extension are obvious but do not encompass the whole lobule; grade 3: collagen fibrils extend and encompass the whole lobule; grade 4: collagen fibrils extend and separate lobule into pseudo-lobule, but mainly shaped in square form; and grade 5: pseudo-lobule shaped mainly in circle form.

Two pathologists who had no knowledge of their sources and each other's assessment examined stained slide independently.

Immunohistochemistry

Liver tissues were fixed in formalin and embedded in paraffin blocks according to standard procedures. Glass slide was cleaned with 95 % ethanol, treated with subbing solution and air-dried. Tissue sections of 4-6 micron thick were cut using microtome and applied to slides; and deparafinized in xylenes using three changes for 5 minutes each. Hydrate sections gradually through graded alcohols: washing in 100 % ethanol twice, then 95 % ethanol twice for 10 minutes each; and washing in deionized water for 1 minutes. Incubate sections for 15 minutes in 0.1 % pepsin at room temperature to expose the antigen masked by formalin fixation and paraffin embedding. Incubate sections with 3 % H₂O₂ and normal non-immunal goat serum for 10 minutes respectively to inactivate endogeneous peroxidase and biotin; incubate sections with primary antibody overnight at 4 °C. Optimal antibody concentration was determined previously. Wash with three changes of PBS for 5 minutes each. Incubate for 20 minutes with biotin-conjugated secondary antibody and avidin biotin enzyme reagent respectively. Wash with three changes of PBS for 5 minutes each. Incubate in peroxidase substrate for 5 minutes, after that dehydrate through alcohols and xylenes. Immediately add 1-2 drops of permanent mounting medium and covered with glass coverlip.

In situ hybridization

The sequence of RNA probe is as follows:

1. TGFβ₁ mRNA

- (1) 5'-CGTTT CACCA GCTCC ATGTC GATGG TGTTG CAGGT-3'
- (2) 5'-CTTGA TTITA ATCTC TGCAA GCGCA GCTCT GCACG-3'
- (3) 5'-TTGGT ATCCA GGGCT CTCCG GTGCC GTGAG CTGTG-3'

2. PDGF mRNA

- (1) 5'-CTCGG CTTCC TCGGC CAGAA CATGG GCGAG GTATC-3'
- (2) 5'-AACCT CACCT GGACT TCTTT CAATT TTGGC TTCTT-3'
- (3) 5'-TTGCA CTCGG CGATC ATGGC CGGCT CAGCA ATGGT-3'
- (4) 5'-GGCTC CAAGG GTCTC CTTC A GTGCC GTCTT GTCAT-3'

3. Col-I mRNA

- (1) 5'-CACAG ATCAC GTCAT CGCAC AACAC CTTGC CGTTG-3'
- (2) 5'-AGCTT CACCG GGACG ACCAG CTTC A CCAGG AGATC-3'
- (3) 5'-TCACT CCTTC TACAT TATAT TCAAA CTGGC PGCCA-3'

4. Col-III mRNA

- (1) 5'-ATTAA CAGAC TTGAG TGAAG TCATA ATCTC ATCGG-3'
- (2) 5'-AGAAT ACAAT CTGTG TTCTT GACCA GGTGA GGTAG-3'
- (3) 5'-GAAGG AGGAG AATCC CGTGG CATGC CAATG AATCT-3'

In situ hybridization was performed as described elsewhere. Briefly, formalin-fixed and paraffin-embedded liver section slides were pretreated by incubation with 0.1 % pepsin, 3 % H₂O₂ and normal non-immunal bovine serum for 10-15 minutes respectively to expose signals masked by formalin fixation and paraffin embedding and inactivate endogeneous peroxidase and biotin. Antisense RNA probe was then added to the sections and incubated together in humidified chamber overnight at 37 °C. After washing with three changes of 2×standard saline citrate (SSC) and 0.2×SSC for 10 minutes each, the sections were subject to incubation with biotin-conjugated secondary antibody and avidin biotin enzyme reagent respectively. Wash with three changes of PBS for 5 minutes each, incubate in peroxidase substrate for 20 minutes, and dehydrate through alcohols and xylenes. One to two drops of permanent mounting medium were immediately added and covered with glass coverlip.

Semiquantitative image analysis

Computer morphometry (CM-2000B Medical Image Analysis Software, Beijing Medical Software Company, China) was used to quantify the optical density of the signal generated by the immunohistochemical and *in situ* hybridization examination. The exact method is described as follows: The video image was generated with a video camera and digitalized for image analysis at 256 gray levels. An optical threshold and filter combination was set to select positive stains. The structure of interest was discriminated automatically by computer and measured for its optical intensity and total area. Staining index was obtained by multiplying the quantified number of optical intensity and total area.

Statistical analysis

Data were analyzed with SAS software. Quantitative data were presented as means ±SD and were compared using *t* test procedure. Frequency data were compared using NPAR1WAY procedure.

RESULTS

CS inhibits fibril deposition and ameliorates liver function of chronic hepatitis

After 10 days (3 times) of CCL₄ administration, rats suffered hepatocyte lipid degeneration, narcosis, and inflammatory cells infiltration, which fulfilled the diagnostic standard for chronic hepatitis.

Specimens from model control group showed apparent formation of fibrotic septa, encompassing regenerated hepatocytes into pseudo-lobules. Regenerated hepatocytes

underwent severe lipraoid degeneration. Specimens from CS group showed only slight fibrogenesis without pseudo-lobule formation.

Although statistical analysis failed to present any significant disparity between quantitative data of histological grading of the two groups, it still indicated that fibrogenesis of CS group was much less severe than that of model control group (Table 1). Compared with model control group, serum contents of HA and LN in CS group were markedly decreased ($P<0.05$), which indicates from another perspective that CS could inhibit hepatic fibrogenesis (Table 2).

Serum contents of ALT and AST in model control group were significantly elevated compared with both normal control and CS groups. However, there was no significant statistical difference between normal control and CS groups ($P>0.05$), which showed that CS could notably ameliorate liver function (Table 2).

CS reduces procollagen I and III mRNA synthesis

Procollagen I and III mRNA synthesis level in liver tissues were determined by *in situ* hybridization and quantified by computer image analyzing system. Positive staining could only be seen at central vein and periportal areas in normal control group. As the model control and CS groups, positive stains were distributed mainly along fibrotic septa other than central vein and periportal areas.

Compared with model control group, staining index of CS group remarkably dropped ($P<0.05$), which suggested that procollagen I mRNA synthesis was strongly inhibited by CS treatment. On the part of procollagen III, despite that there was no significant difference between the two groups, it was also reasonably suggested that CS could inhibit the synthesis of procollagen III mRNA on the consideration of P value (0.0695) (Table 3).

CS reduces TGF β_1 expression

TGF β_1 expression in protein and mRNA level were determined by immunohistochemistry and *in situ* hybridization, respectively. Positive stains were quantified with computer image analyzing system. For the sections of normal control group, positive staining of TGF β_1 and its mRNA was found at central vein and periportal areas. In the sections of model control group and CS group, positive staining could be seen at interstitial cells, inflammatory cells, impaired hepatocytes as well as normal hepatocytes. Fibrotic septa were only slightly stained. TGF β_1 mRNA positive stain distribution was not completely consistent with that of TGF β_1 . More stain was found at fibrotic septa and less at impaired and normal hepatocytes.

Compared with model control group, the staining index of both TGF β_1 and TGF β_1 mRNA in CS group was markedly decreased ($P<0.05$, respectively), indicating that CS could inhibit TGF β_1 mRNA transcription and, thereby, reducing the TGF β_1 expression (Table 3).

CS reduces PDGF expression

PDGF expression in protein and mRNA level was determined, like TGF β_1 , by immunohistochemistry and *in situ* hybridization respectively. Positive staining was quantified with computer image analyzing system. For the sections of normal control group, positive stains of PDGF and its mRNA could be seen at central vein and periportal areas. In the sections of model control group and CS group, positive stains mainly appeared at fibrotic septa.

PDGF expression in CS group dropped dramatically compared with model control group ($P<0.01$). But for PDGF mRNA, there was no significant difference by statistical analysis. In spite of this, the means of two groups still suggested difference. To make sure of this, further studies are needed (Table 3).

Table 1 Histological grading

Group	Grade						
	0	1	2	3	4	5	6
Normal	7						
Model		3	1	2	2	2 ^a	
CS		4	5 ^{ab}				

^a $P<0.05$ vs normal control group, ^b $P<0.05$ vs model control group.

Table 2 Serum content of HA, LN, ALT and AST ($\bar{x}\pm s$)

Groups	HA ($\mu\text{g/L}$)	LN ($\mu\text{g/L}$)	ALT (U/L)	AST (U/L)
Normal	142.4 \pm 51.0	41.6 \pm 2.2	63.6 \pm 11.9	108.6 \pm 27.7
Model	316.5 \pm 94.1 ^a	59.7 \pm 9.8 ^a	224.3 \pm 178.9 ^a	272.6 \pm 130.1 ^a
CS	202.0 \pm 79.3 ^{ab}	50.4 \pm 3.0 ^{ab}	86.0 \pm 34.4 ^b	146.7 \pm 60.2 ^b

^a $P<0.05$ vs normal control group, ^b $P<0.05$ vs model control group.

Table 3 Staining index of procollagen I, III mRNA, TGF β_1 , TGF β_1 mRNA, PDGF and PDGF mRNA in liver tissues ($\bar{x}\pm s$)

Groups	Procoll I mRNA	Procoll III mRNA	TGF β_1	TGF β_1 mRNA	PDGF	PDGF mRNA
Model	2.64 \pm 1.40	0.95 \pm 0.65	1.73 \pm 1.40	3.17 \pm 1.17	1.91 \pm 0.74	0.70 \pm 0.46
CS	1.10 \pm 0.84 ^a	0.36 \pm 0.27 ^c	0.2 \pm 0.14 ^a	1.68 \pm 0.47 ^a	0.87 \pm 0.43 ^b	0.35 \pm 0.34 ^c

^a $P<0.05$, ^b $P<0.01$, and ^c $P>0.05$, vs model control group.

DISCUSSION

In this study, we demonstrated that CS could inhibit hepatic fibrogenesis and retard the development of cirrhosis by evaluating histological grading and serum contents of HA and LN. Its possible mechanism involves inhibiting the synthesis of TGF β_1 mRNA and thereby downregulating the expression of TGF β_1 and PDGF, reducing the deposition of collagen I and III.

CS is a type of traditional Chinese tonic that has already been demonstrated by modern pharmacological researches to have extensively positive effect on a few systems of human body^[13-19]. Recently, some reports suggested that this herb might also have preventive effect on hepatic fibrosis^[4,5]. But the real effect and mechanisms have not been elaborated. This study was designed to evaluate its exact effect on hepatic fibrosis and to investigate its possible mechanism.

Various kinds of chronic liver injury widely spread all over the world and afflicted patients greatly. Effective ways to inhibit fibrogenesis and prevent the development of cirrhosis are of great clinical and academic significance. Although many new agents were being tested, no satisfactory agent with ascertained effectiveness and negligible side effects has appeared as yet. Traditional Chinese herbs were well known for their cheap prices and negligible side effects. Exploration in this area is promising.

We started to treat the rats with CS after 10 days of CCL4 administration. Pathological evaluation showed that rats suffered chronic liver injury in this moment. CS treatment based on this disorder presented its inhibitive effect on preventing the development of cirrhosis. HA and LN are good serum markers of hepatic fibrogenesis^[20]. In this study, serum contents of HA and LN in CS group markedly dropped compared with model control group, which indicates that CS could successfully prevent hepatic fibrogenesis. Histological grading also supported this conclusion.

To address the ways in which this herb yielded in a

significant reduction in fibrosis, we investigated the effect of CS treatment in the expression of TGF β_1 as well as its mRNA. Overexpression of this cytokine was associated closely with fibrogenesis in many ways^[21-25]. It can promote HSC to synthesize collagen I and III, and simultaneously inhibit their decomposition by upregulating the expression of Tissue Inhibitor of Metalproteinase (TIMP), which neutralize the activity of Matrix Metalproteinase (MMP)^[26-28], an important degrading enzyme of collagen I and III. In addition, TGF β_1 could also indirectly promote the HSC proliferation by enhancing the expression of PDGF and its receptor^[21]. One strategy in the development of antifibrotic drug is the exploration of TGF β_1 inhibitors^[21]. Because TGF β_1 expression was regulated by diverse factors in transcription, post-transcription, secretion and releasing levels, the expression of its protein and mRNA varied considerably^[22]. Consequently, analyses in two levels were indispensable. In this study, we determined the expression of this cytokine by immunohistochemistry and *in situ* hybridization to investigate the effect of CS on TGF β_1 expression in the both levels. The results showed that both TGF β_1 and its mRNA expression remarkably decreased in CS group, indicating that CS could downregulate the expression of this important cytokine, which possibly contributed to the reduction of fibrosis.

PDGF is another important cytokine that influences the development of fibrosis. According to the previous reports^[29-33], it is the most potent HSC-proliferation promoter, which plays an important role in fibrogenesis. In spite of its earlier identification and isolation, few pharmacological studies observed the effect of the potential agents on this cytokine. In this study, we initially observed the change of this cytokine responding to CS treatment. Compared with model control group, PDGF expression level in protein of CS group dramatically dropped, indicating that CS could inhibit the PDGF expression. Statistical analysis showed no significant difference of PDGFmRNA expression between the two groups. Whether CS exerts inhibitive effect on PDGF expression in mRNA or directly in protein still remains unclear. Further studies are needed to elucidate the detailed mechanisms.

Pathological feature of hepatic fibrosis is the excessive deposition of ECM components^[34-36]. As the medium of parenchyma cells, constancy of ECM component is essential to the maintenance of liver function. Changes of proportion of ECM components, and the change of their quantities, cause the damage of hepatocytes and the deterioration of liver function. Syntheses of Collagen I and III increase greatly when fibrogenesis occurs, which are mainly responsible for the adverse effects brought about by ECM. As a result, Collagen I and III overshadow other components and become the most important ECM in the development of fibrosis. After nine weeks of CS treatment, expression of procollagen I and III decreased. On one hand, this result further manifests that CS has inhibitive effects on fibrosis; on the other hand, it might be one of the possible explanations for the amelioration of liver function.

CS is a cheap and widely available herb that is well tolerated and has been used for centuries in traditional Chinese medicine without any side effect reported. In this study, we demonstrated that, administered at the stage of chronic hepatitis, CS could successfully inhibit hepatic fibrogenesis and retard the development of cirrhosis. Moreover, it can strikingly ameliorate the liver function. Therefore, we suggest that this herb should serve as a promising antifibrotic agent and deserves further investigations.

REFERENCES

- Lamireau T**, Desmouliere A, Bioulac-Sage P, Rosenbaum J. Mechanisms of hepatic fibrogenesis. *Arch Pediatr* 2002; **9**: 392-405
- Brenner DA**, Waterboer T, Sung Kyu Choi, Lindquist JN, Stefanovic B, Burchardt E, Yamauchi M, Gillan A, Rippe RA. New aspects of hepatic fibrosis. *J Hepatol* 2000; **32** (Suppl 1): 32-38
- Riley TR 3rd**, Bhatti AM. Preventive strategies in chronic liver disease: part II. Cirrhosis. *Am Fam Physician* 2001; **64**: 1735-1740
- Liu YK**, Shen W. Effect of Cordyceps sinensis on hepatocytic proliferation of experimental hepatic fibrosis in rats. *Shijie Huaren Xiaohua Zazhi* 2002; **10**: 388-391
- Ma X**, Qiu DK, Xu J, Zeng MD. Effects of Cordyceps polysaccharides in patients with chronic hepatitis C. *Huaren Xiaohua Zazhi* 1998; **6**: 582-584
- Yang Q**, Yan YC, Gao YX. Inhibitory effect of Quxianruangan Capsulae on liver fibrosis in rats and chronic hepatitis patients. *Shijie Huaren Xiaohua Zazhi* 2001; **9**: 1246-1249
- You H**, Wang B, Wang T. Proliferation and apoptosis of hepatic stellate cells and effects of compound 861 on liver fibrosis. *Zhonghua Ganzhangbing Zazhi* 2000; **8**: 78-80
- Nan JX**, Park EJ, Kim YC, Ko G, Sohn DH. Scutellaria baicalensis inhibits liver fibrosis induced by bile duct ligation or carbon tetrachloride in rats. *J Pharm Pharmacol* 2002; **54**: 555-563
- Wang QC**, Shen DL, Zhang CD, Xu LZ, Nie QH, Xie YM, Zhou YX. Effect of Rangansuopiwan in expression of tissue inhibitor of metalloproteinase-1/2 in rat liver fibrosis. *Shijie Huaren Xiaohua Zazhi* 2001; **9**: 379-382
- Shen M**, Chen Y, Qiu DK, Xiong WJ. Effects of recombinant augmentor of liver regeneration protein, danshen and oxymatrine on rat fibroblasts. *Shijie Huaren Xiaohua Zazhi* 2001; **9**: 1129-1133
- Wang XL**, Liu P, Liu CH, Liu C. Effects of coordination of FZHY decoction on functions of hepatocytes and hepatic satellite cells. *Shijie Huaren Xiaohua Zazhi* 2001; **9**: 663-665
- Yao XX**, Tang YW, Yao DM, Xiu HM. Effect of yigan decoction on the expression of type I, III collagen proteins in experimental hepatic fibrosis in rats. *Shijie Huaren Xiaohua Zazhi* 2001; **9**: 263-267
- Nakamura K**, Yamaguchi Y, Kagota S, Shinozuka K, Kunitomo M. Activation of in vivo Kupffer cell function by oral administration of Cordyceps sinensis in rats. *Jpn J Pharmacol* 1999; **79**: 505-508
- Huang BM**, Hsu CC, Tsai SJ, Sheu CC, Leu SF. Effects of Cordyceps sinensis on testosterone production in normal mouse Leydig cells. *Life Sci* 2001; **69**: 2593-2602
- Chiou WF**, Chang PC, Chou CJ, Chen CF. Protein constituent contributes to the hypotensive and vasorelaxant activities of Cordyceps sinensis. *Life Sci* 2000; **66**: 1369-1376
- Yamaguchi Y**, Kagota S, Nakamura K, Shinozuka K, Kunitomo M. Antioxidant activity of the extracts from fruiting bodies of cultured Cordyceps sinensis. *Phytother Res* 2000; **14**: 647-649
- Huang BM**, Ju SY, Wu CS, Chuang WJ, Sheu CC, Leu SF. Cordyceps sinensis and its fractions stimulate MA-10 mouse Leydig tumor cell steroidogenesis. *J Androl* 2001; **22**: 831-837
- Dai G**, Bao T, Xu C, Cooper R, Zhu JS. CordyMax Cs-4 improves steady-state bioenergy status in mouse liver. *J Altern Complement Med* 2001; **7**: 231-240
- Yang LY**, Chen A, Kuo YC, Lin CY. Efficacy of a pure compound H1-A extracted from Cordyceps sinensis on autoimmune disease of MRL lpr/lpr mice. *J Lab Clin Med* 1999; **134**: 492-500
- Li BS**, Wang J, Zhen YJ, Liu JX, Wei MX, Sun SQ, Wang SQ. Experimental study on serum fibrosis markers and liver tissue pathology and hepatic fibrosis in immuno-damaged rats. *Shijie Huaren Xiaohua Zazhi* 1999; **7**: 1031-1034
- Bissell DM**. Chronic liver injury, TGF-beta, and cancer. *Exp Mol Med* 2001; **33**: 179-190
- Friedman SL**. Cytokines and fibrogenesis. *Semin Liver Dis* 1999; **19**: 129-140
- Chen WX**, Li YM, Yu CH, Cai WM, Zheng M, Chen F. Quantitative analysis of transforming growth factor beta 1 mRNA in patients with alcoholic liver disease. *World J Gastroenterol* 2002; **8**: 379-381
- Gressner AM**, Weiskirchen R, Breitkopf K, Dooley S. Roles of TGF-beta in hepatic fibrosis. *Front Biosci* 2002; **7**: d793-807
- Lewindon PJ**, Pereira TN, Hoskins AC, Bridle KR, Williamson RM, Shepherd RW, Ramm GA. The role of hepatic stellate cells and transforming growth factor-beta (1) in cystic fibrosis liver disease. *Am J Pathol* 2002; **160**: 1705-1715
- Eichler W**, Friedrichs U, Thies A, Tratz C, Wiedemann P. Modu-

- lation of Matrix Metalloproteinase and TIMP-1 Expression by Cytokines in Human RPE Cells. *Invest Ophthalmol Vis Sci* 2002; **43**: 2767-2773
- 27 **Britton RS**, Bacon BR. Intracellular signaling pathways in stellate cell activation. *Alcohol Clin Exp Res* 1999; **23**: 922-925
- 28 **Li D**, Friedman SL. Liver fibrogenesis and the role of hepatic stellate cells: new insights and prospects for therapy. *J Gastroenterol Hepatol* 1999; **14**: 618-633
- 29 **Kuter DJ**. Future directions with platelet growth factors. *Semin Hematol* 2000; **37** (2 Suppl 4): 41-49
- 30 **Pinzani M**. Pdgf and signal transduction in hepatic stellate cells. *Front Biosci* 2002; **7**: D1720-1726
- 31 **Isbrucker RA**, Peterson TC. Platelet-derived growth factor and pentoxifylline modulation of collagen synthesis in myofibroblasts. *Toxicol Appl Pharmacol* 1998; **149**: 120-126
- 32 **Fibbi G**, Pucci M, Grappone C, Pellegrini G, Salzano R, Casini A, Milani S, Del Rosso M. Functions of the fibrinolytic system in human Ito cells and its control by basic fibroblast and platelet-derived growth factor. *Hepatology* 1999; **29**: 868-878
- 33 **Yuan N**, Wang P, Wang X, Wang Z. Expression and significance of platelet derived growth factor and its receptor in liver tissues of patients with liver fibrosis. *Zhonghua Ganzangbing Zazhi* 2002; **10**: 58-60
- 34 **Benyon RC**, Arthur MJ. Extracellular matrix degradation and the role of hepatic stellate cells. *Semin Liver Dis* 2001; **21**: 373-384
- 35 **Neubauer K**, Saile B, Ramadori G. Liver fibrosis and altered matrix synthesis. *Can J Gastroenterol* 2001; **15**: 187-193
- 36 **Schuppan D**, Ruehl M, Somasundaram R, Hahn EG. Matrix as a modulator of hepatic fibrogenesis. *Semin Liver Dis* 2001; **21**: 351-72

Edited by Ma JY

Effect of cisapride on intestinal bacterial and endotoxin translocation in cirrhosis

Shun-Cai Zhang, Wei Wang, Wei-Ying Ren, Bo-Ming He, Kang Zhou, Wu-Nan Zhu

Shun-Cai Zhang, Wei-Ying Ren, Bo-Ming He, Kang Zhou, Wu-Nan Zhu, Department of Gastroenterology, Zhongshan Hospital, Fudan University, Shanghai, 200032, China

Wei Wang, Institute of Materia Medica, Chinese Academy of Science, Shanghai, 200032, China

Supported by the National Natural Science Foundation No.30070340

Correspondence to: Dr. Shun-Cai Zhang, Department of Gastroenterology, Zhongshan Hospital, Fudan University, 180 Fenglin Road, Shanghai 200032, China. zhangsc.zshospital.@net

Telephone: +86-21-64041990-2424

Received: 2002-06-11 **Accepted:** 2002-07-19

Abstract

AIM: To investigate the effects of cisapride on intestinal bacterial overgrowth (IBO), bacterial and endotoxin translocation, intestinal transit and permeability in cirrhotic rats.

METHODS: All animals were assessed with variables including bacterial and endotoxin translocation, intestinal bacterial overgrowth, intestinal transit and permeability. Bacterial translocation (BT) was assessed by bacterial culture of MLN, liver and spleen, IBO by a jejunal bacterial count of the specific organism, intestinal permeability by determination of the 24-hour urinary ^{99m}Tc -DTPA excretion and intestinal transit by measurement of the distribution of ^{51}Cr in the intestine.

RESULTS: Bacterial translocation (BT) and IBO was found in 48 % and 80 % cirrhotic rats respectively and none in control rats. Urinary excretion of ^{99m}Tc -DTPA in cirrhotic rats with BT (22.2 ± 7.8) was greater than those without BT (10.5 ± 2.9). Intestinal transit (geometric center ratio) was significantly delayed in cirrhotic rats (0.31 ± 0.06) and further more delayed in cirrhotic rats with BT (0.24 ± 0.06) than those without BT (0.38 ± 0.11). Cirrhotic rats with IBO had significantly higher rates of intestinal bacterial and endotoxin translocation, slower intestinal transit time and higher intestinal permeability than those without IBO. It was also found that BT was closely associated with IBO and the injury of intestinal barrier. Compared with the placebo group, cisapride-treated rats had lower rates of bacterial/endotoxin translocation and IBO, which was closely associated with increased intestinal transit and improved intestinal permeability by cisapride.

CONCLUSION: These results indicate that endotoxin and bacterial translocation in cirrhotic rats may be attributed to IBO and increased intestinal permeability. Cisapride that accelerates intestinal transit and improve intestinal permeability might be helpful in preventing intestinal bacterial and endotoxin translocation.

Zhang SC, Wang W, Ren WY, He BM, Zhou K, Zhu WN. Effect of cisapride on intestinal bacterial and endotoxin translocation in cirrhosis. *World J Gastroenterol* 2003; 9(3): 534-538
<http://www.wjgnet.com/1007-9327/9/534.htm>

INTRODUCTION

Cirrhotic patients have an increasing susceptibility to bacterial infection, such as spontaneous bacterial peritonitis (SBP) and bacteremia, which are mainly caused by aerobic gram-negative organism of enteric origin^[1,2]. Bacteria of enteric origin crossing the intestinal barrier to the mesenteric lymph nodes (MLN), a phenomenon known as bacterial translocation (BT) has recently been documented to occur commonly in cirrhotic rats compared to normal rats. BT has also been reported to be involved in the development of SBP in experimental models of ascitic cirrhosis^[3-5]. The major mechanisms concerning bacterial translocation are deficiencies in local host immune defense, increased permeability of gut barrier and intestinal bacterial overgrowth (IBO). Certain pathological conditions such as shock, sepsis, trauma, burns, intestinal radiation, antibiotic overdose, malnutrition and immuno-suppression are closely related to BT and endotoxemia^[6-8]. Although it has been showed that several mechanisms are involved in development of BT in liver cirrhosis^[9-13], the increased intestinal permeability and IBO due to intestinal mucous membrane congestion and edema attributed to portal hypertension are considered the most important^[13,14]. However, so far there have been not satisfied methods for prevention and treatment of intestinal endotoxemia. Strategies to reduce the intestinal bacterial translocation (BT) and endotoxemia in patients and experimental models of cirrhosis have mainly focused on the selective intestinal decontamination^[15,16]. In this way the effectiveness of alternative antibiotics might be decreased with time because of the selection of resistant bacterial strains that could subsequently colonize the gut and become a potential source of infection, especially in patients with long-time prophylactic treatment. So nonantibiotic drugs are needed to be evaluated in the treatment and prevention of bacterial and endotoxin translocation in cirrhosis and decided whether or not to be applied to the clinical practice^[17].

Cisapride is a 5-HT₄ agonist that can accelerate the movement of the intestine. Many studies have reported that the intestinal bacterial and endotoxin translocation were closely related to IBO and intestinal hypomotility.

In this study we intend to study the effect of cisapride on intestinal transit and the permeability of gut barrier, two factors that are closely associated with intestinal bacterial and endotoxin translocation in cirrhotic rats.

MATERIALS AND METHODS

One hundred and sixty male Sprague-Dawley rats weighing 180-200 g were included in the study. Animals were caged in a controlled room temperature of 21 °C with a 12-hour light/dark cycle and fed standard rat diet with water *ad libitum*. The study was in accordance with guideline for animal research and was approved by the ethical and research committee of the hospital.

Cirrhotic animal model

Cirrhosis was induced in one hundred and thirty-five rats by subcutaneous injection of 50 % CCl₄-olive oil solution twice

a week at an initial dose of 0.6 ml/100 g. Subsequent dosage was adjusted with body weight changes at a dose of 0.3 ml/100 g for 12 weeks. Seventy rats died during the induction of cirrhosis with a mortality of 50 % on average. At last sixty-five cirrhotic rats were used for further study.

Experimental design

25 rats were assigned as healthy controls (group 1). 65 cirrhotic rats were further divided into three groups. Group 2, which included 25 cirrhotic animals without any treatment, was used to study various parameter changes in cirrhosis. Group 3 was consisted of 20 cirrhotic animals with intragastric administration of cisapride suspension for two weeks and used to determine whether cisapride had effects on BT, endotoxemia, IBO, intestinal transit and intestinal permeability. Another 20 cirrhotic animals receiving equal volume of saline to cisapride suspension were named group 4 and used as cirrhotic controls.

Determination of parameters

Animals were fasted for 8 hours before killed. All experimental procedures were performed in sterile conditions. The animals were anesthetized by injection of 2 % pento-barbital sodium into abdominal cavity at a dose of 25–40 mg/kg. At the first day of experiment the rats were fed 5 μ ci of ^{99m}Tc -diethylenetriamine pentaacetic acid (^{99m}Tc -DTPA) (dissolved in 2 ml water) and housed individually in metabolic cages to collect 24-hour urine for further analysis. At the second day, after another 8-hour fasting animals were given 2 ml water containing 2 μ ci of ^{51}Cr through a gastric tube. Thirty minutes later animals were anesthetized and undergone a laparotomy under strict aseptic conditions. After small intestine was ligated at both ends MLN, liver, spleen and intestine were carefully removed out of the cavity. Blood samples were taken from the inferior vena cava.

Intestinal permeability

Intestinal permeability was determined by the 24-hour urinary excretion of ^{99m}Tc -DTPA. Results were expressed as fractional excretion of the radioactive substance. ^{99m}Tc -DTPA was a macromolecule and rarely absorbed into bloodstream through intestinal mucous membrane. When the intestinal permeability was increased as a result of intestinal mucous membrane injury, The absorption of DTPA into blood stream and thus excretion from urine would be increased. Therefore, increased excretion of DTPA from urine was assumed to be reliable index of intestinal permeability^[18, 19].

Intestinal transit

Measurement of intestinal transit by determining the distribution of ^{51}Cr in the intestine was performed in all animals^[20–22]. Special care was taken to prevent movement of intestinal contents in experimental procedures. After separated from the mesentery intestine was removed out of the abdominal cavity, put longitudinally in a moist container and then divided by the ligation of threads into 5-cm segments from orad to aborad. The radioactivity of every segment was measured with gamma-scintillation. Intestinal transit was expressed as the geometric center of ^{51}Cr distribution within the intestine and was calculated as the sum of the products of the fraction of the total administered dose of radioactivity per segment and the segment number. The geometric center were divided by the total number of segments of each rat to correct the difference in the length of intestine and finally expressed as geometric center ratio, which was regarded to be the most accurate method for measurement of intestinal transit.

BT studies

BT from the intestinal lumen was defined on the basis of

positive culture of MLNs (particularly those draining lymph from ileum and cecum), liver, spleen and blood and excluding the infection from other possible sources. All the samples were immediately stored at -70 °C until detection. MLNs, liver and spleen were washed free of blood with sterile saline solutions (SS) and made 10 % tissue-slurry (1 g tissue plus 10 ml sterile SS), then immediately cultured in agar-blood medium plates.

IBO studies

IBO was defined as a jejunal bacterial count of the specific organism that was more than the mean plus two standard deviations of the same organism count in control rats. For the determination of IBO, 0.1 ml of jejunal contents were obtained under aseptic conditions by needle puncture. Then 20 μ l of samples that were diluted 100 or 1 000 folds respectively were cultured in blood-agar plates. After an incubation period of 24–48 hours, the number of colony-forming units (CFUs) was counted. Moreover, the composition of the isolated flora was determined with standard identification techniques. The results were expressed as CFU/ml of jejunal contents.

Determination of serum endotoxin

All the blood specimens for the endotoxin determination were stored in endotoxin-free tubes. The serum was separated by 8 000 g 10 min. Serum level of endotoxin was determined by limulus ameobatic lysate (LAL) test with LAL kits (purchased from Shanghai medical-chemical institute).

Statistical analysis

Data are presented as means \pm SD or proportions as required. Comparisons of quantitative variables among groups were made with the 1-way ANOVA or its corresponding nonparametric test as required. The χ^2 test was used for comparing proportion. The Spearman or Pearson test was used for correlation analyses when appropriate. A *P* value of <0.05 was considered statistically significant.

RESULTS

BT was found in 12 of 25 (48 %) cirrhotic rats and none in control rats (Table 1, *P*<0.01). IBO was present in 20 of 25 cirrhotic rats (80 %) and none in the control rats. All the 12 cirrhotic rats with BT and 63 % of 13 cirrhotic rats without BT were found having IBO (Table 2). The translocated bacteria were *Escherichia coli* in 10 cirrhotic rats and *Klebsiella P.* and *Enterococcus* in other two rats respectively. The same organism was always found at the same time both in BT and IBO. (Table 3).

BT was observed in 11 of the 20 rats with IBO and in only one of the five rats without IBO (55 % vs 20 %, *P*<0.05) (Figure 1). Endotoxin level was measured in the blood of inferior vena cava of all animals and higher endotoxin level was found in cirrhotic rats. Animals with BT or IBO have higher blood endotoxin level than that without. Intestinal transit was significantly delayed in cirrhotic rats and much more delayed in that with BT. This may result from IBO because cirrhotic rats with IBO have more delayed intestinal transit than that without.

Urinary ^{99m}Tc -DTPA excretion was greatly increased in cirrhotic rats than that of their controls. Although the urinary ^{99m}Tc -DTPA excretion in cirrhotic rats with IBO was more than that without the difference was not significant. Similarly urinary ^{99m}Tc -DTPA excretion in cirrhotic rats with BT was more than that without. All of these showed that severer impairment of mucous membrane barrier that had occurred in cirrhotic rats, which might be the key factor to promote occurrence of BT.

The mortality of rats was similar in both cisapride and placebo-treated animals. BT was present in 1 of the 20 cirrhotic rats treated with cisapride and in 11 of the 20 rats receiving placebo (5 % vs 58 %, *P*<0.01). IBO incidence in cirrhotic rats

receiving cisapride suspension was lower than that treated with placebo. Lower serum endotoxin level and faster intestinal transit was found in cirrhotic rats with cisapride treatment than that in the placebo group. (Table 4) Intestinal permeability as showed by the urinary ^{99m}Tc -DTPA excretion was reduced significantly after cisapride treatment.

Table 1 Characteristics of control and cirrhotic rats

	Control rats	Cirrhotic rats
Number of animal	25	25
IBO(%)	0	20/25(80%) ^b
Total jejunal bacteria contents (CFU/ml)	0.54±0.18	1.59±0.48 ^b
Bacterial translocation(%)	0	12/25(48%) ^b
Endotoxin level(pg/ml)	0.11±0.058	0.648±0.134 ^b
Intestinal transit (geometric center ratio)	0.49±0.08	0.31±0.06 ^a
Intestinal permeability (%urinary excretion of ^{99m}Tc -DTPA)	1.62±0.8	16.1±7.6 ^b

^b $P<0.01$ vs control rats; ^a $P<0.05$ vs control rats.

Table 2 Characteristics of Cirrhotic rats with and without BT

	Cirrhotic rats with BT	Cirrhotic rats without BT
Number of animal	12	13
IBO(%)	100%	63% ^a
Total jejunal bacteria contents (CFU/ml)	2.61±0.56	0.65±0.12 ^b
Endotoxin level(pg/ml)	0.873±0.137	0.440±0.108 ^b
Intestinal transit (geometric center ratio)	0.24±0.06	0.38±0.11 ^a
Intestinal permeability (%urinary excretion of ^{99m}Tc -DTPA)	22.2±7.8	10.5±2.9 ^b

^b $P<0.01$ vs cirrhotic rats with BT; ^a $P<0.05$ vs cirrhotic rats with BT.

Table 3 Bacterial species cultured from mesenteric lymph nodes, liver, spleen, peripheral blood and overgrowth in the jejunum

No.	Mesenteric lymph nodes	Liver	Spleen	Blood	Intestinal bacterial overgrowth
1	E.coli	E.coli	E.coli	-	E.coli
2	E.coli	E.coli	E.coli	E.coli	E.coli
3	E.coli	E.coli	E.coli	E.coli	E.coli
					E.faecalis
4	E.coli	E.coli	E.coli	E.coli	E.coli
5	-	E.coli	-	-	E.coli
6	E.coli	E.coli	-	-	E.coli
	Ps. aeruginosa				Ps. aeruginosa
7	E.coli	-	E.coli	-	E.coli
8	P klebsiella	-	-	-	P klebsiella
	E.coli				E.coli
9	E.coli	E.coli	-	-	E.coli
	P. mirabilis				P. mirabilis
10	-	E.coli	E.coli	-	E.coli
11	P enterococcus	-	SP	-	P enterococcus
	E.coli		enterococcus		E.coli
12	E.coli	-	-	E.coli	E.coli

Abbreviations: E. coli, Escherichia coli; P. mirabilis, Proteus mirabilis; Ps. Aeruginosa, Pseudomonas aeruginosa, P klebsiella: Pneumonia Klebsiella.

Table 4 Effect of cisapride on BT, IBO, serum endotoxin level, intestinal transit and intestinal permeability of cirrhotic rats

	Placebo	Cisapride
Number of animal	20	20
Bacterial translocation (%)	11/20(55%)	2/20(10%) ^b
IBO(%)	16/20(80%)	3/20(15%) ^b
Total jejunal bacteria contents (CFU/ml)	1.60±0.42	0.60±0.58 ^a
Endotoxin level(pg/ml)	0.721±0.123	0.148±0.079 ^b
Intestinal transit (geometric center ratio)	0.33±0.08	0.68±0.16 ^b
Intestinal permeability (%urinary excretion of ^{99m}Tc -DTPA)	17.2±5.98	12.2±5.28 ^a

^b $P<0.01$ vs placebo; ^a $P<0.05$ vs placebo.

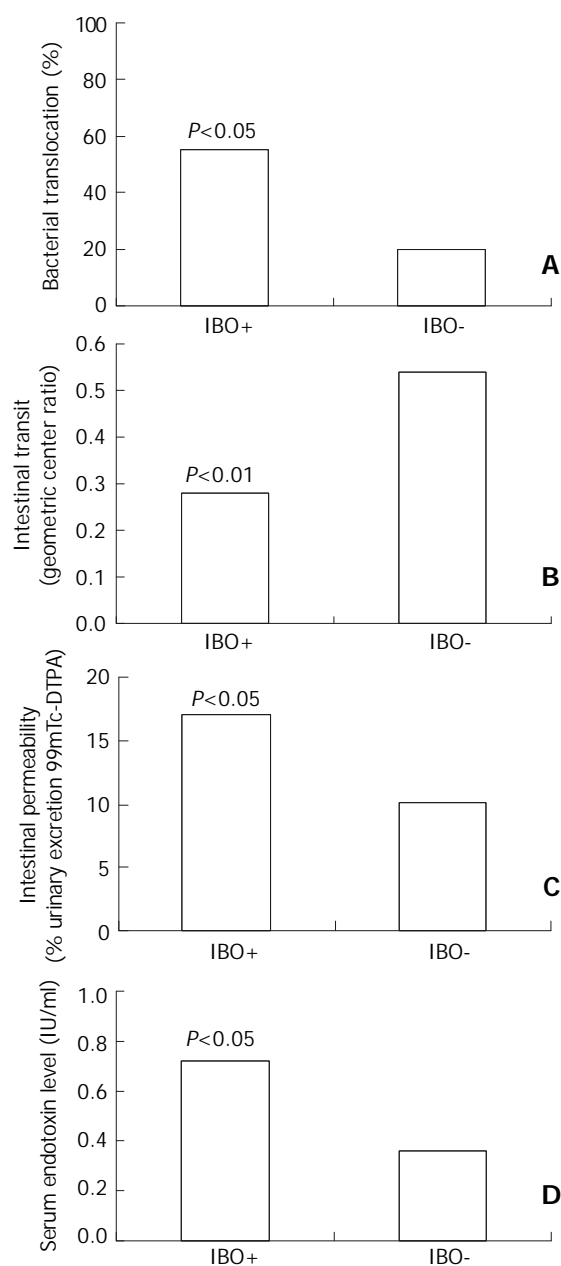


Figure 1 Bacterial translocation, intestinal transit, intestinal permeability and serum endotoxin level in cirrhotic rats with and without IBO (IBO+, IBO-, respectively). Cirrhotic rats with IBO have a higher incidence of BT (A), slower intestinal transit (B), higher intestinal permeability (C) and higher serum endotoxin level (D) than that of cirrhotic rats without IBO.

DISCUSSION

Many studies have shown a high susceptibility to bacterial infection among cirrhotic patients. In recent years, IBO and BT have been suggested to be involved in the pathogenesis of gut-origin bacterial infections, such as SBP, in animal with cirrhosis^[21-23]. Although the phenomenon of BT has been recognized for more than a century, the precise mechanism of BT remains to be elucidated. IBO is postulated to be one of the major factors of BT. Guarner *et al.*^[24,25] have shown that the intestinal aerobic bacterial count in cecal stool is significantly increased in CCl₄ induced cirrhotic rats with BT as compared with without and the prevalence of SBP was found to be significantly higher in cirrhotic patients with IBO than in those without. Reilly JA and Perez-Paramo M have reported that the incidence of IBO was significantly higher in cirrhotic patients with SBP than in those without^[21,22]. Pardo *et al.*^[26] have observed that jejunal IBO were significantly higher in ascitic cirrhotic rats with BT than in those without, for a specific organism BT was always associated with its IBO, which suggests that the IBO favors the development of BT in experimental cirrhosis. In this experimental study, we have observed a direct relationship between the IBO and BT, which also suggests that IBO is one of the major mechanisms that promote BT in experimental models. However, The fact that not all cirrhotic rats with IBO developed BT suggested that other factors may play an important role in development of BT. It had been reported that impairment of gut barrier was a necessary process in the development of BT. Our result that higher value of urinary excretion of ^{99m}Tc-DTPA was seen in BT rats other than in that without was also suggested that the impairment of gut barrier was an important factor in promoting BT.

The mechanisms of gut barrier impairment were not completely elucidated. Some putative mechanisms have been proposed from animal and clinical studies. Portal hypertension in liver cirrhosis may be the most attractive factor in the impairment of gut barrier^[26,27]. However, many studies have showed that poor linear relationship existed between the severity of high portal pressure and the impairment in intestinal permeability and that there was lack of improvement in permeability after reducing portal pressure^[21]. It was possible that increased intra-luminal endotoxin level resulted from IBO played a contributory role in the damage to the gut barrier^[21]. Our results of reduced incidence of IBO and improved intestinal permeability after cisapride treatment have shown the effect of endotoxin on the impairment of gut barrier.

Prevention of IBO was dependent on normal intestinal motility. Intestinal hypomotility was a main cause of IBO in cirrhotic animals^[21,22, 24,25]. This was supported by the delayed intestinal transit in cirrhotic animals with IBO and by the lower incidence of IBO in cirrhotic animals treated with cisapride, a drug that shortens bowel transit time.

During physiological processes, endotoxin is released from the bowel and detoxified by Kupffer cells and hepatocytes. High levels of endotoxin have been noted in cirrhotic patients. A number of previous studies have been shown that the plasma endotoxin level may be potentially helpful in the diagnosis of bacterial infection in patients with cirrhosis^[27]. Recently a study revealed that increased levels of endotoxin indicated the occurrence of gram-negative bacterial infection^[28,29]. In this study, we observed that the serum endotoxin level of the cirrhotic rats, especially those with IBO and BT, was much higher than that of healthy rats. The results suggested that endotoxemia caused by enteric bacteria was common in experimental cirrhosis and positively correlated with IBO and BT.

Several circumstances in cirrhosis could predispose a patient to IBO, such as alcohol abuse, malnutrition, hypochlorhydria,

decreased intraluminal immunoglobulin A or bile salts in the intestine, and disturbances of the small intestinal motility^[6-8,12]. Among which, prolonged intestinal transit, as a consequence of altered intestinal motility seems to play a major role in the development of IBO. Altered small intestinal motility was described in patients with cirrhosis^[8,30,31]. Pardo and his associates^[26] have recently found that alterations in small intestinal motility could result in a prolonged intestinal transit time in cirrhotic patients, which might facilitate the appearance of IBO and the 10-day treatment with prokinetic drug resulted in a marked reduction in jejunal bacterial content and BT in cirrhotic rats^[21], which was coincide with our present study. In addition, and even more important, the prokinetic drug treatment was associated with a dramatic reduction in serum endotoxin level. Although the exact mechanisms by which the prokinetic drug reduce the incidence of BT, endotoxemia and IBO could not be completely elucidated on the basis of the present study, the observations that the serum endotoxin level was positively correlated with jejunal bacterial overgrowth, and that the prokinetic drug administration reduce not only IBO and BT but also endotoxin level, suggested that the beneficial effects of prokinetic drug may be due to the increasing of bowel movement and the promoting of intestinal bacterial and endotoxin elimination, which has been shown by shortened intestinal transit time in cisapride-treated group. Moreover, the administration of prokinetic drug could improve intestinal permeability in cirrhotic rats, which also suggested that increased intestinal permeability in cirrhotic rats was partially due to the damage of intestinal mucous membrane by bacteria overgrowth and high concentrations because cisapride has no direct protective effect on intestinal mucous membrane. In fact, it has been reported that prolonged the OCT could be significantly recovered in cirrhotic patients after cisapride therapy. These results suggested that the beneficial effect of the prokinetic drug on endotoxemia may be due to increasing the abolition of intestinal bacteria through the prokinetic effect. Unfortunately cisapride has lethal side-effect and has been prohibited to be used in treatment of disturbance of intestinal function in human. However, new prokinetic drugs have been available in the market and showed with similar effect on intestinal movement as cisapride. Therefore oral administration of prokinetic drugs might be beneficial to liver diseases by reducing absorption of endotoxin, a substance that is toxic to hepatocytes and could aggravate liver diseases.

In conclusion, the results of our experimental study indicated that the administration of prokinetic drug to cirrhotic rats resulted in a reduction of endotoxemia and BT incidence, which was accompanied by a marked decrease of IBO, reduced intestinal transit time and intestinal permeability. These findings suggested the beneficial effects of prokinetic drug on the prophylaxis of gut origin infection in cirrhosis, which should be taken as an adjuvant or alternative therapy to the selective intestinal decontamination with antibiotics.

REFERENCES

- 1 **Caly WR**, Strauss E. A prospective study of bacterial infections in patients with cirrhosis. *J Hepatol* 1993; **18**: 353-358
- 2 **Bauer TM**, Steinbruckner B, Brinkmann FE, Ditzén AK, Schwacha H, Aponte JJ, Pelz K, Kist M, Blum HE. Small intestinal bacterial overgrowth in patients with cirrhosis: prevalence and relation with spontaneous bacterial peritonitis. *Am J Gastroenterol* 2001; **96**: 2962-2967
- 3 **Llovet JM**, Bartoli R, March F, Planas R, Vinado B, Cabre E, Arnal J, Coll P, Ausina V, Gassull MA. Translocated intestinal bacteria cause spontaneous bacterial peritonitis in cirrhotic rats: molecular epidemiologic evidence. *J Hepatol* 1998; **28**: 307-313
- 4 **Llovet JM**, Bartoli R, Planas R, Vinado B, Perez J, Cabre E, Arnal J, Ojanguren I, Ausina V, Gassull MA. Selective intestinal decon-

- tamination with norfloxacin reduces bacterial translocation in ascitic cirrhotic rats exposed to hemorrhagic shock. *Hepatology* 1996; **23**: 781-787
- 5 **Garcia-Tsao G**, Lee FY, Barden GE, Cartun R, West AB. Bacterial translocation to mesenteric lymph nodes is increased in cirrhotic rats with ascites. *Gastroenterology* 1995; **108**: 1835-1841
- 6 **Casafont F**, Sanchez E, Martin L, Aguero J, Romero FP. Influence of malnutrition on the prevalence of bacterial translocation and bacterial spontaneous bacterial peritonitis in experimental cirrhosis in rats. *Hepatology* 1997; **25**: 1334-1337
- 7 **Plummer JL**, Ossowicz CJ, Whibley C, Ilsley AH, Hall PD. Influence of intestinal flora on the development of fibrosis and cirrhosis in rat model. *J Gastroenterol Hepatol* 2000; **15**: 1307-1311
- 8 **Jackson GD**, Dai Y, Sewell WA. Bile mediates intestinal pathology in endotoxemia in rats. *Infect Immun* 2000; **68**: 4714-4719
- 9 **Madrid AM**, Cumsille F, Defilippi C. Altered small bowel motility in patients with liver cirrhosis depends on severity of liver disease. *Dig Dis Sci* 1997; **42**: 738-742
- 10 **Chang CS**, Chen GH, Lien HC, Yeh HZ. Small intestine dysmotility and bacterial overgrowth in cirrhotic patients with spontaneous bacterial peritonitis. *Hepatology* 1998; **28**: 1187-1190
- 11 **Achord JL**. Mortality associated with spontaneous bacterial peritonitis. *J Clin Gastroenterol* 2001; **33**: 295-298
- 12 **Ramachandran A**, Balasubramania KA. Intestinal dysfunction in liver cirrhosis: its role in spontaneous bacterial peritonitis. *J Gastroenterol Hepatol* 2001; **16**: 607-612
- 13 **Garcia-Tsao G**, Albillos A, Barden GE, West AB. Bacterial translocation in acute and chronic portal hypertension. *Hepatology* 1993; **17**: 1081-1085
- 14 **Veal N**, Auduberteau H, Lemarie C, Oberti F, Cales P. Effects of octreotide on intestinal transit and bacterial translocation in conscious rats with portal hypertension and liver fibrosis. *Dig Dis Sci* 2001; **46**: 2367-2373
- 15 **Runyon BA**, Borzio M, Young S, Squier SU, Guarner C, Runyon MA. Effect of selective bowel decontamination with norfloxacin on spontaneous bacterial peritonitis translocation and survival in an animal model of cirrhosis. *Hepatology* 1995; **21**: 1719-1724
- 16 **Guarner C**, Runyon BA, Heck M, Young S, Sheikh MY. Effect of long-term trimethoprim-sulfamethoxazole prophylaxis on ascites formation, bacterial translocation, spontaneous bacterial peritonitis and survival in cirrhotic rats. *Dig Dis Sci* 1999; **44**: 1957-1962
- 17 **Nanji AA**, Khettry U, Sadrzadeh SM. Lactobacillus feeding reduces endotoxemia and severity of experimental alcoholic liver (disease). *Proc Soc Exp Biol Med* 1994; **205**: 243-247
- 18 **Bjarnason I**, Macpherson A, Hollander D. Intestinal permeability: an overview. *Gastroenterology* 1995; **108**: 1566-1581
- 19 **Campillo B**, Pernet P, Bories PN, Richardet JP, Devanlay M, Aussel C. Intestinal permeability in liver cirrhosis: relationship with severe septic complications. *Eur J Gastroenterol Hepatol* 1999; **11**: 755-759
- 20 **Miller MS**, Galligan JJ, Burks TF. Accurate measurement of intestinal transit in the rat. *J Pharmacol Methods* 1981; **6**: 211-217
- 21 **Reilly JA Jr**, Quigley EM, Forst CF, Rikkers LF. Small intestinal transit in the portal hypertensive rat. *Gastroenterology* 1991; **100**: 670-674
- 22 **Perez-Paramo M**, Munoz J, Albillos A, Freile I, Portero F, Santos M, Ortiz-Berrocal J. Effect of propranolol on the factors promoting bacterial translocation in cirrhotic rats with ascites. *Hepatology* 2000; **31**: 43-48
- 23 **Llovet JM**, Bartoli R, Planas R, Cabre E, Jimenez M, Urban A, Ojanguren I, Arnal J, Gassull MA. Bacterial translocation in cirrhotic rats. Its role in the development of spontaneous bacterial peritonitis. *Gut* 1994; **35**: 1648-1652
- 24 **Guarner C**, Soriano G. Spontaneous bacterial peritonitis. *Semin Liver Dis* 1997; **17**: 203-217
- 25 **Guarner C**, Runyon BA, Young S, Heck M, Sheikh MY. Intestinal bacterial overgrowth and bacterial translocation in cirrhotic rats with ascites. *J Hepatol* 1997; **26**: 1372-1378
- 26 **Pardo A**, Bartoli R, Lorenzo-Zuniga V, Planas R, Vinado B, Riba J, Cabre E, Santos J, Luque T, Ausina V, Gassull MA. Effect of cisapride on intestinal bacterial overgrowth and bacterial translocation in cirrhosis. *Hepatology* 2000; **31**: 858-863
- 27 **Cirera I**, Bauer TM, Navasa M, Vila J, Grande L, Taura P, Fuster J, Garcia-Valdecasas JC, Lacy A, Suarez MJ, Rimola A, Rodes J. Bacterial translocation of enteric organisms in patients with cirrhosis. *J Hepatol* 2001; **34**: 32-37
- 28 **Kuo CH**, Changchien CS, Yang CY, Sheen IS, Liaw YF. Bacteremia in patients with cirrhosis of the liver. *Liver* 1991; **11**: 334-339
- 29 **Chan CC**, Hwang SJ, Lee FY, Wang SS, Chang FY, Li CP, Chu CJ, Lu RH, Lee SD. Prognostic value of plasma endotoxin levels in patients with cirrhosis. *Scand J Gastroenterology* 1997; **32**: 942-946
- 30 **Madrid AM**, Hurtado C, Venegas M, Cumsille F, Defilippi C. Long-Term treatment with cisapride and antibiotics in liver cirrhosis: effect on small intestinal motility, bacterial overgrowth, and liver function. *Am J Gastroenterol* 2001; **96**: 1251-1255
- 31 **Madrid AM**, Brahm J, Antezana C, Gonzalez-Koch A, Defilippi C, Pimentel C, Oksenberg D, Defilippi C. Small bowel motility in primary biliary cirrhosis. *Am J Gastroenterol* 1998; **93**: 2436-2440

Edited by Zhu L

Effects of transmitters and interleukin-10 on rat hepatic fibrosis induced by CCl₄

Xiao-Zhong Wang, Li-Juan Zhang, Dan Li, Yue-Hong Huang, Zhi-Xin Chen, Bin Li

Xiao-Zhong Wang, Li-Juan Zhang, Dan Li, Yue-Hong Huang, Zhi-Xin Chen, Bin Li, Department of Gastroenterology, The Affiliated Union Hospital, Fujian Medical University, Fuzhou, 350001, Fujian Province, China

Supported by Natural Science Foundation of Fujian Province, No. C96042

Correspondence to: Xiao-Zhong Wang, Department of Gastroenterology, The Affiliated Union Hospital, Fujian Medical University, Fuzhou, 350001, Fujian Province, China. drwangxz@public6.fz.fj.cn

Telephone: +86-591-3357896 Ext 8482

Received: 2002-07-31 **Accepted:** 2002-10-12

Abstract

AIM: To study the effects of transmitters ET, AgII, PGI₂, CGRP and GG on experimental rat hepatic fibrosis and the antifibrogenic effects of IL-10.

METHODS: One hundred SD rats were randomly divided into 3 groups: control group (N): intraperitoneal injection with saline 2 ml·kg⁻¹ twice a week; the fibrogenesis group (C): intraperitoneal injection with 50 % CCl₄ 2 ml·kg⁻¹ twice a week; IL-10 treated group (E): besides same dosage of CCl₄ given, intraperitoneal injection with IL-10 4 ug·kg⁻¹ from the third week. In the fifth, the seventh and the ninth week, rats in three groups were selected randomly to collect plasma and liver tissues. The levels of ET, AgII, PGI₂, CGRP and GG were assayed by radioimmunoassay (RIA). The liver fibrosis was observed with silver staining.

RESULTS: The hepatic fibrosis was developed with the increase of the injection frequency of CCl₄. The ET, AgII, PGI₂, CGRP and GG levels in serum of group N were 71.84±60.2 ng·L⁻¹, 76.21±33.3 ng·L⁻¹, 313.03±101.71 ng·L⁻¹, 61.97±21.4 ng·L⁻¹ and 33.62±14.37 ng·L⁻¹, respectively; the levels of them in serum of group C were 523.30±129.3 ng·L⁻¹, 127.24±50.0 ng·L⁻¹, 648.91±357.29 ng·L⁻¹, 127.15±62.0 ng·L⁻¹ and 85.26±51.83 ng·L⁻¹, respectively; the levels of them in serum of group E were 452.52±99.5 ng·L⁻¹, 90.60±44.7 ng·L⁻¹, 475.57±179.70 ng·L⁻¹, 102.2±29.7 ng·L⁻¹ and 38.05±19.94 ng·L⁻¹, respectively. The histological examination showed that the degrees of the rats liver fibrosis in group E were lower than those in group C.

CONCLUSION: The transmitters ET, AgII, PGI₂, CGRP and GG play a significant role in the rat hepatic fibrosis induced by CCl₄. IL-10 has the antagonistic action on these transmitters and can relieve the degree of the liver fibrosis.

Wang XZ, Zhang LJ, Li D, Huang YH, Chen ZX, Li B. Effects of transmitters and interleukin-10 on rat hepatic fibrosis induced by CCl₄. *World J Gastroenterol* 2003; 9(3): 539-543
<http://www.wjgnet.com/1007-9327/9/539.htm>

INTRODUCTION

Hepatic fibrosis is a disease which is characterized by an

increase of type I and type III collagens, proteoglycans fibronectin and hyaluronic acid in extracellular matrix (ECM) deposition^[1-9]. It is an inevitable phase during the formation of liver cirrhosis, which is an irreversible stage of several liver pathological changes^[10-12]. So it is important how to prevent and cure hepatic fibrosis, i.e. antifibrogenetic treatment. Transmitters play an important role in the portal hypertension which is associated with the fibrosis^[13,14]. In our study, the transmitters endothelin (ET), angiotensin II (Ag II), prostacyclin (PGI₂), calcitonin-gene related peptide (CGRP) and glucagon (GG) were selected to explore their effects on hepatic fibrosis induced by CCl₄ and the antifibrogenesis effect of interleukin-10 (IL-10) was explored as well.

MATERIALS AND METHODS

Animals

One hundred clean SD rats weighing 140-180 g were randomly divided into 3 groups. The control group (group N) included 24 rats; the fibrogenesis group (group C) included 40 rats and the IL-10 treated group (group E) included 36 rats, respectively. All the rats were breeding in the routine condition (room temperature 22±2 °C, humidity 55±5 %, lighting 12hrs per day, to drink tap water and eat in any time when they needed, animal food was provided by BK company in Shanghai.).

Establishment of the fibrosis model

Rats in group N were injected intraperitoneally with saline 2 ml·kg⁻¹ twice a week. Rats in group C and group E were injected intraperitoneally with 50 % CCl₄ 2 ml·kg⁻¹ twice a week^[15]. From the third week, rats in group E were injected intraperitoneally with IL-10 4 ug·kg⁻¹ (dissolved in saline)^[16] 20 minutes before they were injected with CCl₄. All injections were performed in Monday and Thursday, rats' body weight was recorded before the injection. In the fifth week, 3 rats in group C and 2 rats in group E died, in the seventh week, total 8 rats in group C and 4 rats in group E died, in the ninth week, total 10 rats in group C, 6 rats in group E and 3 rats in group N died. In 5,7,9 weeks, 10 rats of group C and E and 7 rats in the control group were selected randomly to collect their plasma and liver tissue samples.

Assessment of samples

The blood samples were added into the tubes with 30 µl 10 % EDTA and 40 µl trasylol in ice bath, the tubes were centrifuged at 3 000 rpm for 10 minutes at 4 °C, then the plasma was frozen for the assessment. The plasma levels of ET, Ag II, PGI₂, CGRP and GG were assayed by radioimmunoassay (RIA, kits provided by EastAsia Immune-technology Institute, Beijing). Each plasma sample was taken 100 µl into the tube, then 200 µl buffer and 100 µl antiserum were added into each sample, they were agitated and incubated for 24 hour at 4 °C; then 100 µl ¹²⁵I-marked serum was added, agitated and incubated for 24 hour at 4 °C; also 500 µl precipitation was added, after incubation for 20 min at room temperature, the tubes were centrifuged at 3 500 rpm for 25 min at 4 °C, the upper layer was carefully removed, the cpm account was measured using γ

radioimmuno-counter. The blank control and the standard control was measured respectively at the same time. The liver tissue was made of paraffin section with silver staining.

Statistical analysis

All data were expressed as $\bar{x} \pm s$, *t* test was used for comparison between groups.

RESULTS

Plasma levels of ET, AgII, 6-K-PGF_{1α}, CGRP and GG

The plasma levels of ET, AgII, 6-K-PGF_{1α}, CGRP and GG in group C were higher than those in the control (*P*<0.05). After the intervention of IL-10, the levels of them were decreased, and had no difference with group N (*P*>0.05). Furthermore, their levels were increased with the development of hepatic fibrosis.

Table 1 Plasma levels of ET, AgII, 6-K-PGF_{1α}, CGRP and GG in fibrosis and normal rats (ng·L⁻¹)

	<i>n</i>	ET	AgII	6-K-PGF _{1α}	CGRP	GG
N	21	71.84±60.2	76.21±33.3	313.03±101.71	61.97±21.4	33.62±14.37
C ^a	30	523.30±129.3	127.24±50.0	648.91±357.29	127.15±62.0	85.26±51.83
E ^b	30	452.52±99.5	90.60±44.7	475.57±179.70	102.2±29.7	38.05±19.94

^a*P*<0.05 vs group N, ^b*P*<0.05 vs group N.

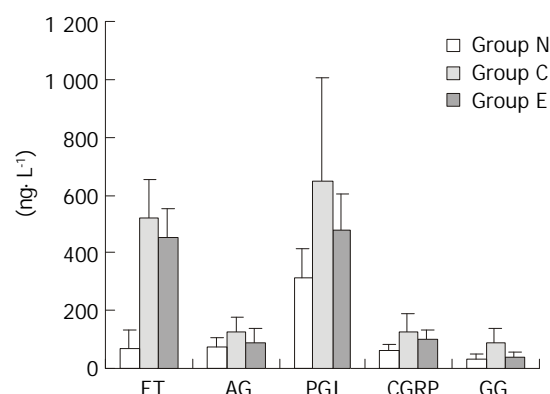


Figure 1 Plasma levels of ET, AgII, 6-K-PGF_{1α}, CGRP and GG in fibrosis and normal rats.

Table 1 and Figure 1 showed that after the treatment of CCl₄, the plasma levels of ET, AgII, 6-K-PGF_{1α}, CGRP and GG were increased, their levels were significantly higher than those in the normal controls (*P*<0.05). After treated with IL-10, their levels were obviously decreased, and there was no significant difference with those in the normal controls. It was showed that when the effective treatment was applied in the fibrosis rats, the levels of these transmitters showed the descending trend. It suggested that the levels of those transmitters were increased in liver fibrosis and they might play important pathogenic roles during the development of liver fibrosis.

Table 2 Plasma levels of ET, AgII, 6-K-PGF_{1α}, CGRP and GG in fibrosis rats (ng·L⁻¹)

Week	<i>n</i>	ET	AgII	6-K-PGF _{1α}	CGRP	GG
No.5	10	421.48±52.3	105.73±36.3	323.15±76.2	88.68±23.2	54.48±18.9
No.7	10	489.80±87.7	131.42±18.9	684.98±214.0	118.14±24.3	55.77±19.2
No.9	10	658.61±102.3	144.58±72.2	1081.61±294.3	174.65±87.7	141.66±50.8

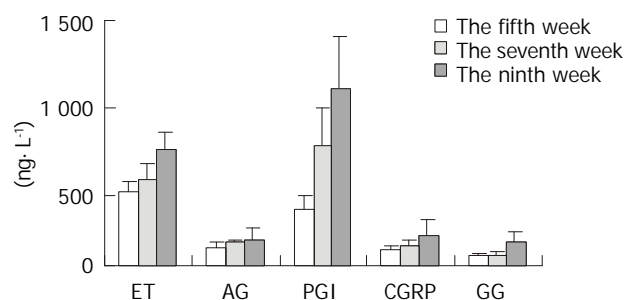


Figure 2 Plasma levels of ET, AgII, 6-K-PGF_{1α}, CGRP and GG in fibrosis rats.

Table 2 and Figure 2 showed that the levels of ET, AgII, 6-K-PGF_{1α}, CGRP and GG were gradually increased and associated with the increase of CCl₄-treated frequency, especially in the ninth week (*P*<0.05). It suggested that there was close relation between the levels of the transmitters and the degrees of liver fibrosis.

Pathological assay

The histological feature showed that liver of control rats had no appreciable alterations (Figure 3). The degree of liver fibrosis in group C was up-going with the increases of the treatment frequency of CCl₄. In the fifth week, few reticular fiber deposited in the periportal tissue space. In the seventh week, the reticular fiber extended with hepatic plate but the full delimitation was not formed, while in the ninth week the integrity fibrous septum was developed in the interlobular septum, sometimes pseudolobular could be seen (Figure 4,5,6). The degrees of inflammation of hepatocytes were decreased evidently in the seventh week after the treatment of IL-10, in the ninth week, the reticular fiber in the interlobular septum was limited remarkably, no pseudolobular could be seen (Figure 7).

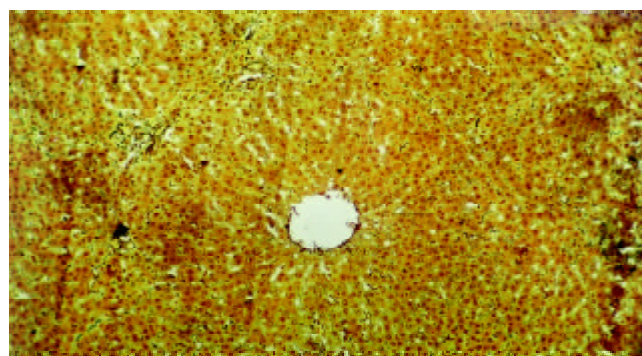


Figure 3 The liver of normal rat (silver staining, ×100).

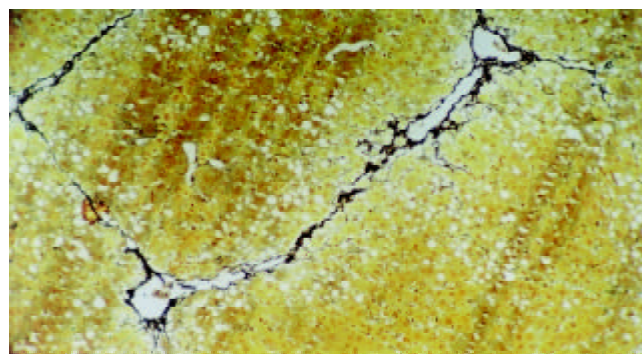


Figure 4 The liver of the rat in group C (the fifth week, silver staining, ×100).

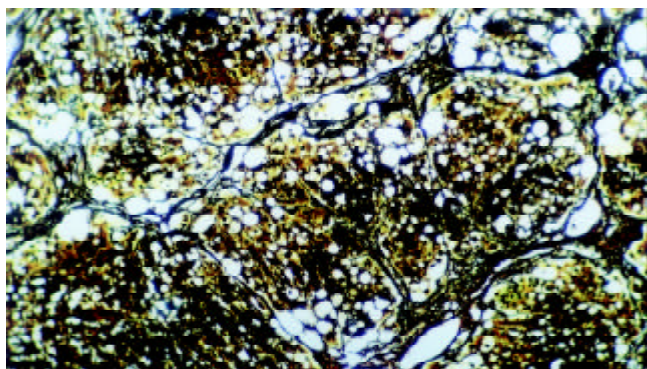


Figure 5 The liver of the rat in group C (the seventh week, silver staining, $\times 100$).

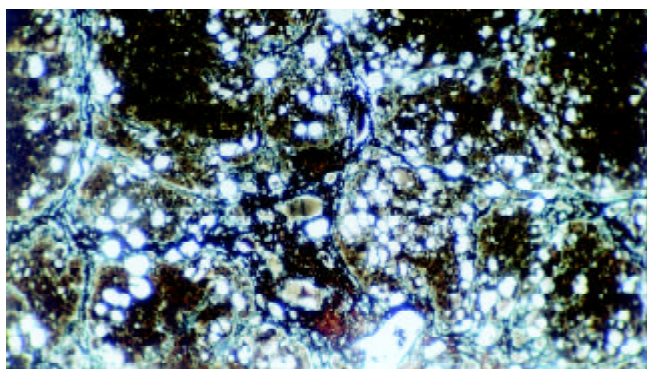


Figure 6 The liver of the rat in group C (the ninth week, silver staining, $\times 100$).

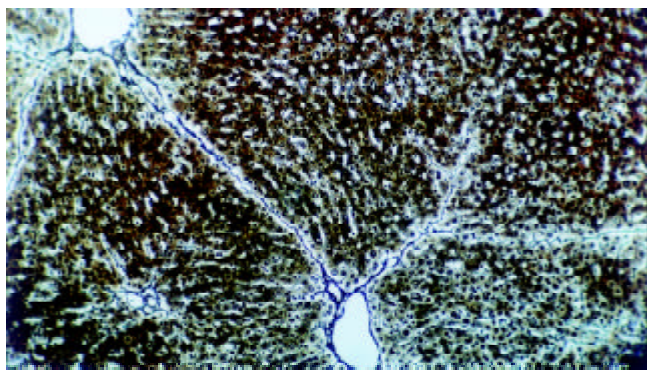


Figure 7 The liver of the rat in group E (the ninth week, silver staining, $\times 100$).

DISCUSSION

Endothelins are a family of polypeptides consisting of 21-amino acids^[17-19]. ET-1 is initially noted for its powerful vasoconstrictor properties^[20-24]. It is markedly overexpressed in different cellular elements in cirrhotic liver tissue, and particularly in sinusoidal endothelial cells and hepatic stellate cells (HSCs) in their activated phenotype located in the sinusoids of the regenerating nodules and at the edges of fibrous septa^[25]. It plays an important role in the regulation of hepatic vascular tone. They elicit biological responses via the ET_A and ET_B receptors. ET-1 induces contraction, proliferation, and collagen synthesis of HSCs *in vitro*, which may be mediated *via* the ET_A receptors^[26]. ET-1 is able to increase $[Ca^{2+}]_i$ in a dose-dependent fashion in HSCs, which results from both intracellular release of Ca^{2+} and extracellular Ca^{2+} influx via a dihydropyridine-insensitive pathway. ET-1-induced contractility of HSCs is maintained through all stages of

activation and is independent of the absolute number of ET_A-binding sites if a threshold level of expression is maintained. It has been shown that ET-1 could act as a cell growth promoter *via* the ET_A receptor to promote the proliferation of smooth muscle cell. Also, ET-1 is able to elicit MAPK (mitogen-activated protein kinase) activity in human HSCs with time-course and dose-response kinetics similar to those reported in mesangial cells through the ET_A receptor. Recent studies have shown that the ETR antagonist modifies the development of portal hypertension in carbon tetrachloride treated rats^[27,28]. Some studies suggest that ET has two effects on HSC^[29]. ET can inhibit the contraction and collagen synthesis in cells that have more ET_B receptors than ET_A receptors; it indicates that ET could restrict the development of liver fibrosis. The difference is linked to the active, contractile HSC phenotype. The cellular sites of action of AgII within the hepatic vasculature are incompletely defined; recent studies have shown that HSCs may be a potential cell target for the AgII actions in the hepatic vasculature^[30]. Two different types of AgII receptors have been described. The AT1 receptors are present in most mesenchymal cells and mediate most of the biological effects of AgII. The AT2 receptors are mainly found in fetal cells, but their physiological role is not completely understood. AgII receptors (AT1 subtype) exist in many cells, including the human HSC^[31], the activated HSCs may be an important target of the AgII in the hepatic vasculature^[32]. The binding of AgII to AT1 receptor induces contraction and proliferation^[33,34]. AgII causes a marked increase in $[Ca^{2+}]_i$ and cell contraction, which largely depends on the entrance of Ca^{2+} through L-type Ca^{2+} channels. In recent years, much attention has been focused on the growth-promoting effects of AgII and it has been found that AgII is also a mitogenic factor for activated HSCs through an MAPK- dependent pathway. So we could hypothesis that AgII plays a role in the proliferation of HSCs and in the progression of liver fibrosis. The inflammation may be the initial fibrogenic event. PGI₂, a potent vasodilator produced by the splanchnic endothelium, would account for much of the observed hyperemia^[35]. Cyclooxygenase blockade reverses the splanchnic hyperemia^[36]. The mechanism for the increase of portal PGI₂ remains unknown. Some have suggested of increase that blood pressure alone will increase the production of PGI₂. Theoretically, damage to any type of liver cell membrane can serve as a source of AA metabolites that initiate fibrosis. In the intact liver, the most probable target cells are the nonparenchymal cells such as endothelial cells. The inflammation may be the initial fibrogenic event. The inflammation involving the release of arachidonic acid (AA) from phospholipids by activation of phospholipase A₂ in damaged cell membranes and formation of bioactive AA metabolites (prostaglandins, thromboxane A₂ and leukotrienes) by way of 5' lipoxygenase pathway is one of the earliest biochemical events in hepatic fibrosis. The concentration of 6-keto-PGF₁ α , the stable metabolite of PGI₂, represents the plasma level of PGI₂. The enhanced production of 6-keto-PGF₁ α increases the TGF- β ₁ gene expression by way of enhancing degranulation of platelets and inflammatory cells which are rich source of the fibrotic cytokine TGF- β ₁^[37]. As we all know, TGF- β ₁ can promote the synthesis and deposition of ECM and inhibit the degradation of ECM^[38,39]. CGRP is a highly potent vasodilator and is widely distributed in nerve fibers with relation to vascular structures^[40]. The circulating CGRP is elevated in liver cirrhosis^[41,42], but little information is known about CGRP in these patients^[43]. Some authors have reported that CGRP could inhibit the lipid peroxidation on the liver, which antagonists the effects of ET^[44]. So it is a protector in the liver fibrosis. Whether the CGRP has effects on the activation of HSC and the synthesis of collagen is not clarified. GG is a stress hormone whose release is stimulated by

catecholamines, cortisol, and growth hormone^[45]. GG plays an important role in the formation of portal hypertension^[46]. The present studies show that plasma GG levels are elevated in cirrhotic patients with portal hypertension. It is also clearly demonstrated that plasma GG levels is increased with the progression of cirrhosis. In addition, positive correlations has been found between plasma GG levels and Pugh's score or liver functions. In our study the increase of GG was associated with the failure of GG's degradation in liver and the hyperexcretion of pancreas. IL-10 is a potent anti-inflammatory cytokine that inhibits the synthesis of pro-inflammatory cytokines by T helper type 1 cells. It is produced locally in the liver and acts in an autocrine or paracrine way. IL-10 can inhibit a range of macrophage effector functions, including nitric oxide and reactive oxygen intermediate production, MHC class II antigen expression, and eicosanoid synthesis. IL-10 can down-regulate expression of adhesion molecules, ICAM-1 and B7, on human monocytes, and also the nuclear transcription factor, nuclear factor κ B. It is able to inhibit chemokine synthesis in T cells, neutrophils, and fibroblasts. Moreover, proinflammatory cytokines synthesis by a wide range of cells, particularly monocytes and macrophages, is profoundly inhibited by IL-10^[47]. Previous reports indicated that IL-10 had a role in the remodeling of the extracellular matrix^[48]. *In vitro*, IL-10 down regulates collagen type I while up regulates metalloproteinase gene expression. It also has antifibrogenic properties by down regulating profibrogenic cytokines, like TGF- β_1 and TNF- α ^[47,49]. Nelson *et al* had treated 24 patients with chronic hepatitis C with IL-10, they found that IL-10 normalized serum ALT levels, decreased hepatic inflammation, reduced liver fibrosis and was well tolerated in patients^[16].

After that treatment of IL-10, all of the transmitters decreased. Therefore, transmitters play important roles in rat hepatic fibrosis induced by CCl₄. IL-10 decreases the levels of these transmitters so it has antifibrogenesis effect.

REFERENCES

- Nie QH, Cheng YQ, Xie YM, Zhou YX, Bai XG, Cao YZ. Methodologic research on TIMP-1, TIMP-2 detection as a new diagnostic index for hepatic fibrosis and its significance. *World J Gastroenterol* 2002; **8**: 282-287
- Nie QH, Cheng YQ, Xie YM, Zhou YX, Cao YZ. Inhibiting effect of antisense oligonucleotides phosphorothioate on gene expression of TIMP-1 in rat liver fibrosis. *World J Gastroenterol* 2001; **7**: 363-369
- Weng HL, Cai WM, Liu RH. Animal experiment and clinical study of effect of gamma-interferon on hepatic fibrosis. *World J Gastroenterol* 2001; **7**: 42-48
- Sun DL, Sun SQ, Li TZ, Lu XL. Serologic study on extracellular matrix metabolism in patients with viral liver cirrhosis. *Shijie Huaren Xiaohua Zazhi* 1999; **7**: 55-56
- Chen PS, Zhai WR, Zhang YE, Zhang JS. The effects of hypoxia on hepatic stellate cell generate collagen and matrix metalloproteinase. *Shijie Huaren Xiaohua Zazhi* 2000; **8**: 586-587
- Liu SR, Gu HD, Li DG, Lu HM. A comparative study of fat storing cells and hepatocytes in collagen synthesis and collagen gene expression. *Xin Xiaohua Bingxue Zazhi* 1997; **15**: 761-762
- Wu J, Zern MA. Hepatic stellate cells: a target for the treatment of liver fibrosis. *J Gastroenterol* 2000; 665-672
- Jiang HQ, Zhang XL. Mechanism of liver fibrosis. *Shijie Huaren Xiaohua Zazhi* 2000; **8**: 687-689
- Wang YJ, Sun ZQ, Quan QZ, Yu JJ. Fat-storing cells and liver fibrosis. *Chin J New Gastroenterol* 1996; **2**: 58-60
- Missale G, Ferrari C, Fiaccadori F. Cytokine mediators in acute inflammation and chronic course of viral hepatitis. *Ann Ital Med Int* 1995; **10**: 14-18
- Wang YJ, Sun ZQ. The cytology and molecular biology investigate advance in liver fibrosis. *Xin Xiaohua Bingxue Zazhi* 1994; **2**: 244-246
- Wang FS, Wu ZZ. Current situation in studies of gene therapy for liver cirrhosis and liver fibrosis. *Shijie Huaren Xiaohua Zazhi* 2000; **8**: 371-373
- Zhang LJ, Wang XZ. Liquid substance and portal hypertension. *Shijie Huaren Xiaohua Zazhi* 2000; **8**: 1280-1281
- Zhang LJ, Wang XZ, Huang YH, Chen ZX. The effects of CGRP, AgII and ET on the liver fibrosis rats. *Shijie Huaren Xiaohua Zazhi* 2001; **9**: 457-459
- Takahara T, Kojima T, Miyabayashi C, Inoue K, Sasaki H, Muragaki Y, Ooshima A. Collagen production in fat-storing cells after carbon tetrachloride intoxication in the rat. Immunoelectron microscopic observation of type I, type III collagens and prolyl hydroxylase. *Lab Invest* 1988; **59**: 509-521
- Nelson DR, Lauwers GY, Lau JY, Davis GL. Interleukin 10 treatment reduces fibrosis in patients with chronic hepatitis C: a pilot trial of interferon nonresponders. *Gastroenterology* 2000; **118**: 655-660
- Zhang Y, Ren XL. Endothelin, nitric oxide and liver cirrhosis. *Chin J New Gastroenterol* 1996; **4**: 40-41
- Cheng RC, Jin XL. The changes of plasma endothelin level in the patient with discompensation liver cirrhosis. *Xin Xiaohua Bingxue Zazhi* 1995; **3**: 110-111
- Li XR, Wu JS, He ZS, Ma QJ. The contents of endothelin in portal vein and peripheral blood of patients with portal hypertension of liver cirrhosis. *Shijie Huaren Xiaohua Zazhi* 1998; **6**: 827
- Liu F, Li JX, Li CM, Leng XS. Plasma endothelin in patients with endotoxemia and dynamic comparison between vasoconstrictor and vasodilator in cirrhotic patients. *World J Gastroenterol* 2001; **7**: 126-127
- Liu BH, Chen HS, Zhou JH, Xiao N. Effects of endotoxin on endothelin receptor in hepatic and intestinal tissues after endotoxemia in rats. *World J Gastroenterol* 2000; **6**: 298-300
- Zhang ZY, Ren XL, Yao XX. Effects of endothelin and nitric oxide in hemodynamics disturbance of cirrhosis. *Shijie Huaren Xiaohua Zazhi* 1998; **6**: 588-590
- Chen S, Liu B, Cai XM, Gu CH. Clinical significance of changes of endothelin and nitric oxide levels in peripheral blood of patients with severe hepatitis. *Shijie Huaren Xiaohua Zazhi* 1999; **7**: 122-124
- Chen YK. The significance of changes of endothelin in patients with severe hepatitis. *Shijie Huaren Xiaohua Zazhi* 1998; **6**: 157
- Pinzani M, Milani S, De Franco R, Grappone C, Caligiuri A, Gentilini A, Tosti-Guerra C, Maggi M, Failli P, Ruocco C, Gentilini P. Endothelin-1 is overexpressed in human cirrhotic liver and exerts multiple effects on activated hepatic stellate cells. *Gastroenterology* 1996; **110**: 534-548
- Reinehr RM, Kubitz R, Peters-Regehr T, Bode JG, Haussinger D. Activation of rat hepatic stellate cells in culture is associated with increased sensitivity to endothelin-1. *Hepatology* 1998; **28**: 1566-1577
- Sogni P, Moreau R, Gomola A, Gadano A, Cailmail S, Calmus Y, Clozel M, Lebrec D. Beneficial hemodynamic effects of bosentan, a mixed ET_A and ET_B receptor antagonist, in portal hypertensive rats. *Hepatology* 1998; **28**: 655-659
- Cho JJ, Hoher B, Herbst H, Jia JD, Ruehl M, Hahn EG, Riecken EO, Schuppan D. An oral endothelin-A receptor antagonist blocks collagen synthesis and deposition in advanced rat liver fibrosis. *Gastroenterology* 2000; **118**: 1169-1176
- Rockey D. Endothelin in hepatic fibrosis-friend or foe? *Hepatology* 1996; **23**: 1698-1700
- Schneider AW, Kald F, Klein CP. Effect of Losartan, an Angiotensin II receptor antagonist, on portal pressure in cirrhosis. *Hepatology* 1999; **29**: 334-339
- Wei HS, Lu HM, Li DG, Zhan YT, Wang ZR, Huang X, Cheng JL, Xu QF. The regulatory role of AT₁ receptor on activated HSCs in hepatic fibrogenesis: effects of RAS inhibitors on hepatic fibrosis induced by CCl₄. *World J Gastroenterol* 2000; **6**: 824-828
- Wei HS, Li DG, Lu HM, Zhan YT, Wang ZR, Huang X, Zhang J, Cheng JL, Xu QF. Effects of AT₁ receptor antagonist, losartan, on rat hepatic fibrosis induced by CCl₄. *World J Gastroenterol* 2000; **6**: 540-545
- Bataller R, Gines P, Nicolas JM, Gorbis MN, Garcia-Ramallo E, Gasull X, Bosch J, Arroyo V, Rodes J. Angiotensin II induces contraction and proliferation of human hepatic stellate cells. *Gastro-*

- enterology* 2000; **118**: 1149-1156
- 34 **Gorbig MN**, Gines P, Bataller R, Nicolas JM, Garcia-Ramalli E, Tobias E, Titos E, Rey MJ, Claria J, Arroyo V, Rodes J. Artial nareuretic peptides angagonizes endothelin-induced calcium increased and cell contraction in culture human hepatic stellate cells. *Heaptology* 1999; **30**: 501-509
 - 35 **Garcia-Pagan JC**, Bosch J, Rodes J. The role of vasoactive mediators in portal hypertension. *Semin Gastrointest Dis* 1995; **6**: 140-147
 - 36 **Yue QL**, Zhang XK, Zhang XR. The changes of contents of nitrix oxide and prostaglandine in gastric mucosa and plasma of rats with portal hypertensive gastropathy. *Shijie Huaren Xiaohua Zazhi* 1999; **7**: 547
 - 37 **Geraci JP**, Mariano MS. Radiation hepatology of the rat: association of the production of prostacyclin with radiation-induced hepatic fibrosis. *Radiat Res* 1996; **145**: 93-97
 - 38 **de Bleser PJ**, Niki T, Rogiers V, Geerts A. Transforming growth factor-beta gene expression in normal and fibrotic rat liver. *J Hepatol* 1997; **26**: 886-893
 - 39 **Sun ZQ**, Wang YJ. The regulate effect of soluble cytokines on liver fibrosis. *Xin Xiaohua Bingxue Zazhi* 1994; **2**: 163-164
 - 40 **Schifter S**. Expression of the calcitonin gene family in medullary thyroid carcinoma. *Peptides* 1997; **18**: 307-317
 - 41 **Wang X**, Wen QS, Huang YX, Zhong YX, Chu YQ, Wang QL. The effects of calcitonin gene-related peptide on portal vein pressure of rats with liver cirrhosis. *Shijie Huaren Xiaohua Zazhi* 1998; **6**: 933
 - 42 **Liu CQ**, Pu J, Li ZX, Liu XF, Zhao YT. The changes of plasma peptides in the patients with liver cirrhosis. *Shijie Huaren Xiaohua Zazhi* 1999; **7**: 1089
 - 43 **Henriksen JH**, Schifter S, Moller S, Bendrsen F. Increased circulating calcitonin in cirrhosis. Relation to severity of disease and calcitonin gene-related peptide. *Metabolism* 2000; **49**: 47-52
 - 44 **Moller S**, Bendtsen F, Schifter S, Henriksen JH. Relation of calcitonin gene-related peptide to systemic vasodilatation and central hypovolemia in cirrhosis. *Scand J Gastroenterol* 1996; **31**: 928-933
 - 45 **Johnson TJ**, Quigley EM, Adrian TE, Jin G, Rikkers L. Glucagon, stress, and portal hypertension Plasma glucagon levels and portal hypertension in relation to anesthesia and surgical stress. *Dig Dis Sci* 1995; **40**: 1816-1823
 - 46 **Greco AV**, Crucitti F, Ghirlanda G, Manna R, Altomonte L, Rebuzzi AG, Bertoli A. Insulin and glucagon concentrations in portal and peripheral veins in patients with hepatic cirrhosis. *Diabetologia* 1979; **17**: 23-28
 - 47 **Kovalovich K**, DeAngelis RA, Li W, Furth EE, Ciliberto G, Taub R. Increased toxin-induced liver injury and fibrosis in interleukin-6-deficient mice. *Hepatology* 2000; **31**: 149-159
 - 48 **Thompson K**, Maltby J, Fallowfield J, McAulay M, Millward-Sadler H, Sheron N. Interleukin-10 expression and function in experimental murine liver inflammation and fibrosis. *Hepatology* 1998; **28**: 1597-1606
 - 49 **Louis H**, Laethem JL, Wu W, Quertinmont E, Degraef C, Van Den Berg K, Demols A, Goldman M, Moine OL, Geerts A, Deviere J. Interleukin-10 controls neutrophilic infiltration, hepatocyte proliferation, and liver fibrosis induced by carbon tetrachloride in mice. *Hepatology* 1998; **28**: 1607-1615

Edited by Xu XQ

A selective tropism of transfused oval cells for liver

Jian-Zhi Chen, Hai Hong, Jin Xiang, Ling Xue, Guo-Qiang Zhao

Jian-Zhi Chen, Hai Hong, Jin Xiang, Ling Xue, Guo-Qiang Zhao,
Department of Pathology, Medical School of Sun Yat-Sen University,
Guangzhou 510080, Guangdong Province, China

Supported by the National Natural Science Foundation of China,
No. 39570348 and 30170473

Correspondence to: Prof. Dr. Guo-Qiang Zhao, Department of
Pathology, Medical School of Sun Yat-Sen University, 74
Zhongshan 2nd Rd., Guangzhou 510080, Guangdong Province,
China. gqzhao@gzsums.edu.cn

Telephone: +86-20-87330743 **Fax:** +86-20-87331679

Received: 2002-06-22 **Accepted:** 2002-07-12

Abstract

AIM: To explore the biological behaviors of hepatic oval cells after transfused into the circulation of experimental animals.

METHODS: Oval cells from male SD rat were transfused into the circulation of a female rat which were treated by a 2-AAF/CCl₄ program, through caudal vein. Sex-determining gene *sry* which located on Y chromosome was examined by PCR and in situ hybridization technique in liver, kidney and spleen of the experimental animals, respectively.

RESULTS: The results of the cell-transplant experiment showed that the *sry* gene was detectable only in the liver but not in spleen and kidney of the experimental rats, and no signals could be detected in the control animals. It can be also morphologically proved that some exogenous cells had migrated into the parenchyma of the liver and settled there.

CONCLUSION: The result means that there are exogenous cells located in the liver of the experimental animal and the localization is specific to the liver. This indicates that some "signal molecules" must exist in the circulation of the rats treated by 2-AAF/CCl₄. These "signal molecules" might play an important role in specific localization and differentiation of transfused oval cells.

Chen JZ, Hong H, Xiang J, Xue L, Zhao GQ. A selective tropism of transfused oval cells for liver. *World J Gastroenterol* 2003; 9 (3): 544-546

http://www.wjgnet.com/1007-9327/9/544.htm

INTRODUCTION

Hepatic oval cells were first described by Opie in 1944 and named as oval cells first by Farber in 1956^[1,2]. Oval cells could be seen at the early stage of hepatocarcinogenesis induced by chemicals in animal and in the liver of human suffering from chronic hepatitis, cirrhosis and other chronic liver diseases^[3-8]. The emergence of oval cells was considered initially to be related to hepatocarcinogenesis. Oval cell was once believed to be a progenitor cell of carcinoma in liver^[9-11]. Recently, more and more evidences showed that oval cell may be a potential stem cell in liver and it could differentiate into hepatocyte and epithelial cell of bile duct in certain conditions^[12,13]. It is believed now that the potential stem cells existing in liver might

play a role in the repair of damaged liver. However, when and how oval cells could be activated still remains unclear. Our aim in this study is to explore the biological behavior of hepatic oval cells after transfused into the circulation of rat for interpreting possible activating mechanisms of hepatic stem cells.

MATERIALS AND METHODS

Culture of oval cells

Hepatic oval cells were isolated from SD male rats and a cell line of OC3 was established by Dr. Xue in our group^[14]. Oval cells were cultivated under a routine condition (37 °C, 5 % CO₂). The cells were collected and suspended in a solution of RPMI-1640 (Gibco BRL) without serum on the day of transfusion experiment, on standby.

Establishment of animal model and transfusion of oval cells

SD female rats, weighing 100-150 g, were used for the establishment of an animal model of liver-damaging. The model was made by means of a 2-AAF/CCl₄ program according to Petersen^[31]. In the experimental group, 2-acetylaminofluorene (2-AAF, Sigma), 2.5 g·L⁻¹ in earthnut oil, was administered to stomach of rats everyday for 14 days. On the 7th day of 2-AAF administering, a Ld50 dose of CCl₄ was given by intraperitoneal injection. Then, the suspended oval cells (5×10⁶ cells per rat) were transfused into the circulation of the rats through caudal vein in 24 hours after CCl₄ injection. In the control group, 1 ml earthnut oil per day was administered to stomach of rats instead of 2-AAF, and without CCl₄ injection, the other treatments was the same as in the experimental group. The animals were sacrificed on the 7th day after transfusion of oval cells. The liver, kidney and spleen of the rats were picked out, respectively and frozen rapidly in liquid nitrogen. The frozen tissues were kept in -80 °C refrigerator.

Isolation of DNA

DNA was extracted from the frozen tissues of liver, kidney and spleen respectively according to the protocol of our laboratory. DNA samples were kept in -80 °C refrigerator.

Primers selection of *sry* gene

The primers selection was according to the DNA sequence of rat *sry* gene from GenBank Database (Accession No.: AJ222688): *Sry*F17: 5' -catctctgacttctctgttgcaa-3', *Sry*R16: 5' -atgctgggattctgttgagcc-3'. The PCR product was 241 bp in length, corresponding to the sequence between 273-514 of rat *sry* gene.

PCR reactions

The DNA samples from liver, kidney and spleen in each experimental group were used as a template in PCR reactions. The reaction cocktails (containing 1 µg Template DNA, 0.125 m mol·L⁻¹ dNTPs, 0.4 µmol·L⁻¹ *sry* F17 primer, 0.4 µmol·L⁻¹ *sry* R16 primer, 1×PCR buffer, 2.5 m mol·L⁻¹ MgCl₂, 1 U Taq-polymerase, add H₂O to 50 µL of total volume) were run on GeneAmp® PCR System 9 600 (AB) with a program combination of Prog. 1 (95 °C, 5 min), Prog. 2 (95 °C, 50 sec; 56 °C, 50 sec; 72 °C, 60 sec; 30 cycles) and Prog. 3 (95 °C, 50 sec; 56 °C, 50 sec; 72 °C, 60 sec). The PCR products were

electrophoresed in 1.2 % agarose, stained with ethidium bromide and photographed.

In situ hybridization

In situ hybridization was carried out according to the protocol described by Zhao^[15]. A DNA probe complementary to rat *sry* gene was labeled with digoxigenin by means of PCR reactions. The sections of liver from rats transfused with oval cells were selected for *in situ* hybridization assay. After deparaffin and rehydrate, the sections were fixed in 4 % paraformaldehyde again. The hybridization (2×SSC, 500 mL·L⁻¹ formamide, 1×Denhardt's solution, 0.5 g·L⁻¹ dextran sulfate, 60 µg·L⁻¹ DIG-Probe) was carried out at 37 °C over night. The hybrids were then revealed by an alkaline phosphatase-conjugated anti-digoxigenin antibody and detected with the detection system of Boehringer Mannheim.

RESULTS

Sry gene was located in Y chromosome and used as a marker of transfused oval cells in female animal. The results of the cell-transplant experiment showed that the *sry* gene was detectable only in the liver but not in the spleen and the kidney of the rats treated by 2-AAF/CCl₄ program, and no signals could be detected in the control animals, neither liver nor spleen and kidney. The distribution of PCR signals of *sry* gene in experimental groups can be seen in Figure 1 and Table 1. On the section of *in situ* hybridization, a cluster of cells with *sry* gene marker could be seen in the parenchyma of the liver of a female rat undergoing oval cell-transplantation (Figure 2A). It was distinguished between sections in the negative and positive controls (Figure 2B and Figure 2C). This result meant that some exogenous cells had migrated into the parenchyma of the liver and settled there.

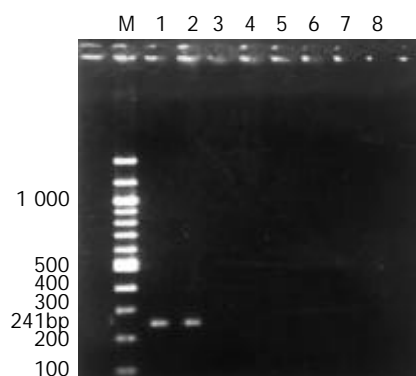


Figure 1 PCR signals of *sry* gene in experimental groups. (M. 100 bp DNA marker; 1. Liver(M): liver of male rat as a positive control; 2. Liver(E): liver of female rat in experimental group; 3. Spleen(E): spleen of female rat in experimental group; 4. Kidney(E): kidney of female rat in experimental group; 5. Liver(C): liver of female rat in control group; 6. Spleen(C): spleen of female rat in control group; 7. Kidney(C): kidney of female rat in control group; 8. Liver(F): liver of female rat negative control).

Table 1 Distribution of PCR signals of *sry* gene in experimental groups

	Liver (M)	Liver (E)	Spleen (E)	Kidney (E)	Liver (C)	Spleen (C)	Kidney (C)	Liver (F)
<i>Sry</i>	+	+	-	-	-	-	-	-

Note: Liver(M): liver of male rat as a positive control; Liver(E): liver of female rat in experimental group; Spleen(E): spleen of female rat in experimental group; Kidney(E): kidney of female

rat in experimental group; Liver(C): liver of female rat in control group; Spleen(C): spleen of female rat in control group; Kidney(C): kidney of female rat in control group; Liver(F): liver of female rat negative control.

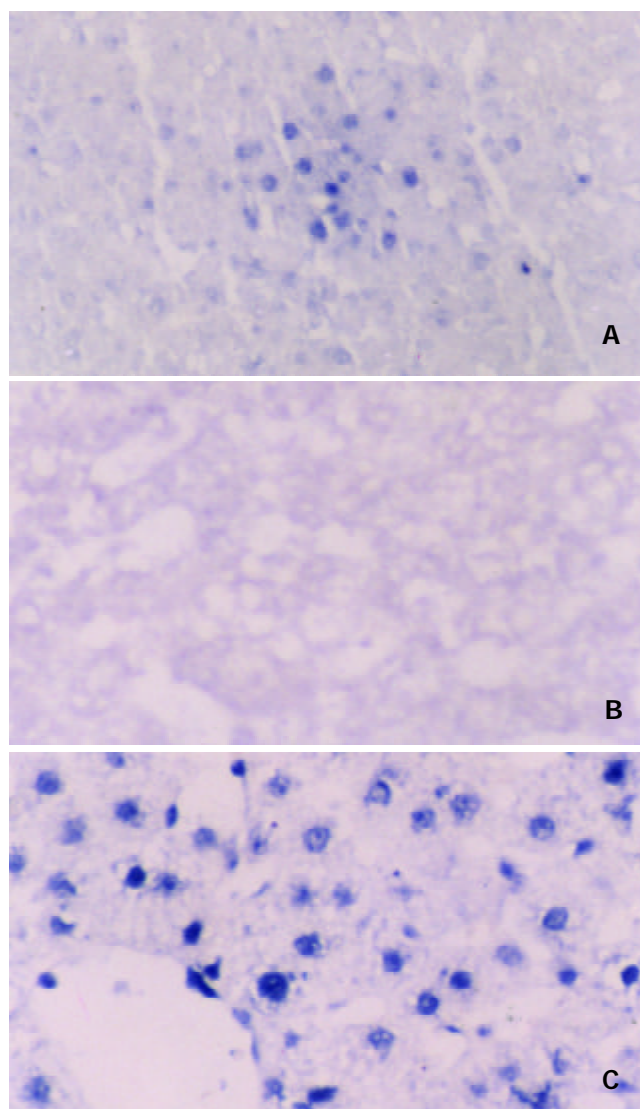


Figure 2 *In situ* hybridization assay of *sry* gene in liver. A. Experimental group, Liver of female rat undergoing oval cell-transplanting. A cluster of cells with *sry* gene marker could be seen in the parenchyma of liver. B. Negative control group, liver of normal female rat. No hybridization signals could be seen. C. Positive control group, liver of normal male rat. Each cell with distinct hybridization signals.

DISCUSSION

As we know, liver has a powerful capacity of regeneration. In general, the injured liver can regenerate itself by self-replication of hepatocyte. So, it is believed that hepatocytes themselves are the functional stem cells of the liver^[16]. Oval cell is now recognized as a potential stem cell existing in liver. But they cannot be seen in normal status. The emergence of oval cells occurs only in a special status in which the liver is damaged severely and the capacity of regeneration of hepatocyte is restrained^[17-20]. At the past, oval cell was believed as a progenitor cell of carcinoma in liver^[9-11,21], because it was often seen at the early stage of hepatocarcinogenesis induced by chemicals^[22-26]. Recently, more and more evidences showed that oval cell could differentiate toward hepatocyte and epithelial cell of bile duct^[12,13,27-30]. So it was guessed that the emergence of oval cells might be relevant to the repair of

damaged liver, and under special conditions the injured liver might produce and release some “signal molecules” which might play an important role in the activation of stem cell. In this study, an animal model of liver-damaging was established by a 2-AAF/CCl₄ program according to Petersen^[31], the capacity of regeneration of hepatocyte was first impaired by 2-AAF and then the liver was damaged severely by CCl₄. In this status the damaged liver might produce a signal of “distress call” to initiate the activation of stem cell. Our results of cell transplantation showed that the *sry* gene was detectable only in the liver but not in the spleen and the kidney of the rats treated by 2-AAF/CCl₄ program, and no signals could be detected in the control animals, neither liver nor spleen and kidney. The results of in situ hybridization also showed that some exogenous cells had migrated into the parenchyma of the liver and settled there. It means that the transfused oval cells have a selective tropism for liver and the driver force might come from the injured liver. All evidences revealed that some “signal molecules” might exist in the circulation of the rats treated by 2-AAF/CCl₄ and the “signal molecules” might be produced and released from the damaged liver. The “signal molecules” might play an important role in the initiation of the activation of stem cell. Further identifying and isolation of these “signal molecules” would be significative for achieving activation and directional inducement of hepatic stem cells.

REFERENCES

- 1 **Opie EL.** The pathogenesis of tumors of the liver produced by butter yellow. *J Exp Med* 1944; **80**: 231-246
- 2 **Farber E.** Similarities in the sequence of early histologic changes induced in the livers of rats by ethionine, 2-acetylaminofluorene and 3'-methyl-4-dimethylaminoazobenzene. *Cancer Res* 1956; **16**: 142-148
- 3 **De Vos R, Desmet V.** Ultrastructural characteristics of novel epithelial cell types identified in human pathologic liver specimens with chronic ductular reaction. *Am J Pathol* 1992; **140**: 1441-1450
- 4 **Crosby HA, Hubscher S, Fabris L, Joplin R, Sell S, Kelly D, Strain AJ.** Immunolocalization of putative human liver progenitor cells in livers from patients with end-stage primary biliary cirrhosis and sclerosing cholangitis using the monoclonal antibody OV-6. *Am J Pathol* 1998; **152**: 771-779
- 5 **Theise ND, Saxena R, Portmann BC, Thung SN, Yee H, Chiriboga L, Kumar A, Crawford JM.** The canals of Hering and hepatic stem cells in humans. *Hepatology* 1999; **30**: 1425-1433
- 6 **Lowes KN, Brennan BA, Yeoh GC, Olynyk JK.** Oval cell numbers in human chronic liver diseases are directly related to disease severity. *Am J Pathol* 1999; **154**: 537-541
- 7 **Malhi H, Irani AN, Gagandeep S, Gupta S.** Isolation of human progenitor liver epithelial cells with extensive replication capacity and differentiation into mature hepatocytes. *J Cell Sci* 2002; **115**: 2679-2688
- 8 **Ma X, Qiu DK, Peng YS.** Immunohistochemical study of hepatic oval cells in human chronic viral hepatitis. *World J Gastroenterol* 2001; **7**: 238-242
- 9 **Goyette M, Faris R, Braun L, Hixson D, Fausto N.** Expression of hepatocyte and oval cell antigens in hepatocellular carcinomas produced by oncogene-transfected liver epithelial cells. *Cancer Res* 1990; **50**: 4809-4817
- 10 **Faris RA, Monfils BA, Dunsford HA, Hixson DC.** Antigenic relationship between oval cells and a subpopulation of hepatic foci, nodules and carcinomas induced by the “resistant hepatocyte” model system. *Cancer Res* 1991; **51**: 1308-1317
- 11 **Sirica AE, Mathis GA, Sano N, Elmore LW.** Isolation, culture, and transplantation of intrahepatic biliary epithelial cells and oval cells. *Pathobiology* 1990; **58**: 44-64
- 12 **Golding M, Sarraf CE, Lalani EN, Anilkumar TV, Edwards RJ, Nagy P, Thorgeirsson SS, Alison MR.** Oval cell differentiation into hepatocytes in the acetylaminofluorene-treated regenerating rat liver. *Hepatology* 1995; **22**: 1243-1253
- 13 **Alison M, Golding M, Lalani EN, Nagy P, Thorgeirsson S, Sarraf C.** Wholesale hepatocytic differentiation in the rat from ductular oval cells, the progeny of biliary stem cells. *J Hepatol* 1997; **26**: 343-352
- 14 **Xue L, Wen J, Zhao G.** The characteristics and significance of oncogenes expression in oval cells cultivated *in vitro*. *Zhonghua Binglixue Zazhi* 1998; **27**: 191-193
- 15 **Zhao GQ, Xue L, Xu HY, Tang XM, Hu RD, Dong J.** *In situ* hybridization assay of androgen receptor gene in hepatocarcinogenesis. *World J Gastroenterol* 1998; **4**: 503-505
- 16 **Forbes S, Vig P, Poulsom R, Thomas H, Alison M.** Hepatic stem cells. *J Pathol* 2002; **197**: 510-518
- 17 **Gournay J, Auvigne I, Pichard V, Ligeza C, Bralet MP, Ferry N.** *In vivo* cell lineage analysis during chemical hepatocarcinogenesis in rats using retroviral-mediated gene transfer: evidence for dedifferentiation of mature hepatocytes. *Lab Invest* 2002; **82**: 781-788
- 18 **Yin L, Lynch D, Illic Z, Sell S.** Proliferation and differentiation of ductular progenitor cells and littoral cells during the regeneration of the rat liver to CCl₄/2-AAF injury. *Histol Histopathol* 2002; **17**: 65-81
- 19 **Faris RA, Konkin T, Halpert G.** Liver stem cells: a potential source of hepatocytes for the treatment of human liver disease. *Artif Organs* 2001; **25**: 513-521
- 20 **Petersen BE.** Hepatic “stem” cells: coming full circle. *Blood Cells Mol Dis* 2001; **27**: 590-600
- 21 **Liao G, Chen J, Ding L.** Relationship between oval cells and preneoplastic lesions induced by 2-acetylaminofluorene in rat liver. *Zhonghua Binglixue Zazhi* 1998; **27**: 87-90
- 22 **Shinozuka H, Lombardi B, Sell S, Iammarino RM.** Early histological and functional alterations of ethionine liver carcinogenesis in rats fed a choline-deficient diet. *Cancer Res* 1978; **38**: 1092-1098
- 23 **Sell S, Hunt JM, Knoll BJ, Dunsford HA.** Cellular events during hepatocarcinogenesis in rats and the question of premalignancy. *Adv Cancer Res* 1987; **48**: 37-111
- 24 **Novikoff PM, Ikeda T, Hixson DC, Yam A.** Characterizations of and interactions between bile ductule cells and hepatocytes in early stages of rat hepatocarcinogenesis induced by ethionine. *Am J Pathol* 1991; **139**: 1351-1368
- 25 **Gera N, Bhatia A, Sood SK.** Light & electron microscopy of proliferating oval cells during early chemical hepatocarcinogenesis. *Indian J Med Res* 1991; **94**: 200-205
- 26 **Evarts RP, Nakatsukasa H, Marsden ER, Hsia CC, Dunsford HA, Thorgeirsson SS.** Cellular and molecular changes in the early stages of chemical hepatocarcinogenesis in the rat. *Cancer Res* 1990; **50**: 3439-3444
- 27 **Yoon BI, Jung SY, Hur K, Lee JH, Joo KH, Lee YS, Kim DY.** Differentiation of hamster liver oval cell following Clonorchis sinensis infection. *J Vet Med Sci* 2000; **62**: 1303-1310
- 28 **Factor VM, Radaeva SA, Thorgeirsson SS.** Origin and fate of oval cells in dipin-induced hepatocarcinogenesis in the mouse. *Am J Pathol* 1994; **145**: 409-422
- 29 **Alpini G, Aragona E, Dabeva M, Salvi R, Shafritz DA, Tavoloni N.** Distribution of albumin and alpha-fetoprotein mRNAs in normal, hyperplastic, and preneoplastic rat liver. *Am J Pathol* 1992; **141**: 623-632
- 30 **Nagy P, Bisgaard HC, Thorgeirsson SS.** Expression of hepatic transcription factors during liver development and oval cell differentiation. *J Cell Biol* 1994; **126**: 223-233
- 31 **Petersen BE, Bowen WC, Patrene KD, Mars WM, Sullivan AK, Murase N, Boggs SS, Greenberger JS, Goff JP.** Bone marrow as a potential source of hepatic oval cells. *Science* 1999; **284**: 1168-1170

Comparative study in the effect of C-type natriuretic peptide on gastric motility in various animals

Hui-Shu Guo, Zheng Jin, Zheng-Yuan Jin, Zhe-Hao Li, Yi-Feng Cui, Zuo-Yu Wang, Wen-Xie Xu

Hui-Shu Guo, Zheng Jin, Zheng-Yuan Jin, Yi-Feng Cui, Zuo-Yu Wang, Wen-Xie Xu, Department of Physiology, Yanbian University College of Medicine, Yanji 133000, Jilin Province China
Wen-Xie Xu, Zhe-Hao Li, Center of experiment, Affiliated Hospital of Yanbian University College of Medicine, Yanji 133000, Jilin Province China

Supported by the National Natural Science Foundation of China, No. 30160028

Correspondence to: Dr. Wen-Xie Xu, Department of Physiology, Yanbian University College of Medicine, Juzi 121, Yanji 133000, Jilin Province China. wenxiexu@ybu.edu.cn

Telephone: +86-433-2660586 **Fax:** +86-433-2659795

Received: 2002-10-17 **Accepted:** 2002-11-14

Abstract

AIM: To investigate the effect of natriuretic peptides on gastric motility in various animals, and the effect of C-type natriuretic peptide (CNP) on spontaneous contraction of gastric smooth muscle in rat, guinea-pig and human in vitro was compared.

METHODS: Spontaneous contraction of gastric smooth muscle was recorded by four channel physiograph.

RESULTS: In the guinea-pig and rat gastric antral circular smooth muscle, CNP markedly decreased the amplitude of spontaneous contraction but it didn't affect the frequency, however, the contractile activity was completely inhibited by CNP in gastric antral longitudinal smooth muscle. In the human gastric antral circular and longitudinal smooth muscle, CNP completely inhibited spontaneous contraction. In the circular smooth muscle of guinea-pig and rat gastric fundus, CNP obviously decreased the amplitude of spontaneous contraction but it didn't affect the frequency, however, the contractile activity was completely inhibited by CNP in smooth muscle of fundus longitudinal. In the circular and longitudinal smooth muscle of guinea-pig gastric body, CNP at first induced a relaxation and then an increase in amplitude of spontaneous contraction (rebound contraction), but the frequency was not changed. After the circular smooth muscle of gastric body was pretreated with atropine, an M receptor blocker, the rebound contraction was abolished; In circular and longitudinal smooth muscle of rat gastric body, CNP induced a transient and slight relaxation and successively followed by the recovery in amplitude of spontaneous contraction but it also didn't affect the frequency. After the smooth muscle was pretreated with atropine, the transient and slight relaxation was replaced by long term and complete inhibition; The percentage of CNP-induced inhibition was $76.77 \pm 6.21\%$ (fundus), $67.21 \pm 5.32\%$ (body) and $58.23 \pm 6.21\%$ (antral) in the gastric circular muscle, however, the inhibitory percentage was $100 \pm 0.00\%$ (fundus), $68.66 \pm 3.55\%$ (body) and $100 \pm 0.00\%$ (antrum) in the gastric longitudinal smooth muscle of guinea-pigs; In the rat, the percentage of CNP-induced inhibition was $95.87 \pm 4.12\%$ (fundus), $94.91 \pm 5.08\%$ (body) and $66.32 \pm 7.32\%$ (antrum) in the gastric circular smooth muscle, but in the longitudinal smooth muscle, CNP completely inhibited the spontaneous

contraction. Using LY83583, a guanylate cyclase inhibitor, and zaparinast as a phosphoesterase inhibitor to inhibit the generation of cGMP, the effect of CNP on the spontaneous contraction was markedly weakened by LY83583, however, the inhibitory effect was enhanced by zaparinast.

CONCLUSION: (1) CNP can obviously inhibit the spontaneous contraction of gastric antral circular and longitudinal smooth muscle in the rat, guinea-pig and human. The order of inhibitory potency is human >rat> guinea-pig. (2) In the same animals, the inhibitory effect of CNP on spontaneous contraction is the most powerful in fundus and the weakest in antrum, in the same position, the inhibitory effect on the circular smooth muscle is more powerful than that on longitudinal smooth muscle. (3) The inhibitory effect of CNP on spontaneous contraction in the gastric smooth muscle is mediated by a cGMP dependent pathway.

Guo HS, Jin Z, Jin ZY, Li ZH, Cui YF, Wang ZY, Xu WX. Comparative study in the effect of C-type natriuretic peptide on gastric motility in various animals. *World J Gastroenterol* 2003; 9(3): 547-552
<http://www.wjgnet.com/1007-9327/9/547.htm>

INTRODUCTION

Since atrial natriuretic peptide (ANP) was isolated from atrium by de Bold *et al* in 1981^[1], brain natriuretic peptide (BNP), C-type natriuretic peptide (CNP), dendroaspis (DNP), micrurus natriuretic peptide (MNP) and ventricular natriuretic peptide (VNP) were successively found. They distribute in all over the body not only in the heart. Among the natriuretic peptides (NP) family, the most studies were focused on ANP, BNP and CNP. The NP family has function of natriuresis-diuresis, vasorelaxation and is able to lower blood pressure and to keep electrolyte homeostasis and so on. CNP was originally found in the central nervous system of the porcine, but it has recently been found in many other systems. In adult mice, the highest CNP expression was detected in the uterus and ovaries, which exceeded the CNP concentrations of the forebrain and brainstem. In contrast, neonatal mice showed highest CNP-mRNA levels in forebrain and brainstem but with lower levels in the skin, tongue, heart, lung, thymus, skeletal muscle, liver, kidney, stomach, and skull^[2]. In the rat, generation and secretion of CNP was demonstrated not only in endothelium but also in vascular smooth muscle cells^[3], and natriuretic peptides gene was expressed^[4] in human coronary arteries. CNP exhibits many functions besides natriuresis-diuresis; for instance, CNP inhibits the growth of vascular smooth muscle cells in the rat^[5] and in has many functions including anti-thrombus and anti-proliferation against vascular smooth muscle cells and myofibroblasts in addition to vasodilation in rabbit^[6,7].

The study on the relationship between CNP and gastrointestinal function has recently become the hot spot. In 1991, Komatsu *et al*^[8] demonstrated that CNP also existed in gastrointestinal and three kinds of NPR receptors was found in both mucosa and muscle tissues of the antrum in the rat by Gower *et al*^[9] in 2000. The study on CNP in gastrointestinal

tract was mainly focused on physiological functions of absorption, secretion and intestinal motility^[10-12]. But few studies reported the regulation of natriuretic peptides on gastric smooth muscles motility. Therefore in the present study, the effect of CNP on spontaneous contraction of gastric smooth muscles in different positions of various animals were investigated.

MATERIALS AND METHODS

Sample preparation

Wista rats (provided by Experimental Animal Center of Yanbian University medical college) of either sex weighing 250 ± 50 g and EWG/B guinea-pigs (provided by Experimental Animal Center of Jilin University medical college) of either sex weighing 300 ± 50 g were euthanized by lethal dose of intravenous pentobarbital sodium (50 mg/kg). The abdomen of each rat was opened along the midline and stomach was removed and placed in a pre-oxygenated Tyrode's solution at room temperature. The mucous layer was removed. Strips (about 2.0×15.0 mm) of gastric antral circular smooth muscle were prepared by cutting along the vertical direction of the longer axis of the stomach and strips of gastric antral longitudinal smooth muscle were prepared by cutting along the longer axis of the stomach. Muscle strips were placed in a chamber. One end of the strip was fixed on the lid of the chamber through glass claw, the other end was attached to an isometric force transducer (TD-112S, JAPAN) to record the contraction. The chamber (2 mL volume) was constantly perfused with pre-oxygenated Tyrode's solution at 1 mL/min. Temperature was maintained at 37.0 ± 0.5 °C by a water bath thermostat (WC/09-05, Chongqing, China). The muscle strips were incubated for at least 40 min before experiments were started. The samples of human stomach were offered by Affiliated Hospital of Yanbian University College of Medicine (As the sample of human gastric was limited, only the gastric antral of human was sampled).

Drugs and solution

Tyrode solution containing ($\text{mmol} \cdot \text{L}^{-1}$) 147 NaCl, 4 KCl, 1.05 $\text{MgCl}_2 \cdot 6\text{H}_2\text{O}$, 0.42 $\text{CaCl}_2 \cdot 2\text{H}_2\text{O}$, 1.81 $\text{Na}_2\text{PO}_4 \cdot 2\text{H}_2\text{O}$, and 5.5 mM glucose was used. Its pH was adjusted to 7.35 by NaOH. C-type natriuretic peptide and LY83583 was diluted to 10^{-7} $\text{mol} \cdot \text{L}^{-1}$. And, Zaprinast was diluted to 10^{-6} $\text{mol} \cdot \text{L}^{-1}$. All drugs above were purchased from Sigma (USA).

Data analysis

All data was expressed as means \pm SD. Statistical significance was evaluated by a *t*-test. Differences were considered to be significant when *P* value was less than 0.05.

RESULTS

Effect of CNP on the spontaneous contraction of the gastric antral smooth muscle in various animals

Different concentrations of CNP obviously inhibited spontaneous contraction in a dose-dependent manner and the percentage of inhibition was 22.8 ± 7.2 %, 44.9 ± 7.6 %, 69.1 ± 12.9 % and 98.2 ± 4.7 % at the concentrations of 1×10^{-8} $\text{mol} \cdot \text{L}^{-1}$, 3×10^{-8} $\text{mol} \cdot \text{L}^{-1}$, 1×10^{-7} $\text{mol} \cdot \text{L}^{-1}$ and 1×10^{-6} $\text{mol} \cdot \text{L}^{-1}$ respectively (Figure 1, $n=7$). The middle dose of CNP 10^{-7} $\text{mol} \cdot \text{L}^{-1}$ was used in following all experiments.

The amplitude of spontaneous contraction in gastric antral circular smooth muscles of guinea-pigs and rats was significantly decreased by CNP and the percentage of inhibition was 58.23 ± 6.21 % and 66.32 ± 7.32 % respectively, however, the frequency was not influenced by CNP (Figure 2A and Figure 2C, Table1.). The spontaneous contraction of the longitudinal smooth muscle was entirely inhibited by CNP in guinea-pigs and rats (Figure 2B and Figure 2D, Table1). In the human gastric

antrum both circular and longitudinal smooth muscles, the spontaneous contraction was also completely inhibited by CNP (Figure 2E and Figure 2F, Table1).

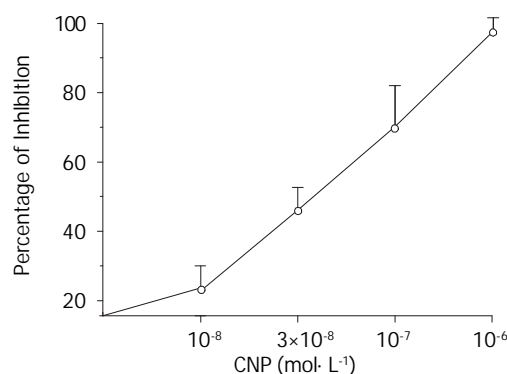


Figure 1 Response of CNP on spontaneous contraction of gastric circular muscle in rats with different concentration.

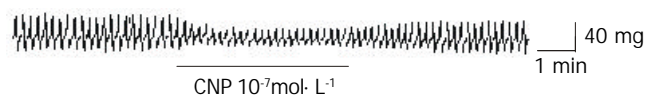


Figure 2A Effect of CNP on spontaneous contraction in gastric antral circular smooth muscle in guinea-pig.

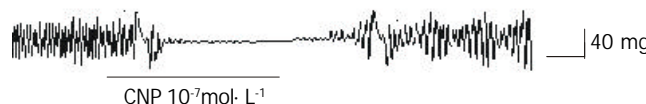


Figure 2B Effect of CNP on spontaneous contraction in gastric antral longitudinal smooth muscle in guinea-pig.

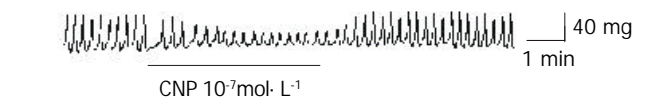


Figure 2C Effect of CNP on spontaneous contraction in gastric antral circular smooth muscle in rat.

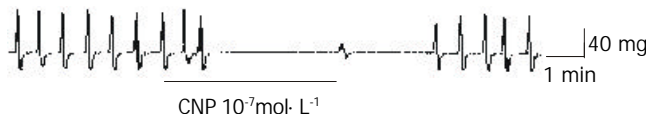


Figure 2D Effect of CNP on spontaneous contraction in gastric antral longitudinal smooth muscle in rat.

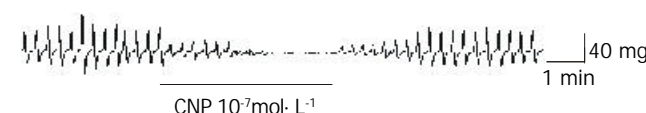


Figure 2E Effect of CNP on spontaneous contraction in gastric antral circular smooth muscle in human.

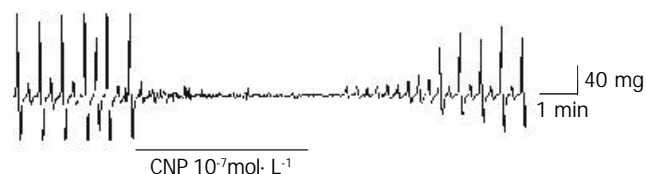


Figure 2F Effect of CNP on spontaneous contraction in gastric antral longitudinal smooth muscle in human.

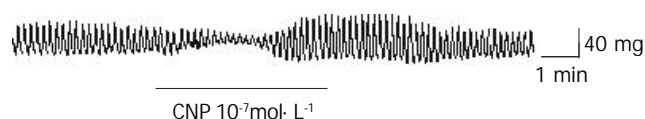
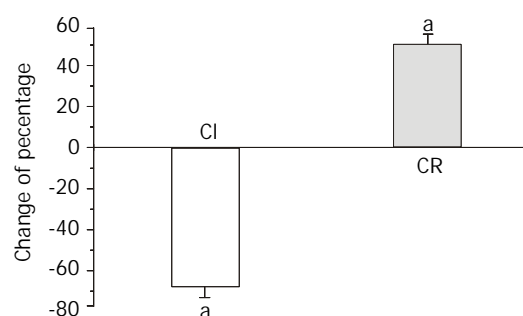
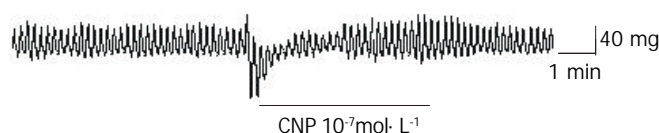
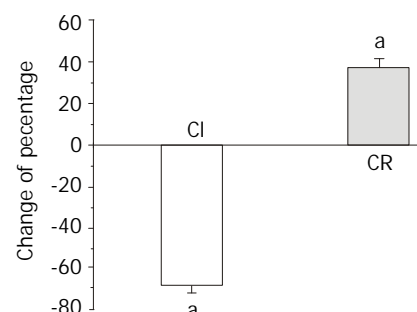
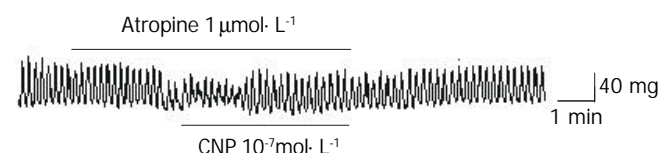
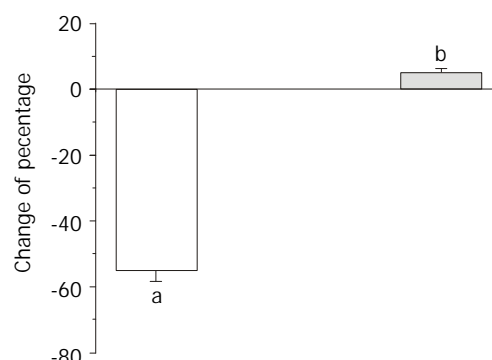
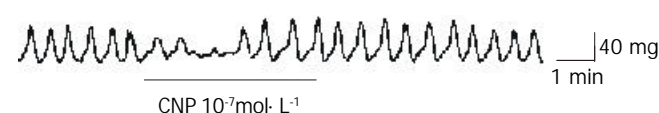
Table 1 Effect of CNP on spontaneous contraction of gastric antral smooth muscle in various animals ($\bar{x} \pm s$)

Species	n	Change of strip motility	
		Amplitude (%)	Frequency (%)
Guinea-pig(C)	6	-58.23 \pm 6.21 ^{a,d}	-10.81 \pm 3.14
Guinea-pig(L)	6	-100.00 \pm 0.00 ^a	-100.00 \pm 0.00 ^a
Rat(C)	8	-66.32 \pm 7.32 ^{a,b,e}	-10.76 \pm 3.21
Rat(L)	8	-100.00 \pm 0.00 ^a	-100.00 \pm 0.00 ^a
Human(C)	4	-100.00 \pm 0.00 ^{a,c}	-100.00 \pm 0.00 ^a
Human(L)	4	-100.00 \pm 0.00 ^a	-100.00 \pm 0.00 ^a

C: circular muscle; L: longitudinal muscle. ^a $P < 0.01$ vs pretreatment; ^b $P < 0.05$ vs Guinea-pig (C) group; ^c $P < 0.01$ vs Guinea-pig (C) group and Rat (C) group; ^d $P < 0.01$ vs Guinea-pig (L) group; ^e $P < 0.01$ vs Rat (L) group.

Effect of CNP on the spontaneous contraction of the gastric body smooth muscle in various animals

CNP-induced response in the gastric body smooth muscle was different from the response in gastric antral smooth muscle in guinea-pigs and rats. In circular and longitudinal smooth muscles of guinea-pig gastric body, CNP first induced a relaxation and successively an increase in the amplitude of spontaneous contraction (rebound contraction), but the frequency was not changed (Figure 3A and C). After the gastric body circular smooth muscle was pretreated with atropine, an M receptor blocker, the rebound contraction was abolished (Figure 3E). In the circular smooth muscle of guinea-pig body, the percentage of inhibition was 67.21 \pm 5.32 % and the percentage of increase was 50.22 \pm 4.67 % (Figure 3B). However, in the longitudinal smooth muscle of guinea-pig body, the percentage of inhibition was 68.66 \pm 3.55 % and the percentage of increase was 38.91 \pm 4.08 % (Figure 3D). The frequency was not affected by CNP in the circular and longitudinal smooth muscles of gastric body of the guinea-pig and the pre-and post treat frequency were 6.44 \pm 0.64, 6.48 \pm 0.67 (circular smooth muscle); 6.53 \pm 0.34, 6.55 \pm 0.29 (longitudinal smooth muscle) respectively. After treated with atropine, the percentages of CNP-induced inhibition and increase were 55.33 \pm 3.23 % and 5.12 \pm 1.19 % respectively in the gastric body circular smooth muscle of the guinea-pig (Figure 3F). In the circular and longitudinal smooth muscles of rat gastric body, CNP induced a transient and a slight relaxation and it was followed by the recovery in an amplitude of spontaneous contraction, but the frequency was not affected by CNP (Figure 4A and C). The percentage of inhibition was 94.91 \pm 5.08 % in the circular smooth muscle of gastric body and 94.34 \pm 5.65 % in the g longitudinal smooth muscle of gastric body (Figure 4B and D) respectively. After the smooth muscle was treated with atropine, the transient and slight relaxation was replaced by long term and complete inhibition. After treated with atropine, the inhibitory duration of contractile activity was lengthened from 1.3 \pm 0.21 min to 4.88 \pm 0.34 min and the rebound contraction disappeared in the gastric body circular smooth muscles of the rat (Figure 4A and E).

**Figure 3A** Effect of CNP on spontaneous contraction in gastric body circular smooth muscle in guinea-pig.**Figure 3B** Effect of CNP on spontaneous contraction in gastric body circular smooth muscle in guinea-pig. ^a $P < 0.01$ vs pretreatment.**Figure 3C** Effect of CNP on spontaneous contraction in gastric body longitudinal smooth muscle in guinea-pig.**Figure 3D** Effect of CNP on spontaneous contraction in gastric body longitudinal smooth muscle in guinea-pig. ^a $P < 0.01$ vs pretreatment.**Figure 3E** Effect of Atropine on CNP-induced spontaneous contraction in gastric body circular smooth muscle in guinea-pig.**Figure 3F** Effect of Atropine on CNP-induced spontaneous contraction in gastric body circular smooth muscle in guinea-pig. ^a $P < 0.01$ vs pretreatment; ^b $P > 0.05$ vs pretreatment.**Figure 4A** Effect of CNP on spontaneous contraction in gastric body circular smooth muscle in rat.

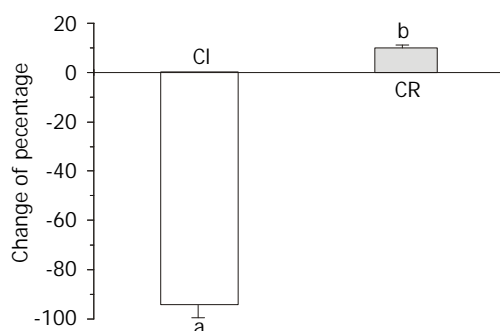


Figure 4B Effect of CNP on spontaneous contraction in gastric body circular smooth muscle in rat. ^a $P < 0.01$ vs pretreatment; ^b $P > 0.05$ vs pretreatment.

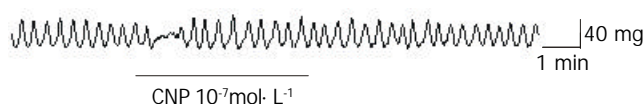


Figure 4C Effect of CNP on spontaneous contraction in gastric body longitudinal smooth muscle in rat.

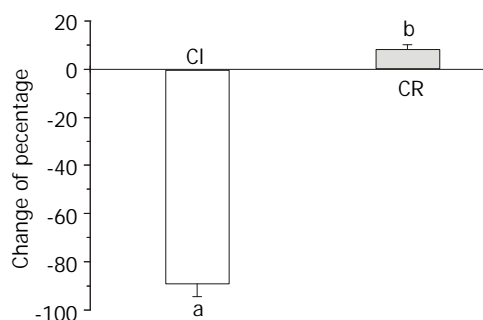


Figure 4D Effect of CNP on spontaneous contraction in gastric body longitudinal smooth muscle in rat. ^a $P < 0.01$ vs pretreatment; ^b $P > 0.05$ vs pretreatment.

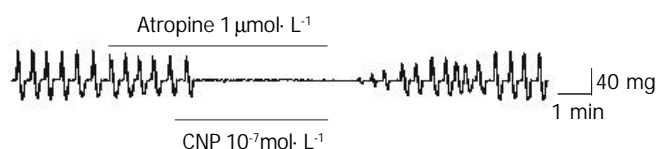


Figure 4E Effect of Atropine on CNP-induced spontaneous contraction in gastric body circular smooth muscle in rat.

Effect of CNP on the spontaneous contraction of the gastric fundus smooth muscle in various animals

CNP diminished the amplitude of the gastric fundus circular smooth muscles of guinea-pigs and rats, and the percentage of inhibition was $76.77 \pm 6.21\%$ and $95.87 \pm 4.12\%$, respectively (Figure 5A and B, Table 2). However, the frequency of spontaneous contraction was not affected by CNP in the g circular smooth muscles of gastric fundus of guinea-pigs and rats (Table 2). The spontaneous contraction of gastric fundus longitudinal smooth muscles of guinea-pigs and rats was completely inhibited (Figure 5C and Figure 5D, Table 2).

Effect of CNP on the spontaneous contraction of gastric smooth muscles in different positions of the same animal

The contractile amplitude was decreased by CNP in the gastric fundus, body and antral circular smooth muscles of the guinea-pig and the percentages of inhibition were $76.77 \pm 6.21\%$, $67.21 \pm 5.32\%$ and $58.23 \pm 6.21\%$ respectively. However, the percentages of inhibition in longitudinal smooth muscle were

$100 \pm 0.00\%$, $68.66 \pm 3.55\%$ and $100 \pm 0.00\%$ respectively (Figure 6A). The contractile amplitude was decreased by CNP in the gastric fundus, body and antral circular smooth muscles of the rat and the percentages of inhibition were $95.87 \pm 4.12\%$, $94.91 \pm 5.08\%$ and $66.32 \pm 7.32\%$, respectively. However, the percentages of inhibition in the longitudinal smooth muscles were $100 \pm 0.00\%$, $94.34 \pm 5.65\%$ and $100 \pm 0.00\%$ (Figure 6B) respectively.

Table 2 Effect of CNP on spontaneous contraction of gastric fundus smooth muscle in various animals ($\bar{x} \pm s$)

Species	n	Change of strip motility	
		Amplitude/%	Frequency/%
Guinea-pig (C)	6	$-76.77 \pm 6.21^{a,b}$	-12.21 ± 3.23
Guinea-pig (L)	6	-100.00 ± 0.00^a	-100.00 ± 0.003^a
Rat (C)	8	$-95.87 \pm 4.12^{a,c,e}$	-94.81 ± 5.19^c
Rat (L)	8	-100.00 ± 0.00^a	-100.00 ± 0.00^a

C: circular muscle; L: longitudinal muscle; ^a $P < 0.01$ vs pretreatment; ^b $P < 0.01$ vs Guinea-pig (L) group; ^c $P < 0.01$ vs Guinea-pig (C) group; ^e $P < 0.01$ vs Rat (L) group.

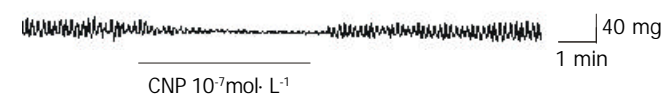


Figure 5A Effect of CNP on spontaneous contraction in gastric fundus circular smooth muscle in guinea-pig.



Figure 5B Effect of CNP on spontaneous contraction in gastric fundus circular smooth muscle in rat.

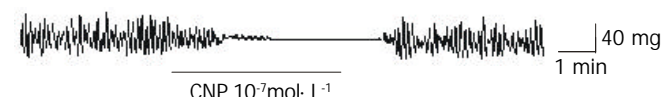


Figure 5C Effect of CNP on spontaneous contraction in gastric fundus longitudinal smooth muscle in guinea-pig.



Figure 5D Effect of CNP on spontaneous contraction in gastric fundus longitudinal smooth muscle in rat.

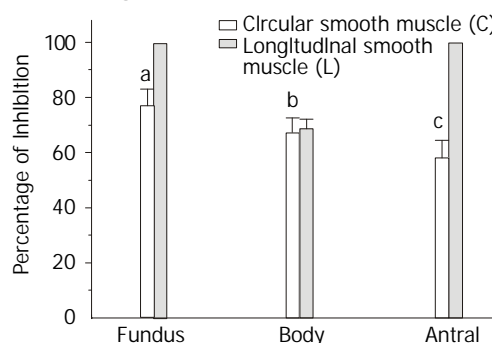


Figure 6A Effect of CNP on spontaneous contraction of different position in guinea-pig. ^a $P < 0.05$ vs Body (C) group and Antral

(C) group; ^a $P < 0.01$ vs Fundus(L) group; ^b $P < 0.01$ vs Fundus(L) group and Antral(L) group; ^c $P < 0.05$ vs Body(C) group; ^c $P < 0.01$ vs Antral(L) group.

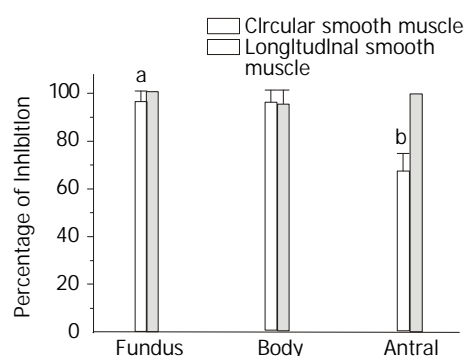


Figure 6B Effect of CNP on spontaneous contraction of different position in rat. ^a $P < 0.01$ vs Antral (C) group; ^b $P < 0.05$ vs Antral (L) group.

Effect of LY83583 and Zaparinast on CNP-induced inhibition in the gastric antral circular smooth muscle

After the gastric antral circular smooth muscle was treated by LY83583 10^{-7} mol·L⁻¹ and zaparinast (10^{-7} mol·L⁻¹) for 15 min to regulate the generation of cGMP, the effect of CNP on gastric motility was observed in the gastric antral circular smooth muscle of the rat. LY83583 markedly diminished the inhibitory effect of CNP on the spontaneous contraction, however, zaparinast enhanced the inhibitory effect of CNP on the spontaneous contraction (Table 3).

Table 3 Effect of LY83583 and Zaparinast on CNP-induced inhibition in gastric circular smooth muscle of rat ($\bar{x} \pm s$)

Group	n	Percentage of inhibition (%)
CNP1	5	63.61±3.68
CNP1+LY	5	54.15±2.97 ^a
CNP2	5	65.67±3.17
CNP2+Zap	5	77.67±5.86 ^b

^a $P < 0.05$ vs CNP1 group; ^a $P < 0.05$ vs CNP2 group.

DISCUSSION

In the present study, the effects of CNP on the spontaneous contraction of gastric smooth muscles in the rat, guinea-pig and human were comparatively investigated. The results indicated that CNP markedly inhibited the spontaneous contraction of gastric antral circular smooth muscles in these three kinds of animals and the order of inhibitory potency was human > rat > guinea-pig; CNP inhibited the contractile activity of gastric fundus circular and longitudinal smooth muscles in the rat and guinea-pig and this response was more obvious in the rat than that in guinea-pig; The effects of CNP on gastric body circular and longitudinal smooth muscles had double-phase, in which CNP first induced a relaxation and then an increase in the amplitude of the spontaneous contraction (rebound contraction) in the rat and guinea-pig. The response was more distinct in the guinea-pig than that in the rat and it disappeared after pretreating with atropine. In the same animal, the CNP-induced inhibition was the most potent in the gastric fundus and the weakest in the gastric antrum, and the inhibition was more obvious in the longitudinal smooth muscle than that in the circular smooth muscle. Using LY83583, a guanylate cyclase inhibitor, and zaparinast as phosphoesterase inhibitor to regulate the generation of cGMP, the effect of CNP on spontaneous contraction was markedly diminished by

LY83583. However, the inhibitory effect was enhanced by zaparinast. It was similar to the result observed in intestinal smooth muscle by Murthy *et al*^[13].

Since CNP was isolated from the central nerve system^[14], previous studies indicated that as a neurotransmitter, CNP exerted functions in the central nervous system^[15] and participated in the regulation of physiological functions in many other systems. CNP was successively found in the cardiovascular system^[16,17], respiratory system^[18], urinary system^[19], reproductive system^[2] and sense system^[20]. Since Komatsu *et al*^[8] found CNP in the gastrointestinal tracts of humans and rats, there were more and more studies on the relationship between CNP and the gastrointestinal tract. But the study on physiological functions of CNP in gastrointestinal tract was mainly focused on absorption, secretion and intestinal motility^[10-12]. Serial studies on natriuretic peptides regulating gastric smooth muscles motility were not reported. In this study, the effect of CNP on gastric motility in various animals, in different positions and in different smooth muscles of the same position of the same animal was comparatively investigated.

In various animals, the effects of CNP on the gastric motility of antrum and fundus smooth muscles presented species diversity. The order of inhibitory potency in gastric antrum was human > rat > guinea-pig, and in gastric fundus, the order was rat > guinea-pig. Analyzing this from the animal characters, It was presumed that either the distribution of the CNP receptor in gastric smooth muscle of three kinds of animals was different or the sensitivity of CNP to CNP receptor in different animal was diverse.

In different positions of the same animal, the effect of CNP on gastric motility exhibited positional diversity. CNP-induced inhibition was the most potent in gastric fundus and the weakest in gastric antrum. The responses may be related to the structure and function of the stomach. It was thought that the muscle layer was the thickest in the gastric antrum and the thinnest in the gastric fundus, and the gastric antrum played an important role in gastric emptying while gastric fundus was related to receptive relaxation. It indicated that the contractile function of the gastric antrum was more potent than the function of gastric fundus. In the same position of the same animal, the inhibition was more obvious in longitudinal smooth muscles than that in circular smooth muscles. The reason was probably that the distribution of CNP receptors showed diversity.

It is well known that NP and NO system are all cGMP-generation system. They play a very important role in regulation of multiple physiological functions. To investigate the mechanism of CNP-induced inhibition, LY83583, a kind of inhibitor of guanylate cyclase, and zaparinast, a phosphoesterase inhibitor were used for observing the effect of CNP on gastric motility in gastric antral circular smooth muscle of the rats. LY83583 markedly diminished the inhibitory effect of CNP on the spontaneous contraction, however, zaparinast enhanced the inhibitory effect of CNP on the spontaneous contraction. It indicated that CNP-induced inhibition on the spontaneous contraction in the gastric smooth muscle *via the cGMP* dependent pathway. Previous studies also supported the theory, for example, CNP dilated the vascular smooth muscle^[21] and relaxed the bronchus smooth muscle^[22] *via cGMP* dependent pathway.

In this present study, the CNP-induced response on spontaneous contraction of the gastric body showed double-phase, in which CNP first induced a relaxation and then inducing rebound contractions in rats and guinea-pigs. The response was more distinct in guinea-pigs than that in rat and it disappeared after pretreated with atropine. The results indicated that cholinergic M receptor participated in this CNP-induced rebound contraction of gastric body smooth muscle in guinea-pigs and rats. Previous studies also indicated that

vagus nerve regulated many functions of NP, for example, ANP promoted gastric acid secretion^[23], ANP, BNP and CNP could all induce bradycardia^[24] and BNP and CNP could enhance vagus-induced response of slowing heart rate^[25]. Then, it was suggested that CNP may facilitate the cholinergic nerve activity in gastric smooth muscles.

CNP may participate in the regulation of gastric motility as gastrointestinal hormone or neurotransmitter. CNP-induced inhibition has species diversity and position diversity in gastric smooth muscles. CNP-induced inhibition on gastric motility may be related to the increase of intracellular cGMP.

REFERENCES

- 1 **De Bold AJ**, Borenstein HB, Veress AT, Sonnenberg H. A rapid and potent natriuretic response to intravenous injection of atrial myocardial extracts in rats. *J Am Soc Nephrol* 2001; **12**: 403-409
- 2 **Stepan H**, Leitner E, Bader M, Walther T. Organ-specific mRNA distribution of C-type natriuretic peptide in neonatal and adult mice. *Regul Pept* 2000; **95**: 81-85
- 3 **Woodard GE**, Rosado JA, Brown J. Expression and control of C-type natriuretic peptide in rat vascular smooth muscle cells. *Am J Physiol Regul Integr Comp Physiol* 2002; **282**: R156-165
- 4 **Casco VH**, Veinot JP, Kuroski de Bold ML, Masters RG, Stevenson MM, de Bold AJ. Natriuretic peptide system gene expression in human coronary arteries. *J Histochem Cytochem* 2002; **50**: 799-809
- 5 **Furuya M**, Yoshida M, Hayashi Y, Ohnuma N, Minamino N, Kangawa K, Matsuo H. C-type natriuretic peptide is a growth inhibitor of rat vascular smooth muscle cells. *Biochem Biophys Res Commun* 1991; **177**: 927-931
- 6 **Wang X**, Xue L, Tong L. Influence of vasoactive peptides on homocysteine-induced proliferation of cultured rabbit vascular smooth muscle cell. *Zhonghua Yixue Zazhi* 1999; **79**: 411-413
- 7 **Ohno N**, Itoh H, Ikeda T, Ueyama K, Yamahara K, Doi K, Yamashita J, Inoue M, Masatsugu K, Sawada N, Fukunaga Y, Sakaguchi S, Sone M, Yurugi T, Kook H, Komeda M, Nakao K. Accelerated reendothelialization with suppressed thrombogenic property and neointimal hyperplasia of rabbit jugular vein grafts by adenovirus-mediated gene transfer of C-type natriuretic peptide. *Circulation* 2002; **105**: 1623-1626
- 8 **Komatsu Y**, Nakao K, Suga S, Ogawa Y, Mukoyama M, Arai H, Shirakami G, Hosoda K, Nakagawa O, Hama N. C-type natriuretic peptide (CNP) in rats and humans. *Endocrinology* 1991; **129**: 1104-1106
- 9 **Gower WR Jr**, Salhab KF, Foulis WL, Pillai N, Bundy JR, Vesely DL, Fabri PJ, Dietz JR. Regulation of atrial natriuretic peptide gene expression in gastric antrum by fasting. *Am J Physiol Regul Integr Comp Physiol* 2000; **278**: R770-780
- 10 **Vuolteenaho O**, Arjamaa O, Vakkuri O, Maksniemi T, Nikkila L, Kangas J, Puurunen J, Ruskoaho H, Leppaluoto J. Atrial natriuretic peptide (ANP) in rat gastrointestinal tract. *FEBS Lett* 1988; **233**: 79-82
- 11 **Brockway PD**, Hardin JA, Gall DG. Intestinal secretory response to atrial natriuretic peptide during postnatal development in the rabbit. *Biol Neonate* 1996; **69**: 60-66
- 12 **Akiho H**, Chijiwa Y, Okabe H, Harada N, Nawata H. Interaction between atrial natriuretic peptide and vasoactive intestinal peptide in guinea pig cecal smooth muscle. *Gastroenterology* 1995; **109**: 1105-1112
- 13 **Murthy KS**, Teng B, Jin J, Makhoulf GM. G protein-dependent activation of smooth muscle eNOS via natriuretic peptide clearance receptor. *Am J Physiol* 1998; **275**: C1409-1416
- 14 **Sudoh T**, Minamino N, Kangawa K, Matsuo H. C-type natriuretic peptide(CNP): A new member of natriuretic peptide family identified in porcine brain. *Biochem Biophys Res* 1990; **168**: 863-870
- 15 **Minerds KL**, Donald JA. Natriuretic peptide receptors in the central vasculature of the toad, *Bufo marinus*. *Comp Biochem Physiol A Mol Integr Physiol* 2001; **128**: 259-268
- 16 **Doyle DD**, Upshaw-Earley J, Bell EL, Palfrey HC. Natriuretic peptide receptor-B in adult rat ventricle is predominantly confined to the nonmyocyte population. *Am J Physiol Heart Circ Physiol* 2002; **282**: H2117-2123
- 17 **Wright RS**, Wei CM, Kim CH, Kinoshita M, Matsuda Y, Aarhus LL, Burnett JC Jr, Miller WL. C-type natriuretic peptide-mediated coronary vasodilation: role of the coronary nitric oxide and particulate guanylate cyclase systems. *J Am Coll Cardiol* 1996; **28**: 1031-1038
- 18 **Nakanishi K**, Tajima F, Itoh H, Nakata Y, Hama N, Nakagawa O, Nakao K, Kawai T, Torikata C, Suga T, Takishima K, Aurues T, Ikeda T. Expression of C-type natriuretic peptide during development of rat lung. *Am J Physiol* 1999; **277**: L996-L1002
- 19 **Meier SK**, Toop T, Donald JA. Distribution and characterization of natriuretic peptide receptors in the kidney of the toad, *Bufo marinus*. *Gen Comp Endocrinol* 1999; **115**: 244-253
- 20 **Suzuki M**, Kitanishi T, Kitano H, Yazawa Y, Kitajima K, Takeda T, Tokunaga Y, Maeda T, Kimura H, Tooyama I. C-type natriuretic peptide-like immunoreactivity in the rat inner ear. *Hear Res* 2000; **139**: 51-58
- 21 **Wennberg PW**, Miller VM, Rabelink T, Burnett JC Jr. Further attenuation of endothelium-dependent relaxation imparted by natriuretic peptide receptor antagonism. *Am J Physiol* 1999; **277**: H1618-1621
- 22 **Borges A**, de Villarroel SS, Winand NJ, de Becemberg IL, Alfonzo MJ, de Alfonzo RG. Molecular and biochemical characterization of a CNP-sensitive guanylyl cyclase in bovine tracheal smooth muscle. *Am J Respir Cell Mol Biol* 2001; **25**: 98-103
- 23 **Puurunen J**, Ruskoaho H. Vagal-dependent stimulation of gastric acid secretion by intracerebroventricularly administered atrial natriuretic peptide in anaesthetized rats. *Eur J Pharmacol* 1987; **141**: 493-495
- 24 **Thomas CJ**, May CN, Sharma AD, Woods RL. ANP, BNP, and CNP enhance bradycardic responses to cardiopulmonary chemoreceptor activation in conscious sheep. *Am J Physiol Regul Integr Comp Physiol* 2001; **280**: R282-288
- 25 **Herring N**, Zaman JA, Paterson DJ. Natriuretic peptides like NO facilitate cardiac vagal neurotransmission and bradycardia via a cGMP pathway. *Am J Physiol Heart Circ Physiol* 2001; **281**: H2318-2327

Edited by Xu XQ

Significance of changes of gastrointestinal peptides in blood and ileum of experimental spleen deficiency rats

Li-Sheng Li, Rui-Yao Qu, Wei Wang, Hua Guo

Li-Sheng Li, Rui-Yao Qu, Wei Wang, Hua Guo, Department of Physiology, Capital University of Medical Sciences, 100054, Beijing, China

Supported by the Traditional Chinese Medicine-Drug Science and Technology Development Foundation, Beijing City (1999-2000)

Correspondence to: Li-Sheng Li, Department of Physiology, Capital University of Medical Sciences, 100054, Beijing, China. lls@sohu.com

Telephone: +86-10-63051492

Received: 2002-09-13 **Accepted:** 2002-10-31

Abstract

AIM: To explore the mechanism of spleen deficiency (SD) by studying the relationship of gastro-intestinal peptides level and ileal electro-mechanical activity of SD rats and cold restrain rats.

METHODS: (1) spleen deficiency (SD) model was established by feeding Houpu: Zhishi: Dahuang in the ratio of 3:3:2, 3 ml/time, for 42 days. (2) The cold restrain stress model: Animals were restrained on grille and placed in a cool water at 18 °C for 3 h. (3) Substance P (SP) and vasoactive intestinal peptide (VIP) levels in all layers of initial part of ileum and blood in rats were measured by radioimmunoassays (RIA) while changes of electric activity and motility in ileum of rats were recorded with electrode and strain gauge.

RESULTS: SP levels in ileum and blood of experimental SD rats were significantly higher than that of the control groups (9.89 ± 5.65 vs 1.22 ± 1.18 , $P < 0.005$, in ileum; 22.7 ± 3.95 vs 6.60 ± 1.47 , $P < 0.001$, in blood) while the VIP levels of the SD rats were significantly lower than that of the controls (3.50 ± 2.01 vs 9.10 ± 4.91 , $P < 0.05$, in ileum; 229.8 ± 62.4 vs 560.4 ± 151.3 , $P < 0.001$, in blood). As compared with the controls, the average frequency of slow electric waves (21.3 ± 0.96 vs 18.2 ± 2.28 , $P < 0.05$) and motility (21.5 ± 0.58 vs 18 ± 2.65 , $P < 0.005$) of SD rats increased obviously and the frequency of fast waves of SD rat also increased. In spontaneous recovery cases, SP levels recovered significantly (compared with the SD groups, 2.99 ± 0.62 vs 9.89 ± 5.65 , $P < 0.001$, in ileum; 14.4 ± 4.22 vs 22.7 ± 3.95 , $P < 0.001$, in blood) but did not drop to normal. After the SD rats treated with Chinese herbs (Jiawei Sijun zi Tang), SP improved (compared with SD cases, 2.20 ± 1.25 vs 9.89 ± 5.65 , ($P < 0.001$), in ileum; 10.7 ± 1.88 vs 22.7 ± 3.95 , ($P < 0.001$), in blood) and VIP in blood also improved (compared with SD rats, 485.7 ± 229.0 vs 229.8 ± 62.4 , $P < 0.01$) while the amplitude of motility decreased apparently (compared with the SD rats, 0.64 ± 0.096 vs 0.89 ± 0.15 , $P < 0.01$). The ileal SP levels of cool stress didn't change while the ileal VIP levels of cool stress became significantly lower than that of the control groups (2.87 ± 0.87 vs 9.10 ± 4.91 , $P < 0.01$). The blood SP levels of cool stress were significantly higher (15.60 ± 1.83 vs 6.60 ± 1.47 , $P < 0.001$) whereas the blood VIP levels of cool stress were significantly lower than that of the control group (153.4 ± 70.46 vs 560.4 ± 151.30 , $P < 0.001$).

CONCLUSION: Changes of SP and VIP levels in initial part

of ileum and blood of SD rats and cool stress rats may be closely related to the gastrointestinal motility disorders presented in SD and cool stress rats. the Chinese herbs (Jiawei Sijun zi Tang) currently used have partially therapeutic effect.

Li LS, Qu RY, Wang W, Guo H. Significance of changes of gastrointestinal peptides in blood and ileum of experimental spleen deficiency rats. *World J Gastroenterol* 2003; 9(3): 553-556

<http://www.wjgnet.com/1007-9327/9/553.htm>

INTRODUCTION

It was well known that Spleen-Stomach theory is an important constituent of the theoretical basis of traditional Chinese Medicine. The spleen here is not synonymous with the spleen in western medicine anatomically, physiologically or pathophysiologically^[1-3]. Conceptually, Spleen-Stomach theory is a comprehensive one. It mainly involves the digestive system, its vegetative nervous system, immunologic function, hemopoiesis, muscle metabolism, endocrine function, hepatic metabolic function, protein, nucleotide, energy, water and salt metabolism.

In recent years, the field of gastrointestinal hormones has expanded at a dazzling speed. The successful isolation of some gastrointestinal hormones and development of sensitive assays for their detection have led to many unexpected findings^[4]. Gastrointestinal hormones as regulatory peptides appear to be major components of bodily integration and have important regulatory actions on physiological function of gastrointestinal tract^[5-17]. Some studies indicated that spleen deficiency syndrome (SDS) was closely related with gastrointestinal hormones^[18-21].

But up to now, the mechanisms of the relationship between gastrointestinal peptides levels and gastrointestinal functional disorder in SD still remain unclear^[22-31]. We tried to explore the relationship between SDS and gastrointestinal hormones by measuring SP and VIP, and by using electrode and highly sensitive strain sensor to record alterations of ileum activity and ileum motility in SD and cool stress rats.

MATERIALS AND METHODS

Experimental animals

Healthy adult male Wistar rats (provided by Experimental Animal center, capital university of medical sciences), weighing 0.12-0.17 kg were used in this study. They were caged in an air conditioned room (23±2 °C).

Sijunzi decoction (SJZD), composed of ginseng, Atractylodes, Poria, Glycyrrhiza, It was prepared by routine method of decocting the crude herbal medicine twice. The filtered medication was preserved in refrigerator at 4 °C.

Fifty rats were randomly divided into five groups: (1) control group: The rats were fed standard rat chow and water ad libitum. (2) experimental SD model group. by feeding Houpu: Zhishi: Dahuang (3:3:2), 3 ml/time, 42 day. (3) Spontaneous recovery group. (4) SJZD treated group. (5) cold stress group: rats were restrained on grille and placed in cool water at 18 °C for 3 h.

Table 3 Changes of electric-mechanical activity in ileum ($\bar{x}\pm s$)

	Main frequency (time/min)		Average frequency (time/min)		Amplitude (time/min)	
	Slow wave	Motility	Slow wave	Motility	Slow wave	Motility
Control group	17.5±2.05	18.5±1.7	18.2±2.28	18±2.65	0.30±0.26	0.43±0.31
SD group	17.4±0.79	18.0±0.69	21.3±0.96 ^b	21.5±0.58 ^a	0.31±0.24	0.89±0.15 ^b
Spontaneous recovery group	16.8±7.8	16.8±1.3	20.5±5.5	19.1±4.85	0.25±0.103	0.77±0.65
Treated group	13.8±3.92	16.1±3.36	20.0±4.04	19.0±3.61	0.14±0.015	0.64±0.096 ^c
Cool stress group	16.5±2.67	15.7±1.1	15.2±2.01	16±2.17	0.27±0.11	0.33±0.12

^a $P<0.005$, vs control group; ^b $P<0.05$, vs control group; ^c $P<0.01$, vs SD group.

Measurements

Radioimmunoassay (RIA) of SP and VIP in these samples was conducted with kits purchased from Beijing HaiKerui Biological technique center. The concentrations of SP, VIP were measured with radioimmunoassay kits. Under anesthesia, the abdomen was opened and the samples were taken as follows: (1) Blood samples of 5-6 ml from the heart were collected in tubes, the plasma was immediately separated by centrifugation, then was frozen and stored at -20 °C until analysis. (2) The initial part of ileal tissue were removed, rinsed and weighed, then were put into a tube with boiling water. The tube was plunged into vigorous boiling water for 3 minutes, then it was cooled down and homogenized for 10 minutes. After centrifugation at 3 000 r/min for 5 minutes, the supernatant was collected and stored at -20 °C until assay.

All groups fasted for 18 h before operating, anesthetized by 20 % urethane, the abdomen was opened, then the silver electrodes and strain gauge were implanted on the initial part of ileum. The changes of electric slow wave and motility of ileum were recorded. Electrode wires were passed through the abdominal muscle and fixed on the skin. All data were handled by a two-channel physiological recorder and a computer.

The cold restrain stress model: Animals were restrained on grille and placed in a cool water at 18 °C for 3 h.

Statistical analysis

Data were expressed as mean \pm standard deviation. Experimental results were analyzed by *t* tests was determined $P<0.05$ was considered statistically significant.

RESULTS

To assess the changes of gut peptides of gastrointestinal functional disorder in SD rats and cold restraint rats, we measured the plasma levels of SP and VIP and those in the initial part of the ileum. SP levels in ileum and blood of experimental SD rats were significantly higher than those of the control groups ($P<0.005$, in ileum; $P<0.001$, in blood) while the VIP levels of the SD rats were significantly lower than those of the controls ($P<0.05$ in Ileum, $P<0.001$, in blood). In spontaneous recovery cases, SP levels recovered significantly (compared with the SD groups, $P<0.001$) and did not drop to normal. After the SD rats were treated with Chinese herbs (Jiawei Sijun Zi Tang), SP was improved (compared with SD cases, $P<0.001$) and VIP in blood was also improved (compared with SD rats, $P<0.01$). SP levels in ileum of cool stress didn't change while the VIP levels were significantly lower than that of the controls groups ($P<0.01$). SP levels in blood of cool stress were significantly higher ($P<0.001$) while the VIP levels were significantly lower than that of the control groups ($P<0.001$), Table 1-2.

As compared with the controls, average frequency of slow electric waves ($P<0.05$) and motility ($P<0.05$) of SD rats

increased obviously while the amplitude of motility decreased apparently ($P<0.05$), Table 3.

Table 1 Changes of SP and VIP in plasma ($\bar{x}\pm s$, $\mu\text{g}\cdot\text{L}^{-1}$)

Group	<i>n</i>	SP	VIP
Control group	7	6.60±1.47	560.40±151.30
SD group	8	22.7±3.95 ^a	229.8±62.4 ^a
Spontaneous recovery group	7	14.4±4.22 ^c	332.7±119.1
Treated group	7	10.7±1.88 ^b	485.7±229.0 ^c
Cool stress group	7	15.60±1.83 ^a	153.4±70.46 ^a

^a $P<0.001$, vs control group; ^b $P<0.001$, vs SD group; ^c $P<0.01$, vs SD group.

Table 2 Changes of SP and VIP in ileum ($W_B/\mu\text{g}\cdot\text{mg}^{-1}$, $\bar{x}\pm s$)

Group	<i>n</i>	SP	VIP
Control group	7	1.22±1.18	9.10±4.91
SD group	8	9.89±5.65 ^a	3.50±2.01 ^c
Spontaneous recovery group	7	2.99±0.62 ^b	4.11±0.83
Treated group	7	2.20±1.25 ^b	4.48±1.14
Cool stress group	7	0.57±0.51	2.87±0.87 ^c

^a $P<0.005$, vs control group; ^b $P<0.001$, vs SD group; ^c $P<0.01$, vs control group.

DISCUSSION

Spleen is one of the five solid organs, which in Traditional Chinese Medicine (TCM), does not completely match the organ designated in western medicine from the standpoint of structure, location and function. It has the functions of digesting food, absorbing and transporting nutrients to the body tissues. The spleen also serves to control the blood and to keep the blood circulating within the vessels, and takes part in the regulation of fluid metabolism^[32-38]. Spleen-Stomach theory forms the basis of diagnostic approach and treatment of Spleen-Stomach disease, Spleen deficiency syndrome is a multisystem and multiorgan functional impairment, but mainly manifest as digestive tract disturbance. Experimental researches on animal model and clinical studies on spleen deficiency syndrome have yielded fruitful results in this field which lead to a better understanding of its mechanism and help open a new avenue for treatment of diseases relevant to Spleen deficiency^[21,39-47]. The Spleen stomach has various physiologic functions. such as: Spleen governs transport and transformation, Spleen-stomach transforms food into nutrients which are the sources of Qi and blood. Stomach governs down-bearing function and spleen governs up-bearing which signify the motility, secretory, assimilative, absorptive and dispersing functions of upper

digestive tract, among which, gut hormones are involved^[20,48-50]. Dysfunction of up-and down-bearing function of spleen-stomach can cause gastrointestinal disturbances and various spleen deficiency syndromes^[1,2,19,20,51,52].

SP and VIP are both important gut Peptides, SP and VIP partly distributed in the mucosa of gastric antrum, the mucosa of the jejunum, ileum. And the central nervous system SP has a wide range of biological actions. In the intestine, VIP markedly stimulates intestinal secretion of electrolytes and hence of water. Its other actions include relaxation of intestinal smooth muscle; sphincters; dilation of peripheral blood vessels; and inhibition of gastric acid secretion.

Our previous studies included: The use of electrode and highly sensitive sensor to record alteration of gut electric activity and motility. To explore the potential role of gut peptides in spleen deficiency (SD), we studied immunoreactive Substance P, VIP, Calcitonin Gene Related Peptide (CGRP) levels in gastric antrum, duodenum and jejunal tissues in experimental SD rats by radioimmunoassays (RIA). The study suggested that motion frequency of several regions in SD rats was lower than that of control and treatment groups, respectively ($P<0.05$). The minimal amplitude of electric activity was also lower than that of control and treatment respectively ($P<0.05$). Correlation between motion frequency and its total amplitude index was different from various regions, the time of MMC was obviously less than that of the control, and the amplitude of motility was significantly higher than that of the control. The SP, VIP levels in antrum of SD rats were obviously less than that of the control, whereas, the SP and VIP levels in duodenum of SD rats were obviously higher than that of control ($P<0.05$), but in jejunum only SP levels increased obviously than that of the control ($P<0.05$). The VIP level in duodenum of SD rats was significantly less than that of treatment group ($P<0.05$), but VIP level of treatment group was higher than that of the control ($P<0.05$). As to CGRP level in antrum and small intestine, there was no obvious difference among the 3 groups.

The present study reveals changes SP and VIP in ileum of SD rats and cool stress rat. All these data imply that changes of SP and VIP levels in the antrum and the small intestine of SD rats may be closely related with the dysmotility of gastrointestinal, malabsorption and diarrhea. The Chinese herb (si junzi Tang) is capable of improving the spleen deficiency significantly and gastrointestinal electro-mechanical activity.

REFERENCES

- Gao R, Li L, Lu Z. Clinical observation on 300 cases of angina pectoris treated by the spleen-stomach regulating method. *J Tradit Chin Med* 1998; **18**: 87-90
- Wu XN. Current concept of Spleen-Stomach theory and Spleen deficiency syndrome in TCM. *World J Gastroenterol* 1998; **4**: 2-6
- Straus E. Gastrointestinal hormones. *Mt Sinai J Med* 2000; **67**: 54-57
- Bierkamp C, Kowalski-Chauvel A, Dehez S, Fourmy D, Pradayrol L, Seva C. Gastrin mediated cholecystokinin-2 receptor activation induces loss of cell adhesion and scattering in epithelial MDCK cells. *Oncogene* 2002; **21**: 7656-7670
- Patten GS, Head RJ, Abeywardena MY, McMurchie EJ. An apparatus to assay opioid activity in the infused lumen of the intact isolated guinea pig ileum. *J Pharmacol Toxicol Methods* 2001; **45**: 39-46
- De Man JG, Moreels TG, De Winter BY, Bogers JJ, Van Marck EA, Herman AG, Pelckmans PA. Disturbance of the prejunctional modulation of cholinergic neurotransmission during chronic granulomatous inflammation of the mouse ileum. *Br J Pharmacol* 2001; **133**: 695-707
- Wise RM, Bass P, Oaks JA. Myoelectric response of the small intestine to the oral presence of the tapeworm *Hymenolepis diminuta*. *J Parasitol* 2001; **87**: 1255-1259
- Stebbing M, Johnson P, Vremec M, Bornstein J. Role of alpha(2)-adrenoceptors in the sympathetic inhibition of motility reflexes of guinea-pig ileum. *J Physiol* 2001; **534**(Pt. 2): 465-478
- Shafik A, El-Sibai O, Ahmed A. Study of the mechanism underlying the difference in motility between the large and small intestine: the "single" and "multiple" pacemaker theory. *Front Biosci* 2001; **6**: B1-5
- Soderholm JD, Perdue MH. Stress and gastrointestinal tract. II. Stress and intestinal barrier function. *Am J Physiol Gastrointest Liver Physiol* 2001; **280**: G7-G13
- Bayer S, Raul F, Boehm N, Klein A, Angel F. Modulatory effects of polyamines and GABA on rat ileal motility *in vitro*. *Gastroenterol Clin Biol* 1999; **23**: 824-831
- Chang IY, Glasgow NJ, Takayama I, Horiguchi K, Sanders KM, Ward SM. Loss of interstitial cells of Cajal and development of electrical dysfunction in murine small bowel obstruction. *J Physiol* 2001; **536**(Pt 2): 555-568
- Shibata C, Murr MM, Balsiger B, Anding WJ, Sarr MG. Contractile activity of circular smooth muscle in rats one year after small bowel transplantation: differing adaptive response of the jejunum and ileum to denervation. *J Gastrointest Surg* 1998; **2**: 463-472
- Pfefferkorn MD, Fitzgerald JF, Croffie JM, Gupta SK, Caffrey HM. Direct measurement of pancreatic enzymes: a comparison of secretagogues. *Dig Dis Sci* 2002; **47**: 2211-2216
- Takeuchi T, Fujita A, Roumy M, Zajac JM, Hata F. Effect of 1DMe, a neuropeptide FF analog, on acetylcholine release from myenteric plexus of guinea pig ileum. *Jpn J Pharmacol* 2001; **86**: 417-422
- Marinovich M, Viviani B, Capra V, Corsini E, Anselmi L, D'Agostino G, Di Nucci A, Binaglia M, Tonini M, Galli CL. Facilitation of acetylcholine signaling by the dithiocarbamate fungicide propineb. *Chem Res Toxicol* 2002; **15**: 26-32
- Venkova K, Sutkowski-Markmann DM, Greenwood-Van Meerveld B. Peripheral activity of a new NK1 receptor antagonist TAK-637 in the gastrointestinal tract. *J Pharmacol Exp Ther* 2002; **300**: 1046-1052
- Yin G, Zhang W, Li G. Therapeutic effect of weikangfu on gastric precancerous disorder with spleen deficiency syndrome and its effect of gastric mucosal zinc, copper, cyclic adenosine monophosphate, superoxide dismutase, lipid peroxide and 3H-TdR lymphocyte conversion test. *Zhongguo Zhongxiyi Jiehe Zazhi* 2000; **20**: 176-179
- Ren P, Huang X, Zhang L. Effect of sijunzi decoction on gastric emptying rate in rat model of spleen deficiency syndrome. *Zhongguo Zhongxiyi Jiehe Zazhi* 2000; **20**: 596-598
- Yin G, Zhang W, Xu F. Effect of Weikangfu granule on ultra-structure of gastric mucosa in patients of precancerosis with spleen deficiency syndrome. *Zhongguo Zhongxiyi Jiehe Zazhi* 2000; **20**: 667-670
- Xu L. Twenty-seven cases of spleen-qi deficiency syndrome treated by heat-producing needling at zusanli. *J Tradit Chin Med* 2000; **20**: 40-41
- Hockerfelt U, Franzen L, Kjorell U, Forsgren S. Parallel increase in substance P and VIP in rat duodenum in response to irradiation. *Peptides* 2000; **21**: 271-281
- Fujimiya M, Inui A. Peptidergic regulation of gastrointestinal motility in rodents. *Peptides* 2000; **21**: 1565-1582
- Chang FY, Doong ML, Chen TS, Lee SD, Wang PS. Vasoactive intestinal polypeptide appears to be one of the mediators in misoprostol-enhanced small intestinal transit in rats. *J Gastroenterol Hepatol* 2000; **15**: 1120-1124
- Huang X, Ren P, Wen AD, Wang LL, Zhang L, Gao F. Pharmacokinetics of traditional Chinese syndrome and recipe: a hypothesis and its verification (I). *World J Gastroenterol* 2000; **6**: 384-391
- Pei WF, Xu GS, Sun Y, Zhu SL, Zhang DQ. Protective effect of electroacupuncture and moxibustion on gastric mucosal damage and its relation with nitric oxide in rats. *World J Gastroenterol* 2000; **6**: 424-427
- Zhang XC, Gao RF, Li BQ, Ma LS, Mei LX, Wu YZ, Liu FQ, Liao ZL. Clinical and experimental study of therapeutic effect of Weixibaonizhuan pills on gastric precancerous lesions. *World J Gastroenterol* 1998; **4**: 24-27
- Xu CT, Pan BR. Current status of gene therapy in gastroenterology. *World J Gastroenterol* 1998; **4**: 85-89

- 29 **Xu CT**, Pan BR. Current medical therapy for ulcerative colitis. *World J Gastroenterol* 1999; **5**: 64-72
- 30 **Yuan HY**, Li Y, Yang GL, Bei DJ, Wang K. Study on the causes of local recurrence of rectal cancer after curative resection: analysis of 213 cases. *World J Gastroenterol* 1998; **4**: 527-529
- 31 **Yamamoto H**, Umeda M, Mizoguchi H, Kato S, Takeuchi K. Protective effect of Irsogladine on monochloramine induced gastric mucosal lesions in rats: a comparative study with rebamipide. *World J Gastroenterol* 1999; **5**: 477-482
- 32 **Yin G**, Zhang W, He X. Histo-cytopathological study on gastric mucosa of spleen deficiency syndrome. *Zhongguo Zhongxiyi Jiehe Zazhi* 1999; **19**: 660-663
- 33 **Zhu L**, Yang ZC, Li A, Cheng DC. Reduced gastric acid production in burn shock period and its significance in the prevention and treatment of acute gastric mucosal lesions. *World J Gastroenterol* 2000; **6**: 84-88
- 34 **Zheng TZ**, Li W, Qu SY, Ma YM, Ding YH, Wei YL. Effects of Dangshen on isolated gastric muscle strips in rats. *World J Gastroenterol* 1998; **4**: 354-356
- 35 **Li W**, Zheng TZ, Qu SY. Effect of cholecystokinin and secretin on contractile activity of isolated gastric muscle strips in guinea pigs. *World J Gastroenterol* 2000; **6**: 93-95
- 36 **Shen XZ**, Koo MWL, Cho CH. Sleep deprivation increase the expression of inducible heat shock protein 70 in rat gastric mucosa. *World J Gastroenterol* 2001; **7**: 496-499
- 37 **Peng X**, Feng JB, Wang SL. Distribution of nitric oxide synthase in stomach wall in rats. *World J Gastroenterol* 1999; **5**: 92
- 38 **Peng X**, Feng JB, Yan H, Zhao Y, Wang SL. Distribution of nitric oxide synthase in stomach myenteric plexus of rats. *World J Gastroenterol* 2001; **7**: 852-854
- 39 **Li L**, Jin NG, Piao L, Hong MY, Jin ZY, Li Y, Xu WX. Hyposmotic membrane stretch potentiated muscarinic receptor agonist-induced depolarization of membrane potential in guinea-pig gastric myocytes. *World J Gastroenterol* 2002; **8**: 724-727
- 40 **Yang WY**, Liang R, Che JX. Clinical study on relation between spleen-qi deficiency syndrome and the pancreatic exocrine function. *Zhongguo Zhongxiyi Jiehe Zazhi* 1996; **16**: 414-416
- 41 **Zhang M**, Zhang Z, Xia T. Effect of sijunzi decoction on serum soluble intercellular adhesive molecule-1, interleukin-15 and monocyte antibody-dependent cell-mediated cytotoxicity in patients of spleen-deficiency. *Zhongguo Zhongxiyi Jiehe Zazhi* 1999; **19**: 270-272
- 42 **Xu MY**, Lu HM, Wang SZ, Shi WY, Wang XC, Yang DX, Yang CX, Yang LZ. Effect of devazepide reversed antagonism of CCK-8 against morphine on electrical and mechanical activities of rat duodenum *in vitro*. *World J Gastroenterol* 1998; **4**: 524-526
- 43 **Lin Z**, Chen JD, Schirmer BD, McCallum RW. Postprandial response of gastric slow waves: correlation of serosal recordings with the electrogastrogram. *Dig Dis Sci* 2000; **45**: 645-651
- 44 **Xu D**, Shen Z, Wang W. Immunoregulation of Youguiyin, Sijunzitan, Taohong Siwutang in treating patients with deficiency of kidney, spleen and blood stasis syndrome. *Zhongguo Zhongxiyi Jiehe Zazhi* 1999; **19**: 712-714
- 45 **Wang ZS**, Cheung JY, Gao SK, Chen JD. Spati-temporal nonlinear modeling of gastric myoelectrical activity. *Methods Inf Med* 2000; **39**: 186-190
- 46 **Tabor S**, Thor PJ, Pitala A, Laskiewicz J. Value of electrogastrographic parameters in evaluation of gastric myoelectrical activity. *Folia Med Cracov* 1999; **40**: 27-42
- 47 **Abo M**, Kono T, Wang Z, Chen JD. Impairment of gastric and jejunal myoelectrical activity during rectal distension in dogs. *Dig Dis Sci* 2000; **45**: 1731-1736
- 48 **Lin X**, Hayes J, Peters LJ, Chen JD. Entrainment of intestinal slow waves with electrical stimulation using intraluminal electrodes. *Ann Biomed Eng* 2000; **28**: 582-587
- 49 **Lin X**, Peters LJ, Hayes J, Chen JD. Entrainment of small intestinal slow waves with electrical stimulation in dogs. *Dig Dis Sci* 2000; **45**: 652-656
- 50 **Abo M**, Liang J, Qian L, Chen JD. Distension-induced myoelectrical dysrhythmia and effect of intestinal pacing in dogs. *Dig Dis Sci* 2000; **45**: 129-135
- 51 **Zeng J**, Dai X, Yang J. 159 sterility patients of yang-deficiency of spleen and kidney treated by shouwu huanjing capsule. *Zhongguo Zhongxiyi Jiehe Zazhi* 1998; **18**: 477-479
- 52 **Muth ER**, Koch KL, Stern RM. Significance of autonomic nervous system activity functional dyspepsia. *Dig Dis Sci* 2000; **45**: 854-863

Edited by Wu XN

Effect of pinaverium bromide on stress-induced colonic smooth muscle contractility disorder in rats

Yun Dai, Jian-Xiang Liu, Jun-Xia Li, Yun-Feng Xu

Yun Dai, Jian-Xiang Liu, Jun-Xia Li, Department of Gastroenterology, First Hospital of Peking University, Beijing 100034, China

Yun-Feng Xu, The Center Laboratory, First Hospital of Peking University, Beijing 100034, China

Correspondence to: Yun Dai, P.O. Box 97-242 Beijing 100016, China. caolanzi@263.net

Telephone: +86-10-66171122-2301

Received: 2002-09-14 **Accepted:** 2002-10-18

Abstract

AIM: To investigate the effect of pinaverium bromide, a L-type calcium channel blocker with selectivity for the gastrointestinal tract on contractile activity of colonic circular smooth muscle in normal or cold-restraint stressed rats and its possible mechanism.

METHODS: Cold-restraint stress was conducted on rats to increase fecal pellets output. Each isolated colonic circular muscle strip was suspended in a tissue chamber containing warm oxygenated Tyrode-Ringer solution. The contractile response to ACh or KCl was measured isometrically on ink-writing recorder. Incubated muscle in different concentrations of pinaverium and the effects of pinaverium were investigated on ACh or KCl-induced contraction. Colon smooth muscle cells were cultured from rats and $[Ca^{2+}]_i$ was measured in cell suspension using the Ca^{2+} fluorescent dye fura-2/AM.

RESULTS: During stress, rats fecal pellet output increased 61 % ($P < 0.01$). Stimulated with ACh or KCl, the muscle contractility was higher in stress than that in control. Pinaverium inhibited the increment of $[Ca^{2+}]_i$ and the muscle contraction in response to ACh or KCl in a dose dependent manner. A significant inhibition of pinaverium to ACh or KCl induced $[Ca^{2+}]_i$ increment was observed at 10^{-6} mol/L. The IC_{50} values for inhibition of ACh induced contraction for the stress and control group were 1.66×10^{-6} mol/L and 0.91×10^{-6} mol/L, respectively. The IC_{50} values for inhibition of KCl induced contraction for the stress and control group were 8.13×10^{-7} mol/L and 3.80×10^{-7} mol/L, respectively.

CONCLUSION: Increase in $[Ca^{2+}]_i$ of smooth muscle cells is directly related to the generation of contraction force in colon. L-type Ca^{2+} channels represent the main route of Ca^{2+} entry. Pinaverium inhibits the calcium influx through L-type channels; decreases the contractile response to many kinds of agonists and regulates the stress-induced colon hypermotility.

Dai Y, Liu JX, Li JX, Xu YF. Effect of pinaverium bromide on stress-induced colonic smooth muscle contractility disorder in rats. *World J Gastroenterol* 2003; 9(3): 557-561
<http://www.wjgnet.com/1007-9327/9/557.htm>

INTRODUCTION

Irritable bowel syndrome (IBS) is a common functional

gastrointestinal disorder in which abdominal pain is associated with changes of bowel habit and abdominal distension^[1,35]. The pathophysiological mechanisms for IBS are not clear and therefore the therapy is usually empirical. Abnormal contraction of intestinal smooth muscle may be important in producing the main IBS symptoms^[2-5,43], thus, modifying the contractility is often the major aim in the treatment of IBS^[6,7]. Pinaverium bromide, a L-type calcium channel blocker with selectivity for the gastrointestinal tract, effectively relieves pain, diarrhea and intestinal discomfort, provides good therapeutic efficacies without significant adverse effects on IBS patients^[8-10].

To evaluate the rational use of calcium channel blockers in colonic motor activity affecting the contraction of smooth muscle and to explore the physiopathology in such functional bowel disorders, we conducted cold-restraint stress on rats to induce fecal pellet output increased, investigated changes in contractility of circular muscle isolated from stressed colon treated with or without pinaverium. In addition, to further clarify the mechanism in the action of pinaverium we cultured colonic smooth muscle cells from rats, analyzed the influence of pinaverium on the free cytoplasmic Ca^{2+} concentration ($[Ca^{2+}]_i$). The circular muscle was chosen because it was the musculature predominantly responsible for propulsive contractile activity.

MATERIALS AND METHODS

Animal model

Male Wister rats, weighing 250-300 g, were housed in individual cages and provided with standard rodent chow and tap water for at least one week prior to the experiment. Room temperature was maintained at 25-28 °C. Rats were deprived of food but not water for 24 h before testing. Rats were studied for 2 h in normal living cages at room temperature (control, no stressed animals) or in wire-mesh restraining cylinders (5.5 cm in diameter \times 18.5 cm in length) placed in a cold (4-6 °C) environment (cold-restraint stressed animals). The quality of fecal pellets expelled by each animal was measured after 2 h.

Recording of contractile responses to the stimulation of agonist

Each animal was killed by cervical dislocation, and the segments of distal colon (4 cm from anus) were removed. Circular smooth muscle strips (2 mm \times 8 mm) were prepared by separating the mucosa and serosa from the muscle layers.

Muscle strips were mounted in individual tissue baths containing warm (37 °C) oxygenated (95 % O_2 and 5 % CO_2) Tyrode-Ringer solution (pH 7.4, composition in mmol/L: 137 NaCl, 5.4 KCl, 0.5 $MgCl_2$, 1.8 $CaCl_2$, 11.9 $NaHCO_3$, 0.4 NaH_2PO_4 , 5 Glucose) and attached to an isometric force transducer. The contractile activity was detected as change of tension, which was generated by circular muscle^[39-41]; the contractile response was measured isometrically on ink-writing recorder and the data were expressed as milli-Newton per square millimeter (mN/mm²).

Muscle strips from the control and stressed rats were randomly stimulated by ACh (10^{-5} mol/L) or KCl (60 mmol/L).

To investigate the effect of pinaverium bromide on muscle contractility, each muscle strip was stimulated by ACh or KCl twice before and twice after introduction of pinaverium (10^{-7} - 3×10^{-5} mol/L) following at least a 15 min equilibration period for each concentration of the blocker in Tyrode-Ringer solution. For a single strip, up to three different concentrations of pinaverium were applied cumulatively. Mean values obtained before and after the treatment of the blocker were compared. The contractile response to pinaverium was expressed as the percent of decreased response in the control recorded immediately before exposure to the calcium channel blocker.

Isolation and culture of colonic smooth muscle cells

Smooth muscle cells were isolated from the colon of rats by two consecutive digestions with collagenase respectively, following the method previously described^[11]. Briefly, after peeling off the serosal and mucosal layers, muscle tissues were minced into small pieces of 2 to 3 mm² and incubated in culture medium A (pH 7.4, composition in mmol/L: 25 HEPES, 120 NaCl, 4 KCl, 2 CaCl₂, 0.6 MgSO₄, 2.6 KH₂PO₄ and 14 glucose) containing 0.1 % collagenase, 0.1 % BSA, and 0.01 % soybean trypsin inhibitor for 40 min at 31 °C, the culture medium was filtered through a nylon mesh. The filtrate, which contained isolated cells, was diluted with enzyme-free culture medium A and centrifuged at 150 g for 5 min. The cell pellet was then diluted in PBS. The remaining tissue from the first incubation was reincubated in culture medium A for 30 min at 31 °C and fragments were dispersed into single cells by passages in and out the inverted wide end of a 5-ml pipette. The acquired cell suspension was filtered through a nylon mesh (500 μm). Isolated cells from the two incubations were pooled and counted. Freshly isolated colonic muscle cells were resuspended in DMEM medium with high glucose (12 mmol/L), sodium pyruvate (1 mmol/L), 10 % heat-inactivated fetal bovine serum and antibiotics (100 UI/mL penicillin G, 100 UI/mL streptomycin, 50 μg/mL gentamicin and 3 μg/mL amphotericin B). Cells were plated in sterile flasks at a density of 5×10^4 cells/mL and incubated at 37 °C in a humidified atmosphere with 5 % CO₂. Culture medium was exchanged every 3 d. Only those cells that were cultured for 14 to 17 days were used for subsequent studies.

Measurement of $[Ca^{2+}]_i$ in colonic smooth muscle cells

After the cultured cells were digested with 0.125 % trypsin, $[Ca^{2+}]_i$ was measured in cell suspension (10^6 cells/mL) using the Ca^{2+} fluorescent dye fura-2/AM as described by Shi *et al*^[11]. Muscle cells were suspended in a modified HEPES buffer containing (in mmol/L) 10 HEPES, 125 NaCl, 5 KCl, 1 CaCl₂, 0.5 MgSO₄ and 5 glucose, and were incubated with 5 μmol/L fura-2/AM for 30 min at 37 °C. The fura-2/AM treated samples were diluted, centrifuged twice, and suspended in 1.5 ml solution with the same composition for immediate measurement of $[Ca^{2+}]_i$. Fluorescence was measured at 510 nm with excitation wavelengths alternating between 340 nm and 380 nm. Autofluorescence value of unloaded cells was subtracted from the fluorescence value of fura-2/AM treated cells. The $[Ca^{2+}]_i$ was calculated from the fluorescence ratio ($R = F_{340}/F_{380}$), $[Ca^{2+}]_i = K_d \cdot (R - R_{min}) / (R_{max} - R)$. The dissociation constant (K_d) of 224 nmol/L was used for fura-2/AM. The maximum and minimum fluorescence value were determined after adding 10 % Triton-X100 and 5 mmol/L EGTA, respectively, in each sample.

To investigate the effect of pinaverium bromide on $[Ca^{2+}]_i$, cells were incubated for 20 min in HEPES buffer containing pinaverium (10^{-7} - 10^{-5} mol/L) before the stimulation of agonists.

Statistical analysis

All values were expressed as $\bar{x} \pm s$. Statistical analysis was done

by one-way analysis of variance and the Student's *t*-test for unpaired observations. $P < 0.05$ was considered statistically significant.

RESULTS

Defecation during stress

Cold-restraint stress significantly increased fecal pellet output. During 2 h, there were 2.40 ± 1.23 fecal pellets in the stressed rats vs 1.49 ± 1.04 in the control ($n = 45$ each, $P < 0.001$). In addition, stressed rats showed a higher incidence of poorly formed fecal pellets, which appeared to contain more fluid.

After the cold-restraint stress for 2 hours, there was no gastric ulcers in rats, and the histological examination on the colon showed that no inflammatory responses (erosion, ulcer, edema, petechia, *etc.*) were found.

Effect of stress on colonic contractility

In the Tyrode-Ringer solution, ACh or KCl induced colonic circular muscle contraction and produced increase in force. Contractility of muscle in the stress group was significantly higher than that in control group ($P < 0.05$) (Table 1).

Table 1 Contractile response to ACh and KCl in colonic circular muscle (mN/mm², $\bar{x} \pm s$)

	ACh (10^{-5} mol/L)	KCl (60 mmol/L)
Control	71.56 ± 19.36 ($n = 8$)	73.85 ± 13.08 ($n = 9$)
Stress	109.66 ± 34.42^a ($n = 8$)	119.54 ± 19.06^a ($n = 8$)

^a $P < 0.05$, vs control.

Effect of Pinaverium on smooth muscle contractility

Pinaverium bromide inhibited the contractile response to ACh or KCl in the control and stressed colonic circular muscle in a dose dependent manner. The IC_{50} value for inhibition of 10^{-5} mol/L ACh induced contraction in the stress group was 1.66×10^{-6} mol/L, and in the control was 0.91×10^{-6} mol/L. Effects of pinaverium on stressed colon were not significantly different from that in the control except for the effects of 3×10^{-6} mol/L and 10^{-5} mol/L. The inhibitory response at the maximum concentration of 3×10^{-5} mol/L pinaverium was 99.57 ± 0.62 % ($n = 8$) and 98.24 ± 1.92 % ($n = 7$), respectively, in the stress and the control group there was no significant difference between them ($P > 0.05$). Concentration-response curve was shown in Figure 1.

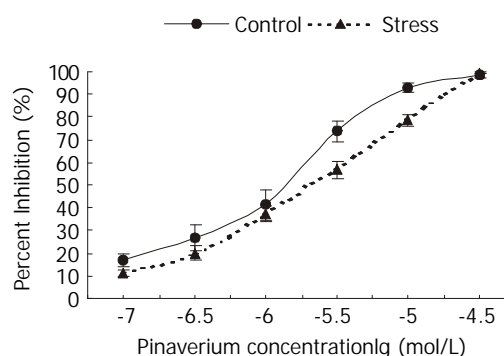


Figure 1 Effect of pinaverium on ACh-induced colonic circular muscle contraction. ^a $P < 0.05$, vs control.

The IC_{50} values for the inhibition of 60 mmol/L KCl induced contraction in the stress group and control group were 8.13×10^{-7} mol/L, and 3.80×10^{-7} mol/L, respectively. Effects of pinaverium on stressed colon were significantly different from

that in the control at 3×10^{-7} mol/L and 10^{-6} mol/L. The inhibitory response of pinaverium at 3×10^{-5} mol/L was 99.68 ± 0.44 % and 99.54 ± 0.65 %, respectively, in the stress and the control group there was no significant difference between them ($P > 0.05$). It was shown in Figure 2.

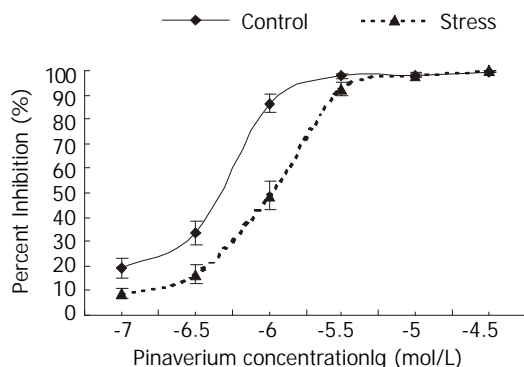


Figure 2 Effect of pinaverium on KCl-induced colonic circular muscle contraction. ^a $P < 0.05$, vs control.

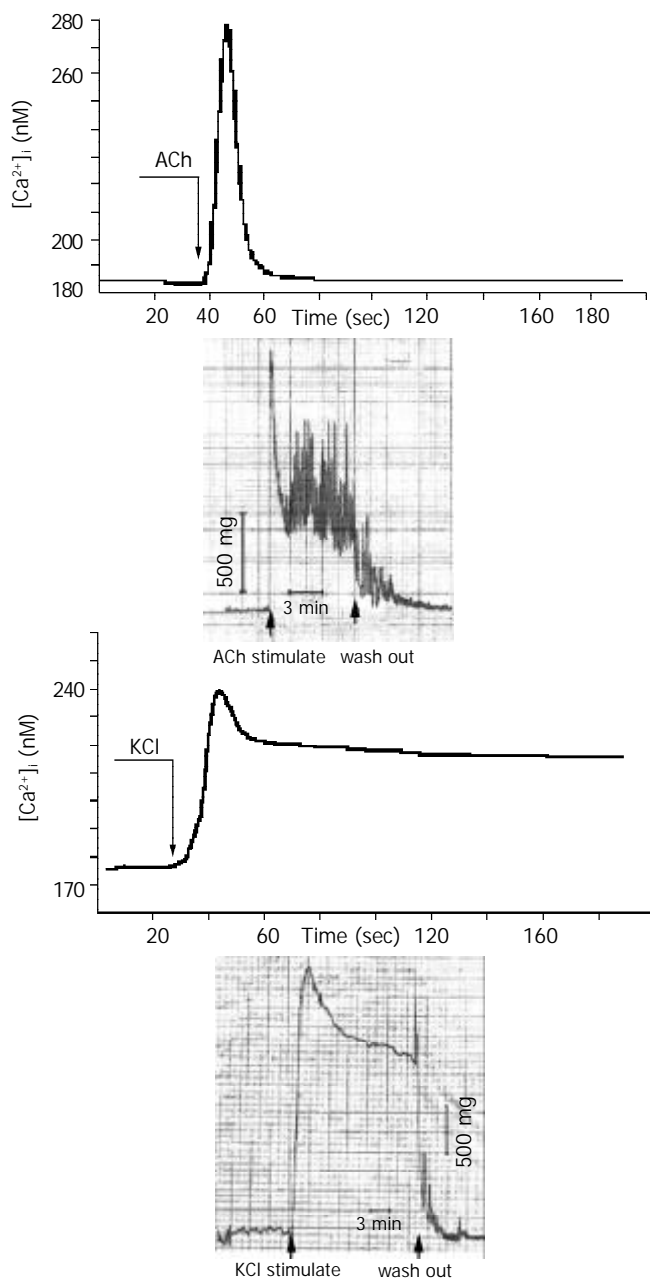


Figure 3 Effect of ACh and KCl on $[Ca^{2+}]_i$ and contraction of colonic smooth muscle.

Effect of Pinaverium on $[Ca^{2+}]_i$

ACh at 10^{-5} mol/L evoked a rapid increase in $[Ca^{2+}]_i$ that reached a peak in 10-15 s (Figure 3A). Similarly, 60 mmol/L KCl increased $[Ca^{2+}]_i$ in colonic muscle cells, the peak $[Ca^{2+}]_i$ was reached at 15-20 s (Figure 3B). Figure 3 also showed that the force of contraction in colonic muscle had no linear relationship with $[Ca^{2+}]_i$, and both velocity and amplitude of $[Ca^{2+}]_i$ increment in contraction were directly related to the force generation.

Pinaverium inhibited the increment of $[Ca^{2+}]_i$ in response to ACh or KCl in a dose dependent manner. A significant inhibition to 10^{-5} mol/L ACh or 60 mM KCl was observed at 10^{-6} mol/L pinaverium, as expressed in Table 2.

Table 2 Effect of pinaverium bromide on the increment of $[Ca^{2+}]_i$ ($\Delta [Ca^{2+}]_i$) in response to ACh and KCl (nmol/L, $\bar{x} \pm s$)

Concentration of pinaverium (mol/L)	ACh (10^{-5} mol/L) (n=7)	KCl (60 mmol/L) (n=6)
0	94.78 ± 15.99	64.61 ± 8.06
10^{-7}	83.57 ± 13.54	55.73 ± 17.39
10^{-6}	34.73 ± 13.98^a	41.71 ± 1.61^a
10^{-5}	27.09 ± 5.64^a	40.34 ± 10.96^a

Figures in this table are the increment of $[Ca^{2+}]_i$ in response to ACh and KCl. $\Delta [Ca^{2+}]_i = [Ca^{2+}]_i \text{ After (ACh, KCl) stimulated} - [Ca^{2+}]_i \text{ Before (ACh, KCl) stimulated}$. ^a $P < 0.05$, vs pinaverium 0 mmol/L.

DISCUSSION

Different types of stresses play important roles in the onset and modulation of IBS symptoms^[12-18]. Our results showed that cold-restraint stress significantly increased fecal pellet output in rats; which appeared to be the results of an increased colonic motility. There was no gastric ulcer or histological changes on the colon in the model of stressed rats, so it was an appropriate animal model to investigate the functional intestinal dysmotility such as IBS. In vitro studies using colonic smooth muscle strips obtained from rats showed that stress was accompanied by an increase in the contractility of muscle, it may be the reason for the colonic dysmotility.

Abnormal contraction of intestinal smooth muscle may be important in the pathology of IBS symptoms, thus, modifying the contractility is often the major aim in treating IBS^[6,7,19]. A new approach to such disorder is based on the fact that Ca^{2+} is involved in the mechanism of excitation-contraction coupling, which directly or indirectly controls the contractility of smooth muscle^[44]. $[Ca^{2+}]_i$ regulates the contractile state of smooth muscle; increase of $[Ca^{2+}]_i$ is the primary stimulus for contraction^[20-22]. Elevation of $[Ca^{2+}]_i$ in contraction is accomplished by Ca^{2+} entry from extracellular and/or intracellular release of Ca^{2+} from sarcoplasmic reticulum. Between these two Ca^{2+} mobilization pathways, Ca^{2+} influx from extracellular plays a major role in the contraction of colonic smooth muscle^[23-29,34]. L-type voltage-dependent Ca^{2+} channel represents the main route of entry of inward Ca^{2+} current that is gated by potential in smooth muscle cells, particularly in the gastrointestinal tract. Thus, activation of Ca^{2+} channel represents the final 'common path' of all mechanisms that regulate muscle contractility^[32,36]. So important are these mechanisms in regulating $[Ca^{2+}]_i$ and the contractile state of smooth muscle that minor defects in function can greatly affect the mechanical activity of colon^[11,30,31,33].

In this study, we investigated the contractile response to KCl and ACh in colonic circular smooth muscle in rats. KCl can induce depolarization of the plasma membrane, activate the voltage-dependent Ca^{2+} channel (dihydropyridine-sensitive L-type Ca^{2+} channel), which results in increase of $[Ca^{2+}]_i$ and

force generation. ACh is one of the most important neurotransmitters in gastrointestinal. ACh can activate Muscarinic M_2 receptors, then non-selective cation channels (NSCC) will be opened. The amount of Ca^{2+} entry through NSCC is controversial, but these channels yield depolarization that activates L-type Ca^{2+} channels, Ca^{2+} entering cells^[25].

We found that the force of contraction in colonic muscle was related nonlinearly to $[Ca^{2+}]_i$; however both velocity and amplitude of $[Ca^{2+}]_i$ increment in muscle cells were directly related to the force generation. Pinaverium bromide is a L-type calcium channel blocker with selectivity for the gastrointestinal used in the treatment of IBS^[37,38,42]. Our work demonstrated that pinaverium inhibited both neurohormonal (ACh) and depolarization (KCl)-induced increment of $[Ca^{2+}]_i$ and contraction of colonic circular muscle in a dose dependent manner. The contractile responses were almost completely blocked at the maximum concentration of 3×10^{-5} mol/L pinaverium, which indicated that repaid influx of Ca^{2+} through L-type calcium channels played a major role in contractions of colon. Pinaverium acted on colonic muscle, and reduced the plateau phase of slow wave, thereby inhibited influx of Ca^{2+} , abolished the accompanying contractile activity^[32]. In normal Ca^{2+} -contain buffer, the contractile responses to ACh and KCl were significantly increased in stress group than those in control group which indicated that more the contractile response was depended on extracellular Ca^{2+} in the stress state and that influx of Ca^{2+} through the cell membrane was increased.

The IC_{50} values (deduced from the concentration-response curves) for inhibition of ACh or KCl induced contraction in the stress group were higher than those in the control group, indicated that increased contractility of stressed colon may in part be due to the increased Ca^{2+} influx through the L-type channels.

Our experiments in insolated circular smooth muscle from rats demonstrated that alterations of the muscle calcium-handling properties was responsible for the increased contractility in colon. However, the precise contribution of these pathways in the intact conscious state can only be speculated. The colonic circular muscle of rat can generate three distinct types of contractions: rhythmic phasic contractions, giant migrating contractions and tone. The amplitudes, durations and motility functions of these contractions differ widely. Because Ca^{2+} is a critical second messenger in the contraction of these cells and the amplitude and duration of cell contraction are correlated with $[Ca^{2+}]_i$, it is likely that the three types of contractions would utilize Ca^{2+} sources differently. The increase of Ca^{2+} influx through L-type channels may be the reason why colonic smooth muscle exhibits hypermotility during stress.

Our study shows that increase of $[Ca^{2+}]_i$ in smooth muscle cells is directly related to the generation of contraction force in colon. L-type Ca^{2+} channels represent the main route of Ca^{2+} entry. Colonic circular muscle hypermotility in rats induced by cold-restraint stress is the result of an increased influx of extracellular Ca^{2+} through L-type Ca^{2+} channels. These studies provide a rationale for the use of pinaverium bromide in the treatment of colonic motor disorders (such as IBS) where excessive contraction need to be suppressed.

REFERENCES

- Janssen HA, Muris JW, Knotterus JA. The clinical course and prognostic determinants of the irritable bowel syndrome: a literature review. *Scand J Gastroenterol* 1998; **33**: 561-567
- Camilleri M. Motor function in irritable bowel syndrome. *Can J Gastroenterol* 1999; **13**: 8A-11A
- Ringel Y, Sperber AD, Drossman DA. Irritable bowel syndrome. *Annu Rev Med* 2001; **52**: 319-338
- Drossman DA. Review article: an integrated approach to the irritable bowel syndrome. *Aliment Pharmacol Ther* 1999; **13**: 3-14
- Collins SM. Peripheral mechanisms of symptom generation in irritable bowel syndrome. *Can J Gastroenterol* 2001; **15**: 14B-16B
- Camilleri M. Review article: clinical evidence to support current therapies of irritable bowel syndrome. *Aliment Pharmacol Ther* 1999; **13**: 48-53
- Camilleri M. Management of the irritable bowel syndrome. *Gastroenterology* 2001; **120**: 652-668
- Lu CL, Chen CY, Chang FY, Chang SS, Kang LJ, Lu RH, Lee SD. Effect of a calcium channel blocker and antispasmodic in diarrhoea-predominant irritable bowel syndrome. *J Gastroenterol Hepatol* 2000; **15**: 925-930
- Bouchoucha M, Faye A, Devroede G, Arsac M. Effect of oral pinaverium bromide on colonic response to food in irritable bowel syndrome patients. *Biomed Pharmacother* 2000; **54**: 381-387
- Scarpignato C, Pelosini I. Management of irritable bowel syndrome: novel approaches to the pharmacology of gut motility. *Can J Gastroenterol* 1999; **13**: 50A-65A
- Shi XZ, Sarna SK. Impairment of Ca^{2+} mobilization in circular muscle cells of the inflamed colon. *Am J Physiol Gastrointest Liver Physiol* 2000; **278**: G234-242
- Mayer EA, Naliboff BD, Chang L, Coutinho SV. Stress and the Gastrointestinal Tract V. Stress and irritable bowel syndrome. *Am J Physiol Gastrointest Liver Physiol* 2001; **280**: G519-524
- Plourde V. Stress-induced changes in the gastrointestinal motor system. *Can J Gastroenterol* 1999; **13**: 26A-31A
- Delvaux MM. Stress and visceral perception. *Can J Gastroenterol* 1999; **13**: 32A-36A
- Bennett EJ, Tennant CC, Piesse C, Badcock CA, Kellow JE. Level of chronic life stress predicts clinical outcome in irritable bowel syndrome. *Gut* 1998; **43**: 256-261
- Tache Y, Martinez V, Million M, Rivier J. Corticotropin-releasing factor and the brain-gut motor response to stress. *Can J Gastroenterol* 1999; **13**: 18A-25A
- Drossman DA, Creed FH, Olden KW, Svedlund J, Toner BB, Whitehead WE. Psychosocial aspects of the functional gastrointestinal disorders. *Gut* 1999; **45**: II25-II30
- Aziz Q, Thompson DG. Brain-gut axis in health and disease. *Gastroenterology* 1998; **114**: 559-578
- De Schryver AMP, Samsom M. New developments in the treatment of irritable bowel syndrome. *Scand J Gastroenterol* 2000; **35**: 38-42
- Li JX, Liu XG, Xie PY, Gu Q, Li J, Zhang Y, Tang CS. The regulation of calcium in the movement of colonic smooth muscle in wrap restraint stress rats. *Zhonghua Neike Zazhi* 2000; **39**: 588-591
- Sanders KM. Invited review: mechanisms of calcium handling in smooth muscles. *J Appl Physiol* 2001; **91**: 1438-1449
- Bolton TB, Prestwich SA, Zholos AV, Gordienko DV. Excitation-contraction coupling in gastrointestinal and other smooth muscles. *Annu Rev Physiol* 1999; **61**: 85-115
- Gibson A, McFadzean I, Wallace P, Wayman CP. Capacitative Ca^{2+} entry and the regulation of smooth muscle tone. *Trends Pharmacol Sci* 1998; **19**: 266-269
- McCarron JG, Flynn ERM, Bradley KN, Muir TC. Two Ca^{2+} entry pathways mediate $InsP_3$ -sensitive store refilling in guinea-pig colonic smooth muscle. *J Physiol* 2000; **525**(Pt 1): 113-124
- Eglen RM. Muscarinic receptor and gastrointestinal tract smooth muscle function. *Life Sci* 2001; **68**: 2573-2578
- Bolton TB, Gordienko DV. Confocal imaging of calcium release events in single smooth muscle cells. *Acta Physiol Scand* 1998; **164**: 567-575
- Young SH, Ennes HS, McRoberts JA, Chaban VV, Dea SK, Mayer EA. Calcium waves in colonic myocytes produced by mechanical and receptor-mediated stimulation. *Am J Physiol* 1999; **276**: G1204-1212
- Petkov GV, Boev KK. Control of the phasic and tonic contractions of guinea pig stomach by a ryanodine-sensitive Ca^{2+} store. *Eur J Pharmacol* 1999; **367**: 335-341
- Henkel CC, Asbun J, Ceballos G, Castillo MC, Castillo EF. Relationship between extra and intracellular sources of calcium and the contractile effect of thiopental in rat aorta. *Can J Physiol Pharmacol* 2001; **79**: 407-414
- Mule F, Serio R. Increased calcium influx is responsible for the sustained mechanical tone in colon from dystrophic (mdx) mice. *Gastroenterology* 2001; **120**: 1430-1437

- 31 **Sarna SK.** *In vivo* signal-transduction pathways to stimulate phasic contractions in normal and inflamed ileum. *Am J Physiol* 1998; **274**: G618-625
- 32 **Boyer JC,** Magous R, Christen MO, Balmes JL, Bali JP. Contraction of human colonic circular smooth muscle cells is inhibited by the calcium channel blocker pinaverium bromide. *Cell Calcium* 2001; **29**: 429-438
- 33 **Khan I.** Molecular basis of altered contractility in experimental colitis: expression of L-type calcium channel. *Dig Dis Sci* 1999; **44**: 1525-1530
- 34 **Niu WX,** Qin XY, Lu YQ, Shi NC, Wang CP. Role of intracellular calcium in contraction of internal anal sphincter. *World J Gastroenterol* 1999; **5**: 183-184
- 35 **Leahy A,** Epstein O. Non-pharmacological treatments in the irritable bowel syndrome. *World J Gastroenterol* 2001; **7**: 313-316
- 36 **Morel N,** Buryi V, Feron O, Gomez JP, Christen MO, Godfraind T. The action of calcium channel blockers on recombinant L-type calcium channel $\alpha 1$ -subunits. *Br J Pharmacol* 1998; **125**: 1005-1012
- 37 **Jayanthi V,** Malathi S, Ramathilakam B, Dinakaran N, Balasubramanian V, Mathew S. Role of pinaverium bromide in south Indian patients with irritable bowel syndrome. *J Assoc Physicians India* 1998; **46**: 369-371
- 38 **Poynard T,** Regimbeau C, Benhamou Y. Meta-analysis of smooth muscle relaxants in the treatment of irritable bowel syndrome. *Aliment Pharmacol Ther* 2001; **15**: 355-361
- 39 **Xie DP,** Li W, Qu SY, Zheng TZ, Yang YL, Ding YH, Wei YL, Chen LB. Effect of areca on contraction of colonic muscle strips in rats. *World J Gastroenterol* 2002; **8**: 350-352
- 40 **Li W,** Zheng TZ, Qu SY. Effect of cholecystokinin and secretin on contractile activity of isolated gastric muscle strips in guinea pigs. *World J Gastroenterol* 2000; **6**: 93-95
- 41 **Zheng TZ,** Li W, Qu SY, Ma YM, Ding YH, Wei YL. Effects of Dangshen on isolated gastric muscle strips in rats. *World J Gastroenterol* 1998; **4**: 354-356
- 42 **Villanueva A,** Dominguez-Munoz JE, Mearin F. Update in the therapeutic management of irritable bowel syndrome. *Dig Dis* 2001; **19**: 244-250
- 43 **Cole SJ,** Duncan HD, Claydon AH, Austin D, Bowling TE, Silk DB. Distal colonic motor activity in four subgroups of patients with irritable bowel syndrome. *Dig Dis Sci* 2002; **47**: 345-355
- 44 **Wang XJ,** Wei JG, Wang CM, Wang YC, Wu QZ, Xu JK, Yang XX. Effect of cholesterol liposomes on calcium mobilization in muscle cells from the rabbit sphincter of Oddi. *World J Gastroenterol* 2002; **8**: 144-149

Edited by Xu XQ

Role of mitochondrial dysfunction in hydrogen peroxide-induced apoptosis of intestinal epithelial cells

Jian-Ming Li, Hong Zhou, Qian Cai, Guang-Xia Xiao

Jian-Ming Li, Hong Zhou, Qian Cai, Guang-Xia Xiao, Institute of Burn Research, Southwest Hospital, Third Military Medical University, Chongqing 400038, China

Supported by the Special Funds for Major State Basic Research of China, No.G1999054202

Correspondence to: Professor Hong Zhou, Institute of Burn Research, Southwest Hospital, Third Military Medical University, Chongqing 400038, China. zhoh64@mail.tmmu.com.cn

Received: 2002-01-11 **Accepted:** 2002-03-05

Abstract

AIM: To study the role of mitochondrial dysfunction in hydrogen peroxide-induced apoptosis of intestinal epithelial cells.

METHODS: Hydrogen peroxide-induced apoptosis of human intestinal epithelial cell line SW-480 was established. Cell apoptosis was determined by Annexin-V and PI double-stained flow cytometry and DNA gel electrophoresis. Morphological changes were examined with light and electron microscopy. For other observations, mitochondrial function, cytochrome c release, mitochondrial translocation and membrane potential were determined simultaneously.

RESULTS: Percentage of apoptotic cells induced with 400 $\mu\text{mol/L}$ hydrogen peroxide increased significantly at 1 h or 3 h after stimulation and recovered rapidly. Meanwhile percentage of apoptotic cells induced with 4 mmol/L hydrogen peroxide increased with time. In accordance with these changes, we observed decreased mitochondrial function in 400 $\mu\text{mol/L}$ H_2O_2 -stimulated cells at 1 h or 3 h and in 4 mmol/L H_2O_2 -stimulated cells at times examined. Correspondingly, swelling cristae and vacuole-like mitochondria were noted. Release of cytochrome c, decreased mitochondrial membrane potential and mitochondrial translocation were also found to be the early signs of apoptosis.

CONCLUSION: Dysfunctional mitochondria play a role in the apoptosis of SW-480 cell line induced by hydrogen peroxide.

Li JM, Zhou H, Cai Q, Xiao GX. Role of mitochondrial dysfunction in hydrogen peroxide-induced apoptosis of intestinal epithelial cells. *World J Gastroenterol* 2003; 9(3): 562-567
<http://www.wjgnet.com/1007-9327/9/562.htm>

INTRODUCTION

Hidden injuries of gut during the early stage of severe burn may contribute to early translocation of bacteria or its endotoxin. Although the mechanisms of gut barrier dysfunction postburn are unclear^[1-10], evidences recently indicate that apoptosis of intestinal epithelial cells after thermal injury may be one of possible factors leading to gut barrier dysfunction^[11,12]. Apoptosis of intestinal epithelial cells induced by excessive reactive oxygen

species released by activated polymorphonuclear leukocytes and vascular endothelial cells plays a role in the pathogenesis of dysfunction of intestinal mucosa. Besides, the role of mitochondrion in the development of apoptosis has been emphasized recently^[13]. We have found that differential expression of mitochondrial genes encoding cytochrome c oxidase and ATPase was involved in apoptosis of intestinal epithelial cells by affecting activities of cytochrome c oxidase and ATPase^[14]. So mitochondrial dysfunction may contribute to the apoptosis of intestinal epithelial cells. In the present study, possible relationship between mitochondrial dysfunction and apoptosis was studied in hydrogen peroxide-induced apoptosis model of SW-480 cells.

MATERIALS AND METHODS

Cell line and culture

Human intestinal epithelial cell line SW-480 stored routinely in our laboratory was cultured in RPMI1640 supplemented with 10 % (V/V) heat-inactivated newborn calf serum (Hyclone), 100 units/ml of penicillin, 0.1 mg/ml streptomycin and 2 mM L-glutamine at 37 °C in a humidified 5 % CO_2 incubator. Confluent cells were prepared for further studies.

Treatment

Experimental cells were treated with 4 mmol/L or 400 $\mu\text{mol/L}$ hydrogen peroxide. Cells without stimulation by hydrogen peroxide were prepared as control.

Transmission electron microscopy

Samples were fixed, embedded and sectioned routinely. Ultrastructural changes of mitochondria were observed with transmission electron microscopy.

Assessment of apoptosis by Annexin-V and PI double-staining flow cytometry

Annexin-V and PI double staining kit (Roche) was used to assess apoptosis in hydrogen peroxide-stimulated SW-480 cells. Ten thousands of cells were counted, and data acquisition and analysis were performed in a Becton Dickinson FACS-can flow cytometer using the CellQuest software.

DNA fragmentation analysis

The DNA fragmentation pattern (DNA ladder) was demonstrated by agarose gel electrophoresis described previously^[15].

Determination of cytochrome c release by cell immunocytochemistry

Cells were grown on glass cover slips. After treated with 4 mmol/L or 400 $\mu\text{mol/L}$ hydrogen peroxide, samples were fixed in 10 % neutral formaldehyde solution for 30 min with PBS rinsing for several times. Then, cells were stained by overnight incubation with 100-fold diluted rabbit anti-human cytochrome c polyclonal antibody (Oncogene) at 4 °C, followed by extensive washing with phosphate-buffered saline and a 30 min incubation with biotin-binding goat anti-rabbit antibody. After another 30 min incubation with horseradish peroxidase conjugated ovalbumin, the specimens were colorized and photographed.

MTT assay

Mitochondrial function was assessed by MTT (3, (4,5-dimethylthiazol-2-yl) 2, 5-diphenyltetrazolium bromide) assay as described previously^[16]. Cells were cultured in 96-well plates 5 000 cells for each well at 37 °C in a humidified 5 % CO₂ incubator. Confluent cells were prepared for further studies. After treated with hydrogen peroxides and washed with phosphate-buffered saline, cells were incubated with MTT (2 µg/ml, Sigma) and RPMI1640 medium without serum at 37 °C for 1 h and dissolved with dimethyl sulfoxide. The absorbance at 570nm, which represented the total mitochondrial function, was recorded.

Measurement of mitochondrial membrane potential

Cells were grown on glass cover slips. After treated with 4 mmol/L or 400 µmol/L hydrogen peroxide, cells were incubated with Rhodamine 123 (1 µmol/L, Molecular probe) and RPMI1640 medium without serum at 37 °C for 30 min, fluorescence intensity was determined by confocal microscope (Leica) with fixed parameters, cells in three random-selected visual fields from each group were scanned and analysed.

Mitochondrial translocation assay

As described previously, cells were seeded in chambered cover slips and preincubated overnight at 37 °C in a humidified 5 % CO₂ air incubator. After the cells were treated with hydrogen peroxide, mitochondria were stained with Rhodamine 123 for 30 min at 37 °C before analysis. The distribution of mitochondria was analyzed with a Zeiss TSTN confocal microscope^[17].

Statistical analysis

Data were summarized as mean ±SD. Student's *t* test was used for multiple comparisons between groups. *P* values less than 0.05 were considered to be statistically significant.

RESULTS

Effects of hydrogen peroxide on apoptosis of SW-480 cells

Percentage of apoptotic cells induced with 400 µmol/L hydrogen peroxide increased significantly at 1 h or 3 h after stimulation and recovered rapidly. Meanwhile percentage of apoptotic cells induced with 4 mmol/L hydrogen peroxide increased with the time, which indicated that the irreversible changes had taken place (Table 1).

Table 1 Percentage of apoptotic cells induced with hydrogen peroxide at different time after stimulation

Group	0 h	1 h	3 h	6 h	12 h	24 h
400 µmol/L	10.93±0.63	19.47±0.36 ^a	19.81±1.82 ^a	12.32±1.67	13.61±1.24	12.72±0.72
4 mmol/L	10.93±0.63	20.84±1.47 ^a	32.25±1.37 ^a	39.48±4.26 ^a	57.91±9.82 ^a	69.05±11.62 ^a

^a*P*<0.05 vs preceding time point (0 h).

Table 2 MTT absorbance (570nm) of SW-480 cells stimulated by hydrogen peroxide

Group	1 h	3 h	6 h	12 h	24 h
Control	1.971±0.101	1.996±0.013	1.867±0.008	2.087±0.126	2.189±0.178
4mmol/L	0.864±0.116 ^a	0.756±0.023 ^a	0.612±0.006 ^a	0.518±0.035 ^a	0.373±0.043 ^a
400mmol/L	1.588±0.005	1.277±0.300 ^a	1.778±0.098	1.599±0.214	1.899±0.031
200mmol/L	1.626±0.262	1.914±0.046	1.941±0.032	1.787±0.033	1.962±0.149
100mmol/L	1.683±0.070	1.973±0.048	1.933±0.094	1.901±0.097	2.079±0.081
50mmol/L	1.865±0.122	1.974±0.080	2.077±0.077	1.876±0.053	1.922±0.048

^a*P*<0.05 vs control at corresponding time point.

DNA fragmentation analysis

DNA ladder in both 4 mmol/L and 400 µmol/L H₂O₂-stimulated groups were clearly observed by DNA fragmentation assay at 1h or 3h after stimulation (Figure 1).

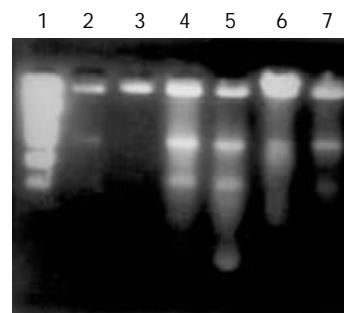


Figure 1 Hydrogen peroxide induced apoptosis of SW-480 cells. 1: PBR322/Hinf I (75, 154, 220, 221, 298, 344, 396, 504, 517, 1632); 2, 3: cells from normal control; 4: 4 mmol/L H₂O₂-stimulated cells (1 h); 5: 4 mmol/L H₂O₂-stimulated cells (3h); 6: 400 µmol/L H₂O₂-stimulated cells (1 h) 7: 400 µmol/L H₂O₂-stimulated cells (3 h).

MTT assay

The MTT assay is based on the conversion of MTT (light yellow) to formazan (blue) by the mitochondrial enzyme succinate dehydrogenase and has been widely used as an indicator of cellular respiration and viability^[3]. We observed decreased mitochondrial function in 400 µmol/L H₂O₂-stimulated cells at 1 h or 3 h after stimulation and in 4 mmol/L H₂O₂-stimulated cells at times examined (Table 2). Interestingly, these changes were in accordance with the apoptosis induced by hydrogen peroxide.

Ultrastructural changes of mitochondria

Swelling cristae and vacuole-like mitochondria were found in hydrogen peroxide -treated cells.

Translocation of mitochondria

Mitochondria were observed to be evolved from an originally scattered, bipolar and nearly symmetric distribution to the asymmetric clustered state in the majority of cells treated with H₂O₂ (Figure 2).

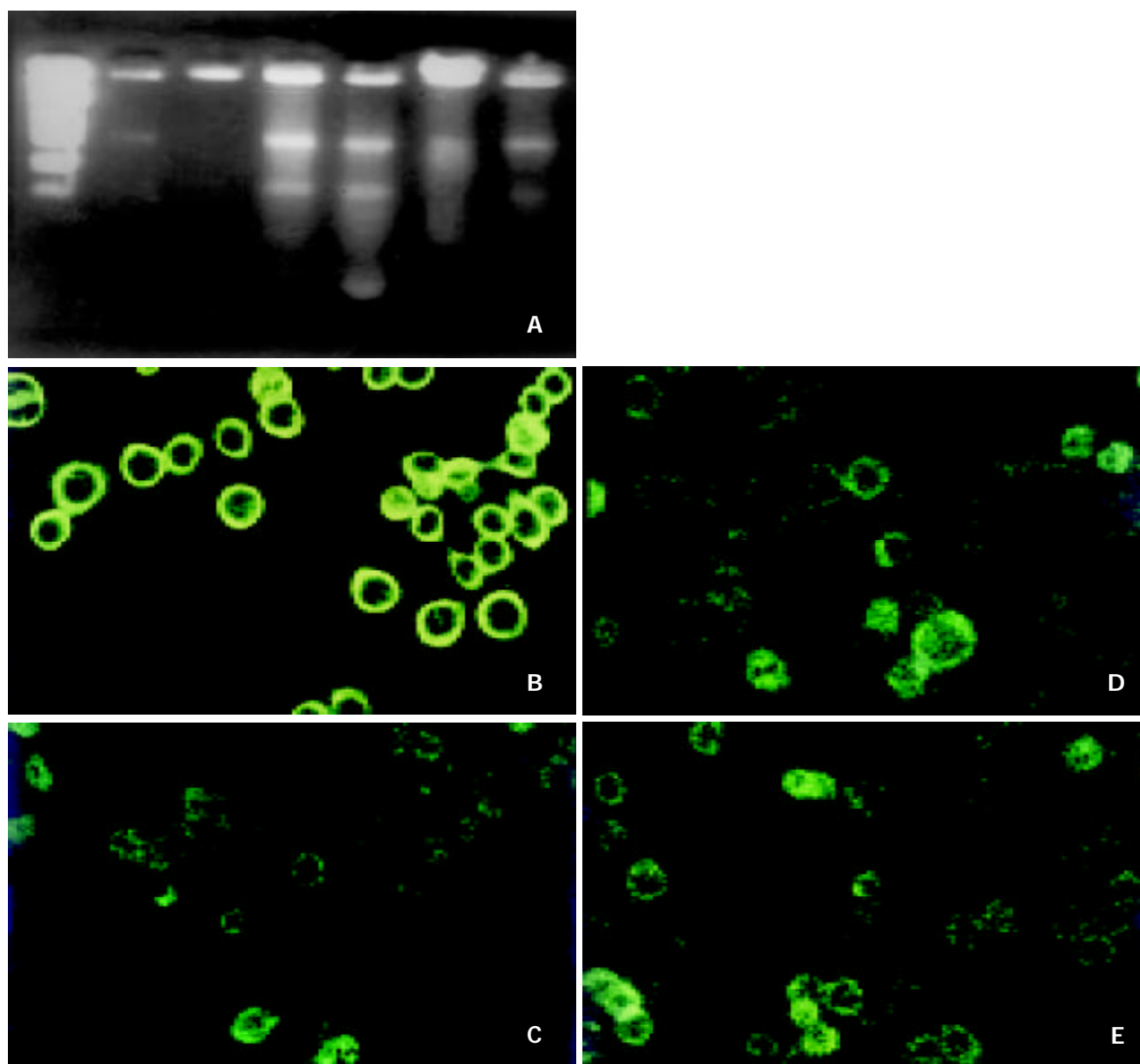


Figure 3a Changes of mitochondrial membrane potential induced by hydrogen peroxide. (A) cells from normal control; (B) 400 $\mu\text{mol/L}$ H_2O_2 -stimulated cells (1 h); (C) 400 $\mu\text{mol/L}$ H_2O_2 -stimulated cells (3 h); (D) 4 mmol/L H_2O_2 -stimulated cells (1h); (E) 4 mmol/L H_2O_2 -stimulated cells (3 h).

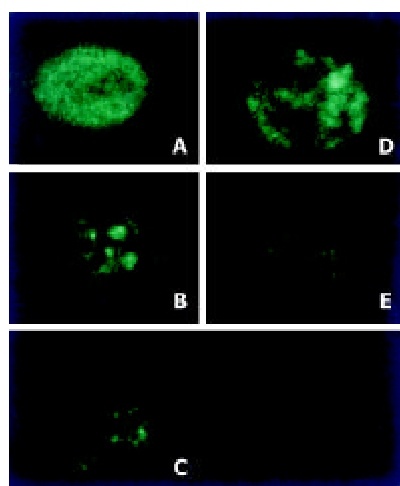


Figure 2 Hydrogen peroxide induced translocation of mitochondria. (A) cells from normal control; (B) 400 $\mu\text{mol/L}$ H_2O_2 -stimulated cells (1 h). (C) 400 $\mu\text{mol/L}$ H_2O_2 -stimulated cells (3 h); (D) 4 mmol/L H_2O_2 -stimulated cells (1 h); (E) 4 mmol/L H_2O_2 -stimulated cells (3 h).

Changes of mitochondrial membrane potential induced by hydrogen peroxide

Decreased mitochondrial membrane potential was observed in cells at 3 h after 400 $\mu\text{mol/L}$ H_2O_2 stimulation and at 1h after 4 mmol/L H_2O_2 treatment (Figure 3a, 3b).

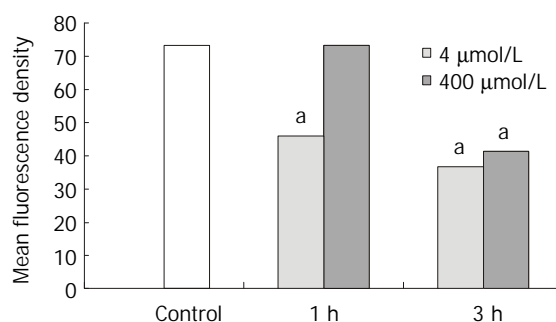


Figure 3b Effects of hydrogen peroxide on mitochondrial membrane potential of SW-480 cells (^a $P < 0.05$ vs control).

Cytochrome c Release

Cytochrome c release could be found in both 400mmol/L and 4mmol/L H₂O₂-stimulated cells 30 min after stimulation by immunochemistry assay (Figure 4).

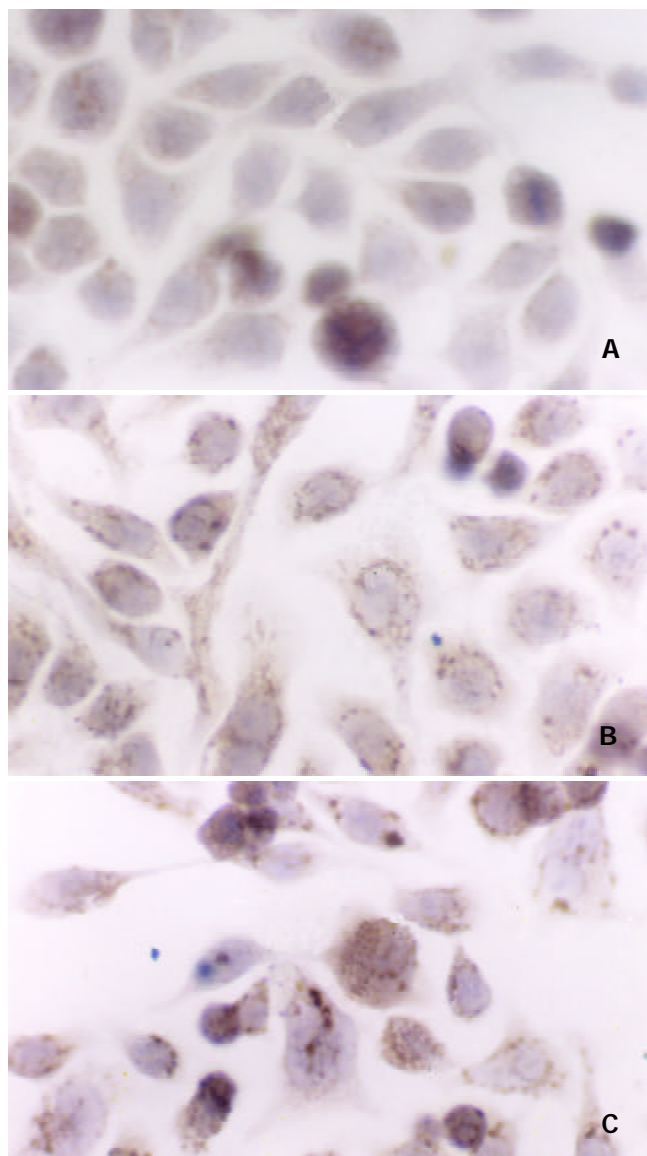


Figure 4 Cytochrome c release in SW-480 cells induced by hydrogen peroxide (S-P×400). A: control cells, B: 400 μmol/L H₂O₂-treated cells (30 min), C: 4 mmol/L H₂O₂-treated cells (30 min).

DISCUSSION

Metabolism of intestinal mucosal epithelium is so active that it is very sensitive to changes of energy supplies in normal conditions^[11]. Many researches have demonstrated that gut is a sensitive organ to be injured postburn^[18-22]. Intestinal mucosal injury can be caused by excessive reactive oxygen species (ROS) released by polymorphonuclear leukocytes and vascular endothelial cells, which is also involved in translocation of intestinal bacteria and its endotoxin.

Our results showed that hydrogen peroxide could lead to injuries of intestinal epithelial cells in the concentration of both 400 μmol/L and 4 mmol/L. From the results of DNA ladders and flow cytometry, apoptosis could be considered one of the main mechanisms for the injury. This indicated that the *in vitro* model of hydrogen peroxide-stimulated SW-480 cells used in the present study could be used to investigate mitochondrial dysfunction in apoptosis of intestinal epithelial cells, and it

also might be helpful to study the role of mitochondria in ROS-induced injuries of intestinal epithelial cells and to clarify mechanism of gut barrier dysfunction.

Role of mitochondria in the pathogenesis of apoptosis has been well defined^[23-27]. Mitochondria, a kind of organelle controlling growing, breeding and dying of eukaryocyte, perform their functions by production of ATP, production of ROS, ROS are also known as signals regulating gene expression and triggering of cell death^[28,29]. Many stimulators like ROS, Ca²⁺ and cytokines could activate caspases by inducing cytochrome c release.

Our results showed that the apoptotic cells were characterized with swelling or vacuole-like mitochondria. It was considered previously that the apoptotic cells manifested condensed chromatin but intact mitochondria. Now much more evidences found that significant changes of mitochondria such as swelling, megamitochondria^[30], mitochondrial pyknosis and disrupted out-membrane have been taken place in many apoptosis models^[31]. Mitochondrial pyknosis was characterized with decreased size and condensed matrix of mitochondria. In apoptotic model of sympathetic neuron triggered by nerve growth factor (NGF) deprivation, the transition from normal to condensed morphology could be reversible following readdition of NGF to the neuron culture^[25]. In addition, the mitochondrial distribution within cells was profoundly affected during apoptosis. Mitochondria were normally dispersed throughout the entire cell. However, during the apoptosis triggered by tumor necrosis factor (TNF-α) a perinuclear clustering of mitochondria could be observed. Both mitochondrial condensation and perinuclear clustering occurred following production of the Bcl-2-related proapoptotic protein Bax in many cell types^[25].

Evidence showed that the spatial distribution of mitochondria evolved from an originally scattered, bipolar or nearly symmetric distribution to an asymmetric, clustered distribution in the majority of the cells within 1 h of treatment of L929 cells with TNF^[17]. Study also indicated that hydrogen peroxide could not lead to the mitochondrial translocation as TNF did^[17]. Interestingly, we found that hydrogen peroxide could induce mitochondrial translocation and massive aggregation by confocal microscopy and 3-D reconstruction technique, which was accompanied by decrease of mitochondrial membrane potential. So our results suggested that mitochondrial translocation may play a role in reactive oxygen species (ROS)-induced injuries of intestinal epithelial cells. As some researches proposed, the condensation of mitochondria may play roles in the inducing of cytochrome c release, generating high ATP levels in energy dependent apoptotic events and facilitating the translocation of mitochondrial proteins to the nucleus. Its mechanism is still uncertain.

The mitochondrial transmembrane potential has been found to be decreased in many apoptosis models, which indicates the opening of a large conductance channel known as the mitochondrial PT pore^[32-36]. PT pore opening results in a volume dysregulation of mitochondria due to the hyperosmolality of the matrix, which causes the matrix space to be expanded. Because the mitochondrial inner membrane with its folded cristae possesses a larger surface area than the outer membrane, this matrix volume expansion can eventually cause the outer membrane rupture, releasing caspase-activating proteins located within the intermembrane space into the cytosol.

We observed that hydrogen peroxide could result in the collapse of mitochondrial membrane potential, if we related it with the release of cytochrome c, we may get the conclusion that hydrogen peroxide caused the release of cytochrome c from mitochondria to cytosol followed by the increased permeability mitochondrial membrane and the opening of mitochondrial

PT pore, which initiated cascade reaction of apoptosis events. This idea has been confirmed by some studies^[37,38].

Recent progress in studies on apoptosis has revealed that cytochrome c is a pro-apoptotic factor^[39]. It is released from its places on the outer surface of the inner mitochondrial membrane at early steps of apoptosis and, combining with some cytosolic proteins, activates conversion of the latent apoptosis-promoting protease pro-caspase-9 to its active form^[39]. Our results also indicated that cytochrome c was released early in hydrogen peroxide-stimulated SW-480 cells.

Our results found that the morphological and functional changes of mitochondria appeared in SW-480 cells treated with hydrogen peroxide and correlated with development of cell apoptosis. Decreased mitochondrial membrane potential or early release of cytochrome c would be the early signs of apoptosis, which suggested mitochondrial dysfunction might be the key event in the development of apoptosis. We also observed mitochondrial translocation, which was reported in TNF-stimulated L929 cells but not in hydrogen peroxide-stimulated cells^[33]. Mitochondrial translocation suggested that cytoskeleton be involved in apoptosis induced by hydrogen peroxide.

Many researches indicated that oxidative stress led to mutation of mitochondrial genes^[40-50]. Researches showed that there are some links between mitochondrial dysfunction and injuries of mitochondrial DNA or abnormal expression of mitochondrial genes in hydrogen peroxide-stimulated vascular endothelial cells and smooth muscle cells^[50]. Our results also indicated that mitochondrial genes were involved in apoptosis of SW-480 cells. Injuries of mitochondrial genes may contribute to early mitochondrial dysfunction. Relationship between response of mitochondrial genes and dysfunctional mitochondria would be the next problem to be answered.

REFERENCES

- Zuo GQ**, Gong JP, Liu CA, Li SW, Wu XC, Yang K, Li Y. Expression of lipopolysaccharide binding protein and its receptor CD14 in experimental alcoholic liver disease. *World J Gastroenterol* 2001; **7**: 836-840
- Meng AH**, Ling YL, Zhang XP, Zhao XY, Zhang JL. CCK-8 inhibits expression of TNF- α in the spleen of endotoxic shock rats and signal transduction mechanism of p38 MAPK. *World J Gastroenterol* 2002; **8**: 139-143
- Wu RQ**, Xu YX, Song XH, Chen LJ, Meng XJ. Relationship between cytokine mRNA expression and organ damage following cecal ligation and puncture. *World J Gastroenterol* 2002; **8**: 131-134
- Li SW**, Gong JP, Wu CX, Shi YJ, Liu CA. Lipopolysaccharide induced synthesis of CD14 proteins and its gene expression in hepatocytes during endotoxemia. *World J Gastroenterol* 2002; **8**: 124-127
- Yu PW**, Xiao GX, Qin XX, Zhou LX, Wang ZQ. The effects of PAF antagonist on intestinal mucosal microcirculation after burn in rats. *World J Gastroenterol* 2000; **6**: 906-908
- Qin RY**, Zou SQ, Wu ZD, Qiu FZ. Influence of splanchnic vascular infusion on the content of endotoxins in plasma and the translocation of intestinal bacteria in rats with acute hemorrhage necrosis pancreatitis. *World J Gastroenterol* 2000; **6**: 577-580
- Wang QG**, He LY, Chen YW, Hu SL. Enzymohistochemical study on burn effect on rat intestinal NOS. *World J Gastroenterol* 2000; **6**: 421-423
- Fu XB**, Yang YH, Sun TZ, Gu XM, Jiang LX, Sun XQ, Sheng ZY. Effect of intestinal ischemia-reperfusion on expressions of endogenous basic fibroblast growth factor and transforming growth factor betain lung and its relation with lung repair. *World J Gastroenterol* 2000; **6**: 353-355
- Fu WL**, Xiao GX, Yue XL, Hua C, Lei MP. Tracing method study of bacterial translocation *in vivo*. *World J Gastroenterol* 2000; **6**: 153-155
- Yang YH**, Fu XB, Sun TZ, Jiang LX, Gu XM. bFGF and TGF β expression in rat kidneys after ischemic/ reperfusional gut injury and its relationship with tissue repair. *World J Gastroenterol* 2000; **6**: 147-149
- Ramzy PI**, Wolf SE, Irtun O, Hart DW, Thompson JC, Herndon DN. Gut epithelial apoptosis after severe burn: effects of gut hypoperfusion. *J Am Coll Surg* 2000; **190**: 281-287
- Wolf SE**, Ikeda H, Matin S, Debroy MA, Rajaraman S, Herndon DN, Thompson JC. Cutaneous burn increases apoptosis in the gut epithelium of mice. *J Am Coll Surg* 1999; **188**: 10-16
- Green DR**, Reed JC. Mitochondria and apoptosis. *Science* 1998; **281**: 1309-1312
- Li JM**, Cai Q, Zhou H, Xiao GX. Effects of hydrogen peroxide on mitochondrial gene expression of intestinal epithelial cells. *World J Gastroenterol* 2002; **8**: 1117-1122
- Zhang C**, Cai Y, Adachi MT, Oshiro S, Aso T, Kaufman RJ, Kitajima S. Homocysteine induces programmed cell death in human vascular endothelial cells through activation of the unfolded protein response. *J Biol Chem* 2001; **276**: 35867-35874
- Salazar JJ**, Van Houten B. Preferential mitochondrial DNA injury caused by glucose oxidase as a steady generator of hydrogen peroxide in human fibroblasts. *Mutation Res* 1997; **385**: 139-149
- De Vos K**, Goossens V, Boone E, Vercammen D, Vancompernelle K, Vandenabeele P, Haegeman G, Fiers W, Grooten J. The 55-kDa tumor necrosis factor receptor induces clustering of mitochondria through its membrane-proximal region. *J Biol Chem* 1998; **273**: 9673-9680
- Cone JB**, Wallace BH, Lubansky HJ, Caldwell FT. Manipulation of the inflammatory response to burn injury. *J Trauma* 1997; **43**: 41-45
- Dries DJ**, Lorenz K, Kovacs EJ. Differential neutrophil traffic in gut and lung after scald injury. *J Burn Care Rehabil* 2001; **22**: 203-209
- Jeschke MG**, Debroy MA, Wolf SE, Rajaraman S, Thompson JC. Burn and starvation increase programmed cell death in small bowel epithelial cells. *Dig Dis Sci* 2000; **45**: 415-420
- Eaves Pyles T**, Alexander JW. Rapid and prolonged impairment of gut barrier function after thermal injury in mice. *Shock* 1998; **9**: 95-100
- Baskaran H**, Yarmush ML, Berthiaume F. Dynamics of tissue neutrophil sequestration after cutaneous burns in rats. *J Surg Res* 2000; **93**: 88-96
- Hengartner MO**. Apoptosis: DNA destroyers. *Nature* 2001; **412**: 27-29
- Hengartner MO**. The biochemistry of apoptosis. *Nature* 2000; **407**: 770-776
- Desagher S**, Martinou JC. Mitochondria as the central control point of apoptosis. *Trends Cell Biol* 2000; **10**: 369-377
- Petit PX**, Susin SA, Zamzami N, Mignotte B, Kroemer G. Mitochondria and programmed cell death: back to the future. *FEBS Letters* 1996; **396**: 7-13
- Finkel E**. The mitochondrion: is it central to apoptosis? *Science* 2001; **292**: 624-626
- Kluck RM**, Bossy Wetzel E, Green DR, Newmeyer DD. The release of cytochrome C from mitochondria: a primary site for Bcl2 regulation of apoptosis. *Science* 1997; **275**: 1132-1136
- Susin SA**, Zamzami N, Castedo M, Hirsch T, Marchetti P, Macho A, Daugas E, Geuskens M, Kroemer G. Bcl-2 inhibits the mitochondrial release of an apoptogenic protease. *J Exp Med* 1996; **184**: 1331-1341
- Wakabayashi T**. Structural changes of mitochondria related to apoptosis: swelling and megamitochondria formation. *Acta Biochim Pol* 1999; **46**: 223-237
- Frey TG**, Mannella CA. The internal structure of mitochondria. *Trends Biochem Sci* 2000; **25**: 319-324
- Hirsch T**, Marzo I, Kroemer G. Role of the mitochondrial permeability transition pore in apoptosis. *Biosci Rep* 1997; **17**: 67-76
- Zamzami N**, Hirsch T, Dallaporta B, Petit PX, Kroemer G. Mitochondrial implication in accidental and programmed cell death: apoptosis and necrosis. *J Bioenerg Biomembr* 1997; **29**: 185-193
- Kroemer G**. Mitochondrial control of apoptosis: an overview. *Biochem Soc Symp* 1999; **66**: 1-15
- Ravagnan L**, Marzo I, Costantini P, Susin SA, Zamzami N, Petit PX, Hirsch F, Goulbern M, Poupon MF, Miccoli L, Xie Z, Reed JC, Kroemer G. Lonidamine triggers apoptosis via a direct, Bcl-2-inhibited effect on the mitochondrial permeability transition

- pore. *Oncogene* 1999; **18**: 2537-2546
- 36 **Larochette N**, Decaudin D, Jacotot E, Brenner C, Marzo I, Susin SA, Zamzami N, Xie Z, Reed J, Kroemer G. Arsenite induces apoptosis via a direct effect on the mitochondrial permeability transition pore. *Exp Cell Res* 1999; **249**: 413-421
- 37 **Anuradha CD**, Kanno S, Hirano S. Oxidative damage to mitochondria is a preliminary step to caspase-3 activation in fluoride-induced apoptosis in HL-60 cells. *Free Radic Biol Med* 2001; **31**: 367-373
- 38 **Smaili SS**, Hsu YT, Sanders KM, Russell JT, Youle RJ. Bax translocation to mitochondria subsequent to a rapid loss of mitochondrial membrane potential. *Cell Death Differ* 2001; **8**: 909-920
- 39 **Skulachev VP**. Cytochrome c in the apoptotic and antioxidant cascades. *FEBS Lett* 1998; **423**: 275-280
- 40 **Simon DK**, Lin MT, Ahn CH, Liu GJ, Gibson GE, Beal MF, Johns DR. Low mutational burden of individual acquired mitochondrial DNA mutations in brain. *Genomics* 2001; **73**: 113-116
- 41 **Wallace DC**. A mitochondrial paradigm for degenerative diseases and ageing. *Novartis Found Symp* 2001; **235**: 247-263
- 42 **Chang SW**, Zhang D, Chung HD, Zassenhaus HP. The frequency of point mutations in mitochondrial DNA is elevated in the Alzheimer's brain. *Biochem Biophys Res Commun* 2000; **273**: 203-208
- 43 **Esposito LA**, Melov S, Panov A, Cottrell BA, Wallace DC. Mitochondrial disease in mouse results in increased oxidative stress. *Proc Natl Acad Sci USA* 1999; **96**: 4820-4825
- 44 **Lu CY**, Lee HC, Fahn HJ, Wei YH. Oxidative damage elicited by imbalance of free radical scavenging enzymes is associated with large-scale mtDNA deletions in aging human skin. *Mutat Res* 1999; **423**: 11-21
- 45 **Bhat HK**, Hiatt WR, Hoppel CL, Brass EP. Skeletal muscle mitochondrial DNA injury in patients with unilateral peripheral arterial disease. *Circulation* 1999; **99**: 807-812
- 46 **Swerdlow RH**, Parks JK, Cassarino DS, Shilling AT, Bennett JP, Harrison MB, Parker WD. Characterization of cybrid cell lines containing mtDNA from Huntington's disease patients. *Biochem Biophys Res Commun* 1999; **261**: 701-704
- 47 **Wei YH**. Oxidative stress and mitochondrial DNA mutations in human aging. *Proc Soc Exp Biol Med* 1998; **217**: 53-63
- 48 **Ide T**, Tsutsui H, Hayashidani S, Kang D, Suematsu N, Nakamura K, Utsumi H, Hamasaki N, Takeshita A. Mitochondrial DNA damage and dysfunction associated with oxidative stress in failing hearts after myocardial infarction. *Circ Res* 2001; **88**: 529-535
- 49 **Swerdlow RH**, Parks JK, Davis JN, Cassarino DS, Trimmer PA, Currie LJ, Dougherty J, Bridges WS, Bennett JP, Wooten GF, Parker WD. Matrilineal inheritance of complex I dysfunction in a multigenerational Parkinson's disease family. *Ann Neurol* 1998; **44**: 873-881
- 50 **Ballinger SW**, Patterson C, Yan CN, Doan R, Burow DL, Young CG, Yakes FM, Van Houten B, Ballinger CA, Freeman BA, Runge MS. Hydrogen peroxide and peroxynitrite induced mitochondrial DNA damage and dysfunction in vascular endothelial and smooth muscle cells. *Circ Res* 2000; **86**: 960-966

Edited by Zhu L

Combined therapy of allantoin, metronidazole, dexamethasone on the prevention of intra-abdominal adhesion in dogs and its quantitative analysis

Xiao-Chen Wang, Chang-Qing Gui, Qing-Shan Zheng

Xiao-Chen Wang, Qing-Shan Zheng, Anhui Provincial Center for Drug Clinical Evaluation & Yijishan Hospital of Wanan Medical Collage, Wuhu 241001, Anhui Province, China

Chang-Qing Gui, Department of Pharmacology, Wanan Medical Collage, Wuhu 241001, Anhui Province, China

Correspondence to: Dr. Qing-Shan Zheng, Anhui Provincial Center for Drug Clinical Evaluation & Yijishan Hospital of Wanan Medical Collage, 93 TuanJieDong Lu, Wuhu 241001, Anhui Province, China. editorys@mail.wh.ah.cn

Telephone: +86-553-573-8350 **Fax:** +86-553-573-8350

Received: 2002-10-30 **Accepted:** 2002-11-19

Abstract

AIM: To observe the preventive effects of combined therapy of AMD (allantoin, metronidazole and dexamethasone in combination) on intra-abdominal adhesion in dogs.

METHODS: 20 dogs of both sexes were used in this study. After laparotomy under anesthesia, 2 cm section of cecal end was clamped and ligated, then 1 cm cecum section was cut and another 1 cm was kept. The cecum stump was closed with purse-string suture. Both parietal and visceral peritonea were stripped for an area of about 3×4 cm². Before the skin closure, the animals were divided into two groups randomly. The abdominal cavities in Group AMD (*n*=10) were rinsed by 200 ml of AMD solution, and with 50 ml left, whereas the control (*n*=10) received the equal volume of normal saline. After 7 d, the degree of intra-abdominal adhesions was evaluated by using the score method of ultrasonography and traditional dissection.

RESULTS: Compared with the control, both the ultrasonography and traditional dissection scores in Group AMD were significantly decreased that marked as 2.0±1.25 vs 3.3±0.82 and 1.91±0.83 vs 3.3±0.82 respectively (*P*<0.01).

CONCLUSION: The combined therapy of AMD is an effective way to prevent intra-abdominal adhesion, and ultrasonography is an useful tool to diagnose intra-abdominal adhesion.

Wang XC, Gui CQ, Zheng QS. Combined therapy of allantoin, metronidazole, dexamethasone on the prevention of intra-abdominal adhesion in dogs and its quantitative analysis. *World J Gastroenterol* 2003; 9(3): 568-571
<http://www.wjgnet.com/1007-9327/9/568.htm>

INTRODUCTION

Intra-abdominal adhesions are almost inevitable to some extent after major abdominal surgery. Weibel and Majno reviewed 289 subjects at post-mortem who had had previous laparotomies, and 67 % of the patients showed adhesions; after multiple operations, the incidence rose to 93 %^[1]. However, there has been little advances in the treatment and prevention

of this complication in recent years. Numerous attempts with agents and surgical techniques often obtain conflicting results^[2,3]. The cause may be mainly, at least partly, due to multi-factor in the adhesion etiology and multi-pathway in the adhesion mechanism^[4-6], which made the adhesions difficult to be prevented by using a single drug or certain measures. Besides, the evaluation of intra-abdominal adhesion was based classically on traditional dissection method, which was impossible to be applied to the clinical settings. In this study, we employed a new reproducible animal model of intra-abdominal adhesion caused by multi-factors, and a new evaluation method by ultrasonography to assess the effects of combined AMD (allantoin, metronidazole and dexamethasone in combination) therapy.

MATERIALS AND METHODS

Materials

Allantoin (Alt) powder with the purity of 99.6 % was obtained from Jiangsu Huanghai Pharmaceutical Factory. Metronidazole (Met) powder was from Tianjing Hebei Pharmaceutical Factory with the purity of 99.85 %. Dexamethasone (Dex) powder was purchased from Roussel Uclaf Co and the purity is 99.6 %. They were dissolved and mixed with 5 % GS, the ratio of Alt: Met:Dex is 50:32:1. The HEWLETT-PACKARD Sonos-2000 Color Ultrasonic Doppler Method Diagnostic Equipment was employed in this study, using a real-time sonolayer SSA-270A ultrasound scanner (Toshiba, Tokyo, Japan) and a 3.5 MHz sector transducer.

Experimental animal

20 adult healthy dogs of both sexes, weighing from 7 to 10 kg were purchased from the Animal Center of Wannan Medical College.

Animal models

The experiment was carried out in clean but not sterile condition. Under 3 % sodium pentobarbital anesthesia (1 ml/kg iv), following shaving and skin disinfecting, the laparotomy was performed through a 5 cm, vertical, midline incision. 2 cm section from the cecal end was clamped and ligated, 1 cm of the section was cut, and the other 1 cm from the ligated site was kept. The cecum stump was closed with the purse-string suture. Then a 3×4 cm² patch of parietal peritoneum corresponding to the cecal was carefully stripped. In addition, both sides of peritoneum along the abdomen incision were scraped for an area of about 3×4 cm². Before skin closure of abdomen, the animals were randomly divided into 2 groups. The abdominal cavity in Group AMD were rinsed by 200 ml of AMD solution and with 50 ml left, whereas the control received the equal volume of normal saline. All the animals were fasted for 8 hours after operation.

Adhesion assessment by ultrasonography

At the seventh day after operation, all the dogs were reanesthetized. Selecting the skin point corresponding to the

appendix, 1 000 ml of normal saline was instilled into the abdominal cavity with a 12G needle to improve the acoustic window^[7]. The whole abdomen was divided into four areas artificially by a horizon through navel and a vertical line through xiphoid (Figure 1), the number and density of adhesion sites were graded on the basis of ultrasonographic findings (Table 1).

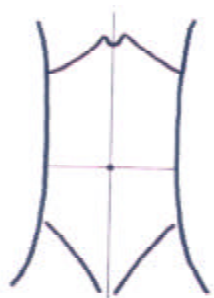


Figure 1 Abridged general view of dog abdomen subregion.

Table 1 Adhesion assessment by ultrasonography

Score	Description
1	Echogenic bands in one area
2	Echogenic bands in two areas
3	Echogenic bands in three areas or alveolate echogenic bands in one area
4	Massive agglutinating adhesion or adhesion between viscera and abdominal wall

Adhesion assessment by traditional dissection

After ultrasonic examination, the dogs were sacrificed and an autopsy examination was carried out with the attention to the number, density and site of the adhesion formation, which was scored by a modified scale by Swolin^[8,9] (Table 2). The highest score for each dog was taken to be further processed.

Table 2 Adhesion assessment by traditional dissection

Score	Description
1	Filmy connections sparated spontaneously
2	Firm adhesions separated by gravity
3	Firm adhesions by traction
4	Dense adhesions requiring sharp dissection

Statistical analysis

Quantitative results were expressed as mean \pm SD. Statistical analysis was performed using Student's *t* test. $P < 0.05$ was considered statistically significant.

RESULTS

One week postoperation animals in control group developed strip or round adhesions (Figure 2), attached either to the closed peritoneal defect or to the midline scar, or connected between the bowels. All the control animals had positive sonographic findings. Transabdominal sonogram clearly showed echogenic bands floating in the abdominal cavity like mice-tails (Figure 3). In more serious subjects, the adhesions were so dense that the sonogram showed alveolate echogenic masses (Figure 4); Some adhesions were formed between the organs in abdominal cavity (Figure 5). All the sonographic positive findings were proved to be the adhesion formation in laparotomy. The adhesion formed in Group AMD was significantly decreased compared with the control group as shown by both ultrasonography and

traditional dissection score that marked as 2.0 ± 1.25 vs 3.3 ± 0.82 and 1.91 ± 0.83 vs 3.3 ± 0.82 respectively ($P < 0.01$).

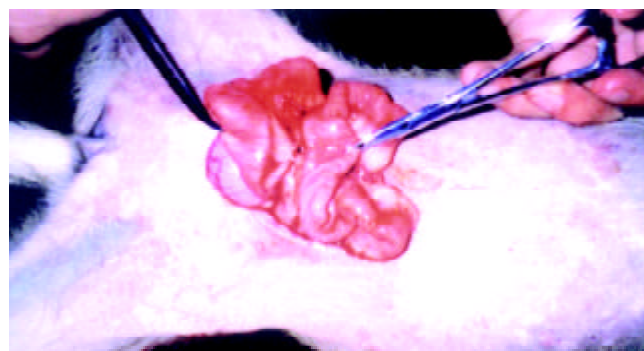


Figure 2 Adhesions between the bowels of animal in control group.

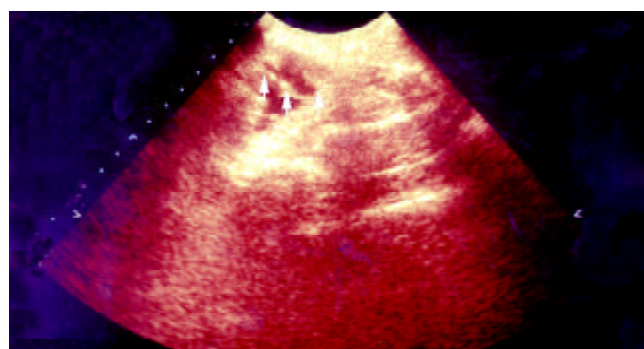


Figure 3A Transabdominal sonogram showed the adhesions between bowels, the adhesion looks like a mouse tail, and the score is 1.

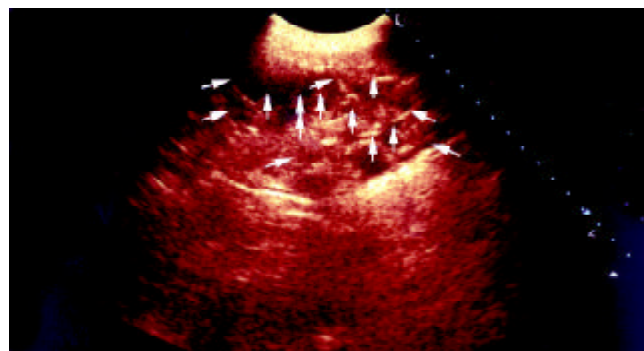


Figure 3B Transabdominal sonogram showed massive agglutinating adhesion between bowels, and the score is 3.

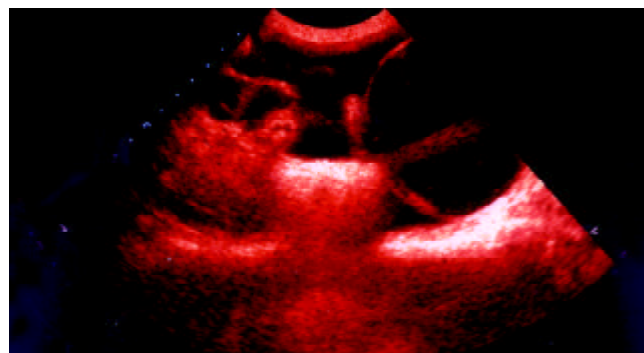


Figure 3C Transabdominal sonogram showed the adhesions between bladder and bowels, and the score is 4.

DISCUSSION

Because of the high incidence of intra-abdominal adhesion formation postoperation, plenty of investigations have been made for the past decades; However, up to the present, satisfactory results have not been achieved yet, which reflected such a fact that there still existed some obstacles waiting to be overcome.

The animal model of intra-abdominal adhesion was such a problem. Traditionally, the model was made mainly on mice, rats and rabbits by a series of America, British investigators in different means^[10-12], however, these small animals were quite different from human beings in phylogenesis, metabolism reactivity and so on. In addition, such model making laid much stress on mechanical trauma, many important factors, such as tissue ischemia, infection, inflammation and exudation^[13-16] were severely neglected, which made the experimental results inconsistent with clinical settings. In the present, study a novel dog model of intra-abdominal adhesion caused by multi-factors was employed, which might reflect really the complexity of etiology and the nature of intra-abdominal adhesion formation.

There are a large number of substances used to combat adhesion formation at present^[17-26], however, because of the multi-factors in the adhesion etiology and multi-pathways in the adhesion mechanism, the single use one or two of these agents could not turn out satisfactory results. Besides, the majority of these agents have been proven to be too toxic to be used^[27-29].

The formation of intra-abdominal adhesion has been attributed to the local depression of plasminogen activator activity (PAA) for more than 3 decades^[30-33]. This deficit permits the deposited fibrin on peritoneal surface to form fibrous adhesion. In this study, we used the combined AMD composed of allantoin, metronidazole and dexamethasone, which was proven to play a role of anti-inflammation, anti-bacteria and anti-exudation by prohibiting the fibrin rich exudate into the abdominal cavity and increasing the activity of endogenous tissue plasminogen activator, to prevent intra-abdominal adhesion postoperation. According to our pilot study, the best proportion of these three drugs was 50:32:1, which made the effectiveness of the combination reinforced, whereas the toxicity didn't increase^[34]. As for the impairment of the combination on wound healing, it was too slight to be noticed, for the intra-abdominal adhesion formed mainly in 6 hours postoperation, after that, the wound healing began to occur while the effect of the combination was gradually disappeared.

Intra-abdominal adhesion failed to be detected by routine ultrasonography. Lee *et al* identified instilling normal saline into abdominal cavity could diagnose the female pelvic lesions^[7], we employed this method to perform an assessment for the intra-abdominal adhesion. It was demonstrated that this method was visible and accurate, the score of intra-abdominal adhesion was well in agreement with that done by the laparotomy. The most notable finding of sonography in the examination of intra-abdominal adhesion was the mouse-tail appearance, which was believed as the sign of adhesion band. In conclusion, we suggested that the combined AMD might be an effective way to prevent intra-abdominal adhesion, and the ultrasonography an useful tool to diagnose intra-abdominal adhesion, and their applications might be valuable to the clinical settings.

REFERENCES

- 1 **Lower AM**, Hawthorn RJ, Ellis H, O'Brien F, Buchan S, Crowe AM. The impact of adhesions on hospital readmissions over ten years after 8849 open gynaecological operations: an assessment from the Surgical and Clinical Adhesions Research Study. *BJOG* 2000; **107**: 855-862
- 2 **Jacobi CA**, Sterzel A, Braumann C, Halle E, Stosslein R, Krahenbuhl L, Muller JM. The impact of conventional and laparoscopic colon resection (CO₂ or helium) on intraperitoneal adhesion formation in a rat peritonitis model. *Surg Endosc* 2001; **15**: 380-386
- 3 **Farmer L**, Ayoub M, Warejcka D, Southerland S, Freeman A, Solis M. Adhesion formation after intraperitoneal and extraperitoneal implantation of polypropylene mesh. *Am Surg* 1998; **64**: 144-146
- 4 **Tulandi T**. Introduction-prevention of adhesion formation: the journey continues. *Hum Reprod Update* 2001; **7**: 545-546
- 5 **Dijkstra FR**, Nieuwenhuijzen M, Reijnen MM, van Goor H. Recent clinical developments in pathophysiology, epidemiology, diagnosis and treatment of intra-abdominal adhesions. *Gastroenterol Suppl* 2000; **232**: 52-59
- 6 **Thompson J**. Pathogenesis and prevention of adhesion formation. *Dig Surg* 1998; **15**: 153-157
- 7 **Li GJ**, Zhou YC, Wu J. A preliminary application of normal saline instilling abdomen cavity in diagnosis of female pelvic lesions. *Zhongguo Chaosheng Yixue Zazhi* 2000; **16**: 535-538
- 8 **Gul A**, Kotan C, Dilek I, Gul T, Tas A, Berktaş M. Effects of methylene blue, indigo carmine solution and autologous erythrocyte suspension on formation of adhesions after injection into rats. *J Reprod Fertil* 2000; **120**: 225-229
- 9 **Tran HS**, Chrzanoski FA Jr, Puc MM, Patel NG, Geldziler B, Malli D, Ramsamooj R, Hewitt CW, DelRossi AJ. An *in vivo* evaluation of a chondroitin sulfate solution to prevent postoperative intraperitoneal adhesion formation. *J Surg Res* 2000; **88**: 78-87
- 10 **Yesildaglar N**, Koninckx PR. Adhesion formation in intubated rabbits increases with high insufflation pressure during endoscopic surgery. *Hum Reprod* 2000; **15**: 687-691
- 11 **Mueller PO**, Hay WP, Harmon B, Amoroso L. Evaluation of a bioresorbable hyaluronate-carboxymethylcellulose membrane for prevention of experimentally induced abdominal adhesions in horses. *Vet Surg* 2000; **29**: 48-53
- 12 **Toosie K**, Gallego K, Stabile BE, Schaber B, French S, de Virgilio C. Fibrin glue reduces intra-abdominal adhesions to synthetic mesh in a rat ventral hernia model. *Am Surg* 2000; **66**: 41-45
- 13 **Sjosten AC**, Ellis H, Edelstam GA. Post-operative consequences of glove powder used pre-operatively in the vagina in the rabbit model. *Sjosten AC. Hum Reprod* 2000; **15**: 1573-1577
- 14 **van den Tol MP**, Haverlag R, van Rossen ME, Bonthuis F, Marquet RL, Jeekel J. Glove powder promotes adhesion formation and facilitates tumour cell adhesion and growth. *Br J Surg* 2001; **88**: 1258-1263
- 15 **Qiu G**, Wang C, Smith R, Harrison K, Yin K. Role of IFN-gamma in bacterial containment in a model of intra-abdominal sepsis. *Shock* 2001; **16**: 425-429
- 16 **Halverson AL**, Barrett WL, Bhanot P, Phillips JE, Iglesias AR, Jacobs LK, Sackier JM. Intraabdominal adhesion formation after preperitoneal dissection in the murine model. *Surg Endosc* 1999; **13**: 14-16
- 17 **Reijnen MM**, de Man BM, Hendriks T, Postma VA, Meis JF, van Goor H. Hyaluronic acid-based agents do not affect anastomotic strength in the rat colon, in either the presence or absence of bacterial peritonitis. *Br J Surg* 2000; **87**: 1222-1228
- 18 **Verco SJ**, Peers EM, Brown CB, Rodgers KE, Roda N, diZerega G. Development of a novel glucose polymer solution (icodextrin) for adhesion prevention: pre-clinical studies. *Hum Reprod* 2000; **15**: 1764-1772
- 19 **Szabo A**, Haj M, Waxman I, Eitan A. Evaluation of seprafilm and amniotic membrane as adhesion prophylaxis in mesh repair of abdominal wall hernia in rats. *Eur Surg Res* 2000; **32**: 125-128
- 20 **Ghellai AM**, Stucchi AF, Chegini N, Ma C, Andry CD, Kaseta JM, Burns JW, Skinner KC, Becker JM. Role of transforming growth factor beta-1 in peritonitis-induced adhesions. *Gastrointest Surg* 2000; **4**: 316-323
- 21 **Kramer K**, Senninger N, Herbst H, Probst W. Effective prevention of adhesions with hyaluronate. *Arch Surg* 2002; **137**: 278-282
- 22 **Cubukcu A**, Alponat A, Gonullu NN. Mitomycin-C prevents reformation of intra-abdominal adhesions after adhesiolysis. *Surgery* 2002; **131**: 81-84
- 23 **Reijnen MM**, Skrabut EM, Postma VA, Burns JW, van Goor H. Polyanionic polysaccharides reduce intra-abdominal adhesion and abscess formation in a rat peritonitis model. *J Surg Res* 2001;

- 101:** 248-253
- 24 **Vela AR**, Littleton JC, O' Leary JP. The effects of minidose heparin and low molecular weight heparin on peritonitis in the rat. *Am Surg* 1999; **65**: 473-477
 - 25 **Ozogul Y**, Baykal A, Onat D, Renda N, Sayek I. An experimental study of the effect of aprotinin on intestinal adhesion formation. *Am J Surg* 1998; **175**: 137-141
 - 26 **Gul A**, Kotan C, Dilek I, Gul T, Tas A, Berktaş M. Effects of methylene blue, indigo carmine solution and autologous erythrocyte suspension on formation of adhesion after injection into rat. *J Reprod Fertil* 2000; **120**: 225-229
 - 27 **Trickett JP**, Rainsbury RM, Green R. Paradoxical outcome after use of hyaluronate barrier to prevent intra-abdominal adhesions. *J R Soc Med* 2001; **94**: 183-184
 - 28 **Reijnen MM**, de Man BM, Hendriks T, Postma VA, Meis JF, Van Goor H. Hyaluronic acid-based agents do not affect anastomotic strength in the rat colon, in either the presence or absence of bacterial peritonitis. *Br J Surg* 2000; **87**: 1222-1228
 - 29 **Haverlag R**, van Rossen ME, van den Tol MP, Bonthuis F, Marquet RL, Jeekel J. Hyaluronate-based coating solution for prevention of surgical adhesions has no major effect on adhesion and growth of intraperitoneal tumour cells. *Eur J Surg* 1999; **165**: 791-795
 - 30 **Edelstam G**, Lecander I, Larsson B, Astedt B. Fibrinolysis in the peritoneal fluid during adhesions, endometriosis and ongoing pelvic inflammatory disease. *Inflammation* 1998; **22**: 341-351
 - 31 **Cheong YC**, Laird SM, Li TC, Shelton JB, Ledger WL, Cooke ID. Peritoneal healing and adhesion formation/reformation. *Hum Reprod Update* 2001; **7**: 556-566
 - 32 **Cao TS**, Liu RH, Sun XM. Experimental study of the effect of methylene blue combined with aprotinin on intraperitoneal adhesion. *Zhongguo Weichang Waikē Zazhi* 2000; **3**: 238-239
 - 33 **Gimbel ML**, Chelius D, Hunt TK, Spencer EM. A novel approach to reducing postoperative intraperitoneal adhesion through the inhibition of insulinlike growth factor I activity. *Arch Surg* 2001; **136**: 311-317
 - 34 **Zheng QS**, Gui CQ, Sun RY, Wang M. A novel animal model of intra-abdominal adhesion and quantitative evaluation with related indices. *Zhongguo Linchuang Yaolixue Yu Zhilixue Zazhi* 2000; **5**: 101-104

Edited by Zhu L

Preparation and identification of anti-transforming growth factor $\beta 1$ U1 small nuclear RNA chimeric ribozyme *in vitro*

Ju-Sheng Lin, Yu-Hu Song, Xin-Juan Kong, Bin Li, Nan-Zhi Liu, Xiao-Li Wu, You-Xin Jin

Ju-Sheng Lin, Yu-Hu Song, Xin-Juan Kong, Nan-Zhi Liu, Xiao-Li Wu, Institute of Liver Diseases, Tongji Hospital, Tongji Medical College, Huazhong University of Science and Technology, Wuhan 430030, Hubei Province, China

Bin Li, You-Xin Jin, State Key Laboratory of Molecular Biology, Institute of Biochemistry and Cell Biology, Shanghai Institutes for Biological Sciences, Chinese Academy of Sciences, Shanghai 200031, China

JS Lin and YH Song contributed equally to this study

Supported by the grant from Chinese Academy of Sciences, No. KSCX2-2-204

Correspondence to: Dr. You-Xin Jin, State Key Laboratory of Molecular Biology, Institute of Biochemistry and Cell Biology, Shanghai Institutes for Biological Sciences, Chinese Academy of Sciences, Shanghai 200031, China. yxjin@sunm.shnc.ac.cn

Telephone: +86-21-64315030-5221

Received: 2002-09-13 **Accepted:** 2002-10-18

Abstract

AIM: To study the preparation and cleavage activity of anti-transforming growth factor (TGF) $\beta 1$ U1 small nuclear (sn) RNA chimeric hammerhead ribozymes *in vitro*.

METHODS: TGF $\beta 1$ partial gene fragment was cloned into T-vector at the downstream of T7 promoter. 32 P-labeled TGF $\beta 1$ partial transcripts as target RNA were transcribed *in vitro* and purified by denaturing polyacrylamide gel electrophoresis (PAGE). Anti-TGF $\beta 1$ ribozymes were designed by computer, then synthetic ribozyme fragments were cloned into the U1 ribozyme vector pZeoU1EcoSpe containing U1 snRNA promoter/enhancer and terminator. 32 P-labeled U1 snRNA chimeric ribozyme transcripts were gel-purified, incubated with target-RNAs at different conditions and autoradiographed after running denaturing PAGE.

RESULTS: Active U1snRNA chimeric ribozyme (U1Rz803) had the best cleavage activity at 50 °C; at 37 °C, it was active, $K_m=34.48$ nmol/L, $K_{cat}=0.14$ min $^{-1}$; while the point mutant ribozyme U1Rz803_m had no cleavage activity, so these indicated the design of U1Rz803 was correct.

CONCLUSION: U1Rz803 prepared in this study possessed the perfect specific catalytic cleavage activity. These results indicate U1 snRNA chimeric ribozyme U1Rz803 may suppress the expression of TGF $\beta 1$ *in vivo*, therefore it may provide a new avenue for the treatment of liver fibrosis in the future.

Lin JS, Song YH, Kong XJ, Li B, Liu NZ, Wu XL, Jin YX. Preparation and identification of anti-transforming growth factor $\beta 1$ U1 small nuclear RNA chimeric ribozyme *in vitro*. *World J Gastroenterol* 2003; 9(3): 572-577

<http://www.wjgnet.com/1007-9327/9/572.htm>

INTRODUCTION

The incidence of liver cirrhosis is still high all over the world, especially in China^[1-6]. Cirrhotic livers are characterized by

extensive fibrosis throughout the entire hepatic parenchyma^[7-12]. Many factors inducing liver injury and inflammation will lead to chronic liver disease, and hepatic fibrosis^[13-22].

TGF $\beta 1$ is an important cytokine in the regulation of the production, degradation, accumulation of extracellular matrix proteins, and that it may play a pivotal role in the fibroproliferative changes that follow tissue damage in many vital organs and tissues, including liver, lung, kidney, skin, heart, and arterial walls^[7,23-27]. In the past decade dramatic advances have been made in the understanding of cellular and molecular mechanisms underlying liver fibrogenesis, it is thought that TGF $\beta 1$ is of crucial importance in rat hepatic fibrosis *in vivo*^[7,28-34]. Inhibition of TGF β can not only prevent liver fibrosis, but also preserve organ function^[30]. So TGF $\beta 1$ has been thought to be an ideal target molecule to prevent the progression of liver fibrosis.

Ribozymes are a class of small catalytic RNA molecules that recognize specific substrate RNA molecules by their complementary nucleotide sequence, cleaving the substrate RNA as an endoribonuclease at enzymatic rates^[35-38]. In the last years ribozyme-mediated inhibition of gene expression in intact cells have been tested many times, but some of them were largely unsuccessful^[39-42]. Factors that contributed to ribozyme efficacy in transfected cell are expression level, stability against rapid degradation, correct folding for exposure to target, and subcellular localization of ribozyme and target. U1 snRNA is a highly expressed stable small RNA (164 nucleotides) involved in both spliceosome and catalytic processing during pre-mRNA splicing. U1small nuclear RNA expression cassette can provide an excellent vehicle for ribozyme delivery and expression in intact cell because of stability, nuclear localization, highly efficient expression^[43-45].

Because TGF $\beta 1$ plays a crucial role in liver fibrosis, in this study we designed ribozymes directed against TGF $\beta 1$ by computer, then cloned them into U1 snRNA chimeric ribozyme vector, it had been proven that it could cleave target RNA efficiently *in vitro* through the cleavage reaction, so it indicated that it might suppress intracellular TGF $\beta 1$ expression, which would provide a new avenue in treatment of liver fibrosis.

MATERIALS AND METHODS

Materials

HSC-T6 cell line is a kind gift from Dr. Scott L. Friedman (Dept of Medicine and Division of Liver Diseases, Mount Sinai School of Medicine). pZeoU1EcoSpe was provided by Dr. Harry C. Dietz (Department of Pediatrics, Medicine and Molecular Biology & Genetics, Johns Hopkins University School of Medicine). pGEM-T vector kit, transcription kit were purchased from Promega Company. Trizol kit, DMEM were purchased from Gibco BRL Company. The PCR primers and ribozyme fragments were synthesized in the Beckman oligo-1 000 DNA synthesizer. Zeocin was purchased from Invitrogen Company. Newborn calf serum was purchased from Hyclone Company. RT-PCR kit, RNase inhibitor, restriction endonucleases, and T4 DNA ligase were purchased from Takara Company. α 32 P UTP was purchased from Beijing Ya-Hui Company.

Methods

Construction of target RNA *in vitro* Total RNA was extracted using Trizol Kit (GIBCO BRL) from cultured HSC-T6 cell, an immortalized rat hepatic stellate cells line (HSC), exhibited an activated phenotype^[46,47]. The upstream primer P1 (5' - GAATTCATTCAGGACTATCAC CTACC-3') in the untranslated region and the downstream primer P2 (5' - AAGCTTTTCTGGT AGAGTTCTACGTG -3') in the open reading frame were selected to amplify a 651-base pair fragment corresponding to bases 279 to 930 of the rat TGF beta 1^[48]. The extracted RNA was reversely transcribed and polymerase chain reaction (PCR) amplified using a pair of primers in one step reverse transcriptase (RT) PCR kit. The PCR products were analyzed and purified on 1 % (w/v) agarose gels. Purified PCR products were ligated into pGEM-T vector. DNA sequencing results showed that the PCR-amplified fragments were cloned into the molecular cloning sites of pGEM-T vector at the downstream of T7 promoter as pTGF β 1. Target RNA was prepared through *in vitro* transcription of PCR-amplified products of pTGF β 1, which contained T7 promoter at the upstream of upper primer. The sequence of the primers for transcription was GAATTCTAATACGACTCACTATAGGGAGGCGGACTACTACGCCAA and TTCTGGTAGAG TTCTACGTG; **TAATACGACTCACTATAG GG** represents T7 promoter. Then PCR product was analyzed and purified by 1 % (w/v) agarose gels electrophoresis as the template for transcription. *In vitro* transcription was carried out at 37 °C for 90 min in a 40 μ L final volume containing 40 mmol/L of Tris·HCl (pH 7.5), 5 mmol/L of DTT, 2 mmol/L of spermidine, 8 mmol/L of MgCl₂, 0.25 mmol/L of ATP, GTP,CTP, 0.05 mmol/L of UTP, 20 μ Ci alpha ³²p-UTP, 80 U T₇ RNA polymerase and 2 μ g purified PCR product. Target RNA was purified by 6 % denaturing gel electrophoresis through cutting off the

autoradiograph bands and soaking in NES (0.5 mol/L NH₄Ac, 0.1 mol/L EDTA, 0.1 % SDS pH 5.4) at 42 °C overnight. the products were precipitated by ethanol, washed twice by 75 % ethanol, dissolved in DEPC H₂O and reserved under -20 °C.

Construction of recombinant plasmid for ribozyme pZeoU1EcoSpe contained the pZeoSV plasmid DNA modified by excising the SV40 promoter, SV40 polyadenylation site, and polylinker at the *Bam*HI sites. In constructing the pZeoU1 EcoSpe, a U1 snRNA expression cassette in pUC13^[49, 50] was excised with *Bam*HI digestion and ligated into the *Bam*HI sites of the modified pZeoSV. Two rounds of site-directed mutagenesis were then performed to change 4 nt flanking the Sm protein binding site of U1 snRNA, creating unique *Eco*RI and *Spe*I restriction sites. The 5' -flanking region of the inserted U1 snRNA expression cassette possessed a promoter/enhancer comparable in strength with the SV40 early promoter^[51]. The ribozymes for TGF β 1 were designed according to the computer software pcFOLD compiled by professor Zuker (Canadian Academy of Science). The homologous possibility with the gene of rat was excluded by consulting with RNA sequence of rat cells from NCBI Genbank. The enclosed vector pZeoU1EcoSpe was cut by *Eco*RI and *Spe*I restriction enzymes and purified by 1 % (w/v) agarose gels electrophoresis. The synthesized oligonucleotides of ribozyme were mixed with equal molar amounts together, then were cloned into the *Eco*RI/*Spe*I sites of pZeoU1EcoSpe to create pU1Rz803. pZeoU1EcoSpe and the reconstruction could be confirmed by DNA sequencing (Figure 1). The oligonucleotides of Rz803 were 5' AATTACATATATACT (G/A)ATGAGTCCGTGAGGACGAAACTGTGT3' and 5' CTAGACACAGTTTCGTCCTCACGGACTCAT(C/T)AGTATATATGT3' ; G and C for activated ribozyme, A and T for inactivated ribozyme.

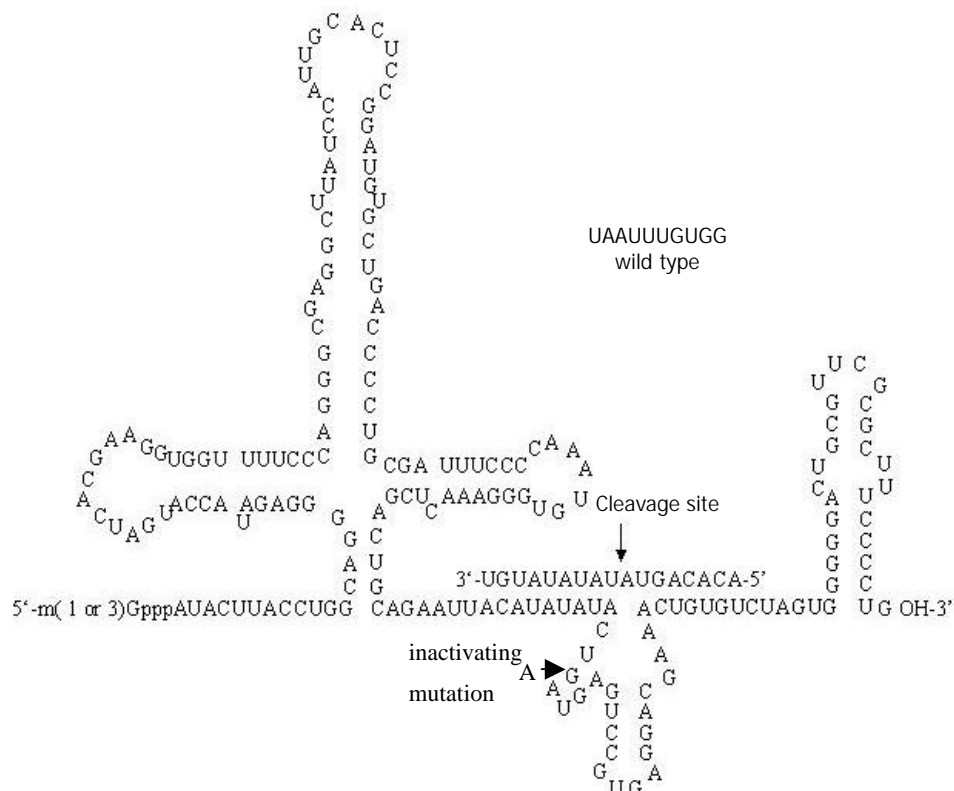


Figure 1 Sequence and predicted structure of U1 snRNA chimeric ribozymes. arrows represent cleavage site and inactivating mutation.

Preparation of ribozymes *in vitro* The templates used for transcription of U1 snRNA chimeric ribozymes were obtained by PCR amplification of pU1Rz803. The primers used for transcription were as follows: upstream primer: 5'-GAATTCTAATACGACTCACTATAGGG GATACTTACC TGGCAGGGGA-3'; downstream primer: 5'-CAGGGGAAAGCGCGAACGCA-3'; **TAATACGA CTCACTATAGGG** represented T7 promoter. The purification of PCR products was the same as that of the template for target RNA. *In vitro* transcription and purification of ribozyme were done as described above.

***In vitro* cleavage reaction of U1Rz803 and U1Rz803_m** U1Rz803, U1Rz803_m and target RNA were quantified by measuring their radioactivity cpm in 1 μ L solution. The cleavage reaction was carried out in 5 μ L solution containing 50 mmol/L Tris·HCl (pH7.5), 20 mmol/L MgCl₂. The molar ratio between ribozyme and target RNA could be estimated according to the cpm value combined with the U number in their RNAs. The initial experiment was: (I) Ribozyme (R): Substrate (S)=1:1(mol/L) ratio, 37 °C, 120 min; (II) the condition as (I), R:S=1:5 (mol/L) ratio, 37 °C, 120 min; (III) the condition as (I), U1Rz803 was incubated with target RNA at different temperatures and at different times. 1 μ L loading buffer (0.25 % Bromophenol Blue, 0.25 % Xylene cyanol FF, 20 mmol/L EDTA and saturated Urea) was added to stop the reaction. The result could be analyzed after running a 6 % denaturing polyacrylamide gel electrophoresis. The cleavage efficiency [CE] was calculated from Bq values of the bands of substrate (S) and products (P) which were cut off from denaturing PAGE. $CE=[P/(P+S)] \cdot 100\%$.

Kinetics studies of the reaction The procedure was described by Uhlenbeck^[52]. The Michaelis constant (K_m) and K_{cat} were determined for the ribozyme by performing multiple turnover kinetics experiments. The volume of kinetics reaction is 15 μ L. Ribozyme concentration was held constant at 5 nmol/L and substrate concentrations ranged from 10 nmol/L to 160 nmol/L. The cleavage reaction was done in the same buffer as described above at 37 °C for 20 minutes. The results were analyzed as above. K_m and K_{cat} were calculated by Lineweaver-Burke method (double- reciprocal plot).

RESULTS

Identification of transcription of target RNA and ribozyme

The length of target RNA transcribed from PCR-amplified template should be 220 nt. In this study the ribozymes were embedded into U1 snRNA, but stem-loop structures of U1 snRNA were maintained. Therefore, the transcripts of PCR-amplified template included U1 snRNA and ribozyme, the transcripts of U1snRNA chimeric ribozyme should be 205 nt. These results (Figure 2) were inconsistent with our design and proven to be correct.

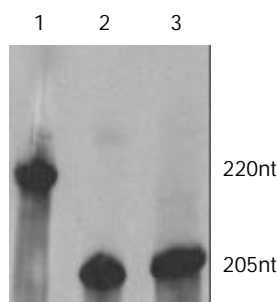


Figure 2 *In vitro* transcripts of target RNA and U1snRNA chimeric ribozymes. 1: transcript of target RNA (220 nt), 2: transcripts of U1Rz803(205 nt), 3: transcripts of U1Rz803_m (205 nt).

In vitro cleavage reaction of U1Rz803 and U1Rz803_m

The cleavage result showed that U1Rz803 was capable of cleaving target RNA *in vitro*. It could cleave target RNA (220 nt) efficiently and exactly to produce two fragment 93 nt/127 nt, while U1Rz803_m showed no *in vitro* cleavage efficacy after 120 min (Figure 3), even at R:S=5:1 (data not shown). At a 1:1 U1Rz803-to-S molar ratio, the cleavage efficiency (CE) was calculated under the condition of 37 °C and 120-minute reaction time, CE=51.36 %. At a 1:5 U1Rz803-to-S molar ratio, CE=27.81 %. This result indicated that the cleavage efficiency increased with increase of ribozyme concentration. The temperature and time would affect the cleavage efficiency.

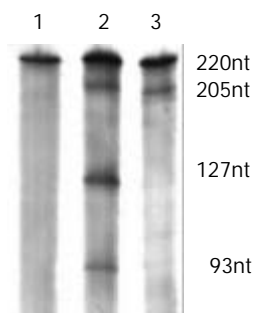


Figure 3 Cleavage of U1Rz803 and U1Rz803_m *in vitro*. 1: Target RNA, 2: target RNA incubated with U1Rz803, 3: target RNA incubated with U1Rz803_m. The ribozymes (205 nt) were shown in this figure because the transcripts were incorporated into alpha ³²P-UTP in the preparation of ribozymes.

Cleavage activity of U1Rz803 *in vitro*

Temperature course When the ratio of U1Rz803 to target RNA was 1:1(molar ratio), the reaction mixture were incubated at different temperature for 90 minutes. The optimal temperature was 50 °C, the cleavage efficacy increased at higher temperatures ranging from 0 °C to 50 °C, but when the temperature was above 50 °C, the cleavage efficacy decreased because the combination of ribozyme and target RNA was weakened (Figure 4).

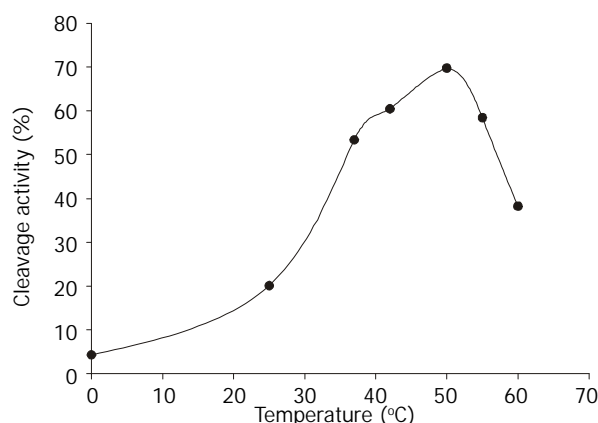


Figure 4 Temperature curve of the cleavage reactions of U1Rz803 prepared *in vitro*.

Time course The cleavage mixture (Rz:substrate=1:5 mol·L⁻¹) were incubated at 37 °C for different times, it was shown that the reaction product increased with increase in incubation time and it was linear within 60 min, CE_{max}=27.81% (Figure 5).

The kinetics of cleavage reaction Under the condition of 37 °C and 20-minute reaction time the cleavage efficiency was calculated at R:S=1:2, 1:4, 1:8, 1:16 and 1:32 (mol/L)ratio. K_m and K_{cat} were obtained by the Lineweaver-Burke method (Figure 6) K_m =34.48 nmol/L, K_{cat} =0.14 min⁻¹.

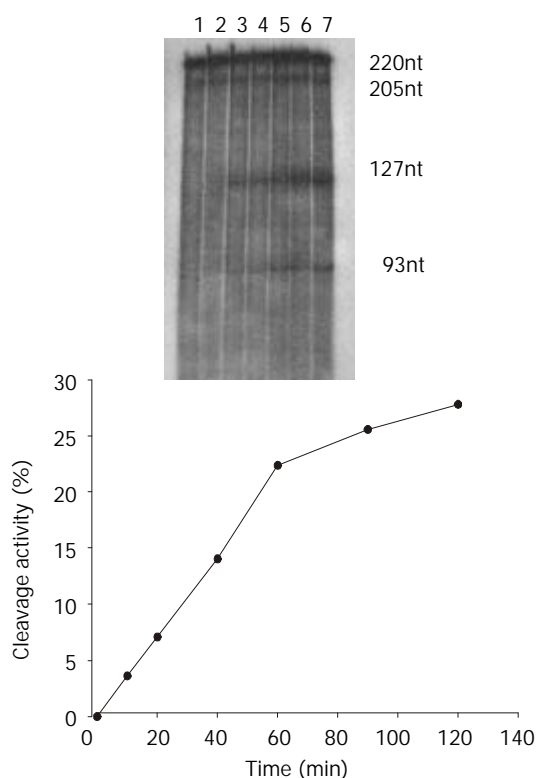


Figure 5 Time course. (A) Specific cleavage of target RNA by U1Rz803 *in vitro* at 37 °C for different times. Lane 1: substrate control; lane 2: incubated for 10 min; lane 3: 20 min; lane 4: 40 min; lane 5: 60 min; lane 6: 90 min; lane 7: 120 min. (B) Time course of cleavage reactions of U1Rz803 prepared *in vitro*.

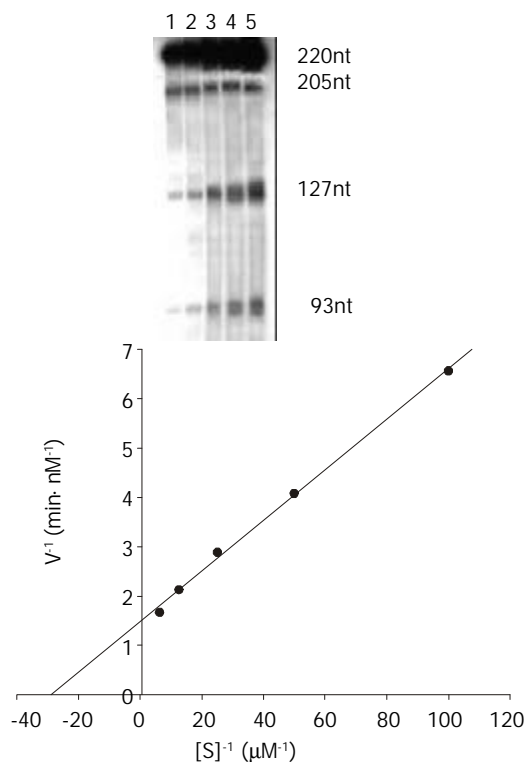


Figure 6 The kinetic of cleavage reaction for U1Rz803. (A) Specific cleavage of target RNA by U1Rz803 for the kinetic of U1Rz803 *in vitro*. U1Rz803 concentration was 5 nmol·L⁻¹, substrate concentration was 10, 20, 40, 80, 160 nmol·L⁻¹ from left to right. (B) Lineweaver-Burk kinetic plots of cleavage reaction for U1Rz803 *in vitro*. U1Rz803 concentration was 5 nmol·L⁻¹, substrate concentration was 160, 80, 40, 20, 10 nmol·L⁻¹ for each dot from left to right. Reactions were performed at 37 °C for 20 minutes.

DISCUSSION

Hepatic fibrosis is a common response to chronic liver injury from many causes, including alcohol, persistent viral infection and hereditary metal overload. To date, reversing the causative agent is the only effective therapy to stop or even reverse the liver fibrosis, but the efficacy is limited. Therefore, the development of effective antifibrotic therapies represents a challenge for modern hepatology. With the knowledge on molecular mechanism underlying pathological fibrosis expanding, there are many antifibrotic therapies based on sound biological mechanisms have been carried out. Ueki *et al* injected a mix of a haemagglutinating virus of Japan (HVJ) liposomes and a plasmid containing the complementary DNA for human hepatocyte growth factor (HGF) into the gluteus muscle of rats treated with dimethylnitrosamine (DMN), a model of persistent liver fibrosis, that could produce the resolution of fibrosis in the cirrhotic liver^[32], but tumorigenicity found in transgenic mice overexpressing HGF^[53] and repetitive *in vivo* transfection are two disadvantages. Qi and Nakamura *et al* prevent liver fibrosis from blockade of TGF beta signal by adenovirus-mediated local expression of a dominant negative type II TGF-beta receptor in the liver of rats treated with DMN, this intervention not only suppressed fibrosis, but also facilitated hepatocyte regeneration, however prolonged period of blocking TGF beta signal could result in unfavorable consequences, such as the inflammation and tissue necrosis^[30,33]. Because TGF β 1 plays a crucial role in liver fibrosis and no report on anti-TGF β 1 ribozyme-mediated cleavage of target RNA for the treatment of liver fibrosis has been published, in this study we designed ribozyme targeting against TGF β 1 and cloned the ribozyme genes into U1 ribozyme vector, prepared U1 snRNA chimeric ribozymes and identified the cleavage activity of ribozymes *in vitro*.

In the previous study on cleavage activity of U1 snRNA chimeric ribozyme *in vitro*, ribozymes were prepared through the transcription of synthesized ribozyme genes containing T7/SP6 promoter, the transcripts only included ribozyme^[43]; but ribozyme structure induced by the secondary structure of long flanking sequences would affect ribozyme's turnover ratio and/or binding activity as the results of less accurate hybridization and less cleavage. In this study we prepared ribozyme by the PCR-amplified templates. The transcripts included U1 snRNA and ribozyme. Compared with the previous study, it may reflect the cleavage activity of U1Rz803 more accurately *in vivo*. From our study, we found that the cleavage activity of U1sn RNA chimeric ribozyme was inferior to that of non-modified ribozyme, the result was not shown in this paper. Trimethylguanosine 5' cap, stable stem-loop structures at both end, high GC content of 3' loop in the structure of U1 snRNA confer resistance to exonucleases *in vivo*^[54]. The hypermethylation of the 5' cap structure and Sm binding site enable U1 snRNA to accumulate in the nucleoplasm, these make U1 snRNA an effective vector for efficient expression and delivery of ribozyme in the nuclear compartment *in vivo*. The transcripts of ribozyme labeled by isotope not only provided convenience for us to isolate ribozyme by cutting off autoradiograph bands, but the transcripts were qualified more accurately than non-labeled transcripts of ribozymes. In this study K_m and K_{cat} of U1Rz803 were measured at 37 °C, not at optimal temperature. Because the ribozyme is used *in vivo* and the temperature *in vivo* is constant at 37 °C, these results may reflect cleavage activity of U1Rz803 in physiological condition.

Ribozymes have all the properties of antisense RNA with the additional feature of catalytic cleavage. To separate antisense from cleavage effect, we created inactive ribozymes by substituting an essential nucleotide of the catalytic core with

an inactive one. The cleavage reaction revealed that U1Rz803 possessed the perfect cleavage activity, while U1Rz803_m possessed no catalytic activity. It can be used as control to exclude antisense effect of ribozyme *in vivo* in order that it is proven that the activity of U1Rz803 is due to catalytic cleavage *in vivo*. The kinetics of U1Rz803 showed that U1Rz803 possessed perfect specific ability of cleaving the TGFβ1 transcripts *in vitro*. These results made U1Rz803 to be worthy of being studied in intact cell and be developed as a nucleic acid drug in the future. However the *in vitro* result cannot completely reflect *in vivo* performance. The secondary and tertiary structure formed by the total TGF beta 1 mRNA transcript in the cell, the subcellular compartment which the ribozyme and target are located in, degradation of ribozyme, the complexes which are formed by ribozyme and ribonucleoprotein within cell and gene delivery system affect expression of ribozyme and cleavage activity of ribozyme. So *in vivo* effect of the ribozyme should be investigated as soon as possible. Experimental analysis of activity of the anti-TGF beta1 ribozyme in HSC-T6 cell is in progress.

ACKNOWLEDGEMENTS

We thanks Mr. F Xu, Mr. G Jiang, Mr.XL Chen, Mr.J Jia, Mr. ZW Wang and Miss W Li for their kind help.

REFERENCES

- Zhu YH**, Hu DR, Nie QH, Liu GD, Tan ZX. Study on activation and c-fos, c-jun expression of *in vitro* cultured human hepatic stellate cells. *Shijie Huaren Xiaohua Zazhi* 2000; **8**: 299-302
- Du WD**, Zhang YE, Zhai WR, Zhou XM. Dynamic changes of type I, III and IV collagen synthesis and distribution of collagen-producing cells in carbon tetrachloride-induced rat liver fibrosis. *World J Gastroenterol* 1999; **5**: 397-403
- Huang ZG**, Zhai WR, Zhang YE, Zhang XR. Study of heteroserum-induced rat liver fibrosis model and its mechanism. *World J Gastroenterol* 1998; **4**: 206-209
- Jia JB**, Han DW, Xu RL, Gao F, Zhao LF, Zhao YC, Yan JP, Ma XH. Effect of endotoxin on fibronectin synthesis of rat primary cultured hepatocytes. *World J Gastroenterol* 1998; **4**: 329-331
- Cheng ML**, Wu YY, Huang KF, Luo TY, Ding YS, Lu YY, Liu RC, Wu J. Clinical study on the treatment of liver fibrosis due to hepatitis B by IFN-α1 and traditional medicine preparation. *World J Gastroenterol* 1999; **5**: 267-269
- Nie QH**, Cheng YQ, Xie YM, Zhou YX, Cao YZ. Inhibiting effect of antisense oligonucleotides phosphorothioate on gene expression of TIMP-1 in rat liver fibrosis. *World J Gastroenterol* 2001; **7**: 363-369
- Friedman SL**. The cellular basis of hepatic fibrosis: mechanism and treatment strategies. *N Engl J Med* 1993; **328**: 1828-1835
- Wang X**, Chen YX, Xu CF, Zhao GN, Huang YX, Wang QL. Relationship between tumor necrosis factor-α and liver fibrosis. *Huaren Xiaohua Zazhi* 1998; **6**: 106-108
- Xu LX**, Xie XC, Jin R, Ji ZH, Wu ZZ, Wang ZS. Effect of selenium in rat experimental liver fibrosis. *Huaren Xiaohua Zazhi* 1998; **6**: 133-135
- Li DG**, Lu HM, Chen YW. Studies on anti-liver fibrosis of tetradrine. *Shijie Huaren Xiaohua Zazhi* 1999; **7**: 171-172
- Wu YA**, Kong XT. Anti-hepatic fibrosis effect of pentoxifylling. *Shijie Huaren Xiaohua Zazhi* 1999; **7**: 265-266
- Liu F**, Liu JX, Cao ZC, Li BS, Zhao CY, Kong L, Zhen Z. Relationship between TGF-β1, serum indexes of liver fibrosis and hepatic-tissue pathology in patients with chronic liver diseases. *Shijie Huaren Xiaohua Zazhi* 1999; **7**: 519-521
- Gu SW**, Luo KX, Zhang L, Wu AH, He HT, Weng JY. Relationship between ductular proliferation and liver fibrosis of chronic liver disease. *Shijie Huaren Xiaohua Zazhi* 1999; **7**: 845-847
- Li BS**, Wang J, Zhen YJ, Liu JX, Wei MX, Sun SQ, Wang SQ. Experimental study on serum fibrosis markers and liver tissue pathology and hepatic fibrosis in immuno damaged rats. *Shijie Huaren Xiaohua Zazhi* 1999; **7**: 1031-1034
- Wang Y**, Gao Y, Huang YQ, Yu JL, Fang SG. Gelatinase a proenzyme expression in the process of experimental liver fibrosis. *Shijie Huaren Xiaohua Zazhi* 2000; **8**: 165-167
- Wang FS**, Wu ZZ. Current situation in studies of gene therapy for liver cirrhosis and liver fibrosis. *Shijie Huaren Xiaohua Zazhi* 2000; **8**: 371-373
- Wang GQ**, Kong XT. Action of cell factor and decorin in tissue fibrosis. *Shijie Huaren Xiaohua Zazhi* 2000; **8**: 458-460
- Liu F**, Wang XM, Liu JX, Wei MX. Relationship between serum TGF-β1 of chronic hepatitis B and hepatic tissue pathology and hepatic fibrosis quantification. *Shijie Huaren Xiaohua Zazhi* 2000; **8**: 528-531
- Li JC**, Ding SP, Xu J. Regulating effect of Chinese herbal medicine on the peritoneal lymphatic stomata in enhancing ascites absorption of experimental hepatofibrotic mice. *World J Gastroenterol* 2002; **8**: 333-337
- Olaso E**, Friedman SL. Molecular regulation of hepatic fibrogenesis. *J Hepatol* 1998; **29**: 836-842
- Pinari M**, Marra F, Carloni V. Signal transduction in hepatic stellate cells. *Liver* 1998; **18**: 2-13
- Alcolado R**, Arthur MIP, Iredale JP. Pathogenesis of liver fibrosis. *Clin Sci* 1997; **92**: 103-112
- Massague J**. The transforming growth factor-beta family. *Annu Rev Cell Biol* 1990; **6**: 597-641
- Sporn MB**, Robert AB. Transforming growth factor-beta: recent progress and new challenges. *J Cell Biol* 1992; **119**: 1017-1021
- Border WA**, Noble NA. Transforming growth factor-beta in tissue fibrosis. *N Engl J Med* 1994; **331**: 1286-1292
- Heldin CH**, Miyazono K, ten Dijke P. TGF-beta signaling from cell membrane to nucleus through SMAD proteins. *Nature* 1997; **390**: 465-471
- Miyazono K**. TGF-beta receptors and signal transduction. *Int J Hematol* 1997; **65**: 97-104
- Friedman SL**. Molecular regulation of hepatic fibrosis, an integrated cellular response to tissue injury. *J Biol Chem* 2000; **275**: 2247-2250
- Bissell DM**, Roulot D, George J. Transforming Growth factor and liver. *Hepatology* 2001; **34**: 859-867
- Qi Z**, Atsuchi N, Ooshima A, Takeshita A, Ueno H. Blockade of type beta transforming growth factor signaling preventing liver fibrosis and dysfunction in the rat. *Proc Natl Acad Sci* 1999; **96**: 2345-2349
- Sanderson N**, Factor V, Nagy P, Kopp J, Kondaiah P, Wakefield L, Roberts AB, Sporn MB, Thorgeirsson SS. Hepatic expression of mature transforming growth factor beta 1 in transgenic mice results in multiple tissue lesions. *Proc Natl Acad Sci* 1995; **92**: 2572-2576
- Ueki T**, Kaneda Y, Tsutsui H, Nakanishi K, Sawa Y, Morishita R, Matsumoto K, Nakamura T, Takahashi H, Okamoto E, Fujimoto J. Hepatocyte growth factor gene therapy of liver cirrhosis in rats. *Nat Med* 1999; **5**: 226-230
- Nakamura T**, Sakata R, Ueno T, Sata M, Ueno H. Inhibition of transforming growth factor beta prevents progression of liver fibrosis and enhances hepatocyte regeneration in dimethylnitrosamine-treated rats. *Hepatology* 2000; **32**: 247-255
- Ueno H**, Sakamoto T, Nakamura T, Qi Z, Atsuchi N, Takeshita A, Shimizu K, Ohashi H. A soluble transforming growth factor beta receptor expressed in muscle prevents liver fibrogenesis and dysfunction in rats. *Hum Gene Ther* 2000; **11**: 33-42
- Persidis A**. Ribozyme therapeutics. *Nat Biotechnol* 1997; **15**: 921-922
- Gibson SA**, Shillito E. Ribozymes. Their functions and strategies for their use. *Mol Biotechnol* 1997; **7**: 125-137
- James HA**, Gibson I. The therapeutic potential of ribozymes. *Blood* 1998; **91**: 371-382
- Muotri AR**, da Veiga Pereira L, dos Reis Vasques L, Menck CF. Ribozymes and the anti-gene therapy: how a catalytic RNA can be used to inhibit gene function. *Gene* 1999; **237**: 303-310
- von Weizsacker F**, Blum HE, Wands JR. Cleavage of hepatitis B virus RNA by three ribozymes transcribed from a single DNA template. *Biochem Biophys Res Commun* 1992; **189**: 743-748
- Beck J**, Nassal M. Efficient hammerhead ribozyme-mediated cleavage of the structured hepatitis B virus encapsidation signal *in vitro* and in cell extracts, but not in intact cells. *Nucleic Acids Res* 1995; **23**: 4954-4962

- 41 **Xu RH**, Liu J, Zhou XQ, Xie Q, Jin YX, Yu H, Liao D. Activity identification of anti-caspase-3 mRNA hammerhead ribozyme in both cell-free condition and BRL-3A cells. *Chin Med J* 2001; **114**: 606-611
- 42 **Xu RH**, Liu J, Xu F, Jiang G, Xie Q, Zhou XQ, Jin YX, Wang DB. Activity identification of chimeric anti-caspase-3 mRNA hammerhead ribozyme *in vitro* and *in vivo*. *Science China(C)* 2001; **44**: 618-627
- 43 **Liu R**, Li W, Karin NJ, Bergh JJ, Adler-Storthz K, Farach-Carson MC. Ribozyme ablation demonstrates that the cardiac subtype of the voltage-sensitive calcium channel is the molecular transducer of 1, 25-dihydroxyvitamin D(3)-stimulated calcium influx in osteoblastic cells. *J Biol Chem* 2000; **275**: 8711-8718
- 44 **Montgomery RA**, Dietz HC. Inhibition of fibrillin 1 expression using U1 snRNA as a vehicle for the presentation of antisense targeting sequence. *Hum Mol Genet* 1997; **6**: 519-525
- 45 **Michienzi A**, Prislei S, Bozzoni I. U1 small nuclear RNA chimeric ribozymes with substrate specificity for the Rev pre-mRNA of human immunodeficiency virus. *Proc Natl Acad Sci* 1996; **93**: 7219-7224
- 46 **Vogel S**, Piantedosi R, Frank J, Lalazar A, Rockey DC, Friedman SL, Blaner WS. An immortalized rat liver stellate cell line (HSC-T6): a new cell model for the study of retinoid metabolism *in vitro*. *J Lipid Res* 2000; **41**: 882-893
- 47 **Kim Y**, Ratziu V, Choi SG, Lalazar A, Theiss G, Dang Q, Kim SJ, Friedman SL. Transcriptional activation of transforming growth factor beta1 and its receptors by the Kruppel-like factor Zf9/core promoter-binding protein and Sp1. Potential mechanisms for autocrine fibrogenesis in response to injury. *J Biol Chem* 1998; **273**: 33750-33758
- 48 **Qian SW**, Kondaiah P, Roberts AB, Sporn MB. cDNA cloning by PCR of rat transforming growth factor beta-1. *Nucleic Acids Res* 1990; **18**: 3059
- 49 **Manser T**, Gesteland RF. Characterization of small nuclear RNA U1 gene candidates and pseudogenes from the human genome. *J Mol Appl Genet* 1981; **1**: 117-125
- 50 **Zhuang Y**, Weiner AM. A compensatory base change in U1 snRNA suppresses a 5' splice site mutation. *Cell* 1986; **46**: 827-835
- 51 **Skuzeski JM**, Lund E, Murphy JT, Steinberg TH, Burgess RR, Dahlberg JE. Synthesis of human U1 RNA. II. Identification of two regions of the promoter essential for transcription initiation at position +1. *J Biol Chem* 1984; **259**: 8345-8352
- 52 **Uhlenbeck OC**. A small catalytic oligoribonucleotide. *Nature* 1987; **328**: 596-600
- 53 **Takayama H**, LaRochelle WJ, Sharp R, Otsuka T, Kriebel P, Anver M, Aaronson SA, Merlino G. Diverse tumorigenesis associated with aberrant development in mice overexpressing hepatocyte growth factor/scatter factor. *Proc Natl Acad Sci* 1997; **94**: 701-706
- 54 **Green MR**. Biochemical mechanisms of constitutive and regulated pre-mRNA splicing. *Annu Rev Cell Biol* 1991; **7**: 559-599

Edited by Wu XN

Analysis of spontaneous, gamma ray- and ethylnitrosourea-induced hprt mutants in HL-60 cells with multiplex PCR

Sheng-Xue Liu, Jia Cao, Hui An, Hua-Min Shun, Lu-Jun Yang, Yong Liu

Sheng-Xue Liu, Jia Cao, Hui An, Hua-Min Shun, Lu-Jun Yang, Yong Liu, Department of Health Toxicology, Preventive Medical College, Third Military Medical University, Chongqing 400038, China
Supported by the National Natural Science Foundation of China, No.39970650

Correspondence to: Dr. Jia Cao, Preventive Medical College, Third Military Medical University, Chongqing 400038, China. caoqq@yahoo.com

Telephone: +86-23-68752271 **Fax:** +86-23-68752277

Received: 2002-10-09 **Accepted:** 2002-11-09

Abstract

AIM: To explore the molecular spectra and mechanism of human hypoxanthine guanine phosphoribosyl transferase (hprt) gene mutation induced by ethylnitrosourea (ENU) and ^{60}Co γ -rays.

METHODS: Independent human promyelocytic leukemia cells (HL-60) mutants at the hprt locus were isolated from untreated, ethylnitrosourea (ENU) and ^{60}Co γ -ray-exposed cells, respectively, and verified by two-way screening. The genetic changes underlying the mutation were determined by multiplex polymerase chain reaction (PCR) amplification and electrophoresis technique.

RESULTS: With dosage increased, survival rate of plated cell reduced (in the group with dosage of ENU with 100-200 $\mu\text{g}/\text{ml}$, $P<0.01$; in the group with dosage of ^{60}Co γ -ray with 2-4 Gy, $P<0.05$) and mutational frequency increased (in the group of ENU 12.5-200.0 $\mu\text{g}/\text{ml}$, $P<0.05$; in the group of ^{60}Co γ -ray with 1-4 Gy, $P<0.05$) significantly. In the 13 spontaneous mutants analyzed, 92.3 % of mutant clones did not show any change in number or size of exon, a single exon was lost in 7.7 %, and no evidence indicated total gene deletion occurred in nine hprt exons. However, deletions were found in 79.7 % of ENU-induced mutations (62.5-89.4 %, $P<0.01$) and in 61.7 % of gamma-ray-induced mutations (28.6-76.5 %, $P<0.01$). There were deletion mutations in all 9 exons of hprt gene and the most of induced mutations were chain deletion with multiplex exons (97.9 % in gamma-ray-induced mutants, 88.1 % in ENU-induced mutants).

CONCLUSION: The spectra of spontaneous mutations differs completely from that induced by ENU or ^{60}Co γ -ray. Although both ENU and γ -ray can cause destruction of genetic structure, mechanism of mutagenesis between them may be different.

Liu SX, Cao J, An H, Shun HM, Yang LJ, Liu Y. Analysis of spontaneous, gamma ray- and ethylnitrosourea-induced hprt mutants in HL-60 cells with multiplex PCR. *World J Gastroenterol* 2003; 9(3): 578-583

<http://www.wjgnet.com/1007-9327/9/578.htm>

INTRODUCTION

Many developments in molecular biology, especially,

polymerase chain reaction (PCR) have made procedure of mutation analysis relatively simple^[1,2]. Classically, Southern hybridization was the primary method for the molecular analysis of deletion mutations. However, southern analysis not only is time-consuming but also provides incomplete results due to the limited resolution of each exon and possible cross-hybridization with pseudogenes. Therefore, using PCR to amplify each individual exon of the hprt gene provides a powerful alternative method to southern analysis^[3]. PCR has been used for the analysis of various mutations in human and Chinese hamster cells. These and other studies of the hprt locus in various mammalian cells have shown a wide spectrum of structural aberrations in the hprt gene, which are induced by physical and chemical mutagens^[4-7]. Ionizing radiation induces deletion mutations and results in genetic alterations, which can be detected by Southern analysis^[8]. Such detectable genetic alterations have been found infrequently after exposure to ultraviolet (UV) light, ethyl methane sulfonate (EMS), ICR-191 and N-ethyl-N-nitrosourea (ENU)^[9-11]. Thus, while conventional missense mutagens induce predominantly point mutations, ionizing radiation induces both point and deletion mutations.

As a part of our ongoing effort to analyze the nature and spectrum of mutations induced by various types of physical and chemical mutagens, we adopted the multiplex PCR technique for the initial screening of deletion mutants. In this paper, we have characterized the molecular nature of mutations induced by γ -ray and ENU at the hprt locus of human promyelocytic leukemia cells.

MATERIALS AND METHODS

Cell culture

HL-60 is a human acute promyelocytic leukemia cell line described earlier by Collins *et al.* HL-60 cells were maintained as an asynchronous, exponentially growing population in RPMI 1640 medium (Sigma, St. Louis, USA) supplemented with 10 % fetal bovine serum (SJQ, Hangzhou, China), 100 U/ml penicillin (Sigma), 100 $\mu\text{g}/\text{ml}$ streptomycin (Sigma), and 2 mM L-glutamine (Gibco, Carlsbad, USA) at 37 °C in an atmosphere of 5 % CO_2 . Preexisting hprt mutants that cannot live in thymidine (Sigma; HAT culture medium) were removed by incubating cells in complete medium supplemented with 10^{-6} M aminopterin (Gibco), 10^{-4} M hypoxanthine (Sigma) and 10^{-5} M HAT culture medium for 24 hours, then the medium was replaced with complete medium containing 10^{-5} M thymidine and 10^{-4} M hypoxanthine and cultured for 48 hours. Following removal this medium, the cells were incubated in normal medium for 7-10 days.

Cytotoxicity

For measuring the cytotoxicity of γ -ray and ENU (Tokyo, Japan), exponentially growing HL-60 cells were treated with different doses of γ -ray and ENU. Initial cell number inoculated was 5.0×10^6 . Sterile distilled water was used as negative control. After incubation, the cells were harvested and washed twice with D-Hank's medium at 37 °C, counted and diluted in normal culture medium and transferred to 96 microwell plates (Gibco),

one single cell was inoculated in 200 μ l medium per well. After incubating for 7 days, colonies per well were counted and the plating efficiency (PE) was calculated with equation:

$$PE = \frac{-\ln(\text{Number of negative well/Number of all wells})}{\text{Number of cells per well}}$$

Mutation experiments

After expression of gene mutations (8 days) HL-60 cells were added in the 96-well microtiter plates to ensure one cell was inoculated per well. After incubating for 7 days, wells with colony formation were counted as positive wells for cloning efficiency (CE). Meanwhile, cells were added in other 96 microwell plates to ensure that each well received 1×10^4 cells in 200 μ l medium containing 1 μ g/ml 6-thioguanine (6-TG; Sigma). After incubating for 8 days, positive wells were counted and mutant frequency (MF) was calculated. Three plates were used for CE and MF in each treatment.

$$MF = \frac{-\ln(\text{Number of negative wells/Number of all wells})}{\text{Number of cells per well} \times CE}$$

Screening, extension and DNA isolation

A single positive clone was transferred from the 96-well plate to a 24-microwell plate (Gibco) with 1 ml screening medium containing 2 μ g/ml 6-TG in each well and cultured for additional 1-2 days. Then, 10^3 cells was transferred to each well in a new 24-microwell plate in HAT culture medium and cultured for 1-3 days. If the cells in a well were obviously dead, the cloned cells of the well were identified as mutated clones and the remaining cloned cells in the 24-microwell were transferred into culture bottles for extension expression. DNA isolation and purification from wild-type cells and hprt-mutated cells was performed with conventional method.

Design, synthesis and appraisal of primers

Eight pairs of oligonucleotide primers were designed by computer software with a minor modification of the literature^[12]. The synthesis and appraisal of the 8 pairs of primers were completed by different laboratories of Beckman Company in Beijing, Cybersyn B. J. in American and the Institute of Cellular Biology of Chinese Academy of Science in Shanghai.

Sequence of 8 pairs of oligonucleotide primers was showed in Table 1. Exons 7 and 8 were amplified simultaneously with same primers, because they are only 163 bp apart. All primers except the exon 1 specific ones enabled amplification of the corresponding exons in the multiplex PCR. It was, however, difficult to include exon 1 primers within the remaining set of all primers without having a spurious synthesis of non-specific signal. In our pre-experiments with several primer pairs in one PCR reaction it was difficult to control and optimize the reaction conditions. In addition, insertions and deletions within exons could occur, therefore we restricted the number of primer pairs in a single PCR reaction in order to confirm the distances among of PCR products based on molecular weights. So, false-negative or false-positive rate was reduced. Following some preliminary experiments, 8 pairs of primers of exons were divided into 3 groups, group one was multiplex PCR including exons 2, 5, 6 and 7/8, group two included exons 3, 4, and 9; in group three, exon 1 was amplified separately. Multiplex PCR method was used to analyze 119 mutants.

PCR analysis

For amplification of hprt exons, 0.5-2.0 μ l of genomic DNA (36-50 ng) was mixed with 50 pmol of each primer in 50 μ l containing 50 mM KCl, 10 mM Tris-HCl (pH8.8), 0.3-1.05

mM MgCl₂, 0.2 mM dNTPs and 2.5 U of Amplitaq DNA polymerase (Shenggong, Shanghai, China). After initial denaturation of the template DNA at 98 $^{\circ}$ C for 7 min, a total of 40 PCR cycles were performed with denaturation at 94 $^{\circ}$ C for 1.5 min, annealing at 52 $^{\circ}$ C for 1.5 min and extension at 72 $^{\circ}$ C for 2.0 min. Exon 1 was synthesized individually with a modified condition: a total of 30 PCR cycles were performed with denaturation at 95 $^{\circ}$ C for 0.5 min, annealing at 64 $^{\circ}$ C for 1.0 min and extension at 72 $^{\circ}$ C for 1 min. The last cycle was extension at 72 $^{\circ}$ C for 7 min. The PCR product (10 μ l) was used for analysis by 3 % agarose gel or by using polyacrylamide gel electrophoresis (Figure 1).

Table 1 Oligonucleotide primers in multiplex PCR of the human HPRT locus

Exons	Primers sequence (5' -3')	Fragment size (bp)
1	F TGG GAC GTC TGG TCC AAG GAT TCA R CCG AAC CCG GGA AAC TGG CCG CCC	626
2	F CCT GAT ATG CTC TCA TTG AAA CA R GCT GCT GAT GTT TGA AAT TAA CAC	211
3	F GTT TAA TGA CTA AGA GGT GTT TG R GAA AAC CTA GTG TTG CCA CAT AA	311
4	F GTG TGT GTA CAT AAG GAT ATA CA R TTC TTC CCT TTC AAG ATA CAT AC	165
5	F GGA AAT ACC GTT TTA TTC ATT GT R GTG CAT ACT AAG TTA GAA AGG TC	125
6	F GTG ACT CTG AAT TTA AAG CTA TG R CTG TGT CAA AAT GTC ATA CAT AC	150
7/8	F GTC TCT CTG TAT GTT ATA TGT CAC R TGC GTG TTT TGA AAA ATG AGT GAG	379
9	F GCT ATT CTT GCC TTT CAT TTC AG R CAA ACT CAA CTT GAA CTC TCA TC	136

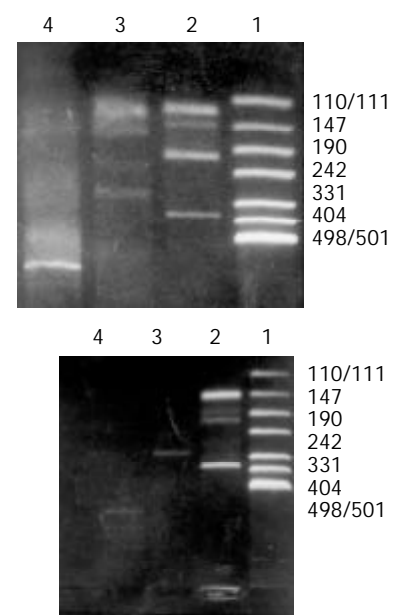


Figure 1 Detection of deletion mutation in human hprt gene by multiplex PCR. (A) PCR products from normal cells; (B) PCR products from one hprt mutant. (1) PUC Mix Marker; (2) Exons 2,5,6,7/8; (3) Exons 3,4,9; (4) Exon 1.

Statistics

All data were analyzed by student's *t* test and total rate test. The statistical difference $P < 0.05$ was considered as significant and $P < 0.01$ as very significant.

RESULTS

Cytotoxicity and mutagenicity of γ -rays and ENU

The HL-60 cells plating efficiency (PE) gradually decreased with increasing concentrations of ENU. There was a significant difference from the control of PE at concentrations above 100.0 $\mu\text{g/ml}$ of ENU. A linear increase of the mutation frequency (MF) with increasing concentration of ENU was found. At 12.5-200.0 $\mu\text{g/ml}$ ENU, MF was 3.5-20.8 times higher than that in the control cultures. The cytotoxicity and mutagenicity of γ -rays were similar to ones of ENU. The HL-60 cells PE gradually decreased with increasing doses of γ -rays. There was a significant difference of PE at doses above 2.0 Gy of γ -rays in comparison with the control. A linear increase of the MF with increasing doses of γ -rays was found. At 1.0-4.0 Gy γ -rays, MF was 3.6-14.2 times higher than that in the control cultures (Table 2).

Table 2 Cytotoxicity and mutagenicity of γ -rays and ENU in HL-60 cells

Type	Dose	PE(%)	CE(%)	MF($\times 10^{-6}$)
Control ($\mu\text{g/ml}$)	0.0	93.01	86.64	5.13
ENU ($\mu\text{g/ml}$)	12.5	75.92	85.91	17.73 ^a
	25.0	70.67	78.62	31.18 ^b
	50.0	61.45	82.67	64.45 ^b
	100.0	45.77 ^b	83.91	82.61 ^b
	200.0	25.63 ^b	67.02	106.70 ^b
γ -ray (Gy)	0.5	91.63	146.0 ^b	12.30
	1.0	69.31	186.0 ^b	18.30 ^b
	2.0	55.34 ^a	108.2	23.20 ^a
	4.0	39.94 ^b	69.0	73.00 ^b

^a $P < 0.05$ vs control group, ^b $P < 0.01$ vs control group.

Multiplex PCR analysis

Analysis of multiplex PCR was done in 13 spontaneous mutants, 59 ENU-induced and 47 γ -rays-induced hprt mutants. Forty-two mutants (35.3 %) of 119 mutants analyzed were found to exhibit no abnormal band in any of the 9 exons, which indicated that these mutants had point mutation without exon deletion or insertion. In 47 of 119 mutants, less than 8 bands were existed for each locus, and showed partial deletions of exons. The remaining 30 mutants had no PCR products, which meant that all exons studied were deleted. Of all mutants analyzed, 64.7 % (77/119) had partial or complete deletions.

Molecular spectrum of HPRT gene

Spontaneously derived, γ -rays- and ENU-induced mutants at the hprt locus were showed in Table 3. The electrophoresis patterns of mutants mainly consisted of three types: "normal pattern" including point mutations, total deletion and partial deletion. γ -rays- (1.0-4.0 Gy) and ENU-induced (12.5-200.0 $\mu\text{g/ml}$) mutant cells showed mutation spectra that were significantly different from the spectra of spontaneous mutations. Total exon deletion did not existed in any spontaneous mutants but in γ -rays- and ENU-induced mutants. The proportions of deletion mutations were quite different between spontaneous mutants and induced mutants, and similar change of γ -rays- and ENU-induced mutants occurred at the hprt locus. Over 60 % deletion mutations were found in these two kind of induced mutants while only 7.7 % deletions were found in spontaneous mutants. The proportion of the "normal pattern" in spontaneous mutants and induced mutants were 92.3 % and less than 40 %, respectively. The clearer dose-response relationship was seen in induction of partial- and whole-deletion mutation than in induction of mutants including and kind of mutations.

Analysis of deletion breakpoints

Distribution of the deletions in the 9 exons of the hprt gene found in the 119 mutants analyzed (Table 4). Deletion mutations were found in all 9 exons of the hprt gene, but number of single exon deletion was very small. Most of γ -rays- (59.6 %) and ENU-induced (67.8 %) mutations were chain deletion with multiple exons.

Table 3 Summary of multiplex PCR analysis of THH-induced HPRT mutants in HL-60 cells

Categories of mutation	Number analyzed	Number showing PCR changes		Percentage deleted	Number showing no change
		Complete deletion	Partial deletion		
Spontaneous	13	0	1/13 (7.7%)	7.7%	12/13 (92.3%)
ENU ($\mu\text{g/ml}$)					
12.5	8	1/8 (12.5%)	4/8 (50.0%) ^a	62.5% ^b	3/8 (37.5%) ^a
25.0	10	2/10 (20.0%)	5/10 (50.0%) ^a	70.0% ^b	3/10 (30.0%) ^b
50.0	10	2/10 (20.0%)	6/10 (60.0%) ^b	80.0% ^b	2/10 (20.0%) ^b
100.0	12	4/12 (33.3%) ^a	6/12 (50.0%) ^a	83.3% ^b	2/12 (16.7%) ^b
200.0	19	7/19 (36.8%) ^a	10/19 (52.6%) ^a	89.4% ^b	2/19 (10.6%) ^b
γ -rays (Gy)					
0.5	7	1/7 (14.3%)	1/7 (14.3%)	28.6%	5/7 (71.4%)
1.0	13	3/13 (23.1%)	5/13 (38.5%)	61.5% ^b	5/13 (38.5%) ^b
2.0	10	3/10 (30.0%) ^a	3/10 (30.0%)	60.0% ^b	4/10 (40.0%) ^b
4.0	17	7/17 (41.2%) ^b	6/17 (35.3%)	76.5% ^b	4/17 (23.5%) ^b

^a $P < 0.05$ vs control group, ^b $P < 0.01$ vs control group.

Table 4 Schematic diagram of the distribution of deletion within nine exons of the human HPRT gene

	Types of exons deletion								Mutation clones	
	1	2	3	4	5	6	7/8	9	Number	Percent (%)
Spontaneous mutants									12	92.3
					— ^a				1	7.7
ENU-induced mutants									12	20.3
	—								3	5.1
			—						2	3.4
				—	—				4	6.8
					—				2	3.4
			—					—	1	1.7
	—	—	—						2	3.4
		—	—	—					2	3.4
				—	—	—	—		2	3.4
						—	—	—	1	1.7
		—	—				—	—	1	1.7
				—	—	—	—	—	3	5.1
		—	—	—	—	—	—	—	1	1.7
	—	—	—	—	—	—	—	—	16	27.1
		—	—	—	—			—	1	1.7
	—				—	—	—		1	1.7
		—			—				2	3.4
		—		—		—	—		2	3.4
					—	—			1	1.7
r-rays-induced mutants									18	38.3
			—						1	2.1
	—	—							1	2.1
			—	—					2	4.3
	—	—	—				—	—	2	4.3
	—	—	—	—			—	—	1	2.1
	—	—	—	—		—	—	—	1	2.1
				—	—	—	—	—	3	6.4
	—	—	—				—	—	1	2.1
				—	—	—	—	—	1	2.1
		—	—	—	—	—	—	—	2	4.3
	—	—	—	—	—	—	—	—	14	29.8

^adeletion of a exon.

DISCUSSION

The X-linked HPRT gene is the most extensively examined mammalian locus for mutagenesis studies^[13-15]. The enzyme is part of the purine salvage pathway, catalyzing the reaction of 5-phosphoribosyl, 1-pyrophosphate with either hypoxanthine or guanine to form precursors that are recycled for use in DNA synthesis. As exploited in mutation analysis, this pathway leads to the killing of wild-type cells exposed to the toxic base analogue 6-TG^[16-18]. Toxicity and mutagenesis of γ -ray and ENU were characterized in HPRT locus forward mutation test, and found that reverse relationship between them was existed. γ -ray and ENU could serve a dual purpose to clone efficiency of HL-60 cell, which have association with dosages.

DNA hybridization used to be a main method in mutation analysis of HPRT gene, and recently PCR has been used in studies of gene mutation, and improved the precision of mutation analysis^[19-21]. HPRT gene mutations were studied with multiplex PCR method. As it was difficult to control and

optimize the reaction conditions in our preliminary study, insertions and deletions within exons could occur, the number of primer pairs in a single PCR reaction was restricted in order to confirm the distances among of PCR products according to their molecular weights, consequently false-negative or false-positive rate were reduced. Therefore, eight pairs of primers were divided into 3 groups: one multiplex PCR included exons 2, 5, 6 and 7/8, second one included exons 3, 4 and 9, and in third one, exon 1 was amplified separately.

ENU is a direct-acting alkylating agent that produces similar ratios of well-characterized ethyl adducts in DNA in solution, in prokaryotes, in cultured mammalian cells, and in various tissues of rats and mice *in vivo*^[22-24]. Several O-ethyl-adducts, including O⁶-ethylguanine, O⁴-ethylthymine, and O²-ethylthymine, have been shown to direct mispairing of bases during DNA replication *in vitro*^[25,26], and the results of site-directed mutations are consistent with the types of base substitutions observed in assays of ENU mutation specificity^[27].

Furthermore, ENU was used as the model agent for developing the *in vivo* hprt mutation assays in mouse, rat, and monkey and for defining the age-dependent relationships between chemical exposure, DNA adduction, and phenotypic expression of hprt mutations in T cells of exposed mice^[28,29].

Ionizing radiation may exert a carcinogenic stimulus, even at low levels of exposure. Such biological effects have been extensively studied. Observed mutation frequencies of γ -ray-induced mutation in HL-60 cells were similar to the results reported previously for X-irradiated human fibroblasts^[30-32]. Our results support the general observation that the majority of ionizing-radiation-induced mutations at the hprt locus are large deletions, about 60 % of mutants of γ -irradiated HL-60 cells exhibited large deletions (1.0-4.0 Gy). These results suggest that the size of genetic alteration appears to be dependent on doses. It is now thought that hprt gene mutations unlikely results from block of transcription and the initial damage leads to irreversible DNA loss.

No obvious differences among the absolute numbers of mutants in all 9 exons of hprt gene were found, meaning that there were no clear "hot spots". However, some reports showed the preferential localization of deletion breakpoints at or toward the 3' end of the hprt gene^[33-35]. Our results suggested that 9 exons of hprt gene are not well distributed, so the controversy might be due to different methods rather than results. As deletion breakpoints are mapped and sequenced more precisely, it may be helpful in clarifying the mechanisms of induced deletion.

REFERENCES

- Mognato M, Ferraro P, Canova S, Sordi G, Russo A, Cherubini R, Celotti L. Analysis of mutational effects at the HPRT locus in human G(o) phase lymphocytes irradiated *in vitro* with r rays. *Mut Res* 2001; **474**: 147-158
- Schwartz JL, Rotmensch J, Sun J, An J, Xu Z, Yu Y, Hsie AW. Multiplex polymerase chain reaction-based deletion analysis of spontaneous, gamma ray- and alpha-induced hprt mutants of CHO-K1 cells. *Mutagenesis* 1994; **9**: 537-540
- Park MS, Hanks T, Jaberaboansari A, Chen DJ. Molecular analysis of gamma-ray-induced mutations at the hprt locus in primary human skin fibroblasts by multiplex polymerase chain reaction. *Rad Res* 1995; **141**: 11-18
- Ward JB, Abdel-Rahman SZ, Henderson RF, Stock TH, Morandi M, Rosenblatt JI, Ammenheuser MM. Assessment of butadiene exposure in synthetic rubber manufacturing workers in Texas using frequencies of hprt mutant lymphocytes as a biomarker. *Chemico-Biological Interactions* 2001; **135-136**: 465-483
- Jones IM, Thomas CB, Haag K, Pleshanov P, Vorobstova I, Tureva L, Nelson DO. Total gene deletions and mutant frequency of the HPRT gene as indicators of radiation exposure in Chernobyl liquidators. *Mut Res* 1999; **431**: 233-246
- Mognato M, Graziani M, Celotti L. Analysis of point mutations in HPRT mutant T-lymphocytes derived from coke-oven workers. *Mut Res* 1999; **431**: 271-278
- Denno G, Gedik C, Wood S, Speit G. Analysis of oxidative DNA damage and HPRT mutations in human after hyperbaric oxygen treatment. *Mut Res* 1999; **431**: 351-359
- Suzuki K, Hei TK. Mutation induction in gamma-irradiated primary human bronchial epithelial cells and molecular analysis of the HPRT mutants. *Mut Res* 1996; **349**: 33-41
- Kiefer J, Schreiber A, Gutermuth F, Koch S, Schmidt P. Mutation induction by different types of radiation at the Hprt locus. *Mut Res* 1999; **431**: 429-448
- Krause G, Garganta F, Vrieling H, Scherer G. Spontaneous and chemically induced point mutations in HPRT cDNA of the metabolically competent human lymphoblastoid cell line, MCL-5. *Mut Res* 1999; **431**: 417-428
- Walker VE, Jones IM, Crippen TL, Meng Q, Walker DM, Bauer MJ, Reilly AA, Bates AD, Nakamura J, Upton PB, Skopek TR. Relationships between exposure, cell loss and proliferation, and manifestation of Hprt mutant T cells following treatment of preweanling, weanling, and adult male mice with N-ethyl-N-nitrosourea. *Mut Res* 1999; **431**: 371-388
- Wei SJ, Chang RL, Cui XX, Merkler KA, Wong CQ, Yagi H, Jerina DM, Conney AH. Dose-dependent differences in the mutational profiles of (-)-(1R, 2S, 3S, 4R)-3,4-dihydroxy-1,2-epoxy-1,2,3,4-tetrahydrobenzo [c]phenanthrene and its less carcinogenic enantiomer. *Cancer Res* 1996; **56**: 3695-3703
- Jie YM, Jia C. Chromosomal composition of micronuclei in mouse NIH3T3 cells treated with acrylamide, extract of Tripterygium hypoglaucom (level) hutch, mitomycin C and colchicines, detected by multicolor FISH with centromeric and telomeric DNA probes. *Mutagenesis* 2001; **16**: 145-149
- Meng Q, Henderson RF, Long LY, Blair L, Walker DM, Upton PB, Swenberg JA, Walker VE. Mutagenicity at the Hprt locus in T cells of female mice following inhalation exposures to low levels of 1, 3-butadiene. *Chemico-Biological Interactions* 2001; **135-136**: 343-361
- Barnett YA, Warnock CA, Gillespie ES, Barnett CR, Livingstone MB. Effect of dietary intake and lifestyle factors on *in vivo* mutant frequency at the HPRT gene locus in healthy human subjects. *Mut Res* 1999; **431**: 305-315
- Aidoo A, Morris SM, Casciano DA. Development and utilization of the rat lymphocyte hprt mutation assay. *Mut Res* 1997; **387**: 69-88
- Loucas BD, Cornforth MN. Postirradiation growth in HAT medium fails to eliminate the delayed appearance of 6-thioguanine-resistant clones in EJ30 human epithelial cells. *Rad Res* 1998; **149**: 171-178
- Recio L, Steen AM, Pluta LJ, Meyer KG, Saranko CJ. Mutational spectrum of 1, 3-butadiene and metabolites 1,2-epoxybutene and 1,2,3,4-diepoxybutane to assess mutagenic mechanisms. *Chemico-Biological Interactions* 2001; **135-136**: 325-341
- Evans HH, Demarini DM. Ionizing radiation-induced mutagenesis: radiation studies in *Neurospora* predictive for results in mammalian cells. *Mut Res* 1999; **437**: 135-150
- da Costa GG, Manjanatha MG, Marques MM, Beland FA. Induction of lacI mutations in Big Blue rats treated with tamoxifen and α -hydroxytamoxifen. *Cancer Letters* 2002; **176**: 37-45
- Turner SD, Wijnhoven SW, Tinwell H, Lashford LS, Rafferty JA, Ashby J, Vrieling H, Fairbairn LJ. Assays to predict the genotoxicity of the chromosomal mutagen etoposide-focussing on the best assay. *Mut Res* 2001; **493**: 139-147
- van Delft JH, Bergmans A, van Dam FJ, Tates AD, Howard L, Winton DJ, Baan RA. Gene-mutation assays in λ lacZ transgenic mice: comparison of lacZ with endogenous genes in splenocytes and small intestinal epithelium. *Mut Res* 1998; **415**: 85-96
- Laws GM, Skopek TR, Reddy MV, Storer RD, Glaab WE. Detection of DNA adducts using a quantitative long PCR technique and the fluorogenic 5' nuclease assay (TaqMan). *Mut Res* 2001; **484**: 3-18
- Sankaranarayanan K. Ionizing radiation and genetic risks X. The potential "disease phenotypes" of radiation-induced genetic damage in humans: perspectives from human molecular biology and radiation genetics. *Mut Res* 1999; **429**: 45-83
- Cosentino L, Heddle JA. Differential mutation of transgenic and endogenous loci *in vivo*. *Mut Res* 2000; **454**: 1-10
- Dobrovolsky VN, Casciano DA, Heflich RH. Tk⁺ mouse model for detecting *in vivo* mutation in an endogenous, autosomal gene. *Mut Res* 1999; **423**: 125-136
- Tates AD, van Dam FJ, Natarajan AT, van Teylingen CM, de Zwart FA, Zwiderman AH, van Sittert NJ, Nilsen A, Nilsen OG, Zahlsen K, Magnusson AL, Tornqvist M. Measurement of HPRT mutations in splenic lymphocytes and haemoglobin adducts in erythrocytes of Lewis rats exposed to ethylene oxide. *Mut Res* 1999; **431**: 397-415
- Casciano DA, Aidoo A, Chen T, Mittelstaedt RA, Manjanatha MG, Heflich RH. Hprt mutant frequency and molecular analysis of Hprt mutations in rats treated with mutagenic carcinogens. *Mut Res* 1999; **431**: 389-395
- Hageman GJ, Stierum RH. Niacin poly(ADP-ribose) polymerase-1 and genomic stability. *Mut Res* 2001; **475**: 45-56
- Sprung CN, Wang YP, Miller DL, Giannini DD, Dhananjaya N, Bodell WJ. Induction of lacI mutations in Big Blue Rat-2 cells treated with 1-(2-hydroxyethyl)-1-nitrosourea: a model system

- for the analysis of mutagenic potential of the hydroxyethyl adducts produced by 1, 3-bis (2-chloroethyl)-1-nitrosourea. *Mut Res* 2001; **484**: 77-86
- 31 **Mills AA**, Bradley A. From mouse to man: generating megabase chromosome rearrangements. *Trends Genetics* 2001; **17**: 331-339
- 32 **Waldren C**, Vannais D, Drabek R, Gustafson D, Kraemer S, Lenarczyk M, Kronenberg A, Hei T, Ueno A. Analysis of mutant quantity and quality in human-hamster hybrid A₁ and A₁-179 cells exposed to ¹³⁷Cs-gamma or HZE-Fe ions. *Adv Space Res* 1998; **22**: 579-585
- 33 **Branda RF**, Lafayette AR, O' Neill JP, Nicklas JA. The effect of folate deficiency on the hprt mutational spectrum in Chinese hamster ovary cells treated with monofunctional alkylating agents. *Mut Res* 1999; **427**: 79-87
- 34 **Mittelstaedt RA**, Smith BA, Chen T, Beland FA, Heflich RH. Sequence specificity of Hprt lymphocyte mutation in rats fed the hepatocarcinogen 2-acetylaminofluorene. *Mut Res* 1999; **431**: 167-173
- 35 **Pluth JM**, O' Neill JP, Nicklas JA, Albertini RJ. Molecular bases of HPRT mutations in malathion-treated human T-lymphocytes. *Mut Res* 1998; **397**: 137-148

Edited by Ren SY

A mouse model of severe acute pancreatitis induced with caerulein and lipopolysaccharide

Shi-Ping Ding, Ji-Cheng Li, Chang Jin

Shi-Ping Ding, Ji-Cheng Li, Chang Jin, Department of Lymphology, Department of Histology and Embryology, Medical College of Zhejiang University, Hangzhou 310031, Zhejiang Province, China

Correspondence to: Dr. Ji-Cheng Li, Department of Lymphology, Department of Histology and Embryology, Medical College of Zhejiang University, Hangzhou 310031, Zhejiang Province, China. lijc@mail.hz.zj.cn

Telephone: +86-571-87217139 **Fax:** +86-571-87217139

Received: 2002-09-13 **Accepted:** 2002-10-17

Abstract

AIM: To establish a non-traumatic, easy to induce and reproducible mouse model of severe acute pancreatitis (SAP) induced with caerulein and lipopolysaccharide (LPS).

METHODS: Thirty-two healthy mature NIH female mice were selected and divided at random into four groups (each of 8 mice), i.e., the control group (NS group), the caerulein group (Cn group), the lipopolysaccharide group (LPS group), and the caerulein+LPS group (Cn+LPS group). Mice were injected intraperitoneally with caerulein only, or LPS only, and caerulein and LPS in combination. All the animals were then killed by neck dislocation three hours after the last intraperitoneal injection. The pancreas and exo-pancreatic organs were then carefully removed for microscopic examination. And the pancreatic acinus was further observed under transmission electron microscope (TEM). Pancreatic weight, serum amylase, serum nitric oxide (NO) concentration, superoxide dismutase (SOD) and malondialdehyde (MDA) concentration of the pancreas were assayed respectively.

RESULTS: (1) NS animals displayed normal pancreatic structure both in the exocrine and endocrine. In the LPS group, the pancreas was slightly edematous, with the infiltration of a few inflammatory cells and the necrosis of the adjacent fat tissues. All the animals of the Cn group showed distinct signs of a mild edematous pancreatitis characterized by interstitial edema, infiltration of neutrophil and mononuclear cells, but without obvious parenchyma necrosis and hemorrhage. In contrast, the Cn+LPS group showed more diffuse focal areas of nonviable pancreatic and hemorrhage as well as systemic organ dysfunction. According to Schmidt's criteria, the pancreatic histologic score showed that there existed significant difference in the Cn+LPS group in the interstitial edema, inflammatory infiltration, parenchyma necrosis and parenchyma hemorrhage in comparison with those of the Cn group, LPS group and NS group ($P<0.01$ or $P<0.05$). (2) The ultrastructure of acinar cells was seriously damaged in the Cn+LPS group. Chromatin margination of nuclei was present, the number and volume of vacuoles greatly increased. Zymogen granules (ZGs) were greatly decreased in number and endoplasmic reticulum exhibited whorls. The swollen mitochondria appeared, the crista of which was decreased in number or disappeared. (3) Pancreatic weight and serum amylase levels in the Cn

+LPS was significantly higher than those of the NS group and the LPS group respectively ($P<0.01$ or $P<0.05$). However, the pancreatic wet weight and serum amylase concentration showed no significant difference between the Cn+LPS group and the Cn group. (4) NO concentration in the Cn+LPS group was significantly higher than that of NS group, LPS group and Cn group ($P<0.05$ or $P<0.01$). (5) The SOD and MDA concentration of the pancreas in the Cn+LPS group were significantly higher than those of NS, LPS and Cn groups ($P<0.05$ or $P<0.01$).

CONCLUSION: The mouse model of severe acute pancreatitis could be induced with caerulein and LPS, which could be non-traumatic and easy to induce, reproducible with the same pathological characteristics as those of SAP in human, and could be used in the research on the mechanism of human SAP.

Ding SP, Li JC, Jin C. A mouse model of severe acute pancreatitis induced with caerulein and lipopolysaccharide. *World J Gastroenterol* 2003; 9(3): 584-589

<http://www.wjgnet.com/1007-9327/9/584.htm>

INTRODUCTION

Severe acute pancreatitis (SAP) is characterized by local pancreatic necrosis as well as systemic organ failure and is still associated with a higher morbidity and mortality despite continuing improvements in critical care^[1-9]. Several animal models have been developed for studying the mechanism, recovery, prognosis and treatment of human SAP^[10-12]. However, these methods such as retrograde pancreatic duct injection, intraductal infusion of sodium taurocholate, closed duodenal loop, pancreatic duct obstruction are so invasive and complex in operation that the mortality of the animals was high^[10-12]. The aim of this study is to establish a SAP animal model induced with caerulein and lipopolysaccharide (LPS), which is non-traumatic, convenient and easy to practise, and reproducible and with the same histopathologic characteristics as those of SAP in human.

MATERIALS AND METHODS

Chemicals

Caerulein and LPS (*Escherichia coli* 0111:B4) were purchased from Sigma Chemical Co. (St. Louis, MO, USA). Assay kits for serum amylase, NO, SOD and MDA concentration were from Nanjing Jiancheng Biological Products Institute (Nanjing, China). Other reagents used were of analytic grade.

Animal and grouping

Thirty-two healthy mature NIH female mice, weighing 22.0-28.0 g, provided by Experimental Animal Center of Zhejiang Academy of Medical Sciences, were selected and divided at random into four groups (each of 8 mice), i.e. the control group (NS group), the caerulein group (Cn group), the

lipopolysaccharides group (LPS group), the caerulein + lipopolysaccharides group (Cn+LPS group).

Establishment of the model of severe acute pancreatitis

All the female NIH mice were fed with a standard diet and fasted for 18 hours before induction of pancreatitis. They received water ad libitum during the experiments. In the NS group, the animals were injected intraperitoneally by normal saline at a dose of 50 ml/kg at a 1 h interval six times. In the Cn group, acute pancreatitis was induced by six intraperitoneal injections of caerulein administered at a dose of 50 µg/kg at a 1 h interval. This pancreatitis was mild, and all animals survived. In the LPS group, the animals were injected intraperitoneally with normal saline (50 ml/kg) six times every one hour prior to the intraperitoneal infusion of LPS (10 mg/kg). In the Cn + LPS group, the mice were induced by LPS challenge after induction of mild pancreatitis, i.e., the mice received intraperitoneal injections of 10 mg/kg LPS immediately after the sixth caerulein injection. Three hours later, all the animals were killed by neck dislocation and the pancreas was carefully dissected from its attachment to the stomach, duodenum and spleen. Fat and tissue excess were trimmed away. The pancreas was rinsed with saline, blotted on paper and weighed. And then, one part was fixed and embedded in paraffin wax for histological analysis; the other part was immediately frozen in liquid nitrogen and stored at -78 °C until the measurement of SOD and MDA concentration. And the liver, kidney and lung were also carefully removed. Blood samples were obtained from femoral artery and were stored at -78 °C until use.

Histological examination

For histological examination, the pancreas was fixed in 10 % formaldehyde for 24 hours, embedded in paraffin, and stained with haematoxylin and eosin. According to Schmidt's standard^[13], a pathologist who was blinded to the treatment protocol scored the tissues for edema, inflammatory infiltration, parenchymal necrosis, and hemorrhage in 20 fields. Grading for edema was scaled as: 0, absent or rare; 1, edema in the interlobular space; 2, edema in the intralobular space; and 3, the isolated-island shape of pancreatic acinus. Inflammation was scored as: 0, absent; 1, mild; 2, moderate; and 3, severe. The parenchyma necrosis was as follows: 0, absent; 1, focal (<5 %); 2, and/or sublobular (<20 %); 3, and/or lobular (>20 %). The parenchyma hemorrhage was scored as: 0, absent; 1, mild; 2, moderate and 3, severe. Liver, kidney and lung sections were similarly stained and assessed for histological changes.

Separate experiment was performed to observe the changes of the pancreas. Pancreatic tissues were double fixed in 2.5 % glutaraldehyde and 1 % osmic acid for 2 hours, then stained with 2 % acetic acid U rapidly, dehydrated in a graded series of alcohol and acetone, embedded in Epon 812 and cut with Leica Ultracut UCT ultramicrotome. Specimens were double stained by acetic acid U and lead citrate fluid and examined with Philips Tecnai 10 TEM operated at 80Kv.

Measurement of serum amylase, NO concentration, SOD and MDA concentration of the pancreas

Serum amylase and NO concentration were assayed according to I-starch chromatometry and a copper-coated cadmium reduction method respectively. The pancreas was isolated and was made homogenate. SOD and MDA concentration of the pancreas were measured by the xanthine oxidase method and the sulfo-barbituric acid method respectively.

Statistical analyse

Data were expressed as means ± SD and analyzed by two-tailed Student's *t* test.

RESULTS

Histological examination

Microscopic examination NS animals displayed normal pancreatic histology both in the exocrine and endocrine. In the LPS group, the pancreas was slightly edematous (Figure 1), with the infiltration of a few inflammatory cells and the necrosis of the adjacent fat tissues. The animals of the Cn group treated with caerulein, showed distinct signs of a mild edematous pancreatitis characterized by interstitial edema (Figure 2), infiltration of neutrophil and mononuclear cells, but without obvious parenchyma necrosis and hemorrhage. The organs, except for the pancreas, showed normal histological characteristics. However, the animals of the Cn+LPS group, which was induced with caerulein and aggravated by subsequent LPS injection, showed the features of a severe form of acute pancreatitis characterized by expansion of interlobular and intralobular spaces caused by moderate to severe interstitial edema, extensive infiltration with inflammatory cells, more diffuse focal areas of nonviable pancreatic parenchyma (Figure 3). Necrosis of peripancreatic fat was also a distinct feature in these animals. In addition, renal cells were swollen (Figure 4A); the lobules of liver was disorganized, with the vacuolization of liver cells (Figure 4B) and a lot of erythrocyte and inflammatory cells also infiltrated in the cavity of pulmonary alveolus (Figure 4C).

According to Schmidt's criteria, the histological score showed that there existed significant difference in the Cn+LPS group in the interstitial edema, inflammatory infiltration, parenchyma necrosis and parenchyma hemorrhage as compared with those of the Cn group, the LPS group and the NS group ($P<0.01$ or $P<0.05$) (Table 1).

Table 1 Comparison of the pancreas lesion between groups ($n=8$)

Groups	Interstitial edema	Inflammatory infiltration	Parenchyma necrosis	Parenchyma hemorrhage
NS	0.0	0.0	0.0	0.0
Cn	1.95±0.26 ^b	1.12±0.22 ^{bc}	0.63±0.09 ^{bd}	0
LPS	0.25±0.03 ^{ad}	0.25±0.43 ^{bd}	0	0
Cn+LPS	2.75±0.43 ^{bc}	2.88±0.33 ^{bc}	2.75±0.33 ^{bd}	1.25±0.26 ^{bd}

^a $P<0.05$, ^b $P<0.01$, vs NS group; ^c $P<0.05$, ^d $P<0.01$, vs Cn group.

Electron microscope examination of the pancreatic acinus

The ultrastructure of acinar cells was normal in the NS group. In the cytoplasm of the acinar cells, a plenty of rough endoplasmic reticulum (RER) and ribosome and a great deal of ZGs appeared. After LPS stimulation, a few cytoplasmic vacuoles formed in acinar cells (Figure 5). In the Cn group, a few cytoplasmic vacuoles in acinar cells also appeared, and ZGs were decreased in number. The RER and the mitochondria was slightly swollen (Figure 6). However, in the Cn+LPS group, the morphological alterations of mouse pancreatic acinar cells were observed under transmission electron microscope. Chromatin margination of nuclei was present (Figure 7A), the number of vacuoles greatly increased and their volume also greatly increased (Figure 7B). ZGs were greatly decreased in number and endoplasmic reticulum exhibited whorls (Figure 7C). The swollen mitochondria appeared, the crista of which was decreased or disappeared (Figure 7D).

Comparison of pancreatic weight and serum amylase

Subsequent experiment showed that pancreatic weight and serum amylase in the Cn +LPS and the Cn group were significantly higher than those in the NS group and the LPS group respectively ($P<0.01$ or $P<0.05$). However, the pancreatic wet weight and serum amylase showed no significant difference between the Cn+LPS and the Cn groups (Table 2).

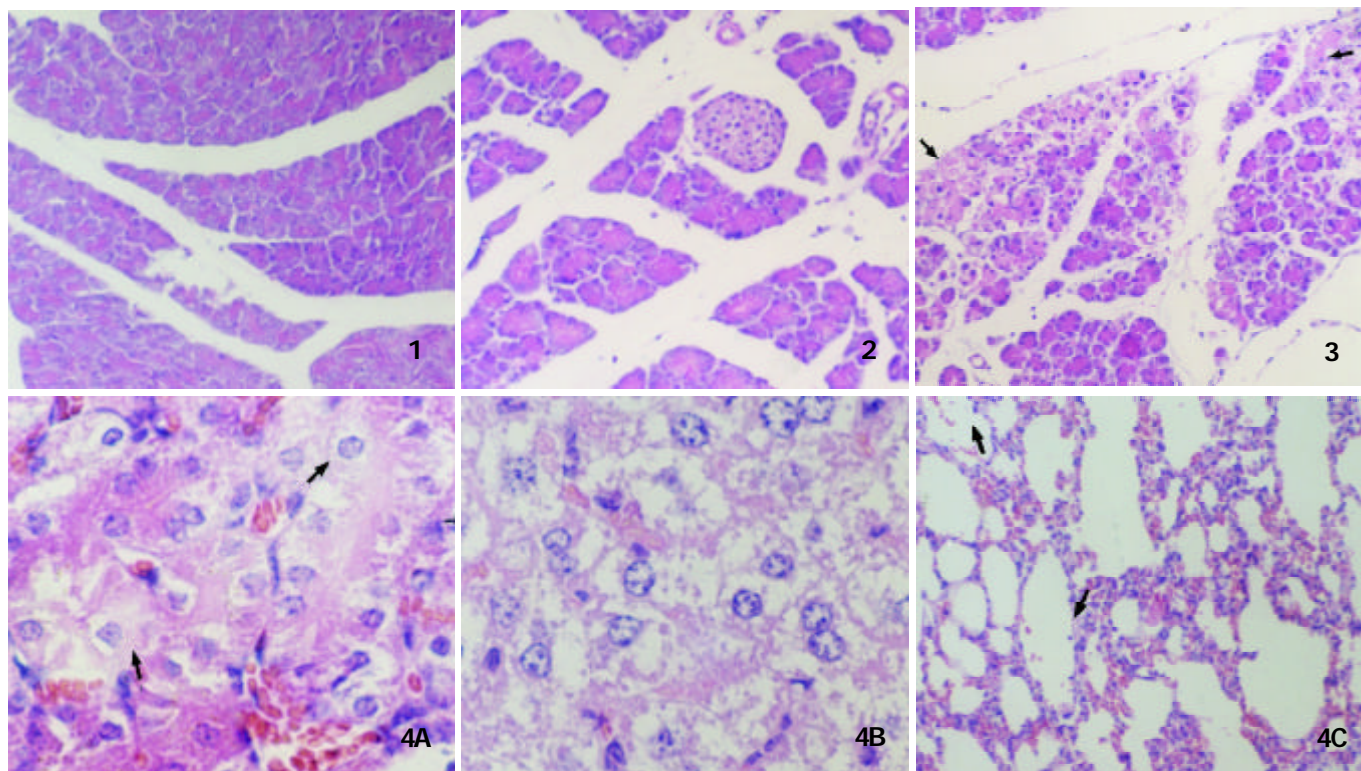


Figure 1 In the LPS group, the pancreas was slightly edematous. $\times 100$.

Figure 2 Microscopic section of the pancreas from the Cn group, showing the features of acute edematous pancreatitis notably interstitial edema. $\times 100$.

Figure 3 In the Cn+LPS group, more diffuse focal areas of nonviable pancreatic parenchyma appeared obviously. $\times 100$.

Figure 4 The histological change of the exo-pancreatic organs in the Cn+LPS group. A: Renal cells were swollen; $\times 100$; B: The vacuolization of liver cells; $\times 400$; C: A lot of erythrocyte and inflammatory cells also infiltrated in the cavity of pulmonary alveolus. $\times 100$.

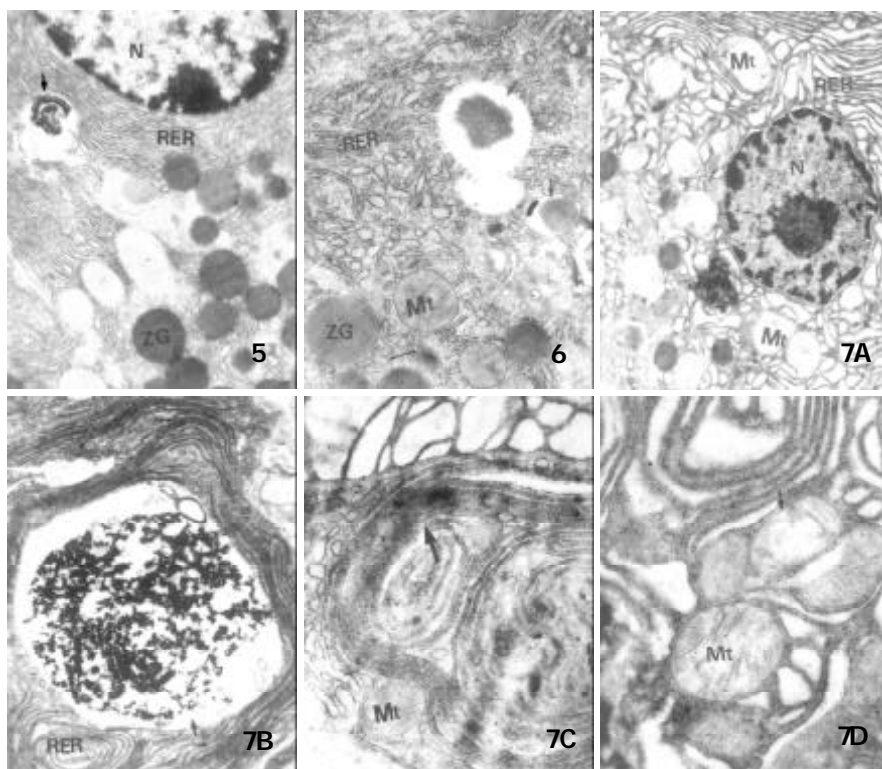


Figure 5 A few cytoplasmic vacuoles formed in acinar cells in the LPS group. $\times 10\ 000$.

Figure 6 In the Cn group, a few cytoplasmic vacuoles in acinar cell appeared, and ZGs were decreased in number. The RER and the mitochondria was slightly swollen. $\times 10\ 000$.

Figure 7 The ultrastructure change of the pancreatic acinus in the Cn+LPS group. A: Chromatin margination of nuclei was present, the swollen mitochondria appeared; $\times 7\ 000$; B: the number of vacuoles greatly increased and their volume also greatly increased; $\times 7\ 000$; C: the endoplasmic reticulum exhibited whorls; $\times 14\ 000$; D: The crista of mitochondria was decreased or disappeared. $\times 20\ 000$.

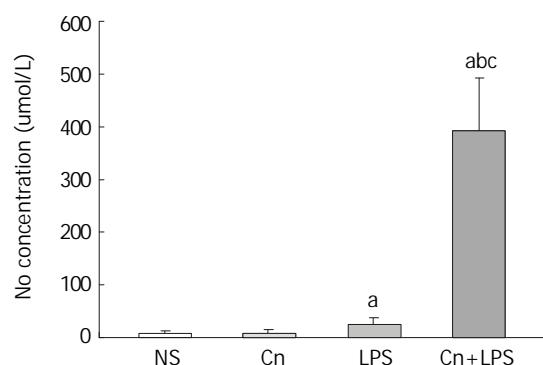
Table 2 Comparison of pancreatic wet weight and serum amylase between groups ($\bar{x}\pm s$)

Groups	Pancreatic weight (mg)	Serum amylase (U/L)
NS	247.70 \pm 30.20	1861.35 \pm 303.36
Cn	337.20 \pm 50.90 ^{bc}	11042.32 \pm 528.03 ^{bd}
LPS	290.10 \pm 39.70 ^a	2385.50 \pm 73.60 ^b
Cn+LPS	380.00 \pm 32.00 ^{bc}	10031.70 \pm 906.19 ^{bd}

^a $P<0.05$, ^b $P<0.01$, vs NS group; ^c $P<0.05$, ^d $P<0.01$, vs LPS group.

Comparison of NO concentration

There was significant difference in the concentration of NO among the groups (Figure 8). The results showed that the concentration of NO in the Cn+LPS group was significantly higher than that in the NS, LPS and Cn groups ($P<0.01$).

**Figure 8** Comparison of NO concentration between groups ($\bar{x}\pm s$) ($n=8$). ^a $P<0.01$, vs NS group; ^b $P<0.01$, vs LPS group; ^c $P<0.05$, vs Cn group.

SOD and MDA concentration of the pancreas

The concentration of SOD and MDA in the pancreas showed significant difference between groups (Table 3). SOD concentration of the pancreas in the Cn+LPS group decreased significantly as compared with that of the NS, LPS and Cn groups. However, MDA concentration of the pancreas in the Cn+LPS group increased significantly compared with that of the NS, LPS and Cn groups.

Table 3 Comparison of SOD and MDA concentration between groups ($\bar{x}\pm s$) ($n=8$)

Groups	SOD concentration (NU/mgprot)	MDA concentration (nmol/mgprot)
NS	151.67 \pm 10.74	0.74 \pm 0.34
Cn	135.73 \pm 10.87 ^a	0.79 \pm 0.31
LPS	136.05 \pm 17.25 ^a	0.97 \pm 0.29
Cn+LPS	85.13 \pm 11.19 ^{bcd}	1.22 \pm 0.24 ^{bd}

^a $P<0.05$, ^b $P<0.01$, vs NS group; ^c $P<0.01$, vs LPS group; ^d $P<0.01$, vs Cn group.

DISCUSSION

Acute pancreatitis may be classified histologically as interstitial edematous or necrotizing according to the inflammatory changes in the pancreatic parenchyma^[14-19]. As for a mild edematous form, the pancreas observed under light microscope showed interstitial edema, interstitial hyperemia and inflammatory cell infiltration and occasionally punctate fat necrosis, but without obvious parenchyma necrosis and hemorrhage^[20-24]. However, a severe necrotizing form is characterized by extensively coagulative necrosis and

hemorrhage as well as systemic organ dysfunction^[25-34]. In the present study, the results showed that the animals of the Cn group, which was treated with caerulein only, showed distinct signs of a mild edematous pancreatitis, indicating that the pancreatic weight and serum amylase became gradually higher than those of the NS group and the LPS group. The microscopic examination showed interstitial edema and inflammatory cell infiltration in the pancreas, and slight parenchyma necrosis and hemorrhage. And the organs except the pancreas, had a normal histological feature. Furthermore, transmission electron microscopic observation of the acinus cells displayed a few cytoplasmic vacuoles in acinar cell, and ZGs were found decreased in number and the RER and the mitochondrion were slightly swollen. In the LPS group which was treated with LPS only, serum amylase and pancreatic weight had an increasing tendency, but the pancreas showed interstitial edema and the formation of a few vacuoles in the cytoplasm of the acinar cells. LPS could not induce acute pancreatitis, which further confirmed Jaworek's findings^[35]. In the Cn+LPS group, which was induced by caerulein and aggravated by subsequent LPS injection, the level of serum amylase and pancreatic weight increased and the pancreas became edematous and the inflammatory cells infiltrated and necrosis and hemorrhage appeared obviously in the pancreas, the ultrastructure of the acinus was destroyed, the organs except the pancreas was lesioned to a different extent. Moreover, in the histological score, there existed significant difference in the Cn+LPS group in the interstitial edema (2.75 \pm 0.43), inflammatory infiltration (2.88 \pm 0.33), parenchyma necrosis (2.75 \pm 0.33) and parenchyma hemorrhage (1.25 \pm 0.26) in comparison with those of caerulein only (1.95 \pm 0.26; 1.12 \pm 0.22; 0.63 \pm 0.09; 0), those of LPS only (0.25 \pm 0.03; 0.25 \pm 0.43; 0; 0) and the NS group (0; 0; 0; 0) ($P<0.01$ or $P<0.05$). It is thus clear that, when induced with caerulein and LPS in combination, the pancreas was destroyed so severely as to result in inflammatory reaction in the body and systemic organ dysfunction. Moreover, the model induced with caerulein and LPS was almost stable under the condition of duplications. Therefore, the mouse model induced with caerulein and LPS was non-traumatic, convenient, easily replicating and bearing the same histological changes as those of human SAP.

Caerulein is a kind of ten-peptide substances, the analog of cholecystokinin, and possesses different biological activities^[36,37]. Caerulein can stimulate the acinar cells to excrete a large amount of digestive enzyme and pancreatic fluid, resulting in a mild edematous pancreatitis characterized by a higher serum amylase level, interstitial edema, leukocyte infiltration and the vacuolation of acinar cells^[36,37]. LPS is a kind of endotoxin, which could activate the mononuclear cell system to release cytokines to switch on systemic inflammation reaction^[38]. Clinically, the endotoxin level was related to the severity of the illness. Therefore, the mechanism to develop severe acute pancreatitis and organ failure with caerulein and LPS might be that caerulein could activate the pancreatin to destroy the pancreas, and detonate inflammatory cells to release inflammation mediators and subsequently LPS challenged the reaction of inflammation medium, thus developing local pancreatitis into severe inflammation reaction in the body^[39-50].

Recent evidence indicated that these cytokines from the inflamed pancreas can activate the production of the inducible nitric oxide (NO) synthase, resulting in overproduction of NO, which acts as a key final cellular and intercellular mediator^[51-53]. In this study, the concentration of NO was significantly higher in the Cn+LPS group, as compared with that of caerulein alone or LPS alone ($P<0.01$). NO as an endothelium-derived relaxing factor (EDRF) and a highly reactive free radical, is produced from the amino acid L-arginine by a family of isoenzymes, the nitric oxide synthases (NOS). Two broad groups can be

identified: constitutive (cNOS) and inducible (iNOS). cNOS is present predominantly as a normal constituent of healthy endothelial cells (endothelial isoform, eNOS) and synthesizes NO in small amounts in response to physical or receptor stimulation. iNOS is not a normal cellular constituent, but can be expressed in a wide variety of cells and generates large amounts of NO in a sustained and largely uncontrolled manner. Excessive production of NO causes vasodilatation and hypotension that is refractory to vasoconstriction, together with increased microvascular permeability and extravascular third spacing. The physiological inability to correct these adverse responses results in end organ hypoperfusion, oedema, initiation of anaerobic metabolism, and end organ dysfunction. Moreover, the reaction of NO with superoxide causes the formation of peroxynitrite, which is a powerful oxidant and cytotoxic agent and may play an important role in the cellular damage associated with the overproduction of NO. The spontaneous reaction of peroxynitrite with proteins makes the nitration of tyrosine residues to form nitrotyrosine, which is a specific nitration product of peroxynitrite and a marker for peroxynitrite induced oxidative tissue damage. It is thus evident that the increase of NO concentration is related to the lesion of pancreas and other organs. In addition, the concentration of SOD as an antioxidant significantly lowered and that of MDA as the lipid peroxide significantly increased, which further indicated that the free radical reaction and oxidation response could be intensified with caerulein and LPS so that a mild edematous form could change subsequently into a severe necrotizing form.

REFERENCES

- 1 **Baron TH**, Morgan DE. Acute necrotizing pancreatitis. *N Engl J Med* 1999; **340**: 1412-1417
- 2 **Pastor CM**, Frossard JL. Are genetically modified mice useful for the understanding of acute pancreatitis. *FASEB J* 2001; **15**: 893-897
- 3 **Lecesne R**, Taourel P, Bret PM, Atri M, Reinhold C. Acute pancreatitis: Interobserver agreement and correlation of CT and MR cholangiopancreatography with outcome. *Radiology* 1999; **211**: 727-735
- 4 **Slavin J**, Ghaneh P, Sutton R, Hartley M, Rowlands P, Garvey C, Hughes M, Neoptolemos J. Management of necrotizing pancreatitis. *World J Gastroenterol* 2001; **7**: 476-481
- 5 **Wu XN**. Treatment revisited and factors affecting prognosis of severe acute pancreatitis. *World J Gastroenterol* 2000; **6**: 633-635
- 6 **Qi QH**, Guo LM. The surgical treatment of acute pancreatitis. *Shijie Huaren Xiaohua Zazhi* 2001; **9**: 416-417
- 7 **Yu CG**, Chen LD, Zhang ZH. Severe acute pancreatitis and infection of pancreas. *Shijie Huaren Xiaohua Zazhi* 2001; **9**: 689-693
- 8 **Zhao M**, Chen RF. Pathogenesis of acute lung injury induced by acute necrotizing pancreatitis. *Shijie Huaren Xiaohua Zazhi* 2001; **9**: 954-957
- 9 **Chen QP**. Enteral nutrition and acute pancreatitis. *World J Gastroenterol* 2001; **7**: 185-192
- 10 **Shang ZM**, Wang BE, Zhang SW, Ci XL. The establishment of the rat model of severe acute pancreatitis. *Shijie Huaren Xiaohua Zazhi* 2000; **8**: 921
- 11 **Tashiro M**, Schafer C, Yao H, Ernst SA, Williams JA. Arginine induced acute pancreatitis alters the actin cytoskeleton and increases heat shock protein expression in rat pancreatic acinar cells. *Gut* 2001; **49**: 241-250
- 12 **Wu WK**. The pathogenesis of acute pancreatitis. *Shijie Huaren Xiaohua Zazhi* 2001; **9**: 410-411
- 13 **Shimizu T**, Shiratori K, Sawada T, Kobayashi M, Hayashi N, Saotome H, Keith JC. Recombinant human interleukin-11 decrease severity of acute necrotizing pancreatitis in mice. *Pancreas* 2000; **21**: 134-140
- 14 **Li JC**. Discussion on the conception of severe acute pancreatitis. *Shijie Huaren Xiaohua Zazhi* 1999; **7**: 1072-1073
- 15 **Wu XN**. Current concept of pathogenesis of severe acute pancreatitis. *World J Gastroenterol* 2000; **6**: 32-36
- 16 **Pezzilli R**, Mancini F. Assessment of severity of acute pancreatitis: a comparison between old and most recent modalities used to evaluate this perennial problem. *World J Gastroenterol* 1999; **5**: 283-285
- 17 **Uhl W**, Buchler MW, Malferteiner P, Begler HG, Adler G, Gaus W. The German pancreatitis study group. A randomized, double blind, multicentre trial of octreotide in moderate to severe acute pancreatitis. *Gut* 1999; **45**: 97-104
- 18 **Hartwig W**, Careter EA, Jimenez RE, Werner J, Fischman AJ, Castillo CF, Warshaw AL. Chemotactic peptide uptake in acute pancreatitis: correlation with tissue accumulation of leukocytes. *J Appl Physiol* 1999; **87**: 743-749
- 19 **Pezzilli R**, Morselli-labate AM, Miniero R, Barakat B, Fiocchi M, Cappelletti O. Simultaneous serum assays of lipase and interleukin-6 for early diagnosis and prognosis of acute pancreatitis. *Clin Chem* 1999; **45**: 1762-1767
- 20 **Zhou ZG**, Chen YD. Influencing factors of pancreatic microcirculatory impairment in acute pancreatitis. *World J Gastroenterol* 2002; **8**: 406-412
- 21 **Chen DL**, Wang WZ, Wang JY. Epidermal growth factor prevents gut atrophy and maintains intestinal integrity in rats with acute pancreatitis. *World J Gastroenterol* 2000; **6**: 762-765
- 22 **Kohut M**, Nowak A, Nowakowska-Dulawa E, Marek T. Presence and density of common bile duct microlithiasis in acute biliary pancreatitis. *World J Gastroenterol* 2002; **8**: 558-561
- 23 **Fleischer F**, Dabew R, Goke B, Wagner AC. Stress kinase inhibition modulates acute experimental pancreatitis. *World J Gastroenterol* 2001; **7**: 259-265
- 24 **Tiscornia OM**, Hamamura S, de Lehmann ES, Otero G, Waisman H, Tiscornia-Wasserman P, Bank S. Biliary acute pancreatitis: a review. *World J Gastroenterol* 2000; **6**: 157-168
- 25 **Frossard JL**, Hadengue A, Pastor CM. New serum markers for the detection of severe acute pancreatitis in humans. *Am J Respir Crit Care Med* 2001; **164**: 162-170
- 26 **Hamano H**, Kawa S, Horiuchi A, Unno H, Furuya N, Akamatsu T, Fukushima M, Nikaido T, Nakayama K, Usuda N, Kiyosawa K. High serum IgG₄ concentrations in patients with sclerosing pancreatitis. *N Engl J Med* 2001; **344**: 732-738
- 27 **Kyriakides C**, Jasleen J, Wang Y, Moore FD, Ashley SW, Hechtman HB. Neutrophils, not complement, mediate the mortality of experimental hemorrhagic pancreatitis. *Pancreas* 2001; **22**: 40-46
- 28 **Luo Y**, Yuan CX, Peng YL, Wei PL, Zhang ZD, Jiang JM, Dai L, Hu YK. Can ultrasound predict the severity of acute pancreatitis early by observing acute fluid collection. *World J Gastroenterol* 2001; **7**: 293-295
- 29 **Wu JX**, Xu JY, Yuan YZ. Effect of emodin and sandostatin on metabolism of eicosanoids in acute necrotizing pancreatitis. *World J Gastroenterol* 2000; **6**: 293-294
- 30 **Qin RY**, Zou SQ, Wu ZD, Qiu FZ. Influence of splanchnic vascular infusion on the content of endotoxins in plasma and the translocation of intestinal bacteria in rats with acute hemorrhage necrosis pancreatitis. *World J Gastroenterol* 2000; **6**: 577-580
- 31 **Yuan YZ**, Gong ZH, Lou KX, Tu SP, Zhai ZK, Xu JY. Involvement of apoptosis of alveolar epithelial cells in acute pancreatitis-associated lung injury. *World J Gastroenterol* 2000; **6**: 920-924
- 32 **Sun XQ**, Fu XB, Zhang R, Lu Y, Deng Q, Jiang XG, Sheng ZY. Relationship between plasma D(-) - lactate and intestinal damage after severe injuries in rats. *World J Gastroenterol* 2001; **7**: 555-558
- 33 **Zhang WZ**, Han TQ, Tang YQ, Zhang SD. Rapid detection of sepsis complicating acute necrotizing pancreatitis using polymerase chain reaction. *World J Gastroenterol* 2001; **7**: 289-292
- 34 **Xia Q**, Jiang JM, Gong X, Chen GY, Li L, Huang ZW. Experimental study of Tong Xia purgative method in ameliorating lung injury in acute necrotizing pancreatitis. *World J Gastroenterol* 2000; **6**: 115-118
- 35 **Jaworek J**, Jachimczak B, Tomaszewska R, Konturek PC, Pawlik WW, Sendur R, Hahn EG, Stachura J, Konturek SJ. Protective action of lipopolysaccharides in rat caerulein-induced pancreatitis: role of nitric oxide. *Digestion* 2000; **62**: 1-13
- 36 **Wagner ACC**, Mazzucchelli L, Miller M, Camoratto AM, Goke B. CER-1347 inhibits caerulein-induced rat pancreatitis JNK activation and ameliorates caerulein pancreatitis. *Am J Physiol Gastrointest Liver Physiol* 2000; **278**: G165-G172

- 37 **Frossard JL**, Bhagat L, Lee HS, Hietaranta AJ, Singh VP, Song AM, Steer ML, Saluja AK. Both thermal and non-thermal stress protect against caerulein induced pancreatitis and prevent trypsinogen activation in the pancreas. *Gut* 2002; **50**: 78-83
- 38 **Vaccaro MI**, Calvo EL, Suburo AM, Sordelli DO, Lanosa G, Iovanna JL. Lipopolysaccharide directly affects pancreatic acinar cell: implications on acute pancreatitis pathophysiology. *Dig Dis Sci* 2000; **45**: 915-926
- 39 **Xia SH**, Zhao XY, Guo P, Da SP. Hemocirculatory disorder in dogs with severe acute pancreatitis and intervention of platelet activating factor antagonist. *Shijie Huaren Xiaohua Zazhi* 2001; **9**: 550-554
- 40 **Yin Y**, Gao NR, Li ZL. Protective effects of ulinostatin on acute lung injury induced by acute necrotizing pancreatitis in rats. *Shijie Huaren Xiaohua Zazhi* 2002; **10**: 558-561
- 41 **Chen H**, Li F, Cheng YF, Sun JB. Pathogenic role of neutrophils in evolution of acute pancreatitis in rats. *Shijie Huaren Xiaohua Zazhi* 2001; **9**: 776-779
- 42 **Yuan YZ**, Lou KX, Gong ZH, Tu SP, Zhai ZK, Xu JY. Effects and mechanisms of emodin on pancreatic tissue EGF expression in acute pancreatitis in rats. *Shijie Huaren Xiaohua Zazhi* 2001; **9**: 127-130
- 43 **Wu K**, Wang BX, Wang XP. Effects of clostridium butyricum on bacterial translocation in rats with acute necrotizing pancreatitis. *Shijie Huaren Xiaohua Zazhi* 2000; **8**: 883-886
- 44 **Gong ZH**, Yuan YZ, Lou KX, Tu SP, Zhai ZK, Xu JY. Effects and mechanisms of somatostatin analogues on apoptosis of pancreatic acinar cells in acute pancreatitis in mice. *Shijie Huaren Xiaohua Zazhi* 1999; **7**: 964-966
- 45 **Wang CH**, Qian KD, Zhu YL, Tang XQ. The significance of TNF and IL-6 level in the patients with acute pancreatitis. *Shijie Huaren Xiaohua Zazhi* 2001; **9**: 1434
- 46 **Okabe A**, Hirota M, Nozawa F, Shibata M, Nakano S, Ogawa M. Altered cytokine response in rat acute pancreatitis complicated with endotoxemia. *Pancreas* 2001; **22**: 32-39
- 47 **Vaquero E**, Gukovsky I, Zaninovic V, Gukovskaya AS, Pandolfi SJ. Localized pancreatic NF- κ B activation and inflammatory response in taurocholate-induced pancreatitis. *Am J Physiol Gastrointest Liver Physiol* 2001; **280**: G1197-G1208
- 48 **Mayer J**, Rau B, Gansauge F, Beger HG. Inflammatory mediators in human acute pancreatitis: clinical and pathophysiological implications. *Gut* 2000; **47**: 546-552
- 49 **Saluja AK**, Bhagat L, Lee HS, Bhatia M, Frossard JL, Steer ML. Secretagogue-induced digestive enzyme activation and cell injury in rat pancreatic acini. *Am J Physiol* 1999; **276**: G835-G842
- 50 **Matsumura N**, Ochi K, Ichimura M, Mizushima T, Harada H, Harada M. Study on free radicals and pancreatic fibrosis-pancreatic fibrosis induced by repeated injections of superoxide dismutase inhibitor. *Pancreas* 2001; **22**: 53-57
- 51 **Simsek I**, Refik M, Yasar M, Ozyurt M, Saglamkaya U, Deveci S, Comert B, Basustaoglu A, Kocabalkan F. Inhibition of inducible nitric oxide synthase reduces bacterial translocation in a rat model of acute pancreatitis. *Pancreas* 2001; **23**: 296-301
- 52 **Gomez-Cambronero L**, Camps B, de La Asuncion JG, Cerda M, Pellin A, Pallardo FV, Calvete J, Sweiry JH, Mann GE, Vina J, Sastre J. Pentoxifylline ameliorates cerulein-induced pancreatitis in rats: role of glutathione and nitric oxide. *J Pharmacol Exp Ther* 2000; **293**: 670-676
- 53 **Schulz HU**, Niederau C, Klonowski Stumpe H, Halangk W, Luthen R, Lippert H. Oxidative stress in acute pancreatitis. *Hepatogastroenterology* 1999; **46**: 2736-2750

Edited by Ma JY

In situ detection of TGF betas, TGF beta receptor II mRNA and telomerase activity in rat cholangiocarcinogenesis

Jian-Ping Lu, Jian-Qun Mao, Ming-Sheng Li, Shi-Lun Lu, Xi-Qi Hu, Shi-Neng Zhu, Shintaro Nomura

Jian-Ping Lu, Department of Pathology, Medical Center of Fudan University (Former Shanghai Medical University), Shanghai 200032, China. Max-Planck-Institute for Cell Biology, Ladenburg 68526, Germany

Jian-Qun Mao, Ming-Sheng Li, Shi-Lun Lu, Xi-Qi Hu, Shi-Neng Zhu, Department of Pathology, Medical Center of Fudan University, (Former Shanghai Medical University), Shanghai 200032, China

Shintaro Nomura, Department of Pathology, Osaka University, School of Medicine, Fukita 565, Japan

Supported by China National Natural Science Foundation, No. 30070846/C03031904

Correspondence to: Jian-Ping Lu, Ph.D. Max-Planck-Institute for Cell Biology, Ladenburg 68526, Germany. lu_jp@hotmail.com

Telephone: +49-6203-106-208 **Fax:** +49-6203-106-122

Received: 2002-10-09 **Accepted:** 2002-11-04

Abstract

AIM: Initial report on the *in situ* examination of the mRNA expression of transforming growth factor betas (TGFβs), TGFβ type II receptor (TβRII) and telomerase activity in the experimental rat liver tissue during cholangiocarcinogenesis.

METHODS: Rat liver cholangiocarcinogenesis was induced by 3'-methyl 4-dimethylazobenzene (3' Me-DAB). *In situ* hybridization was used to examine the TGFβs and TGFβ type II receptor (TβRII) mRNA, *in situ* TRAP was used to check the telomerase activity in the tissue samples.

RESULTS: There was no TGFβs, TβRII mRNA expression or telomerase activity in the control rat cholangiocytes. The expression of TGFβ1, TβRII was increased in regenerative, hyperplastic, dysplastic cholangiocytes and cholangiocarcinoma (CC) cells. The expression of TGFβ2 mRNA was observed in only a part of hyperplastic, dysplastic cholangiocytes. TGFβ3 expression was very weak, only in hyperplastic lesion. There was positive telomerase activity in the regenerative, hyperplastic, dysplastic cholangiocytes, and CC cells. Stroma fibroblasts of these lesions also showed positive TGFβs, TβRII mRNA expression and telomerase activity.

CONCLUSION: There were TGFβs, TβRII expression and telomerase activity in hyperplastic, dysplastic cholangiocytes, cholangiocarcinoma cells as well as in stroma fibroblasts during cholangiocarcinogenesis. Their expression or activity is important in cholangiocarcinogenesis and stroma formation.

Lu JP, Mao JQ, Li MS, Lu SL, Hu XQ, Zhu SN, Nomura S. In situ detection of TGF betas, TGF beta receptor II mRNA and telomerase activity in rat cholangiocarcinogenesis. *World J Gastroenterol* 2003; 9(3): 590-594

<http://www.wjgnet.com/1007-9327/9/590.htm>

INTRODUCTION

Transforming growth factor beta (TGFβ)-TGFβ receptor (TβR) signaling system is important in growth regulating

carcinogenesis and cancer progression^[1,2]. Lacks of the expression of TGFβ and/or TβR, mutation of the related genes were reported in human and animal malignancies^[3-5]. These abnormalities were considered to be the cause of interruption of the growth signal from the TGFβ to the cell nuclear, resulting in the uncontrolled growth of the involved cells. While there are reports on the efficacy of TGFβ which supported that TGFβ was involved in cancer invasion and metastasis^[1, 2, 6].

Hepatocellular carcinoma (HC) and intrahepatic cholangiocarcinoma (CC) are two most common types of liver carcinoma^[7, 8]. Though there are reports on their expression in HC^[9, 10], few reports dealt with the expression of TGFβs and/or TβR in CC. Bile ducts had increased expression of TGFβ1 in inflammatory or obstructive lesions^[11]. TGFβ1 was detected in small amount of cancer cells among 25 of 30 CC cases^[12]. The expression and significance of TGFβs and their receptors during cholangiocarcinogenesis are poorly understood. Stroma fibrosis is one of the characteristics of CC^[7, 8], but the mechanism of excessive stroma formation is not clear.

Telomerase is a key enzyme in the maintenance of the telomeric DNA length^[13]. Telomerase is undetectable in most normal somatic tissues. Its activity was reported in most cancer cell lines as well as cancer tissues from human and experimental animals^[13, 14]. mRNA of telomerase and telomerase-associated protein were detected in CC and its preneoplastic lesions^[15]. It is not clear in which stage the telomerase is activated during cholangiocarcinogenesis.

Liver carcinogenesis was induced by feeding rats with 0.05 % 3'-methyl 4-dimethylazobenzene (3' Me-DAB) in maize flour. The model showed progressive changes from degeneration, necrosis, to cholangiocyte hyperplasia, dysplasia and CC^[16]. We found obviously increased expression of TGFβ and TGFβ type II receptor (TβRII) mRNA and telomerase activity in the proliferative, dysplastic cholangiocytes, CC cells as well as stroma fibroblasts. Here we report these findings and discuss their significance.

MATERIALS AND METHODS

Animals and reagents

Male Wistar rats ($n=100$, weighing 65 ± 10 g) and foods were purchased from the Shanghai Experimental Animal Center of Chinese Academy of Science. All rats received humane care.

3' Me-DAB was purchased from the Tokyo Kasai Co. Ltd. (Tokyo, Japan Cat. 0207). DIG RNA labeling kit (Cat. No. 1175025), DIG nucleic acid detecting kit (Cat. No. 1175041), and Telomerase PCR ELISA kit (Cat. No. 1854666) were bought from Roche, Germany. Mouse anti-proliferating cell nuclear antigen (PCNA), goat anti-vimentin and biotinylated secondary antibodies were purchased from DAKO. ABC Kit was the product of Vector.

Alcian blue (8GS) was the product of Chroma. Sirius red (F3B) was from Sigma. All other reagents were of analytical or molecular biology research grade from Sigma, Merck or Shanghai Analytical Chemical Co.

Experimental design

The rats were divided into Experimental ($n=60$) and Control

($n=40$) Groups randomly and fed with common compound food and tap water during the first week of adaptation. Maize flour containing 0.05 % 3' Me-DAB was prescribed to the Experimental Group rats for 12 weeks to induce liver cancer. The Control Group rats were fed with maize flour only for the 12-week-period. Common compound food was given to all rats after the period. The rats were sacrificed under anesthetization from 4-week to the end of 22-week since 3' Me-DAB feeding.

The liver tissues with macroscopic lesions were sampled. Samples from half of the lesions were fixed in 4 % buffered paraformaldehyde, embedded in paraffin for routine H.E, histochemical staining, immunohistochemistry and *in situ* hybridization. Samples from residual half of the lesions were embedded in OCT compounds, snap frozen, and cryostat section for histochemical staining and *in situ* TRAP reaction. H.E. alcian blue, PAS and sirius red staining were undertaken. The liver lesions were classified into not obvious, hyperplastic or cholangial proliferative, dysplastic proliferative foci and cancer^[7, 8, 14]. The cholangial property of the cells in the lesion was confirmed by positive mucin staining with either serum albumin mRNA expression, or cytoplasmic glycogen.

In situ hybridization

Plasmids containing cDNAs of TGF β 1, 2, 3; T β RII and serum albumin (SA) were proliferated in *E. Coli*. The plasmids were extracted, purified and linearized with specified endonucleases (Table 1). Anti-sense and sense cRNAs were then made and labeled with digoxigenin *in vitro*^[17].

Paraffin embedded tissue samples were sectioned (5 μ m). The sections were deparaffinized in serial xylene and alcohol solvents, transferred into 100 mM PBS (pH7.4) and digested with proteinase K. The sections were pretreated with 4 % buffered paraformaldehyde, PBS, 200 mM HCl, 100 mM TEA-HCl buffer (pH8.0), 100 mM TEA·0.25 % anhydrous acetate, PBS and further dehydrated with serial alcohol. Pre-warmed hybridization solution containing digoxigenin labeled probe was dropped on the pretreated sections, covered with parafilm and incubated in wet chamber for 15 hours at 50 °C. After hybridization, the sections were washed in 5 \times SSC, 2 \times SSC with 50 % formamide and TNE solutions. Non-hybridized probe was digested with RNase A. Digoxigenin labeled probe was detected with alkaline phosphatase labeled anti-digoxigenin antibody and visualized with NBT-BCIP substrate^[17, 18]. Some of the sections were further counterstained with eosin, alcian blue, and/or hematoxylin.

Addition of SA anti-sense probe was used as positive control, sense probes were used as negative controls.

Table 1 Probes and plasmids

Probe	Vector	Endonuclease and promoter		Length of	
		cRNA (-)	cRNA (+)	cDNA	
T β RII	pBluescript II KS(-)	EcoRI T3	Hind III T7	485bp	
TGF β 1	pBluescript II KS(-)	XhoI T3	Hind III T7	400bp	
TGF β 2	pGEM 3ZF(-)	HindIII T7	EcoRI SP6	500bp	
TGF β 3	pGEM 3ZF(-)	BamHI T7	EcoRI SP6	280bp	
SA	pBluescript II KS(-)	HindIII T3	EcoRI T7	620bp	

In situ TRAP

Liver tissues embedded in O.C.T. compounds were sectioned (10 μ m), air-dried shortly for further processing. The *in situ* TRAP was performed as reported^[14, 19]. Briefly, the elongation and PCR mixture was dropped onto cryostat sections and incubated in wet chamber for 30 min at 30 °C. Telomerase was inactivated at 94 °C for 5 min. The elongated telomere

sequence was amplified within GeneAmp *in situ* PCR System 1000 (Perkin-Elmer Co. Foster City, CA 94404) for 30 cycles. Each cycle included: 94 °C for 30 sec, 50 °C for 30 sec, 72 °C for 20 sec. Last cycle was followed by 72 °C for 10 min. The sections were then washed with washing buffer and fixed with 4 % buffered paraformaldehyde.

The sections were further treated with digoxigenin labeled probes, peroxidase labeled anti-digoxigenin antibody and coloration substrate to show the products of amplification. The reaction products were directly photographed before the addition of stop solution. Negative controls included: elongation after inactivation of telomerase, no probe, no antibody or substrate only control.

Immunohistochemical and histochemical reactions

Paraffin sections were routinely deparaffinized and transferred to PBS. PCNA affinity to antibody was recovered by microwave oven treatment of the sections in 10mM TAE. Immunohistochemical detection of PCNA and vimentin was performed following routine procedure^[20].

Alcian blue and sirius red staining were undertaken on paraffin sections. PAS staining was carried out on paraffin as well as frozen sections.

The experiment was undertaken on at least 6 rats from different period of carcinogenesis with lesions of regeneration, hyperplasia, dysplasia and carcinoma foci separately. The experiments on the same sample were duplicated to ensure the results.

RESULTS

The Control Group rats showed no obvious pathologic changes. There was no detectable expression of TGF β 1, 2, 3, T β RII mRNA in the cholangiocytes and bile duct cells from the control rat liver. There was a zonal expression of SA in hepatocytes, stronger at zone 1 and weaker at zone 3. Neither telomerase activity, nor PCNA reaction was detected in the cholangiocytes and bile duct cells. The stellate cells of the sinus were positive to vimentin.

There were successive histological changes in the liver tissue samples in Experimental Group rats: from degeneration and necrosis, regeneration and proliferation, hyperplasia and dysplasia, to carcinoma.

At the early stage, there were massive degeneration and necrosis of the liver tissue samples. No TGF β 1, 2, 3, T β RII expression or telomerase were detected in the degenerative and necrotic liver tissue samples.

Later, regeneration and proliferation of cholangiocytes and hepatocytes were observed. Early in the regenerative and proliferative lesion, there were epithelial cells with edematous stroma. The epithelial cells were scattered in small clusters or forming cell cords, sometimes with lumen in the cords. When the cells differentiate toward cholangiocytes, the cytoplasm of the cells became basophilic without SA or glycogen. There was mucus accumulation in the cytoplasm or in some of the lumens. These cells showed positive TGF β 1 mRNA expression (Figure 1-2). Telomerase activity and PCNA positive nucleus appeared in these epithelial cells.

The proliferation of cholangiocytes continued but the edema of the stroma reduced with time, while vimentin positive fibroblast proliferation appeared in stroma followed by deposition of collagen. At this stage, the cholangiocytes and fibroblasts expressed high level of TGF β 1, 2 and T β RII mRNA (Figure 3-4). These cells were also positive to PCNA and telomerase reactions (Figure 7). TGF β 3 can also be detected transiently in some cholangiocytes. The lesion developed into cholangiocyte hyperplasia with stroma fibrosis (Figure 4, 7).

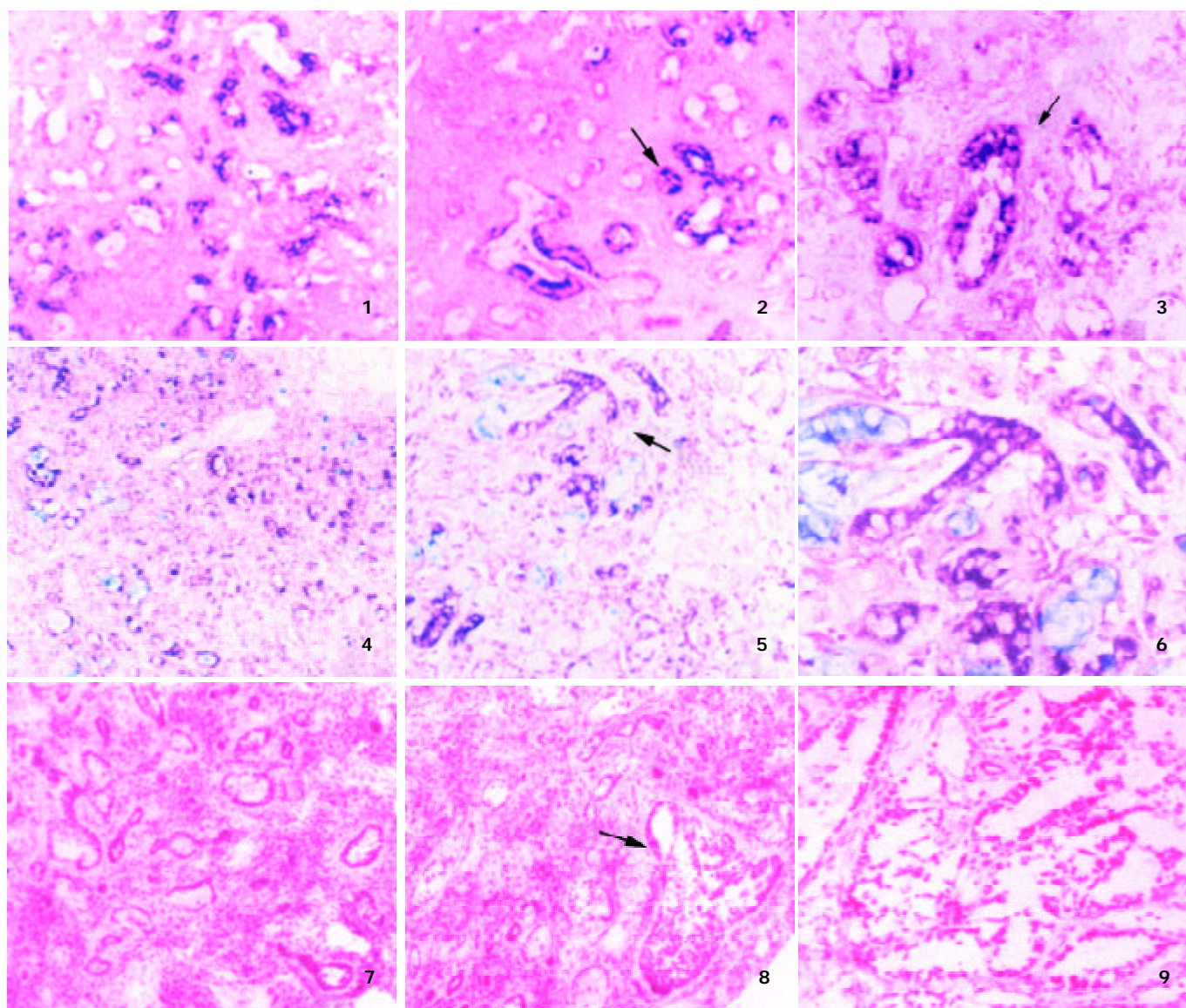


Figure 1-6 *In situ* hybridization showed the mRNA localization (NBT-BCIP purple colored) of TGFβ1 (Figure 1, 2), TGFβ2 (Figure 3), TβR II (Figure 4-6). Figure 1-3 counterstained with eosin; Figure 4-6 counterstained with alcian blue and eosin.

Figure 7-9 *In situ* TRAP shows telomerase activity of the hyperplastic (Figure 7), dysplastic cholangiocytes (Figure 8) and cholangiocarcinoma (Figure 9) in rat liver tissue. Hyperplastic epithelial cells in the stroma form clusters, cords, and ducts (Figure 1, 4, 7). There was mucin formation in some of the ducts (Figure 4) indicating they were cholangiocytes. The hyperplastic cholangiocytes showed TGFβ1, TβR II mRNA expression. (Figure 1, 4). There was telomerase activity in their nuclei (Figure 7). Proliferative cholangiocytes forming duct structures. Some of them had structural and cellular atypia indicating cholangial dysplasia or cholangiocarcinoma in hyperplastic lesion (Figure 2, 3, 5, 6, 8). The expression of TGFβ1, 2, (Figure 2, 3), TβR II (Figure 4-6) and mucin formation in the hyperplastic and dysplastic ducts were uneven (Figure 2-3, 5-6). In Cholangial dysplasia foci and cholangiocarcinoma, there was telomerase activity in the nuclei of cancer cells and stroma fibroblasts (Figure 8-9). (Figure 1, 4, 7, 8×100; Figure 2, 3, 5, 9×200; Figure 6×400).

Later, the cholangiocytes in some areas disappeared with the maturation of fibroblasts to fibrocytes and increased deposition of collagen forming a “burnt-out” picture.

In other areas, the cholangiocytes kept growing with atypical cell morphology, forming irregular cellular clusters, and abortive tubular or glandular structures, indicating cholangiocyte dysplasia. Some of them may accompany with CC. The dysplasia was first found in the liver tissues after 12 weeks of 3’ Me-DAB treatment. Small foci of CC appeared in the liver lesion at the 16th to 20th week of experiment.

There was mucin in the cytoplasm of the dysplastic cholangiocytes, CC cells or in the lumen formed in the cell clusters. The expressions of TGFβ1 and TβRII mRNA in the dysplastic cholangiocytes and CC cells differed greatly from negative to strong positive among different cells and different cell clusters (Figure 2, 5, 6). TGFβ2 mRNA expression was

also uneven in the dysplastic lesions (Figure 3). TGFβ3 expression was undetectable. Most of the dysplastic cholangiocytes and cancer cells showed telomerase activity (Figure 8-9). Strong PCNA positive reaction was observed in the hyperplastic, dysplastic cholangiocytes and CC. The stroma was abundant with proliferative fibroblasts (PCNA and vimentin positive) and collagen deposition. The fibroblasts had positive TGFβ1, TβRII mRNA expression and telomerase activity.

DISCUSSION

The liver tissues from our carcinogenesis model had lesions from cholangiocyte hyperplasia, dysplasia to CC with positive mucin staining with neither albumin mRNA, nor glucagon in the cytoplasm.

TGF β is well known for its effects on fibroblasts which can induce formation of stroma^[1,2,21]. But there is no report on the expression of T β R during experimental cholangiocarcinogenesis. We observed the expression of TGF β 1 and T β R II expression in the fibroblasts of regenerative, dysplastic cholangiocyte lesions and in CC. There was increased fibrous stroma formation around the fibroblasts and fibrocytes. These results supported the function of TGF β -T β R II system in the excessive stroma formation in these lesions.

Present experiment showed that there was no TGF β 1, 2, 3 and T β R II expression in normal bile duct cells. TGF β 1, 2, 3 and T β R II mRNA expression was detected in the repairing and proliferative cholangiocytes. In the dysplastic cholangiocytes and CC cells, their expression varied from negative to strong positive. TGF β 1 protein was also detected in experimental rat and human CC cells^[21-23]. TGF β 1 can suppress the proliferation of epithelium, prevent epithelial carcinogenesis^[1,2]. On the other hand, there are reports that TGF β can not inhibit the cancer growth or even accelerate the cancer invasion^[2,6]. TGF β can suppress the growth of the normal bile duct cell but not the CC cells^[12]. Transgenic mouse with TGF β 1 over expression accelerates hepatocarcinogenesis^[24]. Dominant-negative T β R II mice had accelerated carcinogenesis^[25]. Our results showed that TGF β and T β R II expression accompanied with the cholangiocarcinogenesis procedure.

Cancer progress is related to the reaction between cancer cells and its stroma^[26]. Treatment of Ras-transformed mammary epithelial cells with TGF-beta results in resistant to growth inhibition by TGF-beta. These cells start to secrete TGF-beta, leading to maintenance of the invasive phenotype. The action is dependent on epithelial-stromal interaction^[27]. Our results showed that there was TGF β 1 and T β R II expression in the dysplastic cholangiocytes, CC cells and stroma fibroblasts. Thus, the paracrine and autocrine functions of TGF β 1 are important in supporting the process of cholangiocarcinogenesis.

The expression of TGF β 2 mRNA was only detected in part of hyperplastic, dysplastic cholangiocytes. TGF β 3 mRNA was only weakly positive in some hyperplastic cholangiocytes. There is few reports on the expression of TGF β 2, 3 mRNA in the process of cholangiocarcinogenesis. Their role may be transient.

Phase of telomerase activation during cholangiocarcinogenesis is not specified. Present experiment showed that normal bile duct cells were telomerase negative. There was telomerase activity in the regenerative, hyperplastic, and dysplastic cholangiocytes as well as CC cells. The activation of telomerase occurred in the early stage of cholangio-carcinogenesis. There were also reports on the positive hTR and TP1 mRNA expression in intrahepatic biliary dysplasia^[28]. Increased telomerase activity was reported in dysplastic hepatocytes during hepatocellular carcinogenesis^[29].

The expression of TERT can induce resistance to TGF β growth inhibition^[30]. This may be another reason for the hyperplastic, dysplastic cholangiocytes and CC cells escaping from TGF β -T β R growth suppression in our cholangiocarcinogenesis model.

The telomerase activity is a marker of immortalized or malignant cells^[13,14,31]. In present experiment, telomerase was positive in the proliferating cells no matter they were parenchyma or stroma cells. The phenomenon was observed in other liver proliferative lesions^[14,32]. So that telomerase activation was also a good marker of cell in proliferation.

In summary, this is the first report on the *in situ* detection of TGF β 1, 2, 3, T β R II mRNA and telomerase activity during rat cholangiocarcinogenesis. There is TGF β 1, 2, 3, T β R II mRNA and telomerase activity in the hyperplastic, dysplastic cholangiocytes, CC cells as well as stroma fibroblasts. There is gradual increase of the fibrous stroma (fibrosis) during the

development of CC. It is considered that the expression of TGF β 1, 2, 3, T β R II and telomerase activation has important implication in cholangiocarcinogenesis and cancer stroma formation.

REFERENCES

- 1 **Heldin CH**, Miyazono K, Dijke PT. TGF-signaling from cell membrane to nucleus through SMAD proteins. *Nature*1997; **390**: 465-471
- 2 **Derynck R**, Akhurst RJ, Balmain A. TGF-signaling in tumor suppression and cancer progression. *Nature Genetics* 2001; **29**: 117-129
- 3 **Francis-Thickpenny KM**, Richardson DM, Eel CC, Love DR, Winship IM, Baguley BC, Chenevix-Trench G, Shelling AN. Analysis of the TGF β functional pathway in epithelial ovarian carcinoma. *Brit J Cancer* 2001; **85**: 687-691
- 4 **Jonson T**, Albrechtsson E, Axelsson J, Heidenblad M, Gorunova L, Johansson B, Hoglund M. Altered expression of TGF β receptors and mitogenic effects of TGF β in pancreatic carcinomas. *Int J Oncol* 2001; **19**: 71-81
- 5 **Paterson IC**, Matthews JB, Huntley S, Robinson CM, Fahey M, Parkinson EK, Prime SS. Decreased expression of TGF-beta cell surface receptors during progression of human oral squamous cell carcinoma. *J Pathol* 2001; **193**: 458-467
- 6 **Xiong B**, Yuan HY, Hu MB, Zhang F, Wei ZZ, Gong LL, Yang GL. Transforming growth factor- β 1 in invasion and metastasis in colorectal cancer. *World J Gastroenterol* 2002; **8**: 674-678
- 7 **Ishak KG**, Anthony PP, Sobin LH. Histological Typing of Tumours of the Liver. WHO International Histological Classification of Tumours. Berlin: Springer Verlag, 1994
- 8 **Barwick WK**, Rosai J. Liver. In Rosai J ed. Ackerman's Surgical Pathology 7th ed. Mosby CO. St Louis. 1989: 675-735
- 9 **Rossmann W**, Schulte-Hermann R. Biology of transforming growth factor beta in hepatocarcinogenesis. *Microsc Res Tech* 2001; **52**: 430-436
- 10 **Sasaki Y**, Tsujiuchi T, Murata N, Tsutsumi M, Konishi Y. Alterations of the transforming growth factor-beta signaling pathway in hepatocellular carcinomas induced endogenously and exogenously in rats. *Jpn J Cancer Res* 2001; **92**: 16-22
- 11 **Su WC**, Shiesh SC, Liu HS, Chen CY, Chow NH, Lin XZ. Expression of oncogene products HER2/Neu and Ras and fibrosis-related growth factors bFGF, TGF-beta, and PDGF in bile from biliary malignancies and inflammatory disorders. *Dig Dis Sci* 2001; **46**: 1387-1392
- 12 **Yokomuro S**, Tsuji H, Lunz JG, Sakamoto T, Ezure T, Murase N, Demetris AJ. Growth control of human biliary epithelial cells by interleukin 6, hepatocyte growth factor, transforming growth factor beta1, and activin A: comparison of a cholangiocarcinoma cell line with primary cultures of non-neoplastic biliary epithelial cells. *Hepatology* 2000; **32**: 26-35
- 13 **Holt SE**, Shay JW. Role of telomerase in cellular proliferation and cancer. *J Cell Physiol* 1999; **180**: 10-18
- 14 **Lu JP**, Zhu SN, Song BP, Mao JQ, Li MS, Hayashi K. In situ detection of telomerase activity in hepatic carcinogenesis of rats. *J Shanghai Med Univ* 1999; **26**: 413-416
- 15 **Ozaki S**, Harada K, Sanzen T, Watanabe K, Tsui W, Nakanuma Y. In situ nucleic acid detection of human telomerase in intrahepatic cholangiocarcinoma and its preneoplastic lesion. *Hepatology* 1999; **30**: 914-919
- 16 **Yuan ST**, Hu XQ, Lu JP, Hayashi K, Zhai WR, Zhang YE. Changes of integrin expression in rat hepatocarcinogenesis induced by 3' Me-DAB. *World J Gastroenterol* 2000; **6**: 231-233
- 17 **Wada K**, Nomura S, Mori E, Kitamura Y, Nishizawa Y, Miyake A, Terada N. Changes in levels of mRNAs of transforming growth factor (TGF)-beta1, -beta2, -beta3, TGF-beta type II receptor and sulfated glycoprotein-2 during apoptosis of mouse uterine epithelium. *J Steroid Biochem Mol Biol* 1996; **59**: 367-375
- 18 **Lu JP**. Non-isotopic in situ hybridization technique. *Nanhai Publication* 1996; Haikou, China
- 19 **Lu JP**, Zhu SN, Song BP, Mao JQ, Lu SL. In situ telomerase repeat amplification protocol (TRAP) detecting telomerase activity in human hepatocellular carcinoma. *Acta Histochem Cytochem* 1999; **32**: 477-480
- 20 **Lu JP**, Hayashi K. Transferrin receptor distribution and iron deposition in the hepatic lobule of iron-overloaded rats. *Pathol Int* 1995; **45**: 202-206

- 21 **Mao JQ**, Lu JP, Zhu SN, Li MS, Lu SL, Hayashi K, Nomura S. The significance of TGF β - and its receptor on the difference of stroma formation in experimental rat hepatocellular carcinoma and cholangiocarcinoma. *Chinese Hepatol* 2001; **6**: 23-25
- 22 **Nakatsukasa H**, Evarts RP, Hsia CC, Marsden E, Thorgeirsson SS. Expression of transforming growth factor-beta 1 during chemical hepatocarcinogenesis in the rat. *Lab Invest* 1991; **65**: 511-517
- 23 **Vogelbruch M**, Wellmann A, Maschek H, Schafer MK, Flemming P, Georgii A. Transforming growth factor beta 1 in human liver tumors. *Verh Dtsch Ges Pathol* 1995; **79**: 132-136
- 24 **Factor VM**, Kao CY, Santoni-Rugiu E, Woitach JT, Jensen MR, Thorgeirsson SS. Constitutive expression of mature transforming growth factor beta1 in the liver accelerates hepatocarcinogenesis in transgenic mice. *Cancer Res* 1997; **57**: 2089-2095
- 25 **Kanzler S**, Meyer E, Lohse AW, Schirmacher P, Henninger J, Galle PR, Blessing M. Hepatocellular expression of a dominant-negative mutant TGF-beta type II receptor accelerates chemically induced hepatocarcinogenesis. *Oncogene* 2001; **20**: 5015-5024
- 26 **Lu JP**, Hayashi K. Myofibroblasts and stroma difference between cholangiocarcinoma and hepatocellular carcinoma. *Arch Histopathol D* 1996; **3**: 55-62
- 27 **Oft M**, Peli J, Rudaz C, Schwarz H, Beug H, Reichmann E. TGF-beta1 and Ha-Ras collaborate in modulating the phenotypic plasticity and invasiveness of epithelial tumor cells. *Genes Dev* 1996; **10**: 2462-2477
- 28 **Shimonishi T**, Sasaki M, Nakanuma Y. Precancerous lesions of intrahepatic cholangiocarcinoma. *J Hepatobil Pancreat Surg* 2000; **7**: 542-550
- 29 **Hytioglou P**, Kotoula V, Thung SN, Tsokos M, Fiel MI, Papadimitriou CS. Telomerase activity in precancerous hepatic nodules. *Cancer* 1998; **82**: 1831-1838
- 30 **Stampfer MR**, Garbe J, Levine G, Lichtsteiner S, Vasserot AP, Yaswen P. Expression of the telomerase catalytic subunit, hTERT, induces resistance to transforming growth factor beta growth inhibition in p16INK4A (-) human mammary epithelial cells. *Proc Natl Acad Sci USA* 2001; **98**: 4498-4503
- 31 **Qin LX**, Tang ZY. The prognostic molecular markers in hepatocellular carcinoma. *World J Gastroenterol* 2002; **8**: 385-392
- 32 **Ogami M**, Ikura Y, Nishiguchi S, Kuroki T, Ueda M, Sakurai M. Quantitative analysis and in situ localization of human telomerase RNA in chronic liver disease and hepatocellular carcinoma. *Lab Invest* 1999; **79**: 15-26

Edited by Xu XQ

• CLINICAL RESEARCH •

Postoperative endoscopic surveillance of human living-donor small bowel transplantations

Jie Ding, Chang-Cun Guo, Cai-Ning Li, An-Hua Sun, Xue-Gang Guo, Ji-Yan Miao, Bo-Rong Pan

Jie Ding, Chang-Cun Guo, Cai-Ning Li, An-Hua Sun, Xue-Gang Guo, Ji-Yan Miao, Institute of Digestive Disease, Xijing Hospital, Fourth Military Medical University, Xi'an 710032, Shaanxi Province, China

Bo-Rong Pan, Oncology Center, Xijing Hospital, 127 Changle West Road, Xi'an 710032, China

Correspondence to: Prof. Jie Ding, Institute of Digestive Disease, Xijing Hospital, Fourth Military Medical University, Xi'an 710032, Shaanxi Province, China. charlson_cole@yahoo.com

Telephone: +86-29-3375230

Received: 2002-08-24 **Accepted:** 2002-10-20

Abstract

AIM: To determine the significance of endoscopic surveillance in the diagnosis of acute rejection after human living-donor small bowel transplantations.

METHODS: Endoscopic surveillance was performed through the ileostomy after human living-donor small bowel transplantations. The intestinal mucosa was observed and biopsies were performed for pathological observations.

RESULTS: Acute rejection was diagnosed in time by endoscopic surveillance. The endoscopic and pathological manifestations of acute rejection were described.

CONCLUSION: Endoscopic surveillance and biopsy are reliable methods to diagnose the acute rejection after human living-donor small bowel transplantations.

Ding J, Guo CC, Li CN, Sun AH, Guo XG, Miao JY. Postoperative endoscopic surveillance of human living-donor small bowel transplantations. *World J Gastroenterol* 2003; 9(3): 595-598
<http://www.wjgnet.com/1007-9327/9/595.htm>

INTRODUCTION

Prompt and accurate diagnosis of acute rejection is a key element to ensure the success of human small intestinal transplantation. However due to the limited cases of successful human small intestinal transplantations, little is available for the prompt and accurate diagnosis of acute rejection after the operations. Here we reported the postoperative endoscopic surveillance of acute rejection in 2 cases of human living-donor small bowel transplantations performed in our hospital. We also discussed the significance of endoscopic surveillance and pathological examination of the mucosal biopsy specimen in the diagnosis of acute rejections in this paper.

MATERIALS AND METHODS

Case material

Patient 1, Male, 18 years old, underwent enterectomy because of small bowel necrosis after volvulus with the residual jejunum being only 49 cm in length, had more than 10 defecations in a day with the content being undigested foods, suffered from

severe malnutrition, and was diagnosed as short bowel syndrome. Living-donor small bowel transplantation was performed on the patient on May 20 1999. The donor was his father. The donor and the recipient were ABO compatible (both O type) and their HLA and HLA-DR antigen were semi-compatible. The lymphocytotoxic cross matching test showed reaction <10 %. A 150 cm segment of terminal ileum 20 cm away from the ileocecal valve was removed from the donor. The distal end of graft ileum was anastomosed to the distal end of the recipient ileum. Ileostomy was performed at the terminal end of the graft ileum.

Patient 2, Male, 15 years old, underwent resection of the most part of the small bowel and part of the cecum because of necrosis due to cecum hernia trap. The residual jejunum was only 10 cm in length. The patient defecated shortly after eating. Content of the defecations was undigested food. After 1 year and a half of parenteral nutrition, the patient developed mild liver dysfunction and was diagnosed as short bowel syndrome. Living-donor small bowel transplantation was performed on the patient on Jan 6 2001. The donor was his mother (47 years old). Both the donor and the recipient have a B type in ABO blood type. Their HLA and HLA-DR were semi-compatible. Lymphocytotoxic cross matching test showed <10 % reaction. A 160 cm segment of terminal ileum 20 cm away from the ileocecal valve was removed from the donor. The distal end of graft ileum was anastomosed to the distal end of the recipient ileum. Ileostomy was performed at the terminal end of the graft ileum.

Both patients were given immunosuppressors FK506, MMF and MP together with antibiotics, anticoagulant and nutrition support. Patient 1 developed acute rejection after 67 days after operation. After implosion therapy, the rejection was taken under control, and so far, the patient has survived healthily for 30 months. Patient 2 developed acute rejection after 20 days of the operation, which was controlled after implosion therapy. However acute rejection reoccurred after 80 days of the operation together with severe infection. And the patient died after 5 months of the operation.

Methods

Endoscopic surveillance through the ileostomy was started at 15 days after operation for the patient 1, and 2 days after operation for the patient 2. Endoscopy was performed when discharge from the ileostomy increased or at the case of hemorrhage or other abnormalities. Patients took no food in 12 h before the endoscopic examination, and 1 000 ml 5 % glucose saline was orally taken by the patients to clear the bowels. An Olympus GIF-XQ230 gastroscope was inserted through the ileostomy into the graft bowels for examination. And for a control observation, the gastroscope was extended to pass through the stoma to observe autologous small intestine or colon. Mucosal biopsies were performed at the graft bowels and the autologous small intestine or colon. Then the pathological and microbiological examinations of biopsy specimens were done.

RESULTS

During the 48 days after the operation, 8 times of endoscopic

examinations were performed on patient 1. Biopsies were performed at the same time for pathological examinations. No signs of rejection or infection were seen. After 60 days of the operation, discharge from the ileostomy was increased, and it went up to 1 200 ml at the 66th day. At the 66th day, endoscopy examination was performed, and it was found that the segments of graft bowel 20-35 cm, 40-60 cm and 70-90 cm away from the ileostomy had hyperemia and edema in the mucosa displaying a strong reflection; light yellow mucus was seen on the mucosal surface; patches of mucosal hemorrhage and erosion were also observed; besides, there were several oval-shaped (0.3-0.6 cm in diameter) and linear ulcers (paralleling with the mucosal folds) in the graft bowel; the ulcers were covered with white coat (Figure 1-4). The intestinal wall was quite fragile and easy to bleed. There was much hemorrhage in the biopsy sites after the biopsy. The vermiculation of the graft became weak. The residual autologous small bowel showed no signs of hyperemia, edema, erosion or ulceration. Pathological examination of the biopsy specimen revealed that there were local erosions in the mucosa; some parts of the epithelia showed atrophy in a shape of short column; the goblet cells decreased in size or just disappeared; edema was found universally in the lamina propria; there were infiltrations of neutrophils, plasma cells and lymphocytes in the lamina propria and the muscularis mucosa; there was an increase of the number of neutrophils in the blood vessels. Microbiological examination found no abnormalities. The residual autologous bowel was normal as confirmed by pathological examination in the biopsy specimen. The patient was diagnosed as acute rejection and was treated accordingly. After 3 days of treatment, endoscopic examination was performed, and it was found that the hyperemia and edema abated a lot, the erosions healed up; the ulcers decreased in size and depth and were partly scarred over (Figure 5). Follow-up by endoscopic and pathological examinations detected no lesions thereafter.



Figure 1 Rejection in the graft bowel 40 cm away from the ileostomy.

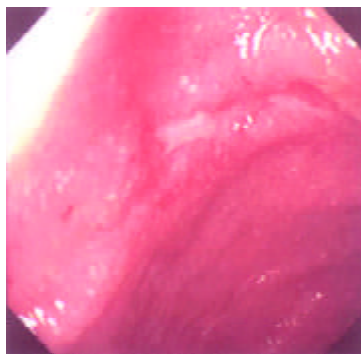


Figure 2 In the rejection of patient 1, we can see the linear ulcer paralleling with the mucosal plica.

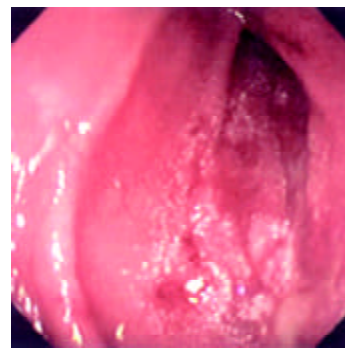


Figure 3 Rejection in the graft segment 50 cm away from the stoma of patient 1.

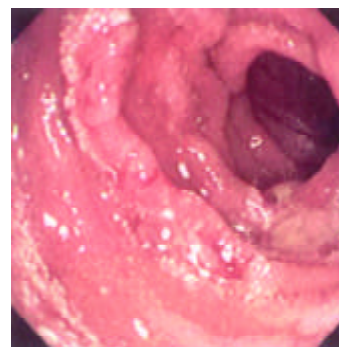


Figure 4 Rejection in the graft bowel 70 cm away from the stoma in patient 1.

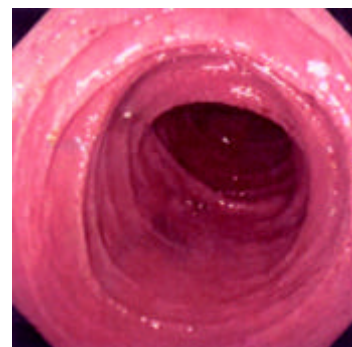


Figure 5 The mucosal edema abated and erosions healed 3 days after treatment. (patient 1).

Endoscopic examinations were performed during the time from the 2nd day to the 17th day after the transplantation. No signs of rejection were detected. However, on day 20 the discharge from the ileostomy increased up to 1 000 ml. Endoscopy was performed on day 22. It was found that: there was severe mucosal hyperemia and edema in the distal end of the graft bowel; patches of hemorrhage and erosions could be seen; a 0.6×1.2 cm oval-shaped longitudinal ulcer was seen 30 cm away from the ileostomy in the graft bowel. The ulcer was shallow and had a flat base with gray coat covering it. The autologous bowel was normal. On day 26, endoscopy was performed again and found that the ulcer was enlarged and deepened with edge raised. Circular broken plica was seen (Figure 6). Pathological examination of the specimen from the lesions suggested that there was acute rejection. No significant changes were seen in the microbiological examination. The autologous bowel showed normal pathological features. After 9 days of anti-rejection treatment, the ulcer became smaller and shallower with no coat on it and showed partial healing (Figure 8). On day 80 after transplantation, the discharge from

the ileostomy increased again. Endoscopy was performed and found that there were multiple lesions of hyperemia and edema in the graft bowel (showing strong reflection under the gastroscope); a great deal of white yellow mucus was seen on the lesions; the bowel lumen at the lesion sites became narrower; and the vermiculation of the graft bowel became weak; in the graft bowel, there were spots or patches of hemorrhage, superficial erosions, and deep round or oval ulcers varying from 0.8-2.0 cm in diameter; the edges of the ulcers showed severe hyperemia and edema. Pathological examination showed that there were ulcerations in the graft bowel; obvious edema could be seen in the lamina propria; the lamina propria and the muscularis mucosa had severe infiltration of neutrophils and lymphocytes. The patient was therefore diagnosed as severe acute rejection. Anti-rejection therapy had no effect on the patient. Follow-up by endoscopies witnessed the enlargement and deepening of the previous ulcers and the formation of new ulcers on the premise of mucosal edema and erosion (Figure 9). Ulcerative hemorrhage was also found.

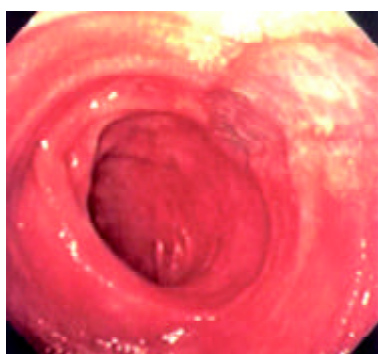


Figure 6 Longitudinal oval- shaped shallow ulcers could be seen in the rejection 30 cm away from the stoma in patient 2.



Figure 7 Part of the shallow ulcers 30 cm away from the stoma was healed after patient 2 was treated for 9 days.

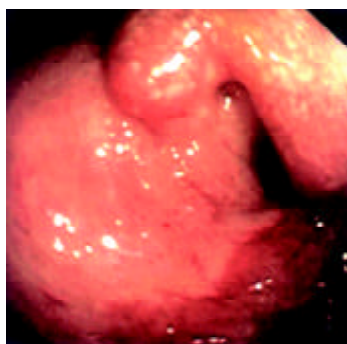


Figure 8 80 d after operation, severe rejection was seen 10 cm away from the ileostomy of the patient 2.



Figure 9 In patient 2, new ulcers formed 109 days after operation, and severe edema could be seen in the mucosa.

DISCUSSION

The significance of endoscopic surveillance

The difficulty of small bowel transplantation lies mainly in the high immunogenicity of the organ. The small bowel is rich in lymphocytes and dendritic cells (DC), especially in the Peyer's patches, lamina propria and the mesenteric nodes. The DC cells have been reported of great importance in the host's rejection to liver graft^[1]. All of the mentioned features of small bowel present a formidable challenge to small bowel transplantation. The major impediment to success of small bowel transplantation is the rejection, which will lead to failure if it is severe. Even though there have been some improvements in the technique of small bowel transplantation, both in human^[2] and animal model^[3], the rejection remains the major cause of failure in transplantation. Therefore, prompt and accurate diagnosis and treatment of rejection is the crux for successful transplantation. Pathological examinations of the mucosal biopsy specimen of the graft serve as the most important and fundamental method in current clinical diagnosis of rejection, for it can well show the characteristics of the rejection and its degree. The biopsy specimen can be openly taken through the stoma or under the endoscopic surveillance. However, typical lesions can not be easily taken by open biopsy, and erosions and ulcerations are often induced near the stoma due to repeated biopsies. Endoscopic surveillance has a good view of the mucosa of the graft bowel and biopsy specimen can be taken precisely at the lesion sites. Now it has been accepted as the most reliable conventional method for surveillance.

Living small bowel transplantation has high tissue compatibility and can reduce the frequency of rejection or its severity. Novel immunosuppressor agents such as FK506 can effectively suppress rejection after transplantation. Living-donor small bowel transplantation was first reported by Deltz *et al*^[4]. Since then, there have been several reports of living small bowel transplantations reported, and most of the transplantations in 1990's were successful^[5]. Compared with cadaveric bowel transplantation, living-donor small bowel transplantation has a lower rate of rejection and infection^[6]. But acute rejection is not uncommon in living small bowel transplantation^[7,8], and if the rejection is severe, it can cause loss of the graft or death of the patients. So, the surveillance, prevention and treatment of the rejection should be paid attention to all the time after the small bowel transplantation. Some indices of enteral function and biochemistry and immunology have been used in immune surveillance after small bowel transplantation in experimental animal, but most of them are under investigation and show no values of clinical practice. The recognition and diagnosis of the rejection are mainly depended on clinical observation, endoscopy and pathological examination. Rejection has no clinical characteristics for diagnosis; the biopsy specimen is not always a mirror of the

situation of rejection; and for definite diagnosis of rejection, the specimen should cover all the layers of the intestinal wall, but the biopsy can easily cause severe complications such as perforation. Therefore, endoscopic examination is the most important method for posttransplant surveillance and diagnosis of rejection.

Method and time for Endoscopy surveillance

Most of the living-donor small bowel transplantations were staged operations, and there was an ileostomy often left for postoperative observation. The graft bowel and the discharge could be observed directly through the ileostomy. And the stoma also provided a passage for the endoscopic surveillance and mucosal biopsy. The endoscopy plays an important role in the assessment of the graft bowel, and in 1999, Kato *et al*^[9] reported the first case of using zoom videoendoscope to evaluate graft bowel mucosa in human intestine transplantation. This method was further proved to be effective to determine the severity of acute cellular rejection and to be able to minimize the times of biopsies^[10]. In this report, with a gastroscopy, we successfully performed endoscopic examinations and mucosa biopsies for 39 times through the stoma in these 2 patients. No complications were observed, which suggested that endoscopy and biopsy are safe and convenient methods for the surveillance of the graft bowel. As for the timing of the endoscopic surveillance, the frequency of endoscopy should be generally 1 or 2 times every week during the first 3 months after the operation. Rejections and other complications of small bowel transplantation such as hemorrhage and thrombosis in mesentery occur most often during the initially several days after the transplantation. So we consider that it is proper to perform endoscopic examination everyday in the first 3 days, and afterwards, the frequency of endoscopy be reduced to once every 2 or 3 days and the intervals between two endoscopies can be prolonged gradually in the following 2 or 3 weeks. Emergency endoscopic examinations should be taken in case of intestinal bleeding and increased discharge from the stoma, etc. As results shown by the study of Sigurdsson and his colleagues, the endoscopy was sensitive enough to diagnose only 63 % of the rejections^[8]. We think it necessary to perform biopsies at the same time. As the rejections have a high anatomic variability in the graft bowel^[11], we recommend that the specimen should be taken at multiple sites in the graft bowel, and residual autologous small should bowel be sampled for the control. If necessary, the specimen should undergo microbiological examination to exclude lesions caused by infection.

Clinical features of acute rejection and its endoscopic manifestations

Acute rejections in human small bowel transplantation often occur early after operation, especially during the first 30 days^[12], but also may happen late beyond the first year after transplantation. Generally, clinical features of rejection show as fever, nausea, vomiting, abdominal pain, diarrhea and increased discharge from the stoma. Under endoscopic observation, mucosal hyperemia and edema, fragile intestine wall, erosion, ulceration and hypoperistalsis can be found. Uleration always suggests the onset of acute rejection. Pathological changes vary with the severity of the rejection. At the early stage, microvillus may become blunt, the goblet cell may disappear, and there may be infiltration of inflammatory cells. And then, there may be crypt inflammation, increased apoptotic cells, and in cases of severe rejection, they

can be mucosa hemorrhage, patchy mucosal exfoliation and formation of small abscesses.

When the discharge from the stoma increased in the 2 patients taking small bowel transplantation in our hospital, the manifestations mentioned above were observed by endoscopic surveillance. Combining the endoscopic and pathological findings together, the acute rejection was diagnosed. After the pulse therapy, the lesions of acute rejection abated or disappeared, which confirmed the diagnosis of acute rejection. Endoscopic surveillance is significant for diagnosing rejection and determining the outcomes of corresponding treatment. According to our experience, when there are mucosal hyperemia, edema, hemorrhage and erosions, they should be regarded them as precautions for rejection; if there are ulcers, it often means the onsets of rejections, in addition to the pathological findings, a prompt diagnosis is warranted; improved situations of the patients and healing ulcers suggests the validity of anti-rejection therapy, while no amelioration, enlargement and deepening of ulcers, hemorrhage or formation of new ulcers are indicators of invalidity of anti-rejection treatment and progress of rejection.

So far, there are no standard criteria for the diagnosis of rejection after human small transplantation, and little is known about the endoscopic characteristics of rejection and pathological changes. But more detailed standard of endoscopic surveillance and pathological examinations will be set with more cases of human small bowel transplantation performed.

REFERENCES

- 1 **Xu MQ**, Yao ZX. Functional changes of dendritic cells derived from allogeneic partial liver graft undergoing acute rejection in rats. *World J Gastroenterol* 2003; **9**: 141-147
- 2 **Zhang WJ**, Liu DG, Ye QF, Sha B, Zhen FJ, Guo H, Xia SS. Combined small bowel and reduced auxiliary liver transplantation: case report. *World J Gastroenterol* 2002; **8**: 956-960
- 3 **Wu XT**, Li JS, Zhao XF, Zhuang W, Feng XL. Modified techniques of heterotopic total small intestinal transplantation in rats. *World J Gastroenterol* 2002; **8**: 758-762
- 4 **Deltz E**, Schroeder P, Gundlach M, Hansmann ML, Leimenstoll G. Successful clinical small-bowel transplantation. *Transplant Proc* 1990; **22**: 2501
- 5 **Margreiter R**. Living-donor pancreas and small-bowel transplantation. *Langenbecks Arch Surg* 1999; **384**: 544-549
- 6 **Cicalese L**, Rastellini C, Sileri P, Abcarian H, Benedetti E. Segmental living related small bowel transplantation in adults. *J Gastrointest Surg* 2001; **5**: 168-172
- 7 **Uemoto S**, Fujimoto Y, Inomata Y, Egawa H, Asonuma K, Pollard S, Tanaka K. Living-related small bowel transplantation: the first case in Japan. *Pediatr Transplant* 1998; **2**: 40-44
- 8 **Sigurdsson L**, Reyes J, Putnam PE, del Rosario JF, Di Lorenzo C, Orenstein SR, Todo S, Kocoshis SA. Endoscopies in pediatric small intestinal transplant recipients: five years experience. *Am J Gastroenterol* 1998; **93**: 207-211
- 9 **Kato T**, O'Brien CB, Nishida S, Hoppe H, Gasser M, Berho M, Rodriguez MJ, Ruiz P, Tzakis AG. The first case report of the use of a zoom videoendoscope for the evaluation of small bowel graft mucosa in a human after intestinal transplantation. *Gastrointest Endosc* 1999; **50**: 257-261
- 10 **Sasaki T**, Hasegawa T, Nakai H, Kimura T, Okada A, Musiaki S, Doi R. Zoom endoscopic evaluation of rejection in living-related small bowel transplantation. *Transplantation* 2002; **73**: 560-564
- 11 **Sigurdsson L**, Reyes J, Todo S, Putnam PE, Kocoshis SA. Anatomic variability of rejection in intestinal allografts after pediatric intestinal transplantation. *J Pediatr Gastroenterol Nutr* 1998; **27**: 403-406
- 12 **Sudan DL**, Kaufman S, Horslen S, Fox I, Shaw Jr BW, Langnas A. Incidence, Timing, and Histologic Grade of Acute Rejection in Small Bowel Transplant Recipients. *Transplant Proc* 2000; **32**: 1199

• CLINICAL RESEARCH •

The effects of the formula of amino acids enriched BCAA on nutritional support in traumatic patients

Xin-Ying Wang, Ning Li, Jun Gu, Wei-Qin Li, Jie-Shou Li

Xin-Ying Wang, Ning Li, Jun Gu, Wei-Qin Li, Jie-Shou Li, Medical School of Nanjing University, Research Institute of General Surgery, Jinling Hospital, Nanjing 210002, Jiangsu Province, China
Supported by the Natural Science Foundation of Jiangsu Province, China (No. BQ 2000014), and the Tenth Five-year Medicine Research Foundation in the CPLA (No. 01Z011)

Correspondence to: Xin-Ying Wang, Research Institute of General Surgery, Jinling Hospital, 305 East Zhongshan Road, Nanjing 210002, Jiangsu Province, China. wxinying@263.net

Telephone: +86-25-4826808-58066 **Fax:** +86-25-4803956

Received: 2002-08-13 **Accepted:** 2002-09-16

Abstract

AIM: To investigate the formula of amino acid enriched BCAA on nutritional support in traumatic patients after operation.

METHODS: 40 adult patients after moderate or large abdominal operations were enrolled in a prospective, randomly and single-blind-controlled study, and received total parenteral nutrition (TPN) with either formula of amino acid (AA group, 20 cases) or formula of amino acid enriched BCAA (BCAA group, 20 cases). From the second day after operation, total parenteral nutrition was infused to the patients in both groups with equal calorie and equal nitrogen by central or peripheral vein during more than 12 hours per day for 6 days. Meanwhile, nitrogen balance was assayed by collecting 24 hours urine for 6 days. The markers of protein metabolism were investigated such as amino acid patterns, levels of total protein, albumin, prealbumin, transferrin and fibronectin in serum.

RESULTS: The positive nitrogen balance in BCAA group occurred two days earlier than that in AA group. The serum levels of total protein and albumin in BCAA group were increased more obviously than that in AA group. The concentration of valine was notably increased and the concentration of arginine was markedly decreased in BCAA group after the formula of amino acids enriched BCAA transfusion.

CONCLUSION: The formula of amino acid enriched BCAA may normalize the levels of serum amino acids, reduce the proteolysis, increase the synthesis of protein, improve the nutritional status of traumatic patients after operation.

Wang XY, Li N, Gu J, Li WQ, Li JS. The effects of the formula of amino acids enriched BCAA on nutritional support in traumatic patients. *World J Gastroenterol* 2003; 9(3): 599-602
<http://www.wjgnet.com/1007-9327/9/599.htm>

INTRODUCTION

Hypermetabolism and increased catabolism can be observed in traumatic patients after operation, which may result in severe disturbance of sugar, lipid and protein metabolism^[1-4], accompanied with the changes on the levels of amino acids in serum^[5,6]. How to adjust the formula of amino acids to improve

the metabolism is an interesting project. There has been no data about formula of amino acid which is fit for nutritional support of patients after trauma yet^[7-11]. The purpose of our study was to investigate the effects of the formula of amino acids enriched BCAA on nutritional support in traumatic patients after operation.

MATERIALS AND METHODS

Subjects

40 adult patients after moderate or large abdominal operations who needed total parenteral nutrition (TPN) for more than 6 days were enrolled in a prospective, randomly and single-blind-controlled study from multiple centers during the period from March 2000 to November 2000. The patients (21 males and 19 females) weighed 45-71 kg and were 20-70 years old without metabolic diseases, malnutrition and dysfunction of liver and kidney. The change of weight in each patient was less than 10 % of that before disease. The patients were divided into two groups in random order, the control group (AA group) supplemented with the formula of amino acid (BCAA 22.8 %) and the study group (BCAA group) with the formula of amino acid enriched BCAA (BCAA 35.9 %).

Experiment protocols

TPN was infused with equal nitrogen and calorie through peripheral or central vein during more than 12 hours per day for 6 days, and began on the 2nd day after operation. The formula included nitrogen ($0.2 \text{ g} \cdot \text{kg}^{-1} \cdot \text{d}^{-1}$), non-protein calorie (NPC, $25 \text{ kcal} \cdot \text{kg}^{-1} \cdot \text{d}^{-1}$), the ratio of NPC to N (125/1), the ratio of lipid to sugar (1/1-3/2).

Collection of samples

Serum samples from all patients were collected on the day before operation and on the 7th day after operation. The amino acid pattern, total protein, albumin, prealbumin, transferrin and fibronectin in serum were detected.

Urine samples: 24-hour urine samples (total volume of urine from 6 am on the first day to 6 am on the second day) of 40 patients were collected from the day before operation to the 7th day after operation to analyze nitrogen balance.

Assays of amino acids, proteins and nitrogen balance

The amino acid pattern in serum was analyzed by the system of high liquid phase amino acid analysis (BECKMAN, USA): 126AA, 166 monitor, 232 reactor, 507 autoloader, golden data station. The total protein (TP) and albumin in serum were respectively detected by the automatic biochemistry analyzer. The serum prealbumin, transferrin, fibronectin were monitored with anti-Pa, anti-Tf, anti-Fn immuno-diffusion board. (Yuhuan reagent Co.) The nitrogen balance was analyzed with the method of Kjeldahl to get the data of nitrogen content in urine.

Statistical analysis

All data were expressed as mean \pm SD. Comparisons between two groups were performed using an unpaired Student's *t* test. Differences were considered statistically significant when $P < 0.05$.

Table 1 The comparability of patients' age, sex and operation

Group	Case	Age(y)	Sex (M/F)	Weigh before operation(kg)	Colectomy	Enterectomy	Miles	Rectal cancer anterior-rectal resection	Abormal trauma	Digestive tract tumor resection
AA	20	20-75	9/11	59.58±12.28	9	4	2	1	1	3
BCAA	20	20-75	12/8	60.38±9.83	7	5	0	2	5	1

Table 2 The changes of prealbumin, fibronectin and transferrin in two groups

	Group	Case	Before transfusion $\bar{x}\pm s$	After transfusion $\bar{x}\pm s$	Difference $\bar{x}\pm s$	<i>P</i> value
Prealbumin						
(g/L)	I	20	0.467±0.294	0.449±0.305	-0.018±0.091	0.305
	II	20	0.296±0.239	0.297±0.250	0.001±0.048	
Fibronectin						
(g/L)	I	20	2.200±0.752	2.112±0.789	-0.085±0.344	0.128
	II	20	2.201±0.792	2.345±1.052	0.144±0.735	
Transferrin (g/L)						
	I	20	0.316±0.171	0.335±0.179	0.019±0.211	0.970
	II	20	0.276±0.107	0.296±0.524	0.018±0.116	

I: AA group (the formula of amino acids); II: BCAA group (the formula of amino acids enriched BCAA).

Table 3 The changes of the amino acid pattern in serum after infusion

	Group	Case	Before infusion $\bar{x}\pm s$	After infusion $\bar{x}\pm s$	P value	Difference $\bar{x}\pm s$	P value
Asparagic acid(umol/L)	I	20	0.0748±0.0672	0.0942±0.0789	0.2580	0.0194±0.0638	0.8728
	II	20	0.0633±0.0413	0.0797±0.0558	0.0999	0.0164±0.0360	
Threonine (umol/L)	I	20	0.1973±0.1554	0.2829±0.2147	0.0354	0.0856±0.1424	0.2415
	II	20	0.1549±0.0863	0.3154±0.2331	0.0065	0.1601±0.1943	
Serine (umol/L)	I	20	0.2320±0.1455	0.2600±0.1701	0.4696	0.0279±0.1456	0.5872
	II	20	0.1981±0.1305	0.2518±0.1576	0.0759	0.0537±0.1086	
Glutacid (umol/L)	I	20	0.2619±0.2755	0.2829±0.2146	0.8237	0.0209±0.3574	0.3334
	II	20	0.2718±0.2409	0.4212±0.3217	0.1275	0.1493±0.3570	
Glycine (umol/L)	I	20	0.3844±0.2695	0.5402±0.3608	0.0173	0.1558±0.2237	0.9325
	II	20	0.3722±0.2207	0.5193±0.3565	0.1028	0.1471±0.3265	
Alanine (umol/L)	I	20	0.5067±0.3043	0.5737±0.4167	0.5325	0.0669±0.4053	0.1322
	II	20	0.4382±0.2862	0.7291±0.5371	0.0111	0.2908±0.3849	
Valine (umol/L)	I	20	0.2959±0.2188	0.2722±0.2168	0.6596	-0.0237±0.2038	0.0264
	II	20	0.2601±0.1494	0.4599±0.3765	0.0249	0.1999±0.3082	
Cysteine (umol/L)	I	20	0.0138±0.0180	0.0209±0.0182	0.1043	0.0057±0.0127	0.9373
	II	20	0.0300±0.0202	0.0350±0.0244	0.5238	0.0050±0.0296	
Methionine (umol/L)	I	20	0.0472±0.0361	0.0590±0.0498	0.3292	0.0118±0.0452	0.4447
	II	20	0.0282±0.0222	0.0516±0.0440	0.0253	0.0234±0.0362	
Isoleucine (umol/L)	I	20	0.1030±0.0728	0.1298±0.0874	0.1973	0.0268±0.0766	0.7457
	II	20	0.0825±0.0586	0.1181±0.0914	0.0730	0.0356±0.0711	
Leucine (umol/L)	I	20	0.2368±0.1699	0.2496±0.1694	0.7556	0.0128±0.1557	0.3377
	II	20	0.1770±0.1113	0.2399±0.1674	0.0698	0.0629±0.1242	
Tyrosine (umol/L)	I	20	0.0774±0.0511	0.0787±0.0631	0.9380	0.0014±0.0659	0.7263
	II	20	0.0584±0.0378	0.0677±0.0528	0.5343	0.0093±0.0563	
Phenylalanine (umol/L)	I	20	0.0897±0.0960	0.1572±0.1323	0.0289	0.0675±0.1074	0.9835
	II	20	0.0736±0.0518	0.1418±0.1277	0.0138	0.0683±0.0939	
Lysine (umol/L)	I	20	0.1888±0.1780	0.2311±0.1984	0.3706	0.0422±0.1767	0.6928
	II	20	0.1124±0.1226	0.1836±0.2403	0.2280	0.0712±0.2187	
Histidine (umol/L)	I	20	0.2517±0.1691	0.2885±0.2054	0.2654	0.0368±0.1227	0.2958
	II	20	0.1907±0.1041	0.2756±0.1778	0.0196	0.0850±0.1249	
Arginine (umol/L)	I	20	0.1214±0.2102	0.2534±0.5048	0.1584	0.1320±0.3433	0.0412
	II	20	0.2038±0.4115	0.0480±0.0678	0.1459	-0.1559±0.3921	
BCAA (umol/L)	I	20	0.6358±0.4556	0.6516±0.4014	0.8631	0.0158±0.3494	0.0785
	II	20	0.5196±0.3128	0.8180±0.6279	0.0325	0.2984±0.4869	

I: AA group (the formula of amino acids); II: BCAA group (the formula of amino acids enriched BCAA).

RESULTS

General clinical data

The age, sex, weight diagnosis and operation of patients were presented in Table 1, and showed the data comparable in both groups.

Nitrogen balance

As shown in Figure 1, the negative nitrogen balance was observed from all patients in both groups after operation, which was significantly improved after TPN infusion. The positive nitrogen balance in study group occurred on the third day after operation, which was earlier two days than that in the control group. On the sixth day after operation, the nitrogen balance in the study group is obviously better than that in the control group ($P<0.05$).

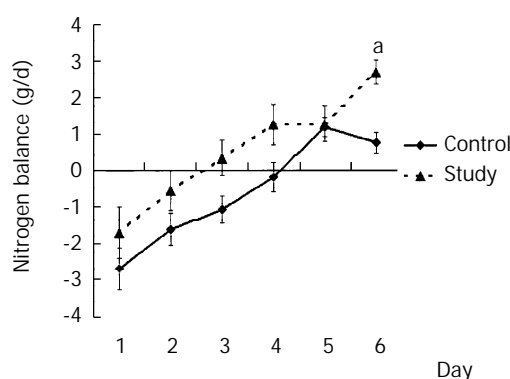


Figure 1 Nitrogen balance after infusion in two groups. ^a $P<0.05$ vs the control group.

Serum levels of prealbumin, fibronectin, and transferrin

The serum levels of prealbumin, fibronectin, and transferrin have no significant difference between two groups (Table 2).

Serum levels of albumin and total protein

There is significant difference before and after study in the serum levels of albumin and total protein of two groups. As shown in Figure 2, contrast to the study group, the serum levels of total protein and albumin decreased greatly in the control group after operation ($P<0.05$).

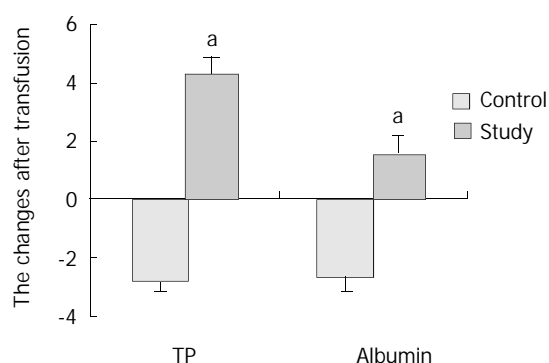


Figure 2 The changes of total protein and albumin after infusion in two groups. ^a $P<0.05$ vs the control group.

The change in the pattern of serum amino acid

The concentration of valine was notably increased ($P=0.02642$) and that of arginine was markedly decreased ($P=0.0412$) in the study group after the formula of amino acids enriched BCAA infusion when compared with the control group. In the study group, the concentrations of valine, threonine, alanine,

methionine, histidine, phenylalanine and BCAA are higher after infusion than those before transfusion ($P<0.05$). In the control group, the concentrations of glycine, histine and phenylalanine are higher after infusion than those before infusion ($P<0.05$). (Table 3).

DISCUSSION

The trauma caused by moderate or large operation may result in disturbance of glucose, lipid and protein metabolism including hypermetabolism and increased catabolism, which may lead to acute protein malnutrition, decline of immunological function and dysfunction of multiple organs^[12-16]. It was reported that the supplement of the special amino acids such as arginine, BCAA and glutamine would improve recovery of patients^[17-24]. Our present study was to observe the effect of the formula of amino acids enriched BCAA on patients after trauma.

In this study, we began to supplement the application of the formula of amino acid enriched BCAA on day 2 after operation to correct patients' hypermetabolism, to normalize the pattern of plasma amino acid concentrations and to improve recovery of patients. BCAA(valine, leucine, isoleucine) can be used as the substrate for energy and glyconeogenesis and as the muscle protein regulator. BCAA can increase the intake of energy by means of oxidization into energy in the tissues without aggrandizing the burden of the liver. As glyconeogenesis substrate, BCAA can also be oxidized in body and produce much energy by the mechanism of circulation between oxidation and alanine synthesis^[25-28]. The valine, leucine and isoleucine per gram molecular can produce 42, 43 and 32 gram molecular ATP respectively, which can supply a lot of energy to the body. The character as the source of energy for these 3 amino acids is that their first carbon can be oxidized and produce phosphate of high energy without glutamic acid, which is helpful for the decline of mechanism of producing energy with glutamic acid during trauma and stress. Because BCAA is mainly metabolized in muscle, the application of the formula of amino acid enriched BCAA can decrease the decompose of visceral protein such as muscle and liver proteins, prevent the loss of amino acids from muscle, correct negative balance, improve protein synthesis and regulate serum amino acids. In addition our results demonstrated the effect was dependent on the dose of BCAA.

Under the stress of trauma, the decompose of muscle protein seriously increases and produces a lot of free amino acids^[29-33], and hyperphenylalaninaemia appears. The ratio of phenylalanine to tyrosine (phe/tyr) rises and the ratio of BCAA to aromatic amino acid (AAA) descends after trauma because of the dysfunction of liver^[34, 35]. The low dose of phenylalanine and the high dose of BCAA in the formula of amino acid enriched BCAA can also improve the pattern of serum amino acids after trauma.

In summary, the nitrogen balance, the synthesis of acute phase proteins and visceral proteins and the pattern of serum amino acid concentrations were measured and compared with two groups after six days of TPN after trauma. Our results demonstrated that the formula of amino acid enriched BCAA could normalize of serum amino acid levels, reduce proteolysis, increase protein synthesis and improve nitrogen balance.

REFERENCES

- 1 **Liang LJ**, Yin XY, Luo SM, Zheng JF, Lu MD, Huang JF. A study of the ameliorating effects of carnitine on hepatic steatosis induced by total parenteral nutrition in rats. *World J Gastroenterol* 1999; 5: 312-315
- 2 **Wu YA**, Lu B, Liu J, Li J, Chen JR, Hu SX. Consequence alimentary reconstruction in nutritional status after total gastrectomy for gastric cancer. *World J Gastroenterol* 1999; 5: 34-37

- 3 **Cui XL**, Iwasa M, Iwasa Y, Ogoshi S. Arginine-supplemented diet decreases expression of inflammatory cytokines and improves survival in burned rats. *JPEN* 2000; **24**: 89-96
- 4 **Mansoor O**, Cayol M, Gachon P, Boirie Y, Schoeffler P, Obled C, Beaufriere B. Albumin and fibrinogen syntheses increase while muscle protein synthesis decreases in head-injured patients. *Am J Physiol* 1997; **273**: E898-902
- 5 **Vente JP**, von Meyenfeldt MF, van Eijk HM, van Berlo CL, Gouma DJ, van der Linden CJ, Soeters PB. Plasma-amino acid profiles in sepsis and stress. *Ann Surg* 1989; **209**: 57-62
- 6 **Wu Y**, Chai JK, Li JY, Diao L. The change in plasma concentration of free amino acids during early postburn stage in severely scalded rats. *Zhonghua Shaoshang Zazhi* 2001; **17**: 215-218
- 7 **Klein S**, Kinney J, Jeejeebhoy K, Alpers D, Hellerstein M, Murray M, Twomey P. Nutrition support in clinical practice: review of published data and recommendations for future research directions. *Am J Clin Nutr* 1997; **66**: 683-706
- 8 **Cao WX**, Cheng QM, Fei XF, Li SF, Yin HR, Lin YZ. A study of preoperation methionine-depleting parenteral nutrition plus chemotherapy in gastric cancer patients. *World J Gastroenterol* 2000; **6**: 255-258
- 9 **Chen QP**. Enteral nutrition and acute pancreatitis. *World J Gastroenterol* 2001; **7**: 185-192
- 10 **Pei WF**, Xu GS, Sun Y, Zhu SL, Zhang DQ. Protective effect of electroacupuncture and moxibustion on gastric mucosal damage and its relation with nitric oxide in rats. *World J Gastroenterol* 2000; **6**: 424-427
- 11 **Bactor DL**, Pillo-Blocka F, Mccrindle BW. Nutrition after cardiac surgery for infants with congenital heart disease. *Nutritim Clinical Practice* 1999; **14**: 111-115
- 12 **Antonio J**, Sanders MS, Ehler LA, Uelmen J, Raether JB, Stout JR. Effects of exercise training and amino-acid supplementation on body composition and physical performance in untrained women. *Nutrition* 2000; **16**: 1043-1046
- 13 **Wang SJ**, Wen DG, Zhang J, Man X, Liu H. Intensify standardized therapy for esophageal and stomach cancer in tumor hospitals. *World J Gastroenterol* 2001; **7**: 80-82
- 14 **Dionigi P**, Alessiani M, Ferrazi A. Irreversible intestinal failure, nutrition support, and small bowel transplantation. *Nutrition* 2001; **17**: 747-750
- 15 **Zhou HP**, Wang X, Zhang NZ. Early apoptosis in intestinal and diffuse gastric carcinomas. *World J Gastroenterol* 2000; **6**: 898-901
- 16 **Zhou ZW**, Wan DS, Chen G, Chen YB, Pan ZZ. Primary malignant tumor of the small intestine. *World J Gastroenterol* 1999; **5**: 273-276
- 17 **Freund HR**, Hanani M. The metabolic role of branched-chain amino acids. *Nutrition* 2002; **18**: 287-288
- 18 **Garcia-de-Lorenzo A**, Ortiz-Leyba C, Planas M, Montejo JC, Nunez R, Ordóñez FJ, Aragon C, Jimenez FJ. Parenteral administration of different amounts of branch-chain amino acids in septic patients: clinical and metabolic aspects. *Crit Care Med* 1997; **25**: 418-424
- 19 **James JH**. Branched chain amino acids in hepatic encephalopathy. *Am J Surg* 2002; **183**: 424-429
- 20 **Bassit RA**, Sawada LA, Bacurau RFP, Navarro F, Martins E, Santos RVT, Caperuto EC, Rogeri P, Rosa LFBPC. Branched-chain amino acid supplementation and the immune response of long-distance athletes. *Nutrition* 2002; **18**: 376-379
- 21 **Bruins MJ**, Soeters PB, Lamers WH, Deutz NE. L-arginine supplementation in pigs decreases liver protein turnover and increases hindquarter protein turnover both during and after endotoxemia. *Am J Clin Nutr* 2002; **75**: 1031-1044
- 22 **Yin L**, Li JS, Guo AQ, Liu FK, Liu FN. The prospective study of metabolic support with individual amino acids after trauma. *Chinese J Surg* 1992; **30**: 659-662
- 23 **Apovian CM**. Nutritional assessment in the elderly: facing up to the challenges of developing new tools for clinical assessment. *Nutrition* 2001; **17**: 62-63
- 24 **Harper AE**, Yoshimura NN. Protein quality, amino acid balance, utilization, and evaluation of diets containing amino acids as therapeutic agents. *Nutrition* 1993; **9**: 460-469
- 25 **Holecck M**. Relation between glutamine, branched-chain amino acids, and protein metabolism. *Nutrition* 2002; **18**: 130-133
- 26 **Kouzetsova L**, Bijlsma PB, van Leeuwen PAM, Groot JA, Houdijk APJ. Glutamine reduces phorbol-12,13-dibutyrate-induced macromolecular hyperpermeability in HT-29Cl.19A intestinal cells. *JPEN* 1999; **23**: 136-139
- 27 **Khan J**, liboshi Y, Cui L, Wasa M, Sando K, Takagi Y, Okada A. Alanyl-glutamine-supplemented parenteral nutrition increases luminal mucus gel and decreases permeability in the rat small intestine. *JPEN* 1999; **23**: 24-31
- 28 **Kudsk KA**, Wu Y, Fukatsu K, Zarzaur BL, Johnson CD, Wang R, Hanna MK. Glutamine-enriched total parenteral nutrition maintains intestinal interleukin-4 and mucosal immunoglobulin A levels. *JPEN* 2000; **24**: 270-274
- 29 **Bush JA**, Wu G, Suryawan A, Nguyen HV, Davis TA. Somatotropin-induced amino acid conservation in pigs involves differential regulation of liver and gut urea cycle enzyme activity. *J Nutr* 2002; **132**: 59-67
- 30 **Meadows GG**, Zhang H, Ge X. Specific amino acid deficiency alters the expression of genes in human melanoma and other tumor cell lines. *J Nutr* 2001; **131**: 3047S-3050S
- 31 **Ratheiser KM**, Pesola GR, Campbell RG, Matthews DE. Epinephrine transiently increases amino acid disappearance to lower amino acid levels in humans. *JPEN* 1999; **23**: 279-287
- 32 **Baggott JE**. Metabolism of methionine derived from deuterated serine infused in a human. *Am J Clin Nutr* 2001; **74**: 701-703
- 33 **Klassen P**, Furst P, Schulz C, Mazariegos M, Solomons NW. Plasma free amino acid concentrations in healthy Guatemalan adults and in patients with classic dengue. *Am J Clin Nutr* 2001; **73**: 647-652
- 34 **Roberts SA**, Thorpe JM, Ball RO, Pencharz PB. Tyrosine requirement of healthy men receiving a fixed phenylalanine intake determined by using indicator amino acid oxidation. *Am J Clin Nutr* 2001; **73**: 276-282
- 35 **de Jonge WJ**, Marescau B, Hooge RD, de Deyn PP, Hallemesch MM, Deutz NEP, Ruijter JM, Lamers WH. Overexpression of arginase alters circulating and tissue amino acids and guanidino compounds and affects neuromotor behavior in mice. *J Nutr* 2001; **131**: 2732-2740

Edited by Zhou YP

• CLINICAL RESEARCH •

Adhesive small bowel obstruction: How long can patients tolerate conservative treatment?

Shou-Chuan Shih, Kuo-Shyang Jeng, Shee-Chan Lin, Chin-Roa Kao, Sun-Yen Chou, Horng-Yuan Wang, Wen-Hsiung Chang, Cheng-Hsin Chu, Tsang-En Wang

Shou-Chuan Shih, Shee-Chan Lin, Chin-Roa Kao, Sun-Yen Chou, Horng-Yuan Wang, Wen-Hsiung Chang, Cheng-Hsin Chu, Tsang-En Wang, Gastroenterology Section, Department of Internal Medicine, Mackay Memorial Hospital, Taipei, Taiwan
Kuo-Shyang Jeng, General Surgery Section, Department of Surgery, Mackay Memorial Hospital, Taipei, Taiwan, China
Shou-Chuan Shih, Mackay Junior School of Nursing, Taipei, Taiwan, China

Correspondence to: Dr. Shou-Chuan Shih, Gastroenterology Section, Department of Internal Medicine, Mackay Memorial Hospital and Mackay Junior College of Nursing, No. 92, section 2, Chang-San North Road, Taipei, Taiwan, China. sschuan@ms2.mmh.org.tw
Telephone: +886-2-25433534 **Fax:** +886-2-27752142
Received: 2002-08-17 **Accepted:** 2002-08-19

Abstract

AIM: To evaluate how long patients with small bowel obstruction caused by postoperative adhesions can tolerate conservative treatment.

METHODS: The records of patients with small bowel obstruction due to postoperative adhesions were retrospectively reviewed. Data collected included the number of admissions, type of management for each admission, duration of conservative treatment, number of repeat laparotomies, and operative findings.

RESULTS: One hundred fifty-five patients with this condition from January 1999 to December 2001, for a total of 293 admissions were enrolled in this study. Medical treatment alone was given in 220 admissions, and repeat laparotomy was performed in 73 admissions. The period of observation in patients managed medically ranged from 2 to 12 days (average: 6.9 days), while for those who underwent surgery, the range was 1 to 14 days (average 5.4 days). At surgery, adhesions were the only finding in 46 cases, while there were intestinal complications in 27, or 9.2 % of all 293 admissions. Fever and leukocytosis greater than 15 000/mm³ were prediction of intestinal complications.

CONCLUSION: With closely monitoring, most patients with small bowel obstruction due to postoperative adhesions could tolerate supportive treatment and recover well averagely within 1 week, although some patients require more than 10 days of observation.

Shih SC, Jeng KS, Lin SC, Kao CR, Chou SY, Wang HY, Chang WH, Chu CH, Wang TE. Adhesive small bowel obstruction: How long can patients tolerate conservative treatment? *World J Gastroenterol* 2003; 9(3): 603-605
<http://www.wjgnet.com/1007-9327/9/603.htm>

INTRODUCTION

Postoperative adhesions are a frequently encountered problem.

They are the most common cause of small bowel obstruction in adults^[1-3]. Clinically, the obstruction may progress to life-threatening complications or follow a more benign course. There is debate about the optimal treatment: surgical or medical management. Some authors have emphasized the importance of early operation for any attack of bowel obstruction because of the possibility of serious sequelae with delayed treatment^[4-6]. However, there is no question that the problem is remitted spontaneously in a significant number of patients, who therefore need not require reoperation^[7-9]. We undertook this retrospective study to evaluate how long patients may safely be treated conservatively, as well as what factors might suggest the need for surgical intervention.

MATERIALS AND METHODS

General data

Cases of small bowel obstruction caused by postoperative adhesions were got from the computerized medical records from January 1999 to December 2001 at Mackay Memorial Hospital, Taipei, Taiwan. The diagnostic criterias for adhesive small bowel obstruction included: (1) history of previous laparotomy (defined as initial laparotomy); (2) clinical features of mechanical ileus, such as vomiting, abdominal pain, abdominal distention and obstipation; (3) obvious evidence of small bowel obstruction on plain x-ray of the abdomen; and (4) exclusion of other organic lesions by radiological contrast study. In patients with a past history of cancer leading to the initial laparotomy or recurrence was ruled out by meticulous examinations (tumor markers, ultrasonography and radiology including CT scan, depending on types of malignancy). Other clinical findings recorded included the presence or absence of fever, tachycardia, rebound tenderness (peritoneal signs), leukocytosis, and elevation of serum amylase and alkaline phosphatase, as well as assessment of the progress and severity of the small bowel obstruction. The diseases or organs accounting for the initial laparotomy in each patient were recorded. The entire medical record for each patient was examined to see how many hospitalizations they had had in the past for adhesion-related small bowel obstruction. The interval between the initial laparotomy and any subsequent admissions were also noted. The management given, medical (conservative) or surgical (re-laparotomy), was recorded, as well as length of stay for each admission and the duration of observation before the final outcome (either resolution with conservative treatment or surgery). Medical management might include any or all of the following: no oral intake; decompression by nasogastric intubation; intravenous fluids, with electrolytes and nutrition as needed; administration of parenteral antibiotics when leukocytosis was present; and regular abdominal x-rays (usually daily). For patients treated surgically, the location of adhesions and the presence or absence of local or systemic complications were identified. Simple obstruction was defined as the presence of adhesions alone, while complicated obstruction included the presence of gangrene and/or strangulation.

RESULTS

During the study period, 155 patients were admitted with the diagnosis of adhesion-related small bowel obstruction. The male to female ratio was 75 to 80, and the age ranged from 18 to 80 years old. The organs involved in the initial laparotomies were the female genital organs in 36 cases (including incidental appendectomy in 5 cases); appendix in 27 cases; colon and rectum in 25 cases (including appendectomy in 3); stomach and duodenum in 19 cases; small bowel in 14 cases; gallbladder, biliary tract and pancreas in 13 cases; and others (including soft tissue trauma, kidney, and spleen) in 21 (Table 1).

Table 1 Initial laparotomy

Organs/types	Number of cases
OB-GYN	36 (5 ^a)
Appendix	27
Colon/Rectum	25 (3 ^a)
Stomach/Duodenum	19
Small intestine	14
Gallbladder/bile duct/pancreas	13
Others (spleen, trauma, etc)	21
Total	155

^awith incidental appendectomy.

The 155 patients had had a total of 293 admissions, with 1 patient being admitted 11 times. The interval between initial laparotomy and subsequent admissions varied widely. The shortest was 2 weeks, while the longest approached 30 years. Of the 293 admissions, medical management alone was used during 220 (75.1 %) admissions. The duration of observation until resolution of bowel obstruction ranged from 2 to 12 days (average 6.9 days, Table 2).

Table 2 Duration of observation in adhesive small bowel obstruction

Duration of observation (days)	Medical treatment: (n=220)	Simple obstruction (n=46)	Complicated obstruction (n=27)
	Admissions	Admissions	Admissions
1	0	2	4
2	15	3	5
3	18	5	3
4	20	6	5
5	26	4	3
6	25	8	2
7	30	6	1
8	19	2	2
9	18	3	1
10	15	2	1
11	19	1	0
12	15	2	0
13	0	1	0
14	0	1	0

Average duration: medical 6.9 days; all re-laparotomy 5.4 days, simple 6.1 days, complicated 4.1 days.

There were 73 admissions in which repeat laparotomy were performed to treat the obstruction (including twice in 2 patients and 3 times in 1 patient). The duration of observation prior to surgery ranged from several hours to 14 days (average 5.4 days, Table 2). At surgery, there was simple obstruction in 46

cases, and there was complicated obstruction in the other 27 (9.2 % of all admissions). The average preoperative observation period was shorter in complicated obstruction than that in simple obstruction (4.1 vs 6.1 days). The comparison of preoperative characteristics in simple and complicated obstruction was shown in Table 3. The site of initial laparotomy did not seem to influence the presence or absence of complications (for easy comparison, the types of initial laparotomies were simply divided into upper and lower abdomen, Table 3). In patients with complicated obstruction, fever was present in 18 (67 %) cases and leukocytosis (greater than 15 000/cu mm) in 20 (74 %) cases. None of the patients with simple obstruction had these findings. No patients in our series died.

Table 3 Comparison of simple and complicated obstruction

	Simple (n=46)	Complicated (n= 27)
Initial laparotomy site		
Upper abdomen	17 (37%)	9 (33%)
Lower abdomen	29 (63%)	18 (67%)
Preoperative clinical findings		
Rebound tenderness	29 (63%)	25 (93%)
Fever >38 °C	0 (0%)	18 (67%)
Tachycardia	15 (33%)	20 (74%)
Leukocytosis>15 000/cumm	0 (0%)	20 (74%)
↑ Hematocrit/ ↑ BUN	20 (43%)	24 (89%)
↑ Serum amylase	2 (4.3%)	10 (37%)
↑ Alkaline phosphatase	3 (6.5%)	7(26%)
Metabolic acidosis	0 (0%)	4 (15%)

DISCUSSION

Formation of adhesions after transperitoneal operation may be both beneficial and deleterious^[10-13]. On one hand, adhesions may localize suture line leakage or isolate an inflammatory process, thus preventing more widespread disease. On the other hand, they may contribute to morbidity, with obstruction being the major serious complication. Small bowel obstruction due to postoperative adhesions develops in 6 % to 11 % of all patients undergoing laparotomy^[9]. It may occur at any time after the initial laparotomy and result in frequent re-admissions in subsequent years^[14, 15]. In our study, adhesive small bowel obstruction followed initial laparotomy in as few as 2 weeks to as long as nearly 30 years. While it may follow any type of laparotomy, it occurs most commonly after manipulation of the lower abdomen and pelvic cavity (appendix, gynecological organs and rectum, Table 1)^[16-18].

There is continuing debating about the ideal approach to patients with adhesive small bowel obstruction^[6, 9]. The process leading to obstruction is dynamic one with twisting and untwisting of bowel segments trapped by adhesions^[12, 13]. There are as yet no totally reliable clinical predictors to differentiate episodes that will resolve spontaneously from those that will require surgery. Even with the imminent onset of bowel strangulation, signs indicating this serious condition, such as fever, leukocytosis and peritoneal signs, are not always present^[14, 19]. This makes determining how long to try conservative management prior to opting for repeat surgery difficult.

In the literature, the incidence of spontaneous recovery with conservative management ranges from 20 % to 60 %^[7, 8, 14]. Some authors recommend only a limited observation period of 24 to 48 hours^[4, 5], but others suggest a longer period is safe, although the recommended upper limit is 5 days^[20, 21]. However, in our experience, an average of 6.9 days was required for spontaneous resolution. The longest period, in 15 cases, was

12 days (Table 2). In all these cases, the patients recovered without any sequelae. This suggested that laparotomy could safely be delayed longer than recommended in the literature. Had we operated in all cases after 5 days, 141 of the 220 patients who eventually had spontaneous remission would have required surgery?

Why conservative treatment may be extended in some patients but not in others probably depends on individual variables. In reports recommending earlier surgical intervention, most of the patients who finally developed bowel complications in fact already had signs of more serious obstruction on initial presentation^[4-6]. In our series, the surgically treated patients had a shorter observation time on average, 5.4 days *vs* 6.9 days for those who resolved spontaneously (Table 2). This suggested that these patients had relatively early onset of signs suggestive of complications. In reported series in which conservative treatment is recommended, most patients who finally recovered spontaneously had no apparent toxic signs throughout the hospital course^[14, 20, 21]. In our experience with reoperation, in only 27 of 73 procedures were actual intestinal complications. It's conceivable that some among the other 46 might have recovered spontaneously had we observed them longer. In fact, none of these 46 episodes were characterized by fever or leukocytosis. The patients chose to undergo surgical intervention mainly because they became inpatient with medical treatment.

Although episodes of small bowel obstruction can be managed conservatively, the adhesions remain. So the possibility of recurrence still exists^[12, 15]. Unfortunately, reoperating to excise the adhesions (adhesiolysis) is not clearly beneficial, since the repeat surgical procedure itself may cause more adhesions^[22]. In addition, the average cost of an admission with surgery is much higher than that of an admission with only medical treatment^[23, 24]. Surgery is thus not a panacea for this condition, and the decision to perform it should only be made after all factors are carefully considered. Certainly, the presence of peritoneal signs, fever, and leukocytosis suggest the need for early surgery. In the absence of these signs, watchful waiting is reasonable.

In conclusion, the actual incidence of serious complications in patients with small bowel obstruction due to postoperative adhesions is low. Most patients can be managed medically. With closely monitoring and in the absence of signs suggestive of complications, an observation period even longer than 10 days before proceeding to surgical intervention appears to be safe.

REFERENCES

- Füzün M**, Kaymak MFE, Harmancioğlu Ö, Astarciöğlu K. Principal causes of mechanical bowel obstruction in surgically treated adults in Western Turkey. *Br J Surg* 1991; **78**: 202-203
- Lee SH**, Ong ETL. Changing pattern of intestinal obstruction in Malaysia: a review of 100 consecutive cases. *Br J Surg* 1991; **78**: 181-182
- McEntee G**, Pender GMD, Mulvin D, McCullough M, Naeeder S, Farah S, Badurdeen MS, Ferraro V, Cham C, Gillham N, Matthews P. Current spectrum of intestinal obstruction. *Br J Surg* 1987; **74**: 976-980
- Otamiri T**, Sjødahl R, Ihse I. Intestinal obstruction with strangulation of the small bowel. *Acta Chir Scand* 1987; **153**: 307-310
- Sosa J**, Gardner B. Management of patients diagnosed as acute intestinal obstruction secondary to adhesions. *Am Surg* 1993; **59**: 125-128
- Mucha PJ**. Small bowel obstruction. *Surg Clin North Am* 1987; **67**: 597-620
- Wolfson PJ**, Bauer JJ, Gelernt IM, Kreel I, Aufses AH Jr. Use of the long tube in the management of patients with small-intestinal obstruction due to adhesions. *Arch Surg* 1985; **120**: 1001-1006
- Brolin RE**, Krasna MJ, Mast BA. Use of tubes and radiographs in the management of small bowel obstruction. *Ann Surg* 1987; **206**: 126-133
- Bass KN**, Jones B, Bulkley GB. Current management of small-bowel obstruction. *Adv Surg* 1997; **31**: 1-34
- Scott-Coombes DM**, Whawell SA, Thompson JN. The operative peritoneal fibrinolytic response to abdominal operation. *Eur J Surg* 1995; **161**: 395-399
- Holmdahl L**, Eriksson E, Eriksson BI, Risberg B. Depression of peritoneal fibrinolysis during operation is a local response to trauma. *Surgery* 1998; **123**: 539-544
- Holmdahl L**, Risberg B. Adhesions: prevention and complications in general surgery. *Eur J Surg* 1997; **163**: 169-174
- Dijkstra FR**, Nieuwenhuijzen M, Reijnen MMPJ, Goor van H. Recent clinical developments in pathophysiology, epidemiology, diagnosis and treatment of intra-abdominal adhesions. *Scand J Gastroenterol* 2000; **232**(Suppl): 52-59
- Tanphiphat C**, Chittmittrapap S, Prasopsunti K. Adhesive small bowel obstruction: a review of 321 cases in a Thai hospital. *Am J Surg* 1987; **145**: 283-287
- Ellis H**, Moran BI, Thompson JN, Parker MC, Wilson MS, Menzies D, McGuire A, Lower AM, Hawthorn RJS, O'Brien F, Buchan S, Crowe AM. Adhesion-related hospital readmissions after abdominal and pelvic surgery: a retrospective cohort study. *Lancet* 1999; **353**: 1476-1480
- Monk BJ**, Berman ML, Montz FJ. Adhesions after extensive gynecologic surgery: clinical significance, etiology and prevention. *Am J Obstet Gynecol* 1994; **170**: 1396-1403
- Al-Took S**, Platt R, Tulandi T. Adhesion-related small-bowel obstruction after gynecologic operations. *Am J Obstet Gynecol* 1999; **180**: 313-315
- Nieuwenhuijzen M**, Reijnen MMPJ, Kuijpers JHC, Goor van H. Small bowel obstruction after total or subtotal colectomy: a 10-year retrospective review. *Br J Surg* 1998; **85**: 1242-1245
- Sarr MG**, Bulkley GB, Zuidema GD. Preoperative recognition of intestinal strangulation obstruction: Prospective evaluation of diagnostic capability. *Am J Surg* 1983; **145**: 176-181
- Hall RI**. Adhesive obstruction of the small intestine: a retrospective review. *Br J Clin Pract* 1984; **38**: 89-92
- Seror D**, Feigin E, Szold A, Allweis TM, Carmon M, Nissan S, Freund HR. How conservatively can postoperative small bowel obstruction be treated? *Am J Surg* 1993; **165**: 121-126
- Ellis H**. The clinical significance of adhesions: focus on intestinal obstruction. *Eur J Surg* 1997; **577**(Suppl): 5-9
- Menzies D**, Parker M, Hoare R, Knight A. Small bowel obstruction due to postoperative adhesions: treatment patterns and associated costs in 110 hospital admissions. *Ann R Coll Surg Engl* 2001; **83**: 40-46
- Ray NF**, Denton WG, Thamer M, Henderson SC, Perry S. Abdominal adhesiolysis: inpatient care and expenditures in the United States in 1994. *J Am Coll Surg* 1998; **186**: 1-9

Edited by Xu XQ

• CLINICAL RESEARCH •

Decision making in right-sided diverticulitis

Li-Rung Shyung, Shee-Chan Lin, Shou-Chuan Shih, Chin-Roa Kao, Sun-Yen Chou

Li-Rung Shyung, Shee-Chan Lin, Shou-Chuan Shih, Chin-Roa Kao, Sun-Yen Chou, Division of Gastroenterology, Department of Internal Medicine, Mackay Memorial Hospital, Taipei, Taiwan, China
Correspondence to: Dr. Li-Rung Shyung, Division of Gastroenterology, Department of Internal, Medicine, Mackay Memorial Hospital, 92, Section 2, Chungshan North Road, Taipei, Taiwan, China. luke.skywalk@msa.hinet.net

Telephone: +886-922988910

Received: 2002-11-29 **Accepted:** 2002-12-22

Abstract

AIM: To evaluate systematically our nine-year experience in treating right-sided diverticulitis of the colon, and to explore its clinical and radiological relationship.

METHODS: The clinical and radiological data of 40 patients with colonic diverticulitis treated in Mackay Memorial Hospital, Taipei, from 1993 through 2002 were reviewed retrospectively.

RESULTS: The average age of the patients with right-sided diverticulitis was 53.1 years, which was 11.6 years younger than that of the patients with left-sided diverticulitis. The preoperative diagnosis of appendicitis was made in 8 of 13 right-sided diverticulitis patients. Nine (69 %) had right lower quadrant abdominal pain for more than 48 hours, and ten patients (77 %) presented with fever. CT findings suggesting acute right-sided diverticulitis including thickening of the intestinal wall and pericolonic inflammation were present in five patients.

CONCLUSION: Right-sided diverticulitis is easily confused with acute appendicitis because it occurs at a somewhat younger age than that in left-sided diverticulitis. Barium enema and CT are helpful for the early diagnosis of right-sided diverticulitis. While clearly not required in the majority of patients with right lower quadrant abdominal pain, barium enema and CT may be helpful in making the decision with a clinical history or physical examinations atypical of acute appendicitis.

Shyung LR, Lin SC, Shih SC, Kao CR, Chou SY. Decision making in right-sided diverticulitis. *World J Gastroenterol* 2003; 9(3): 606-608

<http://www.wjgnet.com/1007-9327/9/606.htm>

INTRODUCTION

Diverticular disease was almost unknown in 1990, but has become the commonest affliction of the colon in Western countries^[1] which was regarded as a deficient disease of Western civilization. The right-sided diverticulitis is more common than left-sided diverticulitis in Far-eastern countries. In a study of 105 patients in Taiwan, China, the incidence of right-sided diverticulosis was 60 %^[2]. The distinction between right-sided diverticulitis and acute appendicitis is often difficult at the time of presentation^[3]. The condition is frequently misdiagnosed and has often been mistreated. During the past nine years, we have treated 13 cases of right-sided diverticulitis

at the Mackay Memorial Medical Center, our experience in relation to the clinical and radiological manifestations was reviewed.

MATERIALS AND METHODS

General data

The pathological reports of medical records at the Mackay Memorial Medical Center were reviewed from January 1993 to June 2002. During this period, there were 40 patients with colonic diverticulitis treated at our institution, we retrospectively reviewed their presentation, diagnostic studies, management and pathology. Colonic diverticulitis was stratified into two groups according to the distribution of diverticula: (1) right-sided diverticulitis with diverticula in the cecum, ascending colon and proximal transverse colon; (2) left-sided diverticulitis with diverticula in the sigmoid and/or descending colon. Clinical details of these patients were shown in Table 1. Presenting symptoms and signs of right-sided diverticulitis patients were shown in Table 2.

Table 1 General data of right-sided and left-sided diverticulitis

	Right-sided diverticulitis	Left-sided diverticulitis
Number	13	27
Male/Female	10/3	20/7
Age (yr)		
Mean±SD	53.15±9.86	64.74±11.28
Range	40-70	44-83
Median	50	68

Table 2 Presenting symptoms and signs (13 cases of total number)

Initial features	Cases number (%)
RLQ abdominal pain for >2 days	9(69)
Nausea/vomiting	2(15)
Diarrhea	2(15)
Leukocytosis	9(69)
Fever	10(77)
Anorexia	1(8)

Statistical analysis

Statistical comparison was performed using Student's *t* test. All analyses were performed with the Stastical Package for the Social Science (SPSS) for windows (Version 10.0) software. The results were considered to be statistically significant at a value of $P<0.05$.

RESULTS

The incidence of right-sided diverticulitis was 33 % in our treated patients. There was no difference between right-sided diverticulitis patients and left-sided diverticulitis patients as regarding to male: female ratio. The age of patients with right-sided diverticulitis was younger than those with left-sided diverticulitis ($P=0.003$, Table1).

Details of their presenting symptoms and signs were shown

in Table 2. The primary complaints among all patients were right lower quadrant abdominal pain for more than two days prior to admission. Nausea and/or vomiting were reported in two patients (15 %) and diarrhea was present in two patients (15 %), but only one of the 13 exhibited anorexia. Ten patients had a fever of more than 37 °C and all of these also had a leukocytosis. The preoperative diagnosis was appendicitis in 8 of the 13 patients in our series. Four patients had performed preoperative barium enemas. In one patient a 4 cm×4.5 cm diverticulum of the proximal transverse colon was identified. In the other three, the barium enema was interpreted as showing a right-sided colonic mass (Figure 1). Six patients had CT scans, of which five correctly diagnosed diverticulitis of the cecum. Diverticulitis of the right colon was correctly diagnosed preoperatively in one patient in whom marked wall thickening of the cecum with classic target appearance was demonstrated (Figure 2). Diverticula was found in one patient. There was no evidence of contrast extravasation in any of the six patients.



Figure 1 Barium contrast roentgenogram demonstrated a right-sided colonic mass. (black arrow head).

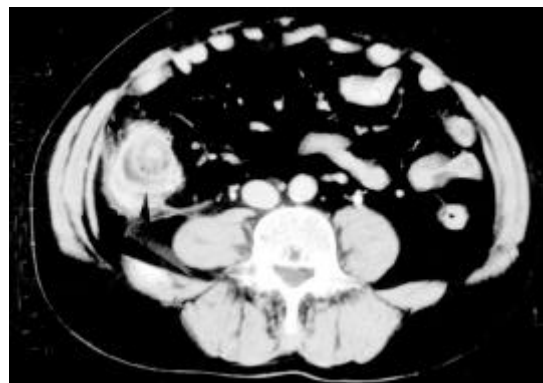


Figure 2 Acute diverticulitis of cecum in 50-year-old man. CT scan clearly showed enhancement of thickened diverticular wall and preservation of wall enhancement pattern of cecum as hyperattenuating inner layer, thickened middle layer of low attenuation, and outer high-attenuation layer (black arrow head).

DISCUSSION

The preoperative distinction between right-sided diverticulitis and appendicitis is extremely difficult to discern based on clinical presentation alone^[4]. In our study, a misdiagnosis of appendicitis was made in 8 of the 13 patients preoperatively which is common in all other reported series^[3-5]. The majority of patients will still undergo laparotomy. The surgeon must make a diagnosis based on operative findings. Hidden diverticula pose a diagnostic dilemma since at laparotomy it may be difficult to distinguish the inflamed mass from Crohn's

disease, malignant lesions of the right colon, a perforated foreign body or even tuberculosis^[3].

Patients with right-sided diverticulitis tend to be younger than those with left-sided diverticulitis^[5]. We compared the age distribution of right-sided diverticulitis and left-sided diverticulitis patients in this study (Table 1).

Clinically, in contrast to appendicitis, relative long history of right lower quadrant abdominal pain, relative lack of systemic toxic signs and low frequency of nausea/vomiting may be helpful in correctly diagnosing right-sided diverticulitis^[2]. The symptoms of right-sided diverticulitis usually begin and remain localized in the right lower quadrant, rather than originating in the epigastrium^[6]. Appendicitis patients typically experience the classic migration of pain to the right lower quadrant at later stage which caused by the stimulation of the visceral afferent nerve fibers that enter the spinal cord at thoracic levels T8 through T10. Nine of our patients presented more than 48 hours after the onset of symptoms (69 %). Eleven of our patients (85 %) had neither nausea, vomiting, nor diarrhea. This absence of vomiting has been noted by others^[7-9].

About one third of patients in this series were right-sided diverticulitis, which differed from other reports in Far-eastern countries^[10-12]. This bias was due to our review was obtained from pathological database of medical records from our hospital, in which some uncomplicated right-sided diverticulitis cases were excluded. Right-sided diverticulitis tends to have a more benign course than that which occurs on the left^[13]. So this differential probably carries little significance, despite our own findings. Diverticular disease is considered as a fiber deficient disease in Western Countries^[1], so duty of the profession is to point the way of prevention of white flour, both brown and white sugar, confectionery, and foods or drinks which contain unnaturally concentrated carbohydrates. But some Eastern racial groups have a higher incidence of right-sided diverticulitis despite a high fiber intake. These findings were coincident to a study from China where about 62 % of right-sided diverticular disease despite a good fiber intake^[14].

Contrast enema studies are the most accurate way to find out the colonic diverticula^[15]. However, because of the risks of extravasation of barium from the perforation in the patients with acute right-sided diverticulitis, barium enema examination should be generally be avoided in patients with suspected acute right-sided diverticulitis and localized peritoneal signs. Criteria for the diagnosis of right-sided diverticulitis include extravasation of barium, narrowed lumen or thickened mucosa, and mass effect^[15]. In our series, barium enema studies were done in four patients who presented a cecal mass in three patients.

In contrast to the barium enema, CT scan demonstrates both the intraluminal and extracolonic manifestations of acute right-sided diverticulitis^[16]. Criteria of CT scan for the diagnosis of right-sided diverticulitis include colonic wall thickening, pericolic fat infiltration (streaky fat), pericolic or distant abscesses, and extraluminal air. In this series, CT scans were obtained preoperatively in six patients with right-sided diverticulitis. CT findings suggesting right-sided diverticulitis were present in five patients. A recent study found that pericolic lymph nodes adjacent to the focal area of colonic thickening are more commonly seen in patients with colonic cancer. Pericolic inflammatory changes are more commonly seen in right-sided diverticulitis^[17]. CT may be helpful for the evaluation of patients with atypical symptoms of acute appendicitis or those who have undergone an appendectomy. Right-sided diverticulitis occurs with greater frequency in Asians. This condition is easily confused with acute appendicitis, since it occurs at a somewhat younger age than those with left-sided diverticulitis. If diagnosed preoperatively, uncomplicated right-sided diverticulitis can be managed conservatively with antibiotic therapy.

REFERENCES

- 1 **Painter NS**, Burkitt DP. Diverticular disease of the colon: a deficient disease of Western civilization. *BMJ* 1971; **2**: 450-454
- 2 **Chiu JH**, Lin JT, Lin JK, Leu SY, Liang CL, Wang FM. Diverticular disease of the colon. *J Surg Asso* 1987; **20**: 102-108
- 3 **Gouge TH**, Coppa GF, Eng K, Ranson JHC, Localio SA. Management of diverticulitis of ascending colon. 10 years' experience. *Am J Surg* 1983; **145**: 387-391
- 4 **Markham NI**, Li AKC. Diverticulitis of the right colon- experience from Hong Kong. *Gut* 1992; **33**: 547-549
- 5 **Fischer MG**, Farkas AM. Diverticulitis of the cecum and ascending colon. *Dis Colon Rectum* 1984; **27**: 454-458
- 6 **Birnbaum BA**, Wilson SR. Appendicitis at the millennium. *Radiology* 2000; **215**: 337-348
- 7 **Arrington P**, Judd C. Cecal diverticulitis. *Am J Surg* 1981; **142**: 56-60
- 8 **Asch M**, Markowitz A. Cecal diverticulitis; report of 16 cases and a review of the literature. *Surgery* 1969; **65**: 906-910
- 9 **Schuler JG**, Bayley J. Diverticulitis of the cecum. *Surg Gynecol Obstet* 1983; **156**: 743-748
- 10 **Wang CH**, Chou LC. The incidence of the diverticular diseases of the colon in T.S.G.H., Taiwan, China. *J Surg Asso* 1979; **12**: 260-266
- 11 **Sugihara K**, Muto T, Morioka Y, Asano A, Yamamota T. Diverticular disease of the colon in Japan. A review of 615 cases. *Dis Colon Rectum* 1984; **27**: 531-537
- 12 **Vajrabukka T**, Saksornchai K, Jimakorn P. Diverticular disease of the colon in a Far-eastern community. *Dis Colon Rectum* 1980; **23**: 151-154
- 13 **Ferzoco LB**, Raptopoulos V, Silen W. Current concepts: acute Diverticulitis. *N Engl J Med* 1998; **338**: 1521-1526
- 14 **Pan G**, Liu T, Chen M, Chang H. Diverticular disease of the colon in China. *Chin Med J* 1984; **97**: 391-394
- 15 **Beranbaum SL**, Zausner J, Lane B. Diverticular disease of the right colon. *AJR* 1972; **115**: 334-348
- 16 **Crist DW**, Fishman EK, Scatarige JC, Cameron JL. Acute diverticulitis of the cecum and ascending colon diagnosed by computed tomography. *Surg Gynecol Obstet* 1988; **166**: 99-102
- 17 **Macari M**, Balthazar EJ. CT of bowel wall thickening: significance and pitfalls of interpretation. *AJR* 2001; **176**: 1105-1116

Edited by Xu XQ

• CLINICAL RESEARCH •

Esophageal ulceration complicating doxycycline therapy

Mohammad A. Al-Mofarreh, Ibrahim A. Al Mofleh

Mohammad A. Al-Mofarreh, Consultant Physician & Gastroenterologist, Poly Clinic, College of Medicine, King Saud University, Riyadh, Saudi Arabia

Ibrahim A. Al Mofleh, Professor of Medicine, College of Medicine, King Saud University, Riyadh

Correspondence to: Prof. Ibrahim A. Al Mofleh, Gastroenterology Div. & Endoscopy Unit, College of Medicine, King Saud University, P.O. Box 2925 (59), Riyadh 11461, Saudi Arabia. iamofleh@yahoo.com

Telephone: +966-1-4671215 **Fax:** +966-1-4671217

Received: 2002-06-27 **Accepted:** 2002-07-27

Abstract

AIM: To report present state of iatrogenic drug-induced esophageal injury (DIEI) induced by medications in a private clinic.

METHODS: Iatrogenic drug-induced esophageal injury (DIEI) induced by medications has been more frequently reported. In a private clinic we encountered 36 cases of esophageal ulcerations complicating doxycycline therapy in a mainly younger Saudi population (median age 29 years).

RESULTS: The most frequent presenting symptoms were odynophagia, retrosternal burning pain and dysphagia (94 %, 75 % and 56 %, respectively). The diagnosis was according to medical history and confirmed by endoscopy in all patients. Beside withdrawal of doxycycline, when feasible, all patients were treated with a proton-pump inhibitor (PPI) and a prokinetic. Thirty patients who reported to the clinic after treatment were improved within 1-7 (median 1.7) days.

CONCLUSION: Esophageal ulceration has to be suspected in younger patients with odynophagia, retrosternal burning pain and/or dysphagia during the treatment with doxycycline.

Al-Mofarreh MA, Al Mofleh IA. Esophageal ulceration complicating doxycycline therapy. *World J Gastroenterol* 2003; 9(3): 609-611

<http://www.wjgnet.com/1007-9327/9/609.htm>

INTRODUCTION

Three decades after the first report of drug-induced esophageal injury (DIEI) induced by potassium therapy^[1], approximately 1 000 cases of DIEI caused by almost 100 different drugs, have been reported in the world literature. Antibiotics have contributed to almost 50 % and doxycycline alone to 27 % of all cases^[2].

The reported DIEI approximate incidence of 4/100 000 is probably underestimated. The actual incidence is apparently much higher for increase of drugs prescription, and they are not all reported^[2,3]. History has been considered sufficient for assuming a clinical diagnosis^[4,5]. Retrosternal pain, sudden odynophagia with or without dysphagia is suspicious of the diagnosis^[2]. History of medication, time of drug intake and amount of concurrent fluid ingested are important^[6,7]. Upper gastrointestinal endoscopy is almost always abnormal and it has been considered as the method of choice to confirm DIEI^[2].

The clinical course is usually uneventful and DIEI may heal after withdrawal of the offending drugs^[5-8].

MATERIALS AND METHODS

General data of patients

In a retrospective analysis of upper gastrointestinal (UGI)-endoscopies performed at Dr. Al Mofarreh's Polyclinic over a period of 9 years, 36 patients who had doxycycline-induced esophageal ulcerations were included in this study. Another seven patients, who had typical symptoms, but had no endoscopy, no ulcer on endoscopy or the offending medication was unknown, were not included.

Methods

The patients were asked history of recent drug intake, the mode, timing of medication and the concurrent amount of fluid ingested.

Endoscopy was performed after a 12 hours fasting using Pentax EPM 3000, EG 2901 videoscope after a local anesthesia with 10 % xylocain spray or 2 % xylocain viscous (Astra, Sweden). Hard print photo documentation was performed in all patients with a color video printer (UP-5000 P, Sony). The number of ulcers, their size, depth and localization at the esophagus were documented.

Patients were treated with withdrawal of doxycycline, when feasible, along with proton-pump inhibitors (PPI) and prokinetics and were requested to report within seven days of management initiation to give feedback on their response of treatment.

RESULTS

Over a period of nine years (from July 1992 to June 2001), 36 patients who complained with sudden odynophagia (34 cases, 94 %), retrosternal burning pain (27 cases, 75 %) and/or dysphagia (20 cases, 56 %) after ingestion of doxycycline capsules, underwent UGI-endoscopy and were found to have esophageal ulcerations. Their age ranged from 12 to 72 (Median: 29) years old and 22 were males. Endoscopy was performed within an average of six days after the onset of symptoms. The median number of ulcers was two (range: 1-9) and one patient had multiple ulcers spread all over the esophagus. The ulcers were localized at the mid, upper and lower esophagus in 24, 6 and 5 patients, respectively. In one patient, the ulcers were scattered all over the esophagus. The ulcers were variable in size, shape and depth (Figure 1-4). No bleeding or significant strictures were encountered in these patients and none of the patients had a pre-existing esophageal disorder. Along with withdrawal of doxycycline when feasible, all patients were treated with PPI and prokinetics. All thirty patients, who reported for follow up, were improved within 1-7 (Median 1.7) days including three patients continued on doxycycline to treat brucellosis.

DISCUSSION

Approximately 100 types of drugs have been incriminated in the etiology of around 1 000 cases of DIEI. The precise mechanism is not well explained. However multiple factors,

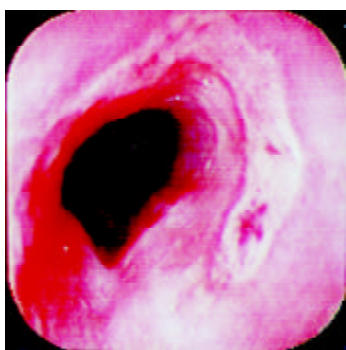


Figure 1 Superficial linear, semicircular esophageal ulcer with partially uncovered eroded mucosa.

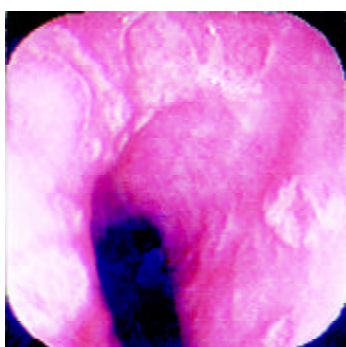


Figure 2 Multiple, variable sized crater-like mid-esophageal ulcer positioned in almost a circular pattern.

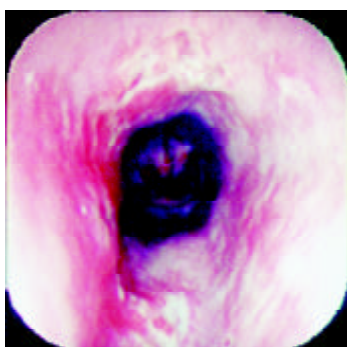


Figure 3 Anterior and posterior superficial mucosal ulcerations.



Figure 4 Deep, butterfly-like mid-esophageal ulceration partially extending in a semi-circular fashion and inducing mild narrowing of the lumen.

including the increasing age, decreased esophageal peristalsis and external compression are predisposing to DIEI^[2]. Furthermore, drugs that have a large size and sticky surface are retained longer in the esophagus^[2,7,9]. A clinical and

experimental study has shown that doxycycline capsules remain three times longer in the esophagus than doxycycline tablets^[10].

Elderly patients are more prone to develop DIEI due to their altered esophageal motility and decreased saliva production. In addition, they more frequently suffer of cardiac disease, require more cardiovascular medication and remain longer in a recumbent position^[7,11,12]. In younger patients, DIEI is mainly caused by antibiotics^[2,5,6]. In our study, majority of patients were young and the only incriminated drug was doxycycline. All patients took doxycycline capsules and shared the same risk factor of taking the medication at bed time with a little amount of fluid. None of these patients suffered from a cardiac or a pre-existing esophageal disease.

The mechanism of esophageal mucosal injury induced by doxycycline capsules may be explained by their acidic effect, gelatinous sticky capsules, increased mucosal concentration and intracellular toxicity^[2,13,14]. The presence of hiatus hernia in patients receiving indomethacin or doxycycline is associated with an increased risk of developing DIEI. The relative risk is 3.96^[15]. The symptoms of DIEI, usually, manifest few hours up to ten days after exposure in form of chest pain, odynophagia and dysphagia, ranked according to their frequency^[7]. In our series, odynophagia, retrosternal burning pain and dysphagia were the commonest symptoms and occurred in 94 %, 80 % and 54 % of patients, respectively.

Although the typical history is sufficient to establish the diagnosis, endoscopy remains the method of choice for detecting DIEI^[3]. Findings on endoscopic biopsies material are non specific^[6,16].

Despite the absence of a significant stricture, dysphagia occurred more frequently in our population compared to other series^[7].

The ulcer varied in size, depth and number. We have previously reported discrete, confluent, linear broad band-formed and butterfly-shaped ulcers partially covered with pseudomembranes. Ulcers were also noted on the opposite site with normal surrounding mucosa^[6]. The majority (66 %) of ulcers were at the mid-esophagus. The presence of mid-esophageal ulceration may raise the possibility of DIEI^[5,6,17,18]. The presence of intact pills or their residues are also important clues for the diagnosis of DIEI^[19].

In agreement with other authors, the main step of treatment in our patients was the withdrawal of the offending drug, however we feel doxycycline treatment could be continued when required with emphasis on patients education in regarding to timing of medication and required amount of fluid^[6]. In addition, patients received a PPIs along with a prokinetics. The value of antacids, anti-secretory drug and PPIs remain questionable in patients without gastroesophageal reflux^[5,7,10]. Apart from sucralfate, no data from the literature have suggested the benefit of acid suppression^[2]. Patients who develop complications in form of hemorrhage or chronic stricture and with unsuccessful surgical intervention require endoscopic management^[3,21].

In the majority of patient, DIEI symptoms resolved within one week (median time: 1.7 days). However, one patient went to the clinic with symptoms persisting over one month following a course of doxycycline and endoscopy revealed esophageal ulcerations. His symptoms were improved soon after initiation of treatment with a PPI and a prokinetic drug and ulcer healing was confirmed by endoscopy. Also the three patients continued with doxycycline to treat brucellosis improved. This observation supported continuation of doxycycline therapy when required and patients education was considered not only as a preventive, but also as a therapeutic measure.

Protracted courses up to six weeks and severe symptoms have also been reported^[22]. Furthermore, severe non-typical

symptoms in form of intractable hiccups have been described after the first dose of doxycycline inducing a lower esophageal ulcer at the gastric junction. The patients' symptoms have been resolved with the medication of omeprazole and sucralfate^[23].

Doxycycline was the only offending drug in this study. A sudden onset of odynophagia, retrosternal pain and/or dysphagia in a healthy individual give a strong evidence of drug induced esophageal injury and necessitate a careful exploration of drug history. Endoscopy is important to determine the type, size, site and depth of injury. Discontinuation of the offending drug, when feasible, is the first step of management acid suppressing agents and prokinetics may be proved helpful. In patients at risk, education and use of alternative medication are important preventive measures.

REFERENCES

- 1 **Pemberton J.** Esophageal obstruction and ulceration caused by oral potassium therapy. *Br Heart J* 1970; **32**: 267-268
- 2 **Kikendall JW.** Pill esophagitis. *J Clin Gastroenterol* 1999; **28**: 298-305
- 3 **Jaspersen D.** Drug-induced esophageal disorders: pathogenesis, incidence, prevention and management. *Drug Safety* 2000; **22**: 237-249
- 4 **Ramirez RA,** Valladares G, Barreda CC. Esophageal ulcers induced by doxycycline: evaluation of 4 cases. *Acta Gastroenterol Latinoam* 1981; **11**: 309-313
- 5 **Bott S,** Prakash C, McCallum RW. Medication-induced esophageal injury. Survey of the literature. *Am J Gastroenterol* 1987; **82**: 758-763
- 6 **Al Mofarreh MA,** Al Mofleh IA. Doxycycline-induced esophageal ulcerations. *Saudi J Gastroenterol* 1998; **4**: 20-24
- 7 **Boyce HW.** Drug-induced esophageal damage: diseases of medical progress. *Gastrointest Endoscopy* 1998; **47**: 547-550
- 8 **Mason SJ,** O' Meara TF. Drug-induced esophagitis. *J Clin Gastroenterol* 1981; **3**: 115-120
- 9 **Hey H,** Jorgensen F, Sorensen K, Hasselbach H, Wamberg T. Esophageal transit of six commonly used tablets and capsules. *BMJ* 1982; **285**: 1717-1719
- 10 **Carlborg B,** Densert O, Lindqvist C. Tetracycline-induced esophageal ulcers. A clinical and experimental study. *Laryngoscope* 1983; **93**: 184-187
- 11 **Bohane TD,** Perralt J, Fowler RS. Esophagitis and esophageal obstruction from quinidine tablets in association with left atrial enlargement. *Aust Peadiatr J* 1978; **14**: 191-192
- 12 **Boyce HW.** Dysphagia after open heart surgery. *Hosp Prac* 1985; **20**: 40-50
- 13 **Bonavina L,** DeMeester TR, McChesney L, Schwizer W, Albertucci M, Bailey RT. Drug-induced esophageal stricture. *Ann Surg* 1987; **206**: 173-183
- 14 **Giger M,** Sonnenberg A, Brandli H, Singeisen M, Guller R, Blum AL. Das tetracyclin-ulkurs der speiserohre. *Dtsch Med Wochenschr* 1978; **103**: 1038-1040
- 15 **Alvarte JF,** Kulkarni SG, Bhatia SJ, Desai SA, Dhawan PS. Prospective evaluation of medication-induced esophageal injury and its relation to esophageal function. *Indian J Gastroenterol* 1999; **18**: 115-117
- 16 **Abraham SC,** Cruz-Correra M, Lee LA, Yardly JH, Wu TT. Alendronate-associated esophageal injury: Pathologic and endoscopic features. *Mod Pathology* 1999; **12**: 1152-1157
- 17 **Kikendall JW,** Friedman AC, Oyewole MA. Pill-induced esophageal injury. Case reports and review of the medical literature. *Dig Dis Sci* 1983; **28**: 174-182
- 18 **Castell DO.** "Pills esophagitis" The case of alendronate. *N Engl J Med* 1996; **335**: 1058-1059
- 19 **O' Meara TF.** A new endoscopic finding of tetracycline-induced esophageal ulcers. *Gastrointest Endosc* 1980; **26**: 106-107
- 20 **De Groen PC,** Lubbe DF, Hirsch LJ. Esophagitis associated with the use of alendronate. *N Engl J Med* 1996; **335**: 1016-1021
- 21 **Kikendall JW.** Pill-induced esophageal injury. *Gastroenterol Clin N Am* 1991; **20**: 835-846
- 22 **Tankurt IE,** Akbaylar H, Yenicerioglu Y, Simsek I, Gonen O. Severe long-lasting symptoms from doxycycline-induced esophageal injury. *Endoscopy* 1995; **27**: 626
- 23 **Tzianetas I,** Habal F, Keystone JS. Short report: Severe hiccups secondary to doxycycline-induced esophagitis during treatment of malaria. *Am J Trop Med Hyg* 1996; **54**: 203-204

Edited by Xu XQ

• CLINICAL RESEARCH •

Endosonography with linear array instead of endoscopic retrograde cholangiography as the diagnostic tool in patients with moderate suspicion of common bile duct stones

Maciej Kohut, Andrzej Nowak, Ewa Nowakowska-Dułała, Tomasz Marek, Roman Kaczor

Maciej Kohut, Andrzej Nowak, Ewa Nowakowska-Dułała, Tomasz Marek, Roman Kaczor, Gastroenterology Department of Silesian Medical Academy, Katowice, Poland

Correspondence to: Maciej Kohut, Department of Gastroenterology, Silesian Academy of Medicine, Medyków 14 40-752 Katowice, Poland. maciej.2250177@pharmanet.com.pl

Telephone: +48-32-7894401 **Fax:** +48-32-2523119

Received: 2002-03-11 **Accepted:** 2002-05-20

Abstract

AIM: To evaluate the diagnostic efficiency of endoscopic ultrasound (EUS) as the main imaging modality in patients with moderate suspicion of common bile duct stones (CBDS).

METHODS: 55 patients with moderate clinical suspicion of CBDS were prospectively included to the study and evaluated with EUS. This study was done in single blind method in the clinical and biochemical data of patients. EUS was done with echo-endoscope Pentax FG 32-UA ($f=5-7.5$ MHz) and Hitachi EUB 405 ultrasound machine. Patients diagnosed with CBDS by EUS were excluded from this study and treated with ERC. All the other patients were included to the follow up study obtained by mail every 6 months for clinical evaluation (need of ERC or surgery).

RESULTS: CBDS was found in 4 patients by EUS. Diagnosis was confirmed in all cases on ERC. The remaining 51 patients without CBDS on EUS were followed up for 6-26 months (meanly 13 months) There were: 40 women, 42 cholecystectomized patients, aged: 55 (mean). Biochemical values (mean values) were as follows: bilirubin: $14.9 \mu\text{mol} \cdot \text{L}^{-1}$, alkaline phosphatase: $95 \text{ IU} \cdot \text{L}^{-1}$, γ -GTP: $131 \text{ IU} \cdot \text{L}^{-1}$, ALT: $50 \text{ IU} \cdot \text{L}^{-1}$, AST: $49 \text{ IU} \cdot \text{L}^{-1}$. Only 1 patient was lost for follow up. In the remaining 50 patients with follow up, there was only 1 (2 %) patient with persistent biliary symptoms in whom CBDS was finally diagnosed by ERC with ES. All other patients remained symptoms free on follow up and did not require ERC or biliary surgery.

CONCLUSION: Vast majority of patients with moderate suspicion of CBDS and no stones on EUS with linear array can avoid invasive evaluation of biliary tree with ERC.

Kohut M, Nowak A, Nowakowska-Dułała E, Marek T, Kaczor R. Endosonography with linear array instead of endoscopic retrograde cholangiography as the diagnostic tool in patients with moderate suspicion of common bile duct stones. *World J Gastroenterol* 2003; 9(3): 612-614

<http://www.wjgnet.com/1007-9327/9/612.htm>

INTRODUCTION

Common bile duct stones mostly come from the gallbladder. Spontaneous passage of bile duct stones to the duodenum is

quite often. Both facts make the presence of bile duct stones a very dynamic state. Precise diagnosis of presence bile duct stones with the minimal invasive method is eagerly awaited and important for the optimal treatment. The clinical suspicion of choledocholithiasis is often difficult to verify. The “gold standard” for bile duct stones diagnosis is still endoscopic retrograde cholangiography (ERC) with endoscopic sphincterotomy (ES) and surgical choledochotomy with choledochoscopy^[1]. Surgical exploration is reserved after failed endoscopic access to the biliary tree. Unfortunately, ERC carries possibility of serious complications. Acute iatrogenic pancreatitis is the most frequent. The need for pre-cut technique during ERC in some patients with difficult access to the papilla exposes the patient to the additional risk of bleeding from the papilla or perforation of the intestine.

The necessity for less invasive imaging modality of biliary tree is obvious. Several imaging modalities including magnetic resonance (MRI), spiral computerised tomography (spiral CT) and EUS are currently under evaluation.

According to several authors - sensitivity, specificity and accuracy of EUS with radial scanning transducer in the diagnosis of bile duct stones are almost the same as the ERC and are described between 84-100 %, 76-100 % and 90-99 %, respectively^[2-11]. The results of EUS with sector scanning transducer in this setting are similar^[12-14]. The sector scanning instruments are cheaper compared with radial scanning instruments. Fine needle aspiration (FNA) monitored under direct ultrasound visual control and Doppler scanning of vessels are additional advantages of sector scanning EUS.

There is only one communication describing the use of EUS (with radial scanning) with intention to replace diagnostic ERC in patients with moderate suspicion of CBDS^[15]. This study of Napoleon *et al.* was neither prospective nor controlled study^[15]. No data about the implementation of EUS with linear array with such intention exist. Thus, a prospective evaluation of the usefulness of EUS with linear array in the evaluation of patients with moderate suspicion of CBDS with intention to avoid ERC or biliary surgery was undertaken.

MATERIALS AND METHODS

Patients

The material comprised of 55 patients with moderate suspicion of bile duct stones treated from January 1996 to March 1997 in the Department of Gastroenterology Silesian Medical Academy. The project of the study was accepted by the Ethical Committee of the Silesian Medical Academy. Informed consent was obtained from every patient.

Inclusion criteria were as stated as follows: 1. clinical suspicion of bile duct stones - biliary colics at present or during the last 6 months prior to the admission. 2. abnormal results of the following biochemical serum tests (at least two times) - bilirubin, transaminases, alkaline phosphatase, γ -glutamylotranspeptidase - at present or in the last 6 months. 3. enlarged bile ducts on conventional ultrasound (US) - at present or in the last 6 months. Bile ducts were evaluated as enlarged

when the diameter of common bile duct exceeded 7 mm in cases with gallbladder *in situ* or 9 mm in post - cholecystectomy cases. 4. patient's data available during follow up (at least 6 months).

Exclusion criterias were as follows: 1. suspicion of bile duct stones on conventional ultrasound. 2. suspicion of biliary or pancreatic malignancy on CT scans. 3. present acute biliary pancreatitis - such patients were directly sent to ERC. 4. present acute cholangitis - treated as acute biliary pancreatitis.

In patients enrolled to the study, case history and a set of mentioned above blood biochemical indexes were collected. In following, conventional ultrasound (US) and EUS as initial imaging methods were performed. Examiners (US, EUS) knew nothing of a patient except for that the patient was suspected for bile duct stones.

In the case of CBDS on US and /or EUS, the patient was sent to ERC and excluded from the follow up study (4 cases). In the case of normal appearance of biliary tree on EUS, the decision to abandon ERC was made and the patient was enrolled to the follow up study (51 cases). The follow up program consisted of postal inquires every three months. We asked the following questions: 1. Did you experience any biliary symptoms - postprandial colics in upper right quadrant of the abdomen? 2. Did you notice any changes in the colour of stools (whitish stools), urine (dark urine) or skin (jaundice) during or after any colic? 3. Did you undergo any investigation in order to evaluate biliary tree (US, ERCP, biliary surgery)?

In the case of recurrence of biliary symptoms during follow up, the patient was admitted to our Gastroenterology Department again. ERC was performed on the in-patient basis. Only patients who completed at least 6 months follow up program were finally evaluated (mean follow up time - 13 months). Demographic and clinical data of patients were shown in Table 1-3.

Table 1 Demographics data of patients (n=51)

Age, [years]	
$\bar{x} \pm s$	55 (± 13)
Minimum	21
Maximum	85
Sex, [Females (%): Males (%)]	40 (78 %): 11 (22 %)
Cholecystectomized cases (%)	42 (82 %)

Table 2 Previous history of patients (up to 6 months prior to hospitalisation) (n=51)

Disease	Cases (%)
Acute biliary pancreatitis	4 (8 %)
Acute cholecystitis	2 (4 %)
Obstructive jaundice	7 (14 %)

Table 3 Biochemical values of patients before EUS (n=51)

Parameter	Cases (*)	Cases with abnormal results (%)
Alkaline phosphatase	45	6 (13%) 95 \pm 70 IU·L ⁻¹
γ -GTP	43	9 (21%) 131 \pm 175 IU·L ⁻¹
ALT	45	6 (13%) 48 \pm 64 IU·L ⁻¹
AST	32	3 (9%) 51 \pm 84 IU·L ⁻¹
Bilirubin	46	1 (2%) 149.6 \pm 100.5 μ mol·L ⁻¹

(*) some biochemical results unavailable in several cases

(*) Normal levels of liver enzymes in our lab:

- Alkaline phosphatase	<110	IU·L ⁻¹
- γ -GTP	<65	IU·L ⁻¹
- ALT	<40	IU·L ⁻¹
- AST	<40	IU·L ⁻¹
- Bilirubin	<17	μ mol·L ⁻¹

EUS

Endoscopic ultrasonography was performed with linear array scanning echoendoscope (Pentax FG 32 UA equipped with HITACHI 405 EUB ultrasonography machine). All EUS procedures were done by the same endosonographer with the experience of 400 EUS examinations (MK). Conscious sedation was achieved with midazolam given intravenously (mean 3,0 mg; range 1-7 mg) in one third patients. In the other two thirds patients midazolam was given orally (7,5 mg) 1,5-2 hours prior to the procedure. Patients were monitored by an anaesthesiologist with the use of ECG monitor and pulsoximetry. Topical pharyngeal anaesthesia with xylocain was used in all patients. EUS was performed with water filling balloon method, starting from the second portion of the duodenum in retrograde direction. EUS was considered positive for the diagnosis of choledocholithiasis if single or multiple hyperechoic structures within biliary tree with acoustic shadowing were found. Patients were diagnosed as stones free in the absence of findings described above. In several cases, antispasmodic agent (Buscopan) was used to control duodenal motility. EUS time was recorded (mean 18 minutes; range 9-37).

RESULTS

EUS was performed successfully with no complications in all 51 cases which were enrolled to the follow up program. Results of EUS showing no stones in the biliary tree in 51 cases could be confirmed in 49 cases during the follow up (96 %). The follow up lasted at least 6 months. The mean follow up time was 13 months (range 6-26 months). Only three patients were followed up for 6 months, the remaining cases were followed up longer. One patient was lost for follow up (2 % of all cases). Another one patient complained of persistent biliary colics on follow up. He was admitted again 3 months after his initial evaluation, as he was found to have complaints on the first postal inquiry. No patients with biliary symptoms were revealed during next postal inquires. In the symptomatic patients, ERC was carried out during the second admission and a single 7 mm stone was found in common bile duct (Figure 1). The stone was extracted after endoscopic sphincterotomy and the patient was discharged without complaints 2 days later.



Figure 1 Common bile duct stone EUS with linear array.

DISCUSSION

According to Cotton, who classified patients before planned cholecystectomy, one can distinguish three groups of patients with different levels of suspicion of CBDS^[16,17]. First group of cases with high risk of CBDS (80-90 %) is characterised by the enlargement over 10 mm of the diameter of common bile duct on US, obstructive jaundice (bilirubin over 20 μ mol·L⁻¹ with the elevation of alkaline phosphatase (3 times above upper limit of the normal value) and the history of acute biliary pancreatitis or acute cholangitis in the last few days. ERC with its possibility of therapeutic intervention should be the diagnostic

tool of first choice in case of strong suspicion of CBDS^[18]. The delay in therapeutic ERC due to the implementation of other imaging tests such EUS, MRI or CT is even unethical in patients with biliary obstruction (cholangitis, acute biliary pancreatitis). However, in case of uncertain reason of obstructive jaundice EUS, MRI or CT can be used to explain the etiology of the jaundice^[7]. Second group of patients, classified as the low risk group (approximately 2 % of cases have CBDS), consists of patients with no relevant case history, normal biochemical values and no abnormalities of biliary tree on US. Preoperative US and intraoperative cholangiography is proposed as the proper approach to the problem of possible CBDS^[16,17]. The third group of patients with moderate risk of CBDS is characterised by suspected (but not documented) acute biliary pancreatitis or obstructive cholangitis in the past, some elevation of alkaline phosphatase level and the diameter of common bile duct between 7 and 10 mm on US.

It is still debatable in the approach to patients with low risk for common bile duct stones. Some authors propose ERC before, after or even during the cholecystectomy^[6,16,19-25]. Spiral CT is proposed as the reliable imaging test for biliary tree evaluation^[9]. MRI is also considered as the possible choice^[26]. One can also learn from the literature that ERC is the only proposal in previously cholecystectomised cases^[16]. However cholecystectomised patients with suspected CBDS are usually old, and ERC can be thought to be even more aggressive approach, that in non cholecystectomised population of patients suspected for biliary lithiasis.

It is well known that EUS with either radial or sector scanning transducers is a powerful tool in the evaluation of patients suspected for biliary tree lithiasis^[2-14]. EUS is as reliable as ERC in the diagnosis of choledocholithiasis.

On the other hand, literatures showing that EUS can really replace ERC in patients with moderate risk of CBDS are curiously few. The only one paper dealing with that problem was appeared in an abstract form only by Napoleon *et al*^[15]. Napoleon *et al.* described the results of a follow up of 238 patients suspected for CBDS and negative EUS (with radial scanning) results. In his group 58 cases were cholecystectomised (24 %). Fourteen cases (6 %) were lost on follow up (median 490 days). ERC was needed due to persistent biliary symptoms (12 %) in 28 cases. However ERC was judged as useful in only 6 cases (3 %). One patient with CBDS, three patients with ampullary sclerosis and two cases with biliary tumors were found on ERC^[15]. The authors concluded that patients suspected for CBDS and negative EUS had a very low risk to need ERC during follow up. They added that EUS but not ERC was the best imaging method in case of moderate suspicion of CBDS^[15].

Our result supported these findings that EUS can be successfully used in older, previously cholecystectomised patients, as our group consisted predominantly of such cases. In conclusion, that EUS with sector scanning transducer (as shown previously for EUS with radial transducers) can be used as the main diagnostic test in patients with moderate risk of CBDS. A large proportion of these patients can avoid ERC or surgical bile ducts exploration in case of negative EUS results.

REFERENCES

- Pitt HA. Role of open choledochotomy in the treatment of choledocholithiasis. *Am J Surg* 1993; **165**: 483-486
- Amouyal G, Amouyal P, Levy P. Value of endoscopic ultrasonography in the diagnosis of idiopathic acute pancreatitis. *Gastroenterology* 1994; **105**: 283
- Amouyal P, Amouyal G, Levy P, Tuzet S, Palazzo L, Vilgrain V, Gayet B, Belghiti J, Fekete F, Bernards P. Diagnosis of choledocholithiasis by endoscopic ultrasonography. *Gastroenterology* 1994; **106**: 1062-1067
- Canto M, Chak A, Stellato T, Sivak MV. Endoscopic ultrasonography vs cholangiography for extrahepatic biliary stones: a prospective study in pre- and post-cholecystectomy pts. *Gastrointest Endosc* 1998; **47**: 439-448
- Denis B, Bas V, Goudot C, Frederic M, Bigard M, Gaucher P. Accuracy of endoscopic ultrasonography in the diagnosis of common bile duct stones. *Gastroenterology* 1993; **104**: 358
- Edmuntowicz S, Aliperti G, Middleton W. Preliminary experience using endoscopic ultrasonography in the diagnosis of choledocholithiasis. *Endoscopy* 1992; **24**: 774-778
- Giovannini M, Roche J, Lapuelle J, Rabbia J, Hoballah H, Rinaldi Y, Dancour M, Pauwells A, Ley G. Multicenter evaluation of EUS using a curved array transducer for assesment of unexplained cholestasis. Result in 121 cases. *Digestive Diseases Week San Francisco* 1996; **339**
- Napoleon B, Pujal B, Pouchon T, Keriven O, Soquet J. Prospective study of the accuracy of endoscopic ultrasonography for the diagnosis bile duct stones. *Endoscopy* 1994; **26**: 238
- Polkowski M, Palucki J, Regula J, Tilszer A, Butruk E. Helical CT cholangiography versus endosonography for suspected bile duct stones-a prospective blinded study in non-jaundiced patients. *Gut* 1999; **45**: 744-749
- Prat F, Amouyal G, Amouyal P, Pelletier G, Fritsch J, Choury AD, Buffet C, Etienne JP. Prospective controlled study of endoscopic ultrasonography and endoscopic retrograde cholangiography in patients with suspected common bile duct lithiasis. *Lancet* 1996; **346**: 75-79
- Sugiyama M, Atomi Y. Endoscopic ultrasonography for diagnosing choledocholithiasis: a prospective comparative study with ultrasonography and tomography. *Gastrointest Endosc* 1997; **45**: 143-146
- Lachter J, Eshef R, Shiller M, Levy A, Sussa A, Yassin K. Linear EUS for bile duct stones. *Gastrointest Endosc* 2000; **51**: 51-54
- Quirk D, Kesley P, Schapiro R, Brugge W. The use of linear-array ultrasonography in the detection of common bile duct stones. *Gastrointest Endosc* 1997; **45**: 178
- Kohut M, Nowakowska-Dulawa E, Marek T, Kaczor R, Nowak A. Accuracy of linear endoscopic ultrasonography in the evaluation of patients with suspected common bile duct stones. *Endoscopy* 2002; **34**: 299-303
- Napoleon B, Keriven-Soquet O, Pujol B, Soquet JC, Ponchon T. Does normal endoscopic ultrasound really avoid ERCP in patients with suspicion of bile duct stone? Study in 238 patients. *Gastrointest Endosc* 1996; **43**: 426
- Cotton PB, Baillie J, Pappas T, Meyers W. Laparoscopic cholecystectomy and the biliary endoscopist. *Gastrointest Endosc* 1991; **37**: 94-97
- Cotton PB. ERCP and laparoscopic cholecystectomy. *Am J Surg* 1993; **165**: 474-478
- Palazzo L. Which test for common bile duct stones? Endoscopic and intraductal ultrasonography. *Endoscopy* 1997; **29**: 655-665
- Deslandres E, Gagner M, Pomp A, Rheault M, Leduc R, Clermont R, Gratton J, Bernard EJ. Intraoperative endoscopic sphincterotomy for common bile duct stones during laparoscopic cholecystectomy. *Gastrointest Endosc* 1993; **39**: 54-58
- Dion Y, Ratelle R, Morin J, Gravel D. Common bile duct exploration: the place of laparoscopic choledochotomy. *Surg Laparosc Endosc* 1994; **6**: 419-424
- Miller R, Kimmelstiel F, Winkler W. Management of common bile duct stones in the era of laparoscopic cholecystectomy. *Am J Surg* 1995; **169**: 273-276
- Neuhaus H, Feussner H, Ungeheuer A, Hoffman W, Classen M. Prospective evaluation of the use of ERCP prior to laparoscopic cholecystectomy. *Endoscopy* 1992; **24**: 745-749
- Rieger R, Sulzbacher H, Woisetchlaeger R, Schrenk P, Wayand. Selective use of ERCP in patients undergoing laparoscopic cholecystectomy. *World J Surg* 1994; **18**: 900-905
- Shim CS, Joo JH, Park CW, Kim YS, Lee JM, Lee MS, Hwang SG. Effectiveness of endoscopic ultrasonography in the diagnosis of choledocholithiasis prior to laparoscopic cholecystectomy. *Endoscopy* 1995; **27**: 428-432
- Widdison A, Longstaff A, Armstrong A. Combined laparoscopic and endoscopic treatment of gallstones and bile duct stones: a prospective study. *Br J Surg* 1994; **81**: 595-597
- de Ledinghen V, Lecesne R, Raymond JM. EUS or magnetic resonance cholangiography? A prospective controlled study. *Gastrointest Endosc* 1999; **49**: 26-31

Crohn's disease and risk of fracture: does thyroid disease play a role?

Nakechand Pooran, Pankaj Singh, Simmy Bank

Nakechand Pooran, Pankaj Singh, Simmy Bank, Division of Gastroenterology Albert Einstein College of Medicine - Long Island Jewish Medical Center, New Hyde Park, New York, USA

Correspondence to: Simmy Bank, M.D., FRCP, Division of Gastroenterology, Long Island Jewish Medical Center, New Hyde Park, NY 11040, USA. simmybank@lij.edu

Telephone: +1-718-4704692 **Fax:** +1-718-3430128

Received: 2002-10-05 **Accepted:** 2002-11-04

Abstract

AIM: To assess the role of thyroid disease as a risk for fractures in Crohn's patients.

METHODS: A cross-sectional study was conducted from 1998 to 2000. The study group consisted of 210 patients with Crohn's disease. A group of 206 patients without inflammatory bowel disease served as controls. Primary outcome was thyroid disorder. Secondary outcomes included use of steroids, immunosuppressive medications, surgery and incidence of fracture.

RESULTS: The prevalence of hyperthyroidism was similar in both groups. However, the prevalence of hypothyroidism was lower in Crohn's patients (3.8 % vs 8.2 %, $P=0.05$). Within the Crohn's group, the use of immunosuppressive agents (0 % vs 11 %), steroid usage (12.5 % vs 37 %), small bowel surgery (12.5 % vs 28 %) and large bowel surgery (12.5 % vs 27 %) were lower in the hypothyroid subset as compared to the euthyroid subset. Seven (3.4 %) Crohn's patients suffered fracture, all of whom were euthyroid.

CONCLUSION: Thyroid disorder was not found to be associated with Crohn's disease and was not found to increase the risk for fractures. Therefore, screening for thyroid disease is not a necessary component in the management of Crohn's disease.

Pooran N, Singh P, Bank S. Crohn's disease and risk of fracture: does thyroid disease play a role? *World J Gastroenterol* 2003; 9(3): 615-618

<http://www.wjgnet.com/1007-9327/9/615.htm>

INTRODUCTION

Recent studies have shown that patients with Crohn's disease have decreased bone density^[1,2] that predisposes to an increased risk of fracture^[3,4]. A chronic inflammatory state with the release of inflammatory cytokines, steroid usage and malnutrition is the proposed mechanism. The co-existence of other medical conditions, which are independently associated with osteoporosis, will further increase the risk of fracture in patients with Crohn's disease. Thyroid disorder is associated with changes in bone metabolism and is an important cause of osteoporosis^[5-7]. Thyroid disorder has also been reported in patients with underlying inflammatory bowel disease (IBD)^[8-12]. One study showed altered thyroid physiology and anatomy in

patients with IBD^[9] and suggests that it may be important to investigate the association between thyroid disorders and Crohn's disease. If patients with Crohn's disease have a higher prevalence of thyroid disease, then screening and treatment of the thyroid disease may reduce the risk of fractures in the Crohn's disease population. Secondly, it has been reported that the presence of hyperthyroidism makes the treatment of inflammatory bowel disease more difficult^[10,13] and, therefore, correcting the thyroid disorder may have an impact on treatment response.

We compared the prevalence of hypothyroidism and hyperthyroidism in patients with Crohn's disease and those without Crohn's disease. To investigate whether co-existing thyroid dysfunction has an impact on the treatment of Crohn's disease, we compared the use of immunosuppressive medications and surgical procedures for the underlying Crohn's disease in patients with and without co-existing thyroid dysfunction.

MATERIALS AND METHODS

Study design and subjects

A retrospective cross-sectional study was conducted at this hospital from 1998 to 2000. The study group included 210 patients with Crohn's disease admitted to the hospital or referred to the endoscopy suite for endoscopic procedures. A control group comprised of 206 consecutive patients who did not have inflammatory bowel disease and who were referred for either screening colonoscopy or esophagogastroduodenoscopy (EGD).

Data collection

Medical records of patients were reviewed to extract information regarding their baseline demographic information, diagnosis and extent of Crohn's disease, presence of thyroid disease and use of either steroid or immunosuppressive agents. The diagnosis of Crohn's disease was made either endoscopically or radiographically. A history of other medical diagnoses (e.g. rheumatoid arthritis, chronic obstructive pulmonary disease) where the potential use of steroids or immunosuppressive agents may be a confounding factor was also recorded. Sample size was calculated based on a reference value of 1 % of thyroid dysfunction in the general population. To detect the difference of 5 % between the two groups with power of 0.8 and a two sided alpha error of 0.05, more than 200 patients were required in both the groups.

Outcome

The primary outcome was the presence of hypothyroidism or hyperthyroidism. Secondary outcomes included the use of immunosuppressive medications and surgery for the Crohn's disease. Thyroid disorder was considered present if the patient had a prior diagnosis of thyroid disorder and was taking thyroid medication (thyroxine, propylthiouracil, methimazole) or had an abnormal thyroid stimulating hormone (TSH) level.

Statistical analysis

Descriptive statistics were reported as proportions, means \pm

standard deviation or median and range. Comparison between groups was done using the Pearson chi-square test for categorical variable (or the Fisher exact test if appropriate) and two-sided student *t*-test for continuous variables (SPSS for Windows, release 10.0, Chicago, IL). $P < 0.05$ was considered significant.

RESULTS

Demographic and clinical characteristics

There were 210 patients with Crohn's disease and 206 controls. The two groups were matched for age (49.24 yr. vs 48.58 yr., $P = 0.68$), sex (88 males/122 females vs 91 males/133 females, $P = 0.29$), and race (153 whites/1 black/34 others vs 118 whites/14 blacks/36 others, $P = 0.34$). The groups differed in body mass index (24.35 kg/m² vs 27.46 kg/m², $P = 0.001$). (Table 1).

Table 1 Comparison of baseline characteristics and thyroid status in patients with Crohn's disease and control group

	Case (n=210)	Control (n=206)	P
Age (years)	49.24±13.71	48.58±18.43	0.68
Sex (M/F)	88/122	91/113	0.29
Body Mass Index (kg/cm ²)	24.35	27.46	0.001
Race (white/black/others)	153/1/34	118/14/36	0.34
Steroid use	75 (35.7%)	None	—
Immunosuppressive therapy	22 (10.4%)	None	—
Hypothyroidism	8 (3.8%)	17 (8.2%)	0.05
Hyperthyroidism	2 (0.01%)	None	0.25

Primary outcome - thyroid dysfunction

In the Crohn's group there were 8 (3.8 %) cases of hypothyroidism and 2 (0.01 %) cases of hyperthyroidism. The control population had 17 (8.2 %) cases of hypothyroidism and 0 (0 %) case of hyperthyroidism. The difference in hypothyroidism showed borderline significance ($P = 0.05$) while hyperthyroidism was not significant ($P = 0.25$) (Figure 1).

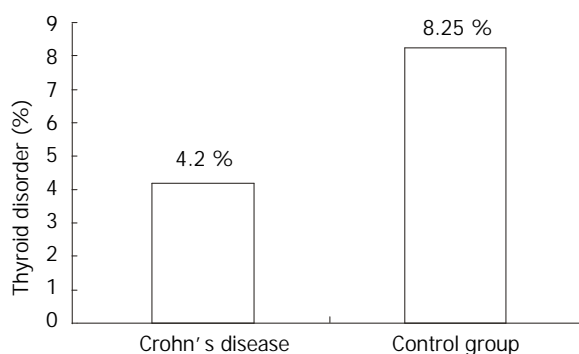


Figure 1 Bar graph showing the prevalence of thyroid disorder in patients with Crohn's disease and in the control group.

Secondary outcome - use of immunosuppressives and surgery

Patients with Crohn's disease were divided into those with hypothyroidism and those without any thyroid disorder. There was clinically higher use of immunosuppressive agents (0 % vs 11 %, $P = 0.59$), steroid usage (12.5 % vs 37 %, $P = 0.15$), small bowel surgery (12.5 % vs 28 %, $P = 0.34$) and large bowel surgery (12.5 % vs 27 %, $P = 0.38$) in Crohn's patients with hypothyroidism in comparison to those who were euthyroid. This difference however, was not statistically significant. (Table 2, Figure 2).

Table 2 Comparison of medical and surgical treatment in patients with hypothyroidism and euthyroidism in Crohn's disease

	Hypothyroidism (n=8)	Euthyroid (n=201)	P
Immunosuppressive medications	None	22 (11%)	0.59
Steroid use	1 (12.5%)	74 (37%)	0.15
Small bowel surgery	1 (12.5%)	56 (28%)	0.34
Large bowel surgery	1 (12.5%)	54 (27%)	0.38

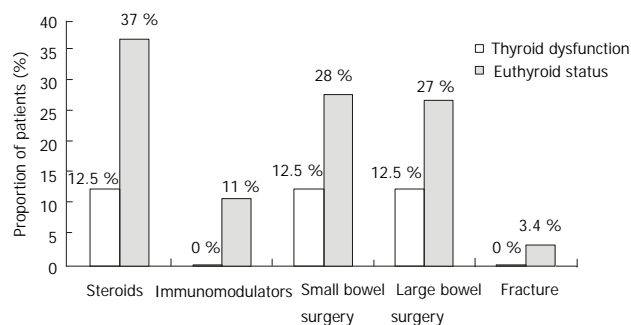


Figure 2 Bar graph showing the usage of steroids, immunosuppressive agents, small bowel surgery, large bowel surgery and fractures in Crohn's patients with thyroid disorder and those without thyroid disorder.

DISCUSSION

Crohn's disease is a chronic illness that is associated with a lower bone mineral density and a higher incidence of fracture^[1-4]. This results in increased morbidity and mortality. Thyroid disorder may potentiate the risk of fracture. The purpose of this study was to investigate whether thyroid disorder contributed to this adverse event and if present, whether thyroid disorder has an impact on the management of Crohn's disease. We did not find a higher prevalence of thyroid disease in our Crohn's population when compared to a control group. In fact, the prevalence of hypothyroidism was less in the Crohn's group. Sub-group analysis of the Crohn's group showed that there was lower usage of steroids, immunosuppressive medications and surgery in those who were also hypothyroid when compared to those who were euthyroid. There were 7 (3.4 %) fractures in the Crohn's population. All of the fractures occurred in those who were euthyroid.

The prophylactic use of a bisphosphonate has been shown to increase the bone mineral density in patients with Crohn's disease^[14]. However, the beneficial effect in lowering the incidence of fracture has not been reported. Due to the lack of an effective prophylactic medication, it becomes important to identify and treat any other co-existing illness that can enhance bone loss and increase the risk of fracture. One common disease that is linked to Crohn's and has an impact on bone metabolism is thyroid disease^[8-12].

In our study, we did not find a difference in the prevalence of thyroid disease between patients with Crohn's disease and our controls. These findings are consistent with two prior studies^[8,12]. Snook *et al*^[8] found a higher prevalence of thyroid disorder in patient with ulcerative colitis, but not Crohn's disease, when comparing patients with IBD to the general population. Hammer *et al*^[12] also found a higher prevalence of thyroid disorder in the ulcerative colitis subset of their IBD population when compared to the general population. The lack of association of clinical thyroid disorder and Crohn's disease is contradicted by the objective findings of Jenerot *et al*^[9]. They showed that patients with IBD had a 35 % higher thyroid

volume and were three times more likely to have an enlarged thyroid. Their finding of thyroid enlargement may be secondary to iodine deficiency, which has been reported in Crohn's disease and is unrelated to functional derangement of the thyroid^[15]. When we subdivided our thyroid disorder into hyperthyroid and hypothyroid, we did not find a difference in the prevalence of hyperthyroid between those with Crohn's disease and controls. Surprisingly, we found a lower prevalence of hypothyroidism in the Crohn's group as compared to controls.

Finding no difference in the prevalence of hyperthyroidism between patients with Crohn's disease and controls has clinical significance. Hyperthyroidism is associated with accelerated bone turnover and shortening of the normal bone remodeling cycle^[6,7]. This results in increased bone metabolism and osteoporosis. Since patients with Crohn's disease do not have a higher prevalence of hyperthyroidism, an elevation of thyroxine levels cannot be the basis for the increased osteoporosis seen in this group of patients. Factors such as chronic inflammation, prolonged steroid usage and malnutrition are the more likely etiological agents for osteoporosis^[16]. Thus, evaluating patients with Crohn's disease for hyperthyroidism should be done on clinical grounds and not as a screening procedure.

Our finding of a lower prevalence of hypothyroidism in our Crohn's population as compared to our controls is similar to those of Hammer *et al.*^[12]. It is possible that since both Crohn's disease and thyroid disorder have a possible autoimmune etiology, treating Crohn's disease with corticosteroids and immune modulating agents may prevent the manifestation of an autoimmune thyroid disorder. The difference in prevalence of hypothyroidism may also be the result of a higher than expected prevalence of hypothyroidism in our control group. The prevalence of hypothyroidism in population based studies varies from 0.5 % to 5 %^[17-19], however, we had an 8 % prevalence of hypothyroidism in our controls. This higher prevalence of hypothyroidism may be explained by the availability of third generation assays for thyroid stimulating hormone (TSH) and increased frequency of screening for thyroid disorder, leading to detection of sub-clinical disease. There is also the possibility of a selection bias in the control group. The controls included people who underwent screening colonoscopy. Those persons are more likely to be health conscious and, therefore, are more likely to visit a physician; thus, this would result in increased screening for thyroid disease as compared to the general population. In addition, the control group had a higher body mass index (BMI) as compared to the Crohn's group. BMI can act as a confounding factor as it is related to both hypothyroidism and reflux symptoms. Hypothyroidism is associated with weight gain^[18,19]. Patients who have a higher BMI are more likely to have reflux symptoms^[20,21] and thus, are more likely to undergo EGD than the general population. Since our controls included patients having EGD, it is possible that our controls contained a higher percentage of people who are hypothyroid. This may be a theoretical concern as a recent, well design; prospective study^[22] did not show an association between obesity and reflux symptoms.

There are concerns that the presence of thyroid disease may have an impact on the management of IBD. Moreover, there are case reports that suggest that thyroid disease needs to be treated in order to successfully treat IBD^[10,13]. We subdivided our Crohn's disease population into those who are euthyroid and those who had thyroid disease. The two groups were compared with regard to steroid usage, use of immune modulating agents, surgery for the management of Crohn's and rate of fracture. There was a higher rate of steroid usage, use of immune modulating agents, and both small and large

bowel surgeries in patients who were euthyroid. For instance, there were seven fractures in the Crohn's group, all of which occurred in patients who were euthyroid. The differences, though clinically significant, were not statistically significant. This is probably due to a small sample size. A larger prospective, controlled study is needed to evaluate this issue. Hypothyroidism is known to decrease metabolism and slow physiological functions. The presence of hypothyroidism may act as endogenous disease modification in patients with Crohn's disease.

Our study was limited by retrospective data collection. This makes it difficult to evaluate and compare disease severity index and extent of disease between Crohn's disease patients who are euthyroid and those who had a thyroid disorder present. It also makes it difficult to establish a temporal relationship between thyroid disease and Crohn's disease. Our results are based on the assumption that patients who were characterized as euthyroid are actually euthyroid. Symptoms may not suggest thyroid disease when it is mild and are often atypical in the elderly^[23-25]. Thus, it is possible that we missed patients with subclinical thyroid disease.

In conclusion, patients with Crohn's disease do not have a higher prevalence of thyroid disease than the general population and, therefore, routine screening for thyroid disease is not a necessary component in the management of Crohn's disease. However, it is apparent that thyroid disease has a significant clinical impact on the course of Crohn's disease, which needs to be studied in a prospective manner.

ACKNOWLEDGEMENT

The authors thank S.D. Rampertab, M.D. for her critical comments on the manuscript.

REFERENCES

- 1 **Silvennoinen JA**, Karttunen TJ, Niemela SE, Manelius JJ, Lehtola JK. A controlled study of bone mineral density in patients with inflammatory bowel disease. *Gut* 1995; **37**: 71-76
- 2 **Andreassen H**, Rungby J, Dahlerup JF, Mosekilde L. Inflammatory bowel disease and osteoporosis. *Scand J Gastroenterol* 1997; **32**: 1247-1255
- 3 **Vestergaard P**, Krogh K, Rejnmark L, Laurberg S, Mosekilde L. Fracture risk is increased in Crohn's disease, but not in ulcerative colitis. *Gut* 2000; **46**: 176-181
- 4 **Bernstein CN**, Blanchard JF, Leslie W, Wajda A, Yu BN. The incidence of fracture among patients with inflammatory bowel disease. A population-based cohort study. *Ann Int Med* 2000; **133**: 759-799
- 5 **Greenspan SL**, Greenspan FS. The effect of thyroid hormone on skeletal integrity. *Ann Int Med* 1999; **130**: 750-758
- 6 **Mosekilde L**, Eriksen EF, Charles P. Effects of thyroid hormone on bone and mineral metabolism. *Endo Metabol Clin NA* 1990; **19**: 35-63
- 7 **Ross DS**. Hyperthyroidism, thyroid hormone therapy, and bone. *Thyroid* 1994; **4**: 319-326
- 8 **Snook JA**, de Silva HJ, Jewell DP. The association of autoimmune disorders with inflammatory bowel disease. *Q J Med* 1989; **72**: 835-840
- 9 **Jarnerot G**, Kagedal B, von Schenck A, Trulove SC. The thyroid in ulcerative colitis and Crohn's disease. V. Triiodothyronine. Effect of corticosteroids and influence of severe disease. *Acta Med Scand* 1976; **199**: 229-232
- 10 **Bonapace ES**, Srinivasan R. Simultaneous occurrence of inflammatory bowel disease and thyroid disease. *Am J Gastroenterol* 2001; **96**: 1925-1926
- 11 **Bianchi GP**, Marchesini G, Gurli C, Zoli M. Thyroid involvement in patients with active inflammatory bowel diseases. *Ital J Gastroenterol* 1995; **27**: 291-295
- 12 **Hammer B**, Ashurst P, Naish J. Diseases associated with ulcerative colitis and Crohn's disease. *Gut* 1968; **9**: 17-21

- 13 **Modebe O**. Autoimmune thyroid disease with ulcerative colitis. *Post Med J* 1986; **62**: 475-476
- 14 **Haderslev KV**, Tjellesen L, Sorensen HA, Staun M. Alendronate increases lumbar spine bone mineral density in patients with Crohn's disease. *Gastroenterol* 2000; **119**: 866-869
- 15 **Janerot G**. The thyroid in ulcerative colitis and Crohn's disease I. Thyroid radioiodide uptake and urinary iodine excretion. *Acta Med Scand* 1975; **197**: 95
- 16 **Andreassen H**, Rungby J, Dahlerup JF, Mosekilde L. Inflammatory bowel disease and osteoporosis. *Scand J Gastroenterol* 1997; **32**: 1247-1255
- 17 **Sawin CT**, Castelli WP, Hershman JM, McNamara P, Bacharach P. The aging thyroid. Thyroid deficiency in the framingham study. *Arch Int Med* 1985; **145**: 1386-1388
- 18 **Dale J**, Daykin J, Holder R, Sheppard MC, Franklyn JA. Weight gain following treatment of hyperthyroidism. *Clin Endo* 2001; **55**: 233-239
- 19 **Pinkney JH**, Goodrick SJ, Katz J, Johnson AB, Mohamed-Ali V, Coppack SW. Leptin and the pituitary-thyroid axis: a comparative study in obese, hypothyroid and hyperthyroid subjects. *Clin Endo* 1998; **49**: 572-583
- 20 **Wajed SA**, Streets CG, Bremner CG, DeMeester TR. Elevated body mass disrupts the barrier to gastroesophageal Reflux. *Arch Surg* 2001; **136**: 1014-1018
- 21 **Wilson LJ**, Ma W, Hirschowitz BI. Association of obesity with hiatal hernia and esophagitis. *Am J Gastroenterol* 1999; **94**: 2840-2844
- 22 **Langergren J**, Bergstrom R, Nyren O. No relation between body mass and gastro-oesophageal reflux symptoms in a swedish population based study. *Gut* 2000; **47**: 26-29
- 23 **Evered DC**, Ormston BJ, Smith PA, Hall R, Bird T. Grades of hypothyroidism. *Brit Med J* 1973; **1**: 657-662
- 24 **Wenzel KW**, Meinhold H, Raffenberg M, Adlkofer F, Schleusener H. Classification of hypothyroidism in evaluating patients after radioiodine therapy by serum cholesterol, T3-uptake, total T4. *Eur J Clin Invest* 1974; **4**: 141-148
- 25 **Bahemuka M**, Hodkinson HM. Screening for hypothyroidism in elderly patients. *Brit Med J* 1975; **2**: 601-603

Edited by Xu XQ

• CLINICAL RESEARCH •

Elevated serum values of procollagen III peptide (PIIIP) in patients with ulcerative colitis who will develop pseudopolyps

Žarko Babić, Vjekoslav Jagić, Zvonko Petrović, Ante Bilić, Kapetanović Dinko, Goranka Kubat, Rosana Troskot, Mira Vukelić

Žarko Babić, Ante Bilić, Rosana Troskot, Division of Hepatogastroenterology, Department of Medicine, Sveti Duh General Hospital, Zagreb, Croatia

Vjekoslav Jagić Department of Laboratory Biochemistry Diagnosis, Sveti Duh General Hospital, Zagreb, Croatia

Zvonko Petrović Department of Pathology, Sveti Duh General Hospital, Zagreb, Croatia

Kapetanović Dinko, Goranka Kubat, Mira Vukelić Department of Radiology, Sveti Duh General Hospital, Zagreb, Croatia

Correspondence to: Assist. Professor Žarko Babić, M.D., Ph.D Fabkovićeva 3, HR-10000 Zagreb, Croatia. zarko.babic@zg.hinet.hr

Telephone: +385-1-3712111 **Fax:** +385-1-3745550

Received: 2002-07-12 **Accepted:** 2002-07-29

Abstract

AIM: To assess the impact of procollagen III peptide as a marker of collagenesis in the development of pseudopolyps in patients with ulcerative colitis.

METHODS: Development of pseudopolyps was monitored in 25 patients with ulcerative colitis classified according to Powell-Tuck index as mild ($n=12$) or moderate ($n=13$) form of disease. Patients with a mild form of disease were treated with oral mesalazine medication (2-4 g/day) and local mesalazine preparation (suppository). Patients with a moderate form of disease received oral mesalazine medication (2-4 g/day), local mesalazine preparation (suppository) and local methylprednisolone at an initial dose of 60 mg/day, followed by dose tapering. How many significant variables (previously determined by analysis of variance) were elevated in the groups with and without pseudopolyp development was observed. ROC analysis for calculation of new index was made.

RESULTS: Serum values of procollagen III peptide (PIIIP), C-reactive protein (CRP) and C4 complement component (C4) were statistically significantly lower in the group of patients free from pseudopolyp development than those who developed one or more pseudopolyps (0.45 ± 0.12 vs 1.42 ± 0.70 , $P < 0.0027$; 7.6 ± 4.7 vs 17.8 ± 9.17 , $P < 0.035$; and 0.46 ± 0.11 vs 0.34 ± 0.16 , $P < 0.068$, respectively) at endoscopic controls with pathohistologically samples during 13 months. There were no statistically significant differences in the values of C3, ceruloplasmin and IgM between the two groups ($P > 0.05$). Discrimination function analysis yielded highest standardized cannon coefficients for PIIIP (0.876), CRP (0.104), C3 (-0.534) and C4 (0.184) ($P < 0.036$). The elevation in two of three laboratory variables (PIIIP, CRP and C4) reached sensitivity of 93 % and specificity of 90 % in the development of pseudopolyps.

CONCLUSION: It is proposed that an increase in two of the three laboratory parameters (PIIIP, CRP and C4) could improve the accuracy of prediction of the development of pseudopolyps. When using PIIIP, CRP and C4 on decision

making, the positive predictive value and accuracy were 90 % and 92 %, respectively.

Babić Ž, Jagić V, Petrović Z, Bilić A, Dinko K, Kubat G, Troskot R, Vukelić M. Elevated serum values of procollagen III peptide (PIIIP) in patients with ulcerative colitis who will develop pseudopolyps. *World J Gastroenterol* 2003; 9(3): 619-621 <http://www.wjgnet.com/1007-9327/9/619.htm>

INTRODUCTION

The role of procollagen and of its metabolites and enzymes involved in the synthesis and degradation of procollagen during the development of ulcerative colitis has already been investigated in a number of studies^[1-6]. Higher levels of procollagen transcripts have been reported in patients with ulcerative colitis as compared with healthy subjects^[4], pointing to an enhanced *de novo* synthesis of all types of collagen in patients with ulcerative colitis^[1,3,4]. Also, the expression of collagenase has been demonstrated to be higher in patients with ulcerative colitis than in normal subjects^[4]. These patients showed hyperexpression of procollagen III RNA transcripts. The elevated level of procollagen messenger RNA correlated with the rate of inflammatory infiltrations^[1,3,4], represented by inflammatory polyps (pseudopolyps). In the process of healing inflammatory desctructed mucosa is changed with the reparatory process^[1-9].

The development of pseudopolyps sometimes is seen in the stage of disease remission^[7,8]. The presence of procollagen and other materials is necessary for polyp formation^[1,9]. The measurement of procollagen may be helpful in the determination of the patient who will develop pseudopolyp formation. Insight to literature of the last 20 years, there were no studies into the predictive value of procollagen III peptide (PIIIP) for polyp development in patients with ulcerative colitis. The aim of the study was to assess the role of PIIIP as a marker of collagen synthesis in the development of pseudopolyps in patients with ulcerative colitis.

MATERIALS AND METHODS

Patients

Twenty-five patients with ulcerative colitis^[7], 11 men with median age of 34 years (aged 30-45) and 14 women with median age 35 years (aged 29-47), were included in the study. Only newly detected patients were enrolled in the study, thus to exclude the effect of previous therapy on collagen formation^[1-7]. Thus the patients were classified according to Powell-Tuck index^[7,8] for disease severity into the groups with mild ($n=12$) and moderate ($n=13$) form of disease. Mild form of disease had no system symptoms, had less then 4 stools over 24 hours. This form of disease was without significant rectal bleeding, had no signs of anemia, had normal body temperature, normal puls rate and had sedimentation rate under 30 mm per hour. Moderate form of disease had 4-6 diarrhoic stools per day, crampy abdominal pain, elevated body

temperature, increased pulse rate, tachycardia, anemia, elevated sedimentation over 30 mm per hour and extraintestinal symptoms (arthritis). Severe form of disease with more than 6 diarrhoic stools per day, more rectal bleeding and severe intestinal and extraintestinal complications, *etc.* were not included in the study, while the therapy for this form of disease can influence the collagen formation^[1-12].

The course of disease was monitored clinically, endoscopically and histologically. The development of pseudopolyps was observed by using endoscopy^[1,7,9-12]. The formation of intraluminal mucosal enlargement with one or more polyps in former or newly inflamed mucosa was observed. Histological criteria for inflammatory polyps (pseudopolyps) were: only the finding of a diffuse colitis with nonspecific inflammation, no granulomas, and involved rectum would be consistent with ulcerative colitis; however, even in cases that the patient might still have some other form of diffuse colitis and the diagnosis of ulcerative colitis is only established by exclusion of all other causes^[13]. The criteria for the diagnosis of epithelial dysplasia and its distinction from the inflammatory and reparative^[14, 15] lesions and neoplasms^[16] that regularly occur in these patients have been established.

Clinical and endoscopic controls were done once monthly during 12 months (12 times), and then once after six months again, what meant totally 13 controls^[7].

Laboratory measurements and new index calculation

PIIIP was measured by using RIA-gnost PIIIP method (Berhingwerke). CRP, C3, C4, IgM and ceruloplasmin were measured by using Turbox Immunonephelometry method (Orion diagnostics).

The significant laboratory variables were determined by using analysis of variance. The contribution of each variable was determined by using the discriminant canonical function on Statistica 5.0 software.

The indexes from three most significant variables were calculated by using ROC analysis. How many significant variables were elevated above laboratory reference values for each patient in two groups (with and without pseudopolyps) was observed. ROC analysis was used to determine the sensitivity, specificity, accuracy and positive predictive value of our new index.

Therapy

The patients with a mild form of disease were treated with oral mesalazine medication (2-4 g/day) and local mesalazine preparation (suppository)^[7]. The patients with a moderate form of disease received oral mesalazine medication (2-4 g/day), local mesalazine preparation (suppository) and oral methylprednisolone at an initial dose of 60 mg/day followed by methylprednisolone dose tapering^[7]. Severe form of disease was excluded with Powell-Tuck index, while therapy for severe form of disease can influence on inflammatory polyps formation^[1-7].

RESULTS

In the group of patients without pseudopolyp development ($n=15$), the levels of PIIIP, C-reactive protein (CRP) and C4 complement component (C4) were statistically significantly lower than those in the group of patients developing pseudopolyps (0.45 ± 0.12 vs 1.42 ± 0.70 , $P<0.0027$; 7.6 ± 4.7 vs 17.8 ± 9.17 , $P<0.035$; and 0.46 ± 0.11 vs 0.34 ± 0.16 , $P<0.068$, respectively). Other parameters, i.e. C3 complement component (C3), ceruloplasmin and IgM, showed no statistically significant differences between the groups of patients with and without pseudopolyp development. Analysis of the discriminative canonical function yielded highest

standardized canonical coefficients for PIIIP (0.876), CRP (0.104), C3 (-0.534) and C4 (0.184) ($P<0.036$), which were then used for subsequent data analysis.

The use of PIIIP, CRP and C4 levels showed that an increase in two of these three laboratory parameters improved the accuracy of prediction of pseudopolyp development. When using PIIIP, CRP and C4 (ROC analysis) on decision making sensitivity was 93 % and specificity 90 %, the positive predictive value and accuracy were 90% and 92%, respectively.

DISCUSSION

In ulcerative colitis patients, inflammatory mucosal destruction is changed by regenerative process (inflammatory polyps (pseudopolyps))^[1-7,13-16]. Collagen is a constituent of connective tissue, thus also of polyps^[1]. In inflammatory bowel diseases, elevated levels of collagen I, III and V are found^[1-3]. Serum level of PIIIP was found to be higher in patients with ulcerative colitis and liver damage, then in patients without liver damage^[9]. Collagenase is regulated by the processes involved in the collagen synthesis (N-terminal propeptide of type III procollagen and C-terminal propeptide of type I procollagen) and degradation (C-terminal telopeptide of type I collagen)^[1]. Degradation of collagens is highly regulated by a cascade of matrix metalloproteases and their tissue inhibitors taken by endoscopic biopsies in patients with inflammatory bowel disease^[8]. The histological severity degree of acute inflammation was correlated well with the expression of metalloproteases gene^[8].

Collagenase can be influenced by glucocorticoid therapy, therefore only newly detected patients were enrolled in the study^[1]. The effect of glucocorticoids on collagenase and collagen degradation has not yet been fully clarified, however, a number of speculative theories have been proposed^[1,3,5,6,9,17]. So, that was the reason why we did not include severe forms of disease in the study, while there was a lot of factors that could have influence on the synthesis of collagen and therefore lead to misinterpretation of results (we tried to succeed "a homogenous sample" according to collagenesis). We found no data about any study predicting pseudopolyps development in patients with inflammatory bowel disease. The development of pseudopolyps is sometimes seen in disease relaps, but not strongly^[1].

Many studies have tackled the issue of predicting disease relapse, however, little has been reported on predicting remission of the disease and none using PIIIP^[1,8,18-22].

The levels of interleukin-1, a potent CRP stimulus, were also monitored^[23]. Serum levels of interleukin-1 receptor antagonist (IL-1ra) may also be an index of ulcerative colitis activity, being low in disease remission^[24]. This parameter may be useful in the differential diagnosis against other IBDs. A group of authors from Aachen prefer the level of interleukin-6 to CRP^[25]. In the present study, CRP levels were among those that, used in combination with other parameters, improved the accuracy of predicting pseudopolyp development, probably pointing not only to inflammation expression but also to the cellular reparatory potential.

The levels of total sialic acid remained increased after the therapy, especially in patients with poor response to therapy with 5-aminosalicylic acid and corticosteroids, while the levels of CRP were normalized after three weeks in most of the patients, irrespective of their therapeutic response^[26].

Endoscopic monitoring of IBD activity should be supplemented by the noninvasive measurement of the levels of α_1 -antitrypsin in stool and serum albumin^[27], the more so, Moran *et al* recommend them as routine markers of the disease endoscopic activity^[28].

The levels of immunoglobulin proved helpful in the

assessment of intestinal resorption, however, in spite of previous belief, had no practical clinical relevance in the determination of disease activity^[29,30]. The results of our study were consistent with these concepts. So, only the values of C4 complement component could be used for subsequent evaluation, and these only in combination with other parameters. Neither were the values of ceruloplasmin as an early inflammation reactant useful for further analysis.

According to Schmoud *et al.*, age is an unfavorable prognostic factor for disease relapse in patients with inflammatory bowel disease (IBD)^[31]. Therefore, the patients included in our study were matched by both sex and age, thus to minimize the impact of these factors on study results.

In the present study, we used the ever more popular method including a combination of factors, providing more accurate information on the real state than each of the factors alone. The role of procollagen should be investigated in a larger sample. Studies with tissue collagen determined before and after therapy may also be expected to yield interesting results. In addition, studies in more severe forms of the disease would be highly interesting, although it might be difficult to differentiate between the collagenase involved in the connective tissue formation in the intestinal wall and the collagenase formed by systemic stimulation of other tissues due to the disease severity^[1,2,6,8,9].

In conclusion, based on the study results, it is proposed that elevation in two of the three laboratory parameters (PIIP, CRP and C4) can improve the prediction of the development of pseudopolyps in patients with ulcerative colitis. When PIIP, CRP and C4 are used in the assessment of pseudopolyp development, the positive predictive value and accuracy were as high as 90 % and 93 %, respectively.

REFERENCES

- Kjeldsen J**, Schaffalitzky OBM, Junker P. Seromarkers of collagen I and III metabolism in active Crohn's disease. Relation to disease activity and response to therapy. *Gut* 1995; **37**: 805-810
- Graham MF**, Diegelmann RF, Elson CO, Lindblad WJ, Gitschalk N, Gay S, Adam J. Collagen content and types in the intestinal strictures of Crohn's disease. *Gastroenterology* 1988; **94**: 257-265
- Matthes H**, Herbst H, Schuppan D, Stallmach A, Milani S, Stein H, Riecken EO. Cellular localisation of procollagen gene transcripts in inflammatory bowel disease. *Gastroenterology* 1992; **102**: 431-442
- Matthes H**, Stallmach A, Matthes B, Herbst H, Schuppan D, Riecken ED. Indications for different collagen metabolism in Crohn's disease and ulcerative colitis. *Med Clin* 1993; **88**: 185-192
- Berg S**, Brodin B, Hesselvik F, Laurent TC, Maller R. Elevated levels of plasma hyaluronan in septicaemia. *Scand J Clin Lab Invest* 1998; **48**: 727-732
- Kaushner I**. The phenomenon of the acute phase response. *Ann NY Acad Sci* 1982; **389**: 39-48
- Rutgeerts P**. Medical therapy of inflammatory bowel disease. *Digestion* 1998; **59**: 453-469
- von Lampe B**, Barthel B, Coupland SE, Riecken EO, Rosewicz S. Differential expression of matrix metalloproteinases and their tissue inhibitors in colon mucosa of patients with inflammatory bowel disease. *Gut* 2000; **47**: 12-14
- Lidenius MH**, Risteli LT, Risteli JP, Taskinen EI, Kellokumpu IH, Hockerstedt KA. Serum aminoterminal propeptide of type III procollagen (S-PIIP) and hepatobiliary dysfunction in patients with ulcerative colitis. *Scand J Clin Lab Invest* 1997; **57**: 297-305
- Walmsley RS**, Ayres RCS, Pounder RE, Allan RN. A simple clinical activity index. *Gut* 1998; **43**: 29-32
- Stallmach A**, Schuppan D, Riese HH, Matthes H, Riecken ED. Increased collagen type III synthesis by fibroblasts isolated from strictures of patients from Crohn's disease. *Gastroenterology* 1992; **102**: 1920-1929
- Modigliani R**. Definition of patient groups: remission. In: Campieri M, Bianchi-Poro G, Fiocchi G, Scholmerich J. eds. Clinical challenges in inflammatory bowel disease- diagnosis, prognosis and treatment. Dordrecht, Boston, London: *Kluwer Academic Publishers* 1998: 85-94
- Goldman H**. Interpretation of large intestinal mucosal biopsy specimens. *Hum Pathol* 1994; **25**: 1150-1159
- Riddell RH**, Goldman H, Ransohoff DF. Dysplasia in inflammatory bowel disease: Standardized classification with provisional clinical applications. *Hum Pathol* 1983; **14**: 931-968
- Pascal RR**. Consistency in the terminology of colorectal dysplasia. *Hum Pathol* 1988; **19**: 1249-1250
- Pascal RR**. Dysplasia and early carcinoma in inflammatory bowel disease and colorectal adenomas. *Hum Pathol* 1994; **25**: 1160-1171
- Dionne S**, Ruemmele M, Seidman EG. Immunopathogenesis of inflammatory bowel disease: role of cytokines and immune cell-enterocyte interactions. In: Bistran BR, Walker-Smith JA. editors. *2nd Nestle Nutrition Workshop Series Clinical & Performance Programme* 1999: 41-62
- Mahmud N**, Stinson J, O'Connell MA, Mantle TJ, Keeling PW, Feely J, Weir DG, Kellehr D. Microalbuminuria in inflammatory bowel disease. *Gut* 1994; **11**: 1599-1604
- Nielsen OH**, Langholz E, Hendel J, Brynskov J. Circulating soluble intercellular adhesion molecule-1 (sICAM-1) in active inflammatory bowel disease. *Dig Dis Sci* 1994; **39**: 1918-1923
- Rowe FA**, Camilleri M, Forstrom LA, Batts KP, Mullan BP, Thomforde GMDunn W, Zinsmeister AR. A pilot study of splenic and whole body retention of autologous radiolabeled leukocytes in the assessment of severity in inflammatory colitis. *Am J Gastroenterol* 1995; **90**: 1771-1775
- Weldon MJ**, Masoomi AM, Britten AJ, Gene J, Finlayson CJ, Joseph AE, Maxwell MD. Quantification of inflammatory bowel disease activity using technetium-99m HMPAO labelled leucocyte single photon emission computerised tomography (SPECT). *Gut* 1995; **36**: 243-250
- Patel RT**, Bain I, Youngs D, Keighely MR. Cytokine production in pouchitis is similar to that in ulcerative colitis. *Dis Colon Rectum* 1995; **38**: 831-837
- Mazlam MZ**, Hodgson HJ. Interrelations between interleukin-6, interleukin-1 beta, plasma C-reactive protein values, and *in vitro* C-reactive protein generation in patients with inflammatory bowel disease. *Gut* 1994; **35**: 77-83
- Propst A**, Propst T, Herold M, Vogel W, Judmaier G. Interleukin-1 receptor antagonist in differential diagnosis of inflammatory bowel disease. *Eur J Gastroenterol Hepatol* 1995; **11**: 1031-1036
- Hotkamp W**, Stollberg T, Reis HE. Serum interleukin-6 related to disease activity but not disease specificity in inflammatory bowel disease. *J Clin Gastroenterol* 1995; **20**: 123-126
- Ricci G**, D' Ambrosi A, Resca D, Masotti M, Alvisi V. Comparison of serum total sialic acid, C-reactive protein, alpha 1-acid glycoprotein and beta 2-microglobulin in patients with non-malignant bowel disease. *Biomed Pharmacother* 1995; **49**: 259-262
- Lindgren S**, Floren CH, Lindgren T, Starck M, Stewnius J, Nassberger L. Low prevalence of anti-neutrophil cytoplasmic antibodies in ulcerative colitis patients with long-term remission. *Eur J Gastroenterol Hepatol* 1995; **7**: 563-568
- Moran A**, Jones A, Asquith P. Laboratory markers of colonoscopic activity in ulcerative colitis and Crohn's colitis. *Scand J Gastroenterol* 1995; **30**: 356-360
- Ivanov AF**, Eroshkina TD, Fomin SA, Musin II, Chirkin VV. The effect of hemosorption on the glycoprotein concentration of the blood serum in inflammatory diseases of the large intestine. *Ter Arkh* 1995; **67**: 36-39
- Philipsen EK**, Bondesen S, Andersen J, Larsen S. Serum immunoglobulin G subclasses in patients with ulcerative colitis and Crohn's disease of different disease activity. *Scand J Gastroenterol* 1995; **30**: 50-53
- Sahmoud T**, Hocht-Boes G, Modigliani R, Bitoun A, Colombel JF, Soule JC, Florent C, Gendre JP, Lerebours E, Sylvester R, Mary JY. Identifying patients with a high risk of relapse in quiescent Crohn's disease. The GETAID groups. The groupe d' Etudes therapeutiques des affections inflammatoires digestives. *Gut* 1995; **37**: 811-818

• CLINICAL RESEARCH •

Synthesis of endotoxin receptor CD14 protein in Kupffer cells and its role in alcohol-induced liver disease

Li-Li Dai, Jian-Ping Gong, Guo-Qing Zuo, Chuan-Xin Wu, Yu-Jun Shi, Xu-Hong Li, Yong Peng, Wu Deng, Sheng-Wei Li, Chang-An Liu

Li-Li Dai, Guo-Qing Zuo, Department of Digestive Disease, the Second College of Clinical Medicine & the Second Affiliated Hospital of Chongqing University of Medical Science, 74 Linjiang Road, Chongqing 400010, China

Jian-Ping Gong, Chuan-Xin Wu, Yu-Jun Shi, Xu-Hong Li, Yong Peng, Wu Deng, Sheng-Wei Li, Chang-An Liu, Department of General Surgery, the Second College of Clinical Medicine & the Second Affiliated Hospital of Chongqing University of Medical Science, 74 Linjiang Road, Chongqing 400010, China

Supported by the National Natural Science Foundation of China, No.39970719, 30170919

Correspondence to: Dr Jian-Ping Gong, Department of General Surgery, the Second College of Clinical Medicine & the Second Affiliated Hospital of Chongqing University of Medical Science, 74 Linjiang Road, Chongqing 400010, China. gongjianping11@hotmail.com

Telephone: +86-23-63766701 **Fax:** +86-23-63822815

Received: 2002-06-24 **Accepted:** 2002-07-22

Abstract

AIM: To observe the synthesis of endotoxin receptor CD14 protein and its mRNA expression in Kupffer cells (KCs), and evaluate the role of CD14 in the pathogenesis of liver injury in rats with alcohol-induced liver disease (ALD).

METHODS: Twenty-eight Wistar rats were divided into two groups: ethanol-fed group and control group. Ethanol-fed group was fed ethanol (dose of 5g·12g·kg⁻¹·d⁻¹) and control group received dextrose instead of ethanol. Two groups were sacrificed at 4 wk and 8 wk, respectively. KCs were isolated and the synthesis of CD14 protein and its mRNA expression in KCs were determined by flow cytometric analysis (FCM) or the reverse transcription polymerase chain reaction (RT-PCR) analysis. The levels of plasma endotoxin and alanine transaminase (ALT) were measured by Limulus Amebocyte Lysate assay and standard enzymatic procedures respectively, and the levels of plasma tumor necrosis factor (TNF)-α and interleukin (IL)-6 were both determined by ELISA. The liver pathology change was observed under light and electric microscopy.

RESULTS: In ethanol-fed group, the percentages of FITC-CD14 positive cells were 76.23 % and 89.42 % at 4 wk and 8 wk, respectively. Compared with control group (4.45 % and 5.38 %), the difference was significant ($P<0.05$). The expressions of CD14 mRNA were 7.56 ± 1.02 and 8.74 ± 1.37 at 4 wk and 8 wk, respectively, which were significantly higher compared with the control group (1.77 ± 0.21 and 1.98 ± 0.23) ($P<0.05$). Plasma endotoxin levels at 4 wk and 8 wk increased significantly in ethanol-fed group (129 ± 21 ng·L⁻¹ and 187 ± 35 ng·L⁻¹) than those in control rats (48 ± 9 ng·L⁻¹ and 53 ± 11 ng·L⁻¹) ($P<0.05$). Mean values of plasma ALT levels increased dramatically in ethanol-fed rats (112 ± 15 IU/L and 147 ± 22 IU/L) than those in the control animals (31 ± 12 IU/L and 33 ± 9 IU/L) ($P<0.05$). In ethanol-fed rats, the levels of TNF-α were 326 ± 42 ng·L⁻¹ and 402 ± 51 ng·L⁻¹ at 4 wk and 8 wk, respectively which were significantly higher than those

in control group (86 ± 12 ng·L⁻¹ and 97 ± 13 ng·L⁻¹) ($P<0.05$). The levels of IL-6 were 387 ± 46 ng·L⁻¹ and 413 ± 51 ng·L⁻¹, which were also higher than control group (78 ± 11 ng·L⁻¹ and 73 ± 10 ng·L⁻¹) ($P<0.05$). In liver section from ethanol-fed rats, there were marked pathological changes including steatosis, cell infiltration and necrosis. No marked pathological changes were seen in control group.

CONCLUSION: Ethanol administration led to a significant synthesis of endotoxin receptor CD14 protein and its gene expression in KCs, which maybe result in the pathological changes of liver tissue and hepatic functional damages.

Dai LL, Gong JP, Zuo GQ, Wu CX, Shi YJ, Li XH, Peng Y, Deng W, Li SW, Liu CA. Synthesis of endotoxin receptor CD14 protein in Kupffer cells and its role in alcohol-induced liver disease. *World J Gastroenterol* 2003; 9(3): 622-626

<http://www.wjgnet.com/1007-9327/9/622.htm>

INTRODUCTION

Our previous studies have shown that the ethanol-fed rats or rats with endotoxemia had higher endotoxin levels in plasma, increased lipopolysaccharide (LPS) receptor CD14 in the liver, and more serious liver injury compared with control rats^[1-6]. But it was unclear where CD14 came from. Accordingly, the purpose of this study is to determine whether Kupffer cells (KCs) synthesize CD14 protein and express its mRNA, and evaluate the role of CD14 protein in alcohol-induced liver disease (ALD).

MATERIALS AND METHODS

Animals and treatments

Twenty-eight adult female Wistar rats weighing 180 g to 220 g were fed *ad libitum* a liquid diet. Animals were divided into two groups: ethanol liquid diet group (ethanol-fed group) and liquid diet group (control group). The rats of ethanol-fed group were fed ethanol, and control group received the same diet but with isocaloric amounts of dextrose instead of ethanol. In ethanol-fed group, the initial dose is 5 g·kg⁻¹·d⁻¹ and the concentration of ethanol within the diet increased up to 12 g·kg⁻¹·d⁻¹ gradually in 8 weeks. All diets were prepared fresh daily. All the animals were anesthetized with sodium pentobarbital (30 mg·kg⁻¹ intraperitoneally) and sacrificed at 4 wk and 8 wk, respectively. Blood was withdrawn from the portal vein and stored at -70 °C before use.

KCs isolation

KCs were isolated with the in situ collagenase perfusion technique, modified as described previously^[7,8]. In brief, the livers were removed after a portal vein perfusion with Hanks' balanced salt solution (HBSS) and the homogenate was digested in a solution of 0.5 g·L⁻¹ collagenase (Type IV, Sigma). The digest was washed thoroughly and plated on plastic dishes in RPMI medium containing 50 mL·L⁻¹ fetal calf serum (FCS).

After 3 h incubation at 37 °C in O₂ and CO₂ (0.95/0.05), nonadherent cells were removed with pipet. The adherent cells were collected with a rubber policeman. KCs purity exceeded 90 % as assessed by light microscopy, and viability was typically greater than 92 % as determined by trypan blue exclusion assay.

Flow cytometric analysis (FCM)

Synthesis of CD14 protein in KCs was examined by FCM^[2,3]. In brief, KCs were incubated with the anti-CD14 polyclonal antibody (0.1 mg·L⁻¹) for 30 mins after washing, cells were incubated with goat anti-rabbit immunoglobulin G labeled with FITC for 30 min, after being washed for three times, and 10 000 cells were analyzed by FCM (Coulter, USA). The percentage and mean fluorescence intensity (MFI) of CD14-positive cells were taken as the indexes.

RNA isolation and complementary DNA synthesis

Total RNA was isolated from KCs with the TRIZOL Reagent (Life Technologies, USA). The quality of RNA was controlled by the intactness of ribosomal RNA bands. 0.5 mg of each intact total RNA samples was reverse-transcribed to complementary DNA (cDNA) with the reverse transcription polymerase chain reaction (RT-PCR) kit (Roche, USA). cDNA was stored at -70 °C until polymerase chain reaction (PCR) analysis.

Determination of CD14 mRNA by RT-PCR

The PCR primers used were CD14: sense (5'-CTCAACCTAGAGCCGTTTCT-3'), anti-sense (5'-CAGGATTGTCAGACAGGTCT-3'); β -actin: sense (5'-ACCACAGCTGAGAGGGAATCG-3'), antisense (5'-AGAGGTCTTTACGGATGTCAACG-3'). The sizes of the amplified PCR products were 267 bp for CD14, and 281 bp for β -actin. The reaction conditions for amplification were as below: denaturation at 93 °C for 1 min, annealing at 57 °C for 2 min, and extension at 71 °C for 1 min for 30 cycles. The PCR products were electrophoresed in 20 g·L⁻¹ agarose gels, and the gels were ethidium bromide stained and video photographed on an ultraviolet transilluminator, and the results were showed with the relative absorbance (Ar: relative optical density, ROD).

Blood endotoxin & ALT

To determinate the endotoxin, blood was collected into pyrogen-free tubes containing heparin. Plasma was immediately separated at 4 °C by centrifugation at 200 g for 8 minutes and stored in pyrogen-free tubes at -70 °C. Plasma endotoxin levels were measured within a week using the Limulus Amebocyte Lysate assay. Serum alanine transaminase (ALT) was measured by standard enzymatic procedures.

Bioassay for cytokines production in plasma

The levels of TNF- α and IL-6 in plasma were determined with enzyme-linked immunosorbent assay (ELISA) kits according to the manufacture's instructions and guidelines (Biosource International, Camarillo, CA).

Liver pathology

Liver samples from left liver lobes were fixed with 100 ml·L⁻¹ buffered formalin or 25 g·L⁻¹ glutaraldehyde immediately. For optical microscope, the tissue blocks were embedded in paraffin, and stained with hematoxylin and eosin (HE). For electronic microscope, the tissue blocks were embedded in Epon 618 resin and ultrathin sections were stained with uranyl acetate and lead citrate. A H-2000 transmission electron microscope was employed.

Statistical analysis

All results were expressed as $\bar{x} \pm s_x$. Statistical differences between means were determined using Student's *t* test. A *P* value of ≤ 0.05 was considered significant.

RESULTS

Binding of FITC to KCs

To confirm the synthesis of CD14 protein in KCs, we examined the binding of FITC to the cells. The percentages of FITC-CD14 positive cells at 4 wk and 8 wk were 4.45 % and 5.38 % in control group, respectively. While in ethanol-fed group, the mean fluorescence intensity (MFI) dramatically increased, the numbers of FITC-CD14 positive cells were 76.23 % and 89.42 % at 4 wk and 8 wk, respectively. There was significant difference when compared to control group ($P < 0.05$).

Expression of CD14 mRNA in KCs

CD14 mRNA expression in both groups KCs was determined with RT-PCR. In control group, there was no significant expression at the level of CD14 mRNA at 4 wk and 8 wk, respectively. However, it was significantly higher in ethanol-fed rats compared with control group ($P < 0.05$, Figure 1).

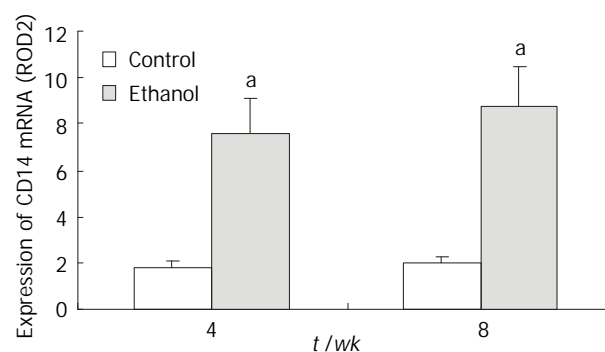


Figure 1 Expression of CD14 mRNA in KCs. ^a $P < 0.05$ vs controls.

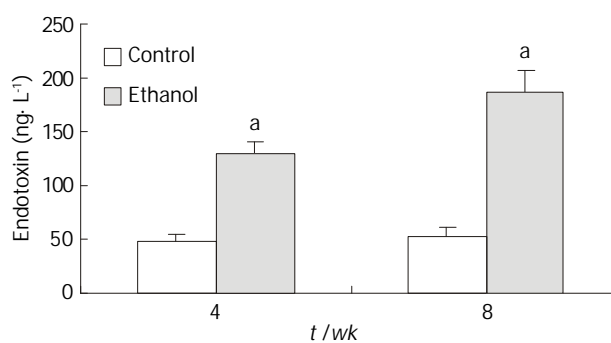


Figure 2 Changes of endotoxin levels. ^a $P < 0.05$, vs controls.

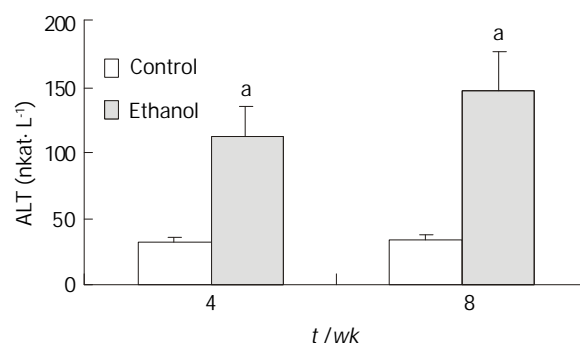


Figure 3 Changes of serum alanine transaminase levels. ^a $P < 0.05$, vs controls.

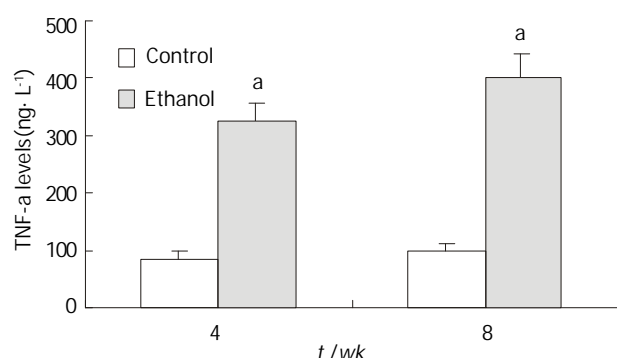


Figure 4 Changes of TNF-α concentrations. ^a $P < 0.05$ vs controls.

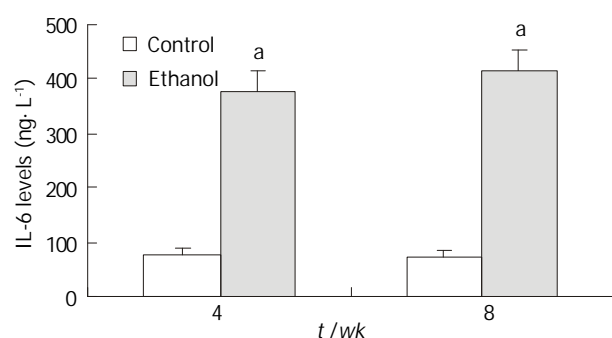


Figure 5 Changes of IL-6 concentrations. ^a $P < 0.05$ vs controls.

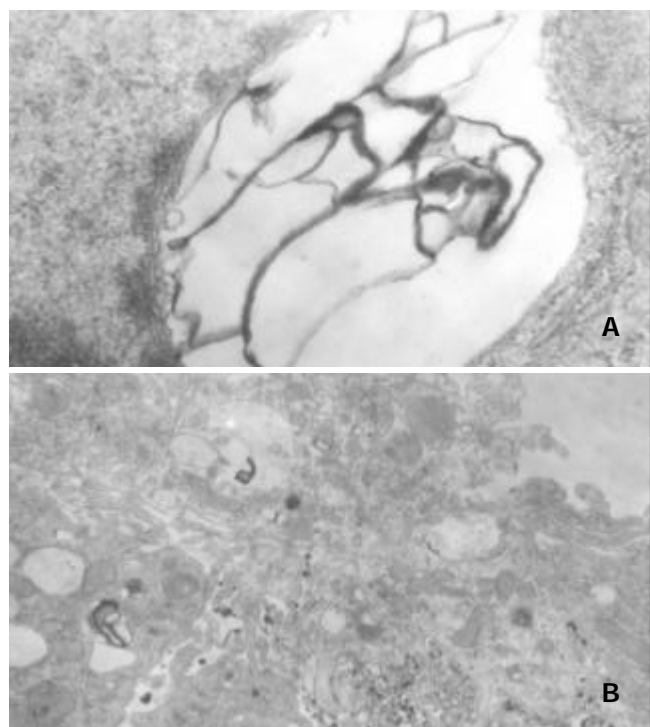


Figure 6 Ethanol-fed rats. A: Huge focal cytoplasmic degeneration in the cytoplasm of hepatocyte TEM×30 000; B: Many focal cytoplasmic degeneration and myelin figures in the cytoplasm of KC TEM×15 000.

Blood endotoxin and ALT levels

Plasma endotoxin levels in ethanol-fed rats increased significantly by ethanol to values of (129 ± 21) ng·L⁻¹ at 4 wk and (187 ± 35) ng·L⁻¹ at 8 wk, the levels of endotoxin were about 2-fold and 3-fold higher than the values of control rats [(48 ± 9) ng·L⁻¹ and (53 ± 11) ng·L⁻¹] ($P < 0.05$, Figure 2). Mean values for ALT in the control animals were (31 ± 12) nkat·L⁻¹ and

(33 ± 9) nkat·L⁻¹ at 4 wk and 8 wk, respectively. Plasma ALT levels were increased dramatically to (112 ± 15) nkat·L⁻¹ and (147 ± 22) nkat·L⁻¹ in ethanol-fed rats after 4 wk and 8 wk, respectively ($P < 0.05$, Figure 3).

Cytokines production in plasma

In ethanol-fed group, the plasma concentrations of TNF-α and IL-6 at 4 wk and 8 wk were 326 ± 42 ng·L⁻¹, 402 ± 51 ng·L⁻¹, 387 ± 46 ng·L⁻¹, and 413 ± 51 ng·L⁻¹, respectively, which were higher than those in control group (86 ± 12) ng·L⁻¹, 97 ± 13 ng·L⁻¹, 78 ± 11 ng·L⁻¹, and 73 ± 10 ng·L⁻¹) ($P < 0.05$, Figure 4 and Figure 5).

Pathological changes

No pathological changes in the liver were observed in the control rats at 4 wk or 8 wk. However, in liver section from rats after 4 wk on ethanol liquid diet, steatosis in both microvesicular and macrovesicular was observed. Few inflammation but accumulation of blood cells in the sinusoidal lining was observed. In liver section from rats after 8 wk on ethanol diet, marked pathological changes (steatosis, cell infiltration and necrosis), KCs proliferation and hypertrophy were detected. Under electron microscopy, huge focal cytoplasmic degeneration and necrosis could be seen in hepatocytes of ethanol-fed rats (Figure 6A). KCs hypertrophy and their surface projections increased as well as, and the phagocytic vacuoles or electron dense phagosomes, Focal cytoplasmic degeneration and many myelin figures in their cytoplasm could also be seen (Figure 6B).

DISCUSSION

Many studies have documented that liver disease could result from the dose- and time-dependent consumption of alcohol^[1,9,10]. However, the mechanisms remain unclear. There appears to be increasing evidences that ethanol toxicity maybe associated with increased levels of endotoxin in plasma^[9,11-16]. Endotoxin or LPS is believed to exert many of its effects on the liver injury via interacting with LBP and CD14^[17-23]. LBP and CD14 are clearly implicated in the molecular and cellular basis of the interaction between endotoxin and monocytes/macrophages. LBP in serum can recognize and bind LPS to form LPS-LBP complexes and activate cells through CD14 receptor on the membrane of these cells, initiate a process leading to the release of cytokines (*e.g.*, tumor necrosis factor-α and interleukins), prostanoids, and other soluble mediators^[9,10,24-29]. The release of these mediators is considered to be an early key step in the pathogenesis of liver disease because they trigger inflammatory events in the liver and alter the parenchymal homeostasis, ultimately initiate liver injury^[30-34]. But, it is not clear where CD14 in liver comes from.

The major goal of this study is to observe the synthesis of CD14 protein and its mRNA expression in KCs in ethanol-fed rats and evaluate the its role in ALD. It was found that endotoxin levels in the plasma of rats treated with ethanol were increased significantly when compared with control animals. The increase in CD14 mRNA levels in the ethanol-fed rats is correlated to inflammation degree and necrosis in the liver of these animals, which developed fatty liver, necrosis, and inflammation. Control rats showed no liver pathological changes. In the present study, we found the severity of pathological changes in ethanol-fed rats was accompanied with the increase in CD14 mRNA in KCs and serum ALT. A similar pattern of changes was observed by Yin *et al*^[12]. They found that blood endotoxin and hepatic CD14 mRNA and protein were increased by ethanol. Therefore, the sensitivity (vulnerability) of rat liver to alcohol-induced injury is directly related to CD14 expression in the liver, leading to the increased production of TNF-α, free radicals, interleukins and other

cytokines^[35-39]. The marked increase in the synthesis of CD14 protein suggests a new mechanism by which alcohol enhanced the LPS-mediated cytokine signaling by the liver macrophages, thus promoting the interaction between alcohol and endotoxins in the development of liver injury^[40-43].

It has been well established that the Liver is the main source of acute reaction protein^[1-6, 8]. However, the mechanism by which the synthesis of CD14 protein and its mRNA expression in the liver increased is thus as yet unclear. It is reported that the synthesis of CD14 protein and its gene expression occurred mainly in monocytes/macrophages, including the cells that reside in the liver (KCs) and these may represent recruitment of inflammatory cells, for example, infiltrating mononuclear cells or macrophages that have high expression of CD14 gene and CD14 protein^[44-48]. The increased CD14 protein may promote monocytes/macrophages response to low level of endotoxin, and lead to NF- κ B activation and production of pro-inflammatory cytokines, which play an important role in alcoholic liver injury^[49-53].

In summary, our results show that ethanol administration led to a significant increase of CD14 protein synthesis and its mRNA expression in KCs when compared with the control rats. The synthesis of CD14 protein and its gene expression may result in greater sensitivity of hepatocytes to endotoxin and lead to the pathological changes of liver tissue and liver functional injury.

REFERENCES

- Zuo GQ**, Gong JP, Liuo CH, Li SW, Wu CX, Yang K, Li Y. Expression of lipopolysaccharide binding protein and its receptor CD14 in experimental alcoholic liver disease. *World J Gastroenterol* 2001; **7**: 836-840
- Li SW**, Gong JP, Wu CX, Shi YJ, Liu CA. Lipopolysaccharide induced synthesis of CD14 protein and its gene expression in hepatocytes during endotoxemia. *World J Gastroenterol* 2002; **8**: 124-127
- Han DW**. Intestinal endotoxemia as a pathogenetic mechanism in liver failure. *World J Gastroenterol* 2002; **8**: 961-965
- Li SW**, Wu CX, Shi YJ, Liu CA. Lipopolysaccharide upregulates expression of CD14 gene and CD14 proteins of hepatocytes in rats. *Zhonghua Ganzangbing Zazhi* 2001; **9**: 103-105
- Gong JP**, Liu CA, Wu CX, Li SW, Shi YJ, Yang K, Li Y, Li XH. Liver sinusoidal endothelial cell injury by neutrophils in rats with acute obstructive cholangitis. *World J Gastroenterol* 2002; **8**: 342-345
- Gong JP**, Han BL. Role of CD14 in activation of Kupffer cell induced by lipopolysaccharide. *Shijie Huaren Xiaohua Zazhi* 1999; **7**: 875-877
- Gong JP**, Han BL. Isolation, culture and identification of liver cells. *Shijie Huaren Xiaohua Zazhi* 1999; **7**: 417-419
- Gong JP**, Wu CX, Liu CA, Li SW, Shi YJ, Yang K, Li Y, Li XH. Intestinal damage mediated by Kupffer cells in rats with endotoxemia. *World J Gastroenterol* 2002; **8**: 923-927
- Jarvelainen HA**, Fang C, Ingelman-Sundberg M, Lindros KO. Effect of chronic coadministration of endotoxin and ethanol on rat liver pathology and proinflammatory and anti-inflammatory cytokines. *Hepatology* 1999; **29**: 1503-1510
- Mathurin P**, Deng QG, Keshavarzian A, Choudhary S, Holmes EW, Tsukamoto H. Exacerbation of alcoholic liver injury by eneral endotoxin in rats. *Hepatology* 2000; **32**: 1008-1017
- Lin H**, Lu M, Zhang YX, Wang BY, Fu BY. Induction of a rat model of alcoholic liver disease. *Shijie Huaren Xiaohua Zazhi* 2001; **9**: 24-28
- Yin M**, Ikejima K, Wheeler MD, Bradford BU, Seabra V, Forman DT, Sato N, Thurman RG. Estrogen is involved in early alcohol-induced liver injury in a rat enteral feeding model. *Hepatology* 2000; **31**: 117-123
- Kono H**, Rusyn I, Yin M, Gabele E, Yamashina S, Dikalova A, Kadiiska MB, Connor HD, Mason RP, Segal BH, Bradford BU, Holland SM, Thurman RG. NADPH oxidase-derived free radicals are key oxidants in alcohol-induced liver disease. *J Clin Invest* 2000; **106**: 867-872
- French SW**. Intragastric ethanol infusion model for cellular and molecular studies of alcoholic liver disease. *J Biomed Sci* 2001; **8**: 20-27
- Enomoto N**, Ikejima K, Yamashina S, Enomoto A, Nishiura T, Nishimura T, Brenner DA, Schemmer P, Bradford BU, Rivera CA, Zhong Z, Thurman RG. Kupffer cell-derived prostaglandin E₂ is involved in alcohol-induced fat accumulation in rat liver. *Am J Physiol* 2000; **279**: G100-G106
- Bautista AP**. Impact of alcohol on the ability of Kupffer cells to produce chemokines and its role in alcoholic liver disease. *J Gastroenterol Hepatol* 2000; **15**: 349-356
- Wu RQ**, Xu YX, Song XH, Chen LJ, Meng XJ. Adhesion molecule and proinflammatory cytokine gene expression in hepatic sinusoidal endothelial cells following cecal ligation and puncture. *World J Gastroenterol* 2001; **7**: 128-130
- Ling YL**, Meng AH, Zhao XY, Shan BE, Zhang JL, Zhang XP. Effect of cholecystokinin on cytokines during endotoxic shock in rats. *World J Gastroenterol* 2001; **7**: 667-671
- Hiki N**, Berger D, Mimura Y, Frick J, Dentener MA, Buurman WA, Seidelmann M, Kaminishi M, Beger HG. Release of endotoxin-binding protein during major elective surgery: role of soluble CD14 in phagocytic activation. *World J Surg* 2000; **24**: 499-506
- Gutsmann T**, Muller M, Carroll SF, Mackenzie RC, Wiese A, Seydel U. Dual role of lipopolysaccharide (LPS)-binding protein in neutralization of LPS and enhancement of LPS-induced activation of mononuclear cells. *Infect Immun* 2001; **69**: 6942-6950
- Heumann D**, Adachi Y, Le Roy D, Ohno N, Yadomae T, Glauser MP, Calandra T. Role of plasma, lipopolysaccharide-binding protein, and CD14 in response of mouse peritoneal exudates macrophages to endotoxin. *Infect Immun* 2001; **69**: 378-385
- Scott MG**, Vreugdenhil ACE, Buurman WA, Hancock REW, Gold MR. Cutting edge: cationic antimicrobial peptides block the binding of lipopolysaccharide (LPS) to LPS binding protein. *J Immunol* 2000; **164**: 549-553
- Kono H**, Wheeler MD, Rusyn I, Lin M, Seabra V, Rivera CA, Bradford BU, Forman DT, Thurman RG. Gender differences in early alcohol-induced liver injury: role of CD14, NF- κ B, and TNF- α . *Am J Physiol Gastrointest Liver Physiol* 2000; **278**: G652-G661
- Lin E**, Calvano SE, Lowry SF. Inflammatory cytokines and cell response in surgery. *Surgery* 2000; **127**: 117-126
- Wang LS**, Zhu HM, Zhou DY, Wang YL, Zhang WD. Influence of whole peptidoglycan of *bjfdobacterium* on cytotoxic effectors produced by mouse peritoneal macrophages. *World J Gastroenterol* 2001; **7**: 440-443
- Bai XY**, Jia XH, Cheng LZ, Qu YD. Influence of IFN α -2b and BCG on the release of TNF and IL-1 by Kupffer cells in rats with hepatoma. *World J Gastroenterol* 2001; **7**: 419-421
- Asea A**, Kraeft SK, Hurt-Jones EA, Stevenson MA, Chen LB, Finberg RW, Koo GC, Calderwood SK. HSP70 stimulates cytokine production through a CD14-dependant pathway, demonstrating its dual role as a chaperone and cytokine. *Nature Med* 2000; **6**: 435-442
- McCaughan GW**, Gorrell MD, Bishop GA, Abbott CA, Shackel NA, McGunness PH, Levy MT, Sharland AF, Bowen DG, Yu D, Slaitini L, Church WB, Napoli J. Molecular pathogenesis of liver disease: an approach to hepatic inflammation, cirrhosis and liver transplant tolerance. *Im ol Rev* 2000; **174**: 172-191
- Hedin KE**, Kaczynski JA, Gibson MR, Urrutia R, Minn R. Transcription factors in cell biology, surgery, and transplantation. *Surg Research Rev* 2000; **128**: 1-5
- Bone-Larson CL**, Simpson KJ, Colletti LM, Lukacs NW, Chen SC, Lira S, Kunkel SL, Hogaboam CM. The role of chemokines in the immunopathology of the liver. *Immunol Rev* 2000; **177**: 8-20
- Marlin M**, Katz J, Vogel SN, Michalek SM. Differential induction of endotoxin tolerance by lipopolysaccharides derived from *porphyromonas gingivalis* and *Escherichia coli*. *J Immunol* 2001; **167**: 5278-5285
- Enomoto N**, Yamashina S, Kono H, Schemmer P, Rivera CA, Enomoto A, Nishiura T, Nishimura T, Brenner DA, Thurman RG. Development of a new, simple rat model of early alcohol-induced liver injury based on sensitization of Kupffer cells. *Hepatology* 1999; **29**: 1680-1689
- Ikejima K**, Enomoto N, Seabra V, Ikejima A, Brenner DA, Thurman RG. Pronase destroys the lipopolysaccharide receptor

- CD14 on Kupffer cells. *Am J Physiol Gastrointest Liver Physiol* 1999; **276**: G591-G598
- 34 **Jarvelainen HA**, Orpana A, Perola M, Savolainen VT, Karhunen PJ, Lindros KO. Promoter polymorphism of the CD14 endotoxin receptor gene as a risk factor for alcoholic liver disease. *Hepatology* 2001; **33**: 1148-1153
- 35 **Shoham S**, Huang C, Chen JM, Golenbock DT, Levitz SM. Toll-like receptor 4 mediates intracellular signaling without TNF- α release in response to cryptococcus neoformans polysaccharide capsule. *J Immunol* 2001; **166**: 4620-4626
- 36 **Kimmings AN**, van Deventer SJH, Obertop H, Rauws EAJ, Huibregtse K, Gouma DJ. Endotoxin, cytokines, and endotoxin binding proteins in obstructive jaundice and after preoperative biliary drainage. *Gut* 2000; **46**: 725-731
- 37 **Guo XW**, Dudman NP. Homocysteine induces expressions of adhesive molecules on leukocytes in whole blood. *Chin Med J* 2001; **114**: 1235-1239
- 38 **LeVan TD**, Bloom JW, Bailey TJ, Karp CL, Halonen M, Martinez FD, Vercelli D. A common single nucleotide polymorphism in the CD14 promoter decreases the affinity of Sp protein binding and enhances transcriptional activity. *J Immunol* 2001; **167**: 5838-5844
- 39 **Nanbo A**, Nishimura H, Muta T, Nagasawa S. Lipopolysaccharide stimulates HepG2 human hepatoma cells in the presence of lipopolysaccharide-binding protein via CD14. *Eur J Biochem* 1999; **260**: 183-191
- 40 **Gordon H**. Detection of alcoholic liver disease. *World J Gastroenterol* 2001; **7**: 297-302
- 41 **Macdonald GA**, Bridle KR, Ward PJ, Walker NI, Houghlum K, George DK, Smith JL, Powell LW, Crawford DH, Ramm GA. Lipid peroxidation in hepatic steatosis in humans is associated with hepatic fibrosis and occurs predominately in acinar zone 3. *J Gastroenterol Hepatol* 2001; **16**: 599-606
- 42 **Calne RY**. Immunological tolerance-the liver effect. *Immunol Rev* 2000; **174**: 280-282
- 43 **Uesugi T**, Froh M, Arteel GE, Bradford BU, Thurman RG. Toll-like receptor 4 is involved in the mechanism of early alcohol-induced liver injury in mice. *Hepatology* 2001; **34**: 101-108
- 44 **Heinrich JM**, Bernheiden M, Minigo G, Yang KK, Schutt C, Mannel DN, Jack RS. The essential of lipopolysaccharide-binding protein in protection of mice against a peritoneal *salmonella* infection involves the rapid induction of an inflammatory response. *J Immunol* 2001; **167**: 1624-1628
- 45 **Neilsen PO**, Zimmerman GA, McIntyre TM. *Escherichia coli* braun lipoprotein induces a lipopolysaccharide-like endotoxic response from primary human endothelial cells. *J Immunol* 2001; **167**: 5231-5239
- 46 **Jersmann HPA**, Hii CST, Hodge GL, Ferrante A. Synthesis and surface expression of CD14 by human endothelial cells. *Infect Immun* 2001; **69**: 479-485
- 47 **Funda DP**, Tuckova L, Farre MA, Iwase T, Moro I, Tlaskalova-Hogenova H. CD14 is expressed and released as soluble CD14 by human intestinal epithelial cells in vitro: lipopolysaccharide activation of epithelial cells revisited. *Infect Immun* 2001; **69**: 3772-3781
- 48 **Le Roy D**, Padova FD, Adachi Y, Glauser MP, Calandra T, Heumann D. Critical role of lipopolysaccharide-binding protein and CD14 in immune responses against gram-negative bacteria. *J Immunol* 2001; **167**: 2759-2765
- 49 **Perera PY**, Mayadas TN, Takeuchi O, Akira S, Zaks-Zilberman M, Goyert SM, Vogel SN. CD11b/CD18 acts in concert with CD14 and Toll-like receptor (TLR) 4 to elicit full lipopolysaccharide and taxol-inducible gene expression. *J Immunol* 2001; **166**: 574-581
- 50 **Gong JP**, Liu CA, Wu CX, Li SW, Shi YJ, Li XH. Nuclear factor κ B activity in patients with acute severe cholangitis. *World J Gastroenterol* 2002; **8**: 346-349
- 51 **Medvebev AE**, Henneke P, Schromm A, Lien E, Ingalls R, Fenton MJ, Golenbock DT, Vogel SN. Induction of tolerance to lipopolysaccharide and mycobacterial components in Chinese hamster ovary/CD14 cells is not affected by overexpression of Toll-like receptor 2 or 4. *J Immunol* 2001; **167**: 2257-2267
- 52 **Jiang Q**, Akashi S, Miyake K, Petty HR. Cutting Edge: Lipopolysaccharide induces physical proximity between CD14 and Toll-like receptor 4 (TLR4) prior to nuclear translocation of NF- κ B. *J Immunol* 2000; **165**: 3541-3544
- 53 **Jarvelainen HA**, Fang C, Ingelman-Sundberg M, Lukkari TA, Sippel H, Lindros KO. Kupffer cell inactivation alleviates ethanol-induced steatosis and CYP2E1 induction but not inflammatory responses in rat liver. *J Hepatol* 2000; **32**: 900-910

Edited by Bo XN

Concomitant hepatocellular adenoma and adenomatous hyperplasia in a patient without cirrhosis

Chuan-Yuan Hsu, Cheng-Hsin Chu, Shee-Chan Lin, Fee-Shih Yang, Tsen-Long Yang, Kuo-Ming Chang

Chuan-Yuan Hsu, Cheng-Hsin Chu, Shee-Chan Lin, Department of Hepatology & Gastroenterology, Mackay Memorial Hospital, Taipei, Taiwan, China

Fee-Shih Yang, Department of Radiology, Mackay Memorial Hospital, Taipei, Taiwan, China

Tsen-Long Yang, Department of Surgery, Mackay Memorial Hospital, Taipei, Taiwan, China

Kuo-Ming Chang, Department of Pathology, Mackay Memorial Hospital, Taipei, Taiwan, China

Correspondence to: Dr. Chuan-Yuan Hsu, Department of Hepatology & Gastroenterology, Mackay Memorial Hospital, No. 92, Chung-Shan N. Road 2 Section, 104 Chung-Shan Area, Taipei, Taiwan, China. erichsu@msl.mmh.org.tw

Telephone: +886-2-25433535

Received: 2002-11-29 **Accepted:** 2002-12-22

Abstract

AIM: Hepatocellular adenoma (HCA) and adenomatous hyperplasia (AH) are rare benign tumors of the liver. HCA is usually found in women who use oral contraceptives. AH usually occurs in patients with liver cirrhosis. Both tumors have potential for malignant transformation.

METHODS: We described a male adult with chronic liver disease (CLD) who had been known to be a hepatitis B carrier (HBV) for years. He was found to have a space-occupying lesion with a suspicion of hepatocellular carcinoma (HCC) by abdominal ultrasonography. His α -fetoprotein (AFP) was normal. Angiographic findings were consistent with the diagnosis of HCC, he wished to avoid an operation, was treated with transcatheter hepatic arterial embolization.

RESULTS: He subsequently consented to surgery, and a right lobectomy was performed. The liver pathology disclosed HCA with nuclear dysplasia and post-embolization effects. In addition, there were multiple small foci of AH with nuclear dysplasia in the resected liver. Although he had some focal areas of cirrhosis-like change or post-embolization effect, the AH was associated only with normal liver tissue.

CONCLUSION: This case confirms that HCA and AH may resemble HCC on imaging studies, and that AH may occur in CLD in the absence of cirrhotic change.

Hsu CY, Chu CH, Lin SC, Yang FS, Yang TL, Chang KM. Concomitant hepatocellular adenoma and adenomatous hyperplasia in a patient without cirrhosis. *World J Gastroenterol* 2003; 9(3): 627-630

<http://www.wjgnet.com/1007-9327/9/627.htm>

INTRODUCTION

Benign hepatic tumors, such as hepatocellular adenoma (HCA) and adenomatous hyperplasia (AH), result from a variety of neoplastic and regenerative proliferative processes. HCA is an uncommon benign tumor of the liver most frequently

occurring in women with long-standing contraceptive steroid use^[1-4, 10, 11]. It usually regresses after discontinuation of contraceptives^[5, 6]. HCA in men has usually been found in association with glycogen storage disease, diabetes, and the use of androgen and anabolic steroids^[7, 10, 11]. HCA is usually solitary, but multiple adenomas have been described, ranging from two nodules to multiple or disseminated lesions of various size. The latter is termed hepatic adenomatosis^[8-10]. Patients may present with a palpable mass over the right upper quadrant. Although most cases are asymptomatic and detected only incidentally, HCA may rupture and lead to life-threatening hemorrhage^[12]. Malignant transformation of HCA is rare, but it may be very difficult to distinguish a benign tumor from a well-differentiated hepatocellular carcinoma (HCC) clinically^[10].

Edmondson first reported adenomatous hyperplasia (AH) of the liver in 1974. He defined it as a regenerative overgrowth with limited growth potential^[13]. AH is the term most commonly used in Japan, while researchers in the United States and Europe call it a macroregenerative nodule (MRN). At the recommendation of the International Working Party Consensus Conference, the terminology for these dysplastic nodules has been standardized^[10]. Based on characterization of cytological and architectural atypia, AH is generally classified as type I MRN (or ordinary AH) and type II MRN (or atypical AH)^[14, 30]. The lesions are usually associated with liver cirrhosis^[14]. The size of AH varies from 5 mm to 10 mm in different series^[10], but a huge AH lesion of 10 cm in diameter has been reported^[29]. AH probably represents one type of malignant precursor^[30]. However, the distinction of AH from well-differentiated HCC, particularly in samples obtained by needle biopsy, can be quite difficult, if not impossible^[10]. Despite several cases reported in the literature, AH remains a poorly understood disease of unknown etiology.

We reported a case with infrequent presentation of both HCA and multiple AH lesions in HBV-related chronic liver disease.

MATERIALS AND METHODS

Case report

A 30-year-old Asian man had been known to be a hepatitis B virus (HBV) carrier for many years. His younger brother had died of HBV-related HCC about 1 year ago. Therefore, he came to the outpatient department (OPD) of Mackay Memorial Hospital (a tertiary referral center) for evaluation of his liver condition. Nine years previously, he had undergone laparotomy at another hospital for a ruptured appendix. He had no history of smoking or alcohol consumption, and he denied use of any medications or exogenous hormones. His alanine aminotransferase (ALT) was 40 U/L (normal: 5-30 U/L), hepatitis B surface antigen (HBsAg) was positive; "e" antigen of hepatitis B (HBeAg) was negative, and AFP 3.33 ng/ml (normal < 6.00 ng/ml). Abdominal sonography demonstrated (a) a space-occupying lesion consistent with HCC, (b) chronic liver disease (CLD), and (c) a gall bladder polyp without stone. The space-occupying hypoechoic lesion, measuring about 24×22 mm in size, was located in the right lobe of the liver (Figure 1).

Because of the abnormal sonographic findings, he was admitted for further assessment and management.

On physical examination, he had no hepatosplenomegaly or abdominal tenderness. In admission, not only the routine hemogram of blood cells and differential count, platelet count, but also prothrombin and activated partial thromboplastin time were normal. The urinalysis and stool for occult blood were negative findings. Biochemistry of blood glucose, protein, albumin, alkaline-phosphatase, aspartate aminotransferase (AST), ALT, total cholesterol, triglycerides, blood urea nitrogen, uric acid, creatinine, potassium, sodium, chloride, and CA19-9 were all normal. The total bilirubin was mildly elevated (1.4 mg/dl, normal range: 0.2-1.3 mg/dl), but the direct bilirubin was normal. The chest X-ray and electrocardiogram were unremarkable. No liver tumor was seen on computed tomography (CT) with or without contrast (Figure 2). On the 6th hospital day, he underwent hepatic angiography that revealed multiple tumor stains in the right lobe of the liver, strongly suggestive of HCC (Figure 3). Given the fact that this patient was hesitant to undergo operation and that there were multiple angiographic lesions, these tumors were embolized with 6 cubic centimetres lipiodol, 6 cubic centimetres lipodox, gelfoam pieces and cephalosporin. The patient subsequently consented to surgery. Indocyanine green (ICG) was 3 % (normal: 0-10 %).

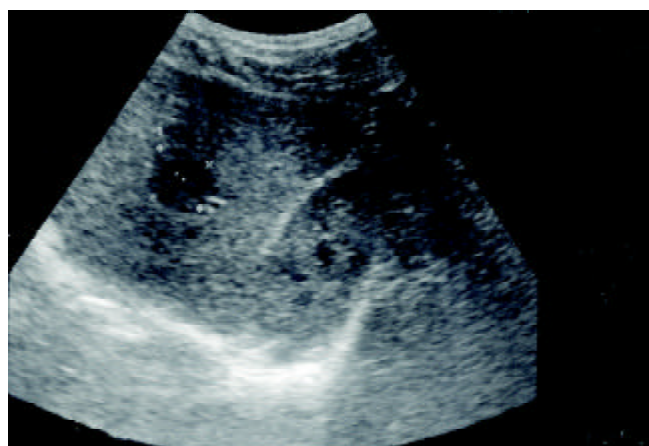


Figure 1 A hypoechoic lesion in the right lobe of the liver, segment S6, 24×22 mm in diameter (asterisks).

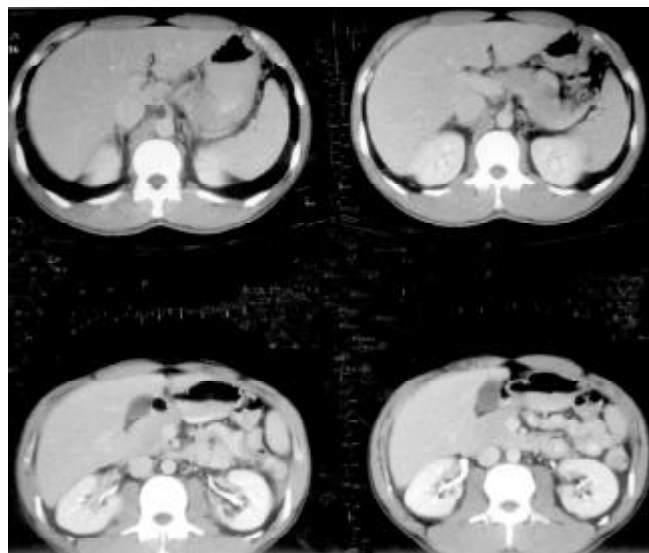


Figure 2 No evidence of hepatocellular tumor seen on upper abdominal CT with contrast.



Figure 3 On angiography, there was an oval hypervascular lesion (black arrows) and multiple scattered tiny hypervascular spots in the right lobe of the liver (white arrows).

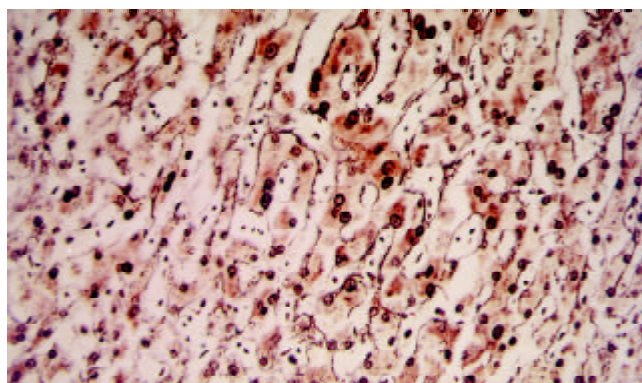


Figure 4 Slightly disarrayed hepatocytes with nuclear dysplasia were found. Besides one-to-two layer reticulin stain, not consistent with HCC, was present. (Reticulin stain, ×250).

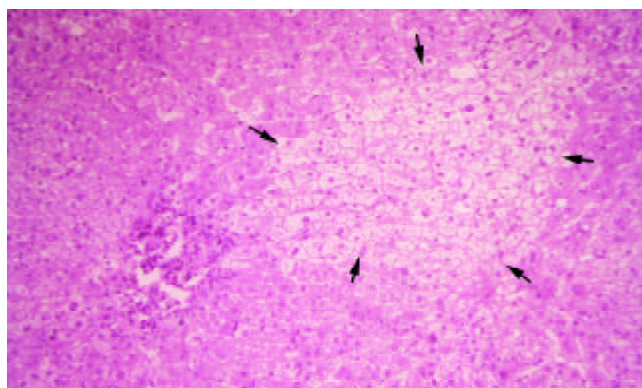


Figure 5 An oval-shape nodule (black arrows) which consisted of disarrayed hepatocytes with nuclear change and clear change in the cytoplasm was surrounded by normal liver tissue. (H&E stain, ×125).

On the 17th hospital day, he underwent total right hepatic lobectomy and cholecystectomy. Grossly on the cut section, there was an easily identifiable, well-defined solitary nodule, 2 cm in the greatest dimension, darker than the surrounding hepatic tissue with a central stellate dark red appearance. The hepatic tissue elsewhere has several 2-4 mm, fairly well-defined dark gray spots. And three areas of subcapsular hemorrhage, the largest 1 cm in diameter, were noted. The surgical margins appeared to be free of tumor involvement.

Microscopically, the main nodule was composed of hepatocytes much larger than the normal cells, with frequent nuclear dysplasia but no apparent increase of nucleus-to-

cytoplasm ratio or mitoses. The arrangement of the hepatocytes in the nodule was disturbed (partially collapsed), which was thought to represent an ischemic-degenerative effect of embolization. However, there was not yet frank infarction except for a focal area in the stellate scar-like lesion in the center. Reticulin staining demonstrated a one-to-two layer arrangement with slight disarray, inconsistent with the appearance of HCC (Figure 4). No biliary ductules were found at the periphery of the stellate area. There was preservation of Kupffer's cells. The lesion was fairly well demarcated from the surrounding normal liver tissue, but it lacked a capsule. The overall appearance indicated a liver cell adenoma post-embolization.

The small gray spots had slightly disarrayed hepatocytes with occasional nuclear dysplasia and clear changes in the cytoplasm, which were arranged in one-to-two-layer thin cords. They had preserved reticulin fibers, in contrast to HCC, and thus were consistent with AH (Figure 5). Excluding the aforementioned lesions, the remaining hepatic tissue was fairly normal except for focal areas with chronic inflammation in the portal triads with bridging fibrosis and possible early cirrhosis. However, post-embolization effect may be considered. The GB was found to have cholesterol polyps.

The patient recovered from surgery uneventfully. He was discharged and followed in the OPD. The other viral markers including HCV and HDV were negative by immunoassay.

DISCUSSION

In regions where HBV is hyper-epidemic, there is a corresponding increase in the incidence of HCC compared to areas with less HBV disease. HBV carriers are more likely than HBV-free individuals to develop HCC. Therefore, in Taiwan, China, with its high prevalence of HBV carriage and incidence of HCC, an HBV carrier presenting with a hepatic mass requires careful evaluation. Therefore, benign lesions must be precisely differentiated from malignant masses.

HCA is a rare benign tumor with a variable sonographic appearance. Cherqui *et al* reported that, of 6 cases, 4 tumors were hyperechoic, 3 hypoechoic, and 1 isoechoic^[15]. Welch *et al* reported that 4 of 13 tumors had mixed echogenicity and 1 was hypoechogenic^[16]. C.H. Hung *et al* reported the appearance of 12 lesions, 1 with isoechoic, 4 with hypoechogenicity, 3 with hyperechogenicity, and the remaining with mixed echogenicity^[7]. The CT scan features of HCA are also very nonspecific. Mathieu *et al* reported 22 cases with 27 tumors that were hyperdense and 5 with hypodense tumors on dynamic CT^[17]. Cherqui *et al* described 3 lesions in 2 of 6 patients had a hyperdense area corresponding to recent hemorrhage, while the others didn't^[15]. Welch *et al* stated that, of 13 cases, 6 tumors were hypodense and 1 was hyperdense^[16]. Magnetic resonance imaging (MRI) may be used, but it is not always helpful in distinguishing HCA from other liver tumor^[11]. Scintigraphy or radionuclide imaging provides a functional assessment of the liver but is helpless for anatomic imaging. Therefore, abdominal sonography, contrast-enhanced CT or MRI are all limited in their ability to discriminate HCA from HCC. However, they do provide helpful information on the size, number, and tumor location, particularly in relation to vascular structures and the biliary tract. It is very important to assess preoperatively.

Angiographic findings may also vary. Kerlin *et al* demonstrated hypervascular tumors in all 15 patients examined, but 7 also had areas of hypovascularity^[1]. Welch *et al* described 9 of 13 cases with hypervascular lesions that also contained small hypovascular area^[16]. As with the other imaging studies, the specificity of angiography is too low to provide a definitive diagnosis, but is helpful in assessing anatomy prior to resection.

Some researchers have suggested using percutaneous fine-needle biopsy^[18], but we are reluctant to do so. HCA is a hypervascular lesion, with a significant risk of hemorrhage if a large-caliber needle is used^[19, 21]. Second, if the lesion turns out to be malignant, there is a risk of tumor seeding along the needle track^[19, 20]. Third, a small sample obtained with a small-bore needle may not be adequate for a histological diagnosis^[21]. Finally, lesions with malignant transformation within an adenoma could be missed, leading to a false-negative biopsy result. Therefore, we did not feel that percutaneous biopsy was appropriate in our patient.

In most reports, AH is considered to begin with small nodules in a cirrhotic liver, progressing to a larger nodule, and then rapidly transforming into a malignant lesion. Hence, AH is thought to be an early stage in hepatocarcinogenesis, especially when the AH is atypical^[14, 30]. While differentiation between malignancy and AH is clinically important, it is also quite difficult. Nomura *et al* reported 4 cases, 2 of which were hypoechogenic and 3 of which had a hyperechoic focus in an area of hypoechoic change; all 4 lesions were missed on CT, and only 1 was detected at angiography^[22]. Again, some authors advise fine-needle biopsy. However, AH is a small liver tumor, usually less than 2 cm in diameter^[10]. An adequate biopsy specimen should be at least 2.5 cm in diameter^[23]. Given the relatively low chance of benefit, it is not worth the risk of biopsy in cases having small area of AH is suspected. Thus, as with HCA, imaging studies are helpful for screening but not for definitive diagnosis of AC, and biopsy is probably not helpful.

AH usually occurs in the presence of liver cirrhosis^[10, 24, 25]. Nevertheless, Gindhart *et al* reported a case of AH of the liver arising spontaneously in an 82-year-old woman without cirrhosis^[26]. Terada *et al* described another case of AH in a patient with chronic active hepatitis^[27]. Theise *et al* incidentally found a small HCC arising in AH in a patient with chronic hepatitis C infection but without cirrhosis^[28]. Furuya *et al* reviewed 345 autopsy cases of chronic liver disease and found one case of AH in a noncirrhotic liver^[25]. In this case, aside from the HCA and AH, most of the liver tissue was normal, except for focal areas of early cirrhosis. The AH lesions all occurred in areas with normal liver tissue, not in conjunction with the focal cirrhosis. AH thus apparently can occur in CLD, not only in patients with cirrhosis. It may represent a malignant precursor in either condition.

In conclusion, this case confirms the difficulty noted in the literature of distinguishing HCA and AH from malignant hepatoma using clinical criteria alone, i.e., history, physical examination, imaging study or biopsy. Surgical intervention for diagnosis, therefore, is undoubtedly required. If that is not possible, very close follow up is recommended. Consideration of the diagnosis of AH should not be limited to patients with liver cirrhosis, since it may occur in CLD of varying etiology, such as HBV. Further research is needed to establish methods for early differentiation of small HCC and benign liver tumors. Until such methods are available, an aggressive, invasive approach is most likely necessary.

ACKNOWLEDGEMENT

Thank Dr. MJ Buttrey for revise elaborately.

REFERENCES

- 1 **Kerlin P**, Davis GL, McGill DB, Weiland LH, Adson MA, Sheedy PF II. Hepatic adenoma and focal nodular hyperplasia: clinical, pathologic, and radiologic features. *Gastroenterology* 1983; **84**: 994-1002
- 2 **Nichols III FC**, van Heerden JA, Weiland LH. Benign liver tumors. *Surg Clin North Am* 1989; **69**: 297-314
- 3 **Edmondson HA**, Henderson B, Benton B. Liver cell adenomas

- associated with the use of oral contraceptives. *N Engl J Med* 1976; **294**: 470-472
- 4 **Thomas R**, Kirsten F, Klaus G, Benno R. Liver tumours in women on oral contraceptives. *The Lancet* 1994; **344**: 1568-1569
- 5 **Edmondson HA**, Reynolds TB, Henderson B, Benton B. Regression of liver cell adenoma associated with oral contraceptives. *Ann Intern Med* 1977; **86**: 180-182
- 6 **Kawakatsu M**, Vilgrain V, Erlinger S, Nahum H. Disappearance of liver cell adenoma: CT and MRI imaging. *Abdom Imaging* 1997; **22**: 274-276
- 7 **Hung CH**, Changchien CS, Lu SN, Eng HL, Wang JH, Lee CM, Hsu CC, Tung HD. Sonographic features of hepatic adenomas with pathologic correlation. *Abdom Imaging* 2001; **26**: 500-506
- 8 **Flejou JF**, Barge J, Menu Y, Degott C, Bismuth H, Potet F, Benhamou JP. Liver adenomatosis. An entity distinct from liver adenoma? *Gastroenterology* 1985; **89**: 1132-1138
- 9 **Chiche L**, Dao T, Salamé E, Galais MP, Bouvard N, Schmutz G, Rousselot P, Bioulac-Sage P, Ségol P, Gignoux M. Liver adenomatosis: reappraisal, diagnosis, and surgical management: eight new cases and review of the literature. *Ann Surg* 2000; **231**: 74-81
- 10 **Elizabeth M**. Brunt. Benign tumors of the liver. *Clin Liver Dis* 2001; **5**: 1-15
- 11 **Patricia J**. Mergo, Pablo R. Ros. Benign lesions of the liver. *Radiol Clin North Am* 1998; **36**: 319-331
- 12 **Ann Simpson Fulcher**, Richard Keith Sterling. Hepatic neoplasms: computed tomography and magnetic resonance features. *J Clin Gastroenterol* 2002; **34**: 463-471
- 13 **Edmondson HA**. Benign epithelial tumors and tumor-like lesions of the liver. In: Okuda K, Peters RL, eds. *Hepatocellular carcinoma*. New York: John Wiley & Sons 1976: 309-330
- 14 **Hytioglou P**, Theise ND, Schwartz M, Mor E, Miller C, Thung SN. Macroregenerative nodules in a series of adult cirrhotic liver explants: Issues of classification and nomenclature. *Hepatology* 1995; **21**: 703-708
- 15 **Cherqui D**, Rahmouni A, Charlotte F, Boulahdour H, Métreau JM, Meignan M, Fagniez PL, Zafrani ES, Mathieu D, Dhumeaux D. Management of focal nodular hyperplasia and hepatocellular adenoma in young women: A series of 41 patients with clinical, radiological and pathological correlations. *Hepatology* 1995; **22**: 1674-1681
- 16 **Welch TJ**, Sheedy PF II, Johnson CM, Stephens DH, Charboneau JW, Brown ML, May GR, Adson MA, McGill DB. Focal nodular hyperplasia and hepatic adenoma: comparison of angiography, CT, US and scintigraphy. *Radiology* 1985; **156**: 593-595
- 17 **Mathieu D**, Bruneton JN, Drouillard J, Pointreau CC, Vasile N. Hepatic adenomas and focal nodular hyperplasia: dynamic CT study. *Radiology* 1986; **160**: 53-58
- 18 **Levy I**, Greig PD, Gallinger S, Langer B, Sherman M. Resection of hepatocellular carcinoma without preoperative tumor biopsy. *Ann Surg* 2001; **234**: 206-209
- 19 **Smith EH**. Complications of percutaneous abdominal fine-needle biopsy. *Radiology* 1991; **178**: 253-258
- 20 **Nakamuta M**, Tanabe Y, Ohashi M, Yoshida K, Hiroshige K, Nawata H. Transabdominal seeding of hepatocellular carcinoma after fine-needle aspiration biopsy. *J Clin Ultrasound* 1993; **21**: 551-556
- 21 **Moulton JS**, Moore PT. Coaxial percutaneous biopsy technique with automated biopsy devices: value in improving accuracy and negative predictive value. *Radiology* 1993; **186**: 515-522
- 22 **Nomura Y**, Matsuda Y, Yabuuchi I, Nishioka M, Tarui S. Hepatocellular carcinoma in adenomatous hyperplasia: detection with contrast-enhanced US with carbon dioxide microbubbles. *Radiology* 1993; **187**: 353-356
- 23 **Caturelli E**, Giacobbe A, Facciorusso D. Percutaneous biopsy in diffuse liver disease: increasing diagnostic yield and decreasing complication rate by routine ultrasound assessment of puncture site. *Am J Gastroenterol* 1996; **91**: 1318-1321
- 24 **Terada T**, Terasaki S, Nakanuma Y. A clinicopathologic study of adenomatous hyperplasia of the liver in 209 consecutive cirrhotic livers examined by autopsy. *Cancer* 1993; **72**: 1551-1556
- 25 **Furuya K**, Nakamura M, Yamamoto Y, Toge K, Otsuka H. Macroregenerative nodule of the liver. A clinicopathologic study of 345 autopsy cases of chronic liver disease. *Cancer* 1988; **61**: 99-105
- 26 **Gindhart TD**, Cimis RJ, Mosenthal WT. Adenomatous hyperplasia of the liver. *Arch Pathol Lab Med* 1979; **103**: 34-37
- 27 **Terada T**, Kitani S, Ueda K, Nakanuma Y, Kitagawa K, Masuda S. Adenomatous hyperplasia of the liver resembling focal nodular hyperplasia in patients with chronic liver disease. *Virchows Arch A Pathol Anat Histopathol* 1993; **422**: 247-452
- 28 **Theise ND**, Lapook JD, Thung SN. A macroregenerative nodule containing multiple foci of hepatocellular carcinoma in a noncirrhotic liver. *Hepatology* 1993; **17**: 993-996
- 29 **Chen LK**, Chang FC, Lai CR, Luo JC, Tsai ST, Hwang SJ. Huge adenomatous hyperplasia of the liver. *J Clin Gastroenterol* 2002; **34**: 272-274
- 30 **Orsatti G**, Theise ND, Thung SN, Paronetto F. DNA image cytometric analysis of macroregenerative nodules (adenomatous hyperplasia) of the liver: Evidence in support of their preneoplastic nature. *Hepatology* 1993; **17**: 621-627

Edited by Xu XQ

• CASE REPORT •

Successful rescuing a pregnant woman with severe hepatitis E infection and postpartum massive hemorrhage

Zhan-Sheng Jia, Yu-Mei Xie, Guo-Wu Yin, Jun-Rong Di, Wei-Pin Guo, Chang-Xing Huang, Xue-Fang Bai

Zhan-Sheng Jia, Yu-Mei Xie, Jun-Rong Di, Chang-Xing Huang, Xue-Fang Bai, Center of Diagnosis and Treatment for Infectious Diseases of PLA, Tangdu Hospital, Fourth Military Medical University, Xi'an 730038, Shaanxi Province

Guo-Wu Yin, Department of Obstetrics and Gynecology, Tangdu Hospital, Fourth Military Medical University, Xi'an 730038, Shaanxi Province

Wei-Pin Guo, Department of Intervention, Tangdu Hospital, Fourth Military Medical University, Xi'an 730038, Shaanxi Province

Correspondence to: Dr. Zhan-Sheng Jia, Center of Diagnosis and Treatment for Infectious Diseases of PLA, Tangdu Hospital, 1 Xinsi Road, Baqiao District, Xi'an 710038, Shaanxi Province, China. jiazsh@fmmu.edu.cn

Telephone: +86-29-3377742 **Fax:** +86-29-3537377

Received: 2002-10-30 **Accepted:** 2002-11-19

Abstract

AIM: To sum up the experience of the successful therapy for the severe hepatitis of pregnant woman with postpartum massive hemorrhage.

METHODS: The advanced therapeutic methods including the bilateral uterine artery embolism, hemodialysis and artificial liver support therapy were performed with comprehensive medical treatments and the course of the successful rescuing the patient was analyzed.

RESULTS: Through the hospitalization of about two months the patient and her neonatus had gotten the best of care in our department and pediatric department separately. Both of them were discharged in good condition.

CONCLUSION: The key points for a successful therapy of the pregnant woman with severe hepatitis are termination of the pregnancy and the control of their various complications. It was suggested that the proper combination of these measures of modern therapy would race against time for renewing of hepatic and renal functions.

Jia ZS, Xie YM, Guo WP, Di JR, Yin GW, Huang CX, Bai XF. Successful rescuing a pregnant woman with severe hepatitis E infection and postpartum massive hemorrhage. *World J Gastroenterol* 2003; 9(3): 631-632

<http://www.wjgnet.com/1007-9327/9/631.htm>

INTRODUCTION

Hepatitis E infection is the most common cause of severe hepatitis in pregnancy, being seriously dangerous for both maternal and fetal life with a mortality rate of 58 %, even up to 100 % if a postpartum massive hemorrhage occurs^[1-4]. A pregnant woman with severe hepatitis E infection complicated with postpartum massive hemorrhage and fulminant hepatic and acute renal failure is presented in this report. With the comprehensive medical treatments in an intensive care setting and three advanced therapeutic measures including bilateral

uterine artery embolism, hemodialysis and artificial liver support therapy, a satisfactory outcome of both the mother and child was achieved.

CASE REPORT

A 24-year-old pregnant woman was admitted to our hospital in May 11th 2002 and presented with a 31-week pregnancy and an 11-day history of asthenia, abdominal distention with deep jaundice. On examination she had a blood pressure of 20/12 kPa, peripheral and facial puffiness, icteric sclera and xanthochromia. The fetal heart rate was 140 beats/min. Laboratory findings showed a normal white blood cell count and a decreased platelet counts ($76 \times 10^9/L$) with a hemoglobin level of 102 g/L. Liver function tests were obvious abnormal (albumin 25.9 g/L, bilirubin 579 $\mu\text{mol/L}$, alanine transaminase 158 IU/L). Prothrombin time activity (PTA) was 21.5 %. The markers of hepatitis virus showed negative for hepatitis A, C and D, positive for anti-HB surface and anti-HE (IgM). So a diagnosis of fulminant hepatic failure of pregnancy (FHFP) with hepatitis E infection was made.

A further clinical course gave a risk signal for the maternal and fetal life. After admission, the gravid woman in the intensive care unit was treated by catharsis with lactulose in order to terminate the pregnancy. With the regular uterine contraction and colporrhagia that appeared as parturient signals, she was immediately sent to the childbearing ward for parturition. After the childbirth of a 1 300 g-weight male baby who was sent to the pediatric care ward, the patient developed postpartum massive hemorrhage. Her blood pressure dropped to 10.7-6.67/6.67-4.0 kPa, at a minimum falling to 0/0 kPa. With the drug hemostasis, such as uterotonic, thromboplasin, and p-amino-merthyl bezoic acid, her colporrhagia could not be stopped. The total of her hemorrhage was about 3 500 ml, and she was on the verge of death. Therefore, it was decided to perform the bilateral uterine artery embolism by the method of intervention. As a result, her colporrhagia was effectively controlled. At the same time fresh blood was transfused together with albumin, and her blood pressure rose up to 15.5/11.5 kPa with the normal vital signs.

After a dangerous delivery the patient underwent a clinical course of exacerbation with hepatic encephalopathy, hepatic renal syndrome, bacterial infection of puerperium and disseminated intravascular coagulation (DIC). The parturient presented fever (to 39.8 °C), oliguria (<400 ml/d) and confusion. The physical signs included severe edema of the whole body, intensive stasis of blood under subcutaneous layer of the abdominal wall and bilateral groin, and huge amount of hemorrhagic ascites. Laboratory study showed that the white blood cell count was $28.8 \times 10^9/L$, N 0.89, Hb $49 \times 10^9/L$, serum creatinine 583.3 $\mu\text{mol/L}$, blood urea nitrogen 24.2 $\mu\text{mol/L}$, blood NH_3 164 $\mu\text{mol/L}$. The tests for DIC revealed thrombocytopenia ($42 \times 10^9/L$), prolonged prothrombin time (PT 32.8 seconds, normal range from 11 to 14 seconds) and active partial thromboplastin time (APTT 88.5 seconds, normal range from 25 to 36 seconds), and hypofibrinogenemia (0.23 g/L).

It was the key time to rescue her hepatic and renal function. The comprehensive medical treatments including diuresis,

hemostasis (antifibrinolytic agents and prothrombin complex) was used with antibiotics for controlling infection and a large number of albumin for improving hypoproteinemia, and in the meanwhile twice hemodialysis for getting rid of the toxic metabolite and the much abundance of her body water were performed. And so the renal and coagulative functions were effectively improved with the increase of her urine volume and the reduction of her whole body edema. However, the improvement of her hepatic function was not significant, total bilirubin remaining at 468 $\mu\text{mol/L}$. Therefore, it was decided that the artificial liver support therapy, an advanced therapeutic approach, was carried out and then the patient got better in her liver function and clinical syndromes with a good appetite. Through the hospitalization of about two mouths the patient and her neonatus had gotten the best of care in our department and pediatric department separately. Both of them were discharged in good condition.

DISCUSSION

Viral hepatitis during pregnancy is common in China^[5-13]. It is one of the most dangerous conditions with a high mortality both for the mother and her fetus, particularly when fulminant hepatic failure occurred^[2,3]. Severe hepatitis is the main cause of FHF in terms of the trimester of gestation^[4]. The pregnant woman with severe hepatitis presents frequently hypodynamia, deep jaundice, coma, hypoproteinemia and sometime acute renal failure^[5]. The patient in this report had a 31-week pregnancy developed severe hepatic dysfunction with deep jaundice (TB 579.9 $\mu\text{mol/L}$, PTA 21.5%), and a positive anti-HE-IgM in her serum, therefore severe hepatitis of pregnancy with HEV infection was diagnosed. It was reported that there were many viruses causing severe hepatitis of pregnancy, but HEV and HBV were frequent, especially HEV infection. The mortality rate was highest (56 %) among HEV infected FHF cases during the third trimester of pregnancy^[4, 14].

Intensive care facilities and an early diagnosis are essential for the management of pregnant patient with severe liver disease^[1,2,14]. The key points for a successful therapy of them are termination of the pregnancy on the proper time and the control of their various complications. It was reported that the severe hepatitis of pregnant woman was with a high mortality rate, even up to 100 % if a postpartum massive hemorrhage and hepatic renal syndrome occur. In this case she presented the very severe hepatic dysfunction and coagulative dysfunctions, and complicated with postpartum massive hemorrhage, bacterial infection, hepatic encephalopathy and hepatic renal syndrome meanwhile or continuously. Therefore the treatments of her were usually very difficult and contradictory.

We considered that the key points of the successful rescuing the patient were on the proper time to adopt three important therapeutic measures. The first was to perform decisively on proper time the bilateral uterine artery embolism by the intervention that is an advanced method with a smaller damage in comparison of the complete hysterectomy and effectively stopped the postpartum massive hemorrhage. The second was to use twice hemodialysis by which removed the toxic metabolite and the abundance of water and the proper comprehensive medical treatments for the improvement of her

renal and coagulative function. The third was to carry out in time the artificial liver support therapy that provides a temporary liver support and promotes the spontaneous liver regeneration in the patient with the remove of toxic metabolic products and the decrease of total bilirubin^[15-18]. It was suggested that the proper combination of these measures of modern therapy would race against time for renewing of hepatic and renal functions, and therefore a better outcome of treatment was anticipated.

REFERENCES

- 1 **Jaiswal SP**, Jain AK, Naik G, Soni N, Chitnis DS. Viral hepatitis during pregnancy. *Int J Gynaecol Obstet* 2001; **72**: 103-108
- 2 **Tank PD**, Nandanwar YS, Mayadeo NM. Outcome of pregnancy with severe liver disease. *Int J Gynaecol Obstet* 2002; **76**: 27-31
- 3 **Yang W**, Shen Z, Peng G, Chen Y, Jiang S, Kang S, Wu J. Acute fatty liver of pregnancy: diagnosis and management of 8 cases. *Chin Med J (Engl)* 2000; **113**: 540-543
- 4 **Hussaini SH**, Skidmore SJ, Richardson P, Sherratt LM, Cooper BT, O'Grady JG. Severe hepatitis E infection during pregnancy. *J Viral Hepat* 1997; **4**: 51-54
- 5 **Yan J**, Chen LL, Luo YH, Mao YF, He M. High frequencies of HGV and TTV infections in blood donors in Hangzhou. *World J Gastroenterol* 2001; **7**: 637-641
- 6 **Yan J**, Ma JY, Pan BR, Ma LS. Study on hepatitis B virus in China. *Shijie Huaren Xiaohua Zazhi* 2001; **9**: 611-616
- 7 **Yuan JM**, Govindarajan S, Gao YT, Ross RK, Yu MC. Prospective evaluation of infection with hepatitis G virus in relation to hepatocellular carcinoma in Shanghai, China. *J Infect Dis* 2000; **182**: 1300-1303
- 8 **Wen YM**. Laboratory diagnosis of viral hepatitis in China: the present and the future. *Clin Chem Lab Med* 2001; **39**: 1183-1189
- 9 **Wang XZ**, Jiang XR, Chen XC, Chen ZX, Li D, Lin JY, Tao QM. Seek protein which can interact with hepatitis B virus X protein from human liver cDNA library by yeast two-hybrid system. *World J Gastroenterol* 2002; **8**: 95-98
- 10 **Wei J**, Wang YQ, Lu ZM, Li GD, Wang Y, Zhang ZC. Detection of anti-preS1 antibodies for recovery of hepatitis B patient by immunoassay. *World J Gastroenterol* 2002; **8**: 276-281
- 11 **Zhang Z**, Wang J, Jiang L. Epidemiological characteristics and risk factors of hepatitis E in Taiyuan. *Zhonghua Yufang Yixue Zazhi* 1997; **31**: 144-146
- 12 **Wu C**, Tao Q. Comparison between homologies of E2/NS1 gene from genotype III Chinese isolates of hepatitis C virus and that from reported isolates. *Chin Med J (Engl)* 1998; **111**: 807-809
- 13 **Guo XC**, Wu YQ. A review: progress of prevention and control on viral hepatitis in China. *Biomed Environ Sci* 1999; **12**: 227-232
- 14 **Luo KX**, Zhang L, Wang SS, Nie J, Yang SC, Liu DX, Liang WF, He HT, Lu Q. An outbreak of enterically transmitted non-A, non-E viral hepatitis. *J Viral Hepat* 1999; **6**: 59-64
- 15 **Hamid SS**, Jafri SM, Khan H, Shah H, Abbas Z, Fields H. Fulminant hepatic failure in pregnant women: acute fatty liver or acute viral hepatitis? *J Hepatol* 1996; **25**: 20-27
- 16 **Strain AJ**, Neuberger JM. A bioartificial liver-state of the art. *Science* 2002; **295**: 1005-1009
- 17 **Nyberg SL**, Hay EJ, Ramin KD, Rosen CB. Successful pregnancy after porcine bioartificial liver treatment and liver transplantation for fulminant hepatic failure. *Liver Transpl* 2002; **8**: 169-170
- 18 **Morsiani E**, Pazzi P, Puviani AC, Brogli M, Valieri L, Gorini P, Scoletta P, Marangoni E, Ragazzi R, Azzena G, Frazzoli E, Di Luca D, Cassai E, Lombardi G, Cavallari A, Faenza S, Pasetto A, Girardis M, Jovine E, Pinna AD. Early experiences with a porcine hepatocyte-based bioartificial liver in acute hepatic failure patients. *Int J Artif Organs* 2002; **25**: 192-202

• CASE REPORT •

Large pedunculated antral hyperplastic gastric polyp traversed the bulbous causing outlet obstruction and iron deficiency anemia: endoscopic removal

Murat Alper, Yusuf Akcan, Olcay Belenli

Murat Alper, Olcay Belenli, Departments of Pathology, University of Abant izzet Baysal, Düzce Medical Faculty, Turkey

Yusuf Akcan, Departments of Gastroenterology, University of Abant izzet Baysal, Düzce Medical Faculty, Turkey

Correspondence to: Dr. Murat Alper, Düzce Tıp Fakültesi Patoloji Ana Bilim Dalı, Konuralp/Düzce, Turkey. malper@ibuduzce-tip.edu.tr

Telephone: +90 380-541 42 13 **Fax:** +90 380-541 42 13

Received: 2002-04-18 **Accepted:** 2002-06-11

Abstract

We present here a large (3 cm) hyperplastic gastric polyp prolapsed into duodenum and caused outlet obstruction and iron deficiency anemia in 60 years old male patient. Endoscopic removal was performed successfully.

Alper M, Akcan Y, Belenli O. Large pedunculated antral hyperplastic gastric polyp traversed the bulbous causing outlet obstruction and iron deficiency anemia: endoscopic removal. *World J Gastroenterol* 2003; 9(3): 633-634

<http://www.wjgnet.com/1007-9327/9/633.htm>

INTRODUCTION

In the literature, it is rarely to see the patients with gastric outlet obstruction due to prolapsing gastric polyps^[1]. Inflammatory fibroid polyp of the gastrointestinal tract is the type most frequently reported^[2]. We present here a large (3 cm) hyperplastic gastric polyp prolapsed into duodenum and caused outlet obstruction and iron deficiency anemia in 60 years old male patient. Endoscopic removal was performed successfully.

CASE

A 60 years old man was admitted to hospital due to severe fatigue, intermittent nausea and vomiting. Undigested food might have been seen in the vomitus. His hemoglobin was 7.6 gr/dl, MCV: 65 and serum iron level: 35 (low); iron binding capacity: 450 (high). All of aforementioned laboratory results indicated that the patient was suffering from iron deficiency anemia. Lower GIS barium enema examination and fiber sigmoidoscopy revealed no pathologic change. In upper endoscopy, initially we saw pyloric canal partially obstructed by a smooth surfaced pili-like structure. When passed to bulbous we observed a large polypoid mass. The biopsies taken were reported as hyperplastic gastric polyp. After re-evaluation of the endoscopic appearance by a second upper endoscopy, we thought that the pili-like structure traversing the pyloric canal might be a stalk of a polyp. Upon dragging the polyp with a controlled force, we were able to bring the polyp back to stomach. It was a pedunculated large antral polyp with a small area eroded on it, which was a possible explanation for blood loss. The polypectomy and removal was performed successfully in toto. The gross appearance (Figure 1) and microscopic examination (Figure 2) revealed a large

hyperplastic polyp with no malignant component in any part. The patient who was regarded cured is under periodic endoscopic followed up. Clinically we transfused two bags of blood and later continued with iron supplementation therapy. Now, the patient is quite well with hemoglobin level of 13.5 gr/dl and has no signs of gastric outlet obstruction, freely consumes a normal diet.

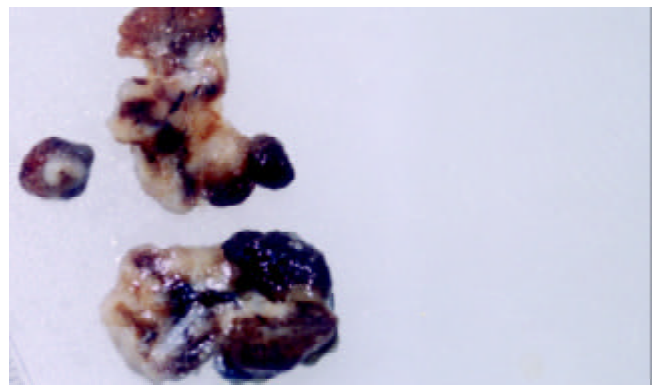


Figure 1 The macroscopic appearance of the polyp.

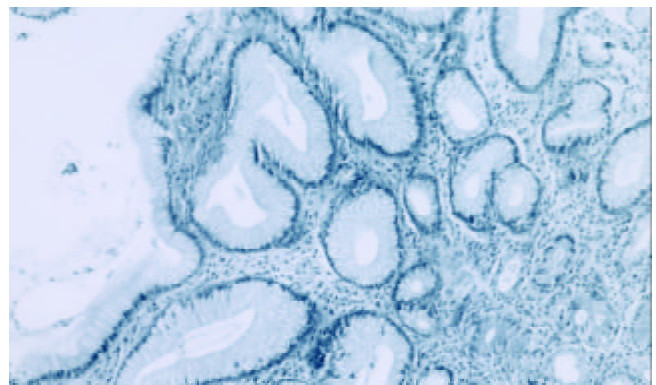


Figure 2 Hyperplastic polyp showing polypoid architecture, foveolar hyperplasia, mild inflammation, and edema. (H&E×200).

DISCUSSION

Histologically, hyperplastic polyp is characterised by a markedly elongated foveolar region: the underlying glands are usually mucous glands. There is a marked lamina propria edema and inflammatory cell infiltration. The frequency of hyperplastic gastric polyps is reported between 1.3 % and 28.3 % in different series of upper gastrointestinal polypectomy^[3,4]. Malignant transformation for hyperplastic polyps is small but the risk may be little bit higher if the polyp is more than 2 cm^[5]. Among the gastric polyps causing outlet obstruction, fibroid polyps are relatively more frequent. Sporadic case reports with other histologic types are

encountered like submucous lipoma^[6]. To the best of our knowledge, there is no hyperplastic gastric polyp with a size of 3 cm originated in the antrum, crossed through the pylorus and captured in the bulb. Rösch *et al*, by now, reported one case of hyperplastic polyp in duodenum formed as a heterotopia of gastric mucosa^[7]. But it was different from our case clinically and with respect to place of formation. In our patient, a 3-cm pediculated polyp had formed in antrum, passed through the pylorus while it was small. Later, it presumably enlarged in bulb so much that it was unable to go back to the stomach. We think so because we hardly take back it to the stomach through pylorus.

Gastric polyps may intussusept to duodenum causing gastric outlet obstruction. If the prolapsed polyp contains a functional antral mucosa over it, that mucosa may keep secreting gastrin due to being placed in the alkaline media of duodenum. In turn this hypergastrinemia may lead to erosion of the prolapsed polyp and blood loss^[8]. Such an assumption could be valid in our case too.

Consequently, large prolapsed polyps can be dragged into stomach by easing the polypectomy procedure with a controlled force, instead of performing it in bulb, which is a narrower space than stomach.

REFERENCES

- 1 **Kumar A**, Quick AU, Carr-Locke DL. Prolapsing gastric polyp, an unusual cause of gastric outlet obstruction: a review of the pathology and management of gastric polyps. *Endoscopy* 1996; **28**: 452-455
- 2 **Johnstone JM**, Morson BC. Inflammatory fibroid polyp of the gastrointestinal tract. *Histopathology* 1978; **2**: 349-361
- 3 **Möckel W**. Hyperplasiogenic gastric polyps and stomach cancer. Endoscopic findings of early stomach cancer in 3 out of 42 biopsies of hyperplasiogenic polyps. *Fortschr Med* 1984; **102**: 635-638
- 4 **Stolte M**, Sticht T, Eidt S, Ebert D, Finkenzeller G. Frequency, location, and age and sex distribution of various types of gastric polyp. *Endoscopy* 1994; **26**: 659-665
- 5 **Gschwantler M**, Pulgram T, Feichtenschlager T, Brownstone E, Gabriel C, Bibus B, Weiss W. Gastric carcinoma arising from a hyperplasiogenic polyp with a diameter of less than 2 centimetres. *Z Gastroenterol* 1995; **33**: 610-612
- 6 **Kallie NR**, Peters JA. Submucous lipoma of the stomach: a case report. *Can J Surg* 1976; **19**: 42-45
- 7 **Rösch W**, Höer PW. Hyperplasiogenic polyp in the duodenum. *Endoscopy* 1983; **15**: 117-118
- 8 **Brooks GS**, Frost ES, Wesselhoeft C. Prolapsed hyperplastic gastric polyp causing gastric outlet obstruction, hypergastrinemia, and hematemesis in an infant. *J Pediatr Surg* 1992; **27**: 1537-1538

Edited by Zhang JZ